

Valeria Patricia Sülsen  
Virginia Susana Martino  
*Editors*

# Sesquiterpene Lactones

Advances in their Chemistry  
and Biological Aspects

 Springer

# Sesquiterpene Lactones

Valeria Patricia Sülsen • Virginia Susana Martino  
Editors

# Sesquiterpene Lactones

Advances in their Chemistry  
and Biological Aspects

 Springer

*Editors*

Valeria Patricia Sülsen  
University of Buenos Aires  
CONICET University of Buenos Aires  
Autonomous City of Buenos Aires  
Buenos Aires, Argentina

Virginia Susana Martino  
University of Buenos Aires  
CONICET University of Buenos Aires  
Autonomous City of Buenos Aires  
Buenos Aires, Argentina

ISBN 978-3-319-78273-7      ISBN 978-3-319-78274-4 (eBook)  
<https://doi.org/10.1007/978-3-319-78274-4>

Library of Congress Control Number: 2018941468

© Springer International Publishing AG, part of Springer Nature 2018

This work is subject to copyright. All rights are reserved by the Publisher, whether the whole or part of the material is concerned, specifically the rights of translation, reprinting, reuse of illustrations, recitation, broadcasting, reproduction on microfilms or in any other physical way, and transmission or information storage and retrieval, electronic adaptation, computer software, or by similar or dissimilar methodology now known or hereafter developed.

The use of general descriptive names, registered names, trademarks, service marks, etc. in this publication does not imply, even in the absence of a specific statement, that such names are exempt from the relevant protective laws and regulations and therefore free for general use.

The publisher, the authors and the editors are safe to assume that the advice and information in this book are believed to be true and accurate at the date of publication. Neither the publisher nor the authors or the editors give a warranty, express or implied, with respect to the material contained herein or for any errors or omissions that may have been made. The publisher remains neutral with regard to jurisdictional claims in published maps and institutional affiliations.

*Cover illustration:* The image corresponds to the leaf surface of *Artemisia annua*, showing glandular trichomes, the site of artemisinin biosynthesis. The image belongs to The CNAP Artemisia Research Project, University of York, UK

Printed on acid-free paper

This Springer imprint is published by the registered company Springer International Publishing AG part of Springer Nature.

The registered company address is: Gewerbestrasse 11, 6330 Cham, Switzerland

*We wish to dedicate this book to our dear colleague, Argentine botanist Gustavo Carlos Giberti, who was the mentor of many Argentine medicinal flora scholars.*

*Gustavo Giberti, PhD (September 7th, 1951–July 2nd, 2017), graduated as Agricultural Engineer from University of Buenos Aires (UBA) in 1976.*

*He attended a postgraduate specialization course at Royal Botanic Gardens, Plant Anatomy Section (Kew, Great Britain), directed by David F. Cutler, PhD (1980–1982), and at Escuela Técnica Superior de Ingenieros Agrónomos, Universidad Politécnica de Madrid (Spain), directed by Prof. César Gómez Campo, PhD (1882–1983). In 2002, he earned a PhD from the University of Buenos Aires in the field of pharmacobotany and pharmacognosy.*

*From 1984 up to 2017, he worked as an Independent Researcher of the Scientific and Technological Research Career of the National Council for Scientific and Technical Research (CONICET) at Instituto de Química y Metabolismo del Fármaco*

*(Institute for Drug Chemistry and Metabolism Studies) (IQUIMEFA-UBA-CONICET), and as curator at the Herbarium of Museo de Farmacobotánica (Pharmacobotany Museum) “Juan Aníbal Domínguez” at the School of Pharmacy and Biochemistry (UBA). He also specialized in economic botany and pharmacobotany. In Argentina, he was an expert in plants of the Aquifoliaceae family, especially, those belonging to the Ilex genus.*

*He has authored more than forty scientific papers and about thirteen book chapters and also contributed largely by helping collect and identify the plant materials employed in the research works carried out at the IQUIMEFA.*

*We will always remember Gustavo for his gentleness and kindness and for his immense generosity to share his knowledge with all of us.*

# Foreword

This book was originally conceived as a smaller project focused only on the anti-parasitic activity of sesquiterpene lactones. After the evaluation of the proposal and taking into account the potential applications of this group of compounds, we decided to expand the scope and to explore chemical and biological aspects by including data on other biological activities and structure-activity studies.

Having obtained collaboration from renowned researchers in the field is, indeed, a dream come true. Virginia Martino, PhD, and César Catalan, PhD, deserve special mention, since they were my research directors and continue to be my mentors in the fields of pharmacognosy and chemistry, especially that of sesquiterpene lactones, respectively. Although they are both retired, they have given me support for the fulfillment of this project.

I am also grateful to those who have relied on and collaborated in this project: Marcus Tullius Scotti, PhD, and Fernando Batista da Costa, PhD (chemotaxonomy); Julián Rodríguez Talou, PhD, and María Perassolo, PhD (biotechnology); Francis Barrios, PhD (organic synthesis); Osvaldo Donadel, PhD (chemistry of natural products); Silvia Cazorla, PhD (trypanosomatids); Nubia Boechat, PhD (antiplasmodial compounds); María Elisa Lombardo, PhD (therapeutic targets and antitrypanosomal drugs); Miguel Sosa Escudero (microscopy); María Victoria Castelli, PhD, and Silvia Noelí López, PhD (antimicrobials); Claudia Anesini, PhD (antitumoral compounds); María Rosario Alonso, PhD (anti-inflammatory compounds); and Thomas J. Schmidt, Dr. rer. nat (structure-activity studies), who has given me access to Research Network Natural Products Against Neglected Diseases (ResNet NPND), which is devoted to the searching of novel natural drugs against neglected diseases.

Gustavo Giberti, PhD, also deserves a special mention in this Foreword. He has died unexpectedly in 2017 and to him we dedicate this book with all our affection. We will cherish in our hearts all the fieldwork and experiences we shared.

I believe the content of this book has met the goals. I would like to thank all the collaborating authors. As for me, I can only say: Mission accomplished!

Valeria P. Sülsen



# Preface

Although some interesting reviews on sesquiterpene lactones have been published, many advances have recently been made in this field, which implies the necessity of an update.

The aim of this book is to review such recent advances made in the study of sesquiterpene lactones, discussing their potential medical applications.

Different aspects will be reviewed, such as the distribution and taxonomy; the biosynthetic pathways; their chemistry, including the synthesis and chemical and biological transformations as well as the analytical isolation and identification procedures most frequently employed. Their biological properties mainly focused on the antimicrobial, antiproliferative, and anti-inflammatory activities and structure-activity studies will be also summarized. An update on the main molecular targets for their antiprotozoal activity will also be presented.

It is expected that this book will serve as a source of information to scientific researchers and postgraduate students, being inspiring for the performance of further studies on the chemistry and the biological activities of this fascinating group of compounds. Finally, the aim of this book is to highlight the importance of sesquiterpene lactones as lead molecules for the development of new therapeutic drugs.

Valeria P. Sülsen  
Virginia S. Martino

# Acknowledgments

We thank Dr. Luis Fernando de O. Furtado, Springer Science + Business Media Editor – Applied Sciences, for inviting us to participate in this editorial project and for believing that we could materialize it.

We also acknowledge Panneerselvam Silembarasan, the Project Coordinator (Books) for Springer Nature, for his guidance and prompt reply to our queries.

We are very grateful to all contributing authors for having embarked in this project and for sharing their knowledge and expertise, as well as for having devoted their time to compiling the literature material and to writing each chapter. We would like to congratulate them for the high quality of their contributions and their predisposition to revise the manuscripts.

We thank Guillermo Nuñez Taquíá, PhD, for English correction.

We kindly acknowledge Dr Caroline M. Calvert, CNAP Manager, HVCfP Network Manager, Department of Biology, University of York, York, UK, for providing the cover image.

We are profoundly thankful to the National Council for Scientific and Technical Research (CONICET), the University of Buenos Aires (UBA), and the National Agency for Scientific and Technological Promotion (ANPCyT) – Science, Technology and Productive Innovation Ministry for supporting this project.

This book entails a complex coordination of efforts and it is the embodiment of the work carried out by many people; we want to express our gratitude to all of them.

# Contents

## Part I Chemical and Biochemical Aspects of Sesquiterpene Lactones

<b>1 Overview</b> .....	3
Valeria P. Sülsen and Virginia S. Martino	
1.1 Introduction .....	4
1.2 Chemical Aspects .....	5
1.3 Some Representative Sesquiterpene Lactones .....	6
1.3.1 Santonin .....	6
1.3.2 Artemisinin .....	9
1.3.3 Parthenolide .....	9
1.3.4 Costunolide .....	9
1.3.5 Dehydroleucodine .....	10
1.3.6 Helenalin .....	10
1.3.7 Thapsigargin .....	10
1.3.8 Arglabin .....	11
1.3.9 Cynaropicrin .....	12
1.4 Adverse Health Effects and Toxicity of Sesquiterpene Lactones ..	12
References .....	13
<b>2 Ancient and Modern Concepts About the Asteraceae Taxonomy</b> ...	19
Gustavo C. Giberti	
2.1 Introduction .....	19
2.2 Asteraceae in Old Times Plant Systematics: Its Influences .....	20
2.3 Towards a “Contemporary” Asteraceae Systematics .....	23
2.4 Conclusion .....	25
References .....	26

<b>3</b>	<b>Chemotaxonomic Study of Sesquiterpene Lactones of Asteraceae: Classical and Modern Methods</b> . . . . .	31
	Mateus Feitosa Alves, Luciana Scotti, Fernando Batista Da Costa, and Marcus Tullius Scotti	
3.1	Introduction . . . . .	32
3.2	Classical Taxonomy . . . . .	33
3.3	Modern Chemotaxonomy . . . . .	36
3.4	Sesquiterpene Lactones Database . . . . .	39
3.5	Conclusion . . . . .	42
	References . . . . .	42
<b>4</b>	<b>Biosynthesis of Sesquiterpene Lactones in Plants and Metabolic Engineering for Their Biotechnological Production</b> . . . . .	47
	María Perassolo, Alejandra Beatriz Cardillo, Víctor Daniel Busto, Ana María Giulietti, and Julián Rodríguez Talou	
4.1	Introduction . . . . .	50
4.2	Biosynthesis of the Isoprenoid Precursors in Plants . . . . .	51
4.2.1	Mevalonate (MVA) Pathway . . . . .	51
4.2.2	2-C-Methyl-D-erythritol 4-phosphate (MEP) Pathway . . . . .	53
4.2.3	Cross-Talk Between MVA and MEP Pathways . . . . .	53
4.2.4	Farnesyl Diphosphate Synthase: Branch Point of Sesquiterpene Lactone Biosynthesis . . . . .	54
4.2.5	Sesquiterpene Lactone Pathway . . . . .	54
4.3	Sesquiterpene Lactone Biosynthetic Pathway Characterisation and Regulation in Medicinal and Aromatic Plants . . . . .	56
4.4	Biotechnological Approaches for the Production of Sesquiterpene Lactones: Plant Cell Culture . . . . .	62
4.5	Metabolic Engineering . . . . .	65
4.5.1	Metabolic Engineering in Plants and Plant Cell Culture . . . . .	66
4.5.2	Metabolic Engineering of the Artemisinin Biosynthetic Pathway . . . . .	67
4.6	Conclusion . . . . .	83
	References . . . . .	84
<b>5</b>	<b>Chemistry of Sesquiterpene Lactones</b> . . . . .	93
	Francis J. Barrios	
5.1	Synthesis of Sesquiterpene Lactones . . . . .	93
5.1.1	General Strategies for the Synthesis of the Germacranolide Skeleton . . . . .	94
5.1.2	Synthesis of the $\alpha$ -Methylene- $\gamma$ -Lactone Moiety . . . . .	94
5.1.3	Strategy to the Total Synthesis of Parthenolide . . . . .	96
5.1.4	Semi-synthesis of Parthenolide . . . . .	98
5.1.5	General Strategies for the Synthesis of Guaianolides . . . . .	99
5.1.6	Semi-synthesis of Guaianolides . . . . .	104
5.2	Chemical Transformation of Sesquiterpene Lactones . . . . .	108
5.2.1	Costunolide and Its Derivatives . . . . .	108

5.2.2	Parthenolide and Analogues . . . . .	109
5.2.3	Artemisinin and Its Derivatives . . . . .	111
5.2.4	Santonin and Its Analogues . . . . .	112
	References. . . . .	114
<b>6</b>	<b>Analytical Procedures. . . . .</b>	<b>119</b>
	Valeria P. Sülsen, Cesar A. N. Catalán, and Virginia S. Martino	
6.1	Structure of Sesquiterpene Lactones . . . . .	120
6.1.1	Skeletal Types of Sesquiterpene Lactones. . . . .	120
6.1.2	Common Side Chains in Sesquiterpene Lactones . . . . .	125
6.2	Extraction. . . . .	125
6.3	Isolation . . . . .	132
6.4	Chromatographic Analysis. . . . .	133
6.4.1	Thin Layer Chromatography . . . . .	133
6.4.2	High-Performance Liquid Chromatography . . . . .	134
6.4.3	Gas Chromatography . . . . .	134
6.5	Conclusion . . . . .	135
	References. . . . .	135
<b>7</b>	<b>Spectroscopic Methods for the Identification of Sesquiterpene Lactones . . . . .</b>	<b>137</b>
	Valeria P. Sülsen, Osvaldo J. Donadel, and Cesar A. N. Catalán	
7.1	General Spectroscopic Characteristics of Sesquiterpene Lactones . . . . .	137
7.1.1	MS Spectra. . . . .	138
7.1.2	IR Spectra. . . . .	139
7.1.3	UV Spectra. . . . .	139
7.1.4	CD Spectra. . . . .	140
7.1.5	NMR Spectra . . . . .	140
7.2	NMR Spectra of Sesquiterpene Lactones . . . . .	148
7.2.1	Guaianolides . . . . .	148
7.2.2	Pseudoguaianolides . . . . .	154
7.2.3	Eudesmanolides . . . . .	160
7.2.4	Germacranolides . . . . .	164
	References. . . . .	171
<b>Part II Biological Activities of Sesquiterpene Lactones</b>		
<b>8</b>	<b>Antitrypanosomal and Antileishmanial Activities . . . . .</b>	<b>175</b>
	Andrés Sánchez Alberti, Natacha Cerny, Augusto Bivona, and Silvia I. Cazorla	
8.1	Introduction to Neglected Tropical Diseases . . . . .	176
8.2	Chagas' Disease and Antitrypanosomal Activities of Sesquiterpene Lactones . . . . .	177
8.3	Leishmaniasis and Antileishmanial Activities of Sesquiterpene Lactones . . . . .	185

8.4	Human African Trypanosomiasis.....	190
8.5	Conclusion.....	192
	References.....	192
<b>9</b>	<b>Antiplasmodial Activity</b> .....	<b>197</b>
	Nubia Boechat, Luiz Carlos da Silva Pinheiro, and Flavia Fernandes da Silveira	
9.1	Introduction.....	198
	9.1.1 Malaria.....	198
	9.1.2 Current Chemotherapy for Malaria.....	199
9.2	Sesquiterpene Lactones as Antiplasmodial Agents.....	209
	9.2.1 Artemisinin and its Semisynthetic Derivatives.....	210
	9.2.2 Other Sesquiterpene Lactones with Antiplasmodial Activity.....	211
	9.2.3 Antimalarial Hybrids Containing Sesquiterpene Lactones.....	213
	9.2.4 Dimer, Trimer and Tetramer Sesquiterpene Lactones.....	216
9.3	Conclusion.....	217
	References.....	218
<b>10</b>	<b>Mode of Action on <i>Trypanosoma</i> and <i>Leishmania</i> spp.</b> .....	<b>223</b>
	María E. Lombardo and Alcira Batlle	
10.1	Introduction.....	223
10.2	Molecular Targets.....	224
	10.2.1 Biosynthesis of Sterols.....	224
	10.2.2 Trypanothione Pathway.....	227
	10.2.3 Purine Salvage Pathway.....	228
	10.2.4 Cysteine Proteinases.....	229
	10.2.5 Trans-sialidase.....	230
	10.2.6 Tubulin.....	231
	10.2.7 Homeostasis of Calcium and Pyrophosphate Metabolism.....	231
	10.2.8 Uptake and Degradation of Heme.....	232
10.3	Oxidative Stress and Apoptosis.....	233
10.4	Natural Sesquiterpene Lactones: Parasitic Effects and Probable Targets in Trypanosomatids.....	234
	References.....	236
<b>11</b>	<b>Contribution of Microscopy for Understanding the Mechanism of Action Against Trypanosomatids</b> .....	<b>241</b>
	Esteban Lozano, Renata Spina, Patricia Barrera, Carlos Tonn, and Miguel A. Sosa	
11.1	Introduction.....	242
	11.1.1 Life Cycle of <i>Trypanosoma cruzi</i> .....	242
	11.1.2 Infection and Disease.....	242
	11.1.3 Morphology and Ultrastructure of <i>T. cruzi</i> .....	243

11.2	How Vulnerable Is <i>T. cruzi</i> ? . . . . .	250
11.2.1	Some Molecular Targets for Trypanocidal Agents . . . . .	250
11.3	In the Search for a Solution Against Parasitic Diseases. . . . .	252
11.3.1	Sesquiterpene Lactones . . . . .	253
11.3.2	Diterpenes . . . . .	253
11.3.3	Effect of Sesquiterpene Lactones and Diterpenes on <i>Trypanosoma cruzi</i> . . . . .	254
11.3.4	Effect of Sesquiterpene Lactones on <i>Leishmania</i> spp. . . . .	265
11.4	Conclusion . . . . .	269
	References. . . . .	269
<b>12</b>	<b>Effects on Other Microorganisms . . . . .</b>	<b>275</b>
	María Victoria Castelli and Silvia Noélf López	
12.1	Introduction . . . . .	276
12.2	Antifungal, Antibacterial, and Antiviral Activity. . . . .	277
12.2.1	Guaianolides and Pseudoguaianolides. . . . .	277
12.2.2	Eudesmanolides . . . . .	281
12.2.3	Germacranolides and Other Related Structures. . . . .	286
12.2.4	Carabranolides . . . . .	292
12.2.5	Dimeric Sesquiterpene Lactones . . . . .	293
12.2.6	Seco-prezizaane Sesquiterpene Lactones . . . . .	295
12.2.7	Cadinanolides . . . . .	296
12.2.8	Microbial Sesquiterpene Lactones. . . . .	297
12.3	Conclusion . . . . .	298
	References. . . . .	299
<b>13</b>	<b>Antiproliferative and Cytotoxic Activities . . . . .</b>	<b>303</b>
	Claudia A. Anesini, María Rosario Alonso, and Renzo F. Martino	
13.1	Introduction . . . . .	306
13.2	In Vitro Studies and Mechanism of Action . . . . .	309
13.3	In Vivo Studies . . . . .	315
13.4	Clinical Trials. . . . .	317
13.5	Conclusion . . . . .	319
	References. . . . .	319
<b>14</b>	<b>Anti-inflammatory Activity . . . . .</b>	<b>325</b>
	María Rosario Alonso, Claudia A. Anesini, and Renzo F. Martino	
14.1	Introduction . . . . .	327
14.2	Inflammatory Pathways Serving as Pharmacological Targets in Inflammatory Diseases. . . . .	328
14.2.1	Inflammatory Cytokines . . . . .	329
14.2.2	Caspase-1 and the Inflammasome Complex Nod-Like Receptor Family Pyrin Domain Containing the Complex NLRP3 . . . . .	331
14.2.3	Nuclear Factor Kappa-Light-Chain-Enhancer of Activated B Cells. . . . .	332

14.2.4	The Janus Kinase (Jak)/Signal Transducers and Activators of Transcription (STATs) Pathway . . . . .	332
14.2.5	Nitric Oxide . . . . .	333
14.2.6	Reactive Oxygen Species. . . . .	333
14.2.7	Mitogen-Activated Protein Kinases. . . . .	334
14.2.8	Lipid Mediators . . . . .	334
14.3	Which Are the Most Currently Used Drugs to Treat Inflammation?. . . . .	335
14.4	Effects of Sesquiterpene Lactones on Inflammatory Pathways . . . . .	338
14.4.1	Effects on the NF- $\kappa$ B Pathway . . . . .	338
14.4.2	Effects on Janus Kinase (Jak)/Signal Transducers and Activators of Transcription (STATs) Pathway . . . . .	340
14.4.3	Effects on Cytokine Production, Maturation, and Release . . . . .	340
14.4.4	Effect on Nitric Oxide, Reactive Oxygen Species, Reactive Nitrogen Species, and Antioxidant Contents. . . . .	341
14.4.5	Effect on the Production of Lipid Mediators. . . . .	341
14.4.6	Effects on Mitogen-Activated Protein Kinase. . . . .	342
14.5	Conclusion . . . . .	342
	References. . . . .	343

### Part III Sesquiterpene Lactones: Medicinal Chemistry Approach

<b>15</b>	<b>Structure-Activity and Activity-Activity Relationships of Sesquiterpene Lactones . . . . .</b>	<b>349</b>
	Thomas J. Schmidt	
15.1	Introduction . . . . .	350
15.2	Structure-Antiprotozoal Activity Relationships. . . . .	350
15.2.1	Anti-trypanosomatid Activity: <i>Trypanosoma brucei</i> . . . . .	350
15.2.2	Anti-trypanosomatid Activity: <i>Trypanosoma cruzi</i> . . . . .	357
15.2.3	Anti-trypanosomatid Activity: <i>Leishmania</i> Species . . . . .	359
15.2.4	Antiplasmodial Activity and SAR (Excluding Artemisinin and Derivatives) . . . . .	360
15.3	Structure-Antitumor Activity Relationships . . . . .	362
15.4	Structure-Anti-inflammatory Activity Relationship. . . . .	367
15.5	Conclusion . . . . .	368
	References. . . . .	369



# Contributors

**Andrés Sánchez Alberti** Cátedra de Inmunología, IDEHU (UBA-CONICET), Facultad de Farmacia y Bioquímica, Universidad de Buenos Aires, Buenos Aires, Argentina

Instituto de Microbiología y Parasitología Médica, IMPaM (UBA-CONICET), Facultad de Medicina, Universidad de Buenos Aires, Buenos Aires, Argentina

**María Rosario Alonso** Universidad de Buenos Aires, Facultad de Farmacia y Bioquímica, Departamento de Farmacología, Cátedra de Farmacología, Buenos Aires, Argentina

CONICET – Universidad de Buenos Aires, Instituto de Química y Metabolismo del Fármaco (IQUIMEFA), Buenos Aires, Argentina

**Mateus Feitosa Alves** Federal University of Paraíba, João Pessoa, PB, Brazil

**Claudia A. Anesini** CONICET – Universidad de Buenos Aires, Instituto de Química y Metabolismo del Fármaco (IQUIMEFA), Buenos Aires, Argentina

Universidad de Buenos Aires, Facultad de Farmacia y Bioquímica, Departamento de Farmacología, Cátedra de Farmacognosia, Buenos Aires, Argentina

**Patricia Barrera** Laboratorio de Biología y Fisiología Celular Dr. Francisco Bertini, Instituto de Histología y Embriología (IHEM-CONICET), Mendoza, Argentina

**Francis J. Barrios** Department of Chemistry and Physics, Bellarmine University, Louisville, KY, USA

**Alcira Batlle** CONICET – Universidad de Buenos Aires, Centro de Investigaciones sobre Porfirinas y Porfirias (CIPYP), Buenos Aires, Argentina

**Augusto Bivona** Cátedra de Inmunología, IDEHU (UBA-CONICET), Facultad de Farmacia y Bioquímica, Universidad de Buenos Aires, Buenos Aires, Argentina

Instituto de Microbiología y Parasitología Médica, IMPaM (UBA-CONICET), Facultad de Medicina, Universidad de Buenos Aires, Buenos Aires, Argentina

**Nubia Boechat** Fundação Oswaldo Cruz, Instituto de Tecnologia em Fármacos Farmanguinhos-Fiocruz, Rio de Janeiro, Brazil

**Víctor Daniel Busto** Universidad de Buenos Aires, Facultad de Farmacia y Bioquímica, Departamento de Microbiología, Inmunología y Biotecnología, Cátedra de Biotecnología, Buenos Aires, Argentina

CONICET-Universidad de Buenos Aires, Instituto de Nanobiotecnología (NANOBIOTEC), Buenos Aires, Argentina

**Alejandra Beatriz Cardillo** Universidad de Buenos Aires, Facultad de Farmacia y Bioquímica, Departamento de Microbiología, Inmunología y Biotecnología, Cátedra de Biotecnología, Buenos Aires, Argentina

CONICET-Universidad de Buenos Aires, Instituto de Nanobiotecnología (NANOBIOTEC), Buenos Aires, Argentina

**María Victoria Castelli** Farmacognosia –Facultad de Ciencias Bioquímicas y Farmacéuticas – CONICET – Universidad Nacional de Rosario, Rosario, Argentina

**Cesar A. N. Catalán** CONICET – Universidad Nacional de Tucumán, Instituto de Química del Noroeste – CONICET (INQUINOA), San Miguel de Tucumán, Argentina

**Silvia I. Cazorla** Laboratorio de Inmunología, Centro de Referencia para Lactobacilos (CERELA-CONICET), Tucumán, Argentina

Instituto de Microbiología y Parasitología Médica, IMPaM (UBA-CONICET), Facultad de Medicina, Universidad de Buenos Aires, Buenos Aires, Argentina

**Natacha Cerny** Cátedra de Inmunología, IDEHU (UBA-CONICET), Facultad de Farmacia y Bioquímica, Universidad de Buenos Aires, Buenos Aires, Argentina

Instituto de Microbiología y Parasitología Médica, IMPaM (UBA-CONICET), Facultad de Medicina, Universidad de Buenos Aires, Buenos Aires, Argentina

**Fernando Batista Da Costa** AsterBioChem Research Team, University of São Paulo, School of Pharmaceutical Sciences of Ribeirao Preto, Ribeirao Preto, SP, Brazil

**Luiz Carlos da Silva Pinheiro** Fundação Oswaldo Cruz, Instituto de Tecnologia em Fármacos Farmanguinhos-Fiocruz, Rio de Janeiro, Brazil

**Flavia Fernandes da Silveira** Fundação Oswaldo Cruz, Instituto de Tecnologia em Fármacos Farmanguinhos-Fiocruz, Rio de Janeiro, Brazil

Programa de Pós-graduação em Química da Universidade Federal do Rio de Janeiro, Rio de Janeiro, Brazil

**Oswaldo J. Donadel** Instituto de Investigaciones en Tecnología Química (INTEQUI), Universidad Nacional de San Luis, San Luis, Argentina

**Gustavo C. Giberti** Universidad de Buenos Aires, Facultad de Farmacia y Bioquímica, Buenos Aires, Argentina

CONICET – Universidad de Buenos Aires. Instituto de Química y Metabolismo del Fármaco – CONICET (IQUIMEFA), Buenos Aires, Argentina

**Ana María Giulietti** CONICET-Universidad de Buenos Aires, Instituto de Nanobiotecnología (NANOBIOTEC), Buenos Aires, Argentina

**María E. Lombardo** Universidad de Buenos Aires, Facultad de Ciencias Exactas y Naturales, Departamento de Química Biológica, Buenos Aires, Argentina

CONICET – Universidad de Buenos Aires, Centro de Investigaciones sobre Porfirinas y Porfirias (CIPYP), Buenos Aires, Argentina

**Silvia Noelí López** Farmacognosia – Facultad de Ciencias Bioquímicas y Farmacéuticas – CONICET – Universidad Nacional de Rosario, Rosario, Argentina

**Esteban Lozano** Laboratorio de Inmunología y Desarrollo de Vacunas, Instituto de Medicina y Biología Experimental de Cuyo (IMBECU, CCT-CONICET), Mendoza, Argentina

**Renzo F. Martino** Universidad de Buenos Aires, Facultad de Farmacia y Bioquímica, Departamento de Microbiología, Inmunología y Biotecnología. Cátedra de Inmunología, Buenos Aires, Argentina

**Virginia S. Martino** CONICET – Universidad de Buenos Aires, Instituto de Química y Metabolismo del Fármaco – CONICET (IQUIMEFA), Buenos Aires, Argentina

**María Perassolo** Universidad de Buenos Aires, Facultad de Farmacia y Bioquímica, Departamento de Microbiología, Inmunología y Biotecnología, Cátedra de Biotecnología, Buenos Aires, Argentina

CONICET-Universidad de Buenos Aires, Instituto de Nanobiotecnología (NANOBIOTEC), Buenos Aires, Argentina

**Thomas J. Schmidt** Institute of Pharmaceutical Biology and Phytochemistry (IPBP), University of Münster, PharmaCampus, Münster, Germany

**Luciana Scotti** Federal University of Paraíba, João Pessoa, PB, Brazil

**Marcus Tullius Scotti** Federal University of Paraíba, João Pessoa, PB, Brazil

**Miguel A. Sosa** Laboratorio de Biología y Fisiología Celular Dr. Francisco Bertini, Instituto de Histología y Embriología (IHEM-CONICET), Mendoza, Argentina

**Renata Spina** Laboratorio de Biología y Fisiología Celular Dr. Francisco Bertini, Instituto de Histología y Embriología (IHEM-CONICET), Mendoza, Argentina

**Valeria P. Sülsen** Universidad de Buenos Aires, Facultad de Farmacia y Bioquímica, Cátedra de Farmacognosia, Buenos Aires, Argentina

CONICET – Universidad de Buenos Aires, Instituto de Química y Metabolismo del Fármaco – CONICET (IQUIMEFA), Buenos Aires, Argentina

**Julián Rodríguez Talou** Universidad de Buenos Aires, Facultad de Farmacia y Bioquímica, Departamento de Microbiología, Inmunología y Biotecnología, Cátedra de Biotecnología, Buenos Aires, Argentina

CONICET-Universidad de Buenos Aires, Instituto de Nanobiotecnología (NANOBIOTEC), Buenos Aires, Argentina

**Carlos Tonn** Instituto de Investigación en Tecnología Química (INTEQUI), Facultad de Química Bioquímica y Farmacia, Universidad Nacional de San Luis, San Luis, Argentina

**Part I**  
**Chemical and Biochemical Aspects of**  
**Sesquiterpene Lactones**

# Chapter 1

## Overview



Valeria P. Sülsen and Virginia S. Martino

**Abstract** Sesquiterpene lactones (STLs) are a group of naturally occurring compounds, most of them found in the Asteraceae family but also present in Apiaceae, Magnoliaceae, and Lauraceae. To date about 8000 compounds have been reported. They consist of a C15 backbone with numerous modifications resulting in a variety of structures but with the common feature of a  $\gamma$ -lactone ring. They are classified in four major groups: germacranolides, eudesmanolides, guaianolides, and pseudoguaianolides, though there are other subtypes. There has been an increasing interest in sesquiterpene lactones due to the wide range of biological activities they present. Among the activities found, antimicrobial, antitumor, anti-inflammatory, antioxidant, antiulcerogenic, molluscicidal, antihelminthic, hepatoprotective and hepatotherapeutic, antiprotozoal, antidepressant, and bitter properties have been described. Besides, they play an important role in the interaction of plants with insects acting as attractants, deterrents, and antifeedants. These compounds were considered at first highly cytotoxic, but chemical transformations have enhanced their biological activities and diminished their cytotoxicity, so considerable attention has been drawn again on them as lead molecules. Artemisinin derivatives, artesunate, and artemether are drugs currently being employed, and dimethylaminoparthenolide, a parthenolide synthetic analogue, and mipsagargin, a prodrug from thapsigargin, are under clinical trials.

A summary with the most important findings about the known sesquiterpene lactones, artemisinin, parthenolide, cynaropicrin, dehydroleucodine, mexicanin, helenalin, costunolide, santonin, arglabin, and thapsigargin, will be given.

---

V. P. Sülsen (✉)

Universidad de Buenos Aires, Facultad de Farmacia y Bioquímica, Cátedra de Farmacognosia, Buenos Aires, Argentina

CONICET – Universidad de Buenos Aires. Instituto de Química y Metabolismo del Fármaco - CONICET (IQUIMEFA), Buenos Aires, Argentina

e-mail: [vsulsen@ffyb.uba.ar](mailto:vsulsen@ffyb.uba.ar)

V. S. Martino

CONICET – Universidad de Buenos Aires. Instituto de Química y Metabolismo del Fármaco – CONICET (IQUIMEFA), Buenos Aires, Argentina

Studies about the adverse health effects, toxicity, and ecological roles of some sesquiterpene lactones are also mentioned.

**Keywords** Sesquiterpene lactones · Chemical aspects · Biological activities · Adverse effects · Toxicity

## 1.1 Introduction

Since ancient times, natural products have played an important role in human health and have constituted one of the main sources of bioactive compounds and templates for synthetic modifications. According to Newman and Cragg (2016), the utilization of natural products and their derivatives in the development of new therapeutic drugs is still a promising approach. Recently, the 2015 Nobel Prize in Medicine has been awarded to Dr. Youyou Tu for the discovery of the natural product artemisinin, which is today an important component of the combined therapy for the treatment of malaria. This award highlighted the importance of the investigation of traditional medicine and drugs coming from natural sources (The Society for Medicinal Plant and Natural Product Research 2017). In the cancer research field, during the 1940–2014 period, 49% of all the small molecules approved for medical use were natural products or their derivatives. In other areas, such as the one corresponding to antimicrobial agents, the use of natural products is also frequent.

Sesquiterpene lactones (STLs) are a group of naturally occurring compounds, generally colorless and bitter in taste. Most of them are found in the Asteraceae family; however, they are also present in Apiaceae, Magnoliaceae, and Lauraceae families (Padilla González et al. 2016). They are mainly found in the leaves and in the flowering heads in a range from 0.001% to 8%/dry weight (Chaturvedi 2011). Some species store large amounts of STLs in leaf trichomes (Amorim et al. 2013).

Sesquiterpene lactones are present in food plants such as lettuce (*Lactuca sativa*) and chicory (*Cichorium intybus*), and star anise (*Illicium verum*) and in many medicinal plants such as feverfew (*Tanacetum parthenium*), qinghaosu (*Artemisia annua*), and yarrow (*Achillea* spp.) (Chaturvedi 2011).

There has been an increasing interest in STLs, mainly for their importance as chemical markers in biosystematic studies and for their wide range of biological activities. Among the activities explored for this group of compounds, antimicrobial, antitumor, anti-inflammatory, antioxidant, antiulcerogenic, molluscicidal, anti-helminthic, hepatoprotective and hepatotherapeutic, antidepressant, and bitter properties have been described. Besides, they play an important role in the interaction of plants with insects acting as attractants, deterrents, and antifeedants (Chaturvedi 2011; Amorim et al. 2013).

Sesquiterpene lactones were considered at first highly cytotoxic. Chemical transformations have enhanced their biological activities and diminished their cytotoxicity, so considerable attention has been drawn again on them as lead molecules.

Artemisinin derivatives, artesunate, and artemether are drugs currently being employed, and dimethylaminoparthenolide, a parthenolide synthetic analogue, and mipsagargin, a prodrug from thapsigargin, are under clinical trials.

To date, about 8000 STLs have been reported (Macias et al. 2013). Some early reviews can be found in the literature about STLs which can be considered as a starting point for the present overview. In Yoshioka et al. (1973), the major skeleton types of STLs and the NMR spectra of 200 naturally occurring compounds are presented. Fischer et al. (1979) and Fischer (1990) summarize the biogenetic considerations concerning the different types of STLs as well as the regulation of their biosynthetic pathways. Rodriguez et al. (1976) and Picman (1986) disclose and discuss some of the more important biological activities of STLs. Other more recent reviews by Chaturvedi (2011) describe the structural characteristics and the biological activities of these compounds, while Chadwick et al. (2013) highlight the importance of STLs, not only for their potential as pharmaceutical agents but also for their importance as nutritional factors and for their physiological role in plants as antioxidants and growth factors, antifeedants, and allelochemicals and as the active constituents of many plants used in traditional medicine. Adekenov (2013) provides an overview of the available technology for the isolation of natural STLs and the chemical modifications to which STLs can be subjected and discusses their potential as source of new biologically active derivatives. In a subsequent publication, Adekenov and Atazhanova (2013) summarize the heteroatom-containing natural STLs, their natural occurrence, isolation methods, and biological activities, while Hohmann et al. (2016) disclose their anti-inflammatory effects. Padilla González et al. (2016) discuss the protective and physiological role of STLs in plants.

## 1.2 Chemical Aspects

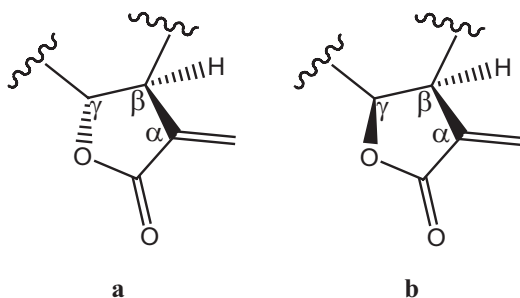
Sesquiterpene lactones consist of a fifteen-carbon (C15) backbone, being the majority cyclic, with numerous modifications and resulting in a variety of structures. A distinctive feature of STLs is the presence of a  $\gamma$ -lactone ring closed toward either C-6 or C-8. This  $\gamma$ -lactone contains, in many cases, an *exo*-methylene group conjugated to the carbonyl group (Padilla González et al. 2016; Picman 1986). The stereochemistry of the lactonization can be either  $\alpha$  or  $\beta$ , since the lactone ring can be fused to the remaining skeleton in either a *trans* or *cis* configuration (*trans*- or *cis*-fused STLs) (Padilla González et al. 2016; Ahern and Whitney 2014). The *trans*-configuration is the most common, and as a rule, the H-7 of STLs is  $\alpha$ -oriented (Fischer 1990) (Fig. 1.1).

In some STLs, the exocyclic methylene is reduced, as is the case of artemisinin, matricin, achillin, and santonin, or the double bond can be endocyclic (Padilla González et al. 2016).

Sesquiterpene lactones are classified in four major groups: germacranolides (10-membered ring), eudesmanolides (6–6 bicyclic compounds), guaianolides, and pseudoguaianolides (5–7 bicyclic compounds) (Yoshioka et al. 1973) (Fig. 1.2). Nevertheless, according to their skeletal arrangement, there are other subtypes of



**Fig. 1.1**  $\alpha,\beta$ -unsaturated  $\gamma$ -lactone moiety present in the sesquiterpene lactones. (a) *trans*-fused lactone ring, (b) *cis*-fused lactone ring



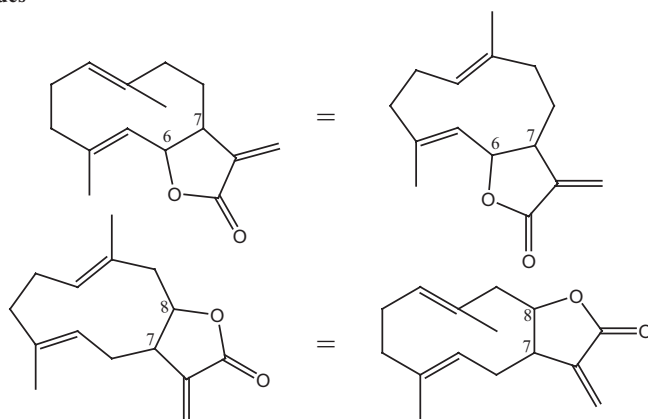
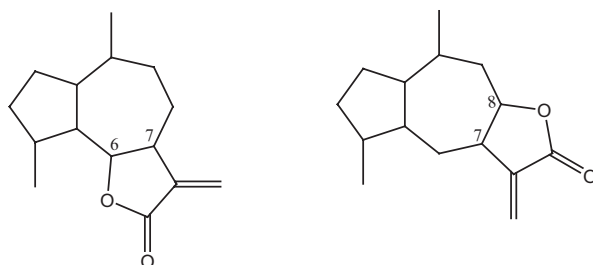
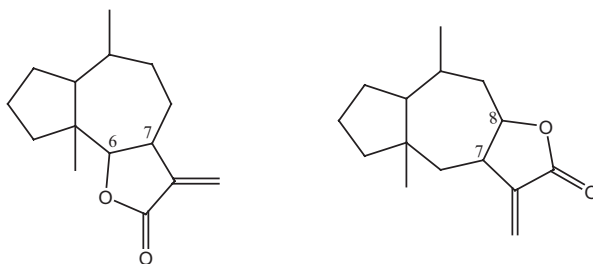
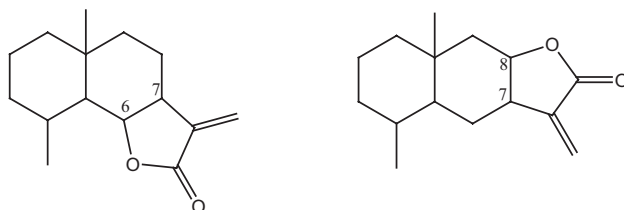
STLs (Fischer et al. 1979; Rodriguez et al. 1976; Picman 1986; Padilla Gonzalez et al. 2016). The suffix “olide” indicates the presence of a lactone group in the structure. The presence of epoxy groups, hydroxyls, and hydroxyls esterified with acetate, which is the most frequent, propionate, isobutyrate, methacrylate, isovalerate, epoxymethacrylate, 2-methylbutanoate, tiglate, angelate, senecioate, epoxyangelate, sarracinate, acetylsarracinate, and other similar residues is frequently found in STLs. Only a few glycosylated lactones or lactones bearing halogen or sulfur atoms in their structures have been described. A cyclopentenone moiety (dehydroleucodin, achillin) and a second  $\alpha,\beta$ -unsaturated lactone ring (mikanolide, deoxyelephantopin) can also be found in STLs (Rodriguez et al. 1976; Picman 1986; Schmidt et al. 2002).

### 1.3 Some Representative Sesquiterpene Lactones

The STLs included in this chapter have been selected based upon the number of studies found in the literature, their biological activities, and/or the fact they are actually being used as medicines or are in clinical trials (Fig. 1.3).

#### 1.3.1 Santonin

Santonin (**1**) is an eudesmanolide present in *Artemisia santonica* and is one of the earliest STLs discovered (1830). This STL has been used as ascaricide and to remove all kind of worms and for the retention of urine and enuresis caused by atony or of other origins. Its pharmaceutical use was abandoned due to its toxic effects. Its anti-inflammatory, antipyretic, and analgesic effects have been reported (al-Harbi et al. 1994). Numerous chemical modifications have been introduced on the santonin structure in order to enhance its antiproliferative activity and cell differentiation on leukemia cells (Khazir et al. 2013; Kweon et al. 2011; Arantes et al. 2010) and its antimalarial activity (Tani et al. 1985). This molecule has been selected as the starting point for the synthesis of other guaianolides and eudesmanolides. Its structure was one of the first to be elucidated among STLs (Birladeanu 2003).

**Germacranolides****Guaianolides****Pseudoguaianolides****Eudesmanolides****Fig. 1.2** Major skeletal types of sesquiterpene lactones

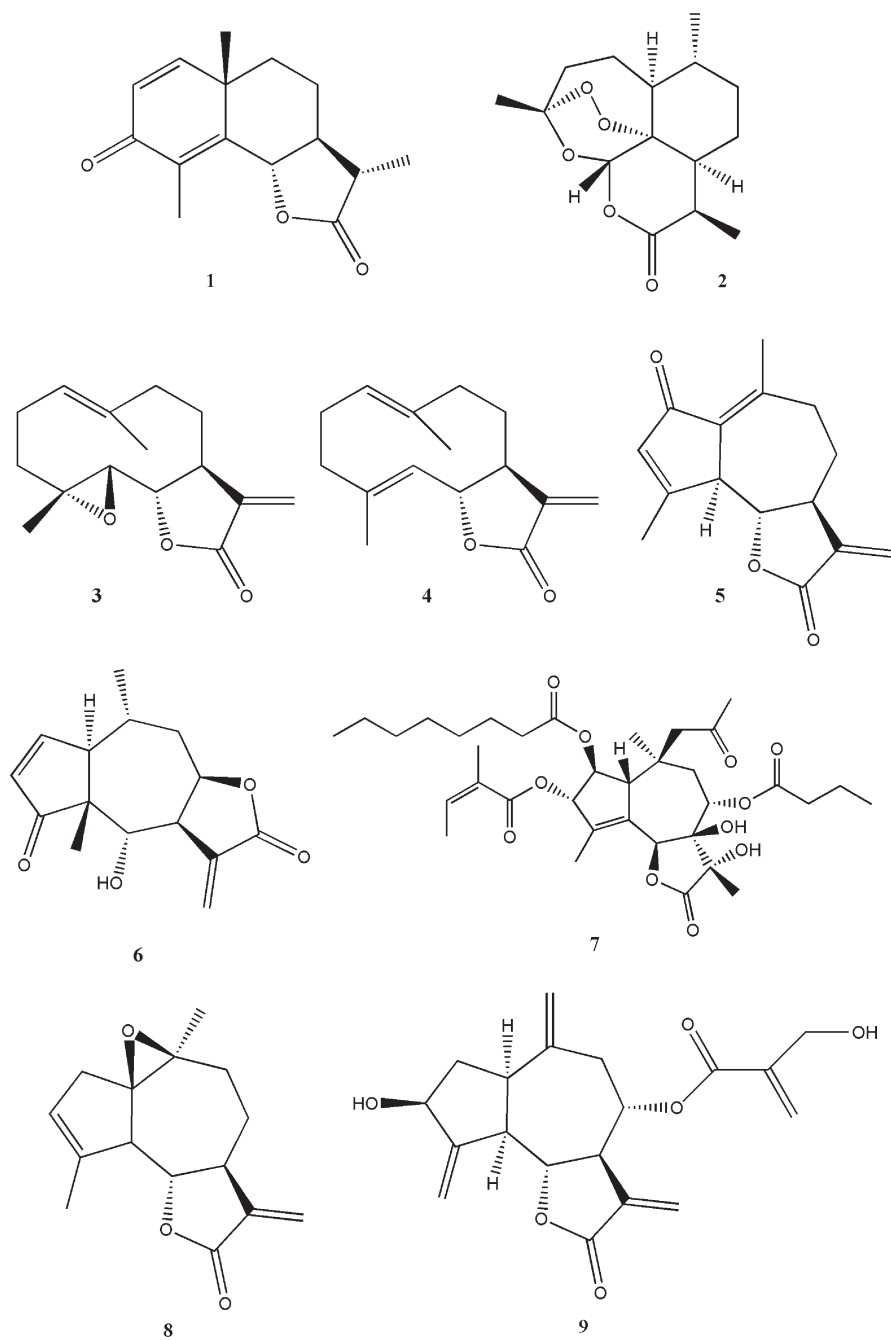


Fig. 1.3 Some representative sesquiterpene lactones

### 1.3.2 Artemisinin

Artemisinin (**2**) is a very particular compound, for it presents an endoperoxide ring in its molecular structure. This STL has been isolated from *Artemisia annua* (Asteraceae). The aerial parts of this plant have been used as febrifuge in Chinese traditional medicine. Nowadays artemisinin and its derivatives are used as antimalarial against chloroquine-resistant *Plasmodium falciparum*. Other activities reported for this STL include leishmanicidal (Lezama Dávila et al. 2007; Ghaffarifar et al. 2015) and anticancer. The latter property is due to its capacity to inhibit cell growth and to induce apoptosis in human hepatocellular carcinoma cells (SMMC-7721) (Deng et al. 2013) and other cell lines (Crespo Ortiz and Wei 2012; Das 2015). Artemisinin also shows antischistosomal activity (Saed et al. 2016). Activity against *Helicobacter pylori* has also been reported (Sisto et al. 2016).

Artemisinin derivatives are currently being assessed in phase I and II trials against lupus nephritis and breast, colorectal, and lung cancers (Lone et al. 2015).

### 1.3.3 Parthenolide

Parthenolide (**3**) is the active principle of feverfew (*Tanacetum parthenium*, Asteraceae). It is a traditional herbal medicine that has been used for centuries for the treatment of migraine, fever, and arthritis (Chaturvedi 2011). This STL has antiproliferative activity on multiple cancer cells such as melanoma; breast, colon, and lung cancer; and leukemia, among others (Wu et al. 2006; Parada Turska et al. 2007; Czyz et al. 2010; Gunn et al. 2011, Mathema et al. 2012). The compound selectivity to exert apoptosis in cancer cells provides an important and novel therapeutic strategy for the treatment of cancer and inflammation-related disorders (Liu 2013).

Other activities have been described for parthenolide such as antiprotozoal (against *Trypanosoma cruzi* and *Leishmania* spp.) (Izumi et al. 2008; Tiunan et al. 2005), anti-inflammatory (Wang and Li 2015), antiherpetic (Onozato et al. 2009), and antiosteoclastogenic (Kim et al. 2014).

### 1.3.4 Costunolide

Costunolide (**4**) is a germacranolide-type STL present in *Saussurea lappa* roots, a traditional Chinese medicinal herb that has anticancer and anti-inflammatory properties. This compound has also been isolated from other plant species such as *Magnolia* sp., *Laurus nobilis*, and *Costus speciosus*, among others. It exhibits a broad spectrum of bioactivities: antidiabetic and antioxidant (Eliza et al. 2009, 2010), anti-inflammatory (Butturini et al. 2014), antiulcerogenic (Zheng et al. 2016), anticlastogenic

(Cheon et al. 2014), and potential anticancer activity. Costunolide exerts its antiproliferative effect by inducing apoptosis through ROS generation (Wang et al. 2016) and cell cycle arrest (Liu et al. 2011; Lin et al. 2016), among other mechanisms. This STL is active on lung carcinoma (Wang et al. 2016; Hua et al. 2016); breast (Roy and Manikkam 2015), colon (Dong et al. 2015), bladder (Rasul et al. 2013), and platinum-resistant ovarian cancer (Yang et al. 2011); hepatoma (Liu et al. 2011); and leukemic (Choi and Lee 2009) cells.

### 1.3.5 *Dehydroleucodine*

Dehydroleucodine (**5**) is a STL isolated from *Artemisia douglasiana* which shows cytotoxic activity against human leukemia cells (Ordoñez et al. 2016) and inhibits the growth of melanoma cells in an animal model (Costantino et al. 2016). It reduces inflammation and gastrointestinal ethanol-induced damage, protecting the gastric mucosa, as demonstrated in in vivo models (Guardia et al. 2003; Wendel et al. 2008; Repetto and Boveris 2010). This compound has inhibitory effect on *T. cruzi* infective forms and *Leishmania mexicana* promastigotes (Jimenez Ortiz et al. 2005; Barrera et al. 2008). Antimicrobial activity against *Pseudomonas aeruginosa* multiresistant strains has also been reported for this compound (Mustafi et al. 2015).

### 1.3.6 *Helenalin*

Helenalin (**6**) is a guaianolide STL isolated from *Arnica montana* and other species of the Asteraceae family. It has been reported to possess cytotoxic (Grippio et al. 1992), hepatoprotective, anti-inflammatory, antioxidant (Lin et al. 2014), and antimicrobial properties against *Staphylococcus aureus* (Boulanger et al. 2007). It affects steroidogenesis in rat adrenocortical cells (Supornsilchai et al. 2006) and has cardiogenic activity (Itoigawa et al. 1987). Trypanocidal effects have also been reported (Schmidt et al. 2002; Jimenez-Ortiz et al. 2005).

### 1.3.7 *Thapsigargin*

Thapsigargin (**7**) is a guaianolide STL isolated from *Thapsia garganica* (Apiaceae). This Mediterranean medicinal plant was mentioned by Hippocrates, Theophrastus, Dioscorides, and Plinius as skin irritant, useful for pulmonary disease, catarrh, and fever and for the relief of rheumatic pains. In search for the skin-irritant principle, thapsigargin was isolated from the fruits and roots, and its structure and absolute configuration were determined between 1980 and 1985. This compound proved to be a potent histamine liberator and a cocarcinogen promoting skin cancer in mice

(Anderson et al. 2016). Nevertheless, the increasing interest in thapsigargin arose with the discovery of its ability to inhibit the sarco-endoplasmic reticulum calcium ATPase (SERCA) pump. The inhibition of this pump produces a high concentration of calcium in the cytosol, which leads to apoptosis. Several analogues have been obtained from thapsigargin, and a prodrug, termed mipsagargin, has been designed. Mipsagargin has shown an acceptable tolerability and a favorable pharmacokinetic profile in patients with solid tumors. Phase I clinical trials have been completed (Mahalingam et al. 2016). This compound has been authorized by the FDA to enter phase II clinical trials on patients suffering from hepatocellular carcinoma who had failed the first-line treatment with sorafenib and also on patients suffering from glioblastoma (Nhu and Christensen 2015). Inspyr Therapeutics Inc. (Texas, USA) has announced the initiation of a phase II clinical trial of mipsagargin for newly diagnosed prostate cancer patients (Inspyr 2016).

### 1.3.8 Arglabin

Arglabin (**8**) is a STL of the guaianolide type isolated for the first time by Adekenov et al. (1982) from *Artemisia glabella*, which is a plant species growing in Kazakhstan. It is present in the above ground parts (leaves, bud flowers, and stems). Later on, arglabin has been reported to be present in *A. myriantha* (Wong and Brown 2002), which is a well-known plant used in Chinese traditional medicine.

Arglabin shows promising antitumor activity against different tumor cell lines. Many derivatives have been obtained, and those bearing bromine and chlorine atoms and an epoxy group on the C(3)=C(4) double bond seem to have an increased antitumor activity. Dimethylamino arglabin, one of these derivatives, has been used to treat lung, liver, and ovarian cancers and is under study in phase I and II clinical trials (Lone et al. 2015). This STL has been patented in the USA and has been registered as an antitumor medicine in the Russian Federation, Kazakhstan, Uzbekistan, Tajikistan, the Kirghiz Republic, and Georgia (Adekenov 2016).

Arglabin acts as antitumor by a different mechanism from artemisinin, thapsigargin derivative, and parthenolide. It inhibits the farnesyl transferase, which is an enzyme that has been demonstrated to be involved in the formation of malignant tumors. Besides, this compound shows other biological activities: it has an inhibitory effect on influenza A virus, it can restore the synthesis of cytokines and other anti-inflammatory mediators acting as anti-inflammatory in *in vivo* models of inflammation (carrageenan, histamine, and formalin models), and it has immunomodulatory activity (Lone et al. 2015). Abderrazak et al. (2016) have demonstrated that arglabin reduces inflammation in pancreatic  $\beta$ -cells *in vivo* and in the INS-1 cell line *in vitro*, thus concluding that it may represent a new promising compound to treat inflammation and type 2 diabetes mellitus.

### 1.3.9 *Cynaropicrin*

Cynaropicrin (**9**) is the bitter principle of *Cynara scolymus*. It is a guaianolide-type STL that has also been isolated from *Saussurea lappa*. This compound inhibits the growth of both *Trypanosoma brucei* (Zimmermann et al. 2013) and *T. cruzi* (Da Silva et al. 2013). It acts as an antiphotoaging agent (Tanaka et al. 2013) and shows cytotoxic activity on leukemic cell lines (Cho et al. 2004), and it has antispasmodic activity (Emerdorfer et al. 2005).

## 1.4 Adverse Health Effects and Toxicity of Sesquiterpene Lactones

The biological properties of STLs are attributed to the  $\alpha$ -methylene- $\gamma$ -lactone group, though other groups such as  $\alpha,\beta$  cyclopentenones, unsaturated side chains, and epoxides may influence their activity. The  $\alpha,\beta$  moiety may react with sulfhydryl groups present in enzymes and other proteins, leading to important toxic effects. The same features that make STLs useful medicines can also be responsible for severe toxicity.

Plants containing these compounds have long been known by farmers due to the observation of contact dermatitis and toxic symptoms in animals. Grazing animals, such as sheep, goats, horses, and cattle, show nasal, ocular, and gastrointestinal irritation upon consumption of certain species (*Centaurea solstitialis*, *C. maculosa*, *C. repens*, *Helenium* spp. and *Hymenoxis* spp., *Eupatorium urticifolium*, *Lactuca virosa*, and *Tanacetum vulgare*).

After feeding on *C. solstitialis* for a long period of time, horses may develop an illness named equine nigrostriatal encephalomalacia (ENE). This is a neurological disorder producing Parkinson-like symptoms and eventually death. Cynaropicrin and other amines present in the species are considered responsible for the symptoms.

Sesquiterpene lactones of the picrotoxane and seco-prezizaane type act as neurotoxins. Epileptoid convulsions have been reported in children consuming fruits of *Coriaria myrtifolia* and *C. ruscifolia*, which contain picrotoxane STLs. *Illicium verum* (Chinese star anise) used as spice can be confused or adulterated with *Illicium anisatum* which presents anisatin, a seco-prezizaane STL that causes tonic and clonic seizures.

There are literature data indicating the toxic effects of STLs on mammalian herbivores, the insecticidal activity, the livestock poisoning, the deleterious effects on animal reproduction, and the capacity to cause contact allergic dermatitis (Heywood et al. 1977).

Studies assessing the genotoxicity of STLs are scarce. Artemisinin, which is currently being used against malaria, has shown embryotoxic effects on rats and rabbits, though no side effects in pregnant women have been reported. Nevertheless, the WHO advises that this antimalarial drug should not be used during the first trimester of pregnancy.

Other genotoxicity studies on helenalin have demonstrated that this STL induces mutations on *Bacillus subtilis*, while hymenoxin alkylates and causes DNA cross-linkage. Other STLs display genotoxic activity through different mechanisms: centratherin induces sister chromatid exchange, and glaucolide B induces structural chromosomal aberrations.

Artemisinin has been demonstrated to alkylate different proteins but not DNA, while artesunate and artemether break DNA through oxidative damage. Aneuploidy has been observed with parthenin (Amorim et al. 2013).

Members of the Asteraceae family have demonstrated to cause dermatitis not only by direct contact but also by the inhalation of airborne allergens. Another example is *Thapsia garganica*, which is known for its skin-irritant properties and from which thapsigargin has been isolated and found to inhibit the SERCA pump. The elevated  $\text{Ca}^{+2}$  levels in the cytoplasm produced by the inhibition of this pump leads to mast cell degranulation and histamine release with the consequent skin irritation.

Moreover, there are reports indicating the presence of STLs in milk and meat as well as the contamination of soils in cultivated areas. This contamination with STLs is due to either leaching or to the incorporation of these compounds from dead plant material that is left behind in the field. *Artemisia annua* is cultivated in Asia and in Africa for the extraction of artemisinin to be used as antimalarial. The cultivated area is increasing to meet the necessities of the infected people. Besides, *A. annua* is also experimentally cultivated in the Netherlands, Switzerland, Finland, and Denmark. A possible contamination of underground water with STLs should be taken into account due to their toxic chronic effects on human health (Knudsmark Jessing and Duke 2014). In the latter report, authors inform about other effects of this compound on insects and other invertebrates and its phytotoxic and other antimicrobial properties and discuss the possible ecological role of this compound under biotic and abiotic stress. Authors conclude that artemisinin is produced as a defense mechanism against biotic factors. Antifungal and antibacterial effects of artemisinin in vitro as well as the insecticidal activity in field experiments are not conclusive. Its accumulation in the trichomes of young leaves and its subsequent decrease in fully developed plants may account for a protective effect against herbivores or pathogens for the young vulnerable plants. Artemisinin is washed off from the leaf surface after the breaking of trichomes and leaches from debris of fallen leaves into the soil, thus exerting an herbicide effect, suggesting its role as an allelochemical. It also reduces and changes the soil microbiota under field conditions.

## References

- Abderrazak A, El Hadri K, Bosc E et al (2016) Inhibition of the inflammasome NLRP3 by arglabin attenuates inflammation, protects pancreatic  $\beta$ -cells from apoptosis, and prevents type 2 diabetes mellitus development in ApoE2Ki mice on a chronic high-fat diet. *J Pharmacol Exp Ther* 357(3):487–494. <https://doi.org/10.1124/jpet.116.232934>
- Adekenov SM (2013) Natural sesquiterpene lactones as renewable chemical materials for new medicinal products. *Eurasian Chem Technol J* 15:163–174



- Adekenov SM (2016) Chemical modifications of arglabin and biological activity of its new derivatives. *Fitoterapia* 110:196–205
- Adekenov SM, Atazhanova GA (2013) Heteroatom-containing natural sesquiterpene lactones and methods for their obtaining. *Eurasian Chem Technol J* 15:195–208
- Adekenov S, Mukhammetzhanov MN, Kagarlitski AN et al (1982) Arglabina a new sesquiterpene lactone from *Artemisia glabella*. *Chem Nat Compd* 18:623–624
- Ahern JR, Whitney KD (2014) Sesquiterpene lactone stereochemistry influences herbivore resistance and plant fitness in the field. *Ann Bot* 113(4):731–740. <https://doi.org/10.1093/aob/mct297>
- al-Harbi MM, Qureshi S, Ahmed MM et al (1994) Studies on the antiinflammatory, antipyretic and analgesic activities of santonin. *Jpn J Pharmacol* 64(3):135–139
- Amorim HR, Gil da Costa RM, Lopes C et al (2013) Sesquiterpene lactones: adverse health effects and toxicity mechanisms. *Crit Rev Toxicol* 43:559–579
- Andersen TG, Quiñonero López C, Manczak T et al (2016) Thapsigargin from *Thapsia* L. to mip-sagargin. *Molecules* 20:6113–6127
- Arantes FF, Barbosa LC, Maltha CR et al (2010) Synthesis of novel  $\alpha$ -santonin derivatives as potential cytotoxic agents. *Eur J Med Chem* 45(12):6045–6051. <https://doi.org/10.1016/j.ejmech.2010.10.003>
- Barrera PA, Jimenez-Ortiz V, Tonn C et al (2008) Natural sesquiterpene lactones are active against *Leishmania mexicana*. *J Parasitol* 94(5):1143–1149. <https://doi.org/10.1645/GE-1501.1>
- Birladeanu L (2003) The stories of santonin and santonin acid. *Angew Chem Int Ed Engl* 42(11):1202–1208
- Boulanger D, Brouillette E, Jaspas F et al (2007) Helenalin reduces *Staphylococcus aureus* infection *in vitro* and *in vivo*. *Vet Microbiol* 119:330–338
- Butturini E, Di Paola R, Suzuki H et al (2014) Costunolide and dehydrocostuslactone, two natural sesquiterpene lactones, ameliorate the inflammatory process associated to experimental pleurisy in mice. *Eur J Pharmacol* 730(1):107–115
- Chadwick M, Trewin H, Gawthrop F et al (2013) Sesquiterpenoid lactones: benefits to plants and people. *Int J Mol Sci* 14:12780–12805. <https://doi.org/10.3390/ijms140612780>
- Chaturvedi D (2011) Sesquiterpene lactones: structural diversity and their biological activities. In: Tiwari VK, Mishra BB (eds) Opportunity, challenge and scope of natural products in medicinal chemistry. Research Signpost, Kerala, pp 313–334. ISBN: 978-81-308-0448-4
- Cheon YH, Song MJ, Kim JY et al (2014) Costunolide inhibits osteoclast differentiation by suppressing c-Fos transcriptional activity. *Phytother Res* 28(4):586–592
- Cho JY, Kim AR, Jung JH et al (2004) Cytotoxic and proapoptotic activities of cynaropicrin, a sesquiterpene lactone, on the viability of leukocyte cancer cell lines. *Eur J Pharmacol* 492(2–3):85–94
- Choi JH, Lee KT (2009) Costunolide-induced apoptosis in human leukemia cells: involvement of c-Jun N-terminal kinase activation. *Biol Pharm Bull* 32(10):1803–1808
- Costantino V, Lobos Gonzalez L, Ibáñez J et al (2016) Dehydroleucodine inhibits tumor growth in a preclinical melanoma model by inducing cell cycle arrest, senescence and apoptosis. *Cancer Lett* 372:10–23
- Crespo Ortiz MP, Wei MQ (2012) Antitumour activity of artemisinin and its derivatives: from a well-known antimalarial agent to a potential anticancer drug. *J Biomed Biotechnol* 2012:247597. <https://doi.org/10.1155/2012/247597>
- Czyz M, Lesiak Mieczkowska K, Koprowska K et al (2010) Cell context-dependent activities of parthenolide in primary and metastatic melanoma cells. *Br J Pharmacol* 160(5):1144–1157
- Da Silva CF, Da Gama JB, De Araujo JS et al (2013) Activities of psilostachyin a and cynaropicrin against *Trypanosoma cruzi* *in vitro* and *in vivo*. *Antimicrob Agents Chemother* 57(11):5307–5305
- Das AK (2015) Anticancer effect of antimalarial artemisinin compounds. *Ann Med Health Sci Res* 5(2):93–102. <https://doi.org/10.4103/2141-9248.153609>

- Deng XR, Liu ZX, Liu F et al (2013) Holotransferrin enhances selective anticancer activity of artemisinin against human hepatocellular carcinoma cells. *J Huazhong Univ Sci Technolog Med Sci* 33(6):862–865
- Dong GZ, Shim AR, Hyeon JS et al (2015) Inhibition of Wnt/ $\beta$ -catenin pathway by dehydrocostus lactone and costunolide in colon cancer cells. *Phytother Res* 29(5):680–686
- Eliza J, Daisy P, Ignacimuthu S et al (2009) Normo-glycemic and hypolipidemic effect of costunolide isolated from *Costus speciosus* (Koen ex. Retz.) Sm. in streptozotocin-induced diabetic rats. *Chem Biol Interact* 179(2–3):329–334
- Eliza J, Daisy P, Ignacimuthu S (2010) Antioxidant activity of costunolide and eremanthin isolated from *Costus speciosus* (Koen ex. Retz) Sm. *Chem Biol Interact* 188(3):467–472. <https://doi.org/10.1016/j.cbi.2010.08.002>
- Emerdorfer F, Bellato F, Noldin VF et al (2005) Antispasmodic effect of fractions and cynaropicrin from *Cynara scolymus* on Guinea pig ileum. *Biol Pharm Bull* 28(5):902–904
- Fischer NH (1990) Sesquiterpene lactones: biogenesis and biomimetic transformations. In: Towers G, Towers H (eds) *Biochemistry of the mevalonic acid pathway to terpenoids*. Plenum Press, New York, pp 161–201
- Fischer NH, Oliver EJ, Fischer HD (1979) The biogenesis and chemistry of sesquiterpene lactones. In: Herz W, Grisebach H, Kirby GW (eds) *Progress in chemistry of organic natural products*, vol 38. Springer, New York, pp 47–390
- Ghaffarifar F, Esavand Heydani F, Dalimi A et al (2015) Evaluation of apoptotic and antileishmanial activities of artemisinin on promastigotes and BALB/C mice infected with *Leishmania major*. *Iran J Parasitol* 10(2):258–267
- Grippio AA, Hall IH, Kiyokawa H et al (1992) The cytotoxicity of helenalin, its mono and difunctional esters, and related sesquiterpene lactones in murine and human tumour cells. *Drug Des Discov* 8(3):191–206
- Guardia T, Juarez AO, Guerreiro E et al (2003) Antiinflammatory activity and effect on gastric acid secretion of dehydroleucodine isolated from *Artemisia douglasiana*. *J Ethnopharmacol* 88(2–3):195–198
- Gunn EJ, Williams JT, Huynh DT et al (2011) The natural products parthenolide and andrographolide exhibit anticancer stem cell activity in multiple myeloma. *Leuk Lymphoma* 52(6):1085–1097
- Heywood VH, Harbone JB, Turner BL (1977) An overture to the Compositae. In: Heywood JB, Harbone JB, Turner BL (eds) *The biology and chemistry of the Compositae*, vol 1. Academic Press, New York/London, pp 1–20
- Hohmann M, Longhi-Balbinot D, Guazelli C et al (2016) Sesquiterpene lactones: structural diversity and perspectives as anti-inflammatory molecules. In: Atta-ur-Rahman FRS (ed) *Studies in natural products chemistry: bioactive natural products*, vol 49. Elsevier, Amsterdam, pp 313–334
- Hua P, Zhang G, Zhang Y et al (2016) Costunolide induces G1/S phase arrest and activates mitochondrial-mediated apoptotic pathways in SK-MES 1 human lung squamous carcinoma cells. *Oncol Lett* 11(4):2780–2786
- Inspyr Therapeutics Inc. (Texas, USA) (2016) Inspyr Therapeutics announces mipsagargin Ph 2 trial for patients with clear cell renal cell carcinoma expressing PSMA. <http://www.inspyrtx.com/news/press-releases/detail/625/inspyr-therapeutics-announces-mipsagargin-ph-2-trial-for>. Accessed 18 Aug 2016
- Itoigawa M, Takeya K, Furukawa H et al (1987) Mode of cardiotoxic action of helenalin, a sesquiterpene lactone, on Guinea pig ventricular myocardium. *J Cardiovasc Pharmacol* 9(2):193–201
- Izumi E, Morello LG, Ueda-Nakamura T et al (2008) *Trypanosoma cruzi*: antiprotozoal activity of parthenolide obtained from *Tanacetum parthenium* (L.) Schultz Bip. (Asteraceae, Compositae) against epimastigote and amastigote forms. *Exp Parasitol* 118(3):324–330
- Jimenez-Ortiz V, Brengio SD, Giordano O et al (2005) The trypanocidal effect of sesquiterpene lactones helenalin and mexicanin on cultured epimastigotes. *J Parasitol* 91(1):170–174
- Khazir J, Singh PP, Reddy DM et al (2013) Synthesis and anticancer activity of novel spiroisoxazoline and spiroisoxazolidine derivatives of  $\alpha$ -santonin. *Eur J Med Chem* 63:279–289. <https://doi.org/10.1016/j.ejmech.2013.01.003>

- Kim J, Cheon Y, Yoon KH et al (2014) Parthenolide inhibits osteoclast differentiation and bone resorbing activity by down-regulation of NFATc1 induction and c-Fos stability, during RANKL-mediated osteoclastogenesis. *BMB Rep* 47(8):451–456
- Knudsmark Jessing K, Duke S (2014) Potential ecological roles of artemisinin produced by *Artemisia annua* L. *J Chem Ecol.* <https://doi.org/10.1007/s10886-014-0384-6>
- Kweon SH, Kim KT, Hee Hong J et al (2011) Synthesis of C (6)-epimer derivatives of diacetoxy acetal derivative of santonin and their inducing effects on HL-60 leukemia cell differentiation. *Arch Pharm Res* 34(2):191–198. <https://doi.org/10.1007/s12272-011-0202-4>
- Lezama Dávila CM, Satoşkar AR, Úc Encalada M et al (2007) Leishmanicidal activity of artemisinin, deoxoartemisinin, artemether and arteether. *Nat Prod Comm* 2(1):1–4
- Lin X, Shijun Z, Renbin H et al (2014) Helenalin attenuates alcohol-induced hepatic fibrosis by enhancing ethanol metabolism, inhibiting oxidative stress and suppressing HSC activation. *Fitoterapia* 95:203–213
- Lin X, Peng Z, Su C (2016) Potential anti-cancer activities and mechanisms of costunolide and dehydrocostuslactone. *Int J Mol Sci* 16(5):10888–10906
- Liu YH (2013) Progress in the research of structure and pharmacological activity of parthenolide (review). *Chin J Pharm Biotechnol* 20(6):586–589
- Liu CY, Chang HS, Chen IS et al (2011) Costunolide causes mitotic arrest and enhances radiosensitivity in human hepatocellular carcinoma cells. *Radiat Oncol* 6:56. <https://doi.org/10.1186/1748-717X-6-56>
- Lone SH, Bhat KA, Khuroo MA (2015) Arglabin: from isolation to antitumor evaluation. *Chem Biol Interact* 240:180–198
- Macías FA, Santana A, Durán AG et al (2013) Guaianolides for multipurpose molecular design. In: Beck J, Coats J, Duke S, Koivunen M (eds) *Pest management with natural products*, vol 1141. ACS, New York, pp 167–188. <https://doi.org/10.1021/bk-2013-1141.ch012>
- Mahalingam D, Wilding G, Denmeade S et al (2016) Mipsagargin, a novel thapsigargin-based PSMA-activated prodrug: results of a first-in-man phase I clinical trial in patients with refractory, advanced or metastatic solid tumours. *Br J Cancer* 114(9):986–994
- Mathema VB, Koh Y, Thakuri BC et al (2012) Parthenolide, a sesquiterpene lactone, expresses multiple anti-cancer and antiinflammatory activities. *Inflammation* 35(2):560–565. <https://doi.org/10.1007/s10753-011-9346>
- Mustafi S, Veisaga ML, López LA et al (2015) A novel insight into dehydroleucodine mediated attenuation of *Pseudomonas aeruginosa* virulence mechanism. *Biomed Res Int* 2015:216097. [doi.org/10.1155/2015/216097](https://doi.org/10.1155/2015/216097)
- Newman DJ, Cragg G (2016) Natural products as sources of new drugs from 1981 to 2014. *J Nat Prod* 79(3):629–661. <https://doi.org/10.1021/acs.jnatprod.5b01055>
- Nhu TQ, Christensen SB (2015) Thapsigargin, origin, chemistry, structure activity relationship and prodrug development. *Curr Pharm Des* 21:5501–5517
- Onozato T, Nakamura CV, Garcia Cortez DA et al (2009) *Tanacetum vulgare*: Antihyper virus activity of crude extract and the purified compound parthenolide. *Phytother Res* 23(6):791–796
- Ordóñez PE, Sharma KK, Bystrom LM et al (2016) Dehydroleucodine, a sesquiterpene lactone from *Gynoxys verrucosa*, demonstrates cytotoxic activity against human leukemia cells. *J Nat Prod* 79(4):691–696. <https://doi.org/10.1021/acs.jnatprod.5b00383>
- Padilla Gonzalez GF, Antunes dos Santos F, Batista Da Costa F (2016) Sesquiterpene lactones: more than protective plant compounds with high toxicity. *CRC Crit RevPlant Sci* 35(1):18–37
- Parada Turska J, Paduch R, Majdan M et al (2007) Antiproliferative activity of parthenolide against three human cancer cell lines and human umbilical vein endothelial cells. *Pharmacol Rep* 59(2):233–237
- Picman A (1986) Biological activities of sesquiterpene lactones. *Biochem Syst Ecol* 14(3):255–281
- Rasul A, Bao R, Malhi M et al (2013) Induction of apoptosis by costunolide in bladder cancer cells is mediated through ROS generation and mitochondrial dysfunction. *Molecules* 18(2):1418–1433

- Repetto MG, Boveris A (2010) Bioactivity of sesquiterpenes: compounds that protect from alcohol-induced gastric mucosal lesions and oxidative damage. *Mini Rev Med Chem* 10(7):615–623
- Rodríguez E, Towers GHN, Mitchell JC (1976) Biological activities of sesquiterpene lactones. *Phytochemistry* 15:1573–1580
- Roy A, Manikkam R (2015) Cytotoxic impact of costunolide isolated from *Costus speciosus* on breast cancer via differential regulation of cell cycle - an *in-vitro* and *in-silico* approach. *Phytother Res* 29(10):1532–1539
- Saeed MEM, Krishna S, Greten HJ et al (2016) Antischistosomal activity of artemisinin derivatives *in vivo* and in patients. *Pharmacol Res* 110:216–226
- Schmidt TJ, Brun R, Willuhm G et al (2002) Antitrypanosomal activity of helenalin and some structurally related sesquiterpene lactones. *Planta Med* 68(8):750–751
- Sisto F, Scaltrito MM, Masia C et al (2016) *In vitro* activity of artemisone and artemisinin derivatives against extracellular and intracellular *Helicobacter pylori*. *Int J Antimicrob Agents* 48(1):101–105
- Supornsilchai V, Söder O, Svechnikov K (2006) Sesquiterpene lactone helenalin suppresses Leydig and adrenocortical cell steroidogenesis by inhibiting expression of the steroidogenic acute regulatory protein. *Reprod Toxicol* 22(4):631–635
- Tanaka YT, Tanaka K, Kojima H et al (2013) Cynaropicrin from *Cynara scolymus* L. suppresses photoaging of skin inhibiting the transcription activity of nuclear factor kappa B. *Bioorg Med Chem Lett* 23(2):518–523
- Tani S, Fukamiya N, Kiyokawa H et al (1985) Antimalarial agents. 1. Alpha-santonin-derived cyclic peroxide as potential antimalarial agent. *J Med Chem* 28(11):1743–1744
- The Society for Medicinal Plant and Natural Product Research (2017) Nobel Prize for the discovery of natural product-derived drugs. <https://www.ga-online.org/events-2/1fpgksc21/Nobel-Prize-for-the-discovery-of-natural-product-derived-drugs->. Accessed 8 Aug 2016
- Tiuman TS, Ueda-Nakamura T, Garcia Cortez DA et al (2005) Antileishmanial activity of parthenolide, a sesquiterpene lactone isolated from *Tanacetum parthenium*. *Antimicrob Agents Chemother* 49(1):176–182
- Wang M, Li Q (2015) Parthenolide could become a promising and stable drug with anti-inflammatory effects. *Nat Prod Res* 29(12):1092–1101
- Wang Z, Zhao X, Gong X (2016) Costunolide induces lung adenocarcinoma cell line A549 cells apoptosis through ROS (reactive oxygen species)-mediated endoplasmic reticulum stress. *Cell Biol Int* 40(3):289–297
- Wendel GH, María AOM, Guzmán JA et al (2008) Antidiarrheal activity of dehydroleucodine isolated from *Artemisia douglasiana*. *Fitoterapia* 79(1):1–5
- Wong HF, Brown GD (2002) Dimeric guaianolides and a fulvenoguaianolide from *Artemisia myriantha*. *J Nat Prod* 65:481–486
- Wu C, Chen F, Rushing JW et al (2006) Antiproliferative activities of parthenolide and golden feverfew extract against three human cancer cell lines. *J Med Food* 9(1):55–61
- Yang YI, Kim JH, Lee KT et al (2011) Costunolide induces apoptosis in platinum-resistant human ovarian cancer cells by generating reactive oxygen species. *Gynecol Oncol* 123(3):588–596
- Yoshioka H, Mabry TJ, Timmerman B (1973) Sesquiterpene lactones. University of Tokio Press, Tokio
- Zheng H, Chen Y, Zhang J et al (2016) Evaluation of protective effects of costunolide and dehydrocostuslactone on ethanol-induced gastric ulcer in mice based on multi-pathway regulation. *Chem Biol Interact* 250:68–77
- Zimmermann S, Oufir M, Leroux A et al (2013) Cynaropicrin targets the trypanothione redox system in *Trypanosoma brucei*. *Bioorg Med Chem* 21(22):7202–7209

# Chapter 2

## Ancient and Modern Concepts About the Asteraceae Taxonomy



Gustavo C. Giberti

**Abstract** This chapter provides an update on the systematics of Asteraceae (formerly known as Compositae), which is the largest vascular plant family. This update includes the changes of concepts that have occurred from the old times of the elementary recognition of the Asteraceae as a natural group of angiosperms in the last decades of the eighteenth century up to the advanced plant systematics trends of the twenty-first century. This contribution is to provide non-scholars in neither botany nor plant systematics some knowledge about this complex mega-family, its infra-familial relationships and the nomenclatural crossroads.

**Keywords** Asteraceae · Plant systematics · New concepts · Cladistic studies · Infra-familial taxonomy

### 2.1 Introduction

Asteraceae Bercht. and J. Presl. nom. Cons. (1820) (=Compositae Giseke, = Synanthereae Cass.), is a phylogenetically advanced cosmopolitan plant family among the dicotyledons that is easily exomorphologically recognized by its typical racemose inflorescence: the flower or pseudanthial head (also named capitulum), formed by a variable (1<sup>1</sup> to numerous) number of sessile, sympetalous, synanthereous and epigynous flowers arising from a common receptacle – this can be either flat, convex or hollow – whole set is surrounded by phyllaries (an uni-pluriseriate bracteal involucre, frequently leaflike).

---

<sup>1</sup>In genera like *Corymbium*, *Echinops*, *Hecastocleis* and *Lagascea*.

G. C. Giberti (✉)

Universidad de Buenos Aires, Facultad de Farmacia y Bioquímica, Buenos Aires, Argentina

CONICET – Universidad de Buenos Aires. Instituto de Química y Metabolismo del Fármaco – CONICET (IQUIMEFA), Buenos Aires, Argentina

e-mail: [vsulsen@ffyb.uba.ar](mailto:vsulsen@ffyb.uba.ar)

The Asteraceae family comprises more than 25,000 plant species distributed in about 1500–1700 genera, thus being the largest plant family among vascular plants. Members of this family are widespread along all continents, except Antarctica. These plants grow from the sea level up to high mountain environments, around 5000 m a. s. l., and also spread from tropical rainforests to arid desert places. The morphological exclusive (or quasi-exclusive) traits of Asteraceae are vast and should deserve a glossary in order to explain their meanings to the lay (for a description of the general morphology of the family, see Cabrera 1974, Freire 2009a, 2013).

About reproductive strategies, so important for a basic discipline as biology, it should be remembered that Asteraceae have proterandrous flowers, and cross-pollination is widespread, occurring through zoophilous pollination, mostly entomophilous (Hymenoptera, Lepidoptera, etc.). However, birds could also perform it in several cases and anemophilous taxa also occur. Several alternatives of sexual expression are shown by various members of this family: dioecy, monoecy, etc. However, selfing and even apomixis are sometimes present, following different evolutive tendencies within this large family. Seed dispersal is also very diversified in different infra-familial groups: cypsela hairiness, pappus consistency and disposition<sup>2</sup> and/or various trichomatous ornamentations (or even the complete flower head receptacle is involved, as in *Xanthium*), either helped or not by some animals, are involved on known strategies for the spatial dispersion of propagules.

On phytochemical grounds, the Compositae/Asteraceae are recognized for storing carbohydrate polymer polyfructosans such as inulin and for the occurrence of polyacetylenes and sesquiterpene lactones and – among other alkaloids – for the hepatotoxic pyrrolizidine compounds, as well as for the absence of iridoid compounds as remarkable characters.

As the wide range of sesquiterpene lactones from this family – more than 8000 compounds have been reported – have been extensively and deeply surveyed everywhere (e.g. Seaman 1982; Seaman and Funk 1983; Hristozov et al. 2007; Zidorn 2008; Scotti et al. 2012; Bruno et al. 2013; among many others), and as it is also considered in the present volume, their details and implications shall not be treated in this chapter.

A miscellaneous list of other types of metabolites like phenolics, diterpenes, amides, cyanogenic glycosides, etc., have also been extensively found in members of Asteraceae (Seaman et al. 1990; Francisco and Pimenta Pinotti 2000; Bohm and Stuessy 2001; Emerenciano et al. 2001; Rios 2012; Granica and Zidorn 2015).

## 2.2 Asteraceae in Old Times Plant Systematics: Its Influences

It is well known that ancient botanical classification systems relied on quite elementary comparative exomorphology traits, and therefore, their scope was obviously very limited, as compared to current standards in plant systematics (Crisci and

---

<sup>2</sup>The wind-moved propagules with a light hairy pappus like in thistles (*Cirsium*, *Carduus*).

López Armengol 1983; Stuessy 2002; Stuessy and Funk 2013). However, influences of such ancient taxonomic systems persist today, among other nomenclatural issues of plant taxonomy (a certain stability of scientific names is still desirable even in the fast-changing advanced biology of today). This situation is exemplified by large and diverse plant families such as the Asteraceae mega-family. Asteraceae's infra-familial-, tribal- and generic-level organization is still under study and is very controversial, a fact quite understandable for such a large and complex taxon. On the other hand, the reverberations entailed by the old infra-familial and generic classification systems – some of them known to be wrong according to current plant systematics concepts – may sometimes reinforce misconceptions held by other groups of scientists (e.g. those engaged on agronomic, phytochemical or ethnopharmacological research, among another group of “users” of basic plant systematics scientific data). Information about accurate field localization (even those out of modern GPS data) of a particular plant species can only be found in old-fashioned generic monographies and/or from aged floristic treatments for the Asteraceae and not in recent papers dealing with current systematic updates of these taxa. Some of such precise chorological information becomes relevant when endangered plant species are considered.

The exact provenance of a given plant species in wild environments becomes increasingly important, keeping in pace with the risk of extinction of such taxon. In such old floras and related papers, still valuable on chorological terms, a non-updated infra-familial systematics is often presented; or even worse, their specific delimitations ought to be reconsidered before a particular phytochemical analysis is performed, especially if any valid chemotaxonomical conclusion could eventually be proposed.

The idea of considering the Asteraceae as a distinctive, recognizable plant family began to achieve wide acceptance among botanists in the last decades of the eighteenth century. This recognition accompanied the widespread use of the old and more imperfect Linnaean classification system, under whose rules, the taxonomical category that we nowadays know as a “plant family”, were still not considered. The correct nomenclature for such taxonomic category, i.e. “family” (Brown 1817), used to be variable in those times, and it was only in the second half of the nineteenth century when most researchers began to refer to a given plant family employing such taxonomical category (and therefore, abandoning older denominations such as “ordines naturales plantarum”, “cohort”, etc.).

As mentioned, a reasonable consensus about the scope and a clear definition of what we actually call the family Asteraceae (or Compositae) has already occurred since the last decade of the eighteenth century (Giseke 1792) and during the early years of the nineteenth century (Berchtold and Presl 1820; de Candolle 1836, 1838; Cassini 1816; Dumortier 1822). Most of the precursor researchers working on the systematics of Compositae agreed on the delimitation of the family; however, controversies and polemical issues about the infra-familial taxonomic arrangement often arouse. For example, de Cassini (1816) accepted 19 tribes within the Compositae, whilst de Candolle (1836, 1838) and Lessing (1832) recognized 8 tribes within the same family: Vernonieae, Eupatorieae, Astereae, Senecioneae,

Cynareae, Mutisieae, Nassauvineae and Cichorieae. In those days, comparative studies based on rough exomorphology studies of plants were paramount, thus disregarding both ontogenical and/or evolutive presumptions whose importance began to be considered about a century later.

Later, in the second half of the nineteenth century, Bentham (1873) made important advances in the infra-familial taxonomy of Compositae. The author divided the family in two main groups: the subfamilies Liguloideae and Tubuloideae. Bentham assigned only one tribe – the Cichorioideae to the Liguloideae – proposing 12 tribes for the second subfamily: Anthemideae, Astereae, Arctotideae, Calenduleae, Cynareae (= Cardueae), Eupatorieae, Helenieae, Heliantheae, Inuleae, Mutisieae, Vernonieae and Senecioneae. In those times, Darwinism and evolution concepts had already appeared in biology, and the influences of such discoveries soon developed. The infra-familial arrangement proposed by Bentham enjoyed considerable importance during the last quarter of the nineteenth century due to Hoffmann's (1894) treatment of the Compositae for Engler and Prantl's *Die Natürlichen Pflanzenfamilien*, which was a respectful classification system for plants. Hoffmann (1894) recognized two subfamilies, Tubiflorae and Liguliflorae, thus completing the 13 tribes previously quoted. Meanwhile, the advances in optics, together with the application of sophisticated techniques, as well as the advances in genetics, cytology and embryology and even the serotaxonomic approaches of the early twentieth century, improved plant anatomical recording of data and plant systematics outputs.

Consequently, Hoffmann's (as an Englerian-based taxonomy, i.e. a long-lasting natural classification system) and Bentham's systems lasted up to the second half of the twentieth century – even exceeding the 1950s. This fact can be exemplified by the existence of many published reports on Asteraceae taxonomy and floristics, among which are those corresponding to Angel L. Cabrera (and to some of his co-workers and disciples such as Sáenz (1981) and Cabrera and Ragonese (1978)). Spanish-born Argentinean botanist A. L. Cabrera (1908–1999) was one of the most prominent South-American synantherologists of the twentieth century. His multiple contributions are reflected in the establishment of several generic keys and important monographic treatments (Cabrera 1962, 1965, 1971a, 1982), as well as his floristic approaches to the same family (Cabrera 1963, 1971b, 1974, 1978), and through his influences on many of his students. As South America is a very important subcontinent in terms of Asteraceae biohistory (Katinas et al. 2007), Cabrera's works have also served as the basis for floristic treatments carried out in some Argentina neighbouring countries (Cabrera and Klein 1973, 1975). Even during more recent years, and although acknowledging more recent approaches to Asteraceae infra-familial systematics carried out by other botanists, Cabrera and his co-workers have still followed Bentham's traditional tribal and generic arrangement for their floristic works on South-American specimens (Cabrera and Freire 1998; Cabrera 1999; Cabrera et al. 2009). The importance of such regional botanical studies, disregarding new or more advanced treatments for the family and/or subordinate taxa, has sometimes been overstressed by plant taxonomy misusers from other disciplines.



### 2.3 Towards a “Contemporary” Asteraceae Systematics

After World War II, novel mathematical approaches to biological classifications began to appear, some of them in the field of phenetics (Sneath and Sokal 1973), which enjoyed considerably influences during the 1960s and 1970s, and later (mainly around cladistics or phylogenetics), through the developments of the German entomologist Willi Hennig’s ideas (Hennig 1966) and many other scientists (Estabrook 1972; Funk and Stuessy 1978; Wiley 1981; Stevens 1991, etc.), a trend which accentuated from the 1970s onwards. In parallel, new data began to be more seriously considered as more useful approaches to plant systematics, as a great amount of novel information on cytogenetics, phytochemistry, exomorphology, plant anatomy, embryology, palynology, plant physiology, molecular biology, ecology, phytogeography, among other disciplines, appeared together with more sensitive laboratory techniques and improved informatics tools, capable of analysing large data sets very quickly.

New insights on the taxonomy of Asteraceae were achieved by several researchers, especially from the 1970s onwards: King and Robinson (1970) have established new study criteria for the Asteraceae upon considering the so-called microcharacters. Few years later, they proposed a new arrangement for the tribe Eupatorieae (King and Robinson 1987) suggesting, for example, the convenience of splitting a big genus like *Eupatorium* into several other equivalent taxa. Another important innovation was the proposition of a new tribe, Liabeae (Robinson and Brettel, 1973; Carlquist 1976). These authors also suggested changes at the infra-familial level, considering two subfamilies, Cichorioideae and Asteroideae, each one comprising six tribes. Wagenitz (1976) was also concerned about Asteraceae systematics. Thus, a great deal of data summarizing the advances in the 1960s and 1970s was presented in the book edited by Heywood et al. (1977).

In parallel, new systematic concepts, techniques and treatments using cladistic approaches appeared and were applied for most plant families (Crisci and Stuessy 1980; Crisci 1982, etc.). Many of these scientists were also engaged on research in the Asteraceae (Crisci 1980; Funk 1985; Katinas 1996 just to quote very few). New studies on tribal systematics were then performed and published, thus introducing modifications to the elementary concepts developed by Cassini and Bentham.

The molecular studies performed by Jansen and Palmer (1987) have also led to major changes in the infra-familial systematics of Asteraceae. These authors proposed the Barnadesiinae (*Barnadesia*, *Chuquiraga* and *Dasyphyllum*) be included as a subtribe within the Mutisieae tribe, due to the presence of a DNA inversion in that group of plants that is absent in the rest of the family. Therefore, Barnadesiinae should constitute a basimorphic subfamily (Barnadesioideae) within the Asteraceae. Obviously, the approaches proposed by Cabrera on Mutisieae (Cabrera 1977) began to change very deeply. These modifications were based not only on molecular but also on micromorphological pollen data, among others, and very miscellaneous informations were responsible of such advances (Katinas 1994; Katinas et al. 2008,

2009; Roque and Funk 2013; Tellería et al. 2013; Funk et al. 2014; Hernández et al. 2015).

According to Robinson and Brettel (1973), the Liabeae tribe and its components have received more attention (Gutiérrez 2003, 2010; Gutiérrez and Luna 2013; Gutiérrez and Katinas 2015).

Bremer (1994) has proposed an infra-familial classification within the Asteraceae. According to cladistic studies using multiple kinds of data sets, his system (Bremer 1994) recognized 3 subfamilies with a total of 18 tribes for the Asteraceae: (1) subfamily Barnadesioideae (Barnadesieae tribe), (2) subfamily Cichorioideae (Mutisieae, Cardueae, Lactuceae, Arctoteae, Vernoniaeae and Liabeae) and (3) subfamily Asteroideae (Inuleae, Gnaphalieae, Plucheeae, Astereae, Anthemideae, Senecioneae, Helenieae, Heliantheae, Calenduleae and Eupatorieae).

However, further studies and molecular approaches (Panero and Funk 2002, 2008) increased to twelve the number of proposed subfamilies within Asteraceae: Barnadesioideae (about 9 genera), Mutisioideae (approximately 44 genera), Stifftioideae (10 genera), Wunderlichioideae (8 genera), Gochnatioideae (5 genera), Hecastocleidoideae (monogeneric subfamily), Carduoideae (more than 100 genera), Pertyoideae (6 genera), Gymnarrhenioideae (1 genus), Cichorioideae (more than 220 genera), Corymbioideae (few genera) and Asteroideae, which remains the largest subfamily, comprising more than 15,000 species which belong to important recognizable tribes, many of them with very large genera such as *Senecio sensu lato*, *Vernonia sensu lato*, *Artemisia* L., *Centaurea* L., *Eupatorium sensu lato*, *Verbesina* L., etc. An obvious tribal reorganization was then also suggested, considering 35 tribes.

Additionally, Jeffrey (2007) has proposed another subfamilial and tribal arrangement for the Asteraceae; however, he recognized only five subfamilies.

Slowly, some of these recent systematic proposals become more and more frequently incorporated on more “traditional” approaches to this mega-family, thus updating some treatments of the family for floristic contributions (Freire 2009a).

Generic and specific studies are also under deep changes due to the use of modern analytical techniques and advanced classification methodologies. A consequence of the evolution in the generic concepts in this family is, for example, within the large tribe Vernoniaeae (comprising more than 1000 species). Among other modifications, Robinson has proposed the creation of several new genera by splitting the large genus *Vernonia* Schreb (Robinson 1999). This is one of the groups within Asteraceae that shows a wide range of cytological characters (different karyotypes, basic chromosome numbers (Dematteis 1997; Angulo and Dematteis 2006, 2015). Among them, *Chrysolea* H. Rob. (Robinson 1988) is one of the taxa segregated from *Vernonia* sl., such as *Lessingianthus* H. Rob. and *Cyrtocymura* H. Rob. (Dematteis 2009a, b). This group is quite complex, and even infraspecific interesting situations have been considered, regardless of the generic final delimitation within the tribe (Dematteis 2004; Freire 2008).

The large *Senecio* genus, *sensu lato*, which comprises around 1000 species, and also its important tribe within the subfamily Asteroideae, the Senecioneae, have also undergone various changes in the light of new systematic evidences (Pelser et al.

2007; Nordenstam et al. 2009; Devos et al. 2010, among many other authors). Furthermore, additional studies performed in several taxa have resulted in the reformulation of several genera and/or in the appearance of new generic concepts, as is the case of the new genus *Xenophyllum* Funk which was segregated from *Werneria* Kunth (Funk 1997).

Anderberg (1989) has splitted Inuleae into three equivalent taxa; as a consequence, such generic reorganization of former components of Inuleae sensu lato began to be treated as separate taxa (Anderberg 1991; Freire and Iharlegui 1997; Anderberg et al. 2005; Freire 2009b).

The tribe Astereae has been revisited (Nesom 1994), and also several genera belonging to it have been studied quite recently (Bonifacino 2009; Bonifacino and Funk 2012).

In order to be brief, no additional details in terms of tribal and/or generic novelties will be mentioned herein; however, the reader may consult the vast literature data published over the last 20 years.

New advanced attempts to understand the Asteraceae systematics are currently being made by the use of sophisticated softwares for crude data analyses (Hristozov et al. 2007; Ernst 2013; Mandel et al. 2015).

Nowadays, facing this enormous, quasi-planetary distributed plant family (Funk et al. 2009), the amount of available information useful for plant systematics is increasing exponentially, along with the development of new well-founded criteria. The development of such criteria can be achieved with the aid of novel study techniques and accompanied by a large availability of herbarium sheets and worldwide plant sample materials. All these processes are directly proportional to an increase in the number of botanists, among other researchers, who are engaged in the study of this family. Consequently, the output in the number and variety of publications is very large. Only a very small fraction of such literature data has been outlined in this chapter.

## 2.4 Conclusion

Perhaps more than in any other plant family, the enormous size and complexity of this vascular plant taxon accounts for the great deal of literature published so far on the subject. It also implies improvements at the infra-familial level as well as changes in the nomenclature. To sum up, the “endless synthesis” that refers to plant systematics research is what makes the infra-familial taxonomy of Asteraceae so complex, variable and fascinating to researchers from very different backgrounds, from old-gone times to our present.

**Acknowledgements** The author wishes to thank CONICET and Universidad de Buenos Aires, Argentina, for the financial support given to his research group and also to the numerous colleagues and fellows for their useful suggestions about botanical issues about Asteraceae.

## References

- Anderberg AA (1989) Phylogeny and reclassification of the tribe Inuleae (Asteraceae). *Can J Bot* 67:2277–2296
- Anderberg AA (1991) Taxonomy and phylogeny of the tribe Gnaphalieae (Asteraceae). *Opera Bot*, vol 104. Council for Nordic Publications in Botany, Copenhagen, pp 1–195
- Anderberg AA, Eldenäs P, Bayer RJ et al (2005) Evolutionary relationships in the Asteraceae tribe Inuleae (incl. Plucheeae) evidenced by DNA sequences of *ndhF*: with notes on the systematic position of some aberrant genera. *Org Divers Evol* 5:135–116
- Angulo MB, Dematteis M (2006) Números cromosómicos en especies sudamericanas de la tribu Vernonieae (Asteraceae) y su implicancia taxonómica. In: Abstracts of the LVII Congreso Nacional de Botánica, Gramado
- Angulo MB, Dematteis M (2015) Karyotypes of some species of the genus *Lessingianthus* (Vernonieae, Asteraceae) and taxonomic implications. *Nordic. J Bot* 33:239–248
- Bentham G (1873) *Compositae*. Bentham G Hooker JD *Genera plantarum* 2 (1):163–533. Lovell Reeve and Co., London
- Bohm BA, Stuessy TF (2001) Flavonoids of the sunflower family (Asteraceae). Springer Science and Business Media/Springer, Wien
- Bonifacino JM (2009) Taxonomic revision of the *Chiliotrichum* group sensu stricto (Compositae: Astereae). *Smithson Contrib Bot* 92:1–118
- Bonifacino M, Funk VA (2012) Phylogenetics of the *Chiliotrichum* group (Compositae, Astereae). The story of the fascinating radiation in the paleate Astereae genera from southern South America. *Taxon* 61(1):180–196
- Bremer K (1994) *Asteraceae: Cladistics and classification*. Timber Press, Portland
- Brown R (1817) Observations on the natural plant family of plants called Compositae. *Trans Linnean Soc* 12(1):41–142
- Bruno M, Bancheva S, Rosselli S et al (2013) Sesquiterpenoids in subtribe Centaureinae (Cass.) Dumort (tribe Cardueae, Asteraceae): distribution, <sup>13</sup>C NMR spectral data and biological properties. *Phytochemistry* 95:19–93
- Cabrera AL (1962/1961) *Compuestas Argentinas, clave para la determinación de los géneros*. *Revista Mus Arg Cienc Nat Bernardino Rivadavia, Bot* 2(5):291–362
- Cabrera AL (1963) *Compuestas*. In: Cabrera AL (ed) *Flora de la Provincia de Buenos Aires*, 6. Colección Científica del Instituto Nacional de Tecnología Agropecuaria (INTA) 4, Buenos Aires
- Cabrera AL (1965) Revisión del género *Mutisia* (Compositae). *Opera Lilloana* 13:5–227
- Cabrera AL (1971a) Revisión del género *Gochmatia*. *Revista del Museo de La Plata, Secc. Bot* 12(66):1–160
- Cabrera AL (1971b) *Compositae*. In: Correa MN (ed) *Flora Patagónica, parte VII*. Colección Científica del Instituto Nacional de Tecnología Agropecuaria (INTA) 8, Buenos Aires
- Cabrera AL (1974) *Compositae, Compuestas*. In: Burkart A (ed) *Flora Ilustrada de Entre Ríos (Argentina), parte VI: Dicotiledóneas Metaclamídeas (Gamopétalas) B: Rubiales, Cucurbitales, Campanulales (Incluso Compuestas)*. Colección Científica del Instituto Nacional de Tecnología Agropecuaria (INTA) 6, pp 106–554
- Cabrera AL (1977) *Mutisieae – systematic review*. In: Heywood VH, Harborne JB, Turner BL (eds) *The biology and chemistry of the Compositae*. Academic Press, London, pp 1039–1066
- Cabrera AL (1978) *Compositae*. In: Cabrera AL (ed) *Flora de la Provincia de Jujuy, República Argentina. X. Colección Científica del Instituto Nacional de Tecnología Agropecuaria (INTA)*, vol 13. INTA, Buenos Aires, pp 9–726
- Cabrera AL (1982) Revisión del género *Nassauvia* (Compositae). *Darwin* 24:283–379
- Cabrera AL, Freire SE (1998) *Compositae V. Asteroideae. Inuleae. Mutisieae*. In: Spichiger R and Ramella L (eds) *Flora del Paraguay, 27. Conservatoire et Jardin botaniques de la Ville de Genève – Missouri Botanical Garden*, pp 9–223

- Cabrera AL, Klein RM (1973) Compostas. Tribe: Mutisieae. In: Reitz R (ed) Flora Ilustrada Catarinense I, Fascículo COMP, Itajaí, pp 1–124
- Cabrera AL, Klein RM (1975) Compostas. Tribe: Senecioneae. In: Reitz R (ed) Flora Ilustrada Catarinense I, Fascículo COMP, Itajaí, pp 127–222
- Cabrera AL, Ragonese AM (1978) Revisión del género *Pterocaulon* (Compositae). Darwin 21(2–4):188–257
- Cabrera AL, Freire SE, Ariza Espinar L (1999) Asteraceae, parte 13. Tribu VIII. Senecioneae. Tribe VIII bis. Liabeae. In: Hunziker AT (ed) Flora Fanerogámica Argentina 62. IMBIV, Córdoba
- Cabrera AL, Dematteis M and Freire SE (2009) Compositae VI. Asteroideae. Senecioneae. Vernonieae. In: Loizeau, P-A (dir) Flora del Paraguay, 39. Conservatoire et Jardin botaniques de la Ville de Genève – Missouri Botanical Garden, pp 9–298
- Carlquist S (1976) Tribal interrelationships and phylogeny of the Asteraceae. Aliso 8:465–492
- Crisci JV (1980) Evolution in the subtribe Nassauviinae (Compositae, Mutisieae): a phylogenetic reconstruction. Taxon 29(2–3):213–224
- Crisci JV (1982) Parsimony in evolutionary theory: law or methodological prescription? J Theor Biol 97:35–41
- Crisci JV, López Armengol MF (1983) Introducción a la teoría y práctica de la taxonomía numérica. Monografía N 26, Serie de Biología, Secretaría General de la Organización de Estados Americanos, Washington DC
- Crisci JV, Stuessy TF (1980) Determining primitive character states for phylogenetic reconstruction. Syst Bot 5:112–135
- de Candolle AP (1836) Compositae. In: de Candolle AP. Prodrum systematis naturalis regni vegetabilis 5. Treuttel et Würtz, Paris, pp 4–695
- de Candolle AP (1838) Mantissa Compositarum. In: Candolle AP de. Prodrum systematis naturalis regni vegetabilis 7. Treuttel et Würtz, Paris, pp 263–307
- de Cassini AHG (1816) Quatrième mémoire sur la famille des Synantherées contenant l'analyse de l'ovaire et des ses accessoires. J Phys Chim Hist Nat Arts 85:5–21
- Dematteis M (1997) Estudios cromosómicos en *Vernonia platensis* (Asteraceae) y especies afines. Bonplandia 9:259–264
- Dematteis M (2004) Taxonomía del complejo *Vernonia rubricaulis* (Vernonieae, Asteraceae). Bonplandia 13:5–13
- Dematteis M (2009a) Revisión taxonómica del género sudamericano *Chrysolaena* (Vernonieae, Asteraceae). Bol Soc Argent Bot 44(1–2):103–170
- Dematteis M (2009b) Tribu Vernonieae. In: Hurrell J A (dir), Flora Rioplatense. Parte 2 Dicotiledóneas, vol. 7a. Buenos Aires, Sociedad Argentina de Botánica, pp 244–266
- Devos N, Barker NP, Nordenstam B et al (2010) A multi-locus phylogeny of *Euryops* (Asteraceae, Senecioneae) augments support for the “cape to Cairo” hypothesis of floral migrations in Africa. Taxon 59(1):57–67
- Dumortier BCJ (1822) Commentationes botanicae. Observations botaniques dédiées à la Société d' Horticulture de Tournay, Tournay
- Emerenciano VP, Militão JS, Campos CC et al (2001) Flavonoids as chemotaxonomic markers for Asteraceae. Biochem Syst Ecol 29:947–957
- Ernst M (2013) Metabolomics in plant taxonomy: the Arnica model. Corrected version of the master's thesis presented to the Post-Graduate Program in Pharmaceutical Sciences. Faculty of Pharmaceutical Sciences of Ribeirão Preto/USP
- Estabrook G (1972) Cladistic methodology: a discussion of the theoretical basis for the introduction of evolutionary history. Annu Rev Ecol Syst 3:427–456
- Francisco IA, Pimenta Pinotti MH (2000) Cyanogenic glycosides in plants. Braz Arch Biol Technol 43(5):487–492
- Freire S (2008) Asteraceae. In: Zuloaga FO, Morrone O and Belgrano MJ (eds) Catálogo de las plantas vasculares del Cono Sur (Argentina, Sur de Brazil, Chile, Paraguay y Uruguay), vol 2. Monogr Syst Bot Missouri Botanical Garden 107, pp 1154–1565

- Freire S (2009a) Generalidades e importancia de las Asteráceas. In: Freire S, Molina AM (eds) Flora Chaqueña -Argentina- Familia Asteraceae. Colección Científica del INTA, Buenos Aires, pp 27–45
- Freire S (2009b) Tribe Gnaphalieae. In: Hurrell JA (ed) Flora Rioplatense - Parte 2 Dicotiledóneas, vol. 7a. Sociedad Argentina de Botánica, Buenos Aires, pp 133–207
- Freire S (2013) Asteraceae. In: Hurrell JA (ed) Flora Rioplatense. Parte 2 Dicotiledóneas, vol 7a, Sociedad Argentina de Botánica, Buenos Aires, pp 12–20
- Freire S, Iharlegui L (1997) Sinopsis preliminar del género *Gamochoaeta* (Asteraceae, Gnaphalieae). Bol Soc Argent Bot 33:23–35
- Funk VA (1985) Cladistics and generic concepts in the Compositae. Taxon 34:72–80
- Funk VA (1997) *Xenophyllum*, a new Andean genus extracted from *Werneria* s.L. (Compositae: Senecioneae). Novon 7:235–241
- Funk VA, Stuessy TF (1978) Cladistics for the practising plant taxonomist. Syst Bot 3:159–178
- Funk VA, Susanna A, Stuessy TF, et al (eds) (2009) Systematics, evolution and biogeography of the compositae. IAPT, pp 965
- Funk VA, Sancho G, Roque N et al (2014) A phylogeny of the Gochnatieae: understanding a critically placed tribe in the Compositae. Taxon 63:859–882
- Giseke PD (1792) Praelectiones in ordines naturales plantarum. BG Hoffman, Hamburg
- Granica S, Zidorn C (2015) Phenolic compounds from aerial parts as chemosystematic markers in the Scorzonnerinae (Asteraceae). Biochem Syst Ecol 58:102–113
- Gutiérrez DG (2003) Reincorporación del género *Liabum* (Asteraceae, Liabeae) a la flora argentina y primer registro de *L. acuminatum* para el país. Darwin 41:55–59
- Gutiérrez DG (2010) *Inkaliabum*, a new Andean genus of Liabeae (Asteraceae) from Perú. Bol Soc Argent Bot 45:363–372
- Gutiérrez DG, Katinas L (2015) Systematics of *Liabum* Adans. (Asteraceae, Liabeae). Syst Bot Monogr 97:1–121
- Gutiérrez DG, Luna M (2013) A comparative study of latex-producing tissues of Liabeae (Asteraceae). Flora 208:33–44
- Hennig W (1966) Phylogenetic systematics. University of Illinois Press, Champaign
- Hernández MP, Katinas L, Arambarri AM (2015) Taxonomic value of histochemical features of the style in early lineages of Asteraceae. Acta Bot Bras 29(4):575–585
- Heywood VH, Harborne JB, Turner BL (eds) (1977) The biology and chemistry of the Compositae. Academic Press, London
- Hoffmann O (1894) Compositae. In: Engler A, Prantl K (eds) Die Natürlichen Pflanzenfamilien, vol 4(5), pp 87–402
- Hristozov D, Da Costa FB, Gasteiger J (2007) Sesquiterpene lactones-based classification of the family Asteraceae using neural networks and *k*-nearest neighbors. J Chem Inf Model 47:9–19
- Jansen RK, Palmer JD (1987) A chloroplast DNA inversion marks an ancient evolutionary split in the sunflower family (Asteraceae). Proc Natl Acad Sci USA 84:5818–5822
- Jeffrey C (2007) Compositae. Introduction and key to the tribes. In: Kubitzki K (ed) The families and genera of vascular plants VIII. Asterales. Springer, Berlin, pp 61–87
- Katinas L (1994) Un nuevo género de Nassauviinae (Asteraceae, Mutisieae) y sus relaciones cladísticas con los géneros afines de la subtribu. Bol Soc Argent Bot 30(1):59–70
- Katinas L (1996) revisión de las especies sudamericanas del género *Trixis* (Asteraceae, Mutisieae). Darwin 34(1–4):27–108
- Katinas L, Gutiérrez DG, Grossi MA et al (2007) Panorama de la familia Asteraceae (=Compositae) en la Argentina. Bol Soc Argent Bot 42(1–2):113–129
- Katinas L, Pruski J, Sancho G et al (2008) The subfamily Mutisioideae (Asteraceae). Bot Rev 74:469–716
- Katinas L, Sancho G, Tellería MC et al (2009) The Mutisieae (Mutisioideae sensu stricto). In: Funk VA et al (eds) Systematics, evolution and biogeography of Compositae. IAPT, Vienna, pp 229–248
- King RM, Robinson H (1970) The new synantherology. Taxon 19:6–11

- King RM, Robinson H (1987) The genera of Eupatorieae (Asteraceae). Monographs in systematic botany from the Missouri botanical garden. Missouri Botanical Garden, St Louis
- Lessing CF (1832) Synopsis generum compositarum earunque dispositionis novae tentamen, monographis multarum Capensium interjectis. Berolini: sumtibus Dunckeri et Humblotii, Leipzig
- Mandel JR, Dikow RB, Funk VA (2015) Using phylogenomics to resolve mega-families. An example from Compositae. *J Syst Evol* 53(5):391–402
- Nesom GL (1994) Subtribal classification of the Astereae (Asteraceae). *Phytologia* 76(3):193–274
- Nordenstam B, Pelser PB, Kadereit JW et al (2009) Senecioneae. In: Funk Vaet al. (eds). Systematics, evolution and biogeography of the Compositae. IAPT, Wien, pp 503–526
- Panero JL, Funk V (2002) Toward a phylogenetic subfamilial classification for the Compositae (Asteraceae). *Proc Biol Soc Wash* 115(4):909–922
- Panero JL, Funk V (2008) The major clades of the Asteraceae (Compositae) revisited. *Mol Phylogenet Evol* 47:757–782
- Pelser PB, Nordenstam B, Kadereit JW et al (2007) An ITS phylogeny of the tribe *Senecioneae* (Asteraceae) and a new delimitation of *Senecio* L. *Taxon* 56:1077–1104
- Rios MY (2012) Natural alkaloids: pharmacology, chemistry and distribution. In: Vallisuta O, Olimat SM (eds) Analytical evaluation of herbal drugs. Drugs discovery and research in Pharmacognosy. Intechopen, Rijeka, pp 107–144
- Robinson HE (1988) Studies in the *Lepidaploa* complex (Vernonieae, Asteraceae) V. The new genus *Chrysolaela*. *Proc Biol Soc Wash* 101:95–158
- Robinson HE (1999) Generic and subtribal classification of American Vernonieae. *Smithson Contrib Bot* 89:1–116
- Robinson H, Brettel RD (1973) Tribal revision in the Asteraceae III. A new tribe, Liabeae. *Phytologia* 25:404–407
- Roque N, Funk VA (2013) Morphological characters add support for some members of the basal grade of Asteraceae. *J Linn Soc Bot* 171(3):568–586
- Sáenz AA (1981) Anatomía y morfología de frutos de Heliantheae (Asteraceae). *Darwin* 23:37–117
- Scotti MT, Emerenciano V, Ferreira MJ et al (2012) Self-organizing maps of molecular descriptors for sesquiterpene lactones and their application to the chemotaxonomy of the Astereceae family. *Molecules* 17(4):4684–4702
- Seaman FC (1982) Sesquiterpene lactones as taxonomic characters in the Asteraceae. *Bot Rev* 48:121–194
- Seaman FC, Funk VA (1983) Cladistic analysis of complex natural products: developing transformation series from sesquiterpene lactone data. *Taxon* 32(1):1–27
- Seaman F, Bohlmann F, Zdero C et al (1990) Diterpenes of flowering plants. Compositae (Asteraceae). Springer, New York
- Sneth PHA, Sokal RR (1973) Numerical taxonomy. The principles and practice of numerical classification. Freeman, San Francisco
- Stevens PF (1991) Character states, morphological variation, and phylogenetic analysis: a review. *Syst Bot* 16:553–583
- Stuessy TF (2002) Morfología profunda en la Sistemática de plantas. Paper presented at the XXVIII Jornadas Argentinas de Botánica, Sociedad Argentina de Botánica, Santa Rosa, 21–25 October 2001
- Stuessy TF, Funk VA (2013) New trends in plant systematics – introduction. *Taxon* 62(5):873–875
- Tellería MC, Sancho G, Funk VA et al (2013) Pollen morphology and its taxonomic significance in the tribe Gochnatieae (Compositae, Gochnatioideae). *Plant Syst Evol* 299:935–948
- von Berchtold FG, Presl JS (1820) O přirozenosti rostlin, obsahujcíc. Krala Wiljma Endersa, Praha
- Wagenitz G (1976) Systematics and phylogeny of the Compositae. *Plant Syst Evol* 125:29–46
- Wiley EO (1981) Phylogenetics: the theory and practice of Phylogenetics systematics. Wiley, New York
- Zidorn C (2008) Sesquiterpene lactones and their precursors as chemosystematic markers in the tribe Cichorieae of the Asteraceae. *Phytochemistry* 69(12):2270–2296

# Chapter 3

## Chemotaxonomic Study of Sesquiterpene Lactones of Asteraceae: Classical and Modern Methods



Mateus Feitosa Alves, Luciana Scotti, Fernando Batista Da Costa, and Marcus Tullius Scotti

**Abstract** Chemotaxonomy is a classification method based on the comparison of similarities of natural compounds among the organisms to be classified. However, it presents some difficulties because the chemical compounds present large variability. Currently, different classification methods are available in chemotaxonomy involving classical and modern taxonomy. Asteraceae is one of the largest families of angiosperms, and its sesquiterpene lactones are considered important taxonomic markers. They have been studied as promising new drug sources as a consequence of their enormous pharmacological potential. With regard to modern methods to study taxonomy, in the last two decades, linear approaches such as principal component analysis and partial least squares as well as other machine learning methods like artificial neural networks, k-nearest neighbors, and self-organizing maps have been used as pattern recognition methods to study the distribution of sesquiterpene lactones among the tribes and genera of Asteraceae. For this purpose, thousands of chemical structures and molecular descriptors that encode different physicochemical features of compounds have been used. Such studies are empowered by computational methods and databases of secondary metabolites. In this sense, systems that are able to manage large databases of sesquiterpene lactones are crucial for more robust chemotaxonomic studies of Asteraceae. The web tool AsterDB ([www.asterbiochem.org/asterdb](http://www.asterbiochem.org/asterdb)) is an interesting database with a friendly interface that contains thousands of chemical structures of secondary metabolites from this family and comprises more than 1000 chemical structures of sesquiterpene lactones. The great evolution in the study of natural products based on computational methods shows that modern and integrated platforms will be available soon for several purposes.

---

M. F. Alves · L. Scotti · M. T. Scotti (✉)  
Federal University of Paraíba, João Pessoa, PB, Brazil

F. B. Da Costa  
AsterBioChem Research Team, University of São Paulo, School of Pharmaceutical Sciences of Ribeirão Preto, Ribeirão Preto, SP, Brazil



**Keywords** Chemotaxonomic methods · Sesquiterpene lactones · Asteraceae · Machine learning · Secondary metabolites database

### 3.1 Introduction

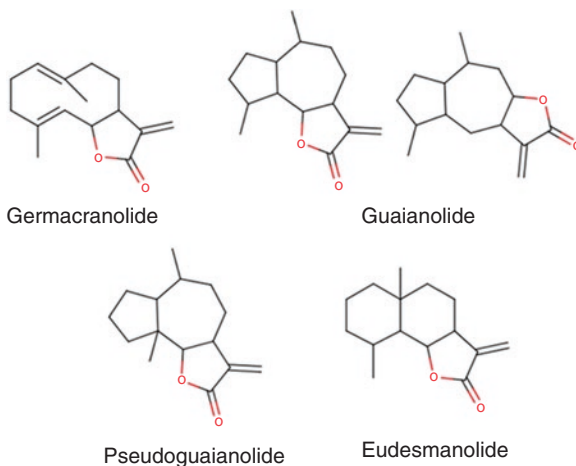
Chemotaxonomy is a classification method based on the comparison of similarities of natural compounds among a group of organisms. Classification criteria may take into account primary (e.g., Calvin leaf acids) or secondary metabolites (e.g., alkaloids, flavonoids, and terpenes), visible particles (e.g., starch grains), and molecular data (e.g., DNA, RNA, and protein sequences) (Alston et al. 1963; Singh 2016).

According to some authors, chemical criteria for classification purposes can present some difficulties at the moment of classification because the chemical compounds are ecologically variable, being their content usually affected by ontogeny, hereditary, and environmental factors. In addition, chemical and morphological characteristics may have evolved at different speed. Thus, within a taxon, primitive chemical characteristics may coexist with the most evolved morphological characteristics. Some experts claim that the classification by molecular data has immense taxonomic value, since it takes into account genetic characteristics. However, time and equipment limitations make it difficult to access the relative degree of advancement of different compounds or classes of compounds in any taxon. Even so, in general terms, molecular, morphological, and chemical characteristics are used to aid in taxonomic classification (Mannheimer 1999; Calabria et al. 2007; Singh 2016).

Currently, different available computational methods, such as artificial neural networks and statistical models, are able to analyze a great number of chemical data, and they therefore help in chemotaxonomic studies. Such approaches have been used in different chemotaxonomy studies (Da Costa et al. 2005). The Kohonen neural network, also named “self-organizing maps” (SOMs), is a simple method that dimensionally organizes complex data into groups according to their relationships (Kohonen 2001). The use of SOMs has been applied to the study of property data of several compounds (Manallack and Livingstone 1999).

Asteraceae is one of the largest Angiosperm families, comprising around 1100 genera and more than 25,000 species distributed into 19 tribes (Heywood 2009; Funk et al. 2005). Due to the enormous pharmacological potential of the biologically active secondary metabolites from several species of this family, they have been studied as promising new drug sources (Schmidt 1999; Schmidt et al. 2009; Merfort 2011; Schmidt et al. 2011; Schmidt et al. 2012a; Chadwick et al. 2013). Species of this family biosynthesize mainly polyacetylenes, phenolics like flavonoids and trans-cinnamic acid derivatives, and terpenoids including diterpenes and the most studied subclass whose members are used as taxonomic markers, i.e., sesquiterpene lactones (STLs) (Seaman 1982; Da Costa et al. 2005).

**Fig. 3.1** Chemical structures of the main skeleton types of sesquiterpene lactones (Seaman 1982)



Sesquiterpene lactones (C-6 or C-8 lactonized sesquiterpenes) are mostly biologically active compounds that belong to the sesquiterpenoid class (Fig. 3.1) (Picman 1986). These compounds present several pharmacological activities, such as antimicrobial (Aljancic et al. 1999), against neglected tropical diseases (Schmidt et al. 2012a, b; Acevedo et al. 2017), anti-inflammatory (Siedle et al. 2004), and antitumor (Schmidt 1999), among others. However, these compounds are highly toxic, causing adverse effects such as contact dermatitis and toxic syndromes in animals. The mutagenic potential of some STLs has also been documented (Schmidt 1999). Such toxic activity is mainly due to the low specificity of the Michael-type addition that takes place when a nucleophile attacks the exocyclic double bond of the lactone ring (Schmidt 1999).

This chapter presents classic and modern approaches to chemotaxonomic studies of STLs of the Asteraceae family.

## 3.2 Classical Taxonomy

The Asteraceae family is characterized by the presence of STLs and furan sesquiterpenes. Lactonized sesquiterpenes are considered good chemical markers (Seaman 1982; Da-Costa et al. 2005). Plant metabolites can be used as a taxonomic criterion for differentiation among species (chemotypes). Another widely used form of classification is cladistics, the most accepted today by the scientific community. Through this technique, organisms are classified according to the order in which they evolved from a common ancestor to whom the most recent ancestors are related to (Seaman 1982).

In addition, evidence of limited biosynthetic routes and influences of chemical and physical characteristics may lead to an erratic distribution of the STLs within the family.

In 1816, botanist Henri Cassini was the first researcher to publish the Asteraceae classification in a diagram showing the interrelation of 19 tribes (Cassini 1816). This arrangement was later revised by Bentham in 1873, who reduced the number of tribes to 13 (Bentham 1873). In 1976, other researchers contributed by introducing a family subclassification based on morphological criteria, therefore facilitating the understanding of the tribal interrelationships within Asteraceae (Carlquist 1976).

In 1987, Bremer introduced a cladogram for Asteraceae, based on the incorporation of chemical, morphological, and molecular characteristics (Bremer 1987). Soon after, he presented a new classification diagram based on morphological criteria giving rise to four subfamilies: Asteroideae, Cichorioideae, Carduoideae, and Barnadesioideae (Bremer 1996; Calabria et al. 2007) (Fig. 3.2).

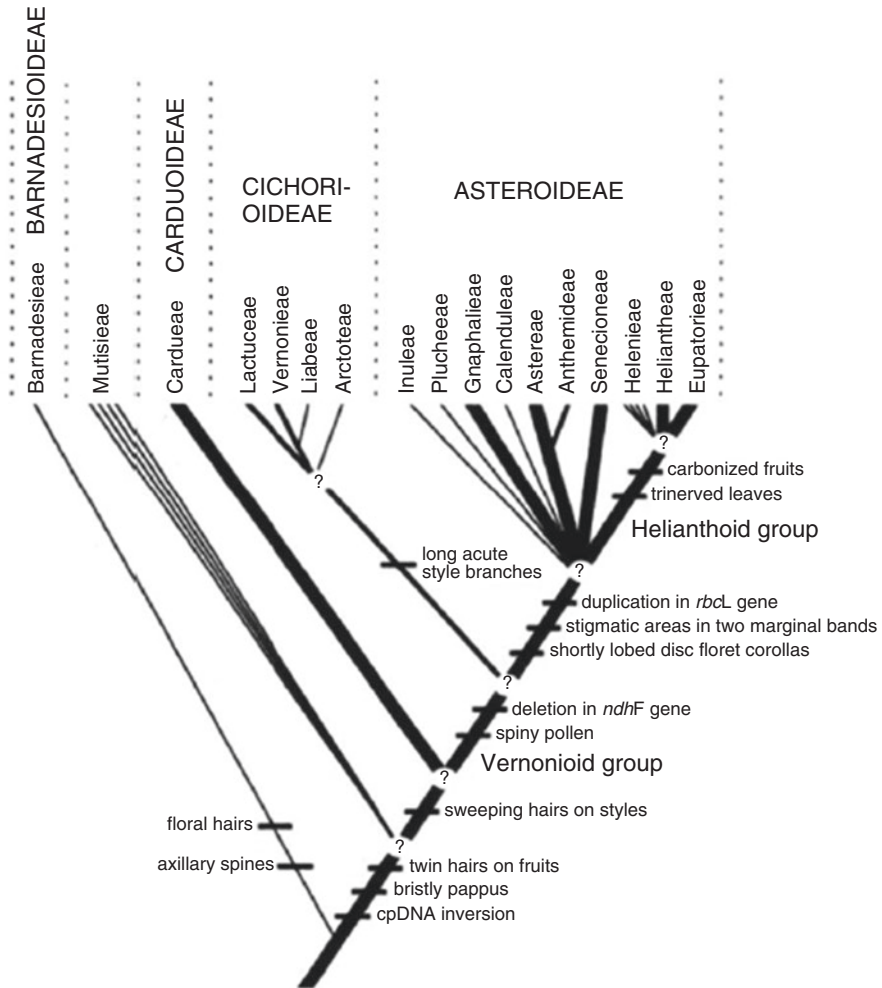


**Fig. 3.2** Classification proposed by Bremer for the tribes and subfamilies of Asteraceae (Bremer 1996)

Seaman (1982) has claimed that STLs could be used as taxonomic markers at various taxonomic levels as long as the used analytical approach was adequate. However, he pointed out that although the biosynthetic pathways for most of these compounds could be proposed, the lack of experimental evidence to support such biogenetic interpretations should be considered when a sesquiterpene-based taxonomic classification was established. Therefore, more sophisticated analytical methods are required to facilitate the sorting of information. Moreover, the author states that cladistic models can be applied to STLs, though with some reservations. This is due to the existence of discontinuous distribution patterns of STLs resulting in the reduction of the confidence level and also because complete data for all taxa included in a study are required for cladistic analysis (Seaman 1982).

In 1998, Gottlieb developed a methodology with a multidisciplinary approach to develop a safe theoretical basis for assessing and measuring biodiversity. This methodology was based on the application of quantitative phytochemistry, and he was able to demonstrate that metabolic mechanisms were analogous to biological mechanisms at cellular, morphological, and ecogeographic levels (Gottlieb et al. 1998). For Gottlieb, the multidisciplinary effort to address a range of issues such as mapping the biological diversity of specific and chemical regions may lead the next generations to prepare for a better understanding of nature (Gottlieb and Borin 2012).

Although they are used for taxonomic classification, secondary metabolites have a restricted taxonomic distribution and can be found in taxonomic groups that are not related to a phylogenetic context (Wink et al. 2010). This irregular occurrence can bring about errors in the taxonomic classification of certain species and is probably due to the fact that certain genes, encoding enzymes involved in the biosynthesis, may or may not be present in all species. Another explanation for the irregular distribution of these secondary metabolites is the interference of fungi in the production of secondary metabolites (Wink 2008). According to Wink (2003), the systematic value of secondary metabolites becomes a matter of interpretation equal to the morphological markers used.

Algorithm-based classification systems replaced the cladistics model for some time. The phenetic model is a classification system based on the observable common phylogeny-independent morphological characteristics existing among organisms. In this method, all the observed characteristics are treated in the same way. From the collected data, a computer processes them through a numerical algorithm creating a coefficient of similarity and obtaining phenograms that will affirm which organisms are morphologically similar to each other. Although they are not subjective, phenograms are circled because they do not explain the fact that individuals can evolve from similar unrelated physical characteristics (Schlee 1975; Williams 1975).

### 3.3 Modern Chemotaxonomy

In 1998, Emerenciano et al. (1998) developed a new method to group chemotaxonomic parameters using 10370 chemical structures of natural products isolated from Asteraceae using evolutionary advancement diagrams. This methodology was widely used to better represent the evolutionary stage of rates at several hierarchical levels. In these diagrams, it could be observed that some tribes did not follow the chemical evolution of the Asteraceae family as regards the biosynthesis of small molecules. According to the authors, this methodology provides a new horizon to help achieve a chemotaxonomic classification of Asteraceae that takes into account the joint interpretation of large and small organic molecules together with botanical data.

Furthermore, Emerenciano et al. (2006) have presented a new methodology that employs the partial least squares (PLS) regression method to evaluate the oxidation stages according to their taxonomic classification. The PLS model was applied using the oxidation data of chemical structures of several secondary metabolites belonging to Asteraceae present in a database containing 27,000 botanical entries. Results showed that there is interdependence among the oxidation of the secondary metabolites of this family at the level of tribes and sub-tribes (Emerenciano et al. 2006).

As for the evaluation of vegetation changes over time, Adamczyk et al. (2013) stated that methodologies based on linear principles, such as the principal component analysis (PCA), are not suitable for the evaluation of these terms because data are not often linear, therefore limiting the analysis of plant alteration over time. To overcome this problem, they proposed the use of self-organized maps (SOMs) to obtain more precise information (Fig. 3.3) (Adamczyk et al. 2013).

**Fig. 3.3** Kohonen's self-organized map (SOM)

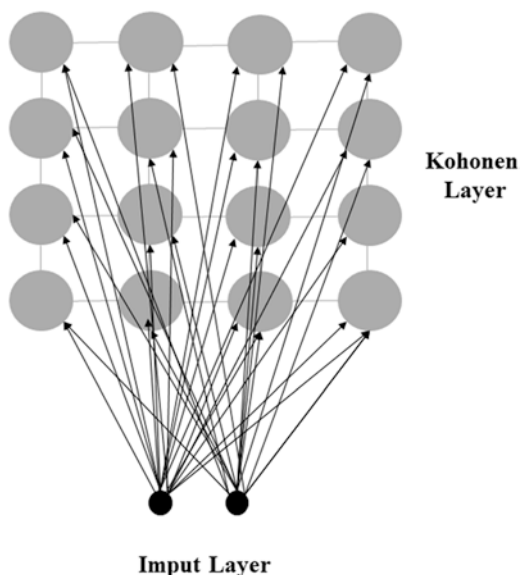


**Table 3.1** Advantages and disadvantages of SOMs

Self-organizing map (SOM)	
<i>Advantages</i>	<i>References</i>
1. It can be used to determine patterns in complex data sets, such as discovering various nonlinear relationships among species, communities, and environmental factors	Adamczyk et al. (2013); Zhang and Yang (2008)
2. It is considered a robust model for nonlinear analysis between variables of non-normal distribution	Adamczyk et al. (2013); Kohonen (1982); Kohonen (2013)
3. The interpretation of the data is easy, since there is a reduction of multidimensional data for a two-dimensional grid	Adamczyk et al. (2013); Park et al. (2006);
4. Its application is already consolidated in other research fields such as ecology	Adamczyk et al. (2013); Bedoya et al. (2009); Zhang and Li (2011)
<i>Disadvantages</i>	<i>References</i>
1. Loss of reasonable information	Adamczyk et al. (2013)
2. The difficulties of finding data recorded in large quantity making it difficult to apply	Adamczyk et al. (2013)

Robust methodologies using artificial neural networks have been developed to detect clusters and patterns that may not be clear even for trained human experts (Scotti et al. 2012). Artificial neural networks are able to simulate a biological neuron in adapted softwares. This method has the advantage of gathering important chemical information when cause-and-effect relationships are still not well understood. Besides, this method can be applied in the fields of object identification and prediction and visualization of chemical data (Ferreira et al. 2004, 2005, Zupan and Gasteiger 1999).

The most commonly used neural network architecture for pattern recognition and classification is the self-organized map (SOM). This method can map multivariate data to a two-dimensional grid, grouping similar patterns close to each other (Scotti et al. 2012). The application of neural networks, such as SOM, has been used to classify Asteraceae tribes using STLs (Da Costa et al. 2005; Hristozov et al. 2007) (Table 3.1).

Using SOMs, Da Costa et al. (2005) have used 144 3D chemical structures to classify 7 sub-tribes within Eupatorieae, Heliantheae, and Vernonieae tribes. The 3D coordinates of the structures were transformed into a structure code with a fixed number of descriptors using the radial distribution function (RDF) code. In this work, the use of neural networks allowed establishing a correlation between chemical structures with the current taxonomic classification of the family. Thus, the authors concluded that neural networks can be used as an aid in the chemotaxonomic classification of STLs.

Hristozov et al. (2007) have used a data set comprising 921 chemical structures of STLs to predict the tribe in which a given STL occurs. The work was carried out using two different structure representations (2D atom counts and 3D RDF) and two supervised classification methods (counter propagation neural networks and  $k$ -nearest neighbors –  $k$ -NN). This study showed that approaches using statistical methods and machine learning tools can be useful to study the relationship between the taxonomic classification and plant chemistry.

With the aim of classifying the Asteroideae subfamily (Asteraceae) using chemical taxonomic markers, a study employing SOMs was performed using 12 chemical classes in different subfamily taxa as variables (Correia et al. 2012). Data showed that it was possible to obtain a satisfactory separation of the tribes into their respective branches. In addition, it was shown that the taxonomic classification obtained with the analysis of secondary metabolites was similar to that obtained by Funk et al. (2005).

In another study (Correia et al. 2008), a chemotaxonomic analysis was performed using SOM, together with a database containing different types of chemical structures belonging to the Heliantheae tribe (Asteraceae). In that study, nine different chemical classes were used as variables. The authors were able to satisfactorily separate, within the same branch, the Helianthinae and Gaillardinae sub-tribes, and also to separate the *Helianthus* and *Pappobolus* genera from the Helianthinae sub-tribe. These data corroborated those from the Stuessy's classification, which were based on the number of chromosomes and morphological data (Correia et al. 2008).

Scotti et al. (2012) have used SOM to classify 1111 STLs extracted from 58 species, 161 genera, 63 sub-tribes, and 15 Asteraceae tribes, which were represented and recorded in two dimensions using the Sistemax software ([sistemax.ufpb.br](http://sistemax.ufpb.br)). In this study, 11 blocks of descriptors (constitutional, functional groups, BCUT, 2D autocorrelations, atom-centered, topological, geometric, RDF, 3D-MoRSE, GETAWAY, and WHIM) were used to separate botanical occurrences. Results demonstrated the existence of similarities among the Heliantheae, Helenieae, and Eupatorieae tribes, as well as between the Anthemideae and Inuleae tribes. These results are in agreement with the systematic classifications proposed by Bremer (1996). Therefore, the authors claimed that the generated SOMs can predict the tribe in which a certain compound is most likely to be found.

Flavonoids belonging to the Asteraceae family were subjected to analysis by SOMs in order to establish phylogenetic relationships among subfamilies and tribes that were classified on the basis of the number of occurrences and oxidation patterns. Results allowed the differentiation between Asteraceae subfamilies and the separation into sub-tribes and tribes according to the degree of methoxylation versus the degree of flavonoid glycosylation. The authors stated that the methodology is a useful tool for the classification of plants (Emerenciano et al. 2007).

### 3.4 Sesquiterpene Lactones Database

The search for chemical structures in databases is costly because several false targets among compounds of natural and synthetic origin can be generated. Therefore, a number of commercially or freely available specialized natural product databases have been developed, and they can be searched with only minimal information, for example, the Dictionary of Natural Products (<http://dnp.chemnetbase.com>); NAPRALERT (Loub et al. 1985; Graham and Farnsworth 2010); Marinlit, for marine natural products; and AntiBase, for microorganism and higher fungi materials (Dabb et al. 2014).

These structures are also available in regional databases, for example, NuBBEDB (Valli et al. 2013), SANCDB (Hatherley et al. 2015), TM-CM (Kim et al. 2015), TCM-Database@Taiwan (Chen 2011), and TCMID (Xue et al. 2013). Many of these databases have been used in research, including virtual screening. In addition, the databases described above include 2D chemical structures, while in some databases, methods and tools to generate 3D structures of small organic molecules have also been incorporated, being often used for studies involving structure-based drug design.

In addition to the databases of natural products with a focus on metabolomic studies involving species metabolites, KNApSAcK Family (Afendi et al. 2012), TIPdb-3D (Tung et al. 2014), and AsterDB ([www.asterbiochem.org/asterdb](http://www.asterbiochem.org/asterdb)) are examples of databases in which it is possible to search for a chemical structure using the species name and other associated information as entries. Nevertheless, they are still not able to carry out correct dereplication because compound information such as exact mass, fragmentation patterns, and geographic data, which have been demonstrated to be very important for this type of studies, are still lacking.

However, focusing only on the information included in the database is not enough to achieve reliable results. In fact, a clean interface, fast search, a user-friendly format, and consistencies across the diversity of operational systems (Microsoft Windows, Mac OS, and Linux platforms) are also necessary. With the aim of including a more concise compound survey and to achieve good results, two new natural product databases, namely, Sistemax ([sistemax.ufpb.br](http://sistemax.ufpb.br)) and AsterDB ([www.asterbiochem.org/asterdb](http://www.asterbiochem.org/asterdb)), have recently been developed, which can be used for chemosystematics studies, dereplication, and botanical correlation.

AsterDB ([www.asterbiochem.org/asterdb](http://www.asterbiochem.org/asterdb)) is a database that contains chemical structures of secondary metabolites from Asteraceae, comprising more than 1000 chemical structures of STLs. AsterDB has been developed in Java programming language for version 8 or higher, also requiring JSP technology version 2.1 or higher. AsterDB uses the MySQL database version 5.5.46-0 for Linux to maintain the system data. The system uses JSP to create the pages with specific information of each molecule and offers dynamic page changes by clicking on certain buttons. Intermediary pages are used to recover information from the database and insert it into the JSP.



Several API are used in the AsterDB implementation. MarvinJS version 15.7.20, from ChemAxon, (<http://www.chemaxon.com>), is the drawing API, and it is integrated to ChemAxon JChem WebServices, an external online service that transforms the drawn structures into SMILES codes, and then a JChem API function turns it into a binary fingerprint. This fingerprint is then used to search structures in the database. AsterDB displays information with respect to the general nomenclature as common structure name, SMILES code, IUPAC name, International Chemical Identifier (InChI), standard InChI hashes (InChIKey), and CAS registry number and some properties such as oxidation number, exact mass, and relative mass.

Additionally, Google Maps, from Google Inc., is an API used to draw maps and locations, and it is used in the system to show a world map containing the registered metabolite location. The API draws the map and receives locations from the database, two variables of double type to represent latitude and longitude. A registered molecule may have multiple locations and species attached to it. Using a JavaScript function, it graphically places the locations on the map. After registering, by clicking on the map, the API sets a marker at the location and adds a line in the coordinates list below the map for each marker on the map, thus allowing to automatically changing the position when the values of either the latitude or the longitude boxes are changed. Using a reverse geocode, which is a function from the Google Maps API, the coordinates are also transformed into an approximate address.

A snapshot of the AsterDB interface is shown in Fig. 3.4. After the user enters the website (<http://143.107.203.160:8080/asterdb/index.jsp>), a structure search option is shown using the MarvinJS API at the top of the screen. Other search options are exhibited in the interface. The home screen of the system with the SMILES, compound name, and species search modes are also visible.

In the first option, the user can perform the search by drawing a structure or skeleton, fragment or substructure, which is important in the cases when only some structural characteristics of the molecule such as functional groups, are available. In addition, it is possible to search by SMILES codes, a chemical notation system capable of representing organic compounds, or species searches. In this last option, it is necessary to input the name of the genus (which presents an auto-completing option), and after being selected, the system presents all of the species registered for the genus, and the user then selects a species to perform the search.

When performing a search, the mechanisms generate a search result page (six results per page), named by its common name; if the compound does not have a common name, IUPAC names are displayed instead. When one of the results is selected, the user has access to the data corresponding to that structure. Data are classified into six different groups.

The first group of results that is displayed is related to the structural representation of the searched molecule. The 2D structure is observed on the interface, on top of which the amplified option appears; by clicking on that option, the system displays a 2D and a 3D representation of the molecule (ChemDoodle). An additional option to save the 2D or 3D structure as an MDL molfile is also offered. The second

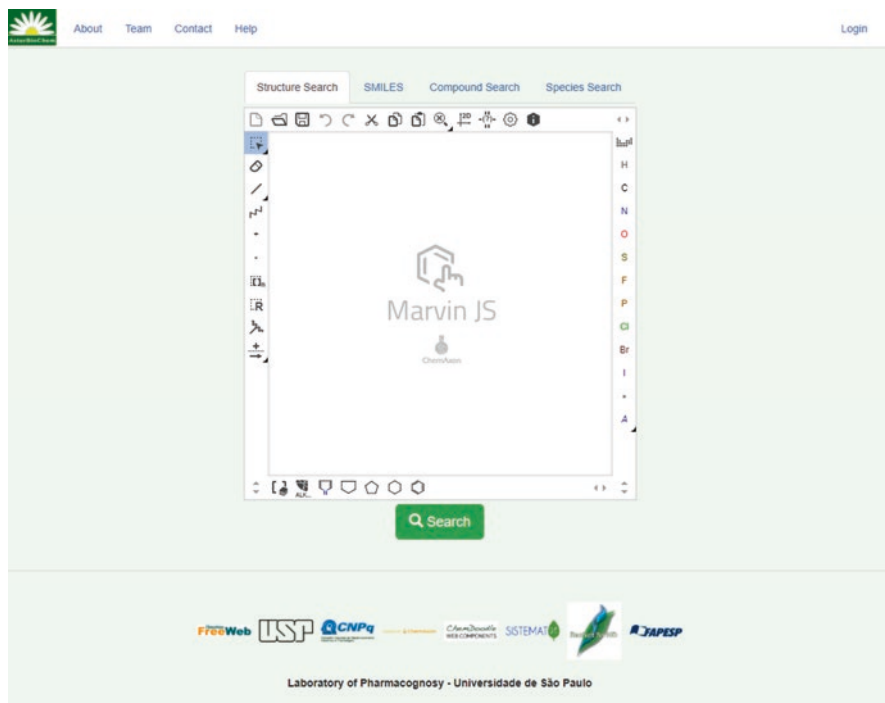


Fig. 3.4 AsterDB interface. (<http://www.asterbiochem.org/asterdb>)

type of result displayed by the system is associated with the compound identification. The common name, SMILES code, IUPAC name, InChI code, InChIKey, and CAS number are all provided.

Compound data results include important characteristics for natural product chemistry. The class of metabolite of the searched molecule and its skeleton provide information about its biosynthetic pathway and aid in chemosystematics and chemotaxonomy studies. Oxidation numbers (NOX), which are calculated based on Hendrickson rules, are fundamental in chemotaxonomy because Gottlieb related oxidation grade of molecules with species evolution (Gottlieb 1989). Molecular masses are calculated using the most abundant isotope of each element (exact mass) and the average atomic mass of each element (relative mass). These data are important for users that work on the purification process and structure elucidation of compounds.

As regards botanical data, the user can find specific information about the taxonomic rank (from family to species) of the plant from which the corresponding chemical structure has been isolated, as well as a bibliographic reference that includes journal name, volume, page, and year. Because many different plant species can synthesize the same compound, there is a register for each species. Data regarding the biological activities of the compound, i.e., type of bioactivity, system,

units, activity values, and bibliographic references, are also available in this section.

Plant species have revealed clear genetic signals of local adaptation (Züst et al. 2012), with one species being able to synthesize or not a certain secondary metabolite depending on its location. Collection-site variations in the compound concentration have also been observed. Because geographical data are an important parameter in natural products research, AsterDB shows the geographical coordinates (latitude and longitude) for each searched molecule and an approximate location of the species from which the metabolite was isolated. Likewise, through the Google Maps API, the user can observe the species location on the world map.

Available and searchable natural product databases show some identical data such as chemical structures and botanical occurrences; some of them are used in virtual screening studies that are useful to optimize the steps of drug design. However, there are several different types of data available in the natural products databases that could be connected, successfully improving the use of information for various applications such as structure elucidation, metabolomics, and drug design, among others.

### 3.5 Conclusion

Several approaches have been used for chemotaxonomic studies of sesquiterpene lactones isolated from plant species belonging to the Asteraceae family. Classical approaches based on compound counts and comparisons with current classifications were used in the past. Over the last decades, classical approaches have been replaced by computer-based tools, which use either statistical methods, such as the principal component analysis or the partial least square regression, or by machine learning techniques, mainly artificial neural networks. More recently, modern databases have been created with the incorporation of important features such as species and structure searches. This great evolution in the computation-based study of natural product area proves that modern and integrated platforms will soon be available.

### References

- Acevedo CH, Scotti L, Alves MF et al (2017) Computer-aided drug design using sesquiterpene lactones as sources of new structures with potential activity against infectious neglected diseases. *Molecules* 22. <https://doi.org/10.3390/molecules22010079>
- Adamczyk JJ, Kurzac M, Park YS et al (2013) Application of a Kohonen's self-organizing map for evaluation of long-term changes in forest vegetation. *J Veg Sci* 24:405–414. <https://doi.org/10.1111/j.1654-1103.2012.01468.x>
- Afendi FM, Okada T, Yamazaki M et al (2012) KNApSAcK family databases: integrated metabolite-plant species databases for multifaceted plant research. *Plant Cell Physiol* 53:e1. <https://doi.org/10.1093/pcp/pcr165>

- Aljancic I, Vajs V, Menkovic N et al (1999) Flavones and sesquiterpene lactones from *Achillea atrata* subsp *multifida*: antimicrobial activity. *J Nat Prod* 62:909–911. <https://doi.org/10.1021/np980536m>
- Alston RE, Turner BL, Mabry TJ (1963) Perspectives in chemotaxonomy. *Science* 142:545–552. <https://doi.org/10.1126/science.142.3592.545>
- Bedoya D, Novotny V, Manolagos ES (2009) Instream and offstream environmental conditions and stream biotic integrity importance of scale and site similarities for learning and prediction. *Ecol Model* 220:2393–2406. <https://doi.org/10.1016/j.ecolmodel.2009.06.017>
- Bentham G (1873) Notes on the classification, history, and geographical distribution of the Compositae. *Bot J Linn Soc* 13:335–557
- Bremer K (1987) Tribal interrelationships of the Asteraceae. *Cladistics* 3:210–253
- Bremer K (1996) Major clades and grades of the Asteraceae. In: Hind DN, Beebte HJ (eds) *Compositae: systematics. Proceedings of the international Compositae conference, Kew, 1994*. Hind DJN (Editor-in-Chief), vol 1, Royal Botanic Gardens, Kew, pp 1–7
- Calabria LM, Emerenciano VP, Ferreira MJP et al (2007) A phylogenetic analysis of tribes of the Asteraceae based on phytochemical data. *Nat Prod Comm* 2:277–285
- Carlquist S (1976) Tribal interrelationships and phylogeny of the Asteraceae. *Aliso* 8:465–492
- Cassini H (1816) Tableau exprimant les affinités des tribus naturelles de famille des Synanthérées. In: *Dictionnaire des Sciences Naturelles*, vol 3. G Cuvier, 2nd edn. Le Normant, Paris
- Chadwick M, Trewin H, Gawthrop F et al (2013) Sesquiterpene lactones: benefits to plants and people. *Int J Mol Sci* 14:12780–12805. <https://doi.org/10.3390/ijms140612780>
- Chen CYC (2011) TCM database@Taiwan: the world's largest traditional Chinese medicine database for drug screening in silico. *PLoS One* 6:e15939. <https://doi.org/10.1371/journal.pone.0015939>
- Correia MV, Scotti MT, Ferreira MJP et al (2008) Self-organizing maps as a new tool for classification of plants at lower hierarchical levels. *Nat Prod Comm* 3:1723–1730
- Correia MV, Fokou HH, Marcelo J et al (2012) Self-organizing maps as a good tool for classification of subfamily Asteroideae. *J Med Plant Res* 6:1207–1218
- Dabb S, Blunt J, Munro M (2014) MarinLit: database and essential tools for the marine natural products community. *Abstracts of Papers of the American Chemical Society*. 248: 25-CINF
- DaCosta FB, Terfloth L, Gasteiger J (2005) Sesquiterpene lactone-based classification of three Asteraceae tribes: a study based on self-organizing neural networks applied to chemo systematics. *Phytochemistry* 66:345–353. <https://doi.org/10.1016/j.phytochem.2004.12.006>
- Emerenciano VP, Rodrigues GV, Alvarenga SAV et al (1998) Um novo método para agrupar parâmetros quimiotaxonômicos *Quím Nova*. 21:125–129
- Emerenciano VP, Cabrol-Bass D, Ferreira MJP et al (2006) Chemical evolution in the Asteraceae. The oxidation-reduction mechanism and production of secondary metabolites. *Nat Prod Comm* 1:495–507
- Emerenciano VR, Barbosa KO, Scotti MT et al (2007) Self-organizing maps in chemotaxonomic studies of asteraceae: a classification of tribes using flavonoid data. *J Braz Chem Soc* 18:891–899
- Ferreira MJP, Brant AJC, Rufino AR et al (2004) Prediction of occurrences of diverse chemical classes in the Asteraceae through artificial neural networks. *Phytochem Anal* 15:389–396. <https://doi.org/10.1002/pca.799>
- Ferreira MJP, Brant AJC, Alvarenga SAV et al (2005) Neural networks in chemosystematic studies of Asteraceae: a classification based on a dichotomic approach. *Chem Biodivers* 2:633–644. <https://doi.org/10.1002/cbdv.200590040>
- Funk VA, Bayer RJ, Keeley S et al (2005) Everywhere but Antarctica: using a supertree to understand the diversity and distribution of the Compositae. *Biol Skr* 55:343–374
- Gottlieb O (1989) The role of oxygen in phytochemical evolution towards diversity. *Phytochemistry* 28:2545–2558. [https://doi.org/10.1016/S0031-9422\(00\)98039-7](https://doi.org/10.1016/S0031-9422(00)98039-7)
- Gottlieb OR, Borin MRMB (2012) Químico-biologia quantitativa: um novo paradigma? *Quím Nova* 35:2105–2114

- Gottlieb OR, Borin MRMB, Pagotto CLAC et al (1998) Biodiversidade: o enfoque interdisciplinar brasileiro. *Cien Saude Colet* 3:97–102
- Graham JG, Farnsworth NR (2010) The NAPRALERT database as an aid for discovery of novel bioactive compounds. In: Mander L, Liu H-W (eds) *Comprehensive natural products II: chemistry and biology*, vol 3. Elsevier, Amsterdam, pp 81–94
- Hatherley R, Brown DK, Musyoka TM et al (2015) SANCDB: a South African natural compound database. *J Cheminform* 7:29. <https://doi.org/10.1186/s13321-015-0080-8>
- Heywood VH (2009) The recent history of Compositae systematics: from daisies to deep achenes, sister groups and metatrees. In: Funk V, Susanna A, Stuessy TF, Bayer RJ (eds) *Systematics, evolution and biogeography of Compositae*. International Association for Plant Taxonomy, Institute of Botany, University of Vienna, Vienna, pp 39–44
- Hristozov D, Da Costa FB, Gasteiger J (2007) Sesquiterpene lactones-based classification of the family Asteraceae using neural networks and k-nearest neighbors. *J Chem Inf Model* 47:9–19. <https://doi.org/10.1021/ci060046x>
- Kim S-K, Nam S, Jang H et al (2015) TM-MC: a database of medicinal materials and chemical compounds in northeast Asian traditional medicine. *BMC Complement Altern Med* 15:218. <https://doi.org/10.1186/s12906-015-0758-5>
- Kohonen T (1982) Self-organized formation of topologically correct feature maps. *Biol Cybern* 43:59–69. <https://doi.org/10.1007/bf00337288>
- Kohonen T (2001) *Self-organizing maps* (springer series in information sciences), 3rd edn. Springer, Heidelberg
- Kohonen T (2013) Essentials of the self-organizing map. *Neural Netw* 37:52–65. <https://doi.org/10.1016/j.neunet.2012.09.018>
- Loub WD, Farnsworth NR, Soejarto DD et al (1985) NAPRALERT - computer handling of natural product research data. *J Chem Inf Comput Sci* 25:99–103. <https://doi.org/10.1021/ci00046a009>
- Manallack DT, Livingstone DJ (1999) Neural networks in drug discovery: have they lived up to their promise? *Eur J Med Chem* 34:195–208. [https://doi.org/10.1016/s0223-5234\(99\)80052-x](https://doi.org/10.1016/s0223-5234(99)80052-x)
- Mannheimer CA (1999) An overview of chemotaxonomy and its role in creating a phylogenetic classification system. *Agricola* 10:87–90
- Merfort I (2011) Perspectives on sesquiterpene lactones in inflammation and cancer. *Curr Drug Targets* 12:1560–1573
- Park YS, Tison J, Lek S et al (2006) Application of a self-organizing map to select representative species in multivariate analysis: a case study determining diatom distribution patterns across France. *Ecol Inform* 1:247–257. <https://doi.org/10.1016/j.ecoinf.2006.03.005>
- Picman AK (1986) Biological activities of sesquiterpene lactones. *Biochem Syst Ecol* 14:255–281
- Schlee D (1975) *Syst Zool* 24:263–268. <https://doi.org/10.2307/2412767>
- Schmidt TJ (1999) Toxic activities of sesquiterpene lactones: structural and biochemical aspects. *Curr Org Chem* 3:577–608
- Schmidt TJ, Nour AMM, Khalid SA et al (2009) Quantitative structure - antiprotozoal activity relationships of sesquiterpene lactones. *Molecules* 14:2062–2076. <https://doi.org/10.3390/molecules14062062>
- Schmidt TJ, Kaiser M, Brun R (2011) Complete structural assignment of serratol, a cembranetype diterpene from *Boswellia serrata*, and evaluation of its antiprotozoal activity. *Planta Med* 77:849–850. <https://doi.org/10.1055/s-0030-1250612>
- Schmidt TJ et al (2012a) The potential of secondary metabolites from plants as drugs or leads against protozoan neglected diseases - part I. *Curr Med Chem* 19:2128–2175
- Schmidt TJ et al (2012b) The potential of secondary metabolites from plants as drugs or leads against protozoan neglected diseases - part II. *Curr Med Chem* 19:2176–2228
- Scotti MT, Emerenciano V, Ferreira MJP et al (2012) Self-organizing maps of molecular descriptors for sesquiterpene lactones and their application to the chemotaxonomy of the Asteraceae family. *Molecules* 17:4684–4702. <https://doi.org/10.3390/molecules17044684>
- Seaman FC (1982) Sesquiterpene lactones as taxonomic characters in the Asteraceae. *Bot Rev* 48:121–595. <https://doi.org/10.1007/bf02919190>

- Siedle B, García Piñeres AJ, Murillo R et al (2004) Quantitative structure - activity relationship of sesquiterpene lactones as inhibitors of the transcription factor NF-kappa B. *J Med Chem* 47:6042–6054. <https://doi.org/10.1021/jm049937r>
- Singh R (2016) Chemotaxonomy: a tool for plant classification. *J Med Plant Stud* 4(2):90–93
- Tung CWCW, Lin YCYC, Chang HSHS et al (2014) TIPdb-3D: the three-dimensional structure database of phytochemicals from Taiwan indigenous plants. *Database* 2014:1–5. <https://doi.org/10.1093/database/bau055>
- Valli M, dos Santos RN, Figueira LD et al (2013) Development of a natural products database from the biodiversity of Brazil. *J Nat Prod* 76:439–444
- Williams WT (1975) Numerical taxonomy. The principles and practice of numerical classification. Peter H. A. Sneath, Robert R. Sokal. *Q Rev Biol* 50:525–526. <https://doi.org/10.1086/408956>
- Wink M (2003) Evolution of secondary metabolites from an ecological and molecular phylogenetic perspective. *Phytochemistry* 64:3–19. [https://doi.org/10.1016/s0031-9422\(03\)00300-5](https://doi.org/10.1016/s0031-9422(03)00300-5)
- Wink M (2008) Plant secondary metabolism: diversity, function and its evolution. *Nat Prod Comm* 3:1205–1216
- Wink M, Botschen F, Gosmann C et al (2010) Chemotaxonomy seen from a phylogenetic perspective and evolution of secondary metabolism. In: Wink M (ed) *Annual plant reviews vol 40 biochemistry of plant secondary metabolism*, 2nd edn. Wiley-Blackwell, Oxford. <https://doi.org/10.1002/9781444320503.ch7>
- Xue R, Fang Z, Zhang M et al (2013) TCMID: traditional Chinese medicine integrative database for herb molecular mechanism analysis. *Nucleic Acids Res* 41:D1089–D1095. <https://doi.org/10.1093/nar/gks1100>
- Zhang JT, Li M (2011, 26-28 July 2011) Self-organizing feature map clustering based on fuzzy equivalence relation and its application in ecological analysis. In: 2011 eighth international conference on fuzzy systems and knowledge discovery (FSKD), Shanghai
- Zhang J, Yang H (2008) Application of self-organizing neural networks to classification of plant communities in Pangquangou nature reserve, North China. *Front Biol* 3:512–517. <https://doi.org/10.1007/s11515-008-0061-7>
- Zupan J, Gasteiger J (1999) *Neural networks in chemistry and drug design*. Wiley, New York
- Züst T, Heichinger C, Grossniklaus U (2012) Natural enemies drive geographic variation in plant defenses. *Science* 338:116–119. <https://doi.org/10.1126/science.1226397>

# Chapter 4

## Biosynthesis of Sesquiterpene Lactones in Plants and Metabolic Engineering for Their Biotechnological Production



María Perassolo, Alejandra Beatriz Cardillo, Víctor Daniel Busto, Ana María Giulietti, and Julián Rodríguez Talou

**Abstract** In the present chapter, we review some aspects of the biosynthesis of sesquiterpene lactones and its regulation in different medicinal and aromatic plants used in the pharmaceutical industry. In this sense, we describe the mevalonate and the 2-C-methyl-D-erythritol 4-phosphate pathways, which generate the corresponding isoprenoid precursors (isopentenyl diphosphate and dimethylallyl diphosphate), as well as the late pathways that lead to sesquiterpene lactone biosynthesis. This chapter also analyses the role of the transcription factors involved in the regulation of sesquiterpene lactone biosynthesis and the different biotechnological approaches that have been developed for sesquiterpene lactone production. In vitro plant cell cultures (comprising micropropagation and plant cell suspension, shoot and root cultures) have emerged as a production platform for many plant secondary metabolites, since they allow their production under controlled conditions and shorter production cycles. The characterisation and isolation of genes involved in the regulation of sesquiterpene lactone biosynthetic pathways have allowed the design of metabolic engineering strategies to increase the production of these metabolites. Moreover, we discuss different strategies to increase sesquiterpene lactone production through genetic engineering. We also focus on the metabolic engineering of the artemisinin biosynthetic pathway in *Artemisia annua*. This metabolic pathway has become a model system not only for the biotechnological production of sesquiterpene lactones but also for the improvement of other plant secondary metabolic pathways. Finally, we analyse the successful expression of the complete artemisinin

---

M. Perassolo · A. B. Cardillo · V. D. Busto · J. R. Talou (✉)  
Universidad de Buenos Aires, Facultad de Farmacia y Bioquímica,  
Departamento de Microbiología, Inmunología y Biotecnología, Cátedra de Biotecnología,  
Buenos Aires, Argentina

CONICET-Universidad de Buenos Aires, Instituto de Nanobiotecnología (NANOBIOTEC),  
Buenos Aires, Argentina  
e-mail: [jrtalou@ffyb.uba.ar](mailto:jrtalou@ffyb.uba.ar)

A. M. Giulietti  
CONICET-Universidad de Buenos Aires, Instituto de Nanobiotecnología (NANOBIOTEC),  
Buenos Aires, Argentina

biosynthetic pathway in *Escherichia coli* and *Saccharomyces cerevisiae*, which has led to the efficient accumulation of artemisinic acid in these microorganisms.

**Keywords** Sesquiterpene lactones · Metabolic engineering · Secondary metabolism · Transcription factors · Plant cell culture · Artemisinin · Yeast · *Escherichia coli*

## Abbreviations

AA	Artemisinic acid
AACT	Acetoacetyl-CoA thiolase
ABA	Abscisic acid
ABREs	ABA-responsive elements
ADHI	Alcohol dehydrogenase 1
ADS	Amorpha-4,11-diene synthase
ALDH1	Aldehyde dehydrogenase
AOC	Allene oxide cyclase
AP2/ERF	APETALA2/ethylene response factor
<i>atoB</i>	Acetoacetyl-CoA thiolase gene
<i>bgl1</i>	$\beta$ -Glucosidase gene
bZIP	Basic leucine zipper
CaMV35S	Cauliflower mosaic virus promoter
CDP-ME	4-Diphosphocytidyl-2-C-methyl-D-erythritol
CDP-ME2P	4-(Cytidine 5'-diphospho)-2-C-methyl-D-erythritol phosphate
CMK	CDP-ME kinase
COS	Costunolide synthase
CPR1	Cytochrome P450 reductase
CYB5	Cytochrome b5
CYP71AV1	Cytochrome P450 monooxygenase
DBR2	Artemisinic aldehyde $\Delta$ 11 (13) reductase
DMAPP	Dimethylallyl diphosphate
DXR	1-Deoxy-D-xylulose 5-phosphate reductoisomerase
DXS	1-Deoxy-D-xylulose 5-phosphate synthase
EMSA	Electrophoretic mobility shift assay
<i>ERG10</i>	Acetoacetyl-CoA thiolase gene
<i>ERG12</i>	Mevalonate kinase
<i>ERG13</i>	HMG-CoA synthase
<i>ERG20</i>	Farnesyl diphosphate synthase gene
<i>ERG8</i>	Phosphomevalonate kinase
FDS	Farnesyl diphosphate synthase
FPP	Farnesyl diphosphate
FRET	Fluorescence resonance energy transfer
GA	Germacrene A



GA-3P	Glyceraldehyde-3-phosphate
GAA	4,11 (13)-Trien-12-oic acid
GAH	Germacrene A hydroxylase
GAO	Germacrene A oxidase
GAS	Germacrene A synthase
GMP	Good manufacturing practices
GSH	Glutathione
GST	Glandular secretory trichomes
GSW1	GLANDULAR TRICHOME-SPECIFIC WRKY 1
GUS	$\beta$ -Glucuronidase reporter gene system
HDR	(E)-4-Hydroxy-3-methylbut-2-enyl diphosphate reductase
HDS	1-Hydroxy-2-methyl-2-(E)-butenyl-4-diphosphate synthase
HMBPP	(E)-4-Hydroxy-3-methylbut-2-enyl diphosphate
HMG-CoA	3-Hydroxy-3-methylglutaryl-CoA
HMGR	HMG-CoA reductase
HMGS	HMG-CoA synthase
IDI	Isopentenyl diphosphate isomerase
<i>idi</i>	Isopentenyl diphosphate isomerase gene
IPP	Isopentenyl diphosphate
<i>ipt</i>	Isopentenyl transferase gene
<i>ispa</i>	Farnesyl diphosphate synthase gene
Ja	Jasmonic acid
MAP	Medicinal and aromatic plants
MCT	2-C-Methyl-D-erythritol 4-phosphate cytidyltransferase
MDS	2-C-Methyl-D-erythritol 2,4-cyclodiphosphate synthase
ME -2,4cPP	2-C-Methyl-D-erythritol 2,4-cyclodiphosphate
MeJ	Methyl jasmonate
MEP	2-C-Methyl-D-erythritol 4-phosphate
MEP	2-C-Methyl-D-erythritol 4-phosphate pathway
MSI	Mass spectrometry imaging
MVA	Mevalonate pathway
<i>mvaA</i>	HMG-CoA reductase gene
<i>mvaS</i>	HMG-CoA synthase gene
MVD	Mevalonate diphosphate decarboxylase
<i>MVD1</i>	Mevalonate diphosphate decarboxylase gene
MVDP	Mevalonate-5-diphosphate
MVK	Mevalonate kinase
MVP	Mevalonate-5-phosphate
PCC	Plant cell culture
PDR	Pleiotropic drug resistance
PMK	Phosphomevalonate kinase
PTS	Parthenolide synthase
PTS	Patchoulol synthase
RNAi	RNA interference
SA	Salicylic acid

SQS	Squalene synthase
SS	Santalene synthase
STLs	Sesquiterpene lactones
STPS	Sesquiterpene synthases
TAR1	TRICHOME AND ARTEMISININ REGULATOR 1
TFs	Transcription factors
tHMRG	Truncated HMG-CoA reductase
TP	Terpene synthase

## 4.1 Introduction

Sesquiterpene lactones (STLs) are terpenoid secondary metabolites that are mainly present in plants. These compounds play important roles in plant physiology as deterrent, defence compounds (phytoalexins), allelochemicals and pollinator attractants (Tholl 2015; Bouvier et al. 2005; Gershenzon and Dudareva 2007). Many STLs are accumulated in specialised tissues like glandular trichomes, oil bodies and resin ducts but also in organs like roots and fruits or even in the whole plant (Nagegowda 2010). STLs also show interesting biological activities such as antibacterial, antimalarial, antifungal, anti-inflammatory and anticancer. In addition, they are used in the cosmetic industry as fragrances (Chadwick et al. 2013; Chaturvedi 2011).

Sesquiterpene lactones are C<sub>15</sub> terpenoids derived from the universal isoprenoid precursor isopentenyl diphosphate (IPP) and its isomer dimethylallyl diphosphate (DMAPP). IPP and DMAPP are synthesized through two independent metabolic routes, the mevalonate (MVA) pathway and the 2-C-methyl-D-erythritol 4-phosphate (MEP) pathway, which are localised in the cytosol and in the chloroplast, respectively (Vranová et al. 2013). The biosynthesis of STLs starts with the cyclization of farnesyl diphosphate (FPP) by a sesquiterpene synthase (SPS). The reaction is followed by a series of oxidations and hydroxylations, carried out by cytochrome P450 enzymes. Finally, the C<sub>15</sub> structure can be modified by alcohol dehydrogenases, reductases and acyl transferases. The diversity of SPS and CYP and their promiscuous enzyme activities result in a great variety of STL structures (Simonsen 2015).

As other secondary metabolic routes, the biosynthesis of STLs is a complex arrangement of enzymatic reactions which are tightly regulated at different levels. Indeed, the MVA, MEP and STL pathways are controlled at the transcriptional and post-transcriptional/translational levels, including feedback regulation (Vranová et al. 2013). Many environmental factors and stimuli, such as light, abiotic stress and pathogens, have been described to affect the STL accumulation and the expression of related genes. In addition, the STL biosynthesis also presents spatial (specific tissue and organ accumulation) and temporal regulation (plant development) (Vranová et al. 2012).

In order to produce these valuable metabolites at the industrial scale, a full elucidation of the biosynthetic pathway and a deep understanding of its regulation are required. In this sense, STL production could be improved through molecular

biology strategies in order to generate genetically modified plants or plant cell cultures or by introducing the full STL biosynthetic pathway in other organisms such as yeast or bacteria (Majdi et al. 2015).

The synthesis of the antimalarial drug, artemisinin, in *Artemisia annua* has been elucidated, and several genes have been overexpressed in *A. annua* plants, thus improving their artemisinin content. Metabolic engineering of the pathway has been also carried out in yeast and bacteria, which proved that STL can be produced efficiently in these expression platforms (Xie et al. 2016). *A. annua* has become a plant model to study STL biosynthesis in plants, allowing the characterisation and isolation of genes involved in other STL pathways. Recently, the full biosynthetic pathway of parthenolide, an anticancer and antimigraine drug present in *Tanacetum parthenium*, has been elucidated, and the gene overexpression in *Nicotiana benthamiana* resulted in parthenolide accumulation (Liu et al. 2014). These advances have been complemented by new techniques of tissue dissection, which allow the isolation of RNA even from very few cells like glandular secretory trichomes (GST) and the construction of specific cDNA libraries (Olofsson et al. 2012). Furthermore, the low cost of transcriptomic sequencing has increased the database identification of genes involved in secondary metabolite production. The transcriptomic analysis resulted in a powerful tool to identify genes encoding enzymes and transcription factors (TFs) of the sesquiterpenoid lactone pathway in *Thapsia laciniata* (thapsigargin, antitumour activity), *Santalum* spp. (santalene, fragrances) and other important medicinal and aromatic plants (Moniodis et al. 2015; Simonsen 2015).

In the present chapter, we review some aspects of STL biosynthesis and the biotechnological approaches for their production. We specifically focus on those plants of medicinal interest and those used in the industry as aromatics.

## 4.2 Biosynthesis of the Isoprenoid Precursors in Plants

As mentioned above, two independent biosynthetic pathways coexist in plants and are responsible for the synthesis of the universal terpenoid precursors IPP and DMAPP: the mevalonate pathway (cytosol) and the 2-C-methyl-D-erythritol 4-phosphate pathway (plastids). On the other hand, the MVA is present in yeast, while the MEP pathway occurs in bacteria.

### 4.2.1 Mevalonate (MVA) Pathway

The condensation of two acetyl-CoA molecules catalysed by the enzyme acetoacetyl-CoA thiolase (AACT) is the first step of the mevalonate pathway (MVA). The second enzymatic step involves the HMG-CoA synthase (HMGS), resulting in the production of 3-hydroxy-3-methylglutaryl-CoA (HMG-CoA). In the third step, the enzyme HMG-CoA reductase (HMGR) converts HMG-CoA to mevalonate (MVA)

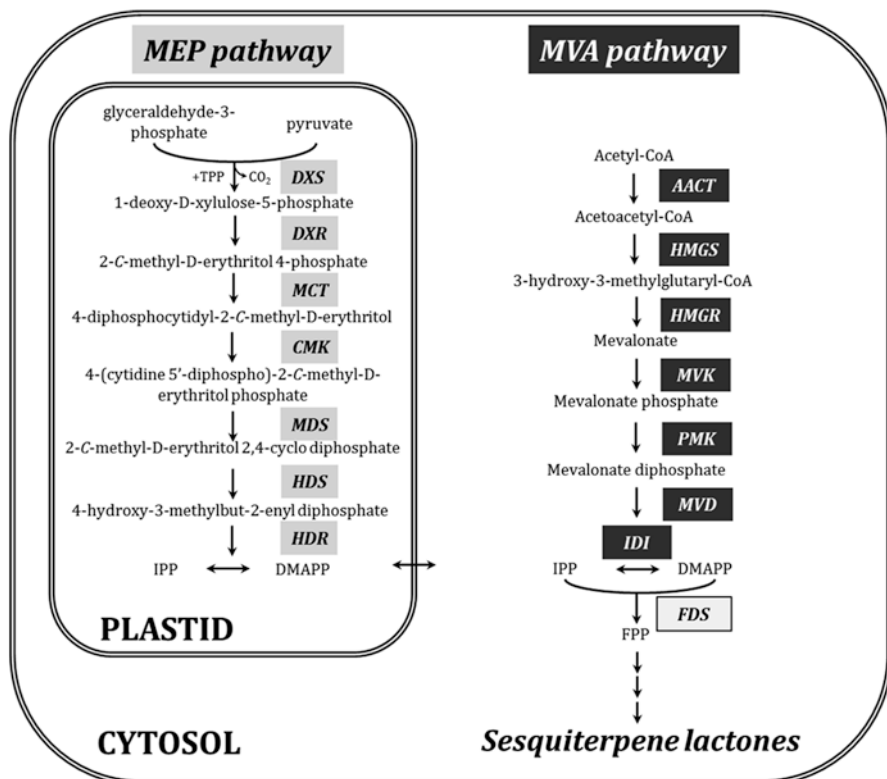


**Fig. 4.1** Schematic representation of the biosynthetic pathways involved in IPP and DMAPP production. *AACT* acetoacetyl-CoA thiolase, *HMGS* HMG-CoA synthase, *HMGR* HMG-CoA reductase, *MVK* mevalonate kinase, *PMK* phosphomevalonate kinase, *MVD* mevalonate diphosphate decarboxylase, *IDI* isopentenyl diphosphate isomerase, *DXS* 1-deoxy-D-xylulose 5-phosphate synthase, *DXR* 1-deoxy-D-xylulose 5-phosphate reductoisomerase, *MCT* 2-C-methyl-D-erythritol 4-phosphate cytidyltransferase, *CMK* CDP-ME kinase, *MDS* 2-C-methyl-D-erythritol 2,4-cyclo-diphosphate synthase, *HDS* 1-hydroxy-2-methyl-2-(E)-butenyl-4-diphosphate synthase, *HDR* (E)-4-hydroxy-3-methylbut-2-enyl diphosphate reductase, *FDS* farnesyl diphosphate synthase

in a double reduction step which requires two NADPH. HMGR is a membrane-bound protein associated to the endoplasmic reticulum (ER) that has been extensively studied in different organisms and described as the rate-limiting step in the MVA pathway. In three successive steps catalysed by the enzymes mevalonate kinase (MVK), phosphomevalonate kinase (PMK) and mevalonate diphosphate decarboxylase (MVD), mevalonate is converted to the final product, IPP (Vranová et al. 2013; Tholl 2015; Vranová et al. 2012). IPP is transformed to DMAPP by the IPP isomerase (IDI) which is localised in different cellular compartments such as the cytosol, chloroplasts and mitochondria (Fig. 4.1).

### 4.2.2 2-C-Methyl-D-erythritol 4-phosphate (MEP) Pathway

The MEP pathway consists of seven enzymatic reactions (Lichtenthaler 1999). The first step is catalysed by the deoxyxylulose phosphate synthase (DXS) and involves the condensation of pyruvate and glyceraldehyde 3-phosphate (GA3P) to produce 1-deoxy-D-xylulose 5-phosphate (DXP). DXP is then converted into 2-C-methyl-D-erythritol 4-phosphate (MEP) by the deoxy-D-xylulose 5-phosphate reductoisomerase (DXR). Both DXS and DXR are considered rate-limiting enzymes in the MEP pathway. In four consecutive reactions, MEP is converted into (E)-4-hydroxy-3-methylbut-2-enyl diphosphate (HMBPP) by 2-C-methyl-D-erythritol 4-phosphate cytidyltransferase (MCT), CDP-ME kinase (CMK), 2-C-methyl-D-erythritol 2,4-cyclodiphosphate synthase (MDS) and 1-hydroxy-2-methyl-2-(E)-butenyl-4-diphosphate synthase (HDS). The last step involves the action of the (E)-4-hydroxy-3-methylbut-2-enyl diphosphate reductase (HDR), which transforms HMBPP into IPP and its isomer DMAPP in a ratio of 5 or 6 to 1 (Vranová et al. 2013; Vranová et al. 2012; Zhao et al. 2013) (Fig. 4.1).

### 4.2.3 Cross-Talk Between MVA and MEP Pathways

It has been generally assumed that the MVA pathway supplies isoprenoid precursors for the synthesis of sterols, sesquiterpenes and triterpenes while the MEP pathway provides precursors to produce monoterpenes, diterpenes and carotenoids. Despite the spatial separation of both pathways, an exchange of IPP and DMAPP between cytosol and plastids has been observed in the synthesis of different terpenoids. Ram et al. (2010) have demonstrated the key role of HMGR in the MVA pathway.  $^{14}\text{C}$ -HMG-CoA was efficiently incorporated into artemisinin; however, the addition of the competitive inhibitor mevinolin inhibited up to 83% the label incorporation into this secondary metabolite. This effect could be reversed by increasing the amount of  $^{14}\text{C}$ -HMG-CoA. Moreover,  $^{14}\text{C}$ -MVA, which is a product of the HMGR, was also incorporated into artemisinin, and incorporation rates were enhanced by increasing concentrations of the labelled compound. On the other hand, the addition of fosmidomycin, which is an inhibitor of the MEP pathway, reduced the artemisinin accumulation by 14%. The authors concluded that the MVA pathway is a major donor of isoprenoid precursors in the biosynthesis of artemisinin and that HMGR is a rate-limiting step in this route. Another study has demonstrated a decrease in artemisinin accumulation when *A. annua* plants were treated with mevinolin and fosmidomycin, inhibitors of the MVA and MEP pathways, respectively (Towler and Weathers 2007). The results obtained proved that IPP from both pathways contribute to the synthesis of this STL. Additionally, a study performed with  $^{13}\text{CO}_2$  confirmed that artemisinin was synthesised from IPP and DMAPP precursors provided by both biosynthetic routes (Schramek et al. 2010). In vivo feeding assays performed with deuterium-labelled

precursors (DXP and mevalonic acid lactone) in intact grape berries have demonstrated that both intermediates were incorporated into STL, which accumulated mainly in the exocarp (May et al. 2013). These results have revealed that the cytosolic and plastidial routes provide isoprenoids intermediates for the production of STL and should be considered for further metabolic engineering strategies.

The MVA and MEP pathways are affected by many environmental, spatial and developmental factors, and such influences depend on plant species and culture system used in each experiment (in vitro culture, hairy roots, suspensions, etc.).

#### **4.2.4 Farnesyl Diphosphate Synthase: Branch Point of Sesquiterpene Lactone Biosynthesis**

Farnesyl phosphate (FPP) is generated from IPP and DMAPP by the action of farnesyl diphosphate synthase (FDS) and is the common precursor of all STLs, sterols, triterpenes and prenylated proteins. FPP is the substrate of squalene synthase (SQS), which is the first step in the synthesis of sterols and brassinosteroids, and consequently an important competitive pathway for isoprenoid precursors (Vranová et al. 2013). FDS is localised mainly in the cytosol and the mitochondria. Overexpression of FDS in *A. annua* resulted in higher artemisinin content than non-transformed plant, proving its role as a rate-limiting step in this pathway (Banyai et al. 2010).

#### **4.2.5 Sesquiterpene Lactone Pathway**

The first step in the biosynthesis of STLs is the cyclisation of FPP catalysed by sesquiterpene synthases (STPS). STPS are mainly located in the cytosol and are characterised by their plasticity, showing the capacity of multiple substrate utilisation. Santalene synthase (SaSSy) from sandalwood (*Santalum album*), which is used in the industry for its essential oil fragrance, produces a mixture of santalenes ( $\alpha$ ,  $\beta$  and epi- $\beta$ -santalene) and  $\alpha$ -exo-bergamotene (Jones et al. 2008; Diaz-Chavez et al. 2013). Two genes encoding STPS in *Arabidopsis thaliana*, *At5g44630* and *At5g23960*, are considered responsible for at least 20 different STLs present in its floral volatiles (Tholl et al. 2005).

One of the best characterised STPS is germacrene A synthase (GAS), which converts FPP into germacrene A (GA). GA is the precursor of many germacranolide-type STLs. The gene encoding GAS has been isolated from several plant species: among them, *A. annua*, *Barnadesia spinosa* (Nguyen et al. 2016), chicory (de Kraker et al. 1998), *T. parthenium* (Liu et al. 2014), sunflower and lettuce. GA is the backbone skeleton for the biosynthesis of costunolides and parthenolides, both of which are of pharmacological interest for their anticancer activity. In a series of oxidation reactions, GA is converted into germacra-1(10), 4,11 (13)-trien-12-oic

acid (GAA) by germacrene A oxidase (GAO), which is a cytochrome P450-like enzyme. GAA is further oxidised by a costunolide synthase to yield costunolide. Recently, a parthenolide synthase (*TpPTS*) from feverfew (*T. parthenium*) was identified; the enzyme catalyses the epoxidation of C4–C5 double bond of costunolide molecules to yield the final product parthenolide, which has antimigraine and anti-cancer activities. In that way, the biosynthesis of parthenolide has become the second STL pathway to be fully elucidated (Liu et al. 2014, Yin et al. 2015).

The most important and commercial valuable STL is the antimalarial drug artemisinin, which is produced by *A. annua*. The artemisinin biosynthetic pathway was the first one to be fully characterised (Fig. 4.2) (Wen and Yu 2011). The first reaction is catalysed by the enzyme amorpha-4,11-diene synthase (ADS) that converts FPP into amorpha-4,11-diene (Chang et al. 2000; Mercke et al. 2000). The following

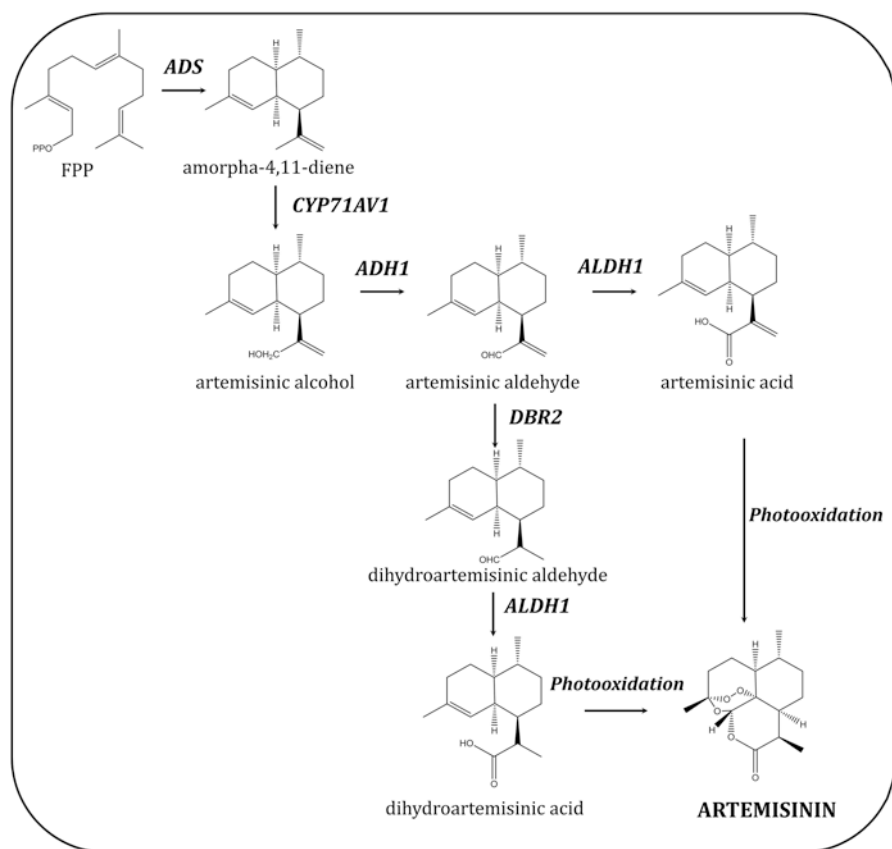


**Fig. 4.2** Schematic representation of the artemisinin biosynthetic pathway in *Artemisia annua*. *ADS* amorpha-4,11-diene synthase, *CYP71AV1* cytochrome P450 monooxygenase, *DBR2* artemisinic aldehyde  $\Delta$ 11 (13) reductase, *ADH1* alcohol dehydrogenase 1, *ALDH1* aldehyde dehydrogenase, *FPP* farnesyl diphosphate

reaction involves a cytochrome P450 monooxygenase (CYP71AV1) and a cytochrome P450 oxidoreductase (CPR) as the native redox partner, which hydroxylates amorpha-4,11-diene to render artemisinic alcohol. The alcohol is then oxidised to artemisinic aldehyde by an alcohol dehydrogenase (ADH1) (Teoh et al. 2006). The artemisinic aldehyde  $\Delta 11$  (13) reductase (DBR2) catalyses the conversion of artemisinic aldehyde into dihydroartemisinic aldehyde (Zhang et al. 2008), which is finally converted to dihydroartemisinic acid by an aldehyde dehydrogenase (ALDH1) (Teoh et al. 2009). Dihydroartemisinin acid is regarded as the immediate precursor of artemisinin. The reaction seems to be a non-enzymatic photooxidation process, although this subject remains under debate (Wen and Yu 2011; Turconi et al. 2014). Artemisinic aldehyde could also be transformed to artemisinic acid (AA) by ALDH1 as an alternative pathway to artemisinin production (Fig. 4.2).

### 4.3 Sesquiterpene Lactone Biosynthetic Pathway Characterisation and Regulation in Medicinal and Aromatic Plants

The STL biosynthesis in plants constitutes a complex network of metabolic pathways that compete for common precursors. In addition, it is also strictly regulated by many environmental, spatial and temporal factors. The biosynthetic enzymatic steps that lead to artemisinin, costunolide and parthenolide production have been fully characterised. Moreover, many TFs that control the transcription of biosynthetic genes have been isolated, which allowed a better comprehension on how these STLs are produced. These findings have constituted a great contribution to the understanding and characterisation of other STL biosynthetic pathways in plants. However, the regulation is specific for each STL pathway. Therefore, it is important to recognise the different factors that regulate the upstream biosynthetic pathways (MVA and MEP) as well as those regulating the STL-specific downstream pathway in each STL-producing plant.

Recently, techniques like mass spectrometry imaging (MSI) and fluorescence resonance energy transfer (FRET)-based nanosensors have allowed the identification of cells and tissues that specifically accumulate secondary metabolites. For instance, MSI studies have shown that the accumulation of STLs in *Helianthus annuus* occurs in the capitate glandular trichomes that are present in the leaves. In this sense, these techniques facilitate transcriptome analyses of different MAPs, thus increasing the bulk of knowledge on STL pathways and their regulation.

*Ginkgo biloba* is one of the most ancient tree species of the plant kingdom and has been used for centuries in traditional Chinese medicine. The main bioactive compounds in the leaf extract are ginkgolides (diterpenes) and bilobalides (sesquiterpenes). A genomic and transcriptomic study allowed the identification of the sequence for a terpene synthase (*GbTP2*) which catalyses the conversion of FPP into (-)- $\alpha$ -bisabolene. The transcript levels of *GbTPS2* were higher in roots and mature leaves than in immature leaves, shoots apices, stem and seeds (Parveen et al. 2015).



*Santalum spicatum* (sandalwood) and other species produce oil that is rich in sesquiterpenes with a high commercial value. The oil is produced in the xylem tissue of mature trees. A study of the xylem transcriptome has shown the presence of most of the transcripts from the MVA pathway, while the transcripts of only two enzymes of the MEP route (DXS and DXR) were found (Moniodis et al. 2015). These results indicate that the MVA pathway is the main supplier of precursors for STL biosynthesis. HMGR seems to be a key step in the pathway, since it showed the highest transcript levels. High transcript levels of at least three terpene synthases (TPS) were found in the xylem, santalene synthase (SS),  $\alpha$ -bisabolol synthase and sesquisabinene B synthase. SS is involved in the biosynthesis of santalol, the main STL present in sandalwood oil. Another abundant transcript found in the transcriptome was the one that encodes a cytochrome P450 of the CYP76 family (*CYP76F39*). This enzyme shows santalene hydroxylase activity and its sequence has 96% identity with the one described in *S. album*. In another study performed in *S. album*, the authors compared the expression pattern of *FDS* and *SS* in mature and immature wood samples. They found a strong correlation between *FDS* and *SS* expression levels with santalol accumulation in mature wood, which suggests that both genes are critical in santalol biosynthesis and are regulated at the developmental level (Jones et al. 2011; Rani et al. 2013).

*Xanthium strumarium* is a traditional medicinal Chinese herb that accumulates the STLs xanthanolides mainly in glandular trichomes. The plant has been used to treat different illnesses such as leucoderma, tuberculosis, herpes, cancer, ulcers and rheumatism. Xanthanolides and other STLs have been associated with most of the biological activities described in *X. strumarium*. A comparative transcriptome study between leaves and glandular trichomes of *X. strumarium* has been carried out. The genes of the MVA and MEP pathways, *IDI* and *FDS*, showed higher expression levels in trichomes than in leaves. These results suggest the existence of a trichome specificity of STL biosynthesis and the participation of MVA and MEP pathways as suppliers of isoprenoid precursors for their synthesis (Li et al. 2016). The same research group performed a microRNA comparative analysis between leaves and trichomes in order to establish the putative post-transcriptional regulation of the STL biosynthesis in *X. strumarium*. MicroRNAs are small non-coding nucleotides that interact with mRNAs by base complementarity resulting in mRNA degradation or translational inhibition of the target genes. The authors found at least two microRNA sequences that target two key enzymes of the upstream terpenoid pathway: HMGR from the MVA pathway and DXS from the MEP pathway. A microRNA sequence targeted to isopentenyl diphosphate isomerase (*IDI*) was also detected in the trichome library (Fan et al. 2015).

Valerian roots are used as anxiolytics and sedatives; these biological activities are attributed to several STLs such as valerenic acid and its precursors, valerenediene and valerenal. Two genes encoding terpene synthases were isolated from a RNA sequencing analysis from roots of *Valeriana officinalis*, *VoTPS1* and *VoTPS2* (Pyle et al. 2012). The heterologous expression in yeast has revealed that *TPS1* catalyses the conversion of FPP to germacrene C/D and *TPS2* generates valerenadiene, 4,7(11)-diene. In a further study, Yeo et al. (2013) have found two genes encoding

TPS, namely, *VoTPS1* and *VoTPS7*. The former has the same enzymatic activity than the *TPS2* found in the previous work, and the latter catalyses the conversion to germacrene C/D. The expression profile of *VoTPS1/7* showed that their transcripts are specifically found in roots. In hairy root cultures, the expression levels of two genes encoding TPS were analysed, and it was found that the expression levels of *VoFDS*, *VoGCS* and *VoVDS* were similar to those found in non-transformed roots (Ricigliano et al. 2016). A putative cytochrome c P450 enzyme (*CYP71D442*) involved in the biosynthesis of STLs has shown the same profile. In methyl jasmonate (MeJ)-treated hairy roots, the transcripts of *VoFDS*, *VoGCS* and *VoVDS* were upregulated after 12, 25 and 36 h of treatment. On the other hand, the *VoCYP71D442* transcript levels were not induced by MeJ, suggesting that this P450 enzyme is not related to the biosynthesis of valerenic acid (Ricigliano et al. 2016).

*Thapsia garganica* and related species produce thapsigargin mainly in roots and fruits. This STL has a potent biological activity against solid tumours. Due to its low solubility, a derivative prodrug is currently being assessed in clinical trials (Andersen et al. 2015). Two encoding genes for STPS, *TgTPS1* and *TgTPS2*, were isolated from a cDNA library and RNA sequencing from roots of *T. garganica*. Both were expressed at high levels in roots. The heterologous expression of both sequences in yeast revealed that *TPS1* produced cadinene while in *TPS2*-expressing yeast, the main product was 6 $\beta$ -hydroxy germacra-1(10),4-diene (kunzeaol) (Pickel et al. 2012). The authors proposed that the latter might be the first enzymatic reaction that leads to the biosynthesis of thapsigargin (Drew et al. 2013). A transcriptomic analysis in *T. laciniata* roots has revealed the presence of several putative genes involved in the biosynthesis of STLs: 5 sesquiterpene synthases, 16 cytochromes P450 of the *CYP71* family and *ALDH* and *ADH* (similar to those present in *A. annua*).

Globe artichoke (*Cynara cardunculus*, *Cynara scolymus*) is a traditional food crop that has also been used with therapeutic purposes in ancient medicine. Globe artichoke accumulates a variety of STLs that are responsible for the classical bitter taste of the plant. Cynaropicrin, which is the main STL present, has shown anti-inflammatory activity and cytotoxicity against cancer cells. Cynaropicrin is formed via the biosynthesis of costunolide, and the three enzymes *GAS*, *GAO* and *COS* have been identified and characterised (Menin et al. 2012). *GAS* has been found in the cytosol, while *GAO* and *COS* were located in the ER. A RT-qPCR analysis of the transcripts has revealed that the genes are highly expressed in mature leaves, as compared with old leaves. These genes were also found to be expressed in callus tissues and the receptacles. The expression pattern correlates with cynaropicrin accumulation, which occurs in the glandular trichomes present in the leaves. A study of the *CcGAO* and *CcCOS* promoters has shown the presence of L1-box *cis*-elements, similar to those found in the genes that are specifically expressed in *Arabidopsis* trichomes (Eljounaidi et al. 2014).

Chicory (*Cichorium intybus*) accumulates STLs that are responsible for the bitterness of the leaves and the stems used in food. Chicory has been used in traditional medicine to promote digestion and appetite. Chicory STLs have shown anticancer, antileukemic, sedative and analgesic activities. de Kraker et al. (2002) have elucidated the complete pathway that leads to the synthesis of costunolide from

FPP. Three enzymes are involved: GAS, germacrene A hydroxylase (GAH) and COS. Costunolide is also the intermediate for the biosynthesis of other STLs such as leucodin and dihydrocostunolide, with these reactions being probably catalysed by a cytochrome P450 enzyme and enoatereductase, respectively. The authors have determined that GAH can also convert amorpha-4,11-diene into amorpha-4,11-dien-12-ol, which is a precursor in the synthesis of artemisinic acid and artemisinin. A transcriptomic analysis of two different chicory cultivars, namely, “Molfettesse” and “Galatina”, has been performed, and it was found that two TFs showed correlation with the expression levels of GAS/GAO and the STL content. One of these TFs belongs to the MYB TF family and its levels correlate positively with GAS/GAO expression. The other is a bHLH TF and its expression correlates negatively with that of GAS/GAO. It has been proposed that these two TFs might regulate the biosynthesis of STL in chicory (Testone et al. 2016).

In *T. parthenium*, the accumulation of STL seems to be regulated by MeJ and salicylic acid (SA). Plants treated with MeJ and SA resulted in the upregulation of genes of the MVA and MEP pathways. The transcript levels of *HMGR*, *DXR* and *HDR* increased upon MeJ and SA addition. MeJ-treated plants showed higher expression levels of these genes than SA-treated plants and in both parthenolide accumulation was higher than in control plants (3.1- and 1.96-fold, respectively) (Majdi et al. 2015). The earlier pathways of terpene biosynthesis also presented a spatial and temporal regulation. The genes involved in these pathways were highly expressed in glandular trichomes and flowers; only the expression levels of *HMGR* were higher in young leaves than in older leaves. The transcript levels of GAS, GAO, COS and PTS, enzymes involved in parthenolide biosynthesis, were induced by the action of MeJ and SA; however this induction was not done coordinately. The expression of *GAS* showed a strong correlation with parthenolide accumulation, which means that GAS could be a crucial step in parthenolide biosynthesis. This correlation was also observed in glandular trichomes and flowers where this STL reached its maximum concentration (Majdi et al. 2011, 2014).

The first attempts to study the regulation of artemisinin biosynthesis were carried out in different plant systems such as in vitro cultures (suspension, hairy roots and seedlings) and plants. Different abiotic and biotic elicitors and other factors such as light and plant development were demonstrated to affect artemisinin production. MeJ, chitosan and fungal pathogen homogenates induced artemisinin production in plant and in in vitro cultures. An increase in artemisinin accumulation was observed in hairy root cultures of *A. annua* treated with *Piriformospora indica* homogenates and MeJ. The addition of *P. indica* extracts induced the transcription of several genes involved in artemisinin biosynthesis: *AaHMRG* (MVA), *AaDXS* and *AaDXR* (MEP) and *AaADS*, *AaCYP71AV1*, *AaALH1* and *AaDBR2* (STL pathway). Similar results were obtained with MeJ elicitation, although *AaDXS* was downregulated (Ahlawat et al. 2014). The addition of both elicitors induced the transcription of all mentioned genes with the exception of *AaDXS* and *AaDBR2*. *AaHMRG* showed the highest increase of transcript levels in all the treatments assayed, which corroborates its role as a rate-limiting step. Lei et al. (2011) have observed that the foliar application of chitosan induced the accumulation of artemisinin and dihydroartemisinin compared

with non-treated plants. Chitosan also activated the transcription of STL pathway genes *AaADS*, *AaCYP71AV1* and *AaDBR2*, even though they showed a different expression response over time. The upstream pathways of STL biosynthesis were also positively affected by chitosan. The expression levels of *HMGR* (MVA) increased 2 h after the addition of chitosan, while the levels of *FDS* transcripts were slightly increased. The *DXS*, *DXR* and *HDR* genes of the MEP pathway were all induced by chitosan. Light was another environmental factor that improved artemisinin accumulation in hairy roots. Increase of light intensity and the period of light irradiation resulted in an increase in the artemisinin content (Liu et al. 2002). The production of artemisinin is also affected by sugars. In fact, *A. annua* seedlings grown in the presence of glucose showed a higher artemisinin content than seedlings grown on sucrose or fructose. Glucose induced the expression of genes encoding the first enzymes involved in the MVA and MEP pathways. *HMRG*, *FDS*, *DXS* and *DXR* were induced after glucose feeding, as compared to control seedlings growing on sucrose. In the same way, the expression levels of *ADS* and *CYP71AV1* were higher than control seedlings. Based on these results, the authors suggested that the carbon source can act as signal involved in the regulation of artemisinin biosynthesis. Arsenault et al. (2010a) have analysed artemisinin production, trichome density and gene expression in the phase of growth that goes from vegetative through reproductive. They found that there was a good correlation between higher levels of trichome density in leaves and artemisinin accumulation. Leaves from the reproductive phase showed a higher density of trichomes per area as well as artemisinin content than those of the vegetative phase. When artemisinin and artemisinic acid (100 µg/ml) were sprayed over vegetative leaves, transcript levels of *CYP* were decreased by both treatments while the expression of *ADS* was negatively affected only by AA. These results suggested that the expression of *ADS* and *CYP71AV1* is regulated by a negative feedback control mediated by AA and, to a lesser extent, by artemisinin (Arsenault et al. 2010b).

Jasmonate (Ja) and MeJ have been shown to elicit the production of secondary metabolites in many plant species, and the response is usually regulated by jasmonate-responsive APETALA2/ethylene response factor (AP2/ERF) TFs (Shen et al. 2016a, b). It has been observed that MeJ induced artemisinin production in plants and plant cell tissue cultures of *A. annua*. A screening from a GST cDNA library resulted in the isolation of two encoding sequences presenting AP2 conserved domains, *AaERF1* and *AaERF2*. After MeJ treatment, both ERF1 and ERF2 were localised in the nucleus and their expression patterns correlated with those of *ADS* and *CYP71AV1*, which are two genes involved in artemisinin biosynthesis. Moreover, yeast one-hybrid and electrophoretic mobility shift assay (EMSA) analyses showed that both TFs bind to conserved sequence motifs of *ADS* and *CYP71AV1* promoters. The overexpression of both TFs resulted in plants with higher artemisinin and artemisinic acid contents in mature leaves of 3-month-old plants, which correlated with higher transcript levels of *ADS* and *CYP71AV1*, as compared to control plants. On the other hand, the silencing of *AaERF1* and *AaERF2* by a RNA interference (RNAi) approach led to lower levels of STL accumulation as well as decreased *ADS* and *CYP71AV1* transcript levels. The experiments undoubtedly proved that AP2/ERF TFs regulate artemisinin accumulation and *ADS* and *CYP71AV1* expression in MeJ-treated plants (Yu et al. 2012).

Lu et al. (2013b) have isolated another AP2/ERF-type TF named *AaORA* from a cDNA library of *A. annua* leaves, which showed high homology sequence with ORCA3, an APE/ERF TF from *Catharanthus roseus*. The profile expression of *AaORA* in different plant tissues was similar to those of *ADS*, *CYP71AV1* and *DBR2*, showing higher transcript levels in bud flowers than in leaves, stems and roots. *AaORA* was specifically expressed in glandular trichomes. The overexpression of *AaORA* induced the transcription of higher levels of *ADS*, *CYP71AV1* and *DBR2* mRNAs, as compared to control lines. Since the *AeERF1* but not the *AeERF2* gene was also upregulated in transgenic plants, the authors hypothesised that *AaORA* might trigger artemisinin production through *AaERF1*.

Ji et al. (2014) have observed that *ADS* and *CYP71AV1* promoters also contained an E-box element with a putative binding site for bHLH TF and searched for candidate sequences in the GST cDNA library mentioned above. The screening resulted in the isolation of an ORF sequence encoding an *AabHLH1* TF. The expression pattern of *AabHLH1* revealed that it was highly expressed in flowers and less expressed in leaves, stems and roots. The authors also studied the effect of abscisic acid (ABA) and chitosan on *AabHLH* and *ADS* expression. They observed that the foliar application of ABA (100 mg/l) and chitosan (150 mg/l) induced *AabHLH* and *ADS* expression coordinately. An EMSA analysis confirmed that *AabHLH1* binds to E-boxes present in *ADS* and *CYP71AV1* promoters. Furthermore, the overexpression of *AabHLH1* performed by a transient expression experiment showed that the transcript levels of *ADS* and *CYP71AV1* were increased. The transient expression assays revealed that the upstream *AaHMGR* gene of the MVA pathway was also activated. The results obtained showed that bHLH1 TF positively regulates artemisinin biosynthesis.

WRKY TFs are involved in the regulation of different processes in plants such as defence, embryogenesis and secondary metabolite biosynthesis. Ma et al. (2009a) have explored the GST of *A. annua* cDNA library and found a specific cDNA sequence expressed in GST (*AaWRKY1*) that showed homology with other WRKY TFs. In *A. annua*, high expression levels of *AaWRKY1* were found in GST, while in flowers, leaves and roots, the expression was much lower. When *A. annua* leaves were treated with MeJ and chitosan, the expression of *AaWRKY1* was rapidly induced, and, in both cases, it preceded the upregulation of *ADS*. An EMSA analysis showed that *AaWRKY1* binds to the W-box motif also present in the *AaADS* promoter. The transient expression of *AaWRKY1* in *A. annua* plants induced the expression of other genes of the STL pathway such as *CYP71AV1*, *HMGR* and *DBR2*. This finding allowed speculating that their promoters also contain W-boxes, although this hypothesis was not corroborated by the authors. The *FDS* expression was not induced by the transient expression of *AaWRKY1*. It has also been observed that the overexpression of *AaWRKY1* in tobacco upregulated the gene expression of the 5-*epi*-aristolochene synthase (*EAS4*), which is a STPS (Ma et al. 2009b).

The basic leucine zipper TF (bZIP) family has been described before to play an important role in ABA signalling regulation in plants. They bind to *cis*-element motifs named ABA-responsive elements (ABREs). By means of a sequence database study, Zhang et al. (2015) have identified a bZIP TF (*AabZIP1*) probably involved in ABA signalling and highly expressed in GST. The levels of *AabZIP1* mRNA were found to be higher in flowers and flower buds than in leaves, stem and roots. Different

types of abiotic stress such as drought and saline triggered the expression of high levels of *AabZIP1* in the same fashion as ABA-treated plants, thus corroborating the participation of this TF in the regulation of stress responses. It has also been demonstrated that *AabZIP1* binds to *ADS* and *CYP71AV1* promoters. Transgenic plants overexpressing *AabZIP1* have shown higher mRNA levels of different genes involved in the artemisinin pathway such as *ADS*, *CYP71AV1*, *DBR2* and *ALDH1*. The authors also observed that ABA induced the upregulation of both *AaERF1* and *AaERF2*, which suggests a possible cross-talk between ABA and Ja signalling.

Recently, the TRICHOME AND ARTEMISININ REGULATOR 1 (TAR1), which is another TF from the AP2/ERF family, has been isolated from GST of *A. annua*. TAR1 plays an important role in trichome development and artemisinin biosynthesis. As expected, TAR1 showed high expression levels in bud flowers and young leaves and particularly in GSTs and in apical meristems. Transgenic plants that constitutively overexpressed TAR1 accumulated more artemisinin, DAA and AA than their non-transgenic counterparts. Moreover, TAR1 activated the expression of *ADS* and *CYP71AV1* but not that of the genes encoding the key enzymes of the MVA (HMGR) and MEP (DXS and DXR) pathways (Tan et al. 2015). An EMSA analysis has revealed that TAR1 was able to bind *cis*-element present in *ADS* and *CYP71AV1* promoters. The authors observed that silencing of TAR1 by RNAi caused a decrease in the artemisinin content in *A. annua* plants, which correlated with the low expression levels of *TAR1*, *ADS*, *CYP71AV1* and *DBR2*. On the other hand, the expression of *DXS* and *DXR* (MEP pathway) was increased. TAR1-RNAi plants also showed abnormal trichome development (Tan et al. 2015).

In summary, several TFs positively regulate artemisinin biosynthesis; they mediate plant development and the response to different stimuli such as phytohormones (ABA, MeJ) and biotic (pathogens and chitosan) and abiotic types of stress (drought and saline). They mainly activate the expression of two key enzymes of the STL pathway, *ADS* and *CYP71AV1* and, to a lesser extent, *DBR2* and *ALDH1*. *ADS* and *CYP71* have been previously described as rate-limiting enzymes of the artemisinin biosynthetic pathway, and they seem to be tightly regulated by these TFs. Although there has been a great advance in the understanding of how these TFs regulate artemisinin biosynthesis, the interaction between them seems to be a complex regulation network that remains unknown.

#### 4.4 Biotechnological Approaches for the Production of Sesquiterpene Lactones: Plant Cell Culture

Many medicinal and aromatic plants are usually slow-growing species, and their products are harvested from wild or agricultural crops with low yields. They are also affected by environmental conditions such as drought, climate changes, pathogens, fires and other natural disasters. Due to these factors, their supply for the industry may become irregular and non-homogenous (Atanasov et al. 2015). In addition, numerous MAP species are difficult to cultivate massively using a conventional

agricultural program, and 20% of them are considered to be in danger of extinction (Kolewe et al. 2008). The chemical synthesis of most of these secondary metabolites, especially STLs, is feasible but commercially non-viable (Wilson and Roberts 2012). The increased demand for these products requires a production platform that can satisfy a continuous supply, a homogeneous production, GMP requirements and a low environmental impact (Rea et al. 2011). In vitro plant cell culture (PCC) has emerged as an alternative production system for many plant secondary metabolites since it can meet all the requirements mentioned above. PCC includes micropropagation, suspension cells and organ cultures (shoots and roots). Micropropagation is a well-established industrial production system for many ornamental, vegetable, forestry and fruit species (Pence 2011). Plant cell suspension cultures (undifferentiated cells) also offer a continuous and homogenous product supply in short growth cycles. The PCC process can be developed in traditional industrial bioreactors used for microorganism or mammalian cell cultures (Atanasov et al. 2015; Eibl and Eibl 2008; Eibl et al. 2009). In many cases, undifferentiated cell cultures usually present low productivities because secondary metabolite accumulation is associated with tissue or organ differentiation. Besides, these cultures are genetically unstable (Mora-Pale et al. 2013). Therefore, the establishment of organ culture shoots and roots constitutes an interesting alternative. These organ cultures usually accumulate secondary metabolites at the same level and pattern as the parent plant. Organ root cultures are genetically and biochemically stable and have become an attractive system to produce secondary metabolites, since the biosynthesis of many of them occurs in the roots. Two kinds of root cultures can be employed: adventitious and hairy roots (Talano et al. 2012). Adventitious root cultures are established after excision of the root from the entire plant and the addition of phytohormones in the culture medium. CBN (Korea) is a company that produces adventitious roots of *Panax ginseng* (ginseng saponins) at a scale of 10 m<sup>3</sup> (Baque et al. 2012). Hairy root cultures are obtained by infection of plant explants with *Agrobacterium rhizogenes*. These cultures can produce high amounts of secondary metabolites and grow at high rates without the addition of growth regulators (Talano et al. 2012). The Swiss company ROOTec Bioactives AG (currently part of Green2Chem, Belgium) has developed a technology for the production of plant natural compounds based on hairy root cultures. The production of secondary metabolite by PCC can also be improved by the manipulation of culture conditions that include inoculum size and age, minerals, carbon source, light, addition of precursors, pH and temperature. Elicitation is another strategy to enhance the production of secondary metabolites. Elicitors are stress conditions or molecules that activate secondary metabolite biosynthesis in plants. MeJ, chitosan, SA, coronatine, yeast extracts and heavy metals, among others, have been extensively used to improve secondary metabolite productivities (Murthy et al. 2014; Wilson and Roberts 2012). These approaches can be combined with in situ product removal (ISPR) strategies that consist of the addition of a second phase in the culture medium. The second phase can be either liquid or solid; in that way, the compounds of interest are incorporated into the second phase and are easily separated from the culture medium (Wilson and Roberts 2012). Moreover, feedback inhibition by product accumulation can be avoided.

**Table 4.1** Different biochemical strategies used to increase artemisinin production in plant cell and tissue cultures

Cell culture	Treatment	Artemisinin production	Reference
Hairy roots	Chitosan	1.8 mg/g dry weight	Putalun et al. (2007)
	MeJ	1.5 mg/g dry weight	
	Yeast extract	0.9 mg/g dry weight	
Hairy roots	Cerebroside elicitor	2.1 mg/g dry weight (16.3 mg/l)	Wang et al. (2009)
	Cerebroside elicitor + SNP	2.2 mg/g dry weight (22.4 mg/l)	
Hairy roots	Oligosaccharide elicitor	1.3 mg/g dry weight (12 mg/l)	Zheng et al. (2008)
	Oligosaccharide elicitor + SNP	2.2 mg/g dry weight (28.5 mg/l)	
Suspensions	Precursor addition	56 mg/l	Baldi and Dixit (2008)
	Yeast elicitor	76 mg/l	
	Combined	115 mg/l	
Suspensions	Cyclodextrin	25.2 µmol/g dry weight	Durante et al. (2011)
	Cyclodextrin + MeJ	27.5 µmol/g dry weight	
Suspensions	MeJ	14.4 µg/g dry weight	Caretto et al. (2011)
	Miconazole (inhibitor)	13 µg/g dry weight	
Hairy roots	MeJ	(13.3 mg/l)	Ahlawat et al. (2014)
	<i>P. indica</i> extracts	(15.6 mg/l)	
	<i>P. indica</i> extracts + MeJ	(19.0 mg/l)	
	FPP (precursor)	(10.3 mg/l)	

*A. annua* plant cell and tissue cultures have been extensively studied as a continuous source of artemisinin, and, in order to produce it at industrial scale, many research groups have employed different plant cell platforms to achieve this goal (Table 4.1). Suspension cell, shoot and hairy root cultures have been used to produce the antimalarial drug. These cultures have been combined with different strategies to improve artemisinin productivities, and some of the variables analysed are summarised in Table 4.1. Elicitation has been the most common, simple and successful approach to improve artemisinin production. Chitosan, MeJ, oligosaccharides and fungal extracts have demonstrated to increase the artemisinin content, as compared to non-treated cultures; in general the artemisinin contents reached values of 1–2.5 mg/g dry weight and concentrations that varied from 10 to 120 mg/l (Putalun et al. 2007; Wang et al. 2009; Zheng et al. 2008; Ahlawat et al. 2014; Durante et al. 2011). The addition of precursors of the artemisinin pathway as well as inhibitors of the competitive steroid pathway has also resulted in higher levels of artemisinin accumulation (Baldi and Dixit 2008; Caretto et al. 2011).

Hairy root cultures have been grown in bioreactors with different configurations (Table 4.2) such as bubble column, airlift, modified stirred tank and mist reactor. Mist bioreactor has shown a better performance than the others for both growth and secondary metabolite production (Patra and Srivastava 2014, 2016; Souret et al. 2003). Moreover, *A. annua* shoot cultures grown in a mist reactor also resulted in an enhanced biomass yield and artemisinin production (3.3- and 1.4-fold) than those grown in a bubble column and multiplate flow reactor (Liu et al. 2003).

Hairy root cultures of *V. officinalis* were also the PCC system chosen for the production of valerenic acid. Transformed roots elicited with MeJ and a *Fusarium graminearum* extract resulted in an increased valerenic acid production that was



**Table 4.2** Bioreactor configurations employed in artemisinin production by plant cell and tissue cultures

Cell culture	Bioreactor	Artemisinin Production	Reference
Hairy roots	Bubble column (3.0 l)	0.27 mg/g dry weight	Patra and Srivastava (2016)
	Mist reactor (3.0 l)	1.12 mg/g dry weight	
Hairy roots	Bubble column (1.5 l)	0.14 µg/g fresh weight	Souret et al. (2003)
	Mist reactor (1.5 l)	0.29 µg/g fresh weight	
Hairy roots	Shake flask	(3.4 mg/l)	Patra and Srivastava (2016)
	Modified stirrer tank (1.5 l)	(4.3 mg/l)	
Hairy roots	Bubble column (1.5 l)	2.94 µg/g dry weight	Kim and Keasling (2001)
	Mist reactor (1.5 l)	0.98 µg/g dry weight	
Shoots	Modified airlift	3.5 mg/g dry weight (14.6 mg/l)	Liu et al. (2003)
	Multiplate flow reactor	3.2 mg/g dry weight (34.4 mg/l)	
	Mist reactor (0.4 l)	1.8 mg/g dry weight (48.2 mg/l)	

6-fold (2.3 mg/g dry weight) and 12-fold (3.02 mg/g dry weight) higher, respectively, than non-elicited roots (0.24 mg/g dry weight). The addition of  $\text{Ca}^{2+}$  and  $\text{Mg}^{2+}$  as abiotic elicitors led to an increase in valerenic acid accumulation that was 8-fold (1.83 mg/g dry weight) and 4.2-fold (1.1 mg/g dry weight) higher than control cultures (0.23 mg/g dry weight). The authors considered the use of these salts as a cost-effective strategy for large-scale production (Torkamani et al. 2014a, b).

Chicory hairy root cultures were found to produce 1.4% dry weight of 8-deoxylactucin glucoside. This amount is two orders of magnitude higher than that produced by roots of chicory plants (Malarz et al. 2002). The accumulation of this STL seems to be affected by light, since hairy roots incubated in the dark produced lower levels (0.88% dry weight) than those of hairy roots incubated under light conditions (1.37% dry weight). In conclusion, hairy roots of chicory could be an alternative system for the production of 8-deoxylactucin glucoside, although these cultures presented a different pattern of STLs after many years of subculture. In *Rudbeckia hirta* hairy roots and suspension cell cultures, light has also been essential to induce the production of pulchelin E (Luczkiewicz et al. 2002). The contents of pulchelin E were higher in transformed roots (14.0 mg/g dry weight) than in suspension cultures (9.0 mg/g dry weight).

Despite all the progress made in the field of secondary metabolite production by PCC, few processes have reached an industrial scale. The main reasons could be the low intrinsic productivities of PCC and the fact that the biosynthetic pathways that lead to secondary metabolite production and their regulation have not been fully elucidated yet.

## 4.5 Metabolic Engineering

Metabolic engineering comprises several strategies that use DNA technology to modify metabolic networks (Paddon and Keasling 2014). Among these strategies, it is possible to (1) overexpress one or various enzymes of the metabolic pathway (generally those involved in rate-limiting steps), (2) downregulate enzymes at

metabolic branching points in order to increase the carbon flux towards the selected pathway, (3) overexpress TFs involved in the regulation of the biosynthetic pathway (in order to increase the expression of several enzymes at the same time) and (4) overexpress other proteins that can indirectly affect STL accumulation (e.g. oncogenes, biosynthetic enzymes of STL-regulating molecules, etc.) (Paddon and Keasling 2014; Majdi et al. 2016).

### 4.5.1 Metabolic Engineering in Plants and Plant Cell Culture

Liu et al. (2014) have been able to isolate and characterise the full biosynthetic pathway that led to parthenolide production. As mentioned above, four genes are responsible for parthenolide accumulation from the universal precursor, FPP in *T. parthenium*: *TpGAS*, *TpGAO*, *TpCOS* and *TpPTS*. The transient expression of the first three genes in *N. benthamiana* plants resulted in the accumulation of costunolide (9.6 µg/g fresh weight). The LC-QTOF-MS analysis of the transformed leaves has revealed that costunolide was found in two conjugated forms with cysteine and glutathione (GSH). In a further experiment, a transient expression of the four genes (*TpGAS*, *TpGAO*, *TpCOS* and *TpPTS*) with *AtHMGR* resulted in the production of free parthenolide to a level up to 2 ng/g fresh weight. The low levels presented were due to the conjugation of parthenolide with cysteine (1368 ng/g fresh weight) and GSH (88 ng/g fresh weight). The co-expression of *AtHMGR* was necessary to increase the carbon flux towards the STL biosynthesis. In *T. parthenium*, costunolides and parthenolides are accumulated in their free forms in glandular trichomes. The presence of the conjugated forms of both STLs in *N. benthamiana* may be a detoxification mechanism. Since parthenolides and costunolides accumulate specifically in trichomes, the authors proposed directing the expression of the full pathway to trichomes to avoid formation of conjugates. In order to improve parthenolide production, the authors suggested that chicory or lettuce could be better heterologous platforms since they naturally accumulate costunolide derivatives in special structures like laticifers located all over the plant. It is interesting to mention that the conjugated versions of parthenolides, i.e. parthenolide-cysteine and parthenolide-GSH, have also shown anticancer activities against different tumours albeit at lower levels than the free parthenolide.

Recently, metabolic engineered hairy roots of *V. officinalis* that overexpress *VoFDP* and *VoVDS* have been established. These genes encode two enzymes involved in valerenic acid and valeranal biosynthesis. The transgenic lines obtained showed higher transcript levels of *VoFDP* and *VoVDS* than control lines although there were differences in the mRNA levels among them. Transgenic lines overexpressing *VoFDP* presented higher levels of valerenadiene, valeranal and β-caryophyllene, which is another STL that competes for the common substrate FPP. The higher STL levels could be due to the increment in FPP cytosolic supply. Recombinant hairy roots overexpressing *VoVDS* showed 1.5- to 4-fold increased valerenic acid contents than the control line and, to a lesser extent, in valeranal and valerenadiene (Ricigliano et al. 2016). On the other hand, the production of β-caryophyllene was not affected.

MeJ elicitation of all transgenic lines produced an increment of STL content, as compared to non-elicited cultures. These results revealed that other enzymatic steps or regulation processes could be limiting STL accumulation.

It is known that the STL biosynthesis and the reaction catalysed by FDS that is responsible for the FPP supply occur in the cytosol. The overexpression of STPs in the cytosol has been the general strategy to increase STL accumulation in transgenic plants, although in many cases, this strategy did not result in higher STL contents. Wu et al. (2006) have hypothesised that the low amounts of STLs registered could be due to a tight regulation at different levels of the biosynthetic pathway. With the aim of corroborating this hypothesis, they redirected the overexpression of FDS (avian source) and the enzyme patchoulol synthase (PTS) to chloroplasts of *Nicotiana tabacum* (Wu et al. 2006). PTS is a sesquiterpene synthase that converts FPP into patchoulol, a main compound of the patchouli essential oil fragrance. Several expression vectors were constructed; *FDS* and *PTS* genes were cloned under the control of strong constitutive promoters with or without a plastid targeting signal sequence (tp). Plastid-targeted enzymes resulted in transgenic plants with 10–30 µg/g fresh weight of patchoulol contents, while the cytosolic engineering of the pathway in plant cells never exceeded 10–12 µg/g fresh weight. The expression of these enzymes in plastid also resulted in the presence of many new STLs that have never been described in *Nicotiana* plants. The same strategy was carried out with *FDS* and *ADS* from *A. annua*, improving amorpho-4,11-diene accumulation to levels of 25 µg/g fresh weight, which are several orders of magnitude higher than those found in transgenic plants with *ADS* targeted to cytosol (Wu et al. 2006). This redirection of the carbon flux of isoprenoid precursors is an interesting approach to increase natural products accumulation in plants.

### 4.5.2 *Metabolic Engineering of the Artemisinin Biosynthetic Pathway*

Since the content of artemisinin in *A. annua* is extremely low (between 0.01% and 0.8% of the plant dry weight), several strategies, briefly described in Sect. 4.4, have been applied to enhance artemisinin accumulation. Moreover, metabolic engineering for artemisinin production became a model system not only for the production of STLs but also for other plant secondary metabolic pathways.

#### 4.5.2.1 **Overexpression of Genes Involved in the Artemisinin Biosynthetic Pathway**

Several authors have reported the overexpression of one or various enzymes involved in artemisinin biosynthesis, not only the specific enzymes responsible for artemisinin synthesis but also those involved in the pathways that generate the precursors of its production (Table 4.2).

One of the enzymes that were overexpressed was the FDS. There is an early report of the expression of a foreign copy of *FDS* (from *Gossypium arboreum*) in hairy roots of *A. annua*, by *A. rhizogenes* genetic transformation. This strategy resulted in an enhanced accumulation of artemisinin in transgenic hairy roots, as compared to control hairy roots (between ~2.5 and 3.0 mg/g dry weight, as compared to ~0.75 mg/g dry weight, respectively) (Chen et al. 1999). The same enzyme expressed in *A. annua* plants resulted in increased levels of artemisinin (~8–10 mg/g dry weight) in five transgenic lines, as compared to those in control lines (~3 mg/g dry weight) (Chen et al. 2000). Other authors have reported the overexpression of FDS from *A. annua*, resulting in three transgenic lines with higher artemisinin content (~0.8–0.9% dry weight), as compared to control lines (~0.65% dry weight) (Han et al. 2006). Another enzyme that has been a target for metabolic engineering was HMGR. Some authors have reported the expression of HMGR from *C. roseus* L. in *A. annua* plants, resulting in higher artemisinin content (up to 0.6 mg/g dry weight, as compared to untransformed lines rendering 0.37 mg/g dry weight) (Nafis et al. 2011). Other authors have reported increases between 17.1 and 22.5%, as compared to control lines (Aquil et al. 2009). In a more recent report, *HMGR* and *FDS* were overexpressed in *A. annua* plants. At least five of the clones analysed showed a higher artemisinin content, as compared to non-transgenic plants. The highest artemisinin accumulation was near 9 mg/g dry weight (1.8-fold increase, as compared to controls) and was accompanied by higher *HMGR* and *FDS* transcript levels, as compared to controls (2.80-fold and 3.68-fold, respectively) (Wang et al. 2011).

Ma et al. have evaluated the terpenoid metabolic profile in a transgenic *A. annua* plant that overexpressed *ADS*. They found that this line showed higher accumulation of artemisinin and artemisinic acid (both ~1.2 mg/g dry weight), as compared to GUS-expressing plants (~0.6 and ~0.8 mg/g dry weight, respectively) (Ma et al. 2009).

Successful results were obtained either overexpressing genes from the general pathway or genes for the specific artemisinin biosynthetic pathway. For instance, the overexpression of *DXR* and co-overexpression of *CYP71A1* and *CPR* in *A. annua* plants have been reported. All transgenic lines showed higher artemisinin content, between 0.62 and 1.21 mg/g dry weight for plants overexpressing *DXR*, as compared to 0.52 mg/g dry weight obtained in control lines (1.21- to 2.35-fold increases), and between 1.46 and 2.44 mg/g dry weight in plants overexpressing *CYP71A1* and *CPR*, as compared to 0.91 mg/g dry weight of control lines (1.61- to 2.69-fold increases) (Xiang et al. 2012). In another report dealing with the co-overexpression of *CYP71A1* and *CPR*, four transgenic lines showed higher artemisinin content (~0.9–1.0 mg/g dry weight), as compared to controls (~0.7 mg/g dry weight), and were accompanied by higher transcript levels of the overexpressed genes, although the increases were different among lines and among genes (Shen et al. 2012).

In the investigation carried out by Alam et al., *HMGR* and *ADS* were co-expressed in *A. annua* plants. Higher levels of *HMGR* and *ADS* transcripts were found in transgenic lines, and in three selected ones, the artemisinin content was ~1.6–1.8 mg/g dry weight, as compared with the 0.2 mg/g dry weight detected in control plants, which represents a ~7-fold increase (Alam and Abdin 2011).

Some authors have addressed this subject by multiple gene engineering, by the co-overexpression of three enzymes, one from the FDS pathway and two from the specific artemisinin pathway. For instance, *FDS*, *CYP71AV1* and *CPR* were overexpressed in *A. annua* plants, resulting in higher expression levels of these genes, although to a different extent among them and among the different transgenic lines obtained. Six transgenic lines showed a significant increase in the artemisinin content, from 1.40 mg/g fresh weight (~1.7-fold) up to 2.98 mg/g fresh weight (~3.6-fold), as compared to 0.83 mg/g fresh weight obtained with the control line (Chen et al. 2013).

Another interesting work on artemisinin production was that performed by Lu et al., who were able to overexpress *ADS*, *CYP71AV1* and *CPR* genes in *A. annua* plants. Although the mRNA levels corresponding to the three genes varied between the eight transgenic lines tested, all of them showed increased artemisinin content, as compared to the control line (between 1.5- and 2.4-fold increases) (Lu et al. 2013a).

Substrate channelling is a relatively new strategy analysed to increase artemisinin production. This strategy is based on the fact that the immediate transference of the product of one enzyme to the next one in a biosynthetic pathway can improve reaction rates. In a recent work, *ADS* has been expressed as a fusion protein with *FDS* in two high artemisinin-producing varieties of *A. annua* (var. Chongqing and var. Anamed), under the control of either CaMV35S or *CYP71AV1* promoter. In both lines, the fusion gene rendered higher transcript levels under the control of the CaMV35S promoter (constitutive) than under the *CYP71AV1* promoter (tissue-specific). As compared to control lines, the transcript levels of *ADS* were higher than those of *FDS*, possibly because *FDS* is highly expressed in wild-type plants. The artemisinin content was increased up to 2–2.5 times in both varieties (around 2.5% dry weight) when the fusion gene was specifically expressed in GST (i.e. under *CYP71AV1* promoter), whereas the CaMV35S promoter was not as effective in improving the artemisinin content (Han et al. 2016).

#### 4.5.2.2 Blockage of Metabolic Competing Routes

Another strategy that has been employed to enhance artemisinin production was the downregulation of metabolic routes that compete with the artemisinin biosynthetic pathway for a common precursor. In the case of artemisinin biosynthesis, FPP becomes a branch point, since it is the precursor of sterol and sesquiterpene biosynthesis. This approach was carried out by Wang et al. who evaluated the suppression of the expression of squalene synthase (*SQS*), the first enzyme in sterol biosynthesis, by expressing an antisense copy of this enzyme in *A. annua* plants. In two transgenic lines, *SQS* expression was reduced, as compared to the control; and the artemisinin content was increased by 22–23%, as compared to the control line (Wang et al. 2012). Zhang et al. have also evaluated the effect of *SQS* suppression by hairpin-RNA-mediated RNAi technique. The expression of *SQS* was significantly suppressed in some of the transgenic lines obtained (up to 60%), resulting in a decrease in the levels of the sterols campesterol, stigmasterol,  $\beta$ -sitosterol and

ergosterol, whereas the artemisinin content was increased up to 31.4 mg/g dry weight (~3.14-fold higher than that of control plants) before the flowering state (Zhang et al. 2009). In another work,  $\beta$ -caryophyllene synthase (CPS) was suppressed by antisense technology. This enzyme is one of the sesquiterpene synthases that competes for the FPP pool. The antisense fragment of *CPS* cDNA was delivered into *A. annua* by *A. tumefaciens*, and the transgenic lines were evaluated in terms of the expression of related genes and the accumulation of related metabolites. As expected, *CPS* expression, as well as the  $\beta$ -caryophyllene content, was reduced in all transgenic lines, whereas the *HMGR*, *FDS*, *ADS*, *CYP71AV1*, *DBR2* and *ALDH1* expressions were enhanced. This was attributed to the high FPP availability, which induced the expression of these genes. The artemisinin production was increased in transgenic lines up to 54.9%, as compared to control lines, and was accompanied by both an increase in dihydroartemisinic acid production (probably due to the higher expression of artemisinin-related enzymes) and a decrease in artemisinic acid content (Chen et al. 2011).

In this sense, Lv et al. have evaluated the effects of the downregulation of the four enzymes that compete with *ADS* for FPP in plants: *CPS*, *BFS*, *GAS* (*STPS*) and *SQS* (Table 4.2). In all the different transgenic lines obtained, artemisinin was increased, as compared to the control line (77, 77, 103 and 71% in anti-*CPS*, anti-*BFS*, anti-*GAS* and anti-*SQS* plants, respectively). Similar results were obtained for the dihydroartemisinic acid content (increases of 132, 54, 130 and 223% in anti-*CPS*, anti-*BFS*, anti-*GAS* and anti-*SQS* plants, respectively). The highest artemisinin content in transgenic lines was ~12 mg/g dry weight (Lv et al. 2016b).

#### 4.5.2.3 Overexpression of Transcription Factors

As mentioned above, the expression of a TF that regulates a whole metabolic pathway is a strategy to increase the amount of a certain compound. As described in Sect. 4.3, several TFs have been described to be involved in the regulation of the artemisinin biosynthesis. Most of them belong to the AP2/ERF family, such as *AaORA*, *AaERF1* and *AaERF2* and *TAR1* (Tan et al. 2015).

The characterisation of *AaERF1* and *AaERF2* has allowed determining that these TFs interact with specific motifs in *ADS* and *CYP71AV1* promoters. Their overexpression in *A. annua* enhanced the accumulation of artemisinin and artemisinic acid (by 19–67% and 11–76% in plants overexpressing *AaERF1* and by 24–51% and 17–121% in plants overexpressing *AaERF2*, respectively) (Yu et al. 2012). The overexpression of *AaORA* led to an increase in its own transcript levels (between 4–14-fold), as well as those of *ADS*, *CYP71AV1*, *DBR2* and *AaERF1* (around 6–13-, 5–17-, 4–13- and 4–12-fold, respectively). The production of artemisinin and dihydroartemisinic acid was higher in transgenic plants, as compared to control plants (by 40–53% and 22–35%, respectively) (Lu et al. 2013b). On the other hand, the overexpression of *TAR1* led to an increase of the corresponding RNA levels (by 12- to 23-fold), and higher artemisinin, dihydroartemisinic acid and artemisinic acid content in leaves (22–38%, 69–130% and 28–164%, respectively) and in flower buds (34–57%, 22–79% and 12–61%, respectively) (Tan et al. 2015).

The AabZIP1 TF has been overexpressed in *A. annua*, resulting in an increase of the corresponding mRNA levels, as compared to those of wild-type (between 20- and 35-fold). The increases in the transcript levels of *ADS* and *CYP71AV1* (6- to 8-fold) were accompanied by an increment in artemisinin and dihydroartemisinic acid production in the transgenic lines by 0.7- to 1.5-fold and 0.3- to 0.8-fold, as compared to the control line, respectively (Table 4.3) (Zhang et al. 2015).

AaWRKY1 is another TF that has been isolated from *A. annua*. Its overexpression (50- to 90-fold increased expression) led to the increase in RNA levels of *ADS* and *CYP71AV1* (1.5- to 3.0-fold and 4.4- to 14.0-fold, respectively) as well as a higher artemisinin content (1.3- to 2.0-fold), as compared to non-transgenic control plants (Jiang et al. 2016).

AaMYC2 is a TF activated by Ja, which is a positive regulator of artemisinin biosynthesis. As a consequence of its overexpression in *A. annua* plants, transcript levels of *ADS*, *CYP71AV1*, *DBR2* and *ALDH1* were increased (1.7- to 8.4-fold, 2.0- to 5.9-fold, 1.2- to 2.9-fold and 1.2- to 2.5-fold, respectively). While the artemisinic acid content was decreased, the artemisinin and dihydroartemisinic acid accumulation was enhanced (by 23–55% and 17–217%, respectively) (Shen et al. 2016a, b).

When the GLANDULAR TRICHOME-SPECIFIC WRKY 1 (AaGSW1) was isolated from *A. annua* and characterised, it was found that its overexpression led to an increase in the transcript levels of *CYP71AV1* (3- to 6-fold) and *ALDH1* (4- to 7-fold). Interestingly, the expression of *ADS* and *DBR2* was enhanced (3- to 5- and 2- to 3-fold, respectively), which was attributed to an increased *AaORA* expression (by 4-fold). Whereas artemisinin and dihydroartemisinic acid were higher in transgenic plants (increases of 55–100 and 50–60%, respectively), artemisinic acid was decreased (by 30–90%, respectively) (Chen et al. 2017).

Lv et al. have reported the overexpression of AaNAC1, which is a transcription factor belonging to the NAC superfamily in *A. annua*. The selection of this TF (from *A. annua* glandular trichome transcriptome) was made on the basis of its abundance and due to the fact that it was induced by SA and MeJ, which are known elicitors of artemisinin production (see Sects. 4.3 and 4.4). In some transgenic lines, the overexpression of *AaNAC1* was accompanied by a significant increase in the mRNA levels of *ADS*, *DBR2* and *ALDH1* but not of *CYP71AV1*, whereas those of *HMGR* remained unchanged. Nevertheless, the content of artemisinin and dihydroartemisinic acid was significantly increased in all transgenic lines (between 14% and 79% and between 30% and 150%, respectively) (Lv et al. 2016a). In a recent work, the *AaMYB1* TF was identified in *A. annua* and characterised. Plants overexpressing *AaMYB1* (either under the *CYP71AV1* or the CaMV35S promoter) showed an increase in artemisinin and dihydroartemisinic acid contents, when compared to control plants (~10 mg/g dry weight artemisinin and ~1.5 mg/g dry weight dihydroartemisinic acid). The accumulation of both compounds were higher in 35S::*AaMYB1* plants (systemic expression; up to ~20 mg/g dry weight artemisinin and up to ~5 mg/g dry weight dihydroartemisinic acid), as compared to p*CYP71AV1*::*AaMYB1* plants (trichome expression; up to ~15 mg/g dry weight artemisinin and up to ~3 mg/g dry weight dihydroartemisinic acid). Genes related to artemisinin biosynthesis were upregulated in both 35S::*AaMYB1* and p*CYP71AV1*::*AaMYB1* plants, especially *CYP71AV1* and *ADS* (Matías-Hernández et al. 2017).

**Table 4.3** Metabolic engineering of the artemisinin biosynthetic pathway carried out in *Artemisia annua* plants or plant cell cultures

Gene(s)	Result	Reference
<i>Overexpression of genes involved in artemisinin biosynthesis</i>		
<i>FDS</i> gene (from <i>G. arboreum</i> ) in <i>A. annua</i> hairy roots	Increased artemisinin content (between ~2.5 and 3.0 mg/g dry weight), as compared to control hairy roots (~0.75 mg/g dry weight)	Chen et al. (1999)
<i>FDS</i> gene (from <i>G. arboreum</i> ) in <i>A. annua</i> plants	Higher artemisinin content (~8–10 mg/g fresh weight), as compared to control lines (~3 mg/g dry weight)	Chen et al. (2000)
<i>FDS</i> in <i>A. annua</i> plants	Increased artemisinin content in three transgenic lines, as compared to control (~0.8–0.9 and ~0.65% dry weight, respectively)	Han et al. (2006)
<i>HMGR</i> (from <i>C. roseus</i> L) in <i>A. annua</i> plants	Higher artemisinin content, up to 0.6 mg/g dry weight, as compared to untransformed lines (0.37 mg/g dry weight)	Nafis et al. (2011)
<i>HMGR</i> (from <i>C. roseus</i> L) in <i>A. annua</i> plants	Increase in artemisinin content, between 17.1 and 22.5%, as compared to control lines	Aquil et al. (2009)
<i>HMGR</i> and <i>FDS</i> genes in <i>A. annua</i> plants	Increased artemisinin content in nine transgenic lines, between 7 and 9 mg/g dry weight (up to 1.8-fold increase), as compared to control Higher <i>HMGR</i> and <i>FDS</i> transcript levels, as compared to control (up to 2.80-fold and 3.68-fold, respectively)	Wang et al. (2011)
<i>ADS</i> gene in <i>A. annua</i> plants	Higher artemisinin and artemisinic acid accumulation (both ~1.2 mg/g dry weight), as compared to control (~0.6 and ~0.8 mg/g dry weight, respectively)	Ma et al. (2009)
<i>DXR</i> , <i>CYP71AV1</i> and <i>CPR</i> in <i>A. annua</i> plants	Higher artemisinin content in plants overexpressing <i>DXR</i> (1.21- to 2.35-fold increases) Higher artemisinin content in plants overexpressing <i>CYP71AV1</i> and <i>CPR</i> (1.61- to 2.69-fold increases)	Xiang et al. (2012)
<i>CYP71AV1</i> and <i>CPR</i> in <i>A. annua</i> plants	Higher artemisinin content in four transgenic lines (~0.9–1.0 mg/g dry weight), as compared to control (~0.7 mg/g dry weight) Higher transcript levels of <i>CYP71AV1</i> and <i>CPR</i> (variations between lines and between genes)	Shen et al. (2012)
<i>HMGR</i> and <i>ADS</i> genes in <i>A. annua</i> plants	Increased artemisinin content (~7-fold increase) in three selected transgenic lines Higher levels of <i>HMGR</i> and <i>ADS</i> transcripts in transgenic lines	Alam and Abdin (2011)
<i>FDS</i> , <i>CYP71AV1</i> and <i>CPR</i> in <i>A. annua</i> plants	Higher artemisinin content (between 1.40 and 2.98 mg/g fresh weight), as compared to control (0.83 mg/g fresh weight) Higher expression levels of <i>FDS</i> , <i>CYP71AV1</i> and <i>CPR</i> (variable between genes and transgenic lines)	Chen et al. (2013)
<i>ADS</i> , <i>CYP71AV1</i> and <i>CPR</i> genes in <i>A. annua</i> plants	1.5- and 2.4-fold increases in artemisinin content	Lu et al. (2013a)

(continued)



**Table 4.3** (continued)

Gene(s)	Result	Reference
<i>ADS::FDS</i> fusion gene in <i>A. annua</i> plants, under CaMV35S or <i>CYP71AV1</i> promoters	Higher transcript level of <i>ADS::FDS</i> gene under CaMV35S than under the <i>CYP71AV1</i> promoter Increased artemisinin content (2–2.5 times; around 2.5% dry weight) in plants expressing <i>ADS::FDS</i> fusion gene under <i>CYP71AV1</i> promoter	Han et al. (2016)
<i>Inhibition of competing metabolic routes</i>		
Suppression of <i>SQS</i> expression (antisense technology)	Increased artemisinin content (by 22–23%, as compared to that of control)	Wang et al. (2012)
Suppression of <i>CPS</i> expression (antisense technology)	Increase in artemisinin content (up to 54.9%, as compared to control lines) Higher expression of <i>HMGR</i> , <i>FDS</i> , <i>ADS</i> , <i>CYP71AV1</i> , <i>DBR2</i> and <i>ALDH1</i> genes	Chen et al. (2011)
Suppression of <i>SQS</i> expression (hairpin-RNA-mediated RNAi)	Increased artemisinin content in some transgenic lines, up to 31.4 mg/g dry weight (~3.14-fold increase) Reduced <i>SQS</i> expression in some transgenic lines obtained (up to 60%)	Zhang et al. (2009)
Downregulation of <i>CPS</i> , <i>BFS</i> , <i>GAS</i> and <i>SQS</i> in <i>A. annua</i> plants	Increased artemisinin content (77, 77, 103 and 71% in anti-CPS, anti-BFS, anti-GAS and anti-SQS plants, respectively) Increased dihydroartemisinic acid content (132, 54, 130 and 223% in anti-CPS, anti-BFS, anti-GAS and anti-SQS plants, respectively)	Lv et al. (2016b)
<i>Overexpression of transcription factors</i>		
<i>AaERF1</i> and <i>AaERF2</i> in <i>A. annua</i> plants	Increased mRNA levels of <i>ADS</i> and <i>CYP71AV1</i> (2- to 8-fold and 1.2- to 5-fold, respectively) Enhanced artemisinin and artemisinic acid accumulation (19–67% and 11–76%, respectively, in plants overexpressing <i>AaERF1</i> and by 24–51% and 17–121%, respectively, in plants overexpressing <i>AaERF2</i> )	Yu et al. (2012)
<i>AaORA</i> in <i>A. annua</i> plants	Increased transcript levels of <i>ADS</i> , <i>CYP71AV1</i> , <i>DBR2</i> and <i>AaERF1</i> (around 6–13-, 5–17-, 4–13- and 4–12-fold, respectively) Higher artemisinin and dihydroartemisinic acid content in transgenic plants (by 40–53% and 22–35%, respectively)	Lu et al. (2013b)
<i>TARI</i> in <i>A. annua</i> plants	Higher artemisinin, dihydroartemisinic acid and artemisinic acid content in leaves (22–38%, 69–130% and 28–164%, respectively) and in flower buds (34–57%, 22–79% and 12–61%, respectively)	Tan et al. (2015)
<i>AabZIP1</i> in <i>A. annua</i> plants	Increased transcript levels of <i>ADS</i> and <i>CYP71AV1</i> (6- to 8-fold) and of <i>DBR2</i> and <i>ALDH1</i> Increased artemisinin and dihydroartemisinic acid content (by 0.7- to 1.5-fold and 0.3- to 0.8-fold, as compared to control, respectively)	Zhang et al. (2015)

(continued)

**Table 4.3** (continued)

Gene(s)	Result	Reference
<i>AaWRKY1</i> gene in <i>A. annua</i> plants	Increase in mRNA levels of <i>ADS</i> and <i>CYP71AV1</i> Increase in artemisinin content (between 1.3- to 2.0-fold)	Jiang et al. (2016)
<i>AaMYC2</i> in <i>A. annua</i> plants	Higher artemisinin (by 23–55%) and dihydroartemisinic acid content (17–217%) and lower artemisinic acid Increased expression of <i>ADS</i> , <i>CYP71AV1</i> , <i>DBR2</i> and <i>ALDH1</i>	Shen et al. (2016a, b)
<i>AaGSWI</i> in <i>A. annua</i> plants	<b>Increased artemisinin and dihydroartemisinic acid content</b> (55–100 and 50–60%, respectively). Lower levels of artemisinic acid (by 30–90%) Increased transcript levels of <i>AaORA</i> , <i>CYP71AV1</i> , <i>ALDH1</i> , <i>ADS</i> and <i>DBR2</i>	Chen et al. (2017)
<i>AaNAC1</i> in <i>A. annua</i> plants	Increase in mRNA levels of <i>ADS</i> , <i>DBR2</i> and <i>ALDH1</i> Increase in artemisinin and dihydroartemisinic acid content (up to 79% and 150%, respectively)	Lv et al. (2016a)
<i>AaMYB1</i> in <i>A. annua</i> plants	Increase in artemisinin and dihydroartemisinic acid contents (up to ~20 and ~5 mg/g dry weight, respectively), when compared to control Higher accumulation when <i>AaMYB1</i> was under CaMV35S promoter than <i>CYP71AV1</i> promoter Higher transcript levels <i>ADS</i> and <i>CYP71AV1</i> and, to a lesser extent, of <i>DBR2</i> , <i>FDS</i> and <i>ALDH1</i> in both 35S:: <i>AaMYB1</i> and <i>pCYP71AV1</i> :: <i>AaMYB1</i> plants	Matías-Hernández et al. (2017)
<i>Expression of unrelated genes</i>		
<i>ipt</i> gene from <i>A. tumefaciens</i> in <i>A. annua</i> plants	Increased artemisinin content (between 30% and 70%) in transformed plants Higher cytokinin levels, increased growth of axillary buds, increased chlorophyll content and lower root mass	Sa et al. (2001)
<i>bgl1</i> from <i>T. reesei</i> in <i>A. annua</i> plants	Artemisinin content varied depending on the position and age of the leaf (increase up to 66.5%) Higher density of glandular trichomes on both leaf and flower surfaces	Singh et al. (2016)
Overexpression of <i>AalCSI</i> in <i>A. annua</i> plants	Increased artemisinin content (up to 1.9-fold), as compared to control lines	Wang et al. (2016)
Overexpression of <i>AaPYL9</i> in <i>A. annua</i> plants	Higher increase in artemisinin content upon ABA treatment in transgenic plants, as compared to control (between 74% and 95% and 33%, respectively) Higher increase in <i>ADS</i> , <i>FDS</i> and <i>CYP71AV1</i> expression levels in transgenic plants after ABA treatment	Zhang et al. (2013)
Overexpression of <i>AOC</i> in <i>A. annua</i> plants	Increased content of artemisinin (by 38–97%), artemisinic acid (by 172–675%) and dihydroartemisinic acid (by 125–248%) Higher transcript levels of <i>FDS</i> , <i>CYP71AV1</i> and <i>DBR2</i>	Lu et al. (2014)

(continued)

**Table 4.3** (continued)

Gene(s)	Result	Reference
<i>rol B</i> and <i>rol C</i> genes in <i>A. annua</i> plants	Increased accumulation of artemisinin (between 2.7- and 9.2-folds), artesunate (between 4- and 12.6-folds) and dihydroartemisinin (1.2–3-folds) in plants expressing <i>rol B</i> Increased accumulation of artemisinin (4–4.6-folds), artesunate (between 4.4- and 9.1-folds) and dihydroartemisinin (1.5–2-folds) in <i>rol C</i> -expressing plants Higher mRNA levels of <i>ADS</i> , <i>CYP71AV1</i> , <i>ALDH1</i> and <i>TFARI</i> . Higher glandular trichome density	Dilshad et al. (2015)
<i>rol ABC</i> genes in <i>A. annua</i> and <i>A. dubia</i> plants	Accumulation of 33.12 (~9-fold increase) and 2.32 mg (~21-fold increase) artemisinin per g dry weight in <i>A. annua</i> and <i>A. dubia</i> shoots, respectively Increased expression of <i>ADS</i> , <i>CYP71AV1</i> and <i>ALDH1</i> genes in both species	Kiani et al. (2016)
<i>AtCRY1</i> in <i>A. annua</i> plants	Increased artemisinin content (by 30–40%) Increased expression of <i>ADS</i> , <i>CYP71AV1</i> and <i>FDS</i>	Hong et al. (2009)

#### 4.5.2.4 Miscellaneous Metabolic Engineering Strategies in Artemisinin-Producing Plants

A different strategy used to increase artemisinin accumulation was to express genes that could indirectly affect its production. For instance, phytohormones are involved in plant growth and physiological changes and also regulate secondary metabolite production. One of the strategies evaluated to increase the artemisinin production was the expression in *A. annua* of an isopentenyl transferase from *A. tumefaciens*. This enzyme is involved in cytokinin biosynthesis in transformed cells and is thought to enhance cytokinin levels in transformed plants. Apart from the increase in the artemisinin content in transformed plants (between 30% and 70%), the levels of iPA and iP were significantly higher and were accompanied by increased growth of axillary buds, increased chlorophyll content and lower root mass (Sa et al. 2001).

Another work that was aimed at increasing the artemisinin accumulation by modifying phytohormone production was that of Singh et al. (2016). The authors evaluated the effect of expressing a  $\beta$ -glucosidase from *Trichoderma reesei*, fused to the vacuole-targeting sequence of chitinase at the C terminus, in *A. annua* plants. This strategy was based on the fact that phytohormones are usually accumulated as glycosylated (inactive) conjugates inside the vacuoles and that their release and conversion into the active form involve the hydrolytic cleavage by glucosidases. Although a higher density of glandular trichomes on both leaf and flower surfaces was observed in transformed plants, the artemisinin content varied depending on the position and age of the leaf, but on average, it increased up to 66.5% when compared to untransformed plants.

Since SA is a phytohormone that has a positive effect on the artemisinin production, the isochorismate synthase from *A. annua* (*AaICS1*, an enzyme involved in SA synthesis) was isolated, characterised and overexpressed. These transgenic plants

showed higher artemisinin content, up to 1.9-fold, as compared to control plants, thus proving to be an interesting alternative to enhance the artemisinin accumulation (Wang et al. 2017).

On the other hand, a report demonstrates an enhanced artemisinin accumulation as a consequence of an increased ABA sensitivity mediated by the overexpression of an ABA receptor (*AaPYL9*). When ABA was applied, both control and transgenic lines showed increased expression of *ADS*, *FDS* and *CYP71AV1*, but not *HMGR*, although in transgenic lines the changes in *ADS*, *FDS* and *CYP71AV1* expression were more dramatic. Regarding the artemisinin content, similar levels were observed in both lines before ABA treatment, whereas after the hormone application, there was a rise in the artemisinin content in transgenic plants, as compared to control plants (between 74–95% and 33%, respectively) (Zhang et al. 2013).

Given the fact that exogenous Ja enhances artemisinin accumulation, Lu et al. have evaluated the overexpression of allene oxide cyclase (AOC), the key enzyme in the biosynthesis of Ja. Transgenic plants resulted in a significant increase in Ja levels, which was accompanied by increases in artemisinin (by 38–97%), dihydroartemisinic acid (by 125–248%) and artemisinic acid (by 172–675%) contents. Moreover, higher transcript levels of *FDS*, *CYP71AV1* and *DBR2* were observed (1.7- to 4.3-fold, 5.8- to 17-fold and 1.5- to 5.1-fold, respectively), whereas no significant changes were observed in the expression of *ADS*, *CPR* and *ALDH1* (Lu et al. 2014).

It is well known that hairy root cultures can produce a high and stable level of secondary metabolites and that this effect is a consequence of the expression of *rol* genes, which are responsible for the phenotypic changes on growth and metabolism. The individual effects of *rolB* and *rolC* expression were evaluated in *A. annua* plants, resulting both in an increase of artemisinin, artesunate and dihydroartemisinin, although the highest production of these metabolites was observed in a line expressing the *rolB* gene. In both cases, higher levels of *ADS*, *CYP71AV1* and *ALDH1* transcripts were detected, as well as a higher glandular trichome density and higher mRNA levels of *TFARI* (trichome-specific fatty acyl-CoA reductase 1, which is supposed to be involved in trichome development) (Dilshad et al. 2015).

In a more recent publication, *rol abc* genes were expressed in *A. annua* and *A. dubia* plants, via *A. tumefaciens* genetic transformation. The expressions of *ADS*, *CYP71AV1* and *ALDH1* genes were significantly higher in transformed plants of both species, although the magnitude of the increase varied among genes. Regarding artemisinin accumulation, while it was highly increased in transformed *A. annua* shoots, as compared to control shoots (33.12 mg/g dry weight and 3.94 mg/g dry weight, respectively), the increase observed in *A. dubia* shoots was less pronounced (2.32 mg/g dry weight vs. 0.11 mg/g dry weight in control lines) (Kiani et al. 2016).

Finally, since environmental conditions affect the production of secondary metabolites, cryptochrome 1 from *Arabidopsis thaliana* (*AtCRY1*), which is a key receptor that perceives light signals, was expressed in *A. annua* plants. Apart from phenotypic changes (colouring of aerial organs, lower height), the artemisinin content of the transgenic lines tested was increased by 30–40%, and it was accompanied by an increase in the transcript levels of *ADS* and *CYP71AV1*, but those of *FDS* were increased in only one of the transgenic lines (Hong et al. 2009) (Table 4.3).

#### 4.5.2.5 Production of Artemisinin in Plant Systems

Several advantages make tobacco an ideal host for artemisinin production: fast growth, the production of high amount of biomass and the fact that there are well-established transformation protocols. The first reports in tobacco dealt with the expression of ADS, the first specific step in artemisinin biosynthesis. Transgenic lines were able to express a functional enzyme and yielded 0.2–1.7 ng/g fresh weight of amorpha-4,11-diene (Wallaart et al. 2001).

The effect of compartmentalisation on the carbon flux and terpenoid accumulation was studied by either the cytosolic or the plastid expression of ADS together with an avian FDS in tobacco. While amorpha-4,11-diene production only reached 0.5 ng/g fresh weight in plants expressing only cytosolic ADS, the plastid co-expression of ADS and FDS led to a drastic increase in amorpha-4,11-diene accumulation (up to 425 mg/g fresh weight), highlighting the advantages of compartmentalisation for critical enzymatic steps (Wu et al. 2006).

Zhang et al. have assayed the production of artemisinin precursors by co-expressing different enzymes of the artemisinin biosynthetic pathway. Plastid expression of FDS and ADS has led to the accumulation of amorpha-4,11-diene (from barely undetectable levels up to 4 µg/g fresh weight). However, when FDS, ADS and CYP71AV1 were co-expressed (the two first in plastids and the other in the cytosol), only artemisinic alcohol and the precursor amorpha-4,11-diene were detected (no accumulation of artemisinic aldehyde or acid was observed). The co-expression of these enzymes together with ALDH1 or both ALDH1 and DBR2 failed to achieve the accumulation of the desired artemisinic or dihydroartemisinic acids, which was attributed to either an impaired oxidation from the corresponding aldehyde in tobacco or the reversion by endogenous enzymes (Zhang et al. 2011).

With a similar objective, transient agroinfiltration experiments were performed in *N. benthamiana*, by using combinations of *HMGR*, *FDS*, *ADS* and *CYP71AV1*. To avoid gene silencing and the use of different promoters, some gene constructs included only one promoter and ribosomal skipping sequences and mitochondrial targeting sequences for compartmentalisation. The co-expression of *FDS*, a truncated version of *HMGR* (tHMGR) and *ADS*, resulted in higher amorpha-4,11-diene accumulation, as compared to the expression of *ADS* alone. The co-expression of *FDS*, tHMGR and *ADS*, together with *CYP71AV1*, resulted in a drastic decrease in amorpha-4,11-diene levels, and although the desired products were not detected, the formation of an unknown compound (up to ~ 40 µg/g fresh weight) was observed. That compound was later identified as artemisinic acid-12-β-diglucoside, being the only metabolite of amorpha-4,11-diene produced and the proof of the functionality of *CYP71AV1* in *N. benthamiana* leaves (van Herpen et al. 2010). In a further study, these authors confirmed the production of artemisinin-related compounds as glycosylated derivatives. They analysed the expression and gene sequences of *DBR2*, *ALDH1* and *CYP71AV1* from two chemotypes of *A. annua* (high artemisinin production, HAP, and low artemisinin production, LAP). The authors found that the chemotype was apparently defined by both the type of *CYP71AV1* (from HAP or LAP plants) and the relative proportion of *DBR2* and *ALDH1*. By performing transient

expression experiments in *N. benthamiana* leaves that combined the expression of *CYP71AV1* with *DBR2* (together with *ADS* and *FDS*, both targeted to the mitochondria and *tHMGR*), a variety of free and glycosylated compounds were detected, including free dihydroartemisinic and artemisinic alcohols and aldehydes (with barely no acids being detected), and mainly conjugated dihydroartemisinic and artemisinic acids. The additional expression of *ALDH1* resulted in an increase in glycosylated artemisinic and dihydroartemisinic acids content (Ting et al. 2013). In order to increase artemisinic and dihydroartemisinic acid content in the apoplast of *N. benthamiana* leaves, these researchers studied the effect the expression of different pleiotropic drug resistance (PDR) transporters and lipid transfer proteins (LTP), isolated from *A. annua*, together with the expression of the biosynthetic pathway of artemisinin. The combined expression of *AaLTP3* and *AaPDR2* led to an increase in the artemisinin and arteannuin B accumulation in the apoplast of *N. benthamiana* leaves (Wang et al. 2016).

Finally, the successful production of artemisinin in tobacco has been reported. This was achieved by constructing a mega-vector that carried a truncated version of *HMGR* from yeast and *CPR*, *CYP71AV1*, *DBR2* and either *ADS* (cytosolic) or *mtADS* (targeted to mitochondria), all these from *A. annua*. Artemisinin accumulation was detected in transgenic lines expressing the cytosolic version of *ADS* (between 0.45 and 0.98  $\mu\text{g/g}$  fresh weight); however, the accumulation levels were even higher when *ADS* was targeted to mitochondria (between 5.0 and 6.8  $\mu\text{g/g}$  fresh weight). The success of this strategy was attributed to several factors, including the expression of *HMGR* to increase the carbon flux through the MVA pathway (which resulted in an increased availability of precursors), the co-expression of *CPR* together with *CYP71AV1* and the use of intense light conditions during tobacco cultivation that might contribute to the spontaneous conversion of dihydroartemisinic acid to artemisinin. Although the levels of artemisinin were lower than those produced by *A. annua*, the process can be further optimised, thus resulting in a promising platform for artemisinin production (Farhi et al. 2011).

#### 4.5.2.6 Heterologous Production of Artemisinin in Microorganisms

While several authors have focused on enhancing the artemisinin production in plants, others have started to work on the heterologous production in microbial systems. The Semi-synthetic Artemisinin Project focused on the alternative production of artemisinin or its precursors by metabolic engineering of microorganisms (Paddon and Keasling 2014). Microbial hosts, such as *Escherichia coli* or *Saccharomyces cerevisiae* are well-known hosts for protein expression. They exhibit several advantages over plant systems, such as ease for genetic manipulation and transformation, fast growth in inexpensive culture media, higher productivities and absence of feedback inhibition due to secretion to the culture media (Majdi et al. 2016). Several authors have reported either the direct production of artemisinin or its precursor, artemisinic acid, followed by a chemical conversion to artemisinin (Paddon and Keasling 2014; Keasling 2012).

**Production in *E. coli*** This microorganism has been employed as a microbial cell factory for the production of target sesquiterpenes or their precursor compounds. In the latter case, specific sesquiterpenes can be obtained from those precursors by synthetic organic chemistry (Majdi et al. 2016). As mentioned above, the Semi-synthetic Artemisinin Project was initiated in 2004 with the aim of producing an artemisinic precursor in an engineered microorganism. *E. coli* was the first microorganism chosen during the initial stages of the project development (Paddon and Keasling, 2014). Several groups had previously engineered the MEP pathway in order to increase the production of isoprenoids in *E. coli* (Farmer and Liao, 2001; Kajiwara et al. 1997; Kim and Keasling, 2001). Increasing the flux through the pathway by balancing the pool of GA3P and pyruvate or overexpressing DXS and IPP isomerase led to an increase in isoprenoids production; however, they were low (at the range of mg/l), most probably due to limitations on the control mechanisms that inhibited synthesis in the native host.

However, and based on previous reports, the Semi-synthetic Artemisinin Project was able to significantly improve the isoprenoids production by a heterologous expression of the *S. cerevisiae* MVA pathway in *E. coli*. The heterologous expression of the *S. cerevisiae* MVA pathway was carried out by introducing two plasmids into *E. coli*: the *MevT* plasmid, which contained the *mevT* operon constituted by *atoB*, *ERG13* and *tHMG1* genes, and the *MevB* plasmid, which contained the *mevB* operon formed by *idi*, *ispA*, *MVD1*, *ERG8* and *ERG12* genes. The *mevT* operon (also called as the “top pathway”) is needed for the conversion of acetyl-CoA to mevalonate, while the *mevB* operon (also called as the “bottom pathway”) is necessary to convert mevalonate into FPP (Fig. 4.3). Both plasmids were coupled with the expression of a synthetic codon-optimised version of the *A. annua* ADS, which resulted in the accumulation of the artemisinin precursor amorpha-4,11-diene. This engineered *E. coli* could produce 112 mg/l of amorpha-4,11-diene (Martin et al. 2003). Nevertheless, the productivity of this strain has been underestimated due to the volatile nature of amorpha-4,11-diene, which evaporates from the fermenter. The presence of amorpha-4,11-diene in the exhaust gas was corroborated by a NMR spectroscopy analysis. The application of an in situ product removal strategy by employing a two-phase partitioning bioreactor with a dodecane organic phase allowed improving the amorpha-4,11-diene production to a final concentration that reached 0.5 g/l (Newman et al. 2006).

On the other hand, despite the high levels of amorpha-4,11-diene produced through the optimisation of the fermentation conditions, it was found that the accumulation of intermediates limited the carbon flux and inhibited cell growth (Pitera et al. 2007). This was due to the fact that the expression of the three enzymes encoded by the *mevT* operon was imbalanced, which led to the accumulation of HMG-CoA that inhibited growth. A synthetic combinatorial approach showed that the reduced expression of HMGS and the overexpression of a truncated HMGR could reduce growth inhibition and HMG-CoA accumulation. Consequently, higher titres of mevalonate were produced. Therefore, it was demonstrated that the carbon flux balancing through the heterologous MVA pathway is a key determinant to optimise isoprenoid biosynthesis in engineered *E. coli* (Pitera et al. 2007).

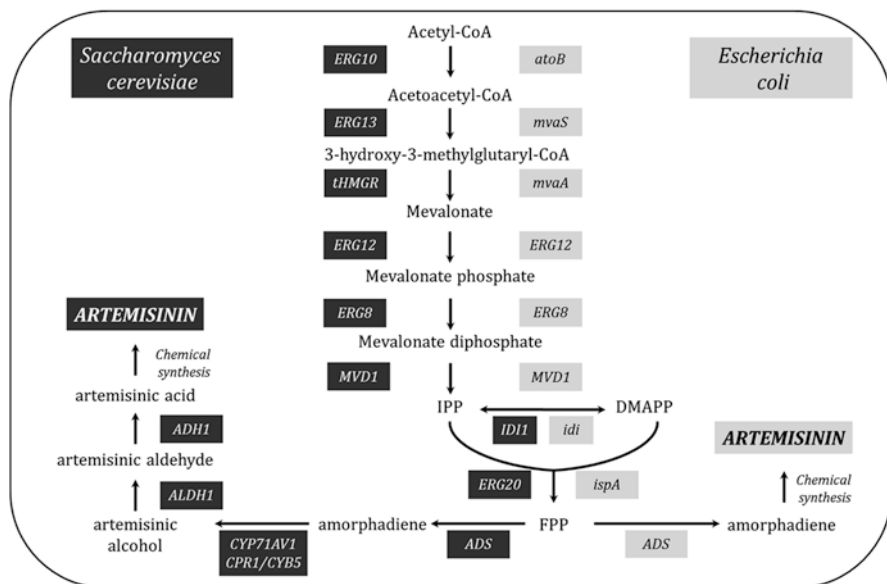


**Fig. 4.3** Metabolic engineering strategies to produce artemisinin in *Saccharomyces cerevisiae* and *Escherichia coli*. *ERG10* and *atoB* acetoacetyl-CoA thiolase, *ERG13* and *mvaS* HMG-CoA synthase, *mvaA* HMG-CoA reductase, *tHMG* truncated HMG-CoA reductase *ERG12* mevalonate kinase, *ERG8* phosphomevalonate kinase, *MVD1* mevalonate diphosphate decarboxylase, *IDI1* and *idi* isopentenyl diphosphate isomerase, *ERG20* and *ispA* farnesyl diphosphate synthase, *ADS* amorpha-4,11-diene synthase, *CYP71AV1* cytochrome P450 monooxygenase, *CYB5* cytochrome b5, *CPR1* cytochrome P450 reductase, *ADH1* alcohol dehydrogenase 1, *ALDH1* aldehyde dehydrogenase, *FPP* farnesyl diphosphate. (Figure adapted from Paddon and Keasling (2014))

Considering that the expression of *mevT* operon led to an imbalance in the carbon flux through the MVA, further efforts were made to improve the production of amorpha-4,11-diene by increasing the mevalonate production. Yeast genes for HMGs and HMGR (the second and third enzymes in the pathway) were replaced with equivalent genes from *Staphylococcus aureus*, which allowed doubling the concentrations of amorpha-4,11-diene (Fig. 4.3). Moreover, amorpha-4,11-diene titres were further increased by developing a novel nitrogen- and carbon-limited fed-batch fermentation process. This optimisation led to an average titre of 27.4 g/l amorpha-4,11-diene. Subsequent chemical conversion of amorpha-4,11-diene to artemisinin would allow achieving the 25 g/l estimated concentration that is required for the commercial feasibility of the artemisinin semi-synthetic production (Tsuruta et al. 2009).

**Production of Artemisinin in Engineered Yeasts** Since P450 enzymes from eukaryotic origin (such as *CYP71AV1*) cannot be correctly expressed in *E. coli* (Paddon and Keasling 2014), *S. cerevisiae* was considered as a host for artemisinin production. The advantages of this system over *E. coli* are the existence in



*S. cerevisiae* of a MVA pathway that produces FPP, and, as it is a eukaryotic organism, the cell environment is more suitable for the expression of plant enzymes (Majdi et al. 2016). Moreover, this system is more industrially robust and less susceptible to phage contamination (Krivoruchko and Nielsen 2015).

One of the first reports of heterologous sesquiterpene production in yeast dealt with the expression of epi-cedrol synthase and the production of epi-cedrol from the endogenous FPP pool. In order to increase epi-cedrol yields, further modifications included the changing of the mating type and the expression of *UPC2-1* (a semi-dominant mutant version of *UPC2*, which is a transcription factor previously demonstrated to increase the carbon flux towards the sterol biosynthesis), a truncated version of HMGR (tHMGR) and FDS. The highest accumulation of epi-cedrol was obtained in a MAT $\alpha$  strain that co-expresses *UPC2-1*, tHMGR and epi-cedrol synthase (Jackson et al. 2003). A few years later, the production of amorpha-4,11-diene was achieved in *S. cerevisiae* CEN.PK113-5D. In this case, *ADS* from *A. annua* was expressed under a galactose-inducible promoter, either after homologous recombination into the host genome or delivered by a suitable yeast expression vector. Although higher amounts of amorpha-4,11-diene were obtained in the plasmid-transformed yeast, as compared to the genomic-transformed one (600 and 100  $\mu\text{g/l}$ , respectively), after a 16-day batch, yields were low, possibly due to an FPP shortage (Lindahl et al. 2006).

The production of artemisinic acid in *S. cerevisiae* was first reported by Ro et al. These authors were able to express an engineered MVA pathway in *S. cerevisiae* (a derivative from the S288C strain), together with the specific enzymes from artemisinin biosynthesis *ADS*, *CYP71AV1* and *CPR* from *A. annua*. Since the expression of *ADS* alone rendered low levels of amorpha-4,11-diene, several modifications were made in the MVA pathway in order to increase FPP formation. By combining the overexpression of two copies of a truncated form of HMGR (tHMGR), the downregulation of *ERG9* (a gene encoding SQS, which competes with *ADS* for FPP) by a methionine repressible promoter (PMET3); the overexpression of *UPC2-1*, which is an activated allele of *UPC2* (a global transcription factor which positively affects the expression of some enzymes from the MVA pathway); and the overexpression of the gene encoding FDS (*ERG20*), the authors achieved a 500-fold increase in amorpha-4,11-diene production (~150 mg/l), as compared to previous reports. Further expression of *CYP71AV1* and *CPR* in this strain led to a high extracellular accumulation of artemisinic acid, up to 115 mg in a 1 liter aerated bioreactor (Ro et al. 2006).

In order to increase amorpha-4,11-diene accumulation in *S. cerevisiae*, Shiba et al. engineered a pyruvate dehydrogenase bypass for enhancing the supply of acetyl-CoA to the MVA pathway. By co-expressing endogenous acetaldehyde dehydrogenase and a mutant version of acetyl-CoA synthetase from *Salmonella enterica*, the carbon flux through the MVA pathway was increased, and consequently, higher amounts of amorpha-4,11-diene were obtained (Shiba et al. 2007).

The research group involved in the Semi-synthetic Artemisinin Project published the development of an industrial fermentation process for the production of artemisinin in yeast. They were able to improve artemisinic acid accumulation up to 2.5 g/l (a ~25-fold increase, as compared to that reported by Ro et al. 2006). The development of a fed-batch process using a defined medium with galactose as both carbon source and as inducer allowed the production of 1.3 g/l of artemisinic acid. The addition of methionine for downregulating *ERG9* (controlled by the *MET3* repressible promoter) increased the artemisinic acid content, up to 1.8 g/l. Finally, the development of an algorithm that controlled both the feed and the agitation led to the maximum production of artemisinic acid (2.5 g/l) (Lenihan et al. 2008). In a following publication, researchers from Amyris Inc. and the University of California developed a process to produce amorpha-4,11-diene from *S. cerevisiae* and a three-step chemical conversion to obtain dihydroartemisinic acid (Westfall et al. 2012). Based on the CEN.PK2 strain, the authors constructed a completely new one, since the CEN.PK2 strain physiology is better characterised and it has high sporulation efficiency, as compared to the previously employed S288C strain. The chromosomal modifications included the overexpression of every enzyme on the MVA pathway and the repression of *ERG9* by the repressible *MET3* promoter. Strains transformed with a plasmid carrying ADS achieved high accumulation of amorpha-4,11-diene (~1,2 g/l), whereas the same strain transformed with a plasmid carrying ADS, *CYP71AV1* and *CPR* produced artemisinic acid, but to a lower extent (~200 mg/l). In a previous report, they had shown that artemisinic acid accumulation led to plasmid instability and the induction of PDR genes in yeasts (Ro et al. 2008). The authors then focused on the amorpha-4,11-diene production, which was improved up to ~40 g/l with further modifications including the deletion of *GAL80* (negative regulator of the galactose regulon) to avoid the need for galactose addition and culture medium optimization. Finally, they developed a chemical process for the conversion of amorpha-4,11-diene to dihydroartemisinic acid, with an overall yield of 48.4% (Westfall et al. 2012).

In one of the latest publications of the researchers involved in the Semi-synthetic Artemisinin Project, the artemisinic acid accumulation in yeasts was reported to reach 25 g/l. In order to achieve this result, Y337 strain (Westfall et al. 2012) was improved by a proper balance between *CYP71AV1* and *CPR1* expression (a reduced *CPR1* expression increased cell viability) (Fig. 4.3), together with the expression of three new genes isolated from *A. annua* (apart from ADS): *CYB5* (encoding cytochrome b5, which enhances the reaction rate of cytochromes P450), *ALDH1* (artemisinic aldehyde dehydrogenase) and *ADH1* (a putative alcohol dehydrogenase). The process was further improved by the development of an extractive fermentation using isopropyl myristate (10% v/v) and a feedback-controlled ethanol pulse-feed process (Paddon et al. 2013).

In a very recent report, the disruption of *PAH1* gene, which encodes phosphatidic acid phosphatase (responsible for the generation of neutral triglycerides from phosphatidic acid) in *S. cerevisiae* through CRISPR/Cas9 technology, provoked a drastic ER proliferation. The co-expression of ADS, *CYP71AV1* and *CPR* from *A. annua* in this yeast strain led to a 2-fold increase in artemisinic acid, as compared to the wild-type strain (Arendt et al. 2017).

#### 4.5.2.7 Metabolic Engineering in Moss

Over the last years, the moss *Physcomitrella patens* has emerged as a biotechnological platform for recombinant protein production in the biopharmaceutical industry. A biotechnological company that employs this biological platform was founded in 1999 for biotherapeutic production. Moreover, this platform has recently been considered for the heterologous production of plant secondary metabolites. In mosses, the haploid phase dominates the growth cycle (protonema), which can be cultured easily under sterile conditions in different suitable containers such as Petri dishes, Erlenmeyer flasks and bioreactors. Mosses grow photoautotrophically in simple media containing inorganic salts without vitamins, sugars or phytohormones. These medium characteristics assure a low risk of contamination, high volume and cost-effective media that enable a simply scaling-up process. Moss tissue cultures are biochemically and genetically stable over time, and they have proved to be very resistant to stress conditions. Genes can be efficiently introduced in *P. patens* tissues by homologous recombination. In addition, these cultures can be preserved under liquid nitrogen for years (Reski et al. 2015; Simonsen et al. 2009).

*P. patens* have been genetically modified in order to overexpress two sesquiterpene synthases, patchoulol synthase (PTS) and santelene synthase (SS). These enzymes are involved in the first steps in the biosynthesis of patchoulol and  $\beta$ -santalene, respectively. They were expressed in the cytosol and in plastids of moss tissue cultures. In cytosol, these enzymes were also co-expressed with a truncated version of the enzyme HMGR (tHMGR). In this tHMGR, the regulatory domain was deleted in order to accomplish enzyme deregulation, which led to increased levels of isoprenoid precursors (Donald et al. 1997). *P. patens* overexpressing PTS in the cytosol accumulated patchoulol to a level of 0.2–0.8 mg/g dry weight. The co-expression of PTS with the tHMGR version resulted in an increase of patchoulol content that reached 1.34 mg/g dry weight. Transgenic lines expressing PTS in plastid accumulated 0.2 mg/g dry weight of patchoulol. *P. patens* overexpressing SS and tHMGR in the cytosol rendered a santelene content of 0.003–0.022 mg/g dry weight, while in cell lines expressing SS alone santelene was not detected. When SS was targeted to chloroplasts, the santelene content was 0.039–0.035 mg/g dry weight, which was the highest yield ever achieved in moss tissues (Zhan et al. 2014). The authors proposed that these results offer the possibility to produce other STLs such as parthenolides or thapsigargin in *P. patens*, although productivities should be increased.

## 4.6 Conclusion

The combination of techniques such as mass spectrometry imaging (MSI), fluorescence resonance energy transfer (FRET)-based nanosensors and laser microdissection together with metabolic analyses (GC-MS, LC-MS, NMR) has allowed identifying and localising the synthesis of secondary metabolites, not only at the level of organs and tissues but also at the cellular level. In addition, it has also allowed performing a more specific analysis of the transcriptome of the cells and tissues producing STLs,

leading to the isolation of new genes involved in their biosynthesis. Provided the biosynthetic pathway is partially or fully elucidated, many putative heterologous hosts can be genetically modified in order to produce the desired metabolites. For instance, metabolic engineering has allowed establishing transgenic plants in *A. annua*, which presented higher concentrations than the plants traditionally used in artemisinin production. It is not always possible to apply this technology to all STL-producing plants, since transformation protocols for some of them have not been developed yet. The alternative may be the use of fast-growing and high biomass producer crops whose agronomic practices are well known. The metabolic engineering in heterologous hosts may have undesirable effects such as the accumulation of STLs in their conjugated forms with cysteine, sugars and glutathione, as is the case of the production of parthenolides in *N. benthamiana*. Some factors must be taken into account for transgenic plant development, such as the availability of lands that are normally intended for crop cultures, public acceptance, environmental impact and the investment required to obtain the approvals of the governmental agencies.

The *in vitro* cultivation of plant cells and organs and the potential use of *P. patens* constitute an alternative to the natural production of STLs since they offer a controlled system and shorter production cycles. The main disadvantage is still their low productivities and the initial investment costs to build an industrial plant equipped with bioreactors. The bulk of knowledge accumulated over decades about the biochemistry, physiology, genetics and scale-up fermentation of microorganisms has allowed yeast and *E. coli* to be considered the first choice to design metabolic engineering cells to produce either STLs or their precursors. Metabolic engineered yeasts have probably shown better performances than *E. coli* because they are able to express more efficiently the cytochrome P450 enzymes involved in STL biosynthesis.

Recently, Sanofi Pasteur has acquired the rights for the production of artemisinin in recombinant yeasts, a development of the Dr. Keasling group from the University of California, but the fall in the market price of artemisinin below \$ 250 per kg caused the process to be economically unachievable (Peplow 2016).

In summary, there are many biotechnological systems available for the industrial production of STLs; however, all of them must be economically competitive when compared to the production and extraction of the metabolites from their natural sources.

## References

- Ahlatw S, Saxena P, Alam P et al (2014) Modulation of artemisinin biosynthesis by elicitors, inhibitor, and precursor in hairy root cultures of *Artemisia annua* L. *J Plant Interact* 9:811–824
- Alam P, Abdin MZ (2011) Over-expression of HMG-CoA reductase and amorpha-4,11-diene synthase genes in *Artemisia annua* L. and its influence on artemisinin content. *Plant Cell Rep* 30(10):1919–1928
- Andersen TB, López CQ, Manczak T et al (2015) Thapsigargin from *Thapsia* L. to mipsagargin. *Molecules* 20(4):6113–6127
- Aquil S, Husaini AM, Abdin MZ et al (2009) Overexpression of the HMG-CoA reductase gene leads to enhanced artemisinin biosynthesis in transgenic *Artemisia annua* plants. *Planta Med* 75(13):1453–1458

- Arendt P, Miettinen K, Pollier J et al (2017) An endoplasmic reticulum-engineered yeast platform for overproduction of triterpenoids. *Metab Eng* 40:165–175
- Arsenault PR, Vail D, Wobbe KK et al (2010a) Reproductive development modulates gene expression and metabolite levels with possible feedback inhibition of artemisinin in *Artemisia annua*. *Plant Physiol* 154(2):958–968
- Arsenault PR, Vail DR, Wobbe KK et al (2010b) Effect of sugars on artemisinin production in *Artemisia annua* L.: transcription and metabolite measurements. *Molecules* 15(4):2302–2318
- Atanasov AG, Waltenberger B, Pferschy-Wenzig EM et al (2015) Discovery and resupply of pharmacologically active plant-derived natural products: a review. *Biotechnol Adv* 33(8):1582–1614
- Baldi A, Dixit VK (2008) Yield enhancement strategies for artemisinin production by suspension cultures of *Artemisia annua*. *Bioresour Technol* 99(11):4609–4614
- Banyai W, Kirdmanee C, Mii M et al (2010) Overexpression of farnesyl pyrophosphate synthase (FDS) gene affected artemisinin content and growth of *Artemisia annua* L. *Plant Cell Tissue Organ Cult* 103:255–265
- Baque MA, Moh SH, Lee EJ et al (2012) Production of biomass and useful compounds from adventitious roots of high-value added medicinal plants using bioreactor. *Biotechnol Adv* 30(6):1255–1267
- Bouvier F, Rahier A, Camara B (2005) Biogenesis, molecular regulation and function of plant isoprenoids. *Prog Lipid Res* 44(6):357–429
- Caretto S, Quarta A, Durante M et al (2011) Methyl jasmonate and miconazole differently affect artemisinin production and gene expression in *Artemisia annua* suspension cultures. *Plant Biol (Stuttg)* 13(1):51–58
- Chadwick M, Trewin H, Gawthrop F et al (2013) Sesquiterpenoids lactones: benefits to plants and people. *Int J Mol Sci* 14(6):12780–12805
- Chang YJ, Song SH, Park SH et al (2000) Amorpha- 4,11-diene synthase of *Artemisia annua*: cDNA isolation and bacterial expression of a terpene synthase involved in artemisinin biosynthesis. *Arch Biochem Biophys* 383:178–184
- Chaturvedi D (2011) Sesquiterpene lactones: structural diversity and their biological activities. In: Tiwari V, Mishra B (eds) Opportunity, challenge and scope of natural products in medicinal chemistry. Research Signpost, Kerala, pp 313–334
- Chen DH, Liu CJ, Ye HC et al (1999) Ri-mediated transformation of *Artemisia annua* with a recombinant farnesyl diphosphate synthase gene for artemisinin production. *Plant Cell Tissue Organ Cult* 57(3):157–162
- Chen DH, Ye HC, Li GF (2000) Expression of a chimeric farnesyl diphosphate synthase gene in *Artemisia annua* L. transgenic plants via *Agrobacterium tumefaciens*-mediated transformation. *Plant Sci* 155(2):179–185
- Chen JL, Fang HM, Ji YP et al (2011) Artemisinin biosynthesis enhancement in transgenic *Artemisia annua* plants by downregulation of the  $\beta$ -Caryophyllene synthase gene. *Planta Med* 77(15):1759–1765
- Chen Y, Shen Q, Wang Y et al (2013) The stacked over-expression of *FDS*, *CYP71AV1* and *CPR* genes leads to the increase of artemisinin level in *Artemisia annua* L. *Plant Biotechnol Rep* 7(3):287–295
- Chen M, Yan T, Shen Q et al (2017) Glandular trichome-specific wrky 1 promotes artemisinin biosynthesis in *Artemisia annua*. *New Phytol* 214(1):304–316
- de Kraker JW, Franssen MCR, de Groot A et al (1998) (+)-Germacrene a biosynthesis—the committed step in the biosynthesis of bitter sesquiterpene lactones in chicory. *Plant Physiol* 117:1381–1392
- de Kraker JW, Franssen MCR, Joerink M et al (2002) Biosynthesis of costunolide, dihydrocostunolide, and leucodin. Demonstration of cytochrome P450-catalyzed formation of the lactone ring present in sesquiterpene lactones of chicory. *Plant Physiol* 129:257–268
- Diaz-Chavez ML, Moniodis J, Madilao LL et al (2013) Biosynthesis of sandalwood oil: *Santalum album* CYP76F cytochromes P450 produce santalols and bergamotol. *PLoS One* 8(9):e75053. <https://doi.org/10.1371/journal.pone.0075053>
- Dilshad E, Cusido RM, Palazon J et al (2015) Enhanced artemisinin yield by expression of *rol* genes in *Artemisia annua*. *Malar J* 14:424

- Donald KA, Hampton RY, Fritz IB (1997) Effects of overproduction of the catalytic domain of 3-hydroxy-3-methylglutaryl coenzyme a reductase on squalene synthesis in *Saccharomyces cerevisiae*. *Appl Environ Microbiol* 63(9):3341–3344
- Drew DP, Dueholm B, Weitzel C et al (2013) Transcriptome analysis of *Thapsia laciniata* Rouy provides insights into terpenoid biosynthesis and diversity in Apiaceae. *Int J Mol Sci* 14(5):9080–9098
- Durante M, Caretto S, Quarta A et al (2011)  $\beta$ -Cyclodextrins enhance artemisinin production in *Artemisia annua* suspension cell cultures. *Appl Microbiol Biotechnol* 90(6):1905–1913
- Eibl R, Eibl D (2008) Design of bioreactors suitable for plant cell and tissue cultures. *Phytochem Rev* 7:593–598
- Eibl R, Werner S, Eibl D (2009) Disposable bioreactors for plant liquid cultures at litre-scale. *Eng Life Sci* 9:156–164
- Eljounaidi K, Cankar K, Comino C et al (2014) Cytochrome P450s from *Cynara cardunculus* L. CYP71AV9 and CYP71BL5, catalyze distinct hydroxylations in the sesquiterpene lactone biosynthetic pathway. *Plant Sci* 223:59–68
- Fan R, Li Y, Li C, Zhang Y (2015) Differential microRNA analysis of glandular trichomes and young leaves in *Xanthium strumarium* L. reveals their putative roles in regulating terpenoid biosynthesis. *PLoS One* 10(9):e0139002. <https://doi.org/10.1371/journal.pone.0139002>
- Farhi M, Marhevka E, Ben-Ari J et al (2011) Generation of the potent anti-malarial drug artemisinin in tobacco. *Nat Biotechnol* 29(12):1072–1074
- Farmer WR, Liao JC (2001) Precursor balancing for metabolic engineering of lycopene production in *Escherichia coli*. *Biotechnol Prog* 17:57–61
- Gershenzon J, Dudareva N (2007) The function of terpene natural products in the natural world. *Nat Chem Biol* 3:408–414
- Han JL, Liu BY, Ye HC et al (2006) Effects of overexpression of the endogenous farnesyl diphosphate synthase on the artemisinin content in *Artemisia annua* L. *J Integr Plant Biol* 48(4):482–487
- Han J, Wang H, Kanagarajan S et al (2016) Promoting artemisinin biosynthesis in *Artemisia annua* plants by substrate channeling. *Mol Plant* 9(6):946–948
- Hong GJ, Hu WL, Li JX et al (2009) Increased accumulation of artemisinin and anthocyanins in *Artemisia annua* expressing the *Arabidopsis* blue light receptor *CRY1*. *Plant Mol Biol Report* 27(3):334–341
- Jackson BE, Hart-Wells EA, Matsuda SPT (2003) Metabolic engineering to produce sesquiterpenes in yeast. *Org Lett* 5(10):1629–1632
- Ji Y, Xiao J, Shen Y et al (2014) Cloning and characterization of AabHLH1, a bHLH transcription factor that positively regulates artemisinin biosynthesis in *Artemisia annua*. *Plant Cell Physiol* 55(9):1592–1604
- Jiang W, Fu X, Pan Q et al (2016) Overexpression of *AaWRKY1* leads to an enhanced content of artemisinin in *Artemisia annua*. *Biomed Res Int* 2016:7314971. <https://doi.org/10.1155/2016/7314971>
- Jones CG, Keeling CI, Ghisalberti EL et al (2008) Isolation of cDNAs and functional characterisation of two multi-product terpene synthase enzymes from sandalwood, *Santalum album* L. *Arch Biochem Biophys* 477(1):121–130
- Jones CG, Moniodis J, Zulak KG et al (2011) Sandalwood fragrance biosynthesis involves sesquiterpene synthases of both the terpene synthase (TPS)-a and TPS-b subfamilies, including santalene synthases. *J Biol Chem* 286(20):17445–17454
- Kajiwarra S, Fraser PD, Kondo K et al (1997) Expression of an exogenous isopentenyl diphosphate isomerase gene enhances isoprenoid biosynthesis in *Escherichia coli*. *Biochem J* 324:421–426
- Keasling JD (2012) Synthetic biology and the development of tools for metabolic engineering. *Metab Eng* 14(3):189–195
- Kiani BH, Suberu J, Mirza B (2016) Cellular engineering of *Artemisia annua* and *Artemisia dubia* with the *rol ABC* genes for enhanced production of potent anti-malarial drug artemisinin. *Malar J* 15(1):252. <https://doi.org/10.1186/s12936-016-1312-8>

- Kim SW, Keasling JD (2001) Metabolic engineering of the nonmevalonate isopentenyl diphosphate synthesis pathway in *Escherichia coli* enhances lycopene production. *Biotechnol Bioeng* 72:408–415
- Kolewe ME, Gaurav V, Roberts SC (2008) Pharmaceutically active natural product synthesis and supply via plant cell culture technology. *Mol Pharm* 5(2):243–256
- Krivoruchko A, Nielsen J (2015) Production of natural products through metabolic engineering of *Saccharomyces cerevisiae*. *Curr Opin Biotechnol* 35:7–15
- Lei C, Ma D, Pu G et al (2011) Foliar application of chitosan activates artemisinin biosynthesis in *Artemisia annua* L. *Ind Crop Prod* 33:176–182
- Lenihan JR, Tsuruta H, Diola D et al (2008) Developing an industrial artemisinic acid fermentation process to support the cost-effective production of antimalarial artemisinin-based combination therapies. *Biotechnol Prog* 24(5):1026–1032
- Li Y, Chen F, Li Z et al (2016) Identification and functional characterization of sesquiterpene synthases from *Xanthium strumarium*. *Plant Cell Physiol* 57(3):630–641
- Lichtenthaler HK (1999) The 1-deoxy-d-xylulose- 5-phosphate pathway of isoprenoid biosynthesis in plants. *Annu Rev Plant Physiol Plant Mol Biol* 50:47–65
- Lindahl AL, Olsson ME, Mercke P et al (2006) Production of the artemisinin precursor amorpha-4,11-diene by engineered *Saccharomyces cerevisiae*. *Biotechnol Lett* 28(8):571–580
- Liu CZ, Guo C, Wang YC et al (2002) Effect of light irradiation on hairy root growth and artemisinin biosynthesis of *Artemisia annua* L. *Process Biochem* 38:581–585
- Liu CZ, Guo G, Wang YC et al (2003) Comparison of various bioreactors on growth and artemisinin biosynthesis of *Artemisia annua* L. shoot cultures. *Process Biochem* 39(1):45–49
- Liu Q, Manzano D, Tanić N et al (2014) Elucidation and in planta reconstitution of the parthenolide biosynthetic pathway. *Metab Eng* 23:145–153
- Lu X, Shen Q, Zhang L et al (2013a) Promotion of artemisinin biosynthesis in transgenic *Artemisia annua* by overexpressing *ADS*, *CYP71AV1* and *CPR* genes. *Ind Crop Prod* 49:380–385
- Lu X, Zhang L, Zhang F et al (2013b) *AaORA*, a trichome-specific AP2/ERF transcription factor of *Artemisia annua*, is a positive regulator in the artemisinin biosynthetic pathway and in disease resistance to *Botrytis cinerea*. *New Phytol* 198(4):1191–1202
- Lu X, Zhang F, Shen Q et al (2014) Overexpression of allene oxide cyclase improves the biosynthesis of artemisinin in *Artemisia annua* L. *PLoS One* 9(3):e91741. <https://doi.org/10.1371/journal.pone.0091741>
- Luczkiewicz M, Zárate R, Dembińska-Migas W et al (2002) Production of pulchelin E in hairy roots, callus and suspension cultures of *Rudbeckia hirta* L. *Plant Sci* 163:91–100
- Lv Z, Wang S, Zhang F et al (2016a) Overexpression of a novel NAC domain-containing transcription factor gene (*AaNAC1*) enhances the content of artemisinin and increases tolerance to drought and *Botrytis cinerea* in *Artemisia annua*. *Plant Cell Physiol* 57(9):1961–1971
- Lv Z, Zhang F, Pan Q et al (2016b) Branch pathway blocking in *Artemisia annua* is a useful method for obtaining high yield Artemisinin. *Plant Cell Physiol* 57(3):588–602
- Ma C, Wang H, Lu X et al (2009a) Terpenoid metabolic profiling analysis of transgenic *Artemisia annua* L. by comprehensive two-dimensional gas chromatography time-of-flight mass spectrometry. *Metabolomics* 5(4):497–506
- Ma D, Pu G, Lei C et al (2009b) Isolation and characterization of *AaWRKY1*, an *Artemisia annua* transcription factor that regulates the amorpha-4,11-diene synthase gene, a key gene of artemisinin biosynthesis. *Plant Cell Physiol* 50:2146–2161
- Majdi M, Liu Q, Karimzadeh G et al (2011) Biosynthesis and localization of parthenolide in glandular trichomes of feverfew (*Tanacetum parthenium* l. Schulz bip.) *Phytochemistry* 72:1739–1750
- Majdi M, Karimzadeh G, Malboobi MA (2014) Spatial and developmental expression of key genes of terpene biosynthesis in *Tanacetum parthenium*. *Biol Plant* 58:379–384
- Majdi M, Abdollahi MR, Maroufi A (2015) Parthenolide accumulation and expression of genes related to parthenolide biosynthesis affected by exogenous application of methyl jasmonate and salicylic acid in *Tanacetum parthenium*. *Plant Cell Rep* 34:1909–1918

- Majdi M, Ashengroph M, Abdollahi MR (2016) Sesquiterpene lactone engineering in microbial and plant platforms: parthenolide and artemisinin as case studies. *Appl Microbiol Biotechnol* 100(3):1041–1059
- Malarz J, Stojakowska A, Kisiel W (2002) Sesquiterpene lactones in a hairy root culture of *Cichorium intybus*. *Z Naturforsch C* 57(11–12):994–997
- Martin VJ, Pitera DJ, Withers ST et al (2003) Engineering a mevalonate pathway in *Escherichia coli* for production of terpenoids. *Nature Biotechnol* 21:796–802
- Matías-Hernández L, Jiang W, Yang K et al (2017) *AaMYB1* and its orthologue *AtMYB61* affect terpene metabolism and trichome development in *Artemisia annua* and *Arabidopsis thaliana*. *Plant J* 90(3):520–534
- May B, Lange BM, Wüst M (2013) Biosynthesis of sesquiterpenes in grape berry exocarp of *Vitis vinifera* L.: evidence for a transport of farnesyl diphosphate precursors from plastids to the cytosol. *Phytochemistry* 95:135–144
- Menin B, Comino C, Portis E et al (2012) Genetic mapping and characterization of the globe artichoke (+)-germacrene synthase gene, encoding the first dedicated enzyme for biosynthesis of the bitter sesquiterpene lactone cynaropicrin. *Plant Sci* 190:1–8
- Mercke P, Bengtsson M, Bouwmeester HJ et al (2000) Molecular cloning, expression, and characterization of amorpha-4,11-diene synthase, a key enzyme of artemisinin biosynthesis in *Artemisia annua* L. *Arch Biochem Biophys* 381:173–180
- Moniodis J, Jones CG, Barbour EL et al (2015) The transcriptome of sesquiterpenoid biosynthesis in heartwood xylem of western Australian sandalwood (*Santalum spicatum*). *Phytochemistry* 113:79–86
- Mora-Pale M, Sanchez-Rodriguez SP, Linhardt RJ et al (2013) Metabolic engineering and *in vitro* biosynthesis of phytochemicals and non-natural analogues. *Plant Sci* 210:10–24
- Murthy HN, Lee EJ, Paek KY (2014) Production of secondary metabolites from cell and organ cultures: strategies and approaches for biomass improvement and metabolite accumulation. *Plant Cell Tissue Organ Cult* 118(1):1–16
- Nafis T, Akmal M, Ram M et al (2011) Enhancement of artemisinin content by constitutive expression of the HMG-CoA reductase gene in high-yielding strain of *Artemisia annua* L. *Plant Biotechnol Rep* 5(1):53–60
- Nagegowda DA (2010) Plant volatile terpenoid metabolism: biosynthetic genes, transcriptional regulation and subcellular compartmentation. *FEBS Lett* 584(14):2965–2973
- Newman JD, Marshall J, Chang M et al (2006) High-level production of amorpha-4,11-diene in a two-phase partitioning bioreactor of metabolically engineered *Escherichia coli*. *Biotechnol Bioeng* 95:684–691
- Nguyen TD, Faraldos JA, Vardakou M et al (2016) Discovery of germacrene A synthases in *Barnadesia spinosa*: the first committed step in sesquiterpene lactone biosynthesis in the basal member of the Asteraceae. *Biochem Biophys Res Commun* 479(4):622–627
- Olofsson L, Lundgren A, Brodelius PE (2012) Trichome isolation with and without fixation using laser microdissection and pressure catapulting followed by RNA amplification: expression of genes of terpene metabolism in apical and sub-apical trichome cells of *Artemisia annua* L. *Plant Sci* 183:9–13
- Paddon CJ, Keasling JD (2014) Semi-synthetic artemisinin: a model for the use of synthetic biology in pharmaceutical development. *Nat Rev Microbiol* 12(5):355–367
- Paddon CJ, Westfall PJ, Pitera DJ et al (2013) High-level semi-synthetic production of the potent antimalarial artemisinin. *Nature* 496(7446):528–532
- Parveen I, Wang M, Zhao J et al (2015) Investigating sesquiterpene biosynthesis in *Ginkgo biloba*: molecular cloning and functional characterization of (E, E)-farnesol and  $\alpha$ -bisabolene synthases. *Plant Mol Biol* 89(4–5):451–462
- Patra N, Srivastava AK (2014) Enhanced production of artemisinin by hairy root cultivation of *Artemisia annua* in a modified stirred tank reactor. *Appl Biochem Biotechnol* 174(6):2209–2222
- Patra N, Srivastava AK (2016) Artemisinin production by plant hairy root cultures in gas- and liquid-phase bioreactors. *Plant Cell Rep* 35(1):143–153



- Pence VC (2011) Evaluating costs for the *in vitro* propagation and preservation of endangered plants. *In Vitro Cell Dev Biol Plant* 47:176–187
- Peplow M (2016) Synthetic biology's first malaria drug meets market resistance. *Nature* 530(7591):389–390
- Pickel B, Drew DP, Manczak T et al (2012) Identification and characterization of a kunzeal synthase from *Thapsia garganica*: implications for the biosynthesis of the pharmaceutical thapsigargin. *Biochem J* 448(2):261–271
- Pitera DJ, Paddon CJ, Newman JD et al (2007) Balancing a heterologous mevalonate pathway for improved isoprenoid production in *Escherichia coli*. *Metab Eng* 9:193–207
- Putalun W, Luealon W, De-Eknamkul W et al (2007) Improvement of artemisinin production by chitosan in hairy root cultures of *Artemisia annua* L. *Biotechnol Lett* 29(7):1143–1146
- Pyle BW, Tran HT, Pickel B et al (2012) Enzymatic synthesis of valerena-4,7(11)-diene by a unique sesquiterpene synthase from the valerian plant (*Valeriana officinalis*). *FEBS J* 279(17):3136–3146
- Ram M, Khan MA, Jha P et al (2010) HMG-CoA reductase limits artemisinin biosynthesis and accumulation in *Artemisia annua* L. plants. *Acta Physiol Plant* 32(5):859–866
- Rani A, Ravikumar P, Reddy MD et al (2013) Molecular regulation of santalol biosynthesis in *Santalum album* L. *Gene* 527(2):642–648
- Rea G, Antonacci A, Lambrea M et al (2011) Integrated plant biotechnologies applied to safer and healthier food production: the Nutra-snack manufacturing chain. *Trends Food Sci Technol* 22:353–366
- Reski R, Parsons J, Decker EL (2015) Moss-made pharmaceuticals: from bench to bedside. *Plant Biotechnol J* 13:1191–1198
- Ricigliano V, Kumar S, Kinison S et al (2016) Regulation of sesquiterpenoid metabolism in recombinant and elicited *Valeriana officinalis* hairy roots. *Phytochemistry* 125:43–53
- Ro DK, Paradise EM, Ouellet M et al (2006) Production of the antimalarial drug precursor artemisinic acid in engineered yeast. *Nature* 440:940–943
- Ro DK, Ouellet M, Paradise EM et al (2008) Induction of multiple pleiotropic drug resistance genes in yeast engineered to produce an increased level of anti-malarial drug precursor, artemisinic acid. *BMC Biotechnol* 8(1):83
- Sa G, Mi M, He-chun Y et al (2001) Effects of *ipt* gene expression on the physiological and chemical characteristics of *Artemisia annua* L. *Plant Sci* 160(4):691–698
- Schramek N, Wang H, Römisch-Margl W et al (2010) Artemisinin biosynthesis in growing plants of *Artemisia annua*. A  $^{13}\text{CO}_2$  study. *Phytochemistry* 71(2–3):179–187
- Shen Q, Chen YF, Wang T et al (2012) Overexpression of the cytochrome P450 monooxygenase (*cyp71av1*) and cytochrome P450 reductase (*cpr*) genes increased artemisinin content in *Artemisia annua* (Asteraceae). *Genet Mol Res* 11(3):3298–3309
- Shen Q, Lu X, Yan T et al (2016a) The jasmonate-responsive AaMYC2 transcription factor positively regulates artemisinin biosynthesis in *Artemisia annua*. *New Phytol* 210(4):1269–1281
- Shen Q, Yan T, Fu X et al (2016b) Transcriptional regulation of artemisinin biosynthesis in *Artemisia annua* L. *Sci Bull* 61:18–25
- Shiba Y, Paradise EM, Kirby J et al (2007) Engineering of the pyruvate dehydrogenase bypass in *Saccharomyces cerevisiae* for high-level production of isoprenoids. *Metab Eng* 9(2):160–168
- Simonsen HT (2015) Elucidation of terpenoid biosynthesis in non-model plants utilizing transcriptomic data. *Next Generat Seq Appl* 2:111
- Simonsen HT, Drew DP, Lunde C (2009) Perspectives on using *Physcomitrella patens* as an alternative production platform for thapsigargin and other terpenoid drug candidates. *Perspect Medicin Chem* 3:1–6
- Singh ND, Kumar S, Daniell H (2016) Expression of beta-glucosidase increases trichome density and artemisinin content in transgenic *Artemisia annua* plants. *Plant Biotechnol J* 14(3):1034–1045
- Souret FF, Kim Y, Wyslouzil BE et al (2003) Scale-up of *Artemisia annua* L. hairy root cultures produces complex patterns of terpenoid gene expression. *Biotechnol Bioeng* 83(6):653–667

- Talano MA, Wevar Oller AL, González PS et al (2012) Hairy roots, their multiple applications and recent patents. *Recent Pat Biotechnol* 6:115–133
- Tan H, Xiao L, Gao S et al (2015) Trichome and artemisinin biosynthesis in *Artemisia annua*. *Mol Plant* 8(9):1396–1411
- Teoh KH, Polichuk DR, Reed DW et al (2006) *Artemisia annua* L. (Asteraceae) trichome-specific cDNAs reveal CYP71AV1, a cytochrome P450 with a key role in the biosynthesis of the antimalarial sesquiterpene lactone artemisinin. *FEBS Lett* 580:1411–1416
- Teoh KH, Polichuk DR, Reed DW et al (2009) Molecular cloning of an aldehyde dehydrogenase implicated in artemisinin biosynthesis in *Artemisia annua*. *Botany* 87:635–642
- Testone G, Mele G, Di Giacomo E et al (2016) Insights into the sesquiterpenoid pathway by metabolic profiling and de novo transcriptome assembly of stem-Chicory (*Cichorium intybus* Cultigroup “Catalogna”). *Front Plant Sci* 8(7):1676
- Tholl D (2015) Biosynthesis and biological functions of terpenoids in plants. *Adv Biochem Eng Biotechnol* 148:63–106
- Tholl D, Chen F, Petri J et al (2005) Two sesquiterpene synthases are responsible for the complex mixture of sesquiterpenes emitted from *Arabidopsis* flowers. *Plant J* 42(5):757–771
- Ting HM, Wang B, Rydén AM et al (2013) The metabolite chemotype of *Nicotiana benthamiana* transiently expressing artemisinin biosynthetic pathway genes is a function of CYP71AV1 type and relative gene dosage. *New Phytol* 199(2):352–366
- Torkamani M, Abbaspour N, Jafari M et al (2014a) Elicitation of valerenic acid in the hairy root cultures of *Valeriana officinalis* L. (Valerianaceae). *Trop J Pharm Res* 13:943–947
- Torkamani M, Jafari M, Abbaspour N et al (2014b) Enhanced production of valerenic acid in hairy root culture of *Valeriana officinalis* by elicitation. *Central Eur. J Biol* 9(9):853–863
- Towler MJ, Weathers PJ (2007) Evidence of artemisinin production from IPP stemming from both the mevalonate and the nonmevalonate pathways. *Plant Cell Rep* 26(12):2129–2136
- Tsuruta H, Paddon CJ, Eng D et al (2009) High-level production of amorpho-4,11-diene, a precursor of the antimalarial agent artemisinin, in *Escherichia coli*. *PLoS One* 4(2):e4489. <https://doi.org/10.1371/journal.pone.0004489>
- Turconi J, Griolet F, Guevel R et al (2014) Semisynthetic artemisinin, the chemical path to industrial production. *Org Process Res Dev* 18:417–422
- van Herpen TWJM, Cankar K, Nogueira M et al (2010) *Nicotiana benthamiana* as a production platform for artemisinin precursors. *PLoS One* 5(12):e14222. <https://doi.org/10.1371/journal.pone.0014222>
- Vranová E, Coman D, Gruissem W (2012) Structure and dynamics of the isoprenoid pathway network. *Mol Plant* 5(2):318–333
- Vranová E, Coman D, Gruissem W (2013) Network analysis of the MVA and MEP pathways for isoprenoid synthesis. *Annu Rev Plant Biol* 64:665–700
- Wallaart TE, Bouwmeester HJ, Hille J et al (2001) Amorpho-4,11-diene synthase: cloning and functional expression of a key enzyme in the biosynthetic pathway of the novel antimalarial drug artemisinin. *Planta* 212(3):460–465
- Wang JW, Zheng LP, Zhang B et al (2009) Stimulation of artemisinin synthesis by combined cerebroside and nitric oxide elicitation in *Artemisia annua* hairy roots. *Appl Microbiol Biotechnol* 85(2):285–292
- Wang Y, Jing F, Yu S et al (2011) Co-overexpression of the *HMGR* and *FDS* genes enhances artemisinin content in *Artemisia annua* L. *J Med Plant Res* 5(15):3396–3403
- Wang H, Song Y, Shen H et al (2012) Effect of antisense squalene synthase gene expression on the increase of artemisinin content in *Artemisia annua*. In: Çiftçi YÖ (ed) *Transgenic plants - advances and limitations*. InTech, Rijeka, pp 397–406
- Wang B, Kashkooli AB, Sallets A et al (2016) Transient production of artemisinin in *Nicotiana benthamiana* is boosted by a specific lipid transfer protein from *A. annua*. *Metab Eng* 38:159–169
- Wang LY, Zhang Y, Fu XQ et al (2017) Molecular cloning, characterisation and promoter analysis of the isochorismate synthase (*AaICS1*) gene from *Artemisia annua*. *J Zhejiang Univ Sci B* 18(8):662–673

- Wen W, Yu R (2011) Artemisinin biosynthesis and its regulatory enzymes: progress and perspective. *Pharmacogn Rev* 5(10):189–194
- Westfall PJ, Pitera DJ, Lenihan JR et al (2012) Production of amorpho-4,11-diene in yeast, and its conversion to dihydroartemisinic acid, precursor to the antimalarial agent artemisinin. *Proc Natl Acad Sci USA* 109(3):E111–E118
- Wilson SA, Roberts SC (2012) Recent advances towards development and commercialization of plant cell culture processes for the synthesis of biomolecules. *Plant Biotechnol J* 10(3):249–268
- Wu S, Schalk M, Clark A et al (2006) Redirection of cytosolic or plastidic isoprenoid precursors elevates terpene production in plants. *Nat Biotechnol* 24(11):1441–1447
- Xiang L, Zeng L, Yuan Y et al (2012) Enhancement of artemisinin biosynthesis by overexpressing *dxr*, *cyp71av1* and *cpr* in the plants of *Artemisia annua* L. *Plant Omics J* 5(6):503–507
- Xie DY, Ma DM, Judd R et al (2016) Artemisinin biosynthesis in *Artemisia annua* and metabolic engineering: questions, challenges, and perspectives. *Phytochem Rev* 15:1093–1114
- Yeo YS, Nybo SE, Chittiboyina AG et al (2013) Functional identification of valerena-1,10-diene synthase, a terpene synthase catalyzing a unique chemical cascade in the biosynthesis of biologically active sesquiterpenes in *Valeriana officinalis*. *J Biol Chem* 288(5):3163–3173
- Yin H, Zhuang YB, Li EE et al (2015) Heterologous biosynthesis of costunolide in *Escherichia coli* and yield improvement. *Biotechnol Lett* 37:1249–1255
- Yu ZX, Li JX, Yang CQ et al (2012) The jasmonate-responsive AP2/ERF transcription factors AaERF1 and AaERF2 positively regulate artemisinin biosynthesis in *Artemisia annua* L. *Mol Plant* 5(2):353–365
- Zhan X, Zhang YH, Chen DF et al (2014) Metabolic engineering of the moss *Physcomitrella patens* to produce the sesquiterpenoids patchoulol and  $\alpha/\beta$ -santalene. *Front Plant Sci* 18(5):636
- Zhang Y, Teoh KH, Reed DW et al (2008) The molecular cloning of artemisinic aldehyde D-11(13) reductase and its role in glandular trichome-dependent biosynthesis of artemisinin in *Artemisia annua*. *J Biol Chem* 283:21501–21508
- Zhang L, Jing F, Li F et al (2009) Development of transgenic *Artemisia annua* (Chinese wormwood) plants with an enhanced content of artemisinin, an effective anti-malarial drug, by hairpin-RNA-mediated gene silencing. *Biotechnol Appl Biochem* 52(3):199–207
- Zhang Y, Nowak G, Reed DW et al (2011) The production of artemisinin precursors in tobacco. *Plant Biotechnol J* 9(4):445–454
- Zhang F, Lu X, Lv Z et al (2013) Overexpression of the *Artemisia* orthologue of ABA receptor, AaPYL9, enhances ABA sensitivity and improves artemisinin content in *Artemisia annua* L. *PLoS One* 8(2):e56697. <https://doi.org/10.1371/journal.pone.0056697>
- Zhang F, Fu X, Lv Z et al (2015) A basic leucine zipper transcription factor, AabZIP1, connects abscisic acid signaling with artemisinin biosynthesis in *Artemisia annua*. *Mol Plant* 8(1):163–175
- Zhao L, Chang WC, Xiao Y et al (2013) Methylerythritol phosphate pathway of isoprenoid biosynthesis. *Annu Rev Biochem* 82:497–530
- Zheng LP, Guo YT, Wang JW et al (2008) Nitric oxide potentiates oligosaccharide-induced artemisinin production in *Artemisia annua* hairy roots. *J Integr Plant Biol* 50(1):49–55

# Chapter 5

## Chemistry of Sesquiterpene Lactones



Francis J. Barrios

**Abstract** Sesquiterpene lactones are a class of bioactive plant products that display an array of biological and pharmacological activities such as antimicrobial, cytotoxic, anti-inflammatory, antiviral, antibacterial, and antifungal. A vast amount of sesquiterpene molecular structures has been reported, and the largest numbers of these types of compounds can be isolated from the Asteraceae (formerly known as Compositae) family. An important feature of these sesquiterpene lactones is the presence of an  $\alpha$ -methylene- $\gamma$ -lactone moiety which can react with nucleophilic sulfhydryl groups present in enzymes, proteins, and glutathione. The differences in the activities found among sesquiterpene lactones are due to the number of alkylating elements, lipophilicity, and chemical environment. This chapter discusses some of the synthetic pathways and summarizes the chemical transformation and biological activities of these sesquiterpene lactones.

**Keywords** Sesquiterpene lactones · Synthesis · Chemical transformation ·  $\alpha$ -Methylene- $\gamma$ -lactone · Germacranolides · Guaianolides

### 5.1 Synthesis of Sesquiterpene Lactones

The assembly of the core skeleton and the formation of the  $\alpha$ -methylene- $\gamma$ -lactone moiety are two essential steps for the synthesis of sesquiterpene lactones exhibiting a variety of skeleton structures. In the following sections, the different routes for the generation of the ten-membered germacrene carbocycle and the hydroazulene skeleton that is characteristic of the guaiane sesquiterpenoid will be presented. Methodologies for the formation of the  $\alpha$ -methylene- $\gamma$ -lactone and strategies for the synthesis and semi-synthesis of germacranolide and guaianolide derivatives will be considered.

---

F. J. Barrios (✉)

Department of Chemistry and Physics, Bellarmine University, Louisville, KY, USA

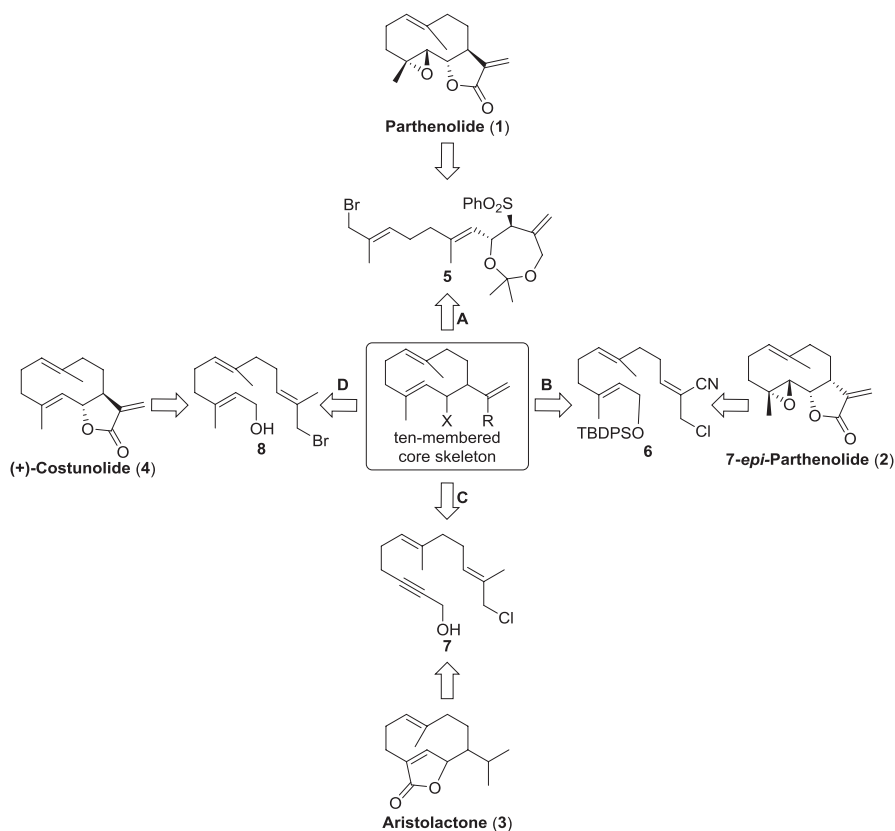
e-mail: [fjavierbarrios@gmail.com](mailto:fjavierbarrios@gmail.com)

### 5.1.1 *General Strategies for the Synthesis of the Germacranolide Skeleton*

Germacranolides are a type of germacrene sesquiterpene lactones that contain a unique ten-membered carbocyclic skeleton that is fused with a  $\gamma$ -lactone. Many classes of cyclic terpenes are made from germacrene intermediates, and it has been demonstrated that these terpenes exhibit a broad range of biological activities. This important intermediate can be converted into other sesquiterpene subclasses such as eudemanes and guaianes, because of the accessibility of germacrene precursors in great quantity (Adio 2009; Bulow and König 2000). Although the total synthesis of germacranolides has been a field of intense research for decades, the synthesis of the ten-membered carbocyclic core has remained a challenge. The cyclodecadiene core is broken down to render cyclized and rearranged fragmented products upon subjection to acidic, basic, and high temperature conditions. Moreover, at room temperature, germacranolides exist as conformer isomers, a phenomenon that creates a challenge for the purification and analysis of the product (Azarken et al. 2008; Minnaard et al. 1999). The general synthetic method for germacrene lactones comprises four basic steps: (a) the synthesis of medium size rings by a direct method, (b) the regio- and stereoselective installation of the (E) and (Z) bonds on the ten-membered ring system, (c) the highly selective introduction of functional groups, and (d) the efficient synthesis of the  $\alpha$ -methylene- $\gamma$ -lactone group. A wide range of methodologies for the synthesis of the ten-membered core skeleton of germacranolides have been reported and are shown in Scheme 5.1. Based on the biosynthetic route of sesquiterpene lactones, the synthesis of parthenolide **1** was accomplished by strategy **A**, in which the synthesis of the ten-membered ring core skeleton starts by the intramolecular  $\alpha$ -alkylation of a sulfone derivative **5** (Yang et al. 2015). The synthesis of 7-*epi*-parthenolide **2** was obtained by strategy **B**, in which the synthesis of the  $\alpha$ -methylene- $\gamma$ -hydroxyl nitrile germacrene system begins with an intramolecular Barbier-type reaction involving compound **6** (Long et al. 2014). In the synthesis of aristolactone **3**, the generation of the germacrene skeleton was performed by method **C**, in which the cyclization of the chloro alcohol **7** precursor is carried out (Marshall et al. 1987). Finally, in strategy **D**, used for the synthesis of costunolide **4**, the bromo alcohol cyclization precursor **8** was used for the generation of the key ten-membered ring skeleton (Shibuya et al. 1986). Baran et al. have achieved the assembly of the carbocyclic terpene backbone, epoxy-germacrenol, by means of a low oxidation state (cyclase phase) followed by oxidative modifications (oxidase phase). This key intermediate allows the access to a wide variety of family members, such as selinanes, guaianes, and elements in a different manner (Foo et al. 2012).

### 5.1.2 *Synthesis of the $\alpha$ -Methylene- $\gamma$ -Lactone Moiety*

The  $\alpha$ -methylene- $\gamma$ -lactone moiety is an important substructural unit found in a vast array of biologically active natural products, such as sesquiterpenoids. They exhibit a variety of biological properties, including antibacterial, cytotoxic,



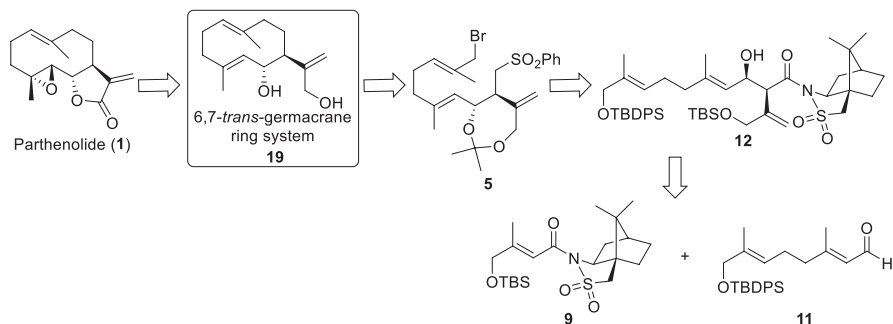
**Scheme 5.1** Selected strategies for the generation of germacranolide ten-membered skeleton

anti-inflammatory, antioxidant, and antimicrobial (Chen et al. 2008; Mang et al. 2006; Reynolds et al. 2003; Siedle et al. 2004; Kummer et al. 2005). Taking into account the significance of this functional group, several strategies have been developed to synthesize  $\alpha$ -methylene- $\gamma$ -lactones; and these methodologies have been applied to the synthesis of natural products, such as sesquiterpene lactones. The preparation of  $\alpha$ -methylene- $\gamma$ -butyrolactones involving the reaction of the  $\gamma$ -butyrolactone enolate with formaldehyde, followed by base-mediated elimination is a commonly used process. Metz et al. have employed this method for the synthesis of the antileukemia agents (–)-eriolanin and (–)-eriolangin (Merten et al. 2004, 2006). A similar approach using lithium diisopropylamine (LDA) and gaseous formaldehyde has been described by Mukai for the total synthesis of (+)-achalensolide (Hirose et al. 2008). Instead of formaldehyde, the Eschenmoser's salt was employed in the total synthesis of the guaianolide arglabin (Kalidindi et al. 2007). During the latter process, a tertiary amine is formed, which traps the lactone enolate derivative with the Eschenmoser's salt. The subsequent methylation reaction followed by the Hofmann elimination provided the desired product. The deprotonation/Eschenmoser's salt

methylation pathway has been used by Kobayashi et al. in the total synthesis of (–) diversifolin, an inhibitor of the NF- $\kappa$ B transcription factor (Nakamura et al. 2009). The ten-membered ring of (–)-diversifolin has been generated through the Grubbs ring-closing metathesis. Then, deprotonation with LDA and subsequent treatment with Eschenmoser's salt afforded the spontaneous generation of the corresponding  $\alpha$ -methylene- $\gamma$ -butyrolactone without the addition of methyl iodide to promote the Hofmann elimination (Mihelcic and Moeller 2003). Another widely employed strategy involves the oxidation of an  $\alpha$ -phenylselenide intermediate followed by  $\beta$ -elimination to introduce unsaturation (Justicia et al. 2008; Fuchs et al. 2007; Arantes et al. 2009). This approach has been employed by Shishido et al. in the synthesis of the antibacterial terpenoid (–)-xanthanin (Yokoe et al. 2008). The treatment of  $\alpha$ -methyl- $\gamma$ -butyrolactone with LDA followed by diphenyl diselenide forms the  $\alpha$ -phenylselenide intermediate. Oxidation and then elimination provided the anticipated methylene lactone. An efficient palladium-catalyzed carbonylation/lactonization sequence was used by Martin et al. to achieve the total synthesis of (+)-8-epixanthatin, a sesquiterpene lactone known to exhibit antimalarial and antitumor activities (Kummer et al. 2005). In the preparation of 6-epicostunolide, Massanet et al. have efficiently applied manganese dioxide to oxidize an allylic alcohol to render the corresponding lactone (Azarken et al. 2008). A one-pot methodology was developed in the early 1970's by Dreiding and Schmidt to synthesize an  $\alpha$ -methylene- $\gamma$ -butyrolactone moiety. They have demonstrated that a functionalized organometallic reagent could be generated by treating 2-bromomethacrylic esters with zinc. The addition of an aldehyde followed by spontaneous cyclization renders  $\alpha$ -methylene- $\gamma$ -butyrolactone. This widely used methodology is one of the simplest and most direct methods for the synthesis of  $\alpha$ -methylene- $\gamma$ -butyrolactone (Kitson et al. 2009). Novel methods for the efficient preparation of  $\alpha$ -methylene- $\gamma$ -butyrolactones have been devised by chemists working in organic synthesis. These methodologies have been applied to develop new compounds for biological screening and to design synthesis routes for the generation of complex natural products.

### 5.1.3 Strategy to the Total Synthesis of Parthenolide

Parthenolide belongs to the sesquiterpene lactone class of natural products and is the active principle isolated from feverfew, a the traditional herbal remedy (Neukirch et al. 2003). It has been demonstrated that parthenolide targets leukemia stem cells with high selectivity in the presence of normal hematopoietic stem cells (Guzman et al. 2005). The asymmetric total synthesis of parthenolide **1** developed by Chen et al. (Yang et al. 2015) has been based on the biosynthetic route of sesquiterpene lactones. This synthetic route involves an aldehyde and a  $\beta$ ,  $\gamma$ -unsaturated chiral sulfonylamide as starting materials from which, after a series of chemical transformations, the synthesis of the desired product is achieved. The strategy **A**, shown in Scheme 5.1, has been used for the generation of the ten-membered carbocyclic ring intermediate of parthenolide **1**. Analyzing the retrosynthetic pathway of Scheme 5.2, compound **1** was

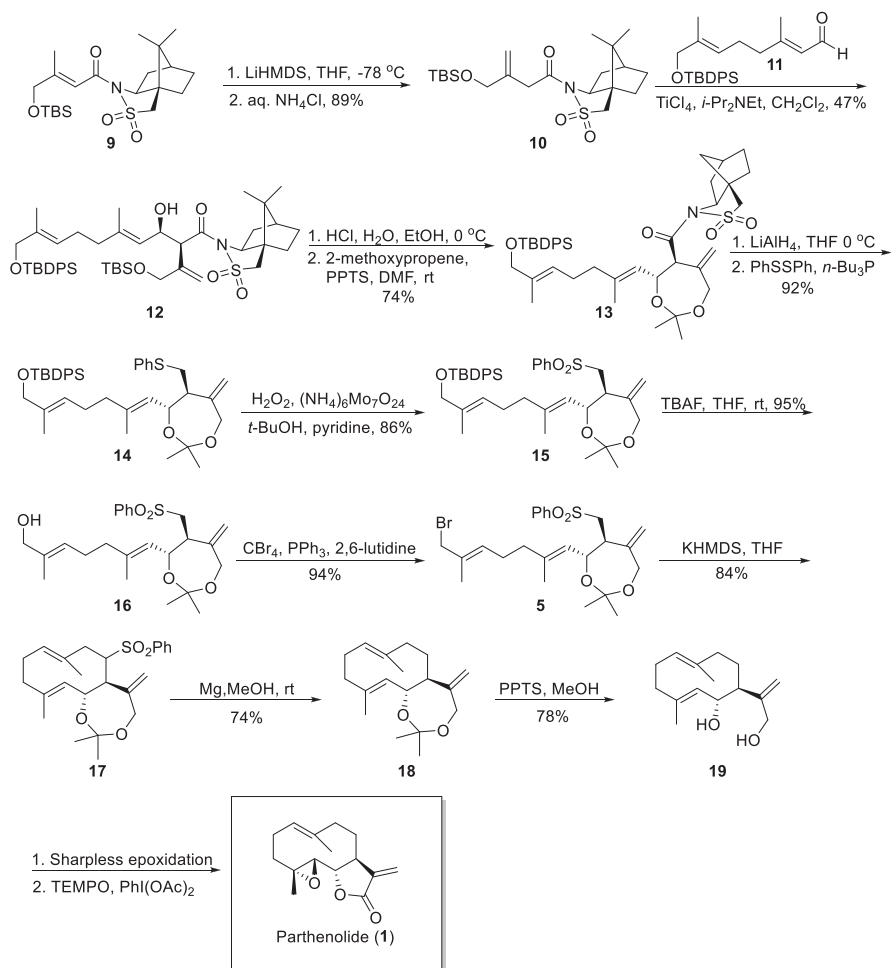


**Scheme 5.2** Retroanalysis to the synthesis of parthenolide (1)

planned to be synthesized from the 6,7-*trans*-germacrane ring system **19** that could be generated from the sulfone **5** through an intermolecular  $\alpha$ -alkylation. Sulfone **5** has been obtained from compound **12** which could be manipulated by the aldol reaction between  $\beta$ ,  $\gamma$ -unsaturated sulfonyl amide **9** and aldehyde **11**.

The steps employed to obtain parthenolide **1** are depicted in Scheme 5.3. The first step was the synthesis of the unsaturated sulfonyl amide **9**, and this was accomplished by a Horner–Wadsworth–Emmons reaction between a ketone and diethylphosphonoacetic acid in two stages, with an overall yield of 59%. The aldol reaction between compound **10** and aldehyde **11** in the presence of titanium tetrachloride ( $\text{TiCl}_4$ ) and di-isopropylethyl amine (*i*-Pr<sub>2</sub>NEt) in dichloromethane ( $\text{CH}_2\text{Cl}_2$ ) afforded compound **12** with the desired 6,7-stereochemistry as the major product and with 47% yield. The selective cleavage of the *tert*-butyldimethylsilyl ether (TBS) protecting group of compound **12** with HCl in ethanol at 0 °C followed by the treatment with 2-methoxypropene furnished acetone **13**. The thioether product **14** was then obtained by a reduction reaction followed by the treatment of the crude product with diphenyl disulfide/tri-*n*-butylphosphine. The oxidation of compound **14** with hydrogen peroxide/ammonium heptamolybdate ( $\text{H}_2\text{O}_2/(\text{NH}_4)_6\text{Mo}_7\text{O}_{24}$ ) in *tert*-butanol (*t*-BuOH) and pyridine provided product **15** in with 86% yield. Removal of the *tert*-butyldiphenylsilyl ether (TBDPS) group of compound **15** with tetrabutylammonium fluoride afforded alcohol **16** with 95% yield. Alcohol **16** was then converted to its corresponding brominated compound **5** with tetrabromomethane ( $\text{CBr}_4$ ), triphenylphosphine ( $\text{PPh}_3$ ), and 2,6-lutidine as a base at 0 °C with 94% yield. The treatment of this compound with four equivalents of potassium bis-(trimethylsilyl)amide (KHMDs) rendered the desired cyclized product **17** with 84% yield. The sulfone moiety on the cyclized product **17** was then removed by adding magnesium/methanol (Mg/MeOH) furnishing product **18** with 74% yield. The solution of pyridinium *p*-toluenesulfonate in methanol has proved to be a good reagent to remove the acetone group of **18** to generate the desired ten-membered carbocyclic germacrene ring intermediate **19**. The Sharpless epoxidation of diol **19** followed by oxidation with 2,2,6,6-tetramethyl-1-piperidinyloxy (TEMPO) and (diacetoxyiodo)benzene ( $\text{PhI}(\text{OAc})_2$ ) afforded parthenolide **1** with 62% yield.

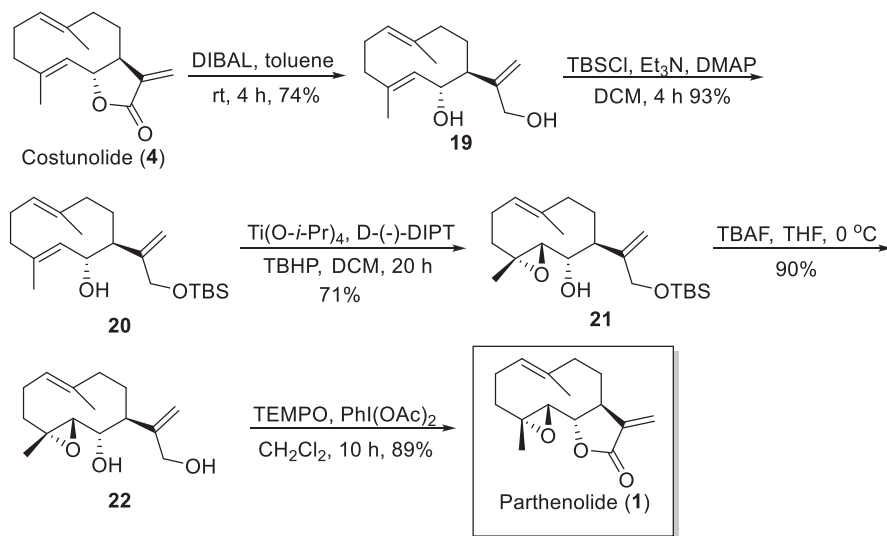




**Scheme 5.3** Synthesis of parthenolide **1**

### 5.1.4 Semi-synthesis of Parthenolide

The semi-synthesis strategy is one that often involves large and complex molecules isolated from natural sources as starting materials. This methodology becomes useful when the precursor molecule contains a structurally complex moiety that is either too costly or too challenging to be generated by total synthesis. The simplest strategy for the synthesis of a complex natural product is to start with molecules that



**Scheme 5.4** Semi-synthesis of parthenolide

already contain the desired germacranolide skeleton and, through a series of chemical transformations, the synthesis of the target molecule is achieved. The stereoselective synthesis of parthenolide **1** involves a protection-free strategy employing the natural product costunolide **4** as starting material (Scheme 5.4) (Long et al. 2013). Costunolide has been found to be a good substrate for the synthesis of parthenolide because this germacranolide is readily isolated from the roots of *Saussurea lappa* (Zhang et al. 2011). Costunolide **4** is treated with diisobutylaluminum hydride (DIBAL) in toluene at room temperature to obtain the key germacrane intermediate **19** with 79% yield. The treatment of **19** with *tert*-butyldimethylsilyl chloride (TBSCl) furnished the protected primary alcohol **20** with a good yield. The selective epoxidation of the C4–C5 bond of compound **20** with titanium isopropoxide ( $\text{Ti(O-}i\text{-Pr)}_4$ ), (–)-diisopropyl D-tartrate (D-(–)-DIPT), and *tert*-butyl hydroperoxide (TBHP) in  $\text{CH}_2\text{Cl}_2$  at room temperature afforded compound **21** with 71% yield. The deprotection of compound **21** followed by oxidation with TEMPO and  $\text{PhI(OAc)}_2$  rendered parthenolide **1** with an 80% yield over two steps.

### 5.1.5 General Strategies for the Synthesis of Guaianolides

Guaianolides are an important and diverse group of biologically active sesquiterpenes. They are often used as scaffolds for the design of new active molecules. The guaianolides central skeletal backbone consists of a 5,7,5-ring system that exists in

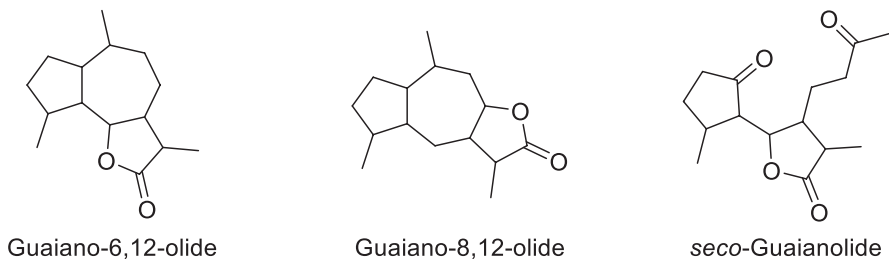
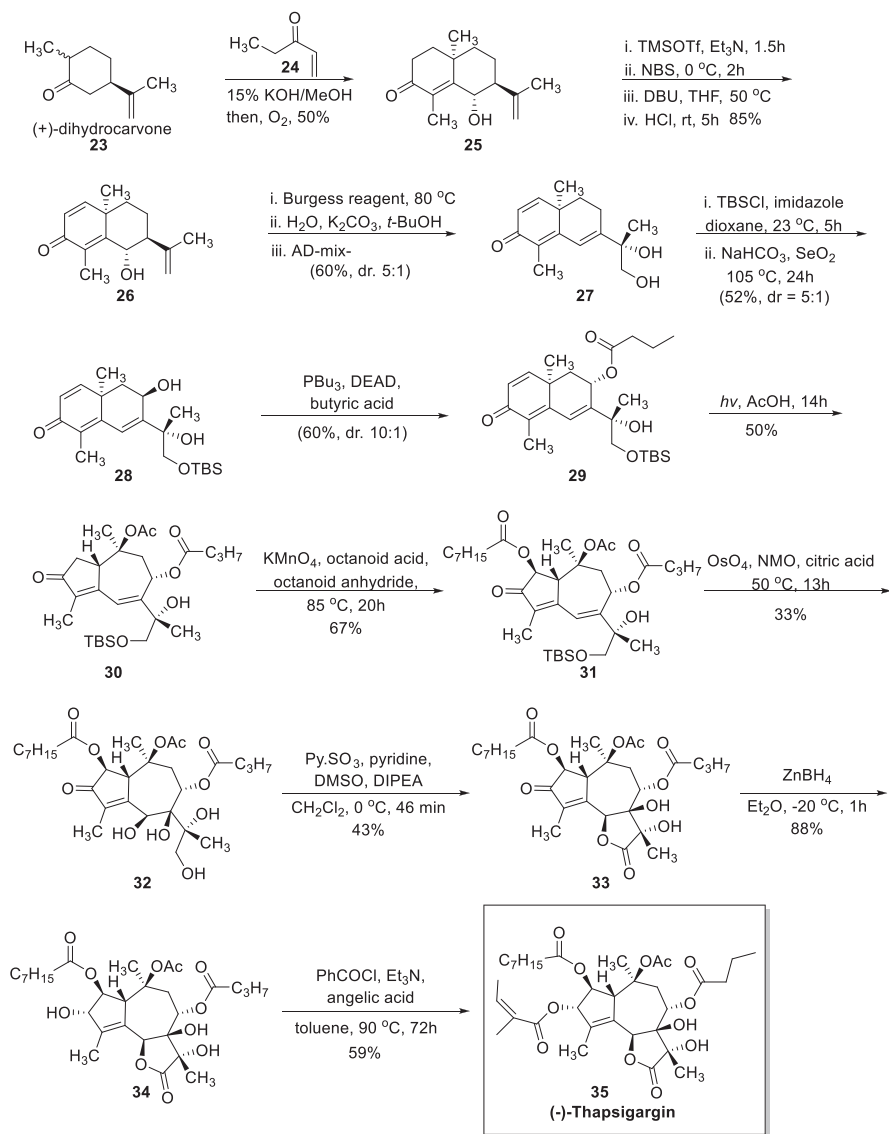


**Fig. 5.1** Guaianolides central skeleton backbone

the forms of the guaian-6,12-olide and the guaian-8,12-olide structures. The least common skeleton is that corresponding to the *seco*-guaianolides, in which a C–C single bond is broken in one of the rings (Fig. 5.1). Several synthetic methodologies for the generation of the hydroazulene skeleton have been developed, including ring rearrangement or enlargement and intra- and intermolecular cycloaddition. The aim of this section is to provide a summary of the relevant and updated synthetic approaches for the synthesis of this important class of natural products.

The use of rearrangement reactions is one of the most common synthetic strategies implemented in the generation of the hydroazulene skeleton of guaianolides. An interesting and convenient methodology developed by Baran et al. includes two key steps: (1) the application of the classic photosantonin rearrangement and (2) the installation of multiple oxygen atoms in the guaianolide skeleton to achieve the scalable total synthesis of (–)-thapsigargin **35** (Scheme 5.5) (Chu et al. 2017). Thapsigargin is known to be a potent inhibitor of the sarco-endoplasmic reticulum  $\text{Ca}^{+2}$  ATP-dependent (SERCA) pump protein, and it has proved to be a good candidate in many medical areas (Andrews et al. 2007). The main challenge in the synthesis of **35** has been to efficiently install six additional oxygen atoms with the correct stereochemical configuration to obtain a guaiane with a high oxidation level. The generation of the skeletal carbons of the target molecule starts with the Robinson annulation and further  $\gamma$ -hydroxylation between (+)-dihydrocarvone **23** and ethyl vinyl ketone **24** affording decalin **25** with 50% yield. The one-pot gram scale bromination/elimination sequence of **25** furnished the dienone **26** with 85% yield. The treatment of compound **26** with the Burgess reagent followed by the chemo- and diastereoselective dihydroxylation of the terminal olefin with AD-mix- $\alpha$  rendered diol **27** with a good yield. The diastereoselective synthesis of the allylic alcohol **28** has been accomplished by first, the selective protection of the primary alcohol and then the in situ allylic C–H oxidation with selenium dioxide ( $\text{SeO}_2$ ). The butyrate was then installed with the required stereochemical configuration at C–8 by the Mitsunobu inversion with butyric acid. The ring enlargement was achieved by the irradiation of a 0.01 M solution of **29** in glacial acetic acid with an Hg lamp. This gram-scale process provided the key guaianolide skeleton intermediate **30** with good stereoselectivity and with 50% yield. The treatment of **30** with potassium per-



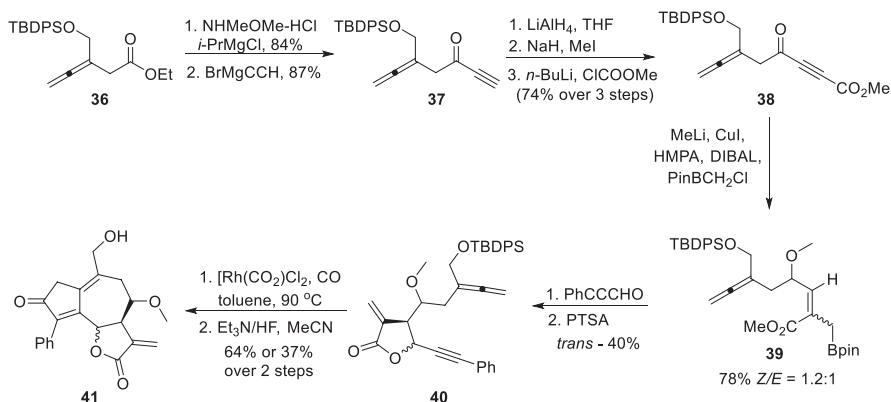
Scheme 5.5 Concise synthesis of (–)-thapsigargin

manganate ( $\text{KMnO}_4$ ) in the presence of octanoic acid and octanoic anhydride under reflux conditions in toluene exerted the desired oxidation to provide the  $\alpha$ -octanoylated enone **31** with 67% yield. Upjohn's modified procedure, which employs citric acid at  $50^\circ\text{C}$ , subsequently provided the tetra-ol **32**. The lactonization of **32** then took place under Parikh–Doering conditions to afford **33**. The final step of their total synthesis consisted of the reduction of **33** with zinc borohydride

followed by acylation with angelic anhydride and benzoyl chloride. The final product was (–)-thapsigargin **35**, which was obtained with 59% yield in 11 steps.

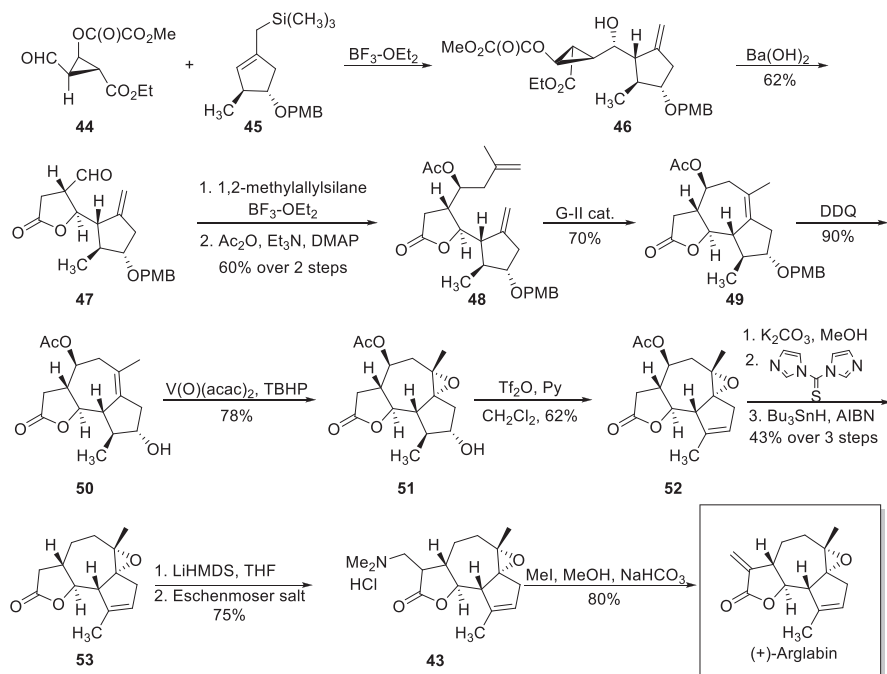
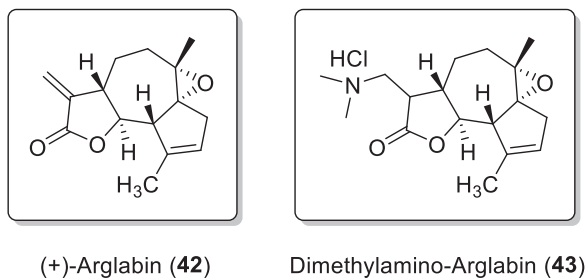
Related strategies have been developed where the hydroazulene backbone is obtained by an intramolecular cycloaddition reaction after the formation of the lactone ring. Recently, Brummond et al. have reported an innovative methodology for the synthesis of highly oxygenated 6,12-guaianolide derivatives (Grillet et al. 2011; Wen et al. 2013). It has been demonstrated that functionalized allene-yne-containing  $\alpha$ -methylene butyrolactones could undergo a cyclocarbonylation reaction in the presence of  $Rh^I$  as a catalyst to afford the 5,7,5-ring system. The synthesis starts with a Johnson–Claisen rearrangement of the monoprotected butynediol to afford the allenyl ester **36**. Ester **36** is then treated with methoxyethyl amine hydrochloride and *i*-PrMgCl to afford the corresponding Weinreb amide, which is converted into the alkyne **37** by treatment with ethyl magnesium bromide. Next, reduction of the carbonyl group of alkyne **37** with lithium aluminum hydride, followed by the formation of the corresponding methyl ether, deprotonation of the terminal alkyne with *n*-butyl lithium, and then the addition of chloromethyl ester gives the alkynoate **38** with 84% yield. The reaction of **38** with diisopropylaluminum hydride (DIBAL), copper (I) iodide (CuI), methyl lithium, and  $ClCH_2BP$  provided alkyl boronates in a *Z/E* ratio of 1.2:1. A complex mixture was obtained after subjecting the alkyl boronate mixture to an allylboration/lactonization step by heating with 3-phenylpropionaldehyde. The lactone *trans*-**40** was then generated in a 2:1 mixture of diastereomers after treatment with *p*-toluenesulfonic acid (PTSA). The subsequent treatment with rhodium biscarbonyl chloride dimer and the removal of the *tert*-butyldiphenylsilyl ether (TBDPS) yielded the cyclocarbonylation product as a mixture of diastereomers (Scheme 5.6).

Another prominent member of one of the largest groups of naturally occurring sesquiterpene lactones is arglabin **42** (Fig. 5.2). This natural product can be isolated from *Artemisia glabella*, and it has proved to be a potent farnesyl transferase inhibi-



**Scheme 5.6** Synthesis of 6,12-guaianolide derivatives

**Fig. 5.2** Structures of sesquiterpene lactones arglabin and dimethylamino arglabin



**Scheme 5.7** Total synthesis of (+)-arglabin

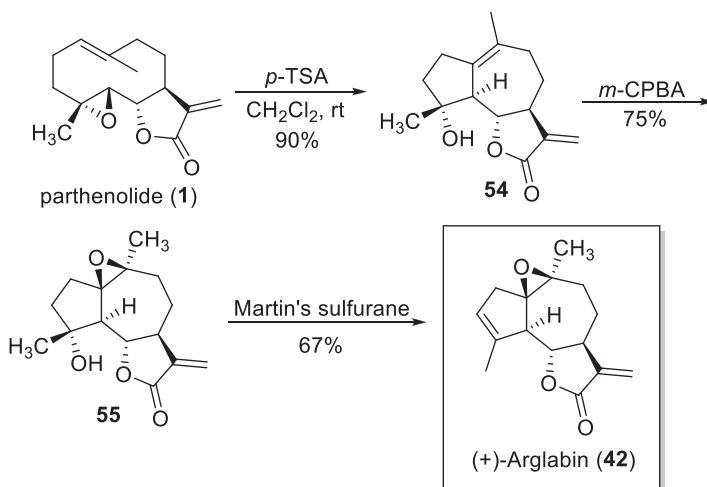
tor with promising antitumor activity and cytotoxicity against human tumor cell lines. To increase bioavailability, arglabin has been converted into its dimethylamine hydrochloride adduct and has been successfully used in Kazakhstan for the treatment of colon, breast, ovarian, and lung cancers (Shaikenov et al. 2001).

The first enantioselective synthesis of arglabin has been accomplished by Reiser et al. using furan derivatives as starting materials (Scheme 5.7) (Kalidindi et al. 2007). A two-step process starting with methyl-2-furoate and involving  $\text{Cu}^{\text{I}}$ -catalyzed asymmetric cyclopropanation followed by ozonolysis afforded

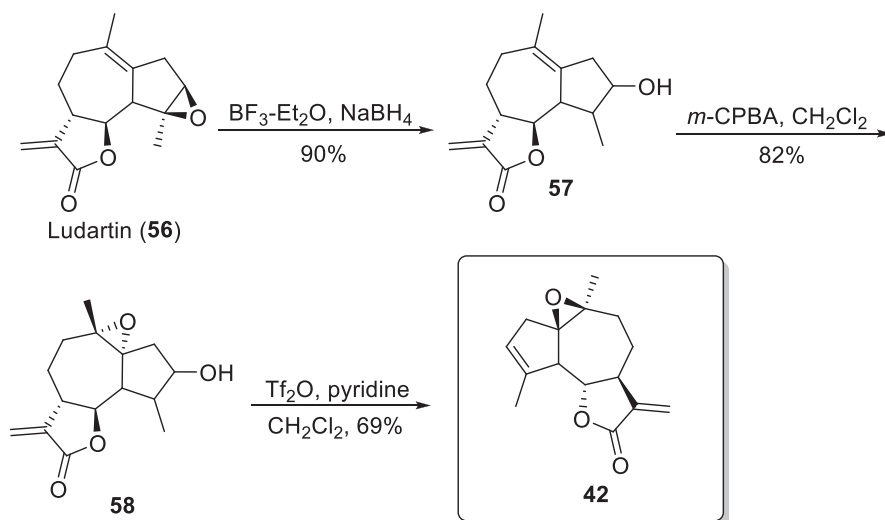
cyclopropanecarbaldehyde **44** in its diastereo- and enantiomerically pure form. The chiral *trans*-substituted allylsilane **45** has been synthesized from furfuryl alcohol by a selective methyl cuprate addition and Ni(II)-catalyzed cross coupling with trimethylsilylmethylenemagnesium chloride. When these two compounds were combined, the formation of **46** proceeded with high stereocontrol where the carbonyl group of **44** is attacked by allylsilane **45** from the face opposite of its methyl group in accordance with the Felkin-Anh paradigm. The saponification of the labile oxalic ester in **46** was induced by the addition of a base, and subsequent lactonization provided the lactone-aldehyde **47**. The synthesis of diene **48** in a 4:1 mixture of diastereomers was accomplished by subjecting compound **47** to a Hosomi–Sakurai allylation with 2-methylallylsilane followed by acylation. The desired guaianolide skeleton **49** was completed by a ring-closing metathesis in the presence of a Grubbs second-generation catalyst. The homoallyl alcohol **50** was generated by PMB deprotection. The desired  $\alpha$ -epoxide **51** was afforded by employing catalytic amounts of vanadyl acetylacetonate (VO(acac)<sub>2</sub>) and *t*-butyl hydroperoxide (TBHP) as the stoichiometric oxidant and with the free hydroxyl group serving as a directing group. Exposure of epoxide **51** to trifluoromethanesulfonic anhydride (Tf<sub>2</sub>O) in the presence of pyridine generated alkene **52** as a single regioisomer. The acetate deprotection followed by the Barton–McCombie protocol provided the deoxygenated product **53**. The final step of this synthesis is to introduce the *exo*-methylene group responsible for the biological activity of sesquiterpene lactones. The alkylation of **53** with the Eschenmoser's salt gave rise to a dimethylamino arglabin derivative **43**. Subsequent quaternization with methyl iodide followed by elimination of trimethylamine afforded the target molecule (+)-arglabin **42** with 80% yield.

### 5.1.6 Semi-synthesis of Guaianolides

In drug discovery, natural products have been the most successful sources. However, these compounds are often generated in small quantities. However, another natural product can serve as starting material for the semi-synthesis of the target drug. The biomimetic semi-synthesis of arglabin **42** has recently been developed from the abundant natural product parthenolide **1** (Scheme 5.8). Parthenolide is readily available from the root bark of *Magnolia delavayi*. It has been demonstrated that parthenolide displays a variety of biological activities and its dimethylamine derivative is being evaluated in a clinical trial (Zhai et al. 2012; Roboz and Guzman 2009; Peese 2010). Parthenolide has been found to be suitable as the starting material for the synthesis of arglabin because it bears a *trans*-6,12 moiety which is key for the synthesis of guaianolides. The treatment of parthenolide **1** with *p*-toluenesulfonic acid (*p*-TSA) afforded micheliolide **54** with excellent yields. The epoxidation of the double bond on the seven-member ring of compound **54** with *m*-chloroperbenzoic acid (*m*-CPBA) furnished the desired  $\beta$ -epoxide **55** as a single stereoisomer. The high stereoselectivity of this process is possible because epoxidation from the top face has to overcome the steric effects from the upward methyl group. It is also



**Scheme 5.8** Transformation of parthenolide into arglabin

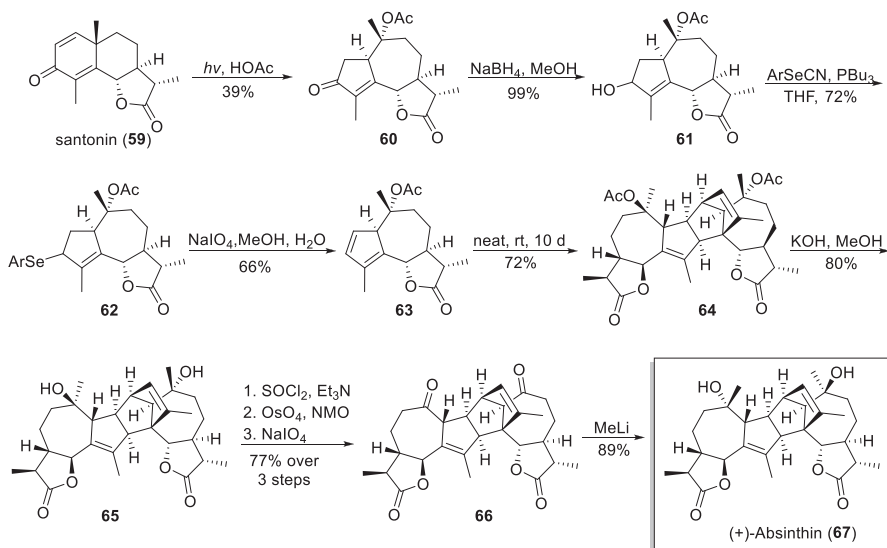


**Scheme 5.9** Semi-synthesis of arglabin from ludartin

known that the hydroxyl substituent can serve as a directing group in the epoxidation of homoallylic alcohols. In the following step, the dehydration of **55** with Martin's sulfurane in  $\text{CH}_2\text{Cl}_2$  afforded arglabin with good yields. This methodology constitutes a convenient and efficient three-step semi-synthesis of arglabin from parthenolide.

The semi-synthesis of arglabin has also been carried out using ludartin **56** as the starting point of the synthesis (Scheme 5.9) (Lone and Bhat 2015). The synthesis

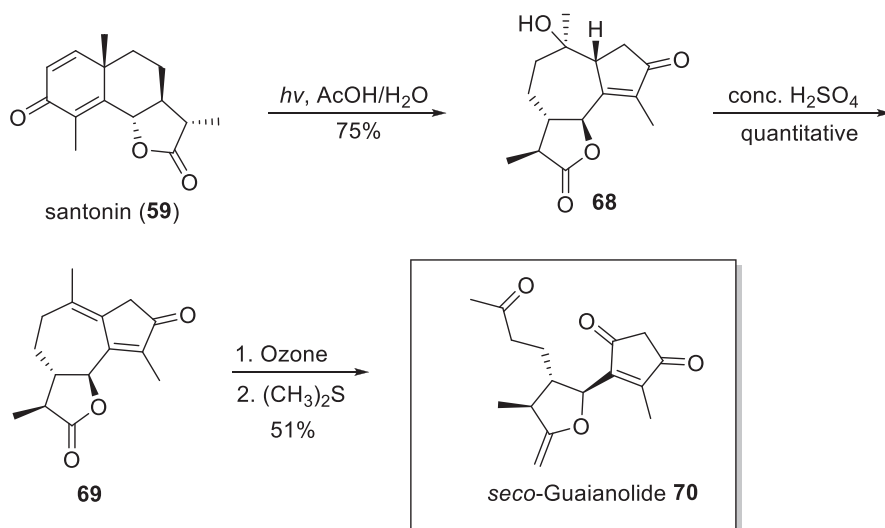




**Scheme 5.10** Synthesis of (+)-absinthin

started with the stereoselective ring opening of the epoxide in ludartin using  $\text{BF}_3 \cdot \text{Et}_2\text{O}$  in a 1:1 mixture of dioxane-water affording compound **57** with good stereoselectivity. The epoxidation of its C(1)10 double bond with *m*-CPBA yielded a mixture of diastereomers which were separated by column chromatography to obtain compound **58**. Finally, dehydration using  $\text{Tf}_2\text{O}$  and pyridine furnished the desired trisubstituted alkene product in arglabin. A concise three-step route for the semi-synthesis of antitumor arglabin from ludartin has been demonstrated. This process had an overall yield of 51%.

In 1953, Herout et al. isolated (+)-absinthin **67** from *Artemisia absinthium* as a dimeric guaianolide. The structural complexity along with its biological activity as a promising anti-inflammatory agent led Zhang et al. to develop the synthesis of this natural product (Scheme 5.10) (Zhang et al. 2005). Using santonin **59** in acetic acid as starting material, the photolysis with an Hg lamp rendered the *O*-acetylisophotosantonin lactone **60**. The reduction of the enone carbonyl with  $\text{NaBH}_4$  provided a mixture of the diastereomeric alcohol **61**. The Mitsunobu aryl selenylation of **61** allowed obtaining selenides **62** and the subsequent treatment with  $\text{NaIO}_4$  led to the formation of the substituted cyclopentadiene **63**. A [4 + 2] Diels-Alder cycloaddition of **63** gave rise to compound **64** with not only high regioselectivity but also with high stereoselectivity. During this process, the steric interactions were minimized because the two Diels-Alder moieties approached each other through the less hindered faces, adopting a head-to-head orientation with respect to the lactone carbonyl groups. The saponification of **64** with a methanolic potassium hydroxide solution followed by acidification with HCl afforded



**Scheme 5.11** Synthesis of *seco*-guaianolide from  $\alpha$ -santonin

*epi*-absinthin **65**. Since the two alcohols had the wrong configuration, diol **65** was converted to diketone **66** by an oxidative degradation. The chemo- and stereoselective installation of the methyl groups completed the synthesis of (+)-absinthin **67** with an overall yield of 18.6%.

Over the last years, and in order to find new bioactive compounds that can act as leads for drug discovery, researchers have focused on *seco*-guaianolides. Recently, Westwood et al. have reported the synthesis and biological evaluation of two *iso-seco*-tanaphartholides (Makiyi et al. 2009). Their study has demonstrated that a late-stage oxidative cleavage reaction in the absence of protecting groups was necessary for the direct synthesis of the natural products and that the *seco*-guaianolides derivatives were inhibitors of the NF- $\kappa$ B signaling pathway. In a different study conducted by Macías et al., the easy preparation of *seco*-guaianolides has been demonstrated (Macias et al. 2012). In their work, the sesquiterpene lactone derivatives were synthesized from commercially available santonin, involving a high-yield photochemical transformation. Specifically,  $\alpha$ -santonin **59** was transformed into the guaianolide isophotosantonin **68** at low temperatures, in the presence of filter solutions, Ni(II) and Co(II), and with a mixture of 16/65 ratio of acetic acid (AcOH) and water. The acid-catalyzed dehydration of the alcohol on molecule **68** provided the diene **69**. Subsequent oxidation of **69** with ozone and dimethyl sulfide provided *seco*-guaianolide **70** (Scheme 5.11).

## 5.2 Chemical Transformation of Sesquiterpene Lactones

The sesquiterpene lactone class of natural products is a large and diverse group of biologically active compounds found in several plant families such as Acanthaceae, Anacardiaceae, Apiaceae, Euphorbiaceae, Lauraceae, Magnoliaceae, Menispermaceae, Rutaceae, Winteraceae, and Hepatideae (Modzelewska et al. 2005; Nam 2006). One important feature of this group of secondary metabolites is the existence of the  $\alpha$ -methylene- $\gamma$ -lactone moiety which is responsible for the biological effects and cytotoxicity. Structure–activity relationship (SAR) investigations have demonstrated that the mechanism of action of these compounds involves the nucleophilic addition of thiols, such as cysteine, to the  $\alpha$ -methylene- $\gamma$ -lactone moiety. However, many of these compounds are poorly soluble in water, and, frequently, the  $\alpha$ -methylene- $\gamma$ -lactone displays a nonselective binding to undesired targets as a Michael acceptor (Ghantous et al. 2010). Furthermore, over the last decade, researchers have been interested in developing new compounds to improve the cytotoxic effects as well as to establish structure–activity relationship.

### 5.2.1 Costunolide and Its Derivatives

Costunolide (**4**, Scheme 5.1), which can be readily extracted from the dried roots of *Saussurea lappa*, has been considered a potential candidate for cancer treatment. It has been reported that costunolide can induce apoptosis in cancer cells and that it suppresses the nuclear transcription factor- $\kappa$ B (NF- $\kappa$ B) activation. It is known that the *exo*-methylene group of the  $\alpha$ -methylene- $\gamma$ -lactone of costunolide is required to elicit cytotoxicity and that its reduction renders an inactive derivative(s) (Sun et al. 2003). A variety of amino adducts of costunolide **4** involving Michael-type addition has been synthesized, and these derivatives have been tested in eight different cell lines (Srivastava et al. 2006). As a rule, several amino derivatives of costunolide have shown higher cytotoxicity and selectivity, with an improved safety index. Overall, all the amino adducts synthesized from dimethyl pyrrolidines, or from piperidines, have exhibited significant antiproliferative activity similar to costunolide **4**. Furthermore, all of the compounds prepared from piperazines proved to be inactive. The structures of the active amino derivatives are illustrated in Fig. 5.3.

Suresh et al. have reported the application of the Heck arylation reaction in the synthesis of costunolide derivatives (Vadaparthi et al. 2015). Under standard Heck reaction conditions, 12 costunolide analogues (**76–85**, Fig. 5.4) have been synthesized after arylation of the  $\alpha$ -methylene- $\gamma$ -lactone and subjected to evaluation for their cytotoxic activities against cervical cancer (HeLa), breast cancer (MCF-7), lung cancer (A549), mouse melanoma (B-16), and prostate cancer (DU-145) cell lines. A broad range of potencies was observed, but when compared to the parent compound costunolide, most of the analogues displayed higher cytotoxicity against the tested cell lines. Compounds **77** and **83** proved to be the most potent compounds

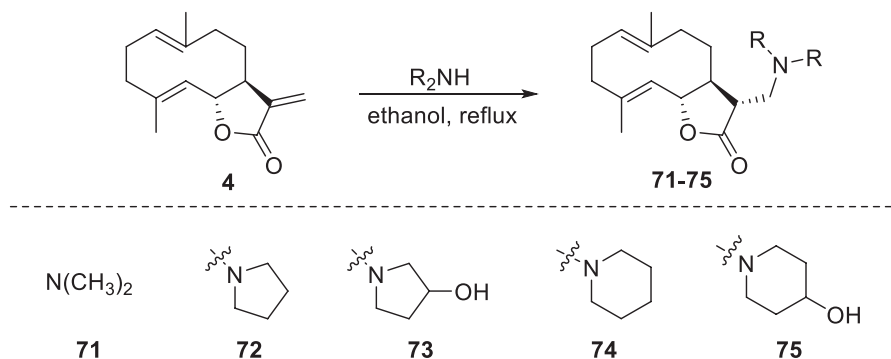


Fig. 5.3 Amino derivatives of costunolide (**4**)

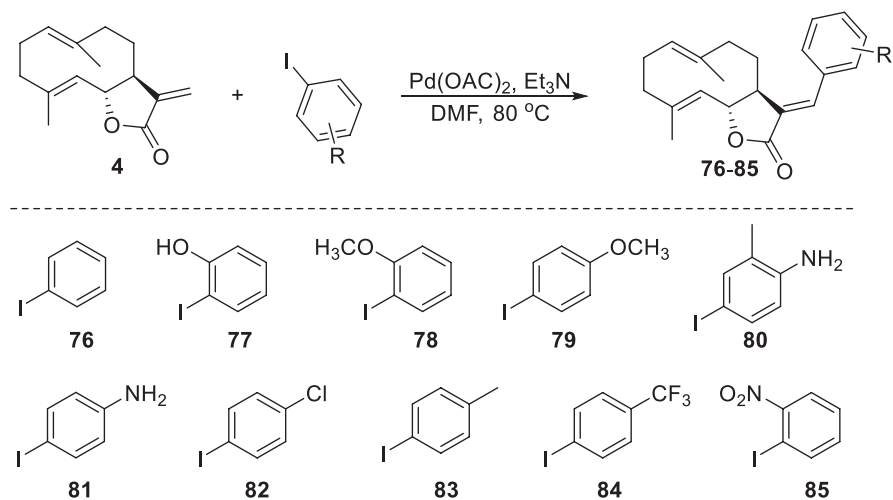


Fig. 5.4 Heck strategy for the synthesis of costunolide analogues **76-85**

against HeLa cells, while compound **82** containing the *p*-chloro substituent showed good activity in all tested cell lines.

### 5.2.2 Parthenolide and Analogues

Parthenolide **1**, is the main active constituent isolated from feverfew (*Tanacetum parthenium*), which is a traditional herbal remedy. This compound belongs to the sesquiterpene lactone class of natural products. Parthenolide **1** is known to have a strong inhibitory effect on NF- $\kappa$ B activation, a process responsible for the strong

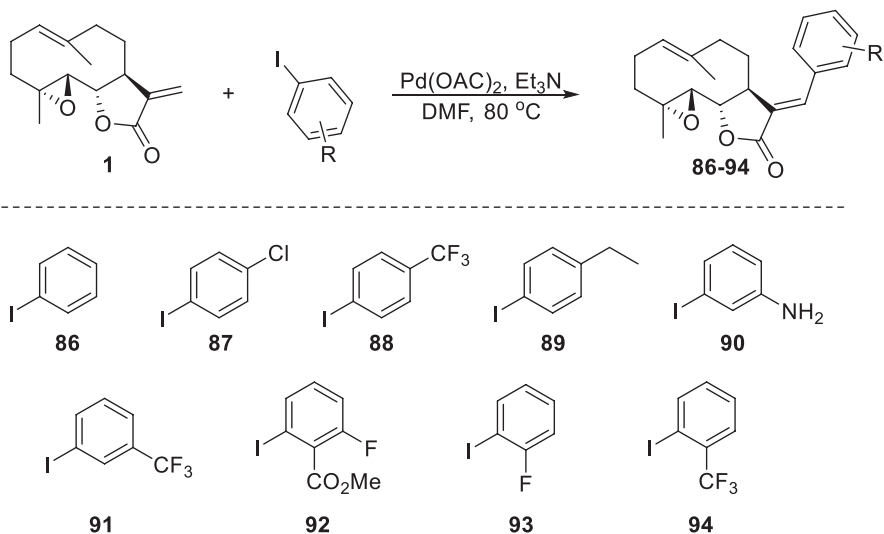
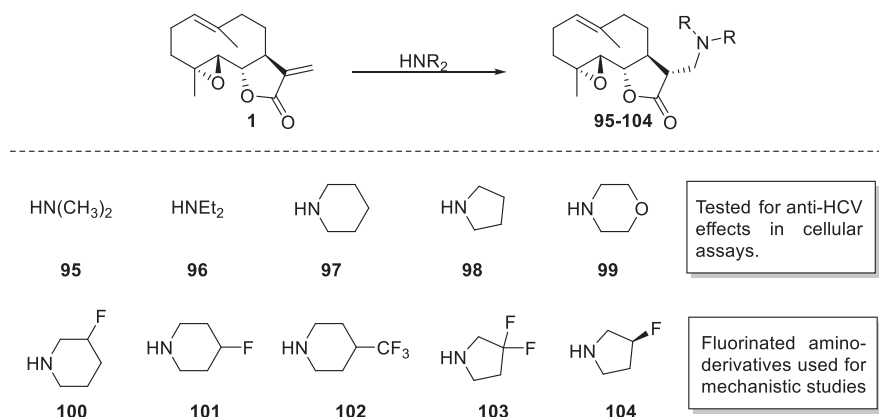


Fig. 5.5 Heck strategy for the synthesis of parthenolide analogues 86–94

anti-inflammatory activity (Kwok et al. 2001a, b). This natural product was demonstrated to selectively target leukemia stem cells while leaving normal hematopoietic cells unaffected. Clinical trials have demonstrated its inadequacy to be used directly, due to the low potency and poor water solubility. As a consequence, researchers have designed new parthenolide derivatives with higher solubility and potency. Colby et al. have successfully applied the palladium-catalyzed arylation reaction of parthenolide with aryl iodide derivatives (Han et al. 2009). To determine the antiproliferative effect, growth inhibition assays with HeLa cells have been conducted. Typically, the authors found that sesquiterpene lactone derivatives bearing electron-withdrawing groups at the *meta*- and *para*-positions retain their activity when compared to the parent compound (Fig. 5.5).

The first amino derivatives of parthenolide have been tested for hepatitis C virus (HCV) infection (Hwang et al. 2006). In that study, it was demonstrated that the seven parthenolide derivatives synthesized from secondary amines (Fig. 5.6) had similar anti-HCV effects to parthenolide. Based on a report demonstrating that parthenolide initiates apoptosis in leukemia stem cells, Crooks et al. have prepared a series of amino adducts of parthenolide from primary and secondary amines (Nasim and Crooks 2008; Neelakantan et al. 2009). It has been demonstrated that dimethylaminoparthenolide (DMAPT) has excellent oral bioavailability, greater aqueous solubility and the outstanding antileukemic activity of parthenolide (Guzman et al. 2007; Hassane et al. 2010). The design, synthesis, and biological evaluation of fluorinated parthenolide amino derivatives have been described by Colby et al. (Fig. 5.6) (Woods et al. 2011). These authors have employed fluorinated aminoparthenolides derived from pyrrolidines and piperidines for mechanistic analysis by <sup>19</sup>F NMR.



**Fig. 5.6** Synthesis of amino derivatives of parthenolide

Studies of their lead compound have demonstrated that the dissociation of the fluorinated amine from the aminoparthenolide prodrug was higher in the presence of glutathione.

### 5.2.3 Artemisinin and Its Derivatives

Artemisinin **105** (ART) is a sesquiterpene lactone containing a peroxide bridge. This compound is obtained from plant *Artemisia annua*. The increase in resistance levels against most of the drugs currently used to treat malaria has led the World Health Organization to use the artemisinin class of compounds as the preferred basis for treatment of infections with *Plasmodium falciparum* strains, cerebral malaria, and malaria in children (Yeung et al. 2004). Artemisinin is an emerging lead compound for malaria treatment that shows a broad range of effectiveness. However, this compound has poor water and oil solubility. In an effort to improve ART bioavailability and efficacy, several artemisinin-like derivatives (ADs) have been synthesized, such as artesunate (ARS), which proved to be more active and less toxic than its parent drug; artemotil, only used in severe cases of malaria; and dihydroartemisinin (DHA), which was found to be more active than ART but thermally less stable (Ploypradith 2004; Krishna et al. 2004; Duthaler et al. 2012). It has been found that polyamines have a significant number of implications of various processes in the malaria parasite. Several amino derivatives of artemisinin have been synthesized, and their mechanism of action has been proposed (Chadwick et al. 2010; Calas et al. 1997; Calas et al. 2000). A new class of amino derivatives of ART with different lipophilic moieties and substituents has been synthesized. The synthesis includes compounds where aliphatic, alicyclic, and aromatic amine groups were introduced through an ethyl ether linker at the C-10 of artemisinin (Fig. 5.7a).

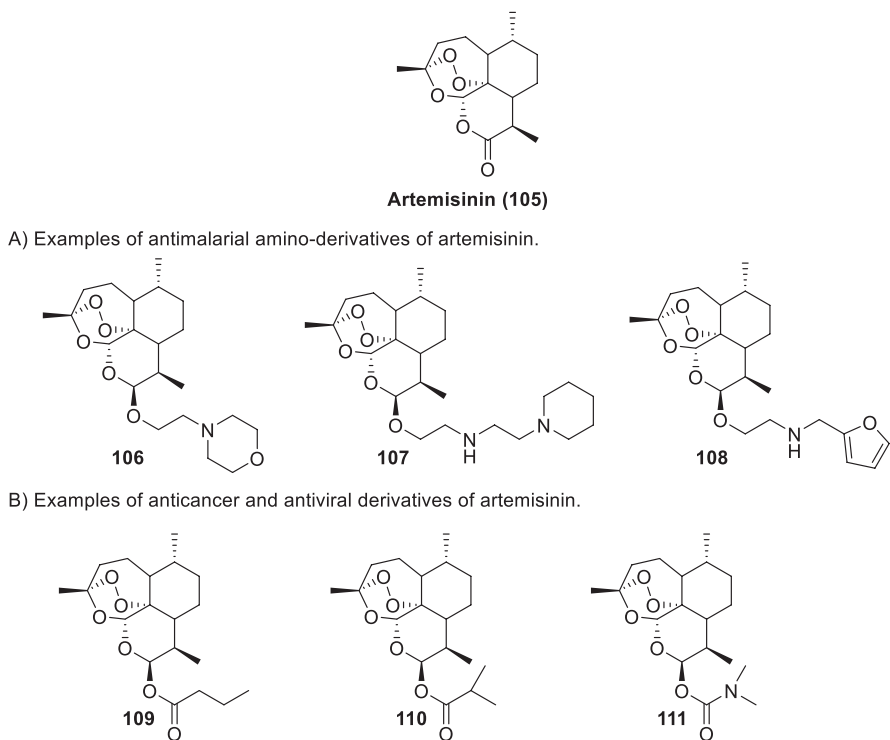
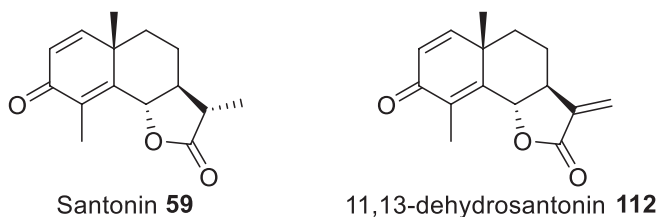


**Fig. 5.7** Chemical structure of artemisinin and its derivatives

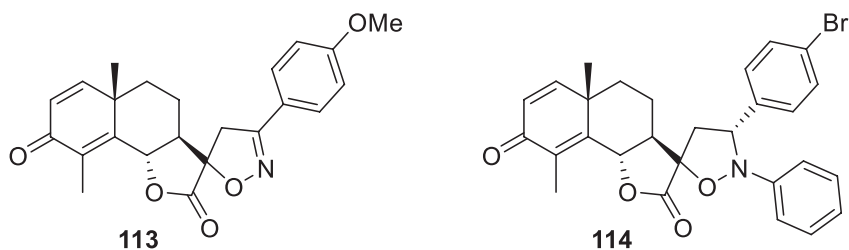
Their antimalarial activity against chloroquine-sensitive (D10) and chloroquine-resistant (Dd2) strains of *Plasmodium falciparum* has been reported. As a rule, all compounds were found to be more potent than chloroquine (CQ) against both strains, and none of the compounds exhibited higher activity against the D10 strain when compared to DHA (Cloete et al. 2012). Several semisynthetic artemisinin derivatives have been evaluated as anticancer and antiviral drugs, and they have shown promising results (Efferth et al. 2008a, b). With the aim of increasing ART solubility and its circulating half-life, Marin et al. have developed the synthesis of artemisinin analogues with bulky groups linked to the C-10 position of DHA (Fig. 5.7b), and their biological activity against liver/colon cancer and viral hepatitis has been tested (Blazquez et al. 2013).

### 5.2.4 Santonin and Its Analogues

Alpha-santonin **59**, a sesquiterpene lactone containing a eudesmane skeleton, has been isolated from *Artemisia santonica*. Over the past decades, researchers have studied its chemical and biochemical transformation along with its pharmacological



A) Spiro-isoxazoline and spiro-isoxazolidine derivatives of santonin.



B) Sesquiterpene lactone with an endo-peroxide functionality.

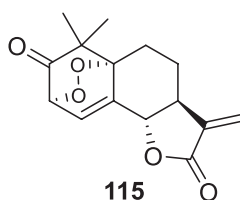


**Fig. 5.8** Chemical structure of  $\alpha$ -santonin and its derivatives

properties. In the past,  $\alpha$ -santonin has been used as anthelmintic, and studies have demonstrated that  $\alpha$ -santonin exhibits important biological properties such as anti-pyretic, anti-inflammatory, and fungicidal (Singh et al. 2001). Additionally, the sesquiterpene lactone  $\alpha$ -santonin has been modified to install the required  $\alpha$ -methylene- $\gamma$ -lactone, and these derivatives exhibited relatively high cytotoxic activity against cancer cells (Arantes et al. 2009). Based on the continuous interest in the design and synthesis of sesquiterpene lactones with anticancer properties, researchers have developed several analogues of  $\alpha$ -santonin. Novel spiro derivatives have been synthesized and tested for their anticancer activity against six human cancer cell lines. Specifically, spiro-isoxazoline and spiro-isoxazolidine derivatives have been prepared by a 1,3-dipolar cycloaddition of 11,13-dehydrosantonin **112** with nitrile oxides and nitrones (Fig. 5.8a). Among the spiro-isoxazoline series, compound **113** has displayed significant activity with  $IC_{50}$  values of 0.02 and 0.2  $\mu M$  in MCF-7 (breast) and A549 (lung) cell lines, respectively. The spiro-isoxazolidine derivative **114** has been evaluated and has shown inhibitory activity against the



central regulator of cancer cell growth and survival NF- $\kappa$ B (Khazir et al. 2013). Santonin derivatives containing the  $\alpha$ -methylene- $\gamma$ -lactone and an endo-peroxide moiety have been synthesized and tested against cancer cell lines (Fig. 5.8b). These compounds have shown high cytotoxicity; however, they were less potent than the control reference compound (Arantes et al. 2010).

## References

- Adio AM (2009) Germacrenes A-E and related compounds: thermal, photochemical and acid induced transannular cyclizations. *Tetrahedron* 65:1533–1552
- Andrews SP, Ball M, Wierschem F et al (2007) Total synthesis of five thapsigargin: guaianolide natural products exhibiting sub-nanomolar SERCA inhibition. *Chemistry* 13:5688–5712
- Arantes FFP, Barbosa LCA, Alvarenga ES et al (2009) Synthesis and cytotoxic activity of alpha-santonin derivatives. *Eur J Med Chem* 44:3739–3745
- Arantes FFP, Barbosa LCA, Maltha CRA et al (2010) Synthesis of novel alpha-santonin derivatives as potential cytotoxic agents. *Eur J Med Chem* 45:6045–6051
- Azarken R, Guerra FM, Moreno Dorado J et al (2008) Substituent effects in the transannular cyclizations of germacranes. Synthesis of 6-epi-costunolide and five natural steiractinolides. *Tetrahedron* 64:10896–10905
- Blazquez AG, Fernandez-Dolon M, Sanchez Vicente L et al (2013) Novel artemisinin derivatives with potential usefulness against liver/colon cancer and viral hepatitis. *Bioorg Med Chem* 21:4432–4441
- Bulow N, Konig WA (2000) The role of germacrene D as a precursor in sesquiterpene biosynthesis: investigations of acid catalyzed, photochemically and thermally induced rearrangements. *Phytochemistry* 55:141–168
- Calas M, Cordina G, Bompard J et al (1997) Antimalarial activity of molecules interfering with *Plasmodium falciparum* phospholipid metabolism. Structure-activity relationship analysis. *J Med Chem* 40:3557–3566
- Calas M, Ancelin ML, Cordina G et al (2000) Antimalarial activity of compounds interfering with *Plasmodium falciparum* phospholipid metabolism: comparison between mono- and bisquaternary ammonium salts. *J Med Chem* 43:505–516
- Chadwick J, Jones M, Chadwick AE et al (2010) Design, synthesis and antimalarial/anticancer evaluation of spermidine linked artemisinin conjugates designed to exploit polyamine transporters in *Plasmodium falciparum* and HL-60 cancer cell lines. *Bioorg Med Chem* 18:2586–2597
- Chen LX, Zhu HJ, Wang R et al (2008) ent-labdane diterpenoid lactone stereoisomers from *Andrographis paniculata*. *J Nat Prod* 71:852–855
- Chu H, Smith JM, Felding J et al (2017) Scalable synthesis of (–)-thapsigargin. *ACS Central Sci* 3:47–51
- Cloete TT, Breytenbach JW, de Koch C et al (2012) Synthesis, antimalarial activity and cytotoxicity of 10-aminoethylether derivatives of artemisinin. *Bioorg Med Chem* 20:4701–4709
- Duthaler U, Huwyler J, Rinaldi L et al (2012) Evaluation of the pharmacokinetic profile of artesunate, artemether and their metabolites in sheep naturally infected with *Fasciola hepatica*. *Vet Parasitol* 186:270–280
- Efferth T, Kah S, Paulus K et al (2008a) Phytochemistry and pharmacogenomics of natural products derived from traditional Chinese medicine and Chinese materia medica with activity against tumor cells. *Mol Cancer Ther* 7:152–161

- Efferth T, Romero MR, Wolf DG et al (2008b) The antiviral activities of artemisinin and artesunate. *Clin Infect Dis* 47:804–811
- Foo K, Usui I, Gootz DC et al (2012) Scalable, enantioselective synthesis of germacrenes and related sesquiterpenes inspired by terpene cyclase phase logic. *Angew Chem Int Ed* 51:11491–11495
- Fuchs S, Berl V, Lepoittevin JP et al (2007) A highly stereoselective divergent synthesis of bicyclic models of photoreactive sesquiterpene lactones. *Eur J Org Chem*:1145–1152
- Ghantous A, Gali-Muhtasib H, Vuorela H et al (2010) What made sesquiterpene lactones reach cancer clinical trials? *Drug Discov Today* 15:668–678
- Grillet F, Huang CF, Brummond KM et al (2011) An allenic Pauson-Khand approach to 6,12-guaianolides. *Org Lett* 13:6304–6307
- Guzman ML, Li XJ, Corbett C et al (2005) Mechanisms controlling selective death of leukemia stem cells in response to parthenolide. *Blood* 106:141a–141a
- Guzman ML, Rossi RM, Neelakantan S et al (2007) An orally bioavailable parthenolide analog selectively eradicates acute myelogenous leukemia stem and progenitor cells. *Blood* 110:4427–4435
- Han CH, Barrios FJ, Riofsky MV et al (2009) Semisynthetic derivatives of sesquiterpene lactones by palladium-catalyzed arylation of the alpha-methylene-gamma-lactone substructure. *J Org Chem* 74:7176–7179
- Hassane DC, Sen S, Minhajuddin M et al (2010) Chemical genomic screening reveals synergism between parthenolide and inhibitors of the PI-3 kinase and mTOR pathways. *Blood* 116:5983–5990
- Hirose T, Miyakoshi N, Mukai C et al (2008) Total synthesis of (+)-achalensolide based on the Rh(I)-catalyzed allenic Pauson-Khand-type reaction. *J Org Chem* 73:1061–1066
- Hwang DR, Chang CW, Lien TW et al (2006) Synthesis and anti-viral activity of a series of sesquiterpene lactones and analogues in the subgenomic HCV replicon system. *Bioorg Med Chem* 14:83–91
- Justicia J, de Cienfuegos LA, Estevez RE et al (2008) Ti-catalyzed transannular cyclization of epoxygermacrolides. Synthesis of antifungal (+)-tuberiferine and (+)-dehydrobrachylaenolide. *Tetrahedron* 64:11938–11943
- Kalidindi S, Jeong WB, Schall A et al (2007) Enantioselective synthesis of arglabin. *Angew Chem Int Ed* 46:6361–6363
- Khazir J, Singh PP, Reddy DM et al (2013) Synthesis and anticancer activity of novel spiro-isoxazoline and spiro-isoxazolidine derivatives of alpha-santonin. *Eur J Med Chem* 63:279–289
- Kitson RR, Millemaggi A, Taylor RJ et al (2009) The renaissance of alpha-methylene-gamma-butyrolactones: new synthetic approaches. *Angew Chem Int Ed Engl* 48:9426–9451
- Krishna S, Uhlemann AC, Haynes RK et al (2004) Artemisinins: mechanisms of action and potential for resistance. *Drug Resist Updat* 7:233–244
- Kummer DA, Brenneman JB, Martin SF et al (2005) Application of a domino intramolecular enyne metathesis/cross metathesis reaction to the total synthesis of (+)-8-epi-xanthatin. *Org Lett* 7:4621–4623
- Kwok BH, Koh BD, Ndubiusi MI et al (2001a) The sesquiterpene lactone parthenolide binds and inhibits IKK beta. *Mol Biol Cell* 12:271a
- Kwok BHB, Koh B, Ndubiusi MI et al (2001b) The anti-inflammatory natural product parthenolide from the medicinal herb feverfew directly binds to and inhibits I kappa B kinase. *Chem Biol* 8:759–766
- Lone SH, Bhat KA (2015) Hemisynthesis of a naturally occurring clinically significant antitumor arglabin from ludartin. *Tetrahedron Lett* 56:1908–1910
- Long J, Ding YH, Wang PP et al (2013) Protection-group-free semisyntheses of parthenolide and its cyclopropyl analogue. *J Org Chem* 78:10512–10518
- Long J, Zhang SF, Wang PP et al (2014) Total syntheses of parthenolide and its analogues with macrocyclic stereocontrol. *J Med Chem* 57:7098–7112

- Macias FA, Santana A, Yamahata A et al (2012) Facile preparation of bioactive seco-guaianolides and guaianolides from *Artemisia gorgonum* and evaluation of their phytotoxicity. *J Nat Prod* 75:1967–1973
- Makiyi EF, Frade RFM, Lebl T et al (2009) Iso-seco-tanaparholides: isolation, synthesis and biological evaluation. *European J Org Chem*:5711–5715
- Mang C, Jakupovic S, Schunk S et al (2006) Natural products in combinatorial chemistry: an andrographolide-based library. *J Comb Chem* 8:268–274
- Marshall JA, Lebreton J, Dehoff BS et al (1987) Stereoselective total synthesis of aristolactone and epiaristolactone via [2,3] wittig ring contraction. *J Org Chem* 52:3883–3889
- Merten J, Frohlich R, Metz P et al (2004) Enantioselective total synthesis of the highly oxygenated 1,10-seco-eudesmanolides eriolanin and eriolangin. *Angew Chem Int Ed* 43:5991–5994
- Merten J, Hennig A, Schwab P et al (2006) A concise sultone route to highly oxygenated 1,10-seco-eudesmanolides – Enantioselective total synthesis of the antileukemic sesquiterpene lactones (–)-eriolanin and (–)-eriolangin. *European J Org Chem* 5:1144–1161
- Mihelcic J, Moeller KD (2003) Anodic cyclization reactions: the total synthesis of alliacol A. *J Am Chem Soc* 125:36–37
- Minnaard AJ, Wijnberg JBPA, de Groot A (1999) The synthesis of germacrane sesquiterpenes and related compounds. *Tetrahedron* 55:2115–2146
- Modzelewska A, Sur S, Kumar SK et al (2005) Sesquiterpenes: natural products that decrease cancer growth. *Curr Med Chem Anticancer Agents* 5:477–499
- Nakamura T, Tsuboi K, Oshida M et al (2009) Total synthesis of (–)-diversifolin. *Tetrahedron Lett* 50:2835–2839
- Nam NH (2006) Naturally occurring NF-kappa B inhibitors. *Mini Rev Med Chem* 6:945–951
- Nasim S, Crooks PA (2008) Antileukemic activity of aminoparthenolide analogs. *Bioorg Med Chem Lett* 18:3870–3873
- Neelakantan S, Nasim S, Guzmán ML et al (2009) Aminoparthenolides as novel anti-leukemic agents: discovery of the NF-kappa B inhibitor, DMAPT (LC-1). *Bioorg Med Chem Lett* 19:4346–4349
- Neukirch H, Kaneider NC, Wiedermann CJ et al (2003) Parthenolide and its photochemically synthesized 1(10)Z isomer: chemical reactivity and structure-activity relationship studies in human leucocyte chemotaxis. *Bioorg Med Chem* 11:1503–1510
- Peese K (2010) New agents for the treatment of leukemia: discovery of DMAPT (LC-1). *Drug Discov Today* 15:322–322
- Ploypradith P (2004) Development of artemisinin and its structurally simplified trioxane derivatives as antimalarial drugs. *Acta Trop* 89:329–342
- Reynolds AJ, Scott AJ, Turner CI et al (2003) The intramolecular carboxyarylation approach to podophyllotoxin. *J Am Chem Soc* 125:12108–12109
- Roboz GJ, Guzman M (2009) Acute myeloid leukemia stem cells: seek and destroy. *Exp Rev Hematol* 2:663–672
- Shaikenov TE, Adekenov SM, Williams RM et al (2001) Arglabin-DMA, a plant derived sesquiterpene, inhibits farnesyltransferase. *Oncol Rep* 8:173–179
- Shibuya H, Ohashi K, Kawashima K et al (1986) Synthesis of costunolide, an antitumor germacranolide, from E,E-farnesol by use of a low-valent chromium reagent. *Chem Lett* 1:85–86
- Siedle B, Garcia-Pineres AJ, Murillo R et al (2004) Quantitative structure – activity relationship of sesquiterpene lactones as inhibitors of the transcription factor NF-kappa B. *J Med Chem* 47:6042–6054
- Singh B, Srivastava JS, Khosa RL et al (2001) Individual and combined effects of berberine and santonin on spore germination of some fungi. *Folia Microbiol* 46:137–142
- Srivastava SK, Abraham A, Bhat B et al (2006) Synthesis of 13-amino costunolide derivatives as anticancer agents. *Bioorg Med Chem Lett* 16:4195–4199
- Sun CM, Syu WJ, Don MJ et al (2003) Cytotoxic sesquiterpene lactones from the root of *Saussurea lappa*. *J Nat Prod* 66:1175–1180

- Vadaparathi PRR, Kumar CP, Kumar K et al (2015) Synthesis of costunolide derivatives by Pd-catalyzed Heck arylation and evaluation of their cytotoxic activities. *Med Chem Res* 24:2871–2878
- Wen B, Hexum JK, Widen JC et al (2013) A redox economical synthesis of bioactive 6,12-guaianolides. *Org Lett* 15:2644–2647
- Woods JR, Mo HP, Bieberich AA et al (2011) Fluorinated amino-derivatives of the sesquiterpene lactone, parthenolide, as F-19 NMR probes in deuterium-free environments. *J Med Chem* 54:7934–7941
- Yang ZJ, Ge WZ, Li QY et al (2015) Syntheses and biological evaluation of costunolide, parthenolide, and their fluorinated analogues. *J Med Chem* 58:7007–7020
- Yeung S, Pongtavornpinyo W, Hastings IM et al (2004) Antimalarial drug resistance, artemisinin-based combination therapy, and the contribution of modeling to elucidating policy choices. *Am J Trop Med Hyg* 71:179–186
- Yokoe H, Yoshida M, Shishido K (2008) Total synthesis of (–)-xanthatin. *Tetrahedron Lett* 49:3504–3506
- Zhai JD, Li DM, Long J et al (2012) Biomimetic semisynthesis of arglabin from parthenolide. *J Org Chem* 77:7103–7107
- Zhang WH, Luo SJ, Fang F et al (2005) Total synthesis of absinthin. *J Am Chem Soc* 127:18–19
- Zhang Q, Cai DF, Liu JH (2011) Matrix solid-phase dispersion extraction coupled with HPLC-diode array detection method for the analysis of sesquiterpene lactones in root of *Saussurea lappa* CB Clarke. *J Chromatogr B Analyt Technol Biomed Life Sci* 879:2809–2814

# Chapter 6

## Analytical Procedures



Valeria P. Sülsen, Cesar A. N. Catalán, and Virginia S. Martino

**Abstract** The aim of this chapter is to provide an introduction to the current methods available for the analysis of plant material containing sesquiterpene lactones, delineate the most widely used extraction methods and provide a brief review of the literature on the subject. A general classification of sesquiterpene lactones, based on their carbocyclic skeletons, is given. The physicochemical properties and methods most commonly used for its extraction from the plant material, including more recent techniques such as supercritical fluid extraction, are analysed. Furthermore, visualization reagents for thin layer chromatography and isolation techniques, using different chromatographic methods, are also described.

**Keywords** Sesquiterpene lactones · Structural types · Extraction · Isolation · Chromatographic analysis · TLC · HPLC · GC · GC-MS

---

V. P. Sülsen (✉)

Universidad de Buenos Aires, Facultad de Farmacia y Bioquímica, Cátedra de Farmacognosia, Buenos Aires, Argentina

CONICET – Universidad de Buenos Aires, Instituto de Química y Metabolismo del Fármaco – CONICET (IQUIMEFA), Buenos Aires, Argentina  
e-mail: [vsulsen@ffyb.uba.ar](mailto:vsulsen@ffyb.uba.ar)

C. A. N. Catalán

CONICET – Universidad Nacional de Tucumán, Instituto de Química del Noroeste – CONICET (INQUINOA), San Miguel de Tucumán, Argentina

V. S. Martino

CONICET – Universidad de Buenos Aires, Instituto de Química y Metabolismo del Fármaco – CONICET (IQUIMEFA), Buenos Aires, Argentina

## 6.1 Structure of Sesquiterpene Lactones

Sesquiterpene lactones (STLs) are a widely distributed kind of secondary metabolites with a 15-carbon skeleton containing an  $\alpha,\beta$ -unsaturated- $\gamma$ -lactone moiety which can be lactonized towards C-6 or C-8 positions with either a *cis* or a *trans* configuration.

### 6.1.1 Skeletal Types of Sesquiterpene Lactones

Sesquiterpene lactones are classified according to their carbocyclic skeletons. The four major groups are germacranolides (10-membered ring), eudesmanolides (6–6 bicyclic compounds), guaianolides and pseudoguaianolides (5–7 bicyclic compounds). There are also several minor types that are described by different authors and will be mentioned herein. The suffix “olide” refers to the lactone group. *Seco*-derivatives are formed by oxidative cleavage of a C-C bond of the five (guaianolides, pseudoguaianolides)- or six (eudesmanolides)-membered ring depending on the type of STL (Yoshioka et al. 1973; Fischer et al. 1979).

#### 6.1.1.1 Germacranolides

The germacranolides, which are based on a cyclodecadiene ring, represent the major group of STLs. Four subtypes of germacranolides can be recognized according to configurational features: germacrolides, melampolides, heliangolides and *cis,cis*-germacranolides (Fig. 6.1).

All germacranolides have in common a cyclodecadiene skeleton with double bonds at C(1)=C(10) and C(4)=C(5) but differ from each other in the configuration of the double bonds:

- Germacrolides: *trans,trans*-germacranolides
- Melampolides: *cis,trans*-germacranolides
- Heliangolides: *trans,cis*-germacranolides
- *Cis,cis*-germacranolides

Germacrolides represent the most common subtype of germacranolides, whilst *cis,cis*-germacranolides are rarely found.

Oxygen functions, apart from the lactone, are frequently present in germacranolide structures: hydroxyl or esterified hydroxyl groups may be present at C-1, C-2, C-3, C-5, C-6, C-8 and C-9. One or both methyl groups can be oxidized to carbinol, aldehyde or carboxyl functions. For example, most melampolides have an oxidized C-14 (aldehyde or carboxylic acid derivatives). Another characteristic is that both or one of the ring double bonds may be transformed to epoxide groups. *Seco*-germacranolides can also be present in some plant species.

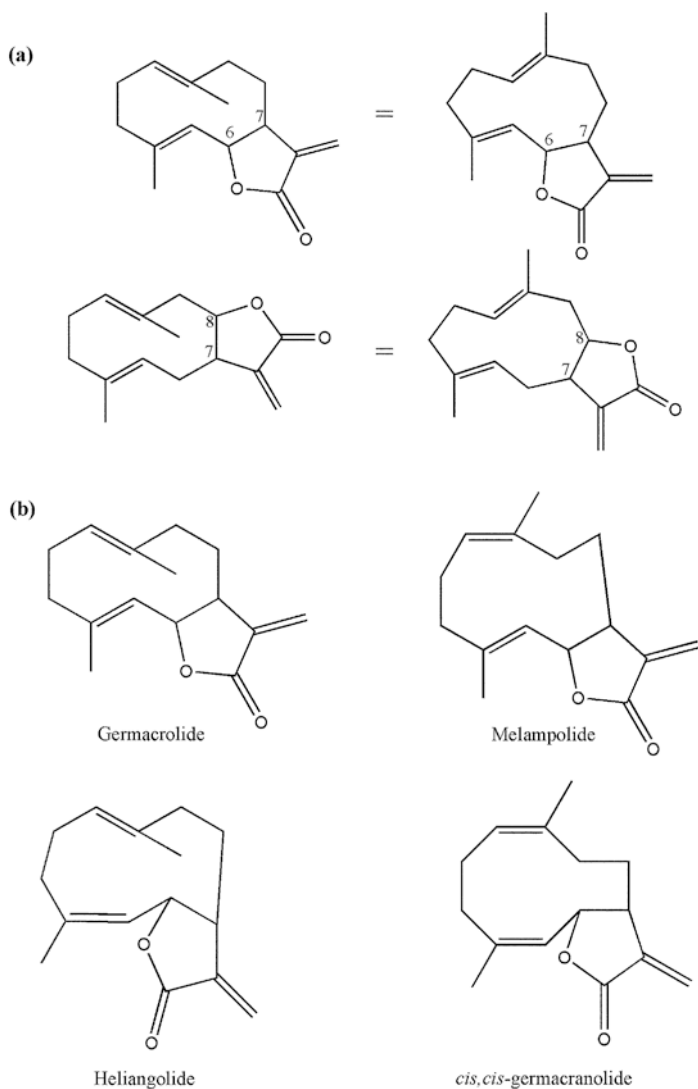


**Fig. 6.1** Structures of 6,7- and 7,8-lactonized germacranolides (a) and germacranolide subtypes according to the  $C_1 = C_{10}$  and  $C_4 = C_5$  double-bond configuration (b)

### 6.1.1.2 Eudesmanolides

These are 6–6 bicyclic compounds, based on the eudesmane skeleton. Members of this group could be lactonized 6,7 or 7,8, being the first most common. In this sense, most compounds have a 6,7-*trans*-lactonized moiety with an *exo*-methylene group between C-11 and C-13. The corresponding 11,13-dihydro derivatives have also been described. Compounds 7,8-lactonized may occur as *cis*- or *trans*- $\gamma$ -lactones.

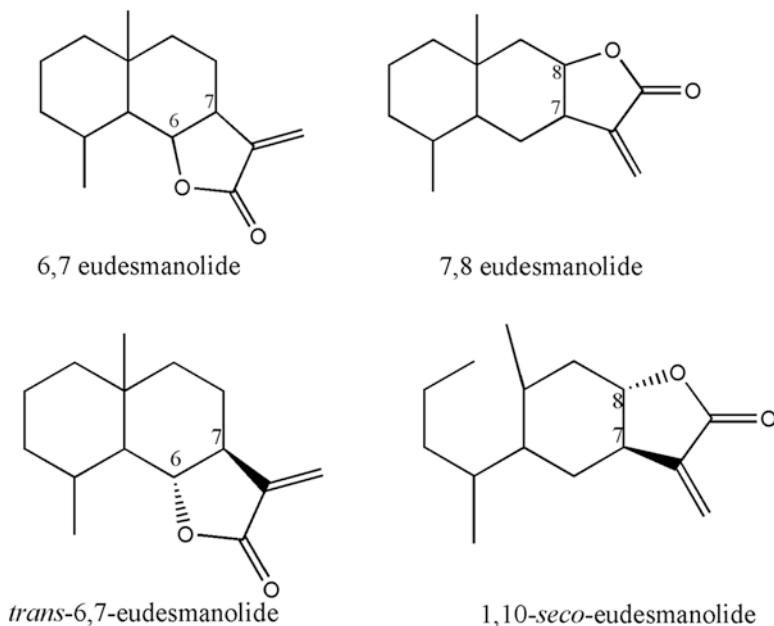


**Fig. 6.2** Structures of 6,7 and 7,8 eudesmanolides, *trans*-6,7-eudesmanolide and 1,10-*seco*-eudesmanolide

Most of the compounds of this group show double bonds at C(3)=C(4), C(4)=C(5) or C(5)=C(15) or have epoxide groups at these positions. Hydroxyl and/or ketone functions are common at C-1, C-3 and C-8. *Seco*-eudesmanolides can be also found in nature (Fig. 6.2).

### 6.1.1.3 Guaianolides

Guaianolides are STLs based on the guaiane skeleton. Together with their 4,5-*seco*-derivatives, known as xanthanolides, these are one of the largest groups of STLs (Fig. 6.3).

#### 6.1.1.4 Pseudoguaianolides

Pseudoguaianolides are 5–7 bicyclic compounds with a methyl group at the C-5 ring junction. They can be lactonized towards C-6 or C-8 (Fig. 6.4a). The other methyl group is present at C-10. Pseudoguaianolides can be divided into two groups according to the stereochemistry of the C-10 methyl group:

- Ambrosanolides, with a  $\beta$  methyl group at C-10 (Fig. 6.4b)
- Helenanolides, with an  $\alpha$  methyl group at C-10 (Fig. 6.4b)



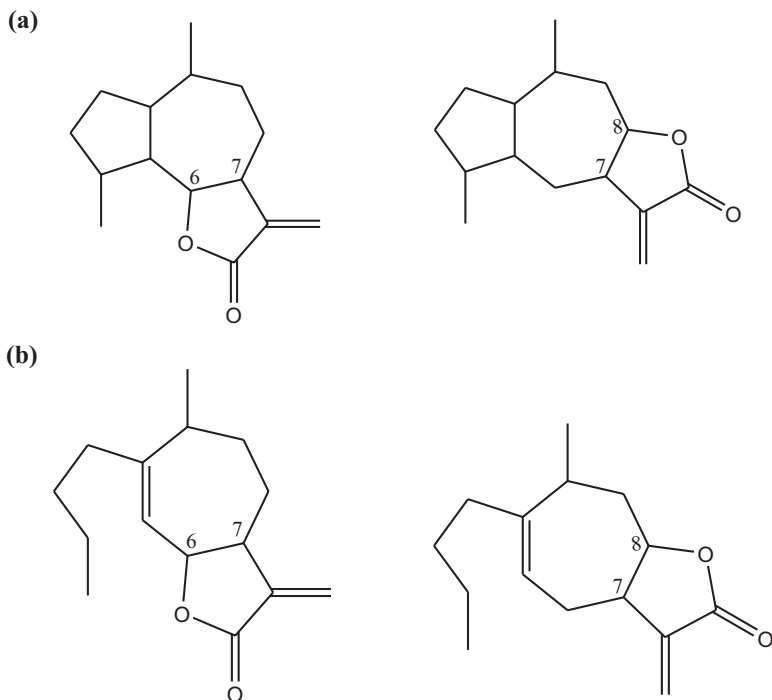


**Fig. 6.3** Structures of 6,7 and 7,8 guaianolides (a) and xanthanolides (b)

Most ambrosanolides are *cis*-lactonized towards C-6. On the other hand, all helenanolides have its lactone ring closed towards C-8 and lactonized either *cis* or *trans*. Cleavage between C-3 and C-4 or C-4 and C-5 can occur giving *seco*-pseudoguaianolides. Oxidative cleavage of ambrosanolides and helenanolides give the corresponding *seco*-derivatives: *seco*-ambrosanolides and *seco*-helenanolides (Fig. 6.5a). Psilostachynolides (psilostachyin A, B and C), produced by members of genus *Ambrosia* (Asteraceae), are examples of *seco*-ambrosanolides (Fig. 6.5b).

The nor-pseudoguaianolides are pseudoguaianolides that have lost a carbon atom and can be found occasionally in nature. They are usually C-15 nor-pseudoguaianolides due to loss of the methyl group on C-5.

#### 6.1.1.5 Other Classes of Sesquiterpene Lactones

- Bisabolonolides: STLs based on a bisabolane skeleton.
- Drimanolides: STLs based on a drimane skeleton. The most common structures have a C-10  $\beta$  methyl group.
- Eremophilinolides: STLs derived from eudesmanolides lactonized at C-8 and formed by migration of the methyl group of C-10 to C-5.

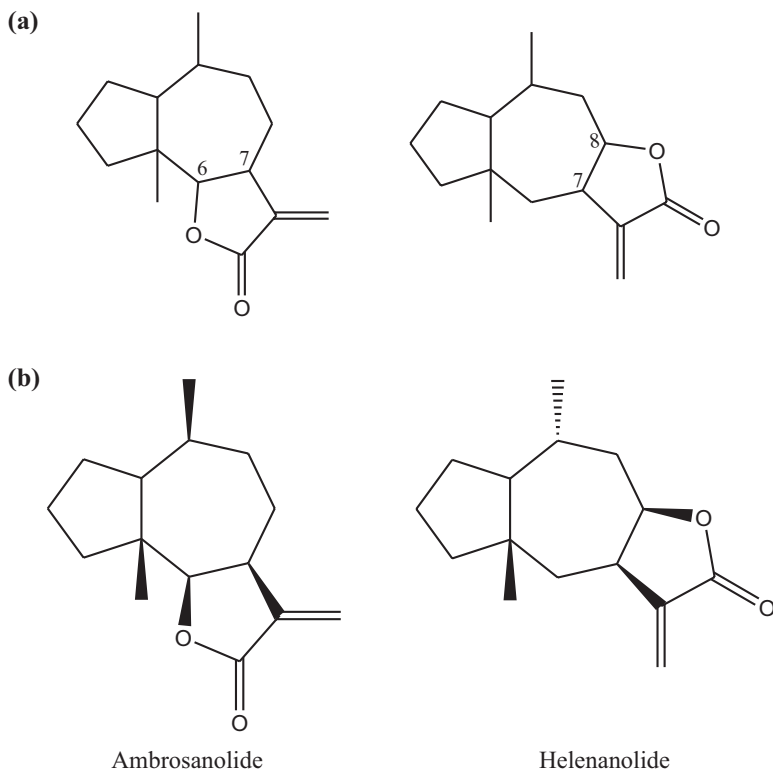


**Fig. 6.4** Structures of 6,7- and 7,8-lactonized pseudoguaianolides (a). A 6,7-*cis*-lactonized ambrosanolide and a 7,8-*cis*-lactonized helenanolide (b)

- Fukinanolides or bakkenolides: STLs containing a fukinane ring. They are derived from eremophilanolides by cleavage of the C(8)–C(9) bond and formation of a new C(7)–C(9) bond.
- Elemanolides: STLs derived from germacranolides by Cope transformation (e.g. miscandenin).
- Germafurenolides: germacranolides that have a furane ring at C-7 and C-8 in their structure.
- Tutinanolides (picrotoxins): they are STLs isolated from genera of the Orchidaceae family. They are generally highly oxidized and frequently contain nitrogen in their structure.
- Cadinanolides: they are STLs based on a cadinane skeleton. Artemisinin belongs to this group of STLs.

The general structure of bisabolenolides, drimanolides, eremophilanolides, fukinanolides (bakkenolides), elemanolides, germafurenolides, tutinanolides (picrotoxins) and cadinanolides are shown in Fig. 6.6.

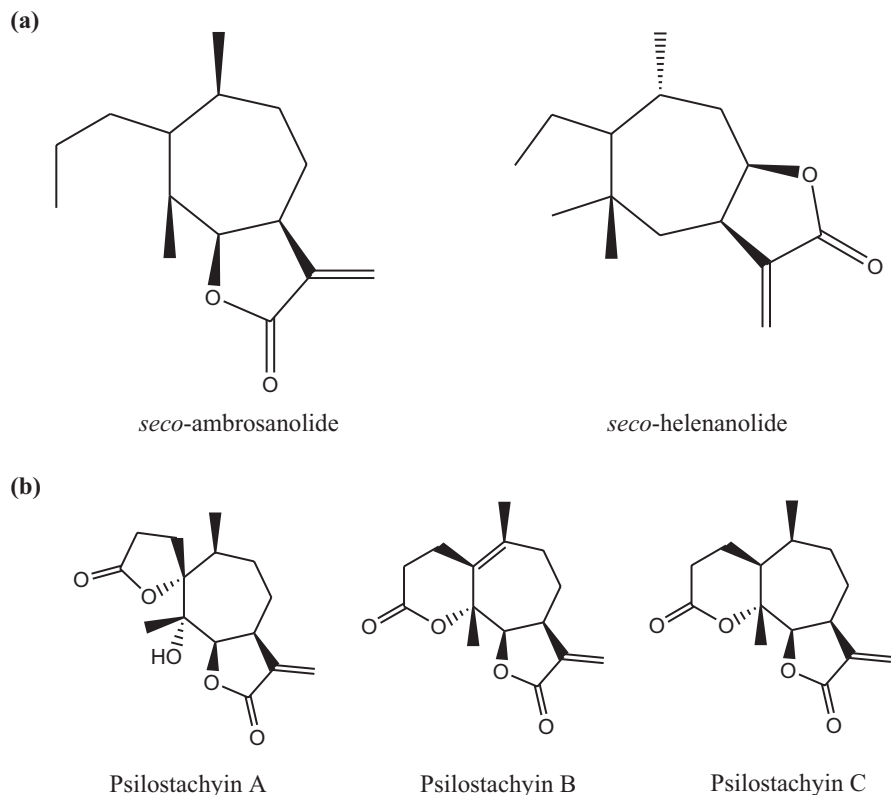


**Fig. 6.5** Structures of a 4,5-*seco*-ambrosanolide and a 3,4-*seco*-helenanolide (a) and psilostachynolides (b)

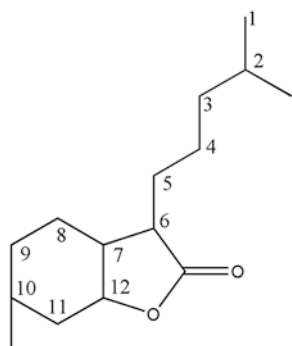
### 6.1.2 Common Side Chains in Sesquiterpene Lactones

Acetate groups are commonly found in the structure of STLs. Some of the most frequent side chains are shown in Fig. 6.7 (Fischer et al. 1979; Hernandez et al. 1995). Other less common side chains are represented in Fig. 6.8 (Cuenca et al. 1992).

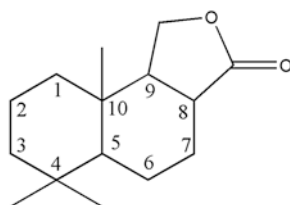
## 6.2 Extraction

Although hundreds of new STLs have been reported over the last years, there has been not much novelty regarding techniques used for their extraction and isolation.

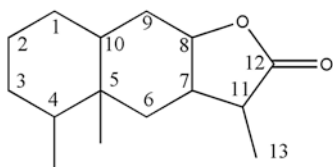
Sesquiterpene lactones are secondary metabolites present mainly in the leaves and flowering parts, though sometimes they are present in roots. The concentration



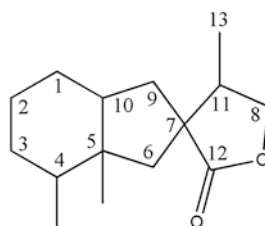
Bisabolonolide



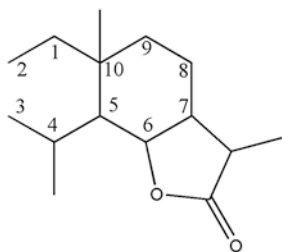
Drimanolide



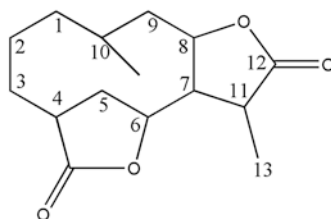
Eremophilonolide



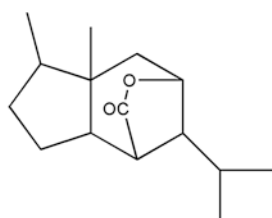
Fukinanolide



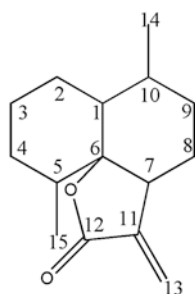
Elemanolide



Germafuranolide



Picrotoxinin type



Cadinanolide

**Fig. 6.6** Structures of other classes of sesquiterpene lactones

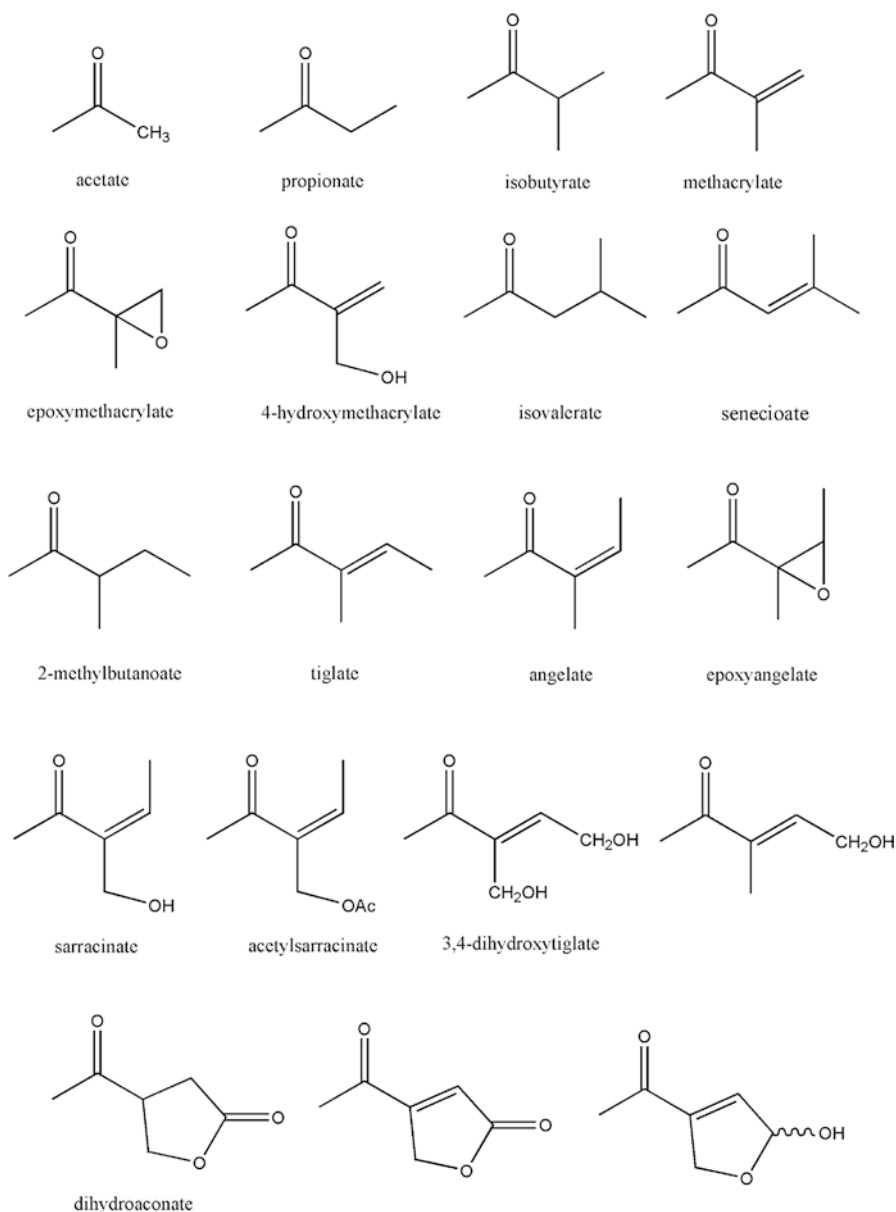


**Fig. 6.7** Most frequent side chains present in sesquiterpene lactones

of these compounds in the plant material ranges from 0.01% to 8% dry weight. They are generally found in a free form and rarely as glycosides.

These compounds are colourless crystalline, gummy or oily compounds and bitter in taste. They present low volatility and many of them are thermolabile. Due to their lipophilic character, they are soluble in non-polar solvents and insoluble in water.

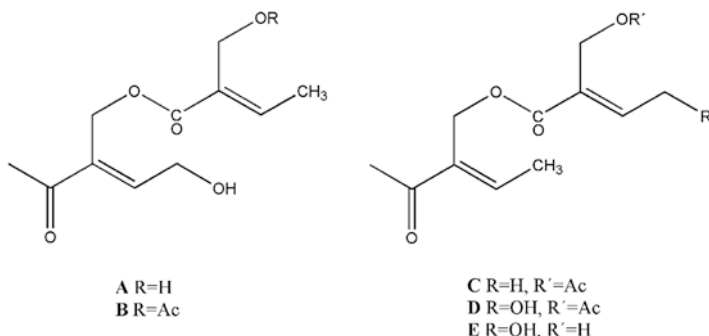


**Fig. 6.8** Less common side chains present in sesquiterpene lactones

Generally, the most used solvents for the extraction of STLs are chloroform, dichloromethane, ethyl acetate, diethyl ether and toluene. Acetone, methanol, ethanol and hydroalcoholic mixtures have been used occasionally. Generally the extraction is carried out by maceration at room temperature. Other extraction procedures such as soaking or Soxhlet extraction can be applied for different periods of time from seconds to days.

As an example of a general procedure, the dried ground plant sample is extracted with dichloromethane or chloroform at room temperature for 24 h. The extract is filtered and concentrated to dryness under vacuum, the residue taken in ethanol and the ethanol solution is mixed with an aqueous solution of lead acetate. Thus, the most polar compounds present in the extract precipitate and separate by paper filtration. The hydroalcoholic filtrate is then partitioned with chloroform. The organic layer, containing the STLs, is taken to dryness under vacuum (Domínguez 1979).

Another option consists in obtaining the chloroform extract by maceration of the plant material at room temperature. After filtering and solvent evaporation, the residue is dissolved in ethanol at 60 °C and diluted with water. The hydroalcoholic suspension is then extracted successively with hexane and chloroform. Sesquiterpene lactones are concentrated in the chloroform fraction (Catalan et al. 2003; Krautmann et al. 2007).

Another extraction method reported in the literature consists in obtaining a dewaxed crude extract. For this purpose, the dried entire leaves are soaked one by one in chloroform for 20 s at room temperature with a gentle shaking. The chloroform extract is then concentrated to dryness and the residue taken in methanol at 50 °C. After cooling, distilled water is added dropwise to precipitate waxes. After filtering, the hydromethanolic filtrate is then evaporated at reduced pressure. This procedure yields a dewaxed extract containing STLs and diterpenes (Mercado et al. 2010).

The use of entire leaves as starting material in the extraction methods described above is justified since STLs are generally produced and stored in the glandular trichomes on the leaf surface. Besides, the use of a short period of time would not

allow the extraction of other metabolites present in the internal parts of the plant material.

In this sense, Mercado (2011) have compared two procedures for the extraction of STLs in “yacon” (*Smallanthus sonchifolius*) leaves:

- A. One of the procedures consists in obtaining the glandular trichomes by scraping the surface of fresh leaves. Glandular trichomes are then extracted with chloroform for 10 min at room temperature with magnetic stirring. The extract is concentrated under vacuum.
- B. The other procedure is named “foliar washing”. This technique consists in soaking each leaf (individually) in a cube with chloroform or dichloromethane for 20 s with a gentle swinging movement. When all the leaves have been washed, the obtained extract is evaporated at reduced pressure and the residue taken in methanol at 50 °C. After cooling, distilled water is added dropwise to precipitate waxes which are collected by filtration. The hydromethanolic filtrate is evaporated at reduced pressure to yield a dewaxed extract.

The residues obtained with both A and B procedures were dissolved in dichloromethane and analysed by thin layer chromatography (TLC) and gas chromatography/mass spectrometry (GC/MS). Results demonstrated that the composition of STLs was essentially the same in both extracts (Figs. 6.9 and 6.10). In the extract obtained by procedure A, the presence of high-chain hydrocarbons was detected. This phenomenon was due to the absence of a dewaxing step in procedure A (Table 6.1).

The time of extraction was also evaluated by Mercado (2011) by using the foliar washing procedure. Periods of times of 20, 40, 120, 420 and 1020 s were employed in order to determine the optimal time for STL extraction. The best results were obtained by soaking the leaves during 20 s. This period of time allows the complete extraction of STLs together with other metabolites present in the surface of the leaves (waxes) with minimum extraction of other compounds present inside the leaves. Longer times led to the extraction of other metabolites (chlorophyll and other compounds) that complicate the analysis and subsequent separation of the STLs.

Although glycosylation is not a common feature in STLs, when glycosylated STLs are of interest, methanol, ethanol or ethanol-water mixtures can be used for their extraction and isolation.

A thorough description of extraction and isolation procedures for most of the representative STLs, such as santonin, artemisinin, alantolactone, parthenolide, arglabin and others, can be found in the literature (Adekenov 2013).

Due to the lipophilicity of STLs, medium polarity organic solvents are generally used for their extraction. When scaling up these methods for an industrial production, they are labour intensive and have the disadvantage of using large quantities of toxic solvents. Therefore, more environmentally friendly methods should be employed. Supercritical fluid extraction (SFE), using liquid CO<sub>2</sub>, has been demonstrated to be an efficient extraction method, for example, for the extraction of

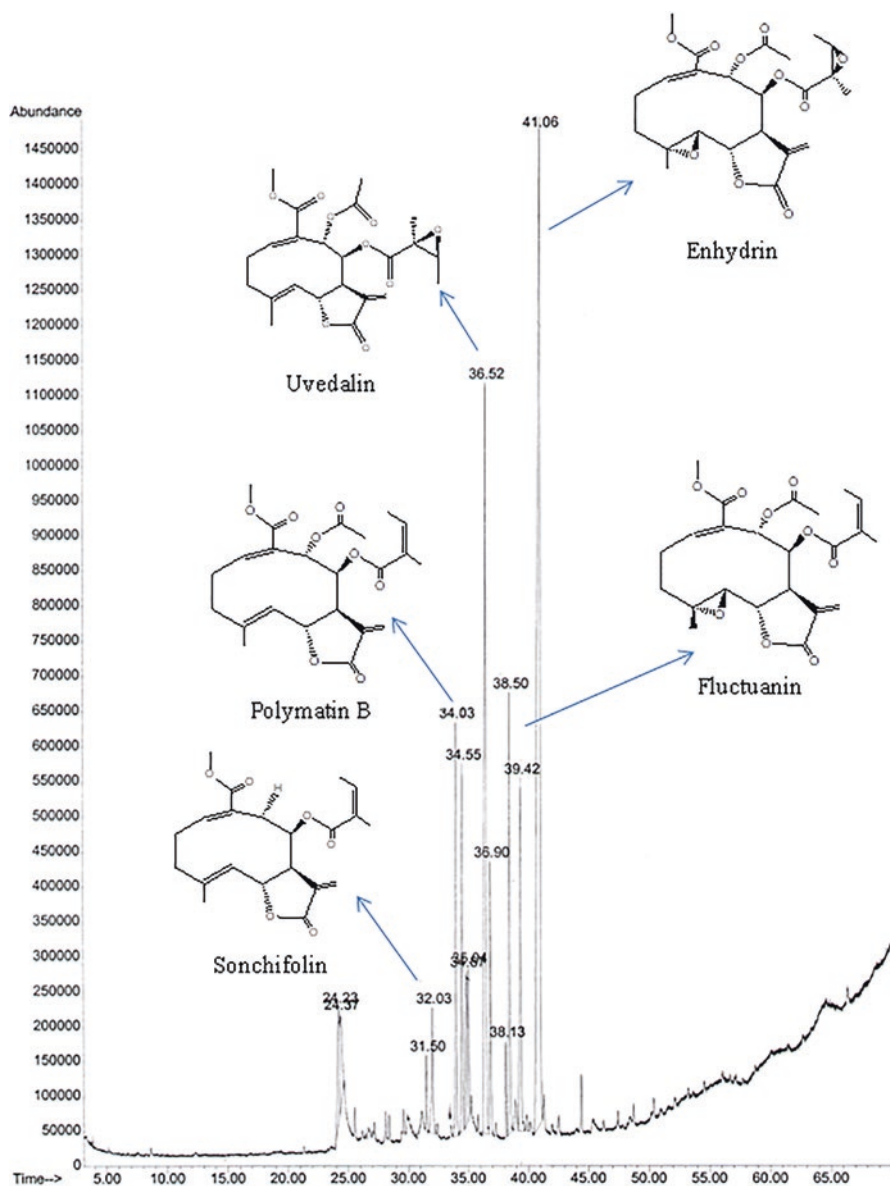


**Fig. 6.9** Gas chromatographic profile of the residue obtained from *Smilax sonchifolia* leaves by extraction procedure A (Mercado 2011)

arglabin. Using SFE, the yield of arglabin was almost four times higher than that obtained when chloroform was used (Adekenov 2013). Adekenov (2016) has studied the arglabin yield under different SFE extraction conditions such as temperature, pressure and extraction time.



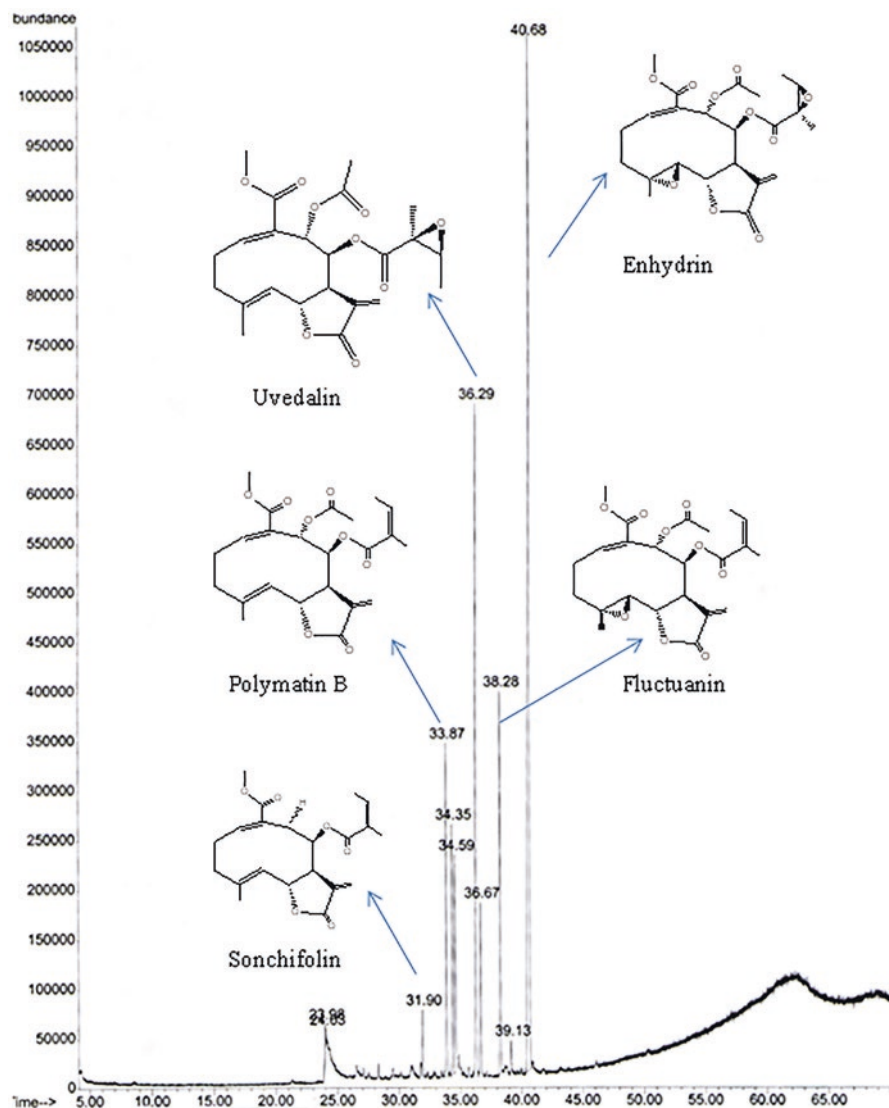


**Fig. 6.10** Gas chromatographic profile of the residue obtained from *Smilax sonchifolius* leaves by extraction procedure B (Mercado 2011)

Another method with low solvent consumption that can be used for the extraction of STLs is microwave-assisted extraction (MAE). In the case of artemisinin, MAE has proved to be more efficient allowing a higher recovery of the STL than that obtained with the classical solvent extraction. Pressurized solvent extraction (PSE) using elevated temperatures and pressure has been also applied to artemisinin extraction (Ivanescu et al. 2015).

**Table 6.1** Percentages of the main sesquiterpene lactones present in CHCl<sub>3</sub> extracts (procedures A and B) of *Smilax sonchifolius* leaves

Compounds	% of the compounds <sup>(a)</sup>	
	Procedure A	Procedure B
Enhydrin	37.5 ± 0.7	45.2 ± 1.5
Fluctuanin	7.8 ± 0.3	11 ± 1.0
Uvedalin	15.5 ± 0.5	16.7 ± 0.6
Polymatin B	7.2 ± 0.3	5.8 ± 0.7
Sonchifolin	2.8 ± 0.3	1.7 ± 0.3
Others <sup>a</sup>	29.2 ± 1.1	18.3 ± 1.6

Adapted from Mercado (2011)

<sup>a</sup>The determination was performed by GC/MS

### 6.3 Isolation

Purification of the STLs present in crude extracts can be done by repeated open column chromatography (CC) or flash CC on silica gel or aluminium oxide eluting with hexane:EtOAc, hexane:acetone (Ivanescu et al. 2015) or dichloromethane:EtOAc mixtures (Adekenov 2013).

Generally, the dewaxed extract (described in Sect. 6.2) is fractionated by CC using silica gel employing CHCl<sub>3</sub> or CH<sub>2</sub>Cl<sub>2</sub> with increasing amounts of EtOAc (10–40%) as mobile phases. Fractions are commonly analysed by TLC and Fourier-transform infrared (FT-IR) spectroscopy and sometimes by nuclear magnetic resonance (NMR). Fractions exhibiting  $\gamma$ -lactone carbonyl absorption in the IR spectra (1755–1790 cm<sup>-1</sup>) are then analysed by GC/MS (Krautmann et al. 2007; Mercado et al. 2010; Catalan et al. 2003).

Preparative reversed phase high performance liquid chromatography (RP-HPLC) is also employed for the separation and purification of STLs. This method employs C8, C18 or phenylhexyl columns and either refractive index detector or UV detector at 220 nm, using MeOH:H<sub>2</sub>O mixtures as mobile phase (Krautmann et al. 2007; Mercado et al. 2010; Cuenca et al. 1988; Catalan et al. 2003).

Another technique employed for the separation and purification of STLs is high-speed centrifugal chromatography (HSCC) which has been successfully applied for the isolation of arglabin and some glycosylated STLs (Adekenov 2013; Cai et al. 2014). The main advantage of this liquid-liquid partition technique is that it avoids the loss of yield due to adsorption onto a solid matrix.

The last step in the purification of STLs consists in a recrystallization of the obtained compound using 96% EtOH or mixtures of hexane:EtOAc, heptane:EtOAc or EtOH:H<sub>2</sub>O.

## 6.4 Chromatographic Analysis

Chromatographic techniques are very useful in phytochemical analysis as they can provide information about the complexity and types of compounds present in a crude extract. They are very useful in monitoring the fractions of a separation by CC and for the isolation and identification of a given compound. Thin layer chromatography using selective detection reagents and hyphenated techniques such as HPLC-MS is very useful for the detection of these compounds in crude extracts. Conventional open CC is the most frequently used method for the separation of natural products in general. This methodology does not need specialized equipment and it is easy to perform (Hosttetman et al. 2008).

The successful exploitation of known techniques together with the improvements to existing methods and the continuous development of new techniques to overcome analytical problems make chromatographic methods an important tool in the isolation and discovery of new compounds (Harborne, 1998).

### 6.4.1 Thin Layer Chromatography

Thin layer chromatography is a simple and fast method for the preliminary search for STLs in crude plant extracts. The most commonly used stationary phase is silica gel. The plates are developed with some of the following solvent systems:

- $\text{CH}_2\text{Cl}_2$ :acetone (3:1; 4:1; 5:1)
- $\text{CHCl}_3$ :EtOAc (6:1; 4:1; 3:2; 1:3)
- Hexane:EtOAc (7:3; 1:1; 3:7)
- $\text{CHCl}_3$ :methanol (9:1; 19:1; 99:1)
- $\text{CHCl}_3$ :EtO<sub>2</sub> (4:1; 5:1)
- Benzene:acetone (4:1)
- Benzene:EtOAc (5:5)
- Benzene:methanol (9:1)
- Benzene:ether (2:3)
- Toluene:EtOAc (3:2; 1:1; 2:3)
- Cyclohexane:acetone (1:1)
- Hexane:THF:methanol (5:5:1)
- Petroleum:ether: $\text{CHCl}_3$ :EtOAc (2:2:1)

These same solvent systems can be used for monitoring the resulting fractions from CC separation.

General visualization reagents such as  $\text{KMnO}_4$ , concentrated  $\text{H}_2\text{SO}_4$  followed by heating or exposure to iodine vapours and UV light observation at 254 nm, can be used for the detection of STLs (Picman et al. 1980). Sesquiterpene lactones appear as brown spots when iodine vapours are used. After spraying with concentrated  $\text{H}_2\text{SO}_4$  and heating for 5 min at 100–110 °C, STLs are detected as green, brown,

yellow, red or blue spots. The colour produced by some STLs may be related to structural characteristics (Harborne 1998).

Other visualization reagents used for the detection of STLs produce distinctive colours with the individual compounds on TLC plates:

- Vanillin sulphuric acid: purple, blue, green, red colours (\*) (Picman et al. 1980).
- Anisaldehyde sulphuric acid: mauve, red-brown, black-blue, orange, yellow and grey colours (\*) (Nowak et al. 2010).
- Five percent solution of aluminium chloride in ethanol: purple or brown colour on the plate. Yellow, brown and green fluorescence under UV light at 366 nm is evident only 10–15 min after heating at 120 °C (Villar et al. 1984).
- One percent methanolic resorcinol – 5% phosphoric acid (1:1) (Harborne 1998).

(\*) Colours are observed after spraying and heating at 100–110 °C for 3–5 min.

### 6.4.2 High-Performance Liquid Chromatography

High-performance liquid chromatography has been demonstrated to be a suitable tool for the detection and quantification of STLs in plant extracts and for monitoring the purification of STLs together with TLC. Reverse phase methods are of choice. Most common columns used are C8 and C18 but phenylhexyl columns are also used. Most used mobile phases are mixtures of acetonitrile:water or methanol:water. Acetonitrile is preferable since the methanol cut-off (205 nm) may interfere with some STL absorption maximum.

Exceptionally, some analytical normal phase techniques employ silica gel columns using mixtures of dichloromethane:methanol, EtOAc:hexane, tert-butyl-methyl ether:methanol and n-hexane:acetonitrile:methanol as mobile phases (Merfort 2002).

The ultraviolet low absorption of STLs is the main problem when ultraviolet diode array detector (UV-DAD) detector is employed. Derivatization methods have been developed in order to increase the sensitivity and allow the detection of STLs at higher wavelengths. For example, parthenolide can be effectively quantified in this way (Merfort 2002).

### 6.4.3 Gas Chromatography

Gas chromatography coupled to MS can be a useful tool for the separation and identification of STLs. However, this method cannot be applied in all cases since some STLs are thermolabile or are not volatile enough. This difficulty can be overcome through derivatization or transformation of these compounds (Ivanescu et al. 2015). Generally, non-polar capillary columns and oven temperature ranging from 180 to 300 °C are used.

For example, the *Artemisia pallens* extract has successfully been analysed by GC-MS allowing the identification of its main compounds (Ivanescu et al. 2015). Excellent results have also been obtained in the case of *Smilax sonchifolius* (Mercado et al. 2010), in which a selective mass detector (quadrupole) coupled to a GC was used.

Mercado et al. (2010) recommend the following conditions for analysing STLs by GC/MS:

- Column: 5% phenylmethylsiloxane
- Ionization energy: 70 eV
- Carrier gas: helium at 1.2 ml/min
- Injector temperature: 220 °C
- GC/MS interphase temperature: 280 °C
- Ion source temperature: 230 °C
- Selective mass detector temperature: 150 °C
- Oven conditions: temperature from 180 to 300 °C at 2 °C/min and held at 300 °C for 10 min

The samples are dissolved in dichloromethane (25 µl/mg of STL mixture). Percentages are reported as the means of at least three runs and calculated from the total ion chromatogram (TIC).

## 6.5 Conclusion

The extraction and isolation of sesquiterpene lactones can be achieved using conventional methods with organic solvents or, more recently, by environmentally friendly techniques such as supercritical extraction. Separation and purification of individual compounds can be performed mainly by column chromatography, semi-preparative HPLC and recrystallization. Several chromatographic methods (TLC, HPLC, GC), altogether with combined techniques (HPLC/DAD; GC/MS), have been successfully applied for the analysis, separation and quantification of several sesquiterpene lactones.

## References

- Adekenov SM (2013) Natural sesquiterpene lactones as renewable chemical materials for new medicinal products. *Euras Chem Tech J* 15:163–174
- Adekenov SM (2016) Chemical modification of arglabin and biological activity of its new derivatives. *Fitoterapia* 110:196–205
- Cai W, Zhang JY, Li GL et al (2014) Isolation and purification of sesquiterpene lactones from *Ixeris sonchifolia* (bunge) hance by high-speed countercurrent chromatography and semi-preparative high performance liquid chromatography. *Trop J Pharm Res* 13(12):2065–2069

- Catalan CAN, Cuenca M, Hernandez L et al (2003) *cis,cis*-Germacranolides and melampolides from *Mikania thapsoides*. *J Nat Prod* 66(7):949–953
- Cuenca MR, Bardon A, Catalan CA et al (1988) Sesquiterpene lactones from *Mikania micrantha*. *J Nat Prod* 51(3):625–626
- Cuenca MR, Borkosky S, Catalan CA et al (1992) A cadinanolide and other sesquiterpene lactones from *Mikania haenkeana*. *Phytochemistry* 31(10):3521–3525
- Domínguez XA (1979) Métodos de investigación fitoquímica. Limusa, México
- Fischer NH, Oliver EJ, Fischer HD (1979) The biogenesis and chemistry of sesquiterpene lactones. In: Herz W, Grisebach H, Kirby GW (eds) *Progress in chemistry of organic natural products*, vol 38. Springer, New York, pp 47–390
- Harborne JB (1998) *Phytochemical methods. A guide to modern techniques of plant analysis*. Chapman & Hall, London
- Hernandez LR, Catalán CAN, Cerda García Rojas CM et al (1995) Guaianolides from *Stevia gilliesii*. *Nat Prod Lett* 6:215–225
- Hosstetman K, Gupta M, Marston A et al (2008) Handbook of strategies for the isolation of bioactive natural products. Secab and Cyted, Bogotá
- Ivanescu B, Miron A, Corciova A (2015) Sesquiterpene lactones from *Artemisia* genus: biological activities and methods of analysis. *J Anal Methods Chem* 2015:247685. <https://doi.org/10.1155/2015/247685>
- Krautmann M, de Riscalca EC, Burgueño-Tapia E et al (2007) C-15-functionalized eudesmanolides from *Mikania campanulata*. *J Nat Prod* 70(7):1173–1179
- Mercado MI (2011) Ph.D. thesis, Universidad Nacional de Tucumán
- Mercado MI, Coll Aráoz MV, Grau A et al (2010) New acyclic diterpenic acids from yacon (*Smallanthus sonchifolius*) leaves. *Nat Prod Commun* 5(11):1721–1726
- Merfort I (2002) Review of the analytical techniques for sesquiterpenes and sesquiterpene lactones. *J Chromatogr A* 967(1):115–130
- Nowak G, Dawid-Pač R, Urbańska M et al (2010) TLC of selected sesquiterpenoids of the Asteraceae family. *Acta Soc Bot Pol* 80(3):193–196
- Picman AK, Ranieri RL, Towers GHN et al (1980) Visualisation reagents for sesquiterpene lactones and polyacetylenes on thin layer chromatograms. *J Chromatogr A* 189:187–198
- Villar A, Rios JL, Simeón S et al (1984) New reagent for the detection of sesquiterpene lactones by thin-layer chromatography. *J Chromatogr A* 303(1):306–308
- Yoshioka H, Mabry J, Timmermann BN (1973) *Sesquiterpene lactones: chemistry, NMR and plant distribution*. University of Tokyo Press, Tokyo

# Chapter 7

## Spectroscopic Methods for the Identification of Sesquiterpene Lactones



Valeria P. Sülsen, Osvaldo J. Donadel, and Cesar A. N. Catalán

**Abstract** The most widely used spectroscopic methods for the identification of sesquiterpene lactones are discussed. The most distinctive and characteristic signals in the UV, IR, MS,  $^1\text{H-NMR}$  and  $^{13}\text{C-NMR}$  spectra are discussed. In addition, some examples of the application of these techniques for the structure elucidation of some representative sesquiterpene lactones with different skeletal types are presented.

**Keywords** UV · CD · IR · MS ·  $^1\text{H-NMR}$  ·  $^{13}\text{C-NMR}$  · 2D techniques

### 7.1 General Spectroscopic Characteristics of Sesquiterpene Lactones

Spectroscopic methods are fundamental in the structural determination of the different skeletons of sesquiterpene lactones (STLs). The most important are mass spectrometry (MS), infrared and ultraviolet absorption spectrometry (IR and UV, respectively), circular dichroism (CD), nuclear magnetic resonance spectrometry (NMR) and X-ray diffraction (Budesinsky and Saman 1995).

---

V. P. Sülsen

Universidad de Buenos Aires, Facultad de Farmacia y Bioquímica, Cátedra de Farmacognosia, Buenos Aires, Argentina

CONICET – Universidad de Buenos Aires, Instituto de Química y Metabolismo del Fármaco – CONICET (IQUIMEFA), Buenos Aires, Argentina

O. J. Donadel

Instituto de Investigaciones en Tecnología Química (INTEQUI),  
Universidad Nacional de San Luis, San Luis, Argentina

C. A. N. Catalán (✉)

CONICET – Universidad Nacional de Tucumán, Instituto de Química del Noroeste – CONICET (INQUINOA), San Miguel de Tucumán, Argentina  
e-mail: [ccatalan@fbqf.unt.edu.ar](mailto:ccatalan@fbqf.unt.edu.ar)

### 7.1.1 MS Spectra

The mass spectrometric behaviour of STLs varies widely. Fragmentation patterns are quite different depending on the skeletal type involved. The main application of mass spectroscopy by electron impact ionization is to determine the elemental composition of the compound studied. In structurally simple STLs, the base peak frequently corresponds to the molecular ion. However, when STLs with hydroxyl and/or ester side chains are analysed, the peak corresponding to the molecular ion is often missing. This phenomenon is due to the loss of water and/or the side chain by a rearrangement of McLafferty. In such cases, the acyl ion of the ester group is usually observed as an intense peak that often represents the base peak of the mass spectrum. This drawback can usually be overcome by using fast atom bombardment (FAB) ionization. The FAB-mass spectrum contains a peak corresponding to the  $[M + H]^+$  ion (Budesinsky and Saman 1995). In the spectra corresponding to STLs containing hydroxyl and/or acetoxy groups, the M-18 and M-60 peaks can be found (Domínguez 1979).

Mass spectra of germacranolides display differences due to the variation in the skeleton and substitution patterns. The parent peak and ester side chains attached to the ten-membered ring can be detected. In compounds containing hydroxyls and/or ester functions, the parent peak is frequently missing due to the loss of either water or side chain. In this latter case, the acylium group of the ester group is generally the base peak (Fischer et al. 1979).

In eudesmanolides, as in germacranolides and other types of STLs, the position of the oxygen substituents changes the fragmentation pattern. In eudesmanolides with C(1)-OH, the most common fragmentation is the cleavage of the C(1)-C(10) and the C(4)-C(5) bonds showing a fragment at  $m/z = 167$ . The M-CH<sub>3</sub>, M-H<sub>2</sub>O and M-CO ions may be generated, and the elements of the lactone ring could split up to generate peaks of different intensities (Abdullaev et al. 1979).

The fragmentation pattern of guaianolide-type STLs depends on the nature of substituents and the presence of double bonds. In the case of 1,2-epoxyguaianolides, the electron impact causes the breakdown of M<sup>+</sup> with elimination of substituents and cleavage of rings A and B (A, cyclopentane ring; B, cycloheptane ring). The mass spectra of 1,2-dihydroxyguaianolides show stability of the M<sup>+</sup>. The elimination of substituents and the cleavage of ring A have also been observed. The presence of a system C(1)=C(10), C(2)=O and C(3)=C(4) conjugated bonds, and also of C(5)=C(6), stabilizes the M<sup>+</sup>, and the most important fragment process is the elimination of the lactone ring. The presence of OH groups at C-3 and C-8 does not change the stability of the M<sup>+</sup> (Plugar et al. 1987).

Pseudoguaianolides render weak parent peaks in the mass spectrum, together with slightly lower  $m/e$  value peaks corresponding to the loss of water and methyl, acetyl and carbonyl groups, among others (Matsueda 1972; Tsai et al. 1969; Sülsen 2009).

The mass spectrum corresponding to helenalin and related pseudoguaianolides (helenanolides), such as mexicanin I, tenulin and baldulin, bearing the 4-, 6- and 8-oxygenation pattern with the double bond in the five-membered ring, has been



analysed (Tsai et al. 1969). Thus, the presence of peaks at  $m/z$  95, 96, 122, 123 and 124 is characteristic in the mass spectrum of this type of compounds.

The ambrosanolides psilostachyin, psilostachyin C and peruvian are known to produce common peaks at  $m/z$  96, which are attributed to the presence of the exomethylene  $\gamma$ -lactone moiety as well as peaks at  $m/z$  91 corresponding to the tropylium ion ( $C_7H_7^+$ ). Psilostachyin C also generates a peak at  $m/z$  67 corresponding to the  $\delta$ -lactone function (Sülsen 2009).

Two groups of pseudoguaianolides with OH groups in any of the positions C-1, C-6, C-8 or C-10 and lactonized either towards C-6 (A) or C-8 (B) have been established by Cortes et al. (1977). Compounds lactonized towards C-6 show the same fragmentation pattern with ions at ( $M^+ - CH_3$ ), ( $M^+ - H_2O$ ), [ $M^+ - (CH_3 + H_2O)$ ], [ $M^+ - (15 + 28)$ ], 123, 95 and 67. Apart from these, other fragments can be detected at  $m/z$  [ $M^+ - (28 + 18)$ ], 191, 175, 165, 140, 137, 124 and 97. Compounds of group B display a similar fragmentation pattern to those of group A. One of the differences observed is that compounds of the B group do not show a fragment  $m/z$  at ( $M^+ - CH_3$ ) attributed to the loss of the  $CH_3$  group at C-5. Fragments which show the loss of water ( $M^+ - H_2O$ ) and cetene ( $M^+ - C_2H_2O$ ) can also be found. The loss of cetene is a consequence of the breakdown of the linkages C(2)–C(3) and C(4)–C(5), giving the ion at  $m/z$  222.

In dimeric STLs, high-resolution mass spectrum (HRMS) shows the dissociation of the dimer into its two components.

### 7.1.2 IR Spectra

Infrared spectroscopy is also an extremely useful tool for the detection of functional groups (carbonyl, hydroxyl, double and triple bonds, etc.) present in a molecule. Besides, it is particularly useful for detecting STLs in fractions and extracts, through the presence of the band corresponding to the  $\gamma$ -lactone ring. The carbonyl stretching of  $\alpha,\beta$ -unsaturated- $\gamma$ -lactones generates an intense absorption band at 1750–1790  $cm^{-1}$  that allows detecting their presence even when they are in a small percentage. The exomethylene group generates absorption signals at 1665, 1405, 965 and 890  $cm^{-1}$ . Saturated STLs generate absorption bands at ca. 1770  $cm^{-1}$  (Nakanishi 1962).

### 7.1.3 UV Spectra

Ultraviolet spectroscopy is generally employed for compounds containing an appropriate chromophore. The UV absorption of STLs occurs at low wavelengths, and such phenomenon correlates with the number of unsaturations present in the molecule. Saturated STLs absorb at near 200 nm or lower, while  $\alpha,\beta$ -unsaturated STLs show maximal absorptions in the range of 205–225 nm. The presence of cyclohexenone or cyclopentenone groups in eudesmanolides and guaianolides, respectively, determines a  $\lambda_{max}$  of 214–230 nm (Domínguez 1979).

### 7.1.4 CD Spectra

The stereochemistry of some STLs has been determined by CD. The  $\alpha$ -methylene- $\gamma$ -lactone chromophore group shows a Cotton effect (due to a  $n-\pi^*$  transition) in the 245–260 nm range. The Stocklin-Waddell-Geissman rule correlates the signal obtained through the Cotton effect with the position (12,6-resp. 12,8-olide) and stereochemistry (*cis* or *trans*) of the lactone ring (Budesinsky and Saman 1995).

### 7.1.5 NMR Spectra

NMR spectroscopy plays an extremely important role in the structural analysis of STLs. The advances in 1D ( $^1\text{H-NMR}$ ,  $^{13}\text{C-NMR}$ , DEPT) and 2D (HMBC, HSQC, edited HSQC, HMBC, COSY and ROESY) methodologies have allowed determining the structure of a large number of lactones.

#### 7.1.5.1 $^1\text{H-NMR}$

In all types of STLs, the proton signals corresponding to the hydrogen atoms on C-6, C-7, C-8 and C-13 are characteristic because they are involved in the lactone closure positions and the presence or absence of a C(11)–C(13) double bond. Valuable structural information is obtained with the  $^1\text{H-NMR}$  spectrum (chemical shifts, multiplicity of the signals and coupling constant values). The couplings between the different signals are evidenced using 2D-COSY. The direct and indirect correlation of carbons and protons can be performed by HSQC and HMBC.

Stereochemical information can be obtained from the vicinal and long-range coupling constant values and the nuclear Overhauser effect (NOE) enhancement, which depends on the distance between the corresponding protons (Budesinsky and Saman 1995).

The common feature in  $^1\text{H-NMR}$  spectra of STLs containing an  $\alpha$ -methylene- $\gamma$ -lactone moiety is the presence of two doublets with  $J = 1-4$  Hz, generally one below and the other above 6 ppm (generally in the range of 5–6.5 ppm). These signals are due to the C-13 methylene protons, with the lower field signal corresponding to the proton oriented towards the lactone carbonyl group (Hb). The signals for H-13a and H-13b generally appear both as a doublet by allylic coupling with H-7, and they are found in all exomethylene- $\gamma$ -lactones closed either towards C-6 or C-8. In a C(6)- $\alpha,\beta$ -unsaturated- $\gamma$ -lactone with an  $\alpha$ -hydroxyl group at C-8 (Fig. 7.1), in addition to the allylic coupling with H-7, a geminal coupling ( $J \geq 1$  Hz) between H-13a and H-13b is observed. In these cases, C-13 protons appear as a doublet of doublets (*dd*), and H-13a (the proton located *trans* to the  $\gamma$ -lactone carbonyl) appears at a lower field, as compared with the same proton present in compounds that do not contain the 8- $\alpha$ -hydroxyl group (Fischer et al. 1979; Yoshioka et al. 1973). In 11,13-dihydro-STLs, C-13 protons appear as a doublet at  $\sim 1.14$  ppm ( $J = 7$  Hz).

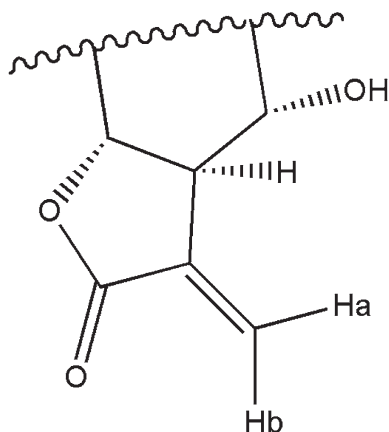


**Fig. 7.1** Partial structure of a sesquiterpene lactone containing C(6)- $\alpha,\beta$ -unsaturated- $\gamma$ -lactone and an  $\alpha$ -hydroxyl group at C-8

Protons present in methyl groups linked to a secondary carbon generate a doublet at 0.98–1.20 ppm, whereas protons present in methyl groups linked to a tertiary carbon appear as a singlet at 0.76–1.22 ppm.

**Germacranolides** *Trans*-lactones produce larger allylic couplings ( $J \geq 3$  Hz) between H-7 with H-13a and H-13b than *cis*-lactones ( $J \leq 3$  Hz). This phenomenon has been observed with 7,6-lactonized germacrolides and melampolides.

**Eudesmanolides** In 7,8-lactonized eudesmanolides, the lactone proton C(8)-H appears as a *ddd* or a *dt* at ca. 4.5 ppm. The allylic coupling between H-7 and C-13 protons of eudesmanolides is in accordance with that of germacranolides. The 7,8-*cis*-lactonized eudesmanolides show  $J_{7,13}$  values of 1.5 Hz or below, while 7,6 *trans*-lactonized compounds exhibit  $J_{7,13}$  couplings equal or greater than 3 Hz.

In the case of 11,13-dihydro-eudesmanolides, the C-6 lactonic proton appears as a broadened triplet (as in the case of  $\alpha$ -santonin). This broadening is due to a long-range coupling between H-6 and H-11, and it is also observed in 11,13-dihydro-elemanolides. None of the 11,13-unsaturated compounds show this triplet broadening (Yoshioka et al. 1973).

**Guaianolides** In the  $^1\text{H-NMR}$  spectrum of a guaianolide-type STLs, H-6 appears either a doublet or a multiplet depending on the number of protons at C-4. In C(6)- $\gamma$ -lactones of the guaianolide type, the stereochemistry of a hydroxyl group at C-8 could be determined. A positive shift ( $\sim 0.5$  ppm), in relation to a compound without a C-8-hydroxyl group, for H-13a (with concurrent geminal coupling), implies an  $\alpha$ -orientation of C(8)-OH. In contrast, a negative result denotes a  $\beta$ -orientation of C(8)-OH. These considerations can also be applied to germacranolides, eudesmanolides and elemanolides (Yoshioka et al. 1973).

**Pseudoguaianolides** In pseudoguaianolides, the C-6 proton appears as a doublet at 4.45–4.96 ppm ( $J = 10$  Hz), and the H-7 proton generates a multiplet at 3.43 ppm. In this type of compounds, one of the C-4 protons couples with C-15 protons.

### 7.1.5.2 $^{13}\text{C}$ -NMR

The  $^{13}\text{C}$ -NMR of STLs is generally obtained with proton decoupling, eliminating the splitting generated by the  $^{13}\text{C}$ - $^1\text{H}$  spin interactions and allowing the  $^{13}\text{C}$  signals to appear as singlets. By  $^{13}\text{C}$ -NMR it is possible to determine the number and type of carbons present in the molecule. A characteristic signal of all STLs is due to the lactonic carbons that appear at  $\sim 170$  ppm.

Information about other carbon atom types can be obtained from the chemical shifts. Thus, carbonyl carbons appear at 210–160 ppm, olefinic carbons appear at 160–110 ppm, aliphatic carbons with electronegative substituents appear at 110–55 ppm, and other aliphatic carbons generate a signal at 55–5 ppm. The  $^{13}\text{C}$ -NMR data for some representative STLs are shown in Fig. 7.2. The  $^1\text{H}$ -NMR and  $^{13}\text{C}$ -NMR characteristic signals of the most common ester side chains found in STLs are presented in Table 7.1.

Structural assignments of STL carbons can be performed in combination with other 1D-NMR methods such as INEPT, DEPT and APT which allow the discrimination of carbons according to the number of protons bonded directly to them (C, CH,  $\text{CH}_2$  and  $\text{CH}_3$ ).

**Germacranolides** As described in Chapter 6, germacranolides have four isomeric forms which differ from each other in the double-bond configurations, i.e. germacrolides, melampolides, heliangolides and *cis,cis*-germacranolides. They all have a cyclodecadiene skeleton with double bonds in positions 1–10 and 4–5. The double-bond configurations influence the conformation of the ten-membered rings. Conformational equilibria have been described for some 12,8-germacranolides, while in 12,6-germacranolides, the occurrence of conformational equilibrium is less common. At room temperature, some germacranolides with 10,14-exocyclic double bonds give unresolved  $^{13}\text{C}$ -NMR spectra. Conformational interconversion can be evidenced in the  $^{13}\text{C}$ -NMR spectra, and NOE experiments allow establishing the number of conformers for each STL. In this regard, experiments with variable temperature are very useful and informative.

Generally, 7,6-lactonized germacrolides have a fixed conformation in solution, while 7,8-lactonized germacrolides can exist in more than one conformation. In the case of melampolides, the conformational interconversion gives rise to broadened signals for the ten-membered ring, especially C-9. Conformational changes can also occur in heliangolides and *cis,cis*-germacranolides.

Resonances of the C-14 and C-15 methyl groups of germacranolides arising at  $\delta > 20$  ppm indicate a *Z* configuration, while values lower than 20 ppm indicate *E*

### Germacranolides

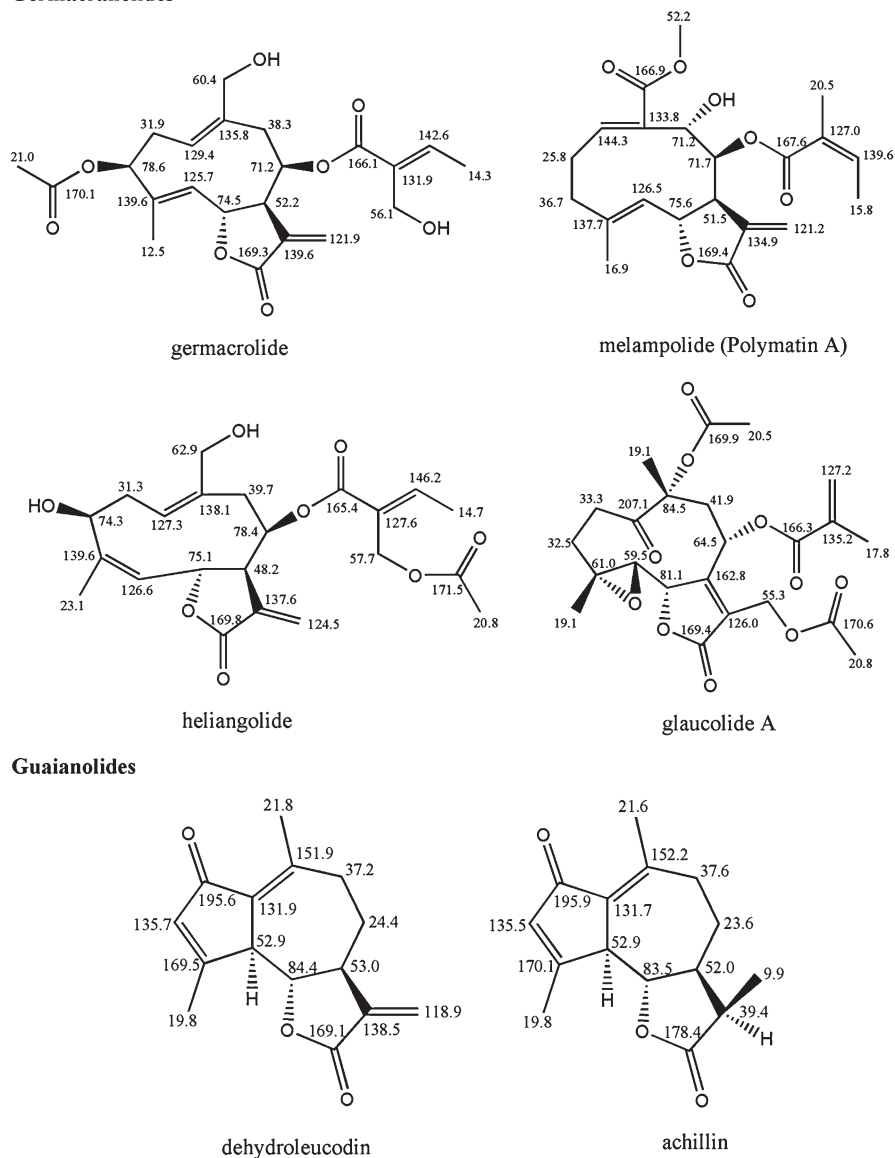
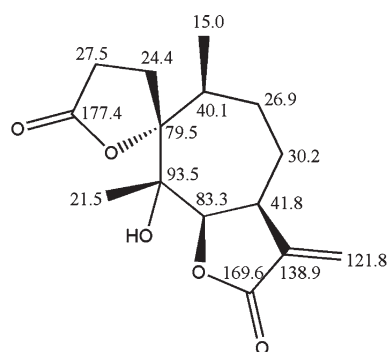
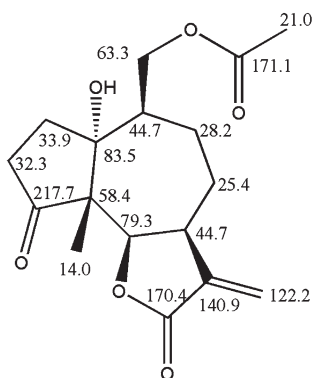
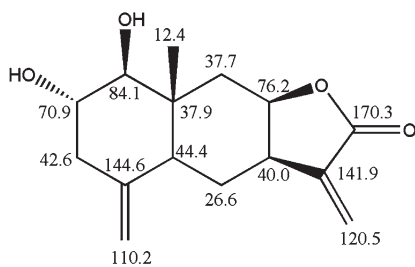


Fig. 7.2  $^{13}\text{C}$ -NMR data for some representative sesquiterpene lactones

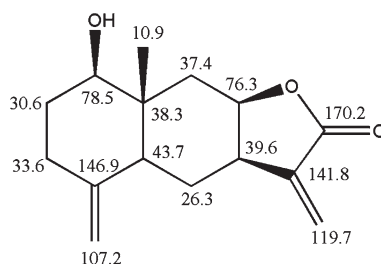
configuration. In 11,13-dihydro sesquiterpene lactones, the configuration of the 11-methyl group can be determined by  $^{13}\text{C}$ -NMR where chemical shifts of 12–15 ppm and <10 ppm indicate an  $\alpha\text{CH}_3$  and  $\beta\text{CH}_3$  configuration, respectively. However, exceptions to this rule have been reported with  $\text{CH}_3$  groups occurring at 10–12 ppm.

**Pseudogainolides**

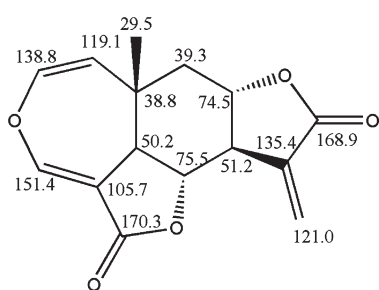
psilostachyin

**Eudesmanolides**

ivasperin



asperilin

**Elemanolides**

miscandenin

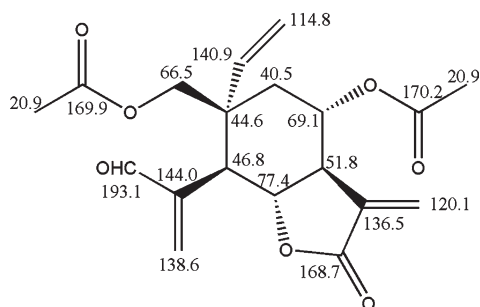
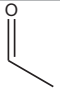
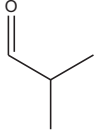
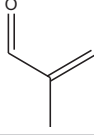
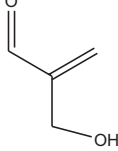
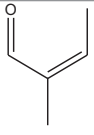
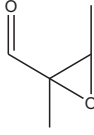
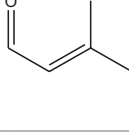
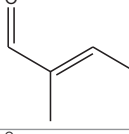
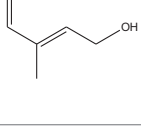


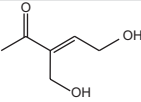
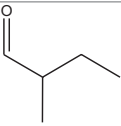
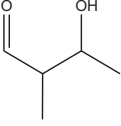
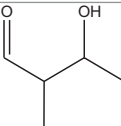
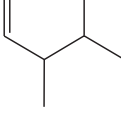
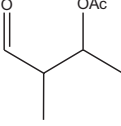
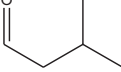
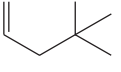
Fig. 7.2 (continued)

**Table 7.1**  $^1\text{H-NMR}$  and  $^{13}\text{C-NMR}$  characteristic signals of most common ester side chains found in sesquiterpene lactones

Side chain	Abbreviation	Structure	$^1\text{H-NMR}^a$	$^{13}\text{C-NMR}$
Acetate	Ac		2.08 <i>s</i>	1' 170.0 2' 21.0
Isobutyrate	iBu		2.57 <i>hept</i> (7.0) H-2' 1.19 <i>d</i> (7.0) H-3' 1.15 <i>d</i> (7.0) H-4'	1' 175.4 2' 34.1 3' 19.0 4' 19.0
Methacrylate	Meacr		6.31 <i>br s</i> H-3'a 5.69 <i>br s</i> H-3'b 1.97 <i>br s</i> H-4'	1' 165.9 2' 135.4 3' 126.6 4' 18.3
Methacrylate-4-hydroxy	Meacr-4-OH		6.17 <i>br s</i> H-3'a 5.86 <i>d</i> (1.2) H-3'b 4.28 <i>br s</i> H-4'	1' 164.9 2' 138.8 3' 126.9 4' 62.3
Angelate	Ang		6.19 <i>qq</i> (7.0, 1.5) H-3' 2.04 <i>dq</i> (7.0, 1.5) H-4' 1.87 <i>quintet</i> (1.5) H-5'	1' 167.4 2' 126.9 3' 139.5 4' 15.8 5' 20.4
Epoxyangelate	EpoxyAng		3.01 <i>q</i> (5.2) H-3' 1.18 <i>d</i> (5.2) H-4' 1.46 <i>s</i> H-5'	1' 170.2 2' 59.3 3' 59.9 4' 13.6 5' 19.1
Senecioate	Sen		5.62 <i>br s</i> H-2' 2.14 <i>br s</i> H-4' 1.92 <i>br s</i> H-5'	1' 165 2' 115.9 3' 157.5 4' 27.3 5' 20.2
Tiglate	Tig		6.95 <i>qq</i> (7.0, 1.0) H-3' 1.83 <i>br d</i> (7.0) H-4' 1.85 <i>br s</i> H-5'	1' 166.9 2' 127.8 3' 138.8 4' 14.5 5' 12.2
Tiglate-4-hydroxy	Tig-4-OH		6.74 <i>tq</i> (6, 1.5) H-3' 4.32 <i>d</i> (6) H-4' 1.80 <i>d</i> (1.5) H-5'	1' 166.1 2' 127.6 3' 141.6 4' 59.7 5' 12.8

(continued)

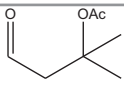
**Table 7.1** (continued)

Side chain	Abbreviation	Structure	<sup>1</sup> H-NMR <sup>a</sup>	<sup>13</sup> C-NMR
Tiglate-4,5-dihydroxy	Tig-4,5-di-OH		6.90 <i>t</i> (6.0) H-3' 4.43 <i>d</i> (6.0) H-4'a,b 4.36 <i>br d</i> (13) H-5'a 4.33 <i>br d</i> (13) H-5'b	1' 165.8 2' 131.8 3' 144.3 4' 59.1 5' 57.3
2-methyl butyrate	2-MeBu		2.41 <i>sext</i> (7.0) H-2' 1.66 <i>ddq</i> (14.0, 7.0, 7.0) H-3'a 1.48 <i>ddq</i> (14.0, 7.0, 7.0) H-3'b 1.13 <i>d</i> (7.0) H-5' 0.91 <i>t</i> (7.0) H-4'	1' 175.2 2' 41.2 3' 26.7 4' 16.0 5' 11.5
2-methyl butyrate-3-hydroxy <i>Erythro</i>	2-MeBu-3-OH <i>erythro</i>		4.11 <i>qd</i> (6.5, 3.0) H-3' 2.56 <i>qd</i> (7.0, 3.0) H-2' 1.23 <i>d</i> (7.0) H-5' 1.22 <i>d</i> (6.5) H-4'	1' 173.9 2' 45.8 3' 68.1 4' 20.1 5' 10.8
2-methyl butyrate-3-hydroxy <i>Threo</i>	2-MeBu-3-OH <i>threo</i>		3.94 <i>quint</i> (7.0) H-3' 2.55 <i>quint</i> (7.0) H-2' 1.25 <i>d</i> (7.0) H-5' 1.20 <i>d</i> (7.0) H-4'	1' 174.0 2' 47.2 3' 69.4 4' 20.7 5' 13.7
2-methyl butyrate-3-acetate <i>Erythro</i>	2-MeBu-3-OAc <i>erythro</i>		5.22 <i>qd</i> (6.5, 5.0) H-3' 2.68 <i>qd</i> (7.0, 5.0) H-2' 1.27 <i>d</i> (6.5) H-4' 1.22 <i>d</i> (7.0) H-5' OAc: 2.03 <i>s</i>	1' 172.0 2' 44.3 3' 70.4 4' 17.7 5' 11.3 OAc 170.2, 20.9
2-methyl butyrate-3-acetate <i>Threo</i>	2-MeBu-3-OAc <i>threo</i>		5.11 <i>quint</i> (6.5) H-3' 2.68 <i>qd</i> (7.0, 6.5) H-2' 1.26 <i>d</i> (6.5) H-4' 1.17 <i>d</i> (7.0) H-5' OAc: 2.06 <i>s</i>	1' 172.8 2' 44.3 3' 70.8 4' 17.6 5' 12.2 OAc 170.4, 21.1
Isovalerate	iVal		2.21 <i>s</i> H-2'a,b 2.08 <i>hept</i> (7.0) H-3' 0.95 <i>d</i> (7.0) H-4' 0.95 <i>d</i> (7.0) H-5'	1' 172.0 2' 43.2 3' 25.6 4' 22.3 5' 22.3
Isovalerate-3-hydroxy	iVal-3-OH		2.56 <i>d</i> (15.0) H-2'a 2.25 <i>d</i> (15.0) H-2'b 1.31 <i>s</i> H-5' 1.29 <i>s</i> H-4'	1' 170.9 2' 46.8 3' 69.2 4' 29.3 5' 29.2

(continued)



**Table 7.1** (continued)

Side chain	Abbreviation	Structure	<sup>1</sup> H-NMR <sup>a</sup>	<sup>13</sup> C-NMR
Isovalerate-3-acetate	iVal-3-OAc		2.95 <i>d</i> (14.5) H-2'a 2.85 <i>d</i> (14.5) H-2'b 1.53 <i>s</i> H-5' 1.53 <i>s</i> H-4' OAc: 2.00 <i>s</i>	1' 170.5 2' 44.4 3' 79.2 4' 26.5 5' 26.5 OAc 169.2, 22.3

<sup>a</sup>*br* broad, *s* singlet, *d* doublet, *t* triplet, *q* quartet, *quint* quintet, *sext* sextet, *hept* heptet

**Eudesmanolides** The rule related to the configuration of C-11 methyl group explained above can also be applied for the analysis of eudesmanolides. The C-13 chemical shifts of santonin and some other eudesmanolides have been used to determine the stereochemistry of the  $\gamma$ -lactone ring fusion and the configuration of the C-11 methyl group. In  $\alpha$ -santonin, the 11-methyl group appears at 12.5 ppm, while in  $\beta$ -santonin it does at 9.9 ppm (Budesinsky and Saman 1995).

**Guaianolides** HETCOR spectra allow the assignment of C-7, C-11 and C-13, while long-range HETCOR, in combination with NOE experiments, permits the assignments of C-4 and C-5. In some of these compounds, the configuration of C-11, in epimers, has been determined by the chemical shifts of C-13 and C-8. A peak at  $\delta$ ~94.6–95.4 ppm is characteristic of an allylic C-1 with a hydroperoxy group (Budesinsky and Saman 1995).

**Pseudoguaianolides** Most of ambrosanolides and helenanolides have *trans*-fused five- and seven-membered rings and differ in the configuration of the methyl group at C-10, being  $\beta$  in ambrosanolides and  $\alpha$  in helenanolides. The lactone closure typically occurs at C-6 in ambrosanolides and at C-8 in helenanolides. However, a few exceptions of compounds with *cis*-fused 5,7 rings and 12,8 ambrosanolides have been reported.

The signals of C-14 and C-15 methyl groups are sensitive to the reduction of 2–3 and 11–13 double bonds. This effect has been observed in pseudoguaian-12,8-olides and is probably due to conformational changes of the seven-membered ring from chair to boat (Budesinsky and Saman 1995).

In psilostachynolides, which are di-lactones, two signals are observed: one corresponding to a  $\gamma$ -lactone carbonyl carbon ( $\delta$  ~ 170 ppm) and the other to either another  $\gamma$ -lactone or a  $\delta$ -lactone carbonyl carbon ( $\delta$  160–177 ppm) (Borges del Castillo et al. 1981).

**Other Sesquiterpene Lactone Types** The <sup>13</sup>C-NMR of elemanolides shows characteristic signals for the C-1, C-2, C-3 and C-4 olefinic carbons. Most eremophilanolides have *cis*-fused six-membered rings and a 7-11 double bond. According to the configuration of C-8, the stereochemistry of these compounds can be either 8 $\beta$ -steroidal or 8 $\alpha$ -non-steroidal. Chemical shifts for C-1, C-4, C-5, C-7 and C-10 appear upfield in 8 $\beta$ -eremophilanolides.

## 7.2 NMR Spectra of Sesquiterpene Lactones

In this section, the  $^1\text{H}$ -NMR and  $^{13}\text{C}$ -NMR spectroscopic characteristics of some STLs belonging to the different structural types will be presented and analysed.

### 7.2.1 Guaianolides

In the guaiane nucleus, the assignments corresponding to the hydrogens of the 6, 7 and 8 positions are of importance since they are the closing points of the lactone system and where the closure stereochemistry is defined.

Peroxyeupahakonin A (**1**) and B (**2**), eupahakonin A (**3**) and B (**4**) and eupahakonin A (**5**) and B (**6**) (Fig. 7.3) are guaianolide-type STLs that have been isolated from *Eupatorium chinense* var. *hakonense* (Ito et al. 1982). Eupahakonin B has been also isolated from *Stevia satureiaefolia* (Sosa et al. 1984). Eupahakonin A (**3**) and B (**4**) and eupahakonin A (**5**) and B (**6**) are regioisomers of the double bond at C-10, respectively.

A characteristic of these compounds is a *trans*-diaxial relationship between the protons at C(5)–C(6) and C(6)–C(7), which was observed in the signal for H-6. This proton (H-6) appears as a doublet of doublets at  $\delta$  4.50 ( $J = 8.5, 11$  Hz),  $\delta$  4.52 ( $J = 9, 10$  Hz),  $\delta$  4.46 ( $J = 8.5, 11$  Hz) and  $\delta$  4.46 ( $J = 9, 10$  Hz) for **1**, **2**, **3** and **4**, respectively (Table 7.2).

The exocyclic methylene protons gave two singlets at  $\delta$  5.03 and 5.09 in the  $^1\text{H}$ -NMR spectrum of **2**, instead of the broad singlet due to the C-10 vinyl-methyl protons as occur in **1**.

The chemical shift of H-5 in **3** ( $\delta$  2.85) indicated that the hydroxyl group was  $\alpha$ , because of the upfield shift ( $\Delta$  0.51) in comparison with H-5 in **1** ( $\delta$  3.36). An  $\alpha$ -orientation of H-8 was determined by NOE experiments.

The  $^1\text{H}$ -NMR spectra of eupahakonin A and eupahakonin B were similar. The differences between them are the presence of the vinyl-methyl group and the absence of exocyclic methylene protons. These facts indicate that these compounds are regioisomers of the double bond at C-10.

In the  $^{13}\text{C}$ -NMR spectra of peroxyeupahakonin A (**1**) and B (**2**), the presence of seven oxygenated carbon atoms can be determined. The peaks at  $\delta$  94.6 in **1** and  $\delta$  95.4 in **2** were characteristic of an allylic carbon (C-1) bearing a hydroperoxy group (Table 7.3).

The  $^1\text{H}$ -NMR spectra of eupahakonin A and eupahakonin B were similar. The differences between them are the presence of the vinyl-methyl group and the absence of exocyclic methylene protons. These facts indicate that these compounds could be regioisomers of the double bond at C-10. The  $^1\text{H}$ -NMR and  $^{13}\text{C}$ -NMR data of compounds **1**–**6** are detailed in Tables 7.2 and 7.3, respectively (Ito et al. 1982).

The guaianolide STL (**7**) (Fig. 7.4) was isolated from *Mikania mendocina* by Bardón et al. (1996). Spectroscopic data ( $^1\text{H}$ -NMR and  $^{13}\text{C}$ -NMR) are presented in Tables 7.4 and 7.5.

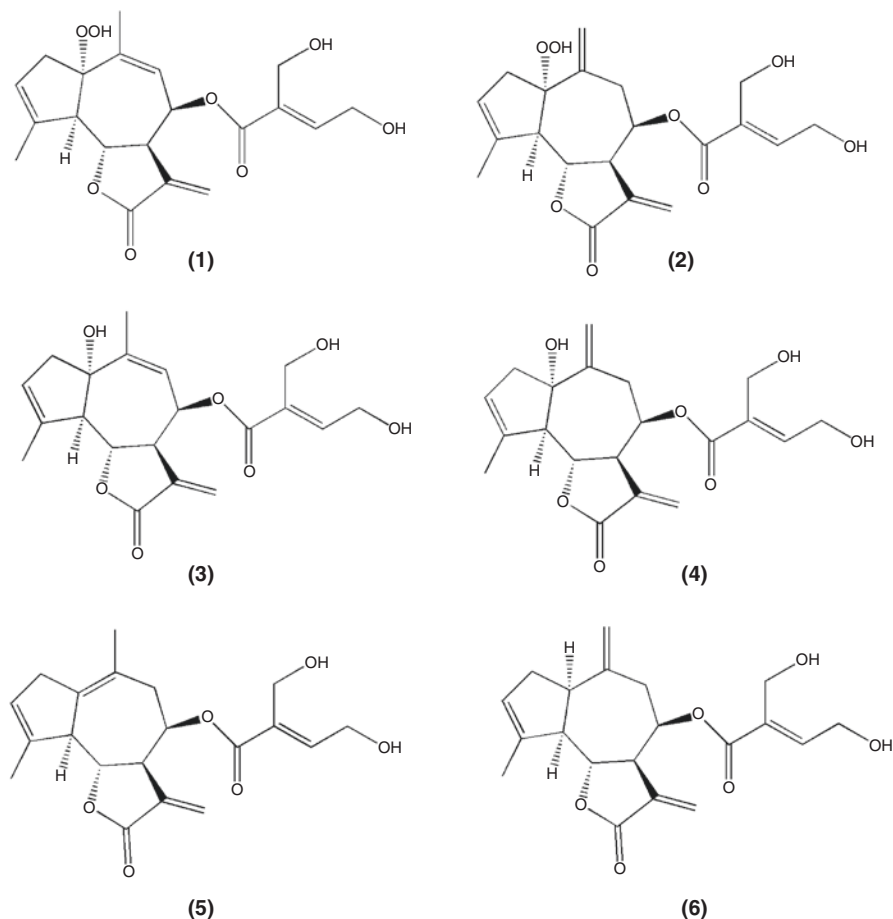


**Fig. 7.3** Chemical structures of peroxyeupahakonin A (1) and B (2), eupahakonin A (3) and B (4) and eupahakonin A (5) and B (6)

This compound has an acetylated hydroxymethylene group at C-4 showing signals at  $\delta$  4.58 in the  $^1\text{H-NMR}$  and  $\delta$  67.9 ppm in the  $^{13}\text{C-NMR}$ . The stereochemistry at C-1, C-4 and C-10 was determined by NOEs of H-7 with H-1, of H-15 with H-8 and of H-8 with H-14.

Estafietin (8) (Fig. 7.5) is the main sesquiterpene lactone of *Stevia alpina* (de Heluani et al. 1989). The  $^1\text{H-NMR}$  and  $^{13}\text{C-NMR}$  data of this guaianolide are presented in Tables 7.6 and 7.7.

Estafietin (8), as other STLs, showed the signals of vinyl protons corresponding to an exomethylene- $\gamma$ -lactone at  $\delta$  5.48 and 6.21 ppm and two other signals at 4.88 and 4.95 ppm corresponding to the protons of an isolated exocyclic methylene group. The signal at  $\delta$  1.62 ppm (singlet), which integrates for 3H, was attributed to the protons of the methyl group (C-15).

**Table 7.2** <sup>1</sup>H-NMR data of compounds **1**, **2**, **3**, **4**, **5** and **6**

Proton	Compounds					
	<b>1</b> <sup>a</sup>	<b>2</b> <sup>b</sup>	<b>3</b> <sup>a</sup>	<b>4</b> <sup>a</sup>	<b>5</b> <sup>c</sup>	<b>6</b> <sup>c</sup>
H-1	–	–				3.17
H-2	2.58 <i>m</i>	2.90	2.56 <i>m</i>	2.62 <i>m</i> 2.75 <i>m</i>	3.03 <i>s</i>	2.48 <i>m</i>
H-3	5.40 <i>s</i> ( <i>br</i> )	5.60	5.58 <i>s</i> ( <i>br</i> )	5.60	5.57	5.53
H-5	3.36 <i>d</i> (11)	2.90	2.85 <i>s</i> ( <i>br</i> ) (11)	2.86 <i>d</i> ( <i>br</i> ) (10)	3.40 <i>d</i> ( <i>br</i> ) (10)	2.81 <i>t</i> ( <i>br</i> ) (9)
H-6	4.50 <i>dd</i> (8.5; 11)	4.52 <i>dd</i> (9; 10)	4.46 <i>dd</i> (8.5; 11)	4.46 <i>dd</i> (9; 10)	4.12 <i>t</i> (10)	4.48 <i>dd</i> (9;10.5)
H-7	3.59 <i>m</i>	3.40 <i>m</i>	3.60 <i>m</i>	3.59 <i>m</i>	3.06 <i>m</i>	3.17
H-8	5.88 <i>dd</i> ( <i>br</i> ) (3; 6.3)	5.60	5.88 <i>dd</i> ( <i>br</i> ) (3; 6)	5.60 <i>d</i>	5.60 <i>m</i>	5.60 <i>m</i>
H-9	5.70 <i>dd</i> ( <i>br</i> ) (1; 6.3)	2.49 <i>dd</i> (3.2;14.5) 3.14 <i>dd</i> (3.9;14.5)	5.48 <i>m</i>	2.36 <i>dd</i> (3.5;14) 3.19 <i>dd</i> (3.9;14)	2.61 <i>m</i>	2.55 <i>d</i> (5)
H-13	5.57 <i>d</i> (3) 6.11 <i>d</i> (3.4)	5.65 <i>d</i> (3.2) 6.18 <i>d</i> (3.7)	5.56 <i>d</i> (3.2) 6.10 <i>d</i> (3.8)	5.58 <i>d</i> (3.5) 6.10 <i>d</i> (3.8)	5.44 <i>d</i> (3) 6.15 <i>d</i> (3.5)	5.52 <i>d</i> (3) 6.22 <i>d</i> (3.8)
H-14	0.92 <i>s</i> ( <i>br</i> )	5.03 <i>s</i> , 5.09 <i>s</i>	1.92 <i>m</i>	5.07 <i>s</i>	1.61 <i>s</i>	4.86 <i>s</i> 4.98 <i>s</i>
H-15	1.92 <i>s</i> ( <i>br</i> )	1.84 <i>s</i> ( <i>br</i> )	1.96 <i>s</i> ( <i>br</i> )	1.81 <i>s</i> ( <i>br</i> )	1.97 <i>s</i> ( <i>br</i> )	1.84 <i>s</i> ( <i>br</i> )
H-3',4',5'	6.75 <i>t</i> (5.8,H-3') 4.30 <i>d</i> (5.8,H-4') 4.20 <i>s</i> (H-5')	6.80 <i>t</i> (5.8,H-3') 4.35 <i>d</i> (5.8,H-4') 4.27 <i>s</i> (H-5')	6.77 <i>t</i> (5.8,H-3') 4.35 <i>d</i> (5.8,H-4') 4.22 <i>s</i> (H-5')	6.80 <i>t</i> (5.8,H-3') 4.32 <i>d</i> (5.8,H-4') 4.22 <i>s</i> (H-5')	6.80 <i>t</i> (5.8,H-3') 4.38 <i>d</i> (5.8,H-4') 4.31 <i>s</i> (H-5')	6.79 <i>t</i> (5.8,H-3') 4.35 <i>d</i> (5.8,H-4') 4.28 <i>s</i> (H-5')

Ito et al. (1982)

<sup>a</sup>d<sub>6</sub>-Me<sub>2</sub>CO<sup>b</sup>CD<sub>3</sub>OD<sup>c</sup>CDCl<sub>3</sub>

From the seeds of *Scorzonera divaricata*, Yong-Jin Yang et al. (2016) have isolated several metabolites, among which the sulphated STLs **9**, **10** and **11** were present (Fig. 7.6).

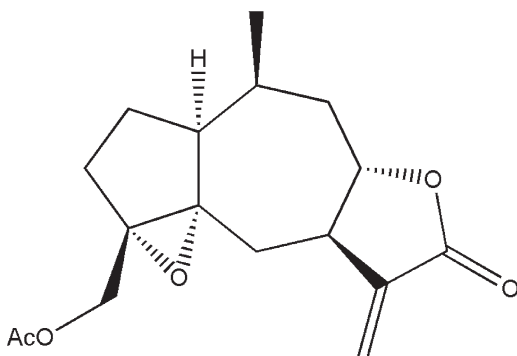
NMR studies allowed assigning the characteristic signals of hydrogen atoms at positions 6, 7, 8, 13, 14 and 15, as well as the corresponding carbons (Table 7.8).

Cha et al. (2011) have reported the isolation of three new STLs from *Ixeris dentata*, in addition to other nine known structures (Fig. 7.7). Assignments were based on the coupling patterns that are characteristic of compounds **12** and **13** highlighting the proton coupling pattern at δ 4.85 ppm (1H, dd, *J* = 10.4, 10.4 Hz), corresponding to C-6 and which indicates a *trans*-diaxial arrangement of C-5 (α), C-6 (β) and C-7 (α) protons, strongly suggesting the existence of a guaian-type STL skeleton. However, with the exception of the signals generated by protons H-3, H-4, H-5 and H-15, the chemical shifts and coupling constants of all proton signals of **12** were very similar to

**Table 7.3**  $^{13}\text{C}$ -NMR data for compounds **1**, **2**, **3**, **4**, **5** and **6**

Carbon	Compounds					
	<b>1</b> <sup>a</sup>	<b>2</b> <sup>b</sup>	<b>3</b> <sup>a</sup>	<b>4</b> <sup>a</sup>	<b>5</b> <sup>c</sup>	<b>6</b> <sup>c</sup>
1	94.6	95.4	83.4	84.5	125.2	47.6
2	44.2	43.3	47.7	47.8	37.9	37.3
3	123.4	125.6	123.6	125.4	125.4	126.6
4	142.7	144.5	145.5	147.0	139.9	139.6
5	60.7	59.8	66.4	64.8	56.4	56.4
6	78.9	79.3	79.0	79.7	79.9	80.0
7	48.2	48.5	48.2	47.8	55.3	48.5
8	67.9	68.0	67.8	68.7	66.7	68.2
9	122.8	37.1	119.6	36.7	37.6	40.3
10	141.7	137.5	142.2	139.2	136.7	143.1
11	135.6	135.5	135.9	136.3	135.2	134.4
12	169.0	169.3	169.0	169.1	169.1	169.4
13	121.6	121.5	121.2	121.1	119.5	122.0
14	24.4	118.1	24.9	115.8	24.1	116.4
15	17.8	16.9	17.9	17.1	17.7	16.7
1'	166.4	166.4	166.5	166.2	165.9	165.8
2'	131.8	132.1	132.0	132.2	131.1	131.3
3'	145.9	145.8	145.9	145.9	144.1	143.9
4'	59.2	58.7	59.2	59.1	58.7	58.8
5'	56.9	56.3	57.0	56.9	56.7	56.9

Ito et al. (1982)

<sup>a</sup>d<sub>6</sub>-Me<sub>2</sub>CO<sup>b</sup>C<sub>5</sub>D<sub>5</sub>N<sup>c</sup>CDCl<sub>3</sub>**Fig. 7.4** Chemical structure of the guaianolide (**7**) isolated from *Mikania mendocina*

those of **13** (8-epiisolipidiol) isolated from *Crepis capillaris* and *C. conyzifolia* (Table 7.9) (Kisiel 1983; Kisiel and Michalska 2001; Rychlewska and Kisiel 1991).

Shi et al. (2016) have reported the isolation of two new structures of the guaiane-type STLs, **14** and **15** from *Ainsliaea spicata* (Fig. 7.8). The NMR spectra of **14** showed similar signals to the known STL diaspanolide A (**16**), such as two exocyclic

**Table 7.4**  $^1\text{H}$ -NMR data for compound **7**

Proton	Compound <b>7</b> <sup>a</sup>
H-1	3.03 <i>br d</i> (8.0)
H-2	2.15–2.25
H-2'	1.60 <i>m</i>
H-3	2.44 <i>dt</i> (16.8;6.4)
H-3'	2.25–2.40
H-6	2.95 <i>dd</i> (17.6;5.0)
H-6'	2.30–2.40
H-7	3.22 <i>m</i>
H-8	4.04 <i>ddd</i> (12.4;9.6;2.8)
H-9	2.04 <i>dt</i> (5.0;12.4)
H-9'	2.25–2.40
H-10	2.20
H-11	–
H-13	6.25 <i>d</i> (3.2)
H-13'	5.48 <i>d</i> (3.0)
H-14	0.85 <i>d</i> (7.2)
H-15	4.58 <i>s</i>

Bardón et al. (1996)

<sup>a</sup> $\text{CDCl}_3$ **Table 7.5**  $^{13}\text{C}$ -NMR data for compound **7**

Carbon	Compound <b>7</b> <sup>a</sup>
1	53.6
2	24.2
3	36.2
4	–
5	–
6	43.7
7	42.4
8	79.6
9	40.6
10	33.4
11	138.4
12	169.1
13	120.4
14	14.4
15	67.9

Bardón et al. (1996)

<sup>a</sup> $\text{CDCl}_3$ 

double bonds [ $\delta$  4.99 ppm (1H, s, H-14a), 5.05 ppm (1H, s, H-14b), 5.28 ppm (1H, t,  $J = 2.2$  Hz, H-15a), 5.43 ppm (1H, t,  $J = 2.2$  Hz, H-15b)] and signals at  $\delta\text{C}$  143.1 ppm (C-10), 116.4 ppm (C-14), 148.3 ppm (C-4), 114.3 ppm (C-15), and one lactone group [ $\delta$  4.00 ppm (1H, t,  $J = 9.9$  Hz, H-6) and  $\delta$  178.6 (C-12), 79.1 (C-6)].

**Fig. 7.5** Chemical structure of estafietin (**8**)

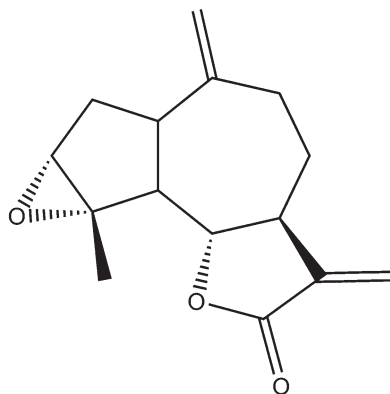


**Table 7.6**  $^1\text{H-NMR}$  data for compound **8**

Proton	Compound <b>8</b> <sup>a</sup>
H-1	2.98 <i>ddd</i> (10.5;8;8)
H-2a	2.07 <i>dd</i> (14;8)
H-2b	1.80 <i>ddd</i> (14;10.5;1)
H-3	3.40 <i>br s</i>
H-5	2.31 <i>dd</i> (11;8)
H-6	4.07 <i>dd</i> (11;9)
H-7	2.87 <i>dddd</i> (11.5;8.5;5;3.5;3)
H-8a	~2.20
H-8b	1.55 <i>m</i>
H-9a	~2.20
H-9b	~2.20
H-13a	6.21 <i>d</i> (3.5)
H-13b	5.48 <i>d</i> (3)
H-14a	4.95 <i>br s</i>
H-14b	4.88 <i>d</i> (1.5)
H-15	1.62 <i>s</i>

de Heluani et al. (1989)

<sup>a</sup> $\text{CDCl}_3$

An outstanding difference was the presence of an additional oxygenated methine signal [ $\delta$  3.77 ppm (1H, m),  $\delta$  75.1 ppm (C-8)] in the NMR spectra of **14** instead of the signal corresponding for a methylene at C-8 found for compound **16**, indicating that **14** is a hydroxylated derivative of compound **16**.

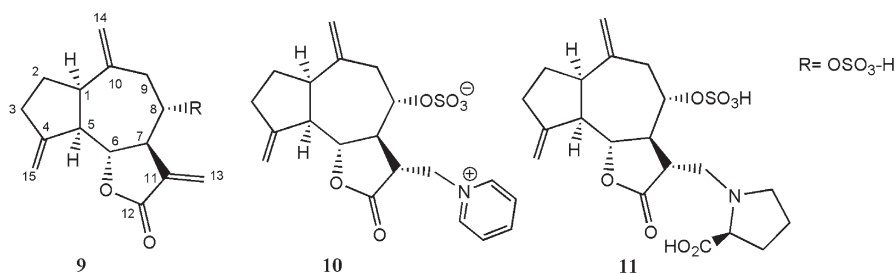
Joel et al. (2011) have reported the identification of a STL of the guaianolide type named dehydrocostus lactone (**17**) (Fig. 7.9). The  $^1\text{H}$ - and  $^{13}\text{C}$ -NMR spectra (Table 7.10) exhibited the typical signals of three exocyclic methylene groups at  $\delta$  4.83 ppm, 4.91 ppm, 5.08 ppm, 5.28 ppm, 5.50 ppm and 6.23 ppm, which correspond to the signals assigned to C-14 ( $\delta$  112.85 ppm), C-15 ( $\delta$  109.86 ppm) and C-13 ( $\delta$  120.40 ppm), respectively. The signal at  $\delta$  3.98 ppm (t,  $J = 9.3$  Hz) corresponds to H-6, where the lactone ring is closed (C-6:  $\delta$  85.45 ppm).

Chaves and de Oliveira (2003) have reported the identification of the guaianolide  $8\beta$ -hydroxyzaluzanin D (**18**). The  $^1\text{H-NMR}$  spectrum exhibited two characteristic

**Table 7.7**  $^{13}\text{C}$ -NMR data for compound **8**

Carbon	Compound <b>8</b> <sup>a</sup>
1	44.79
2	32.86
3	62.24
4	64.96
5	50.71
6	79.42
7	43.78
8	28.85
9	28.52
10	146.55
11	140.43
12	168.34
13	118.37
14	114.29
15	18.59

de Heluani et al. (1989)

<sup>a</sup>C<sub>6</sub>D<sub>6</sub>**Fig. 7.6** Chemical structures of compounds **9**, **10** and **11**

doublets at  $\delta$  6.42 ppm and 5.62 ppm ( $J = 3.8$  and 3.2 Hz, respectively) corresponding to an exocyclic methylene group conjugated to a  $\gamma$ -lactone (H-13a and H-13b) (Fig. 7.10). The exocyclic methylene groups at C-10 and C-4 generated singlets at  $\delta$  4.99 ppm (H-14a) and 5.10 ppm (H-14b) and two triplets ( $J = 2.0$  Hz) at  $\delta$  5.32 ppm (H-15a) and 5.52 ppm (H-15b).

Neves et al. (1999) have reported the isolation of STLs **19–21** from *Targionia lorbeeriana* (Fig. 7.11). The  $^1\text{H}$ -NMR showed characteristic signals of guaianolide-type STLs. Compounds **20** and **21** differ from **19** in that they have one less methylene group which is replaced by a methyl and an acetyloxy group in **20** and by a methine proton C(11)-H and a methyl in **21** (Table 7.11).

## 7.2.2 Pseudoguaiinolides

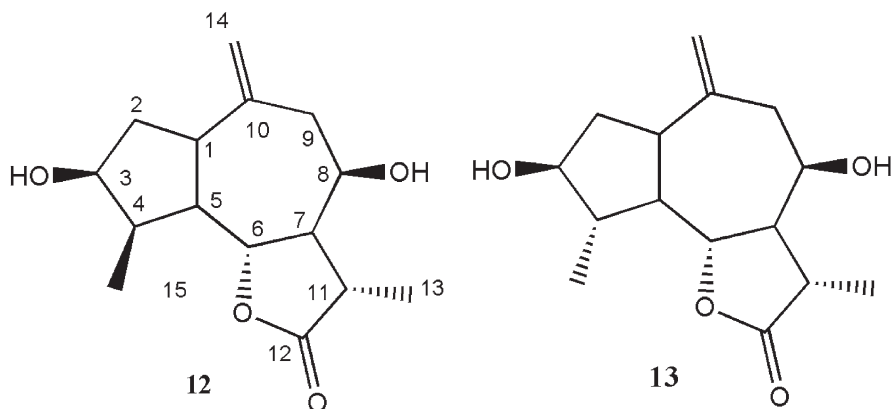
Psilostachyin C (**22**) and psilostachyin (**23**) (Fig. 7.12) have been isolated from *Ambrosia scabra* and *A. tenuifolia*, respectively (Sülsen 2009). However, these compounds have also been isolated from other *Ambrosia* species. These compounds



**Table 7.8**  $^1\text{H-NMR}$  and  $^{13}\text{C-NMR}$  chemical shifts and coupling constants corresponding to the sulphated sesquiterpene lactones **9**, **10** and **11**

Position	<b>9</b>		<b>10</b>		<b>11</b>	
	$\delta^{\text{H}}$ (J in Hz)	$\delta^{\text{C}}$	$\delta^{\text{H}}$ (J in Hz)	$\delta^{\text{C}}$	$\delta^{\text{H}}$ (J in Hz)	$\delta^{\text{C}}$
4		152.4		153.8		153.2
6 $\beta$	4.05 ( <i>t</i> , 10.0)	80.1	4.07 ( <i>t</i> , 9.6)	q	4.16 ( <i>t</i> , 9.6)	82.9
7 $\alpha$	2.95 ( <i>t</i> , 9.2)	49.6	2.53 ( <i>brdd</i> , 10.8, 9.6)	50.9	2.55 ( <i>brdd</i> , 10.4, 9.6)	51.1
8 $\beta$	4.48 ( <i>dt</i> , 9.2, 4.4)	80.2	4.43 ( <i>dt</i> , 9, 5.6)	82.6	4.41 ( <i>dt</i> , 8.4, 6.0)	81.5
11		139.2	3.48 ( <i>td</i> , 10.6, 3.3)	48.3	3.43 ( <i>td</i> , 10.4, 4.0)	43.5
12		177.8		177.8		178.7
13a	6.23 ( <i>d</i> , 2.8)	124.4	4.82 ( <i>brd</i> , 11.2)	62.2	3.61 ( <i>brt</i> , 9.2)	56.5
13b	6.07 ( <i>d</i> , 3.2)		5.11 ( <i>dd</i> , 13.4, 3.4)		3.67 ( <i>dd</i> , 12.8, 5.2)	
14a	4.96 ( <i>s</i> )	117.6	4.96 ( <i>s</i> )	116.7	4.99 ( <i>s</i> )	116.0
14b	4.957 ( <i>s</i> )		4.85 ( <i>s</i> )		4.88 ( <i>s</i> )	
15a	5.09 ( <i>s</i> )	111.2	5.01 ( <i>s</i> )	110.7	5.07 ( <i>s</i> )	110.0
15b	4.92 ( <i>s</i> )		4.91 ( <i>s</i> )		4.97 ( <i>s</i> )	

Yong-Jin Yang et al. (2016)

**Fig. 7.7** Chemical structures of compounds **12** and **13**

are pseudoguinolides specifically classified as ambrosanolides since they all have the C-15 methyl group  $\beta$ - oriented.

The  $^1\text{H-NMR}$  and  $^{13}\text{C-NMR}$  data of psilostachyin C (**22**) are presented below:

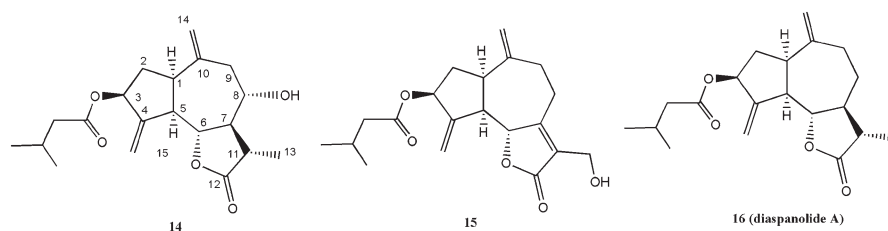
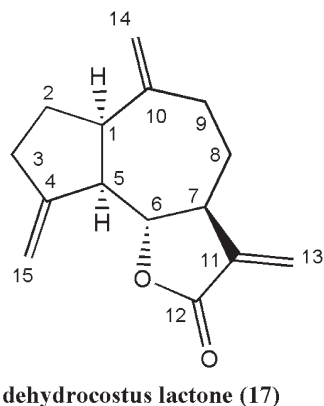
**$^1\text{H-RMN}$  (500 MHz,  $\text{CDCl}_3$ )**  $\delta$  (ppm) 1.00 (3H, *d*, 7.5 Hz), 1.29 (3H, *s*), 1.68 (1H, *qt*, 2.5; 7; 14 Hz), 1.70–1.80 (2H), 1.92 (1H, *ddd*, 2.5; 5.1; 12.6 Hz), 2.05 (1H), 2.16 (1H, *m*, 3.8 Hz), 2.45 (1H, *ddd*, 6; 12; 19 Hz), 2.64 (1H, *ddd*, 2; 5.5; 18 Hz), 3.40 (1H, *m*, 3 Hz), 4.63 (1H, *d*, 9.5 Hz), 5.48 (1H, *d*, 3 Hz), 6.24 (1H, *d*, 3 Hz)

**$^{13}\text{C-RMN}$  (500 MHz,  $\text{CDCl}_3$ )**  $\delta$  169.55 (C-12), 168.85 (C-4), 138.35 (C-11), 120.45 (C-13), 89.81 (C-5), 86.22 (C-6), 43.20 (C-1), 41.37 (C-7), 35.35 (C-10), 31.70 (C-9), 30.96 (C-6), 24.02 (C-2), 22.55 (C-8), 18.98 (C-15), 14.41 (C-14)

**Table 7.9**  $^1\text{H}$ -NMR and  $^{13}\text{C}$ -NMR chemical shifts and coupling constants corresponding to STLs **12** and **13**

Position	<b>12</b>		<b>13</b>	
	$\delta^{\text{H}}$ ( $J$ in Hz)	$\delta^{\text{C}}$	$\delta^{\text{H}}$ ( $J$ in Hz)	$\delta^{\text{C}}$
3	4.44 ( <i>ddd</i> , $J = 10.4, 6.0, 6.0$ )	73.4	3.95 ( <i>ddd</i> , $J = 12.8, 10.4, 8.8$ )	78.5
4	2.43 ( <i>ddq</i> , $J = 7.2, 6.0, 6.0$ )	41.2	2.20 ( <i>ddq</i> , $J = 10.4, 8.8, 7.2$ )	48.0
6	4.85 ( <i>dd</i> , $J = 10.4, 10.4$ )	77.1	4.64 ( <i>dd</i> , $J = 10.8, 10.4$ )	81.3
7	2.02 ( <i>ddd</i> , $J = 10.4, 10.4, 2.2$ )	55.6	2.06 ( <i>ddd</i> , $J = 10.8, 10.8, 2.4$ )	57.1
8	4.16 ( <i>ddd</i> , $J = 4.0, 3.5, 2.2$ )	63.6	4.17 ( <i>br m</i> )	64.0
11	3.22 ( <i>dq</i> , $J = 10.4, 7.2$ )	37.1	3.23 ( <i>dq</i> , $J = 10.8, 7.2$ )	37.4
12		179.6		179.5
13	1.26 ( <i>d</i> , $J = 7.2$ )	132	1.28 ( <i>d</i> , $J = 7.2$ Hz)	136
14a	5.16 ( <i>s</i> )	114.2	5.15 ( <i>s</i> )	115.7
14b	5.20 ( <i>s</i> )		5.25 ( <i>s</i> )	

Kisiel (1983), Kisiel and Michalska (2001), and Rychlewska and Kisiel (1991)

**Fig. 7.8** Chemical structures of compounds **14**, **15** and **16****Fig. 7.9** Chemical structure of dehydrocostus lactone (**17**)

In the  $^1\text{H}$ -RMN spectrum, two doublets at  $\delta$  6.24 and  $\delta$  5.48 ppm corresponding to the exomethylene protons of C-13 (H-13a and H13b) were observed.

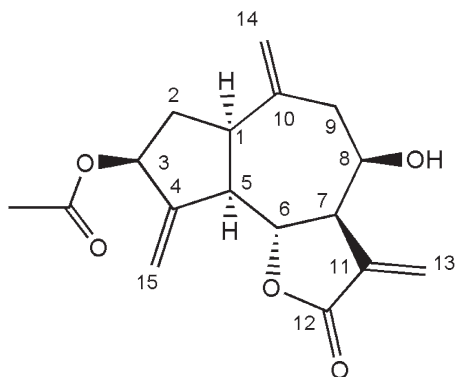
The multiplicity and  $J$  values calculated in the  $^1\text{H}$ -NMR spectrum indicate that the proton at 2.45 ppm was axial, while protons showing signals at 2.65 and 1.68 ppm were equatorials.

**Table 7.10**  $^1\text{H}$ -NMR and  $^{13}\text{C}$ -NMR chemical shifts and coupling constants corresponding to dehydrocostus lactone (**17**)

Position	<b>17</b>	
	$\delta^1\text{H}$ ( $J$ in Hz)	$\delta^1\text{C}$
4		151.43
6	3.98 ( <i>t</i> , 9.3)	85.46
7	2.89	45.36
8a	2.25	31.16
8b	2.17	
11		139.98
12		170.49
13a	6.23 ( <i>d</i> , 3.4)	120.40
13b	5.50 ( <i>d</i> , 2.9)	
14a	4.91 ( <i>brs</i> )	112.85
14b	4.83 ( <i>brs</i> )	
15a	5.28 ( <i>brd</i> , 2.4)	109.86
15b	5.08 ( <i>brd</i> , 1.9)	

Joel et al. (2011)

**Fig. 7.10** Chemical structure of  $8\beta$ -hydroxyzaluzanin D (**18**)



**$8\beta$ -hydroxyzaluzanin D (**18**)**

In the COSY spectrum, the doublet of three protons with  $J = 7.5$  Hz at  $\delta$  1.00 ppm (C-14 methyl) showed to be coupled with a proton at  $\delta$  2.16 ppm (multiplet) located on a methyne carbon (C-10, 35.35 ppm) as seen in the HSQC spectrum.

These observations indicate that the methyl and methyne groups are located contiguously.

The signals at 2.45 and 2.64 (ddd) ppm correspond to protons of the same methylene group, located on carbon that appears at 30.96 ppm (C-3).

In the  $^{13}\text{C}$ -NMR spectrum, two signals attributed to carbonyl groups can be seen at  $\delta$  169.55 (C-12) and 168.85 (C-4). The lowest intensity resonance of C-12 is explained because this atom (a  $\gamma$ -lactone carbonyl) has a larger relaxation time than the C-4 ( $\delta$ -lactone carbonyl) (Borges del Castillo et al. 1981). Two olefinic carbons, C-11 and C-13, appeared at  $\delta$  138.35 and 120.45 ppm, respectively. The signals at  $\delta$  89.81 and 86.22 ppm indicate a linkage to oxygen and are attributed to C-5 and C-6, respectively.

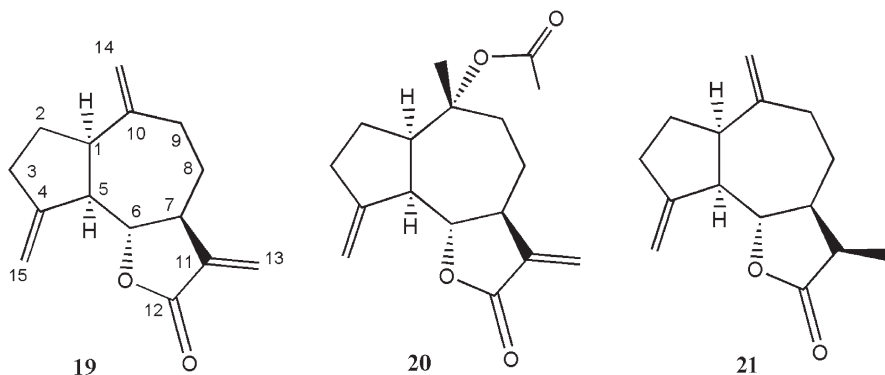


**Fig. 7.11** Chemical structures of compounds **19**, **20** and **21**

**Table 7.11**  $^1\text{H-NMR}$  and  $^{13}\text{C-NMR}$  chemical shifts and coupling constants corresponding to compounds **19**, **20** and **21**

Position	<b>19</b>		<b>20</b>		<b>21</b>	
	$\delta^{\text{H}}$ ( $J$ in Hz)	$\delta^{\text{C}}$	$\delta^{\text{H}}$ ( $J$ in Hz)	$\delta^{\text{C}}$	$\delta^{\text{H}}$ ( $J$ in Hz)	$\delta^{\text{C}}$
4		150.9		039.3		150.3
6	3.97( <i>dd</i> , 9.0)	85.1	4.01 ( <i>dd</i> , 10.2, 9.5)	80.4	4.04 ( <i>dd</i> , 10, 8.8)	85.1
7	2.90 ( <i>m</i> )	45.0	2.98 ( <i>m</i> )	44.3	2.42 ( <i>m</i> )	44.8
8a	1.46 ( <i>m</i> )	30.9	1.57 ( <i>m</i> )	24.2	1.44 ( <i>m</i> )	28.7
8b	2.27 ( <i>m</i> )		2.12 ( <i>m</i> )		1.82 ( <i>m</i> )	
10		148.8		86.0		151.7
11		139.5		141.2		39.3
12		170.0		170.1		179.9
13a	6.21 ( <i>d</i> , 3.4)	119.9	6.17 ( <i>d</i> , 3.4)	119.5	1.16 ( <i>d</i> , 7.8)	11.3
13b	5.49 ( <i>d</i> , 2.9)		5.45 ( <i>d</i> , 3.4)			
14a	4.90 ( <i>s</i> )	112.4	1.51 <i>s</i>	26.1	4.87 ( <i>brs</i> )	111.7
14b	4.82 ( <i>s</i> )				4.77 ( <i>s</i> )	
15a	5.27 ( <i>dd</i> , 2.2)	109.04	5.19 ( <i>d</i> , 2.4)	110.6	5.20 ( <i>d</i> , 2)	109.3
15b	5.07 ( <i>dd</i> , 2.2)		5.03 ( <i>d</i> , 2.2)		5.05 ( <i>dd</i> , 2, 1)	

Neves et al. (1999)

The  $^1\text{H-NMR}$  and  $^{13}\text{C-NMR}$  data of psilostachyin (**23**) are presented below:

**$^1\text{H-RMN}$  (500 MHz,  $\text{CDCl}_3$ )**  $\delta$  (ppm) 1.03 (3H, *d*, 7.5 Hz), 1.20 (3H, *s*), 1.57 (1H, *m*), 1.72 (1H, *dt*, 10.5 Hz) 1.95 (2H, *dd + dd*), 2.20 (2H, *m*), 2.50 (3H, *m*), 2.70 (1H, *m*), 3.40 (1H, *m*), 4.97 (1H, *d*, 9.5 Hz), 5.55 (1H, *d*, 3 Hz), 6.27 (1H, *d*, 3 Hz)

**$^{13}\text{C-RMN}$  (500 MHz,  $\text{CDCl}_3$ )**  $\delta$  (ppm) 177.30 (C-4), 169.65 (C-12), 138.92 (C-11), 121.83 (C-13), 93.50 (C-5), 83.29 (C-6), 79.65 (C-1), 41.80 (C-7), 40.14 (C-10), 30.22 (C-8), 27.50 (C-3), 26.92 (C-9), 24.40 (C-2), 21.50 (C-15), 14.99 (C-14)

The  $^1\text{H-NMR}$  spectrum of psilostachyin shows the characteristic signals at  $\delta$  6.27 and 5.55 (doublets) corresponding to H-13b and H-13a, respectively. The signals at

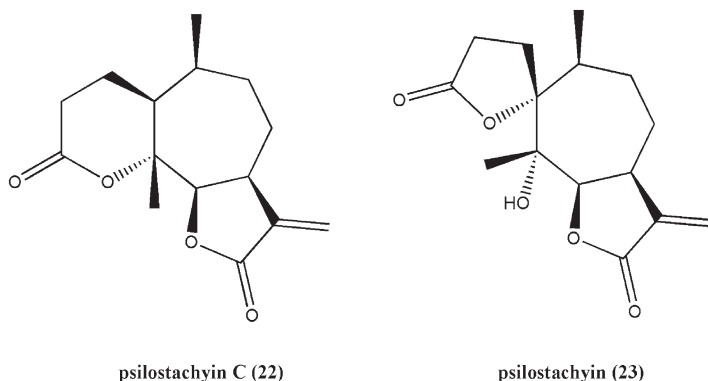
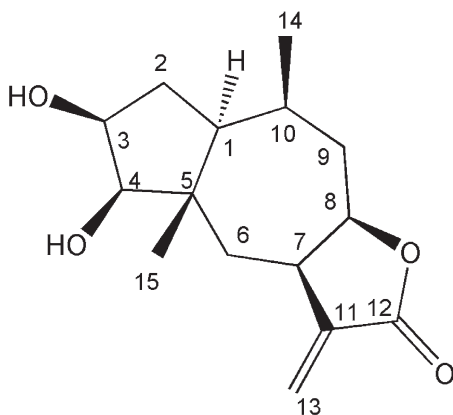


Fig. 7.12 Chemical structures of psilostachyin C (22) and psilostachyin (23)

Fig. 7.13 Chemical structure of cumenin (24)



$\delta$  1.20 and 1.03, which integrate for 3H each, correspond to the protons of the  $\text{CH}_3$  groups C-15 (singlet) and C-14 (doublet), respectively. The doublet at 4.97 (1H) was assigned to the C-6 lactonic proton and the multiplet at  $\delta$  3.40 to the C-7 proton.

The quaternary carbon (C-1) connected to CH showed a signal at  $\delta$  93.50 ppm which indicates a linkage to oxygen (Sülsen 2009). The spiro- $\gamma$ -lactone closed at C-1 and the OH group at C-5 exhibited distinctive signals at  $\delta$  177.3 ppm for a saturated  $\gamma$ -lactone carbonyl (C-4) and  $\delta$  93.5 ppm for a quaternary carbonyl (C-5). The signal of C-1 appears at 79.65 ppm. All the remaining signals could be assigned by using HSQC, HMBC, COSY and ATP experiments (Sülsen 2009).

Sülsen et al. (2013) and Martino et al. (2015) have reported the isolation of cumenin (24) from *Ambrosia tenuifolia* (Fig. 7.13). This compound is a STL based on a pseudoguaianolide skeleton. The  $^1\text{H-NMR}$  spectrum shows the characteristic signals at  $\delta$  6.26 ppm (d,  $J = 2.3$  Hz, 1H) and 5.61 ppm (d,  $J = 2.3$  Hz, 1H) corresponding to H-13a and H-13b, respectively, which are typical of an exocyclic methylene group of a  $\alpha,\beta$ -unsaturated lactone (Table 7.12).

**Table 7.12**  $^1\text{H}$ -NMR and  $^{13}\text{C}$ -NMR chemical shifts and coupling constants of cumenin (**24**)

Position	$\delta\text{H}$ (J in Hz)	$\delta\text{C}$
<b>3</b>	4.21 ( <i>m</i> )	68.4
<b>4</b>	3.51 ( <i>d</i> , 7)	77.1
<b>6</b>	1.95 ( <i>m</i> )	40.7
	1.59 ( <i>m</i> )	
<b>7</b>	3.13 ( <i>m</i> )	37.8
<b>8</b>	4.68 ( <i>ddd</i> , 2; 8)	80.1
<b>10</b>	1.95( <i>m</i> )	30.4
<b>11</b>		139.8
<b>12</b>		169.9
<b>13</b>	6.26 ( <i>d</i> , 2.3)	123.0
	5.61 ( <i>d</i> , 2.3)	
<b>14</b>	1.04 ( <i>d</i> , 2.3)	16.7
<b>15</b>	0.98 s	17.8

The singlet at  $\delta$  0.98 ppm is attributed to the protons of the tertiary methyl group (H-15) and the signal at  $\delta$  1.04 ppm (doublet) to the protons of a secondary methyl group (H-14).

### 7.2.3 Eudesmanolides

Several eudesmanolides have been isolated from *Mikania campanulata* by Krautmann et al. (2007). The  $^1\text{H}$ -NMR and  $^{13}\text{C}$ -NMR spectrum data of one of the STLs, (1S,4S,5S,6S,7S,10R)-1-hydroxy- 15-acetoxyeudesm-11(13)-en-6,12-olide (**25**) (Fig. 7.14), are presented in Tables 7.13 and 7.14.

The  $^1\text{H}$ -NMR spectrum of **25** (Table 7.13) shows two characteristic  $\alpha$ -methylene- $\gamma$ -lactone doublets assigned to H-13a and H-13b at  $\delta$  6.06 ( $J = 3.3$  Hz) and 5.40 ( $J = 3.0$  Hz), respectively, whose  $J$  values, larger than 3.0 Hz, are indicative of a *trans*-lactone ring. Resonances for an acetate methyl and a quaternary methyl appeared at  $\delta$  2.06 and 0.97, respectively. Other resonances were the AB portion of an ABX system showing a triplet at  $\delta$  4.32 ( $J = 10.4$  Hz) and a double doublet at  $\delta$  4.03 ( $J = 10.4, 3.5$  Hz) assigned to the C-15 methylene protons, a double doublet at  $\delta$  3.94 ( $J = 11.5$  and 10.6 Hz, H-6), a double doublet at  $\delta$  3.50 (3.8 and 2.4 Hz, H-1), a multiplet at  $\delta$  2.48 (H-7) and a double doublet at  $\delta$  2.35 ( $J = 11.5$  and 5.2 Hz, H-5). Collectively this data indicate a 6,12-*trans*-lactonized eudesmanolide with an O-acetyl substituent at C-15 and a hydroxyl group at C-1, as shown in structure **25**. The relative configuration was established from coupling constants for H-1, H-5, H-6 and H-7 and NOESY.

The chemical shift of C-7 indicates also a *trans*-lactonization at C-6. In *cis*-lactones closed at C-6, the signal of C-7 appears between 39 and 43 ppm. When a  $\beta$ -oriented -OR group is present in C-14, this carbon resonates at higher fields ( $\delta$  11.5–14.0 ppm) than when the -OR group is  $\alpha$ -oriented ( $\delta$  17.0–21.0 ppm).

**Fig. 7.14** Chemical structure of compound **25**

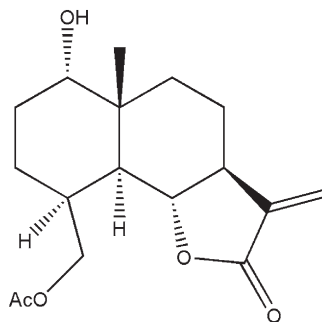


**Table 7.13**  $^1\text{H-NMR}$  data for compound **25**

Proton	Compound <b>25</b> <sup>a</sup>
H-1	3.50 <i>br dd</i> (3.8;2.4)
H-2 $\alpha$	1.58 <i>m</i>
H-2 $\beta$	1.92 <i>m</i>
H-3 $\alpha$	1.88
H-3 $\beta$	1.60 <i>m</i>
H-4	2.41 <i>m</i>
H-5	2.35 <i>dd</i> (11.5;5.2)
H-6	3.94 <i>dd</i> (11.5;10.6)
H-7	2.48 <i>m</i>
H-8 $\alpha$	2.05 <i>m</i>
H-8 $\beta$	1.58 <i>m</i>
H-9 $\alpha$	2.00 <i>m</i>
H-9 $\beta$	1.24 <i>m</i>
H-13 $\alpha$	6.06 <i>d</i> (3.3)
H-13 $\beta$	5.40 <i>d</i> (3.0)
H-14	0.97 <i>s</i>
H-15a	4.32 <i>t</i> (10.4)
H-15b	4.03 <i>br dd</i> (10.4;3.5)
OAc	2.06 <i>s</i>

Krautmann et al. (2007)

<sup>a</sup> $\text{CDCl}_3$

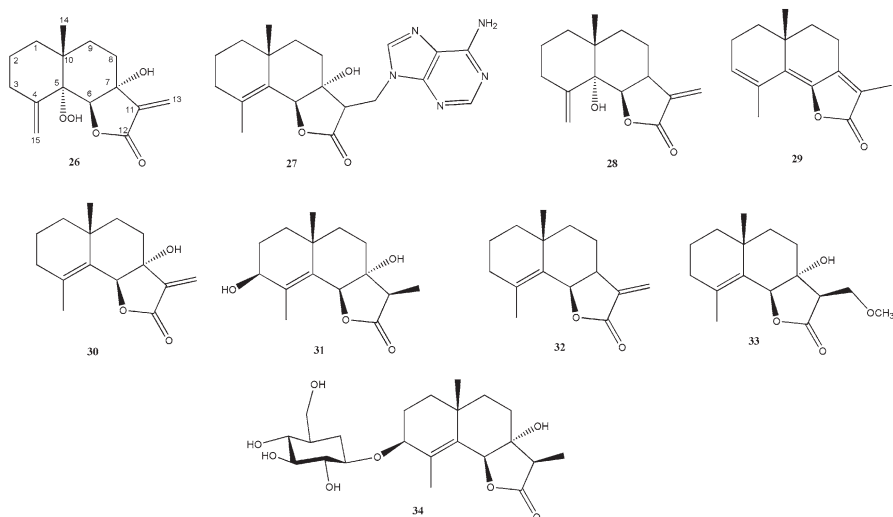
Emani et al. (2017) have reported the isolation of four new eudesmanolides from *Sphaeranthus indicus*: compounds **26–29** and eudesmanolides **30–34** that had been previously reported (Atta-Ur-Rahman et al. 1989; Shekhani et al. 1990, 1991; Jadhav et al. 2007) (Fig. 7.15).

Two signals corresponding to olefinic protons at  $\delta$  5.79 ppm and 6.19 ppm, which correlated with the signal of an olefinic carbon at  $\delta$  119.7 ppm, a carbonyl carbon at  $\delta$  167.8 ppm and a quaternary carbon at  $\delta$  75.7 ppm, were present in the NMR spectra of **26**. Besides, an oxymethine proton signal at  $\delta$  4.75 ppm revealed the presence of an  $\alpha$ -methylene- $\gamma$ -lactone moiety, which is characteristic of 7-hydroxyeudesmanolides compounds. The proton spectrum also showed the pres-

**Table 7.14**  $^{13}\text{C}$ -NMR data for compound **25**

Carbon	Compound <b>25</b> <sup>a</sup>
1	73.5
2	24.4
3	20.2
4	32.5
5	43.2
6	80.4
7	50.5
8	21.4
9	35.8
10	40.0
11	139.5
12	170.8
13	117.0
14	20.8
15	62.9
OAc	171.4 20.9

Krautmann et al. (2007)

<sup>a</sup> $\text{CDCl}_3$ **Fig. 7.15** Chemical structures of compounds **26–34**

ence of signals at  $\delta$  5.38 ppm (1H, s, H-15a),  $\delta$  5.28 ppm (1H, s, H-15b),  $\delta$  2.42–2.26 ppm (2H, m, H-3),  $\delta$  1.81–1.72 ppm (2H, m, H-2a, 8a) and  $\delta$  1.20–1.12 ppm (2H, m, H-8b, H-9b). Compound **27** displayed signals at  $\delta$  3.57 ppm (1H, t,  $J$  = 6.8 Hz, H-11), 2.13–1.98 ppm (2H, m, H-3), 1.86–1.79 ppm (2H, m, H-2a, 8a), 1.75 ppm (3H, s, Me-15) and 1.05 ppm (3H, s, H-14) and two quaternary olefinic carbons at  $\delta$  126.9 ppm (C-4) and 138.7 ppm (C-5). The presence of a hydroxyl



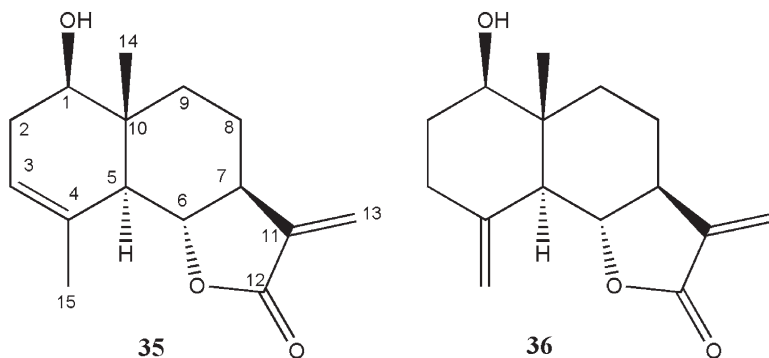


**Fig. 7.16** Chemical structures of santamarine (**35**) and reynosin (**36**)

function at C-7 was determined through a proton signal that was interchangeable with D<sub>2</sub>O at  $\delta$  5.50 ppm and through its HMBC correlations with the C-7 ( $\delta$  75.8 ppm) and C-6 ( $\delta$  79.2 ppm) oxygenated carbons, a methylene carbon at  $\delta$  24.2 ppm (C-8) and a methine carbon at  $\delta$  51.7 ppm (C-11). These data suggested the presence of a sesquiterpene moiety similar to 7-hydroxyphenylanilide, with an 11,13-dihydro modification and with an adenine moiety. The compound was therefore described as (11 $\alpha$ , 13-dihydro-7 $\alpha$ -hydroxyfrullanolide-13-yl)-adenine (**27**).

The chemical shifts and coupling constants for 5 $\alpha$ -hydroxyisosphærantholide (**28**) were  $\delta$  6.08 ppm (1H, d,  $J$  = 0.8 Hz, H-13a), 5.55 ppm (1H, d,  $J$  = 0.8 Hz, H-13b), 5.30 ppm (1H, s, H-15a), 5.02 ppm (1H, d,  $J$  = 1.2 Hz, H-15b), 4.26 ppm (1H, d,  $J$  = 4.4 Hz, H-6), 2.59–2.50 ppm (1H, m, H-3a), 2.22–2.01 ppm (1H, m, H-3b), 1.89 ppm (2H, dt,  $J$  = 4.4 Hz, 13.6 Hz, H-1a, H-9a), 1.78–1.66 ppm (1H, m, H-8b), 1.57–1.51 ppm (1H, m, H-2b), 1.13–1.06 ppm (2H, m, H-1b, H-9b) and 0.98 ppm (3H, s, H-14).

For 11 $\alpha$ ,13-dihydro-eudesman-3,5,7(11)-triene-6 $\alpha$ -12-olide (**29**), values were  $\delta$  5.84–5.82 ppm (1H, m, H-3), 2.70–2.64 ppm (2H, m, H-2), 2.32–2.30 ppm (2H, m, H-8), 2.13 ppm (3H, d,  $J$  = 1.2 Hz, H-15), 1.89 ppm (3H, s, H-13), 1.67–1.51 ppm (4H, m, H (M, 1H) and 1.07 ppm (3H, s, H-14).

Coronado-Aceves et al. (2016) have reported the isolation of the STLs santamarine (**35**) and reynosin (**36**) from the chloroform extract of *Ambrosia confertiflora* (Fig. 7.16). The spectroscopic data of these compounds are given below:

**Santamarine (35):** <sup>1</sup>H-NMR (CDCl<sub>3</sub>, 400 MHz):  $\delta$  3.68 ppm (1H, dd,  $J$  = 9.9 Hz, 6.6 Hz, H-1),  $\delta$  5.35 ppm (1H, m, H-3),  $\delta$  2.37 ppm (1H, m, H-5),  $\delta$  3.95 ppm (1H, t,  $J$  = 11 Hz, H-6),  $\delta$  2.50 ppm (1H, m, H-7),  $\delta$  5.41 ppm (1H, d,  $J$  = 3.1 Hz, H-13),  $\delta$  6.08 ppm (1H, d,  $J$  = 3.2 Hz, H-13); <sup>13</sup>C-NMR (CDCl<sub>3</sub>, 100 MHz):  $\delta$  75.4 ppm (C-1),  $\delta$  121.4 ppm (C-3),  $\delta$  133.6 ppm (C-4),  $\delta$  81.7 ppm (C-6),  $\delta$  51.2 ppm (C-7),  $\delta$  139.1 ppm (C-11),  $\delta$  171.0 ppm (C-12),  $\delta$  117.0 ppm (C-13),  $\delta$  11.2 ppm (C-14),  $\delta$  23.5 ppm (C-15).

**Reynosin (36):** <sup>1</sup>H-NMR (CDCl<sub>3</sub>, 400 MHz):  $\delta$  1.38 ppm (1H, m, H-3),  $\delta$  2.10 ppm (1H, m, H-3),  $\delta$  2.12 ppm (1H, m, H-5),  $\delta$  4.03 ppm (1H, t,  $J$  = 10.9 Hz, H-6),  $\delta$  2.54 ppm (1H, m, H-7),  $\delta$  6.09 ppm (1H, d,  $J$  = 3.2 Hz, H-13),  $\delta$  5.41 ppm (1H, d,  $J$  = 3.0 Hz, H-13),  $\delta$  4.87 ppm (1H, d,  $J$  = 0.9 Hz, H-15),  $\delta$  4.99 ppm (1H, d,

$J = 0.9$  Hz, H-15);  $^{13}\text{C}$ -NMR ( $\text{CDCl}_3$ , 100 MHz):  $\delta$  78.4 ppm (C-1),  $\delta$  35.9 ppm (C-3),  $\delta$  142.7 ppm (C-4),  $\delta$  79.8 ppm (C-6),  $\delta$  49.8 ppm (C-7),  $\delta$  139.5 ppm (C-11),  $\delta$  170.8 ppm (C-12),  $\delta$  117.2 ppm (C-13),  $\delta$  11.8 ppm (C-14),  $\delta$  110.9 ppm (C-15).

These compounds differ from each other in the NMR signals of protons and carbons of positions 3, 4 and 15.

## 7.2.4 Germacranolides

Examples of the structural elucidation of different germacranolide subtypes are given.

### 7.2.4.1 Germacrolides

The germacrolide STLs mikanolide (**37**), deoxymikanolide (**38**) and dihydromikanolide (**39**), also known as mikanolide type STLs, have been isolated from several *Mikania* species (Laurella et al. 2017; Cuenca et al. 1988; Cuenca 1995; Rufatto et al. 2012) (Fig. 7.17).

Mikanolide (**37**) exhibits the characteristic signals of H-13a and H-13b (doublets) at 6.45 ppm ( $J = 3.6$  Hz) and 6.02 ppm (3.3 Hz), respectively, and a dddd corresponding to H-7 at 3.25 ppm. The presence of a second  $\alpha,\beta$ -unsaturated lactone group was evidenced in the  $^1\text{H}$ -NMR by a broad singlet at 7.20 ppm (H-5) and by a double doublet at 5.31 ppm (H-6) ( $J_{5,6} = 1.6$  Hz and  $J_{6,7} = 3.5$  Hz).

The  $^{13}\text{C}$ -NMR spectrum shows signals for two lactonic carbonyl carbons at 167.7 ppm (C-12) and 170.3 ppm (C-5). The other two carbons that are bases of lactones, C-6 and C-8, arise at 83.2 ppm and 77.0 ppm, respectively. Carbon 5, the carbon that is in  $\beta$  position with respect to  $\alpha,\beta$ -unsaturated system, appears at 147.3 ppm. The signals for C-9, C-10 and C-14 arise at 43.7 ppm, 21.7 ppm and 57.4 ppm (Cuenca 1995).

The  $^1\text{H}$ -NMR spectra of deoxymikanolide (**39**) shows some differences with respect to mikanolide. It does not show the signals of H-2 and H-3, which appear as doublets at 3.37 ppm and 4.04 ppm, respectively. In this case, the signals of H-2 $\alpha$  and H-2 $\beta$  and H-3 $\alpha$  and H-3 $\beta$  appear at 1.51 and 2.13 ppm and 2.73 ppm (br dd) and 2.58 ppm (ddd), respectively.

In the  $^{13}\text{C}$ -NMR of deoxymikanolide, there are two less signals of carbons linked to oxygen with respect to mikanolide. In contrast, two signals attributed to methylene carbons, C-2 and C-3, appear at 23.0 and 22.3 ppm.

In the case of dihydromikanolide (**38**), H-13 appears as a doublet at 1.43 ppm instead of the doublets of H-13a and H-13b. These protons are coupled to H-11 at 2.67 ppm as a double quartet. The high value of the  $J_{7,11}$  (12.3 Hz) dictates an  $\alpha$  position of the methyl group.

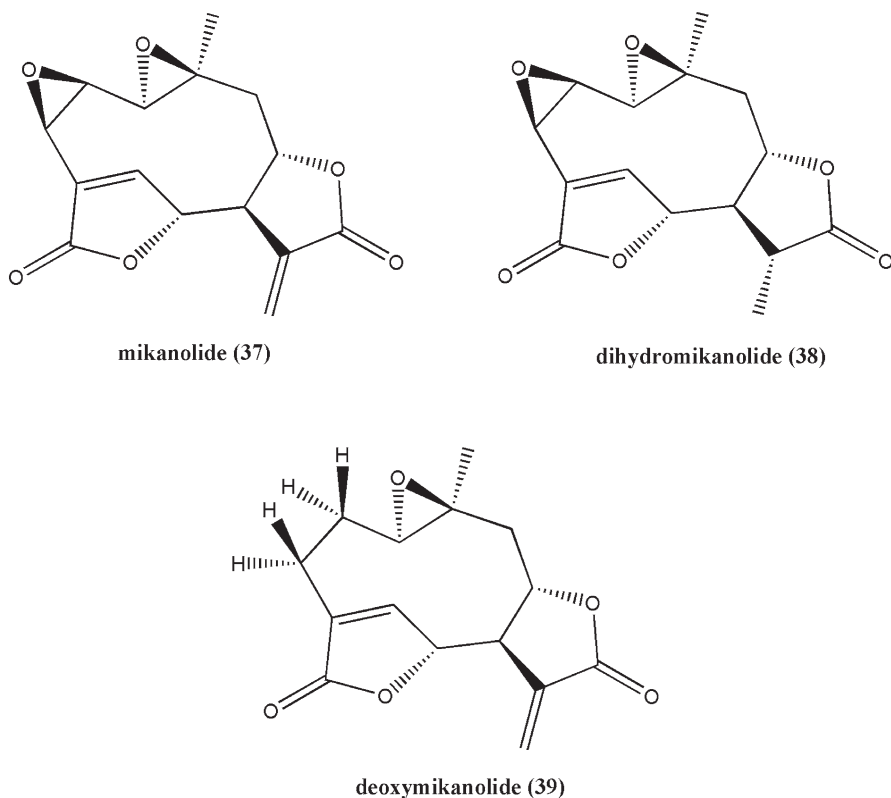


**Fig. 7.17** Chemical structures of mikanolide (37), dihydromikanolide (38) and deoxymikanolide (39)

#### 7.2.4.2 Melampolides

Some melampolides have been isolated from the aerial parts of *Mikania cordifolia* (Asteraceae) (Gutierrez et al. 1987). Two of them are the compounds **40** and **41** (Fig. 7.18).

Both compounds have shown the H-13 doublets at 6.62 and 5.50 ( $J = 3$  Hz) and the two vinylic protons at 5.38–5.36 ppm (t) and 5.04 ppm (dd) corresponding to H-1 and H-5, respectively. The proton under the lactone oxygen (H-8) appears at  $\delta$  3.55 ppm as a broad multiplet (Table 7.15). The signals at  $\delta$  2.29 ppm and 2.17 ppm are due to H-9a and H-9b. In this type of compounds, H-15 allylic protons appear generally as singlets at approximately  $\delta$  4.58–4.59 ppm (Gutierrez et al. 1987; Catalán et al. 2003). The  $J$  values of H-5 with H-6 and H-7 with H-13a and H-13b are in accordance with a *Z* configuration of the 4,5-double bond.

In the  $^{13}\text{C}$ -NMR spectra, the pairs of olefinic carbons C-1, C-10 and C-4, C-5 of the ten-membered ring appear at  $\delta$  125.6, 138.4 and 139.6, 127.4 ppm, respectively (Table 7.16).

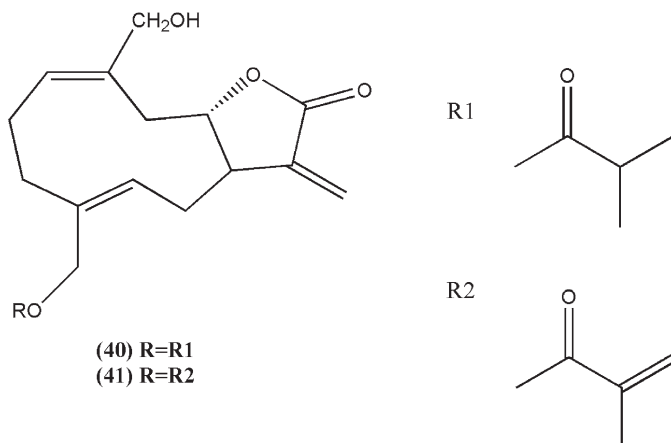


Fig. 7.18 Chemical structures of compounds **40** and **41**

Table 7.15  $^1\text{H-NMR}$  data for compounds **40** and **41**

Proton	Compound <b>40</b> <sup>a</sup>	Compound <b>41</b> <sup>a</sup>
H-1	5.38 <i>br t</i> (8)	5.36 <i>br t</i>
H-5	5.04 <i>dd</i> (11;5)	5.04 <i>dd</i>
H-7	~2.2 <i>m</i>	~2.2 <i>m</i>
H-8	3.55 <i>dt</i> (8;3.5)	3.55 <i>dt</i>
H-9a	2.29 <i>dd</i> (14;3.5)	2.29 <i>dd</i>
H-9b	2.17 <i>dd</i> (14;3.5)	2.17 <i>dd</i>
H-13a	6.08 <i>d</i> (3)	6.08 <i>d</i>
H-13b	4.98 <i>d</i> (3)	4.98 <i>d</i>
H-14a,b	3.92 <i>br</i>	3.92 <i>br</i>
H-15a	4.51 <i>d</i> (12)	4.54 <i>d</i>
H-15b	4.25 <i>d</i> (12)	4.32 <i>d</i>
2'	2.40 <i>m</i>	–
3'a	1.06 <i>d</i> (7)	5.26 <i>br</i>
b		4.98 <i>br</i>
4'	1.06 <i>d</i> (7)	1.82 <i>br</i>

Gutierrez et al. (1987)

<sup>a</sup>C<sub>6</sub>D<sub>6</sub>

### 7.2.4.3 Heliangolides

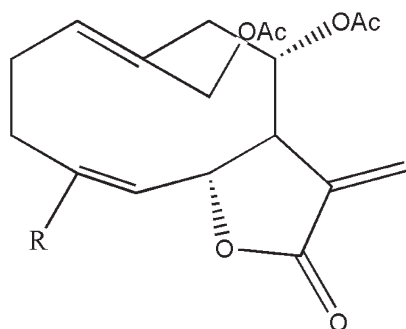
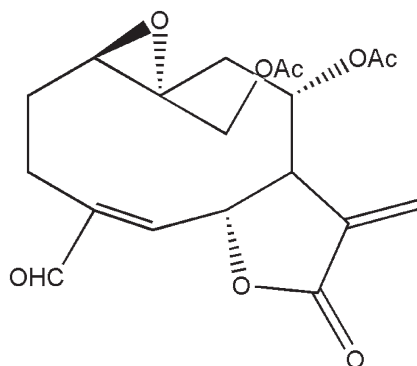
Four heliangolides (**42–45**) (Fig. 7.19) have been reported in *Mikania minima* (Cuenca et al. 1993).

In the  $^1\text{H-NMR}$  the small  $J$  values of H-7 with H-13a and H-13b ( $J_{7,13}\sim 1$  Hz) and a small  $J_{6,7}$  value ( $J_{6,7}\sim 1$  Hz) are indicative of heliangolide type STLs. The chemical shift of H-5 of **44** and **45** indicates that H-5 is *cis* to the aldehyde function (Table 7.17). In **43**, location of the second acetate on C-14 rather than C-15 was evident from the allylic coupling between H-1 and the CH<sub>2</sub>O- signals at lower field (Cuenca et al. 1993).

**Table 7.16**  $^{13}\text{C}$ -NMR data for compounds **40** and **41**

Carbon	Compound <b>40</b> <sup>a</sup>	Compound <b>41</b> <sup>a</sup>
1	125.6	125.6
2	28.4	28.4
3	29.5	29.5
4	139.6	139.6
5	127.4	127.4
6	31.1	31.1
7	46.5	46.5
8	84.1	84.1
9	34.7	34.7
10	138.4	138.4
11	135.8	136.1
12	169.7	169.7
13	120.7	120.7
14	66.2	66.2
15	63.1	63.3
1'	176.5	165.9
2'	33.9	135.75
3'	18.8	125.8
4'	18.8	18.2

Gutierrez et al. (1987)

<sup>a</sup> $\text{CDCl}_3$ **(42)**  $\text{R}=\text{CH}_2\text{OAc}$ **(43)**  $\text{R}=\text{CH}_2\text{OH}$ **(44)**  $\text{R}=\text{CHO}$ **(45)****Fig. 7.19** Chemical structures of compounds **42**, **43**, **44** and **45**

**Table 7.17** <sup>1</sup>H-NMR data of compounds **42**, **43**, **44** and **45** (500 MHz, CDCl<sub>3</sub>)

Proton	Compounds			
	<b>42*</b>	<b>43*</b>	<b>44</b>	<b>45</b>
H-1	5.59 <i>br dd</i>	5.60 <i>br dd</i>	5.49 <i>br dd</i>	2.87 <i>dd</i>
H-2a	2.56 <i>m</i>	2.56 <i>m</i>	2.61 <i>dddd</i>	2.26 <i>m</i>
H-2b	2.21 <i>m</i>	2.21 <i>m</i>	1.98 <i>dddd</i>	1.55 <i>m</i>
H-3a	2.44 <i>ddd</i>	2.40 <i>m</i>	2.85 <i>ddd</i>	2.75 <i>dd</i>
H-3b	2.15 <i>m</i>	2.09 <i>m</i>	2.12 <i>ddd</i>	2.26 <i>m</i>
H-5	5.44 <i>dd</i>	5.48 <i>dddd</i>	6.27 <i>br d</i>	6.37 <i>d</i>
H-6	5.08 <i>dd</i>	5.09 <i>dd</i>	5.30 <i>br dd</i>	5.70 <i>dd</i>
H-7	2.94 <i>dddd</i>	2.95 <i>dddd</i>	3.03 <i>dddd</i>	2.96 <i>dddd</i>
H-8	5.04 <i>ddd</i>	5.04 <i>ddd</i>	5.09 <i>ddd</i>	5.24 <i>dd</i>
H-9a	2.75 <i>dd</i>	2.76 <i>br dd</i>	2.77 <i>dd</i>	2.79 <i>dd</i>
H-9b	2.28 <i>dd</i>	2.27 <i>br dd</i>	2.28 <i>dd</i>	1.36 <i>dddd</i>
H-13a	6.41 <i>br s</i>	6.40 <i>br s</i>	6.50 <i>d</i>	6.50 <i>d</i>
H-13b	5.78 <i>br s</i>	5.70 <i>br s</i>	5.86 <i>d</i>	5.86 <i>d</i>
H-14a	4.76 <i>br d</i>	4.72 <i>br s</i>	4.78 <i>br d</i>	4.41 <i>br d</i>
H-14b	4.71 <i>br d</i>		4.73 <i>br d</i>	4.23 <i>dd</i>
H-15	4.54 <i>br s</i>	4.13 <i>br s</i>	9.45 <i>br s</i>	9.52 <i>s</i>
Ac	2.14 <i>s</i> , 2.10 <i>s</i>	2.14 <i>s</i> , 2.01 <i>s</i>	2.16 <i>s</i> , 1.07 <i>s</i>	2.20 <i>s</i> , 2.02 <i>s</i>

Cuenca et al. (1993)

(\*) some signals broadened at room temperature

#### 7.2.4.4 Cis,cis-germacranolides

Catalán et al. (2003) reported the isolation of six new *cis,cis*-germacranolides from *Mikania thapsoides*. One of them, compound **46** (Fig. 7.20), shows in the <sup>1</sup>H-NMR spectra the characteristic  $\alpha$ -methylene- $\gamma$ -lactone doublets at  $\delta$  6.31 ppm ( $J = 3.6$  Hz) and 5.58 ( $J = 3.1$  Hz) corresponding to H-13a and H-13b, respectively (Table 7.18). The constant values ( $>3$  Hz) indicate a *trans* ring lactonization, since a *cis*-lactone presents a small coupling constant values, generally  $<2$  Hz.

A pair of doublets at  $\delta$  4.30 and 3.87 ppm ( $J = 12.6$  Hz) were assigned to CH<sub>2</sub>-15 and the other at  $\delta$  4.51 and 4.42 ppm ( $J = 12.9$  Hz) to CH<sub>2</sub>-14. The H-8 and H-5 show signals at  $\delta$  4.54 ( $J = 7.4, 4.3, 2.4$  Hz) and  $\delta$  4.64 ( $J = 3.6, 3.4$  Hz), respectively.

The signal of H-3 ( $\delta$  3.09 ppm) shows a long-range *W*-type coupling with that of H-5 at  $\delta$  4.20 (ddd,  $J = 3.6, 3.4, 1.0$  Hz) which indicates a  $\beta$ -oriented epoxide between C-3 and C-4.

The presence of three carbonyls, six olefinic carbons and six sp<sup>3</sup> carbons bearing oxygen can be detected in the <sup>13</sup>C-NMR spectra (Table 7.19). The chemical shift of C-8 at  $\delta$  84.3 ppm indicates a *trans*-lactonization to C-8. In *cis*-lactones closed to C-8, this signal is shown at  $\delta$  70–79 ppm. The signal of C-14 at  $\delta$  68.4 ppm indicates an *E* configuration of the C(1) = C(10) double bond. This observation and the relative stereochemistry of all chiral centres were confirmed by NOESY experiments.

**Fig. 7.20** Chemical structure of compound **46**

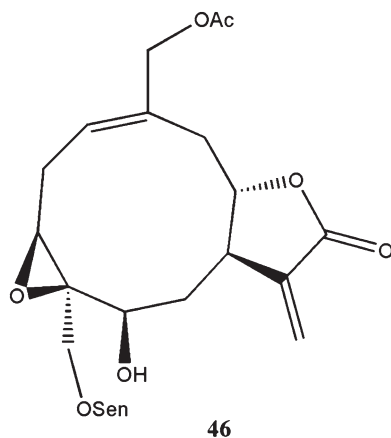


**Table 7.18**  $^1\text{H-NMR}$  data for compound **46** (300 MHz,  $\text{CDCl}_3$ )

Proton	Compound <b>46</b>
H-1	5.89 <i>m</i>
H-2 $\alpha$	2.65 <i>m</i>
H-2 $\beta$	3.10 <i>br q</i> (11.2)
H-3 $\alpha$	3.09
H-5	4.64 <i>br dd</i> (3.6,3.4)
H-6 $\alpha$	2.21 <i>ddd</i> (16,3.4,1.6)
H-6 $\beta$	2.10 <i>ddd</i> (16,10.7,3.6)
H-7	2.99 <i>dddd</i> (10.7,7.4,3.6,3.1,1.6)
H-8	4.54 <i>ddd</i> (7.4,4.3,2.4)
H-9 $\alpha$	2.57 <i>dd</i> (15.1,2.4)
H-9 $\beta$	3.34 <i>dd</i> (15.1,4.3)
H-13a	6.31 <i>d</i> (3.6)
H-13b	5.58 <i>d</i> (3.1)
H-14a	4.51 <i>d</i> (12.9)
H-14b	4.42 <i>d</i> (12.9)
H-15a	4.30 <i>d</i> (12.6)
H-15b	3.87 <i>d</i> (12.6)
2'	5.65 <i>hept</i> (1.3)
4'	2.18 <i>br d</i> (1.3)
5'	1.91 <i>br d</i> (1.3)
AcO	2.03 <i>s</i>

Catalán et al. (2003)

#### 7.2.4.5 Other Germacranolides

Stefani et al. (2006) have reported the isolation of some germacranolides (**47**, **48**, **49**) (Fig. 7.21) from *Dimerostemma episcopale* and from *D. brasilianum*.

Compound **49** differs from **48** in the presence of an additional double bond at C-3 as well as by the lack of the two 1,10- and 4,5-epoxy rings. This information

**Table 7.19**  $^{13}\text{C}$ -NMR data for compound **46** ( $\text{CDCl}_3$ )

Carbon	Compound <b>46</b>
1	127.3
2	27.2
3	60.5
4	61.8
5	69.4
6	35.5
7	36.7
8	84.3
9	31.0
10	134.6
11	140.2
12	169.6
13	121.4
14	68.4
15	66.0
1'	165.4
2'	114.6
3'	159.3
4'	20.3
5'	27.4
AcO	170.5, 20.6

Catalán et al. (2003)

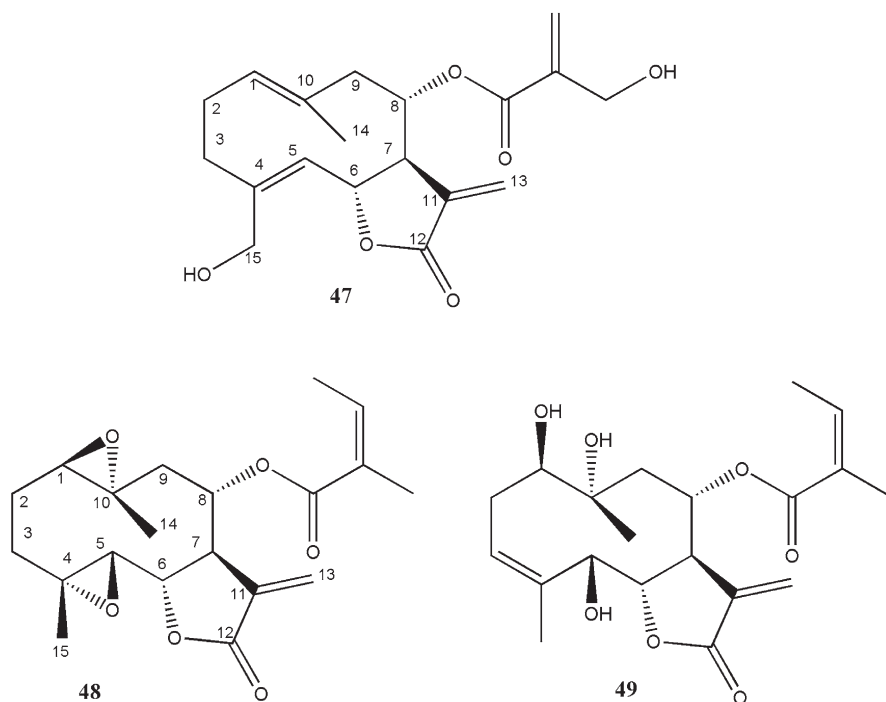


**Fig. 7.21** Chemical structures of compounds **47**, **48** and **49**



was easily taken from  $^{13}\text{C}$ -NMR data, since no signals were observed between  $\delta$  56.0 ppm and 67.0 ppm, and a pair of olefinic signals appeared at  $\delta$  125.4 ppm and 134.2 ppm. The chemical shift of H-15 ( $\delta$  1.67 ppm, s, 3H), which is typical of a methyl group attached to olefinic carbon atoms, along with its correlation with C-3 ( $\delta$  125.4 ppm) and C-4 ( $\delta$  134.2 ppm) in the HMBC spectrum, indicates the presence of the olefinic bond between C-3 and C-4. Additionally, this bond is also confirmed by the correlation observed between H-3 ( $\delta$  5.70 ppm, dd) and C-3 ( $\delta$  125.4 ppm) in the HSQC spectrum.

## References

- Abdullaev UA, Rashkes YV, Tarasov VA et al (1979) Mass spectra of some sesquiterpene lactones of the eudesmane series with a  $\text{C}_1$ -OH group. *Chem Nat Compd* 15:28–32
- Atta-Ur-Rahman, Shekhani MS, Perveen S et al (1989) 7-hydroxyfrullanolide, an antimicrobial sesquiterpene lactone from *Sphaeranthus indicus* Linn. *J Chem Res S* 13:68
- Bardón A, Cardona L, Catalán CAN et al (1996) 15-Norguaianolides and germacranolides from *Mikania mendocina*. *Phytochemistry* 41(3):845–849
- Borges del Castillo J, Manresa-Ferrero MT, Rodríguez Luis F et al (1981)  $^{13}\text{C}$  NMR study of psilostachyinolides from some *Ambrosia* species. *Magn Reson Chem* 17(3):232–234
- Budesinsky M, Saman D (1995) Carbon  $^{13}\text{C}$  NMR spectra of sesquiterpene lactones. In: Webb G (ed) , vol vol 30. Academic Press, London, pp 231–475
- Catalán CA, Cuenca M, Hernández LR et al (2003) cis,cis-Germacranolides and melampolides from *Mikania thapsoides*. *J Nat Prod* 66(7):949–953
- Cha M-R, Choi YH, Choi C et al (2011) New guaiane sesquiterpene lactones from *Ixeris dentata*. *Planta Med* 77:380–382
- Chaves JS, de Oliveira DCR (2003) Sesquiterpene lactones and other chemical constituents of *Mikania hoehnei* R. *J Braz Chem Soc* 14(5):734–737
- Coronado-Aceves EW, Velázquez C, Robles-Zepeda RE et al (2016) Reynosin and santamarine: two sesquiterpene lactones from *Ambrosia confertiflora* with bactericidal activity against clinical strains of *Mycobacterium tuberculosis*. *Pharm Biol* 54(11):2623–2628
- Cortes E, Romero MC, Romo J (1977) Espectrometría de masas de lactones sesquiterpénicas de la serie de los pseudoguaianolidos II. *Rev Latinoamer Quim* 8:168–171
- Cuenca MDR (1995) Ph.D. thesis, University of Tucumán
- Cuenca MDR, Bardon A, Catalán CAN et al (1988) Sesquiterpene lactones from *Mikania micrantha*. *J Nat Prod* 51(3):625–626
- Cuenca MDR, Borkosky S, Catalán CAN et al (1993) Sesquiterpene lactones of *Mikania minima*. *Phytochemistry* 32(6):1509–1513
- de Heluani CS, de Lampasona MP, Catalan CAN et al (1989) Guaianolides, heliangolides and other constituents from *Stevia alpina*. *Phytochemistry* 28(7):1931–1935
- Domínguez XA (1979) Métodos de investigación fitoquímica. Limusa, México
- Emami LR, Ravada SR, Garaga MR et al (2017) Four new sesquiterpenoids from *Sphaeranthus indicus*. *Nat Prod Res* 17:1–8
- Fischer NH, Oliver EJ, Fischer HD (1979) The biogenesis and chemistry of sesquiterpene lactones. In: Herz W, Grisebach H, Kirby GW (eds) *Progress in chemistry of organic natural products*, vol 38. Springer, New York, pp 47–390
- Gutierrez A, Oberti JC, Sosa V et al (1987) Melampolides from *Mikania cordifolia*. *Phytochemistry* 26(8):2315–2320
- Ito K, Sakakibara Y, Haruna M (1982) Seven guaianolides from *Eupatorium chinense*. *Phytochemistry* 21(3):715–720
- Jadhav RB, Sonawane KB, Deshpande NR et al (2007) Two new eudesmanolides from *Sphaeranthus indicus* (Linn). *Indian J Chem* 46B(121):379–381

- Joel DM, Chaudhuri SK, Plakhine D et al (2011) Dehydrocostus lactone is exuded from sunflower roots and stimulates germination of the root parasite *Orobanche Cumana*. *Phytochemistry* 72:624–634
- Kisiel W (1983) Two new guaianolides from *Crepis capillaries*. *Polish J Chem* 57:139–143
- Kisiel W, Michalska K (2001) Sesquiterpenoids and phenolics from *Crepis conyzifolia*. *Z Naturforsch* 56c:961–964
- Krautmann M, de Riscalca EC, Burgueño-Tapia E et al (2007) C-15-functionalized eudesmanolide from *Mikania campanulata*. *J Nat Prod* 70(7):1173–1179
- Laurella LC, Cerny N, Bivona AE et al (2017) Sesquiterpene lactones from *Mikania* species display *in vitro* activity against *Trypanosoma cruzi* and *Leishmania* sp. *PLoS Negl Trop Dis* 11(9):e0005929. <https://doi.org/10.1371/journal.pntd.0005929>
- Martino R, Beer MF, Elso O et al (2015) Sesquiterpene lactones from *Ambrosia* spp. are active against a murine lymphoma cell line by inducing apoptosis and cell cycle arrest. *Toxicol In Vitro* 29:1529–1536
- Matsueda S (1972) Studies on sesquiterpenelactones. VII. Mass spectra of pseudoguaiane-sesquiterpenelactones. *Yakugaku Zasshi* 92(7):905–907
- Nakanishi K (1962) Infrared absorption spectroscopy. Holden-Day, Inc., San Francisco and Nankodo Company Limited, Tokyo
- Neves M, Morais R, Gafner S et al (1999) New sesquiterpene lactones from the Portuguese liverwort *Targionia lorbeeriana*. *Phytochemistry* 50:967–972
- Plugar VN, Rashker YV, Saitbaeva IM et al (1987) Fragmentation of sesquiterpene lactones related to leucomisin. *Chem Nat Compd* 23:80–84
- Rehman NU, Hussain H, Al-Riyami SA et al (2016) Lyciumaside and lyciumate: a new diacylglycoside and sesquiterpene lactone from *Lycium shawii*. *Helv Chim Acta* 99:1–4
- Rufatto LC, Gower A, Schwambach J et al (2012) Genus *Mikania*: chemical composition and phytotherapeutical activity. *Rev Bras Farmacogn* 22(6):1384–1403
- Rychlewska U, Kisiel W (1991) Structure of the naturally occurring sesquiterpene lactone 8-epiisolipidiol. *Acta Crystallogr C* 47:129–132
- Shekhani MS, Shah PM, Yasmin A et al (1990) An immunostimulant sesquiterpene glycoside from *Sphaeranthus indicus*. *Phytochemistry* 29:2573–2576
- Shekhani MS, Shah PM, Khan KM et al (1991) New eudesmanolides from *Sphaeranthus indicus*. *J Nat Prod* 54:882–885
- Shi Z-R, Zhang X-Y, Zeng R-T et al (2016) Sesquiterpenoids from *Ainsliaea spicata* and their cytotoxic and NO production inhibitory activities. *Phytochem Lett* 18:87–94
- Sosa VE, Oberti JC, Prasad JS et al (1984) Flavonoids and eupahakonenin B from *Stevia sature-iaefolia*. *Phytochemistry* 23(7):1515–1516
- Stefani R, Schorr K, Tureta JM et al (2006) Sesquiterpene lactones from *Dimerostemma* species (Asteraceae) and *in vitro* potential anti-inflammatory activities. *Z Naturforsch C* 61(9–10):647–652
- Sülsen V (2009) Ph.D. thesis, University of Buenos Aires
- Sülsen V, Cazorla S, Frank F et al (2013) Natural terpenoids from *Ambrosia* species are active *in vitro* and *in vivo* against human pathogenic trypanosomatids. *PLoS Negl Trop Dis* 7(10):e2494
- Tsai L, Highet RJ, Herz W (1969) The mass spectra of pseudoguaianolides related to helenalin. *J Org Chem* 34(4):945–948
- Yang YJ, Yao J, Jin XJ et al (2016) Sesquiterpenoids and tirucallane triterpenoids from the roots of *Scorzonera divaricate*. *Phytochemistry* 124:86–98
- Yoshioka H, Mabry J, Timmermann BN (1973) Sesquiterpene lactones: chemistry, NMR and plant distribution. University of Tokyo Press, Tokyo

**Part II**  
**Biological Activities of Sesquiterpene**  
**Lactones**

# Chapter 8

## Antitrypanosomal and Antileishmanial Activities



Andrés Sánchez Alberti, Natacha Cerny, Augusto Bivona,  
and Silvia I. Cazorla

**Abstract** The so-called neglected tropical diseases, which are endemic in 149 tropical and subtropical countries, affect more than 1 billion people annually, including 875 million children in developing economies. These diseases are responsible for over 500,000 deaths per year and are characterized by long-term disability and severe pain. Neglected tropical diseases include Chagas' disease, human African trypanosomiasis, and leishmaniasis, among others. The current chemotherapeutic treatments are clearly out-of-date and inadequate because of the toxic effects, the generation of resistance, and frequent inefficacy and because the route and long-term schedules of administration are not adapted to the field conditions. Taken these drawbacks into account, the search for active compounds that provide the basis for the development of new therapies capable of generating curing against *T. cruzi* and *Leishmania* spp. infections is highly desirable.

Natural products are an increasing source of new drugs. In recent decades, the Asteraceae family has been extensively studied due to the large number and variety of active compounds that can be extracted from each species. Among them, sesquiterpene lactones are characteristic phytochemicals within this family. The antiprotozoal activity against *Trypanosoma cruzi*, *Leishmania* spp., and *Plasmodium* spp. has been reported for these compounds, making them interesting leads for future drug design.

---

A. S. Alberti · N. Cerny · A. Bivona  
Cátedra de Inmunología, IDEHU (UBA-CONICET), Facultad de Farmacia y Bioquímica,  
Universidad de Buenos Aires, Buenos Aires, Argentina

Instituto de Microbiología y Parasitología Médica, IMPaM (UBA-CONICET), Facultad de  
Medicina, Universidad de Buenos Aires, Buenos Aires, Argentina

S. I. Cazorla (✉)  
Laboratorio de Inmunología, Centro de Referencia para Lactobacilos (CERELA-CONICET),  
Tucumán, Argentina

Instituto de Microbiología y Parasitología Médica, IMPaM (UBA-CONICET), Facultad de  
Medicina, Universidad de Buenos Aires, Buenos Aires, Argentina  
e-mail: [scazorla@cerela.org.ar](mailto:scazorla@cerela.org.ar)

**Keywords** *Trypanosoma cruzi* · *Trypanosoma brucei* · *Leishmania* spp. · Sesquiterpene lactones · Neglected tropical diseases · Chemotherapy · Active compounds · Natural products

## 8.1 Introduction to Neglected Tropical Diseases

Parasitic diseases caused by protozoa, such as Chagas' disease, leishmaniasis, sleeping illness, and malaria, are considered neglected tropical diseases (NTDs), a diverse group of communicable diseases that occur in tropical and subtropical areas (WHO 2017a). Nevertheless, nowadays, NTDs are reported to be present everywhere, affecting more than one billion people and costing billions of dollars each year (WHO 2017b). The real health impact of NTDs may be underestimated due to the fact that many NTD infections are asymptomatic and are associated with longer incubation periods (Fenwick 2012). Children suffer the most devastating symptoms, which include malnutrition, cognitive impairment, stunted growth, and inability to attend school, while infection in adults can result in social isolation as well as inability to work (Cheuka et al. 2016). Poverty, illiteracy, negligent mentality, inadequate sanitation, climate conditions, high vector habitats density, and proximity of infected domestic animals are the main causes of NTDs.

Current clinically used drugs against NTDs are far from ideal, with unwanted physiological effects, such as nausea, vomiting, and disorders of the digestive tract (Castro et al. 2006; Sundar and Chakravarty 2013). Moreover, some anti-NTD drugs are known to cause teratogenesis and organ damage (Srivastava et al. 2016). For example, for the treatment of Chagas' disease, benznidazole and nifurtimox cannot be administered neither to pregnant women nor to patients with hepatic and renal insufficiency. For the treatment of malaria, the use of quinine, along with clindamycin, is restricted in the first trimester of pregnancy, while artemisinin-based combination therapies are recommended during the second and third trimesters (Manyando et al. 2012). Besides the low effectivity of nifurtimox and benznidazole in the chronic phase of *Trypanosoma cruzi* infection, the increase in the number of cases of resistance and the high risk of death entailed by the use of melarsoprol, an arsenic derivative for treating the chronic phase of human African trypanosomiasis, are some examples of the limitations of some chemotherapies currently used for NTDs.

Other limitations associated with current chemotherapeutic agents include the widespread drug resistance (Sundar and Chakravarty 2013; Barros de Alencar et al. 2017), lengthy treatment duration, and complicated drug administration procedures which may be a challenge in the resource-poor communities affected by the NTDs (Pink et al. 2005).

The discovery and development of drugs for NTDs are faced with a number of challenges (Paucar et al. 2016; Molyneux et al. 2017). Firstly, the investment in these therapeutic areas by major pharmaceutical companies is not financially attractive, owing to the prospect of poor financial returns (Pink et al. 2005). An ideal NTD drug should have availability, affordability, more parasiticidal than static potential, ability to scavenge the organism without harming of host's cells, and rapid action onset. However, finding a biochemical or chemical agent that acts as a

drug devoid of toxic effects is almost utopic. Plant-based drugs are of great interest as alternative medications, since they are believed to be devoid of such side effects.

Natural products and their derivatives are potential leads for new therapies against NTDs. We want to highlight the immense therapeutic potential that remains untapped in natural product-derived compounds. Although different classes of metabolites have demonstrated comparable and, in some cases, superior potency along with better toxicity profiles, as compared to standard drugs, none of the promising leads have been assessed in clinical trials. Some natural product compounds could provide templates for further medicinal chemistry optimization programs.

One of the most studied plant families in the natural products research field is the Asteraceae (formerly known as Compositae). Asteraceae is the largest family of flowering plants that are present in every continent, principally in the New World (Herrera Acevedo et al. 2017). Some molecules found in this family have been successfully used in humans against parasite diseases, such as artemisinin, an antimalarial sesquiterpene lactone (STL), the discovery of which led to the 2015 Nobel Prize for Medicine and Physiology (Nobel Prize 2015).

Artemisinin, which has the most rapid action against the malaria caused by *Plasmodium falciparum*, opened the panorama of research into new therapeutics for leishmaniasis, trypanosomiasis, and schistosomiasis. Several studies have demonstrated the great potential of STLs as alternatives to the current chemotherapy agents employed against NTDs and the relationship between the antiprotozoal activities with their chemical structure.

STLs are secondary metabolites characteristic of the Asteraceae family which have shown in vitro and in vivo activity, and some promising molecules have emerged from these studies.

## 8.2 Chagas' Disease and Antitrypanosomal Activities of Sesquiterpene Lactones

Chagas' disease (CD), which is caused by the protozoan *Trypanosoma cruzi*, is the parasitic disease with the highest impact in the Americas, affecting about seven million people, mainly in the poorest regions of Central and South America (da Silva et al. 2017). Traditionally associated to endemic countries, the epidemiology of CD is changing with an increase in the number of cases in non-endemic countries, mainly, due to human immigration and relocation of vectors. It is also noteworthy that some reactivation of infections mainly appears due to *T. cruzi*-HIV coinfections (Teixeira et al. 2011). This underscores the global impact of the disease as well as the urgent need for the development of new antitrypanosomal agents with lower toxicity and higher activity, particularly for the chronic phase of the disease (Izumi et al. 2011; Veiga-Santos et al. 2015; Sánchez and Ramírez 2013).

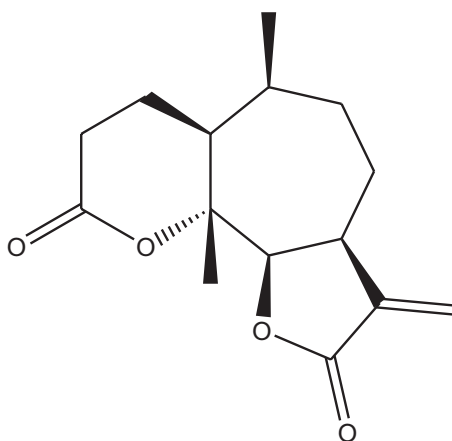
*Trypanosoma cruzi* infection involves different forms and hosts along its life cycle. *T. cruzi* presents an indirect life cycle involving mammals as definitive hosts. In these hosts, the parasite develops in two forms: the circulating non-replicative trypomastigotes and the intracellular replicative amastigotes. CD is mainly trans-

mitted by Reduviidae hematophagous insects that, upon feeding on an infected mammal, ingest blood trypomastigotes. In the insect's gut, trypomastigotes will transform into epimastigotes, which is the replicative extracellular form of the parasite (Jimenez et al. 2008). Trypomastigotes then differentiate into infective metacyclic trypomastigotes in the triatomine's hindgut and are deposited with the feces when the insect feeds on a vertebrate. These parasite forms enter the mammal body when the individual scratches the skin wound caused by the insect's bite or through permissive mucosa or conjunctive membranes, being able to invade almost any nucleated cell. Additionally, the parasite can be transmitted congenitally and orally by ingestion of parasite-contaminated food (Chatelain 2016; Coura 2015).

The main challenge of CD pharmacotherapy is the inability of anti-*T. cruzi* agents to reach infected cells and destroy the intracellular parasites, because the plasma membrane and complex microenvironment of the host's cells prevent the selective and massive delivery of drugs to the intracellular amastigote nests (Prokop and Davidson 2008). Thus, a drug or a drug delivery system that provides a high volume of distribution, long plasmatic half-life, and high efficacy in both the acute and the chronic phases of the infection is desirable (Branquinho et al. 2014).

*Trypanosoma cruzi* presents a variety of invasion and infection mechanisms and is able to parasitize different tissues and organs which have their own particular responses against the parasite. Therefore, treatment strategies should consider more than one therapeutic target. Probably, the success of future treatments for parasitic diseases lays on the combination of the conventional anti-parasitic drugs with other synthetic or natural compounds, which could modulate the immune response (Castillo et al. 2013; Molina-Berríos et al. 2013) or present a different mechanism of action. Therefore, a multidrug approach for the treatment of these NTDs could be more effective and better tolerated.

The trypanocidal activity of STLs has been demonstrated, both in vivo and in vitro, which makes them a promising guide for the design of novel trypanocidal agents (Muschiatti and Ulloa 2016). In this sense, Sülsen et al. (2011) have shown that psilostachyin C (**1**) isolated from *Ambrosia scabra* was active against the different stages of *T. cruzi*.



**psilostachyin C (1)**

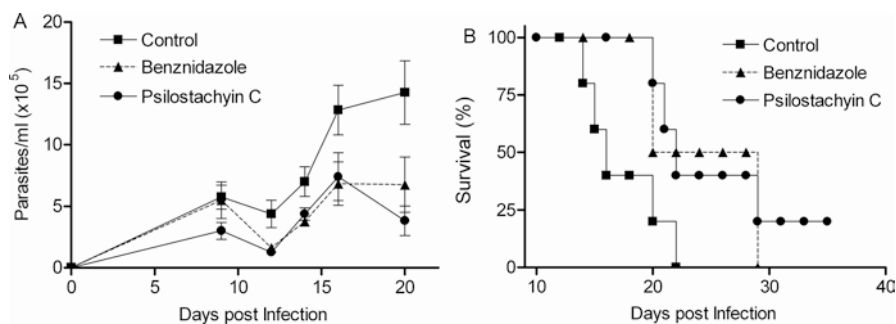
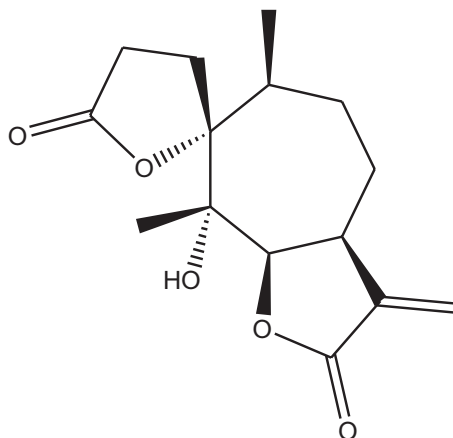


**Fig. 8.1** In vivo psilostachyin C trypanocidal activity. Parasitemia levels (a) and survival curves (b) during the acute infection

For this compound, parasite growth inhibitory concentration (50%,  $IC_{50}$ ) values of 0.6  $\mu\text{g/ml}$ , 3.5  $\mu\text{g/ml}$ , and 0.9  $\mu\text{g/ml}$  for epimastigotes, trypomastigotes, and amastigotes, respectively, were reported. Moreover, the cytotoxic concentration in mammal cells ( $CC_{50}$ ) for psilostachyin C was 87.5  $\mu\text{g/ml}$ , showing a good selectivity index (SI), which is used to compare the toxicity for mammalian cells and the activity against the parasites. In that work, the authors also observed a significant reduction in the number of circulating parasites in an in vivo experiment. Infected mice treated for 5 days with 1 mg/kg body weight/day of psilostachyin C showed a reduction of parasitemia levels with respect to the control group ( $7.4 \pm 1.2 \times 10^5$  parasites/ml vs.  $12.8 \pm 2.0 \times 10^5$  parasites/ml) (Fig. 8.1).

Recently, through bioassay-guided techniques performed on the organic extract of *Smilax sonchifolius*, the same group isolated new antitrypanosomal STLs. The authors isolated three active compounds against *T. cruzi* epimastigotes, enhydrin ( $IC_{50}$ , 0.84  $\mu\text{M}$ ), uvedalin ( $IC_{50}$ , 1.09  $\mu\text{M}$ ), and polymatin B ( $IC_{50}$ , 4.90  $\mu\text{M}$ ), of which, only the first two compounds presented activity against *T. cruzi* trypomastigotes ( $IC_{50}$ , 33.4  $\mu\text{M}$  and 25.0  $\mu\text{M}$ , respectively) (Frank et al. 2013). Employing the same methodology, peruvín and psilostachyin (2) were tested against *T. cruzi* epimastigotes, obtaining low values of  $IC_{50}$  (6.2  $\mu\text{M}$  and 4.4  $\mu\text{M}$ , respectively), where psilostachyin was more active on trypomastigotes ( $IC_{50}$  of 2.7  $\mu\text{M}$ , as compared with 200  $\mu\text{M}$  obtained by peruvín) (Sülßen et al. 2008). Psilostachyin was then selected for in vivo testing. After a lethal challenge with *T. cruzi*, 100% of psilostachyin-treated mice survived and presented lower parasitemia levels than control mice.

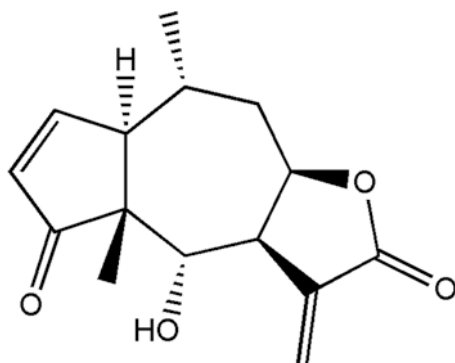




**psilostachyin (2)**

Against *T. cruzi*, the same authors also described an additive effect of two STLs with similar structures. These STLs have been reported to act on different targets. Psilostachyin, which is obtained from *Ambrosia tenuifolia*, interacts with hemin, while psilostachyin C, which is obtained from *Ambrosia scabra*, inhibits the synthesis of sterols. In these two cases, parasite death is caused by apoptosis after 4 h of treatment (Sülsen et al. 2016).

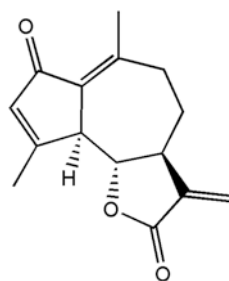
Schmidt et al. (2002) have described the anti-trypanocidal activities of helenanolate and eudesmanolate STL types. In an in vitro study, the authors found helenalin (3) as the most promising molecule they tested against *Trypanosoma brucei* and *Trypanosoma cruzi* (IC<sub>50</sub>, 0.051 and 0.695 μM, respectively). Besides, authors showed that bifunctional alkylants like helenin present a high selective toxicity towards the parasites, as compared to monofunctional STLs. This compound then also proved to be effective against the insect stage of the parasite (IC<sub>50</sub>, 1.9 μM), although this stage was less sensitive than the infective form (Jimenez-Ortiz et al. 2005). Interestingly, parasite DNA fragmentation and exposure of phosphatidylserine on the parasite's surface was observed upon treatment with helenalin or dehydroleucodine in both epimastigotes and trypomastigotes. The latter finding led the authors to propose that these STLs act by inducing programmed cell death (Jimenez et al. 2014). Considering that conventional anti-chagasic drugs present a different mechanism of action, a combination treatment between benznidazole and/or nifurtimox plus helenin was proposed as a novel approach against *T. cruzi* (Jimenez et al. 2014).



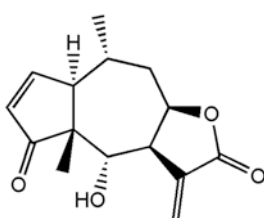
**helenalin (3)**

Guaianolide-type STL, are related to oxidative stress damage to the parasite. Among this type of STLs, 11,13-dehydrocompressanolide was isolated from *Tanacetum parthenium* (Cogo et al. 2012). This compound was effective against all *T. cruzi* stages (IC<sub>50</sub> for epimastigotes: 18.5 μM, IC<sub>50</sub> for amastigotes: 66.6 μM and IC<sub>50</sub> for trypomastigotes: 5.7 μM). The combination of this compound with benznidazole has also been studied, reporting a synergistic effect only for epimastigotes. More importantly, the authors have found a nearly additive effect between both compounds, against the infective form of *T. cruzi*.

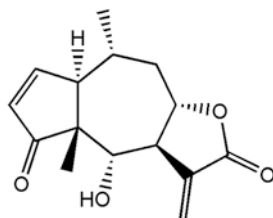
In 2012, Lozano et al. (2012) tested the effect of three other STLs, dehydroleucodine (4), helenalin (3), and mexicanin (5), and a diterpene (5-epi-icetexone) on the Y strain of *T. cruzi*. At 48 h of treatment, the number of amastigotes was lower than in control cells. This effect was observable at concentrations of 1.5–3.8 μM, which caused low cytotoxicity to host cells. Cultures treated with the compounds showed a decreased percentage of infected cells, and also a reduced release of trypomastigotes to the extracellular medium was observed. In all cases, helenalin was the most potent STL.



**dehydroleucodine (4)**



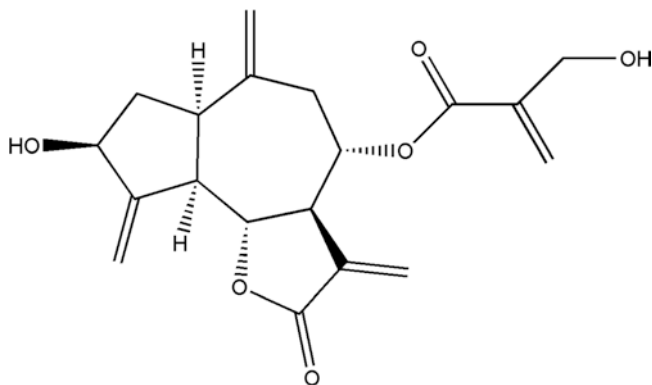
**helenalin (3)**



**mexicanin (5)**

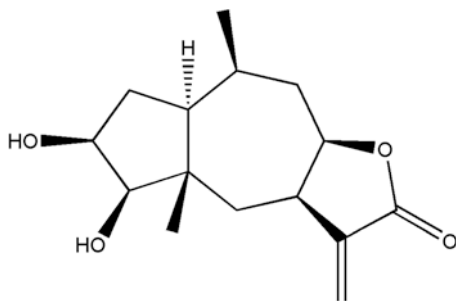
Even though cynaropicrin (6) displays activity toward salivary trypanosomas (African trypanosomiasis), the efficacy of this STL against stercorarian trypanoso-

mas (American trypanosomiasis) seems to be less promising (in vitro  $IC_{50}$ , 4.4  $\mu$ M) (Zimmermann et al. 2012). This finding was also confirmed later in in vivo studies, where cynaropicrin-treated mice failed to control *T. cruzi* infection during the acute phase (Da Silva et al. 2013).



**cynaropicrin (6)**

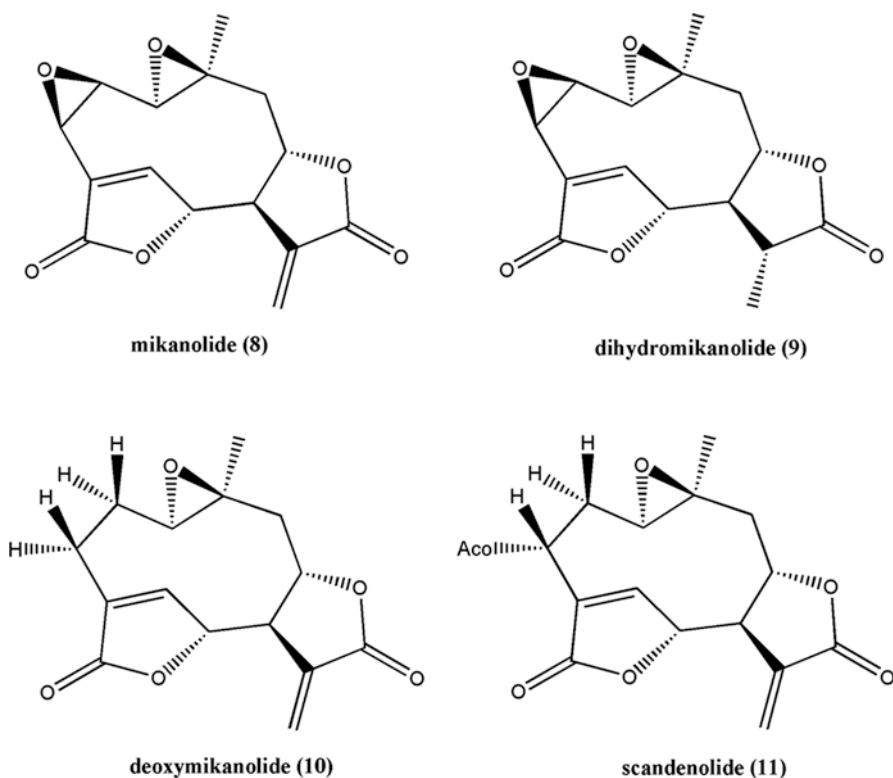
In 2013, Sülsen et al. isolated the STLs cumanin (7), psilostachyin, and cordilin. Cumanin and cordilin were found to be active against *Trypanosoma cruzi* epimastigotes showing  $IC_{50}$  values of 12 mM and 26 mM, respectively. Moreover, these compounds are active against bloodstream trypomastigotes, regardless of the *T. cruzi* strain (RA and K98) tested. Psilostachyin and cumanin were also active against amastigote forms, with  $IC_{50}$  values of 21 mM and 8 mM, respectively. Besides, the authors found that cumanin and psilostachyin exhibited an additive effect in their trypanocidal activity. In an in vivo model of *T. cruzi* infection, cumanin was more active than benznidazole, producing an eightfold reduction in parasitemia levels during the acute phase of the infection, as compared to the control group, and more importantly, a reduction in mortality, with 66% of the animals surviving, in comparison with 100% mortality in the control group.



**cumanin (7)**

The *in vitro* and *in vivo* activities against *T. cruzi* were evaluated for two STLs: psilostachyin A and cynaropicrin. Results showed that although these STLs presented quite considerable trypanocidal effects *in vitro*, with cynaropicrin being more effective than psilostachyin A, both STLs failed to control infections by Y and Colombian strains of *T. cruzi*. These data demonstrated that although cynaropicrin is a promising drug against African trypanosomes, this drug is not effective in acute mouse models of *T. cruzi* infection, when compared to benznidazole (da Silva et al. 2013).

Recently, the isolation of mikanolide (8), deoxymikanolide (9), dihydromikanolide (10), and scandenolide (11), by bioassay-guided fractionation, from *Mikania variifolia* and *Mikania micrantha* dichloromethane extracts has been achieved.



Mikanolide, deoxymikanolide, and dihydromikanolide were active against *T. cruzi* epimastigotes with  $IC_{50}$  values of 0.7  $\mu\text{g/ml}$ , 0.08  $\mu\text{g/ml}$ , and 2.5  $\mu\text{g/ml}$ , respectively. Mikanolide, deoxymikanolide, and dihydromikanolide were also active against the infective forms of the parasites, with  $IC_{50}$  values of 2.1, 1.5, and 0.3  $\mu\text{g/ml}$  for trypomastigotes and 4.5, 6.3, and 8.5  $\mu\text{g/ml}$  for amastigotes, respectively (Laurella et al. 2017). Moreover, the deoxymikanolide treatment decreased the parasitemia levels and the weight loss associated with the acute phase of the parasite infection. More importantly, while 100% of control mice died on day 22 post infection, 70% of deoxymikanolide-treated mice survived to a lethal *T. cruzi* infection (Fig. 8.2).

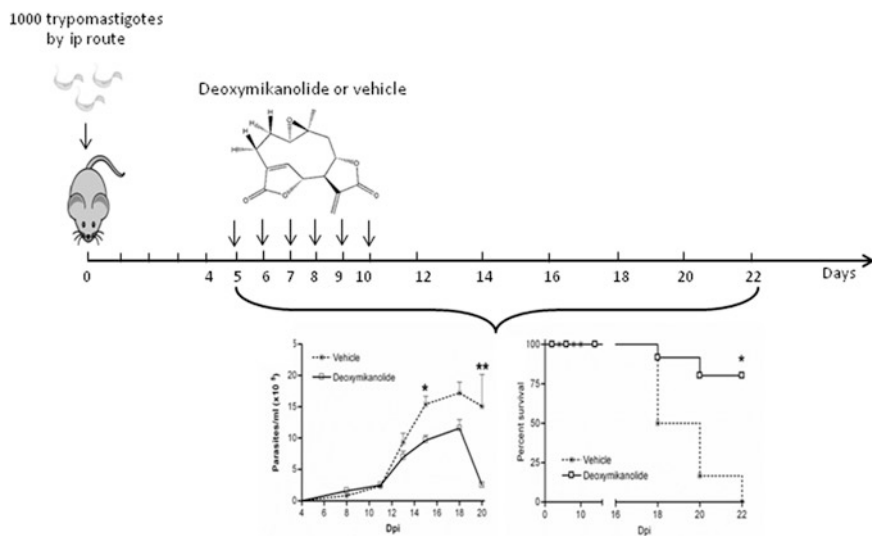


**Fig. 8.2** Treatment of *Trypanosoma cruzi*-infected mice with deoxymikanolide

Recently, the in vivo activity of a new drug, lychnopholide (LYC), was studied by Branquinho et al. (2014). LYC was loaded in nanocapsules (NC), and its effects were compared to those of free LYC and benznidazole against *T. cruzi*. Infected mice were treated in the acute phase with 2.0 mg/kg/day free LYC, LYC-poly- $\epsilon$ -caprolactone NC (LYC-PCL), and LYC-poly(lactic acid)-co-polyethylene glycol NC (LYC-PLA-PEG) or with 50 mg/kg/day benznidazole solution by the intravenous route. Animals infected with the CL strain, and treated 24 h after infection for 10 days, exhibited a 50% decrease of parasitemia when treated with LYC-PCL NC and 100% cure when treated with benznidazole. Nevertheless, 100% of the animals treated during the asymptomatic period for 20 days with these formulations or LYC-PLA-PEG NC were cured. Animals infected with the Y strain and treated 24 h after infection for 10 days by LYC-PCL NC were cured. Free LYC reduced the parasitemia and improved mice survival, but none of the mice was cured. LYC-loaded NC showed higher cure rates, reduced parasitemia, and increased survival when used in doses two to five times lower than those used for benznidazole. This study confirms that LYC can be a potential new treatment for Chagas' disease. Furthermore, the long half-life of PLA-PEG NC in the blood and its ability to improve LYC efficacy demonstrated that this formulation is more effective in reaching the parasite in vivo.

### 8.3 Leishmaniasis and Antileishmanial Activities of Sesquiterpene Lactones

Leishmaniasis is an anthroponotic and zoonotic disease caused by approximately 20 protozoan parasite species of the genus *Leishmania*, which are transmitted to humans by more than 30 different species of phlebotomine sandflies (Akhoundi et al. 2016). According to the clinical manifestations, the three main forms of leishmaniasis are cutaneous (CL), mucocutaneous (MCL), and visceral (VL) (Steverding 2017; Karimkhani et al. 2017). Visceral leishmaniasis or kala-azar is the most severe form of the disease, being fatal in the absence of treatment (Sundar and Rai 2002). There are reports indicating that even 5–10% of patients that are under medication die (Belo et al. 2014). About 12 million people are currently infected in 98 countries, approximately with 2 million new cases and 20,000–50,000 deaths each year (WHO 2017a; b).

*Leishmania major* and *L. tropica* are the primary cause of CL in the Old World, while *L. braziliensis* and *L. mexicana* are responsible for CL infection in the New World. MCL is principally caused by *L. braziliensis*, although other species (*L. amazonensis*, *L. panamensis*, and *L. guyanensis*) have also been described (Hoyos et al. 2016). In the Indian subcontinent, Asia, and East Africa, VL is caused by *L. donovani*, while *L. infantum* is responsible for infections in Europe, North Africa, and Latin America (Cheuka et al. 2016). The clinical outcome of the disease is influenced by the pathogenic species, as well as the state of the host's immunity. If the immune response has the capacity to fight the infection, the skin lesions associated with CL are often self-healing with concomitant development of lifelong resistance to reinfection (Sacks and Noben-Trauth 2002). In the case of immunity failure, the disease becomes chronic, with infection progressing to the reticuloendothelial system resulting in VL which is systemic and non-healing (Von Stebut and Udey 2004).

These parasites exhibit a heteroxenous life cycle, alternating between intracellular amastigotes in the mammalian host and flagellate promastigotes in the sandfly vector. Metacyclic promastigotes (the infective form) are introduced into the skin by the bite of the vector and taken up by mononuclear phagocytes, where they proliferate as non-flagellate amastigotes and remain in this stage for the duration of their life cycle in the mammalian. These stages can also be reproduced in liquid medium cultures, where the parasites show high invasiveness toward macrophages and fibroblasts.

For over five decades, the main treatment has consisted of pentavalent antimonial compounds, such as sodium stibogluconate and meglumine antimoniate, the efficacy of which is between 80% and 95% (Vasconcellos Ede et al. 2006). Other second-line antileishmanial chemotherapeutics include miltefosine (Prajapati et al. 2013). However, serious concerns of its teratogenicity may limit its use. The long half-life (152 h) of this compound could cause the emergence of drug resistance (Mukhopadhyay et al. 2011). A combination of pentavalent antimonials and paromomycin is also recommended, despite their significant side effects (Barrett and Croft 2012; Sundar and Chakravarty 2013). They are low-cost antileishmanial

drugs, easily available in endemic regions; however, resistance phenomena (Singh et al. 2016) and toxicity are observed in some regions in the case of long-term treatments (up to 28 days of parenteral administration) (Croft et al. 2003). Therefore, the search for new compounds is needed.

Several studies testing *in vitro* and *in vivo* activities of numerous STLs have been performed in the search for new compounds effective against VL. The STL 8-epixanthatin 1 $\beta$ ,5  $\beta$ -epoxide isolated from the Sudanese plant *Xanthium brasili-cum* is a terpenoid metabolite that has displayed noteworthy *in vitro* leishmanicidal potency against *L. donovani*, with an IC<sub>50</sub> value of 0.6  $\mu$ M and a minimal cytotoxicity on rat myoblast cells (Nour et al. 2009). Moreover, axenically cultured *L. donovani* amastigotes were incubated with three anthecotulide-type linear STLs, anthecotulide, 4-hydroxyanthecotulide, and 4-acetoxyanthecotulide isolated from *Anthemis auriculata*, and a significant antileishmanial activity was observed. However, these compounds cannot be considered as future drugs due to the high *in vitro* cytotoxic activity against mammalian L6 cells (Karioti et al. 2009).

Six germacranolide STLs were isolated from *Calea zacatechichi* and tested on *L. donovani*. Calealactone C and calein D were found to be active with IC<sub>50</sub> values of 1.9 and 2.2  $\mu$ M, respectively. More importantly, the values were similar to those obtained with the reference drug pentamidine (IC<sub>50</sub> 2.9  $\mu$ M) (Wu et al. 2011). Avolio et al. (2014) proposed inuloxin A, isolated from the aerial parts of *Inula viscosa*, as a promising new antileishmanial lead against *L. donovani* with an IC<sub>50</sub> of 6.9  $\mu$ g/ml, which is a value that is near the effective dose of pentamidine.

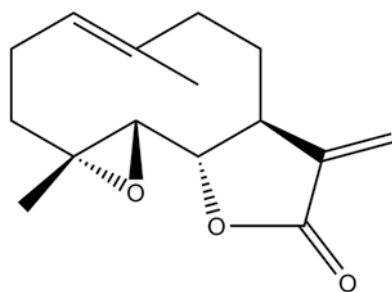
In other studies, the activity of seven hirsutinolide-type STLs isolated from *Pseudelephantopus spiralis* was studied against *L. infantum* expressing luciferase activity. Results showed that the hirsutinolides were more active against the intracellular stage of the parasite than against promastigotes, thus being adequate to prevent the intracellular replication of the parasites in the mammalian reservoir. Piptocarphins A displayed the strongest activity against the promastigotes and axenic amastigotes of *L. infantum*, with IC<sub>50</sub> values of 9.5 mM and 2.0 mM, respectively. These values are similar to the IC<sub>50</sub> of the reference drug miltefosine against promastigotes (8.8 mM). Unfortunately, these compounds were not selective, displaying cytotoxic effects toward macrophages (Girardi et al. 2015).

A dichloromethane extract of *Anthemis nobilis* flower cones has shown promising *in vitro* activity against *L. donovani*, with IC<sub>50</sub> values of  $1.40 \pm 0.07$   $\mu$ g/ml. A comprehensive profiling of the most active fractions afforded 19 STLs, including 15 germacranolides, 2 seco-sesquiterpenes, 1 guaianolide STL, and 1 cadinane acid. Several known STLs were identified as nobilin, 3-epi-nobilin, 8-methacrylate nobilin, hydroxyisonobilin, 1,10-epoxynobilin, and cadinane acid. A submicromolar activity was observed only against *L. donovani* after treatment with nobilinson A, guaianonobilin, and seconobilin A, but without suitable selectivity values (IC<sub>50</sub>, 0.38–0.81  $\mu$ M; SI, 3–7) (De Mieri et al. 2017).

Moreover, other authors such as Sülsen et al. (2008) are in the search of promising compounds against CL. By bioassay-guided fractionation, the authors found two STLs from *Ambrosia tenuifolia*, peruvin and psilostachyin, which displayed IC<sub>50</sub> values of 1.5  $\mu$ M and 0.4  $\mu$ M, respectively, for *L. mexicana* promastigotes, and

also have trypanocidal activity. Three STLs, isolated from plants native to the Cuyo Region (Argentina), were found to be active against *L. mexicana* promastigotes: helenalin (Hln) ( $IC_{50}$ , 1.9  $\mu$ M), dehydroleucodine (DhL) ( $IC_{50}$ , 3.8  $\mu$ M), and mexicanin I (Mxc) ( $IC_{50}$ , 1.9  $\mu$ M). These compounds also induced a significant reduction in the number of parasites per cell, interfering with parasite growth and being more effective than the reference drug ketoconazole used as control (Barrera et al. 2008). This effect was irreversible for Hln even after short periods of exposure (3 h), but it was partially reversible for Mxc and DhL, indicating that lactones can interfere rapidly with certain vital processes. However, an effect of DhL and Mxc was still observable 48 h after the removal of the compounds. These compounds remained effective against the parasites up to 72 h after preincubation in the STL-containing medium. Moreover, these compounds exhibited low cytotoxicity for mammalian cells. The authors suggested that these compounds can affect the parasite's life cycle, possibly through multiple mechanisms (Barrera et al. 2013).

Parthenolide (12) is a very common STL that is present in several species of the Asteraceae family. Tiuman et al. (2005) have purified this compound from the hydroalcoholic extract of the aerial parts of *Tanacetum parthenium* and reported its leishmanial activity against promastigotes ( $IC_{50}$ , 0.37  $\mu$ g/ml) and also against axenic and intracellular amastigotes of *L. amazonensis* ( $IC_{50}$  values of 1.3  $\mu$ M and 2.9  $\mu$ M, respectively). More importantly, parthenolide showed no cytotoxic effects against J774G8 macrophages and did not cause lysis of sheep red blood cell when it was used at higher concentrations than those that inhibited promastigote growth (Tiuman et al. 2005, 2014). The enzymatic activity of cysteine protease increased following the treatment of promastigotes with parthenolide (Tiuman et al. 2005). This compound inhibits interleukin-12 production in lipopolysaccharide-stimulated macrophages (Kang et al. 2001) and could inhibit the expression of intercellular adhesion molecule-1 (ICAM-1) induced by interleukin-1, tumor necrosis factor alpha, and, less strongly, gamma interferon (Piela-Smith and Liu 2001). The modulation of the molecular expression may be an additional mechanism by which feverfew mediates the anti-inflammatory effects.



**parthenolide (12)**

Recently, Rabito et al. (2014) have assessed the effect of the intramuscular injection of the STL-rich dichloromethane fraction of *Tanacetum parthenium* for 4 weeks



to find a significant reduction ( $p = 0.0010$ ) in the growth and size of footpad lesions in BALB/c mice infected with  $1 \times 10^7$  *L. amazonensis* metacyclic promastigotes. It should be borne in mind that the main STLs present in the dichloromethane fraction are parthenolide and 11,13-dehydrocompressanolide.

The organic and aqueous extracts of *Mikania micrantha*, *M. parodii*, *M. periplo-cifolia*, and *M. cordifolia* were tested on *L. braziliensis* promastigotes (Laurella et al. 2012). The bioassay-guided fractionation of *M. micrantha* organic extract led to the identification of two active fractions. The chromatographic profile and infrared analysis of these fractions revealed the presence of STLs. At a concentration of 100  $\mu\text{g/ml}$ , the organic extracts of *M. micrantha* and *M. parodii* displayed leishmanicidal activity with growth inhibition rates above 85%. At the lowest concentration tested (1  $\mu\text{g/ml}$ ), *M. micrantha* was the most active extract causing an inhibition of  $77.8 \pm 1.1\%$ .

The antileishmanial activities of an STL-rich preparation—a leaf rinse extract (LRE) from *Tithonia diversifolia*—was tested against the main causative agent of MCL. Results revealed that LRE is a rich source of potent leishmanicidal compounds, with an  $\text{IC}_{50}$  value of  $1.5 \pm 0.50$   $\mu\text{g/ml}$  against *L. braziliensis* promastigotes (H3227 MHOM/BR/94/H-3227) originally isolated from a human case of MCL in the state of Ceará, Brazil. Therefore, eight STLs from the LRE were initially assessed for their leishmanicidal activity against *L. braziliensis* promastigotes. One of them did not present any significant leishmanicidal effect ( $\text{IC}_{50} > 50$   $\mu\text{g/ml}$ ). Another STL had a cytotoxic effect on macrophages (4.5  $\mu\text{g/ml}$ ). Five leishmanicidal STLs with the highest level of selectivity were further evaluated against the intracellular parasites (amastigotes) using peritoneal macrophages. Tirofundin 3-*O*-methyl ether, tagitinin F, and a guaianolide were able to cause a significant reduction in the internalization of parasites after 48 h, as compared to the negative control ( $p < 0.05$ ) (de Toledo et al. 2014).

Sosa et al. (2016) have evaluated 17 STLs, isolated from five species of the tribe *Vernonieae*, for their in vitro activity against *L. amazonensis* and *L. braziliensis* promastigotes. As all these natural compounds were found to have potent to mild antileishmanial properties, a quantitative structure-activity relationship study has also been performed. The most active compounds against *L. braziliensis* were isodeoxyelephantopin and deoxyelephantopin, which bear two lactone rings in their structure, showing  $\text{IC}_{50}$  values 1.45  $\mu\text{M}$  and 1.34  $\mu\text{M}$ , respectively, followed by a goyazensolide natural derivative, showing an  $\text{IC}_{50}$  value of 1.60  $\mu\text{M}$  against *L. amazonensis*.

The efficacy of different STLs against *Leishmania* species causing both cutaneous and visceral forms has been reported. Two terpenoid metabolites, isoiguesterin and its analogue, 20-*epi*-isoiguesterinol, both isolated from *Salacia madagascariensis* (Celastraceae), have strong submicromolar leishmanicidal potency against both *L. donovani* and *L. mexicana* ( $\text{IC}_{50}$ , 0.20  $\mu\text{M}$  and 0.082  $\mu\text{M}$ , respectively) (Thiem et al. 2005).

The combination therapy with antileishmanial drugs is currently considered as one of the most rational approaches to lower the treatment failure rate and to limit the spreading of drug resistance phenomena (Gazanion et al. 2011; Mwololo et al.

2015). In that sense, Mutiso et al. (2011) have recently studied the in vitro and in vivo activities of diminazene (Dim), artesunate (Art), and the combination of Dim and Art (Dim-Art) against *L. donovani* strain NLB-065. The two drugs have been previously shown to be effective against different protozoan diseases (Macharia et al. 2004; Oliario et al. 2001). In vitro, the Dim-Art combination showed an  $IC_{50}$  value of  $2.28 \pm 0.24$   $\mu\text{g/ml}$ , while the values obtained for each compound were  $9.16 \pm 0.3$   $\mu\text{g/ml}$  and  $4.64 \pm 0.48$   $\mu\text{g/ml}$ , respectively. In that study the  $IC_{50}$  for amphotericin B was  $0.16 \pm 0.32$   $\mu\text{g/ml}$  against stationary phase promastigotes of *L. donovani* strain NLB-065. The in vivo evaluation in the *L. donovani* BALB/c mice model indicated that treatments with the combined drug therapy at doses of 12.5 mg/kg for 28 consecutive days induced a significant ( $p < 0.001$ ) reduction in the parasite burden in the spleen, as compared to the single drug treatments at the same dosages (Mutiso et al. 2011). The lack of complete elimination of parasites by neither the Dim-Art combined therapy nor amphotericin B may be attributed to the delayed beginning of treatments of infected mice. Furthermore, the treatment was administered when most of the mice presented severe symptoms of the disease. Besides, in cases of advanced disease, such treatment would have been efficient had it been administered for a longer period of time. Further studies are needed to determine the most suitable combination ratio of the two compounds. The survival rates of 100% obtained in the animals treated with artesunate, Dim-Art, or amphotericin B up to the end of the experimental period may be attributed to the significant reduction of the parasite load achieved by the administration of those compounds. Fifty percent of the animals treated with Dim, and over 80% of mice in the control group died before termination of the experiment. A parasite load of at least 130 parasites per 500 nucleated spleen cells was recorded in each animal that died from any of these two groups. No side effects attributable to the dosages employed were observed.

The discovery of a drug that can be applied for the treatment of both kinetoplastid infections could be an important solution, especially in Argentina, where endemic areas overlap and sometimes differential diagnoses between them are not possible by conventional serological techniques (Frank et al. 2003). In this sense, Sülsen et al. (2008) have reported for the first time the trypanocidal and leishmanicidal activities of two STLs, psilostachyin and peruvín, isolated by bioassay-guided fractionation of the organic extract of *Ambrosia tenuifolia* (Asteraceae). The inhibitory activity of psilostachyin and peruvín on *Leishmania* promastigotes was studied after 120 h by a [ $^3\text{H}$ ]-thymidine uptake assay. The  $IC_{50}$  values were 0.12 and 0.39  $\mu\text{g/ml}$  for psilostachyin and peruvín, respectively.

Sülsen et al. (2013) have also isolated the STL cumanin from *Ambrosia elatior*, whereas two other STLs, psilostachyin and cordilin, were isolated from *A. scabra*. Apart from the activity of these STL against *T. cruzi*, cumanin proved to have leishmanicidal activity with growth inhibition values greater than 80% at a concentration of 5 mg/ml (19 mM), against both *L. braziliensis* and *L. amazonensis* promastigotes. Together, these results suggest that psilostachyin, peruvín, and cumanin could be considered potential candidates for the development of new antiprotozoal agents against both Chagas' disease and leishmaniasis.

At present, improved methodologies and greater knowledge of the chemical structures of compounds permit rational drug design that may replace empirical screening. In addition, molecular techniques have allowed determining the complete DNA sequence of the parasites' genome, thus permitting the identification of possible targets for drug action. However, empirical screening should not be undervalued, since this methodology may also allow identifying new chemical structures effective against protozoa parasites as well as bacteria and viruses.

## 8.4 Human African Trypanosomiasis

Human African trypanosomiasis (HAT), also known as sleeping sickness, is caused by the protozoan parasites *Trypanosoma brucei rhodesiense* and *Trypanosoma brucei gambiense*. HAT impacts 70 million people living in 1.55 million km<sup>2</sup> of sub-Saharan Africa (Aksoy et al. 2017). Both protozoa are transmitted by tsetse fly species. Endemic areas do not overlap, with Uganda being the only country endemic for both forms, albeit in different areas of the country (Keating et al. 2015).

Humans are the main reservoir host for *T. b. gambiense*, while cattle or wild bovids serve as the main reservoir host for *T. b. rhodesiense*. Animal to human, animal to animal, and human to human transmission occur with *T. b. rhodesiense*. Transmission varies as a function of vector density and biting behavior. The disease normally affects remote rural communities where people are exposed to the bite of the tsetse fly during their daily outdoor activities.

Epidemic outbreaks can be devastating, substantially reducing productivity, with a mortality rate of almost 100% when the disease is untreated. Both parasites are initially found in the bloodstream, but after a period, they penetrate the central nervous system, giving rise to the worst and fatal manifestation of the disease. All current drugs to treat HAT are inadequate due to poor efficacy, detrimental side effects, and the requirement for parenteral administration, which is not appropriate for rural African settings. Drugs to treat the early-stage infection (pentamidine and suramin) are well tolerated, relatively easy to administer, and effective. However, the drugs used for the advanced disease (melarsoprol) and eflornithine, which is ineffective for the acute rhodesiense form, have to cross the blood brain barrier to exert the effect. These drugs are toxic (particularly melarsoprol), often causing severe and sometimes fatal side effects, and have to be administered under costly medical supervision.

Several natural products have been extensively tested for the treatment of sleeping illness. A dichloromethane extract of *Anthemis nobilis* flower cones has shown promising in vitro antiprotozoal activity against *L. donovani*, as mentioned above, and also against *Trypanosoma brucei rhodesiense* (IC<sub>50</sub>, 1.43 ± 0.50 µg/ml) (De Mieri et al. 2017). The authors identified several known STLs, among which, the furanoheliangolide derivative presented the highest in vitro potency and selectivity against *T. b. rhodesiense* bloodstream trypomastigotes (IC<sub>50</sub>, 0.08 ± 0.01 µM; SI,

63). These findings were in agreement with those reported by Schmidt et al. (2014), who identified a furanoheliangolide-type compound as the most active STL against *T. b. rhodesiense*. Unfortunately, the limited amount of furanonobilin that could be isolated precluded an in vivo study.

In the course of a larger screening study of 1800 plant and fungal extracts, Julianti et al. (2011) have reported that the ethyl acetate extract of *Saussurea costus* roots potently inhibited the growth of *T. b. rhodesiense*. The subsequent HPLC-based activity profiling led to the identification of the STLs arbusculin B,  $\alpha$ -cyclocostunolide, costunolide, and dehydrocostuslactone. These compounds were tested for in vitro antitrypanosomal activity and cytotoxicity, to find values of  $IC_{50}$  ranging from 0.8 to 22  $\mu$ M,  $CC_{50}$  values ranging from 1.6 to 19  $\mu$ M, and SI values ranging from 0.5 to 6.5.

Gökbulut et al. (2012) have identified two STLs from the flowering aerial parts of *Inula montbretiana*, 9  $\beta$ -(3',4'-epoxy-3'-methylpentanoyloxy)-parthenolide and 9  $\beta$ -(3'-oxo-2'-methylbutanoyloxy)-parthenolide, as the most active constituent against *T. b. rhodesiense* ( $IC_{50}$ : 0.26  $\mu$ g/ml) and with low cytotoxic activity ( $SI \cong 9$ ) against rat skeletal myoblasts (L6 cell line).

In another study, the STL deoxyelephantopin, isolated by ethyl acetate partition from the *Elephantopus scaber* Linn methanolic extract, showed an  $IC_{50}$  value of 0.070  $\mu$ M against *T. b. rhodesiense*. This compound presented the highest activity value out of 70 extracts screened from Malaysian plants (Zahari et al. 2014). The antiprotozoal principle, which was isolated from the ethyl acetate partition through a solvent fractionation and crystallization process, was identified as deoxyelephantopin.

The effectiveness of STLs against trypanosomatid infections is reinforced by the study carried out by Zimmermann et al. (2012), who screened 1800 plant and fungal extract libraries with antiprotozoal activity. Through an HPLC-based activity profiling approach, cynaropicrin was identified as the first natural plant product effective against *T. brucei* in vitro ( $IC_{50}$ , 0.2  $\mu$ M). Besides, a significant reduction in the parasitemia was observed upon cynaropicrin treatment in an acute mouse model of African trypanosomiasis (pentamidine and melarsoprol). This finding indicates that cynaropicrin is a promising candidate against this infection. Sato et al. (2015) have described the synthesis of a cynaropicrin deuterated derivative by replacing the side chain of natural cynaropicrin. This achievement constitutes a potential contribution to the study of cynaropicrin as a lead molecule.

Two hundred and seven extracts were prepared from 60 plants from South Africa and screened in vitro for activity against *T. b. rhodesiense* (Mokoka et al. 2013). Among the most remarkable results are the activities found for *Psoralea pinnata* ( $IC_{50}$ , 0.15  $\mu$ g/ml), *Schkuhria pinnata* ( $IC_{50}$ , 2.04  $\mu$ g/ml), and *Vernonia mespilifolia* ( $IC_{50}$ , 1.01  $\mu$ g/ml) against *T. b. rhodesiense*. The HPLC-based activity profiling was used to identify the active constituents in the extracts, and the germacranolide STLs schkuhrin I and II from *S. pinnata* and cynaropicrin from *V. mespilifolia* were identified, with  $IC_{50}$  values of 0.9  $\mu$ M, 1.5  $\mu$ M, and 0.23  $\mu$ M, respectively.

## 8.5 Conclusion

All these studies have clearly demonstrated the great potential of STLs against NTDs. Since most of these biologically active compounds have been isolated from plants, natural products represent an important reservoir of leading molecules for the development of new therapeutics. Nowadays, plant products represent about half of the drugs in use. Besides, compounds of natural origin are feasible to be chemically improved either in terms of efficacy and selectivity or to achieve optimum pharmacokinetic and pharmacodynamic properties.

In addition, an interesting strategy is the development and identification of drug combinations, either of new or of existing compounds with different chemical structures, with the aim of reducing the side effects, duration of treatment, and therefore the risk of developing resistance.

## References

- Akhoundi M, Kuhls K, Cannet A et al (2016) A historical overview of the classification, evolution, and dispersion of *Leishmania* parasites and sandflies. *PLoS Negl Trop Dis* 10(3):e0004349. <https://doi.org/10.1371/journal.pntd.0004349>. Erratum in: *PLoS Negl Trop Dis* 10(6):e0004770
- Aksoy S, Buscher P, Lehane M et al (2017) Human African trypanosomiasis control: achievements and challenges. *PLoS Negl Trop Dis* 11(4):e0005454. <https://doi.org/10.1371/journal.pntd.0005454>
- Avolio F, Rimando AM, Cimmino A et al (2014) Inuloxins A-D and derivatives as antileishmanial agents: structure-activity relationship study. *J Antibiot* 67(8):597–601. <https://doi.org/10.1038/ja.2014.47>
- Barrera PA, Jimenez-Ortiz V, Tonn C et al (2008) Natural sesquiterpene lactones are active against *Leishmania mexicana*. *J Parasitol* 94(5):1143–1149. <https://doi.org/10.1645/GE-1501.1>
- Barrera P, Sülsen VP, Lozano E et al (2013) Natural sesquiterpene lactones induce oxidative stress in *Leishmania mexicana*. *Evid Based Complement Alternat Med* 163404. <https://doi.org/10.1155/2013/163404>
- Barrett MP, Croft SL (2012) Management of trypanosomiasis and leishmaniasis. *Br Med Bull* 104:175–196. <https://doi.org/10.1093/bmb/lds031>
- Barros de Alencar MV, de Castro E, Sousa JM et al (2017) Diterpenes as lead molecules against neglected tropical diseases. *Phytother Res* 31(2):175–201. <https://doi.org/10.1002/ptr.5749>
- Belo VS, Struchiner CJ, Barbosa DS et al (2014) Risk factors for adverse prognosis and death in American visceral leishmaniasis: a meta-analysis. *PLoS Negl Trop Dis* 8(7):e2982. <https://doi.org/10.1371/journal.pntd.0002982>
- Branquinho RT, Mosqueira VC, de Oliveira-Silva JC et al (2014) Sesquiterpene lactone in nanostructured parenteral dosage form is efficacious in experimental Chagas disease. *Antimicrob Agents Chemother* 58(4):2067–2075. <https://doi.org/10.1128/AAC.00617-13>
- Castillo C, Ramírez G, Valck C et al (2013) The interaction of classical complement component C1 with parasite and host calreticulin mediates *Trypanosoma cruzi* infection of human placenta. *PLoS Negl Trop Dis* 7(8):e2376. <https://doi.org/10.1371/journal.pntd.0002376>
- Castro JA, de Mecca MM, Bartel LC (2006) Toxic side effects of drugs used to treat Chagas' disease (American trypanosomiasis). *Hum Exp Toxicol* 25(8):471–479
- Chatelain E (2016) Chagas disease research and development: is there light at the end of the tunnel? *Comput Struct Biotechnol J* 15:98–103. <https://doi.org/10.1016/j.csbj.2016.12.002>

- Cheuka PM, Mayoka G, Mutai P et al (2016) The role of natural products in drug discovery and development against Neglected Tropical Diseases. *Molecules* 22(1). <https://doi.org/10.3390/molecules22010058>
- Cogo J, De Oliveira Caleare A, Ueda-Nakamura T et al (2012) Trypanocidal activity of guaianolide obtained from *Tanacetum Parthenium* (L.) Schultz-Bip. and its combinational effect with benznidazole. *Phytomedicine* 20(1):59–66. <https://doi.org/10.1016/j.phymed.2012.09.011>
- Coura JR (2015) The main sceneries of Chagas disease transmission. The vectors, blood and oral transmissions – a comprehensive review. *Mem Inst Oswaldo Cruz* 110(3):277–282. <https://doi.org/10.1590/0074-0276140362>
- Croft SL, Vivas L, Brooker S (2003) Recent advances in research and control of malaria, leishmaniasis, trypanosomiasis and schistosomiasis. *East Mediterr Health J* 9(4):518–533
- De Mieri M, Monteleone G, Ismajili I et al (2017) Antiprotozoal activity-based profiling of a dichloromethane extract from *Anthemis nobilis* flowers. *J Nat Prod* 80(2):459–470. <https://doi.org/10.1021/acs.jnatprod.6b00980>
- Fenwick A (2012) The global burden of neglected tropical diseases. *Public Health* 126(3):233–236. <https://doi.org/10.1016/j.puhe.2011.11.015>
- Frank FM, Fernández MM, Taranto NJ et al (2003) Characterization of human infection by *Leishmania spp.* in the Northwest of Argentina: immune response, double infection with *Trypanosoma cruzi* and species of *Leishmania* involved. *Parasitology* 126(Pt 1):31–39
- Frank FM, Ulloa J, Cazorla SI et al (2013) Trypanocidal activity of *Smalanthus sonchifolius*: identification of active sesquiterpene lactones by bioassay-guided fractionation. *Evid Based Complement Alternat Med* 627898. <https://doi.org/10.1155/2013/627898>
- Gazanion E, Vergnes B, Seveno M et al (2011) *In vitro* activity of nicotinamide/antileishmanial drug combinations. *Parasitol Int* 60(1):19–24. <https://doi.org/10.1016/j.parint.2010.09.005>
- Girardi C, Fabre N, Paloque L et al (2015) Evaluation of antiplasmodial and antileishmanial activities of herbal medicine *Pseudelephantopus spiralis* (Less.) Cronquist and isolated hirsutinolide-type sesquiterpenoids. *J Ethnopharmacol* 170:167–174. <https://doi.org/10.1016/j.jep.2015.05.014>
- Gökbulut A, Kaiser M, Brun R et al (2012) 9 $\beta$ -hydroxyparthenolide esters from *Inula montbretiana* and their antiprotozoal activity. *Planta Med* 78(3):225–229. <https://doi.org/10.1055/s-0031-1280371>
- Herrera Acevedo C, Scotti L, Feitosa Alves M et al (2017) Computer-aided drug design using sesquiterpene lactones as sources of new structures with potential activity against Infectious Neglected Diseases. *Molecules* 22(1):79. <https://doi.org/10.3390/molecules22010079>
- Hoyos CL, Cajal SP, Juarez M et al (2016) Epidemiology of American Tegumentary Leishmaniasis and *Trypanosoma cruzi* infection in the Northwestern Argentina. *Biomed Res Int* 2016:6456031
- Izumi E, Ueda-Nakamura T, Dias Filho BP et al (2011) Natural products and Chagas' disease: a review of plant compounds studied for activity against *Trypanosoma cruzi*. *Nat Prod Rep* 28(4):809–823. <https://doi.org/10.1039/c0np00069h>
- Jimenez V, Paredes R, Sosa MA et al (2008) Natural programmed cell death in *T. cruzi* epimastigotes maintained in axenic cultures. *J Cell Biochem* 105(3):688–698. <https://doi.org/10.1002/jcb.21864>
- Jimenez V, Kemmerling U, Paredes R et al (2014) Natural sesquiterpene lactones induce programmed cell death in *Trypanosoma Cruzi*: a new therapeutic target? *Phytomedicine* 21(11):1411–1418. <https://doi.org/10.1016/j.phymed.2014.06.005>
- Jimenez-Ortiz V, Brengio SD, Giordano O et al (2005) The Trypanocidal effect of Sesquiterpene lactones Helenalin and Mexicanin on cultured Epimastigotes. *J Parasitol* 91(1):170–174. <https://doi.org/10.1645/GE-3373>
- Julianti T, Hata Y, Zimmermann S et al (2011) Antitrypanosomal sesquiterpene lactones from *Saussurea costus*. *Fitoterapia* 82(7):955–959. <https://doi.org/10.1016/j.fitote.2011.05.010>
- Kang BY, Chung SW, Kim TS (2001) Inhibition of interleukin-12 production in lipopolysaccharide-activated mouse macrophages by parthenolide, a predominant sesquiterpene lactone in *Tanacetum parthenium*: involvement of nuclear factor-kappaB. *Immunol Lett* 77(3):159–166

- Karimkhani C, Wanga V, Naghavi P et al (2017) Global burden of cutaneous leishmaniasis. *Lancet Infect Dis* 17(3):264. [https://doi.org/10.1016/S1473-3099\(16\)30217-1](https://doi.org/10.1016/S1473-3099(16)30217-1)
- Karioti A, Skaltsa H, Kaiser M et al (2009) Trypanocidal, leishmanicidal and cytotoxic effects of anthecotulide-type linear sesquiterpene lactones from *Anthemis auriculata*. *Phytomedicine* 16(8):783–787. <https://doi.org/10.1016/j.phymed.2008.12.008>
- Keating J, Yukich JO, Sutherland CS et al (2015) Human African trypanosomiasis prevention, treatment and control costs: a systematic review. *Acta Trop* 150:4–13. <https://doi.org/10.1016/j.actatropica.2015.06.003>
- Laurella LC, Frank FM, Sarquiz A et al (2012) *In vitro* evaluation of antiprotozoal and antiviral activities of extracts from Argentinean *Mikania* species. *ScientificWorldJournal* 121253. <https://doi.org/10.1100/2012/121253>
- Laurella LC, Cerny N, Bivona AE et al (2017) Sesquiterpene lactones from *Mikania* species display *in vitro* activity against *Trypanosoma cruzi* and *Leishmania* sp. *PLoS Negl Trop Dis* 11(9):e0005929. <https://doi.org/10.1371/journal.pntd.0005929>
- Lozano E, Barrera P, Salinas R et al (2012) Sesquiterpene lactones and the diterpene 5-epi-icetexone affect the intracellular and extracellular stages of *Trypanosoma cruzi*. *Parasitol Int* 61(4):628–633. <https://doi.org/10.1016/j.parint.2012.06.005>
- Macharia JC, Bourdichon AJ, Gicheru MM (2004) Efficacy of Trypan: a diminazene based drug as antileishmanial agent. *Acta Trop* 92(3):267–272
- Manyando C, Kayentao K, D'Alessandro U et al (2012) A systematic review of the safety and efficacy of artemether-lumefantrine against uncomplicated *Plasmodium falciparum* malaria during pregnancy. *Malar J* 11:141. <https://doi.org/10.1186/1475-2875-11-141>
- Mokoka TA, Xolani PK, Zimmermann S et al (2013) Antiprotozoal screening of 60 south African plants, and the identification of the antitrypanosomal germacranolides schkuhrin I and II. *Planta Med* 79(14):1380–1384. <https://doi.org/10.1055/s-0033-1350691>
- Molina-Berrios A, Campos-Estrada C, Henriquez N et al (2013) Protective role of acetylsalicylic acid in experimental *Trypanosoma cruzi* infection: evidence of a 15-epi-lipoxin A<sub>4</sub>-mediated effect. *PLoS Negl Trop Dis* 7(4):e2173. <https://doi.org/10.1371/journal.pntd.0002173>
- Molyneux D, Savioli L, Engels D (2017) Neglected tropical diseases: progress towards addressing the chronic pandemic. *Lancet* 389(10066):312–325. [https://doi.org/10.1016/S0140-6736\(16\)30171-4](https://doi.org/10.1016/S0140-6736(16)30171-4)
- Mukhopadhyay R, Mukherjee S, Mukherjee B et al (2011) Characterisation of antimony-resistant *Leishmania donovani* isolates: biochemical and biophysical studies and interaction with host cells. *Int J Parasitol* 41(13–14):1311–1321. <https://doi.org/10.1016/j.ijpara.2011.07.013>
- Muschietti L, Ulloa J (2016) Natural sesquiterpene lactones as potential trypanocidal therapeutic agents: a review. *Nat Prod Comm* 11(10):1569–1578
- Mutiso JM, Macharia JC, Barasa M et al (2011) *In vitro* and *in vivo* antileishmanial efficacy of a combination therapy of diminazene and artesunate against *Leishmania donovani* in BALB/c mice. *Rev Inst Med Trop Sao Paulo* 53(3):129–132
- Mwololo SW, Mutiso JM, Macharia JC et al (2015) *In vitro* activity and *in vivo* efficacy of a combination therapy of diminazene and chloroquine against murine visceral leishmaniasis. *J Biomed Res* 29(3):214–223. <https://doi.org/10.7555/JBR.29.20140072>
- Nobel Prize (2015). <https://www.nobelprize.org/nobelprizes/medicine/laureates/2015/press.html>. Accessed 30 Jul 2017
- Nour AM, Khalid SA, Kaiser M et al (2009) The antiprotozoal activity of sixteen asteraceae species native to Sudan and bioactivity-guided isolation of xanthanolides from *Xanthium brasili-cum*. *Planta Med* 75(12):1363–1368. <https://doi.org/10.1055/s-0029-1185676>
- Olliaro PL, Nair NK, Sathasivam K et al (2001) Pharmacokinetics of artesunate after single oral administration to rats. *BMC Pharmacol* 1:12
- Paucar R, Moreno-Viguri E, Pérez-Silanes S (2016) Challenges in Chagas disease drug discovery: a review. *Curr Med Chem* 23(28):3154–3170
- Piela-Smith TH, Liu X (2001) Feverfew extracts and the sesquiterpene lactone parthenolide inhibit intercellular adhesion molecule-1 expression in human synovial fibroblasts. *Cell Immunol* 209(2):89–96

- Pink R, Hudson A, Mouriès MA et al (2005) Opportunities and challenges in Antiparasitic drug discovery. *Nat Rev Drug Discov* 4:727–740
- Prajapati VK, Sharma S, Rai M et al (2013) *In vitro* susceptibility of *Leishmania donovani* to miltefosine in Indian visceral leishmaniasis. *Am J Trop Med Hyg* 89(4):750–754. <https://doi.org/10.4269/ajtmh.13-0096>
- Prokop A, Davidson JM (2008) Nanovehicular intracellular delivery systems. *J Pharm Sci* 97(9):3518–3590. <https://doi.org/10.1002/jps.21270>
- Rabito MF, Britta EA, Pelegrini BL et al (2014) *In vitro* and *in vivo* antileishmanial activity of sesquiterpene lactone-rich dichloromethane fraction obtained from *Tanacetum parthenium* (*L.*) *Schultz-Bip.* *Exp Parasitol* 143:18–23. <https://doi.org/10.1016/j.exppara.2014.04.014>
- Sacks D, Noben-Trauth N (2002) The immunology of susceptibility and resistance to *Leishmania major* in mice. *Nat Rev Immuno* 2(11):845–858
- Sánchez LV, Ramírez JD (2013) Congenital and oral transmission of American trypanosomiasis: an overview of physiopathogenic aspect. *Parasitology* 140(2):147–159. <https://doi.org/10.1017/S0031182012001394>
- Sato T, Hara S, Sato M et al (2015) Synthesis of cynaropicrin-d(4). *Bioorg Med Chem Lett* 25(23):5504–5507. <https://doi.org/10.1016/j.bmcl.2015.10.065>
- Schmidt TJ, Brun R, Willuhn G et al (2002) Anti-Trypanosomal activity of Helenalin and some structurally related Sesquiterpene lactones. *Planta Med* 68(8):750–751. <https://doi.org/10.1055/s-2002-33799>
- Schmidt TJ, Da Costa FB, Lopes NP et al (2014) *In Silico* prediction and experimental evaluation of furanohelianiogolide sesquiterpene lactones as potent agents against *Trypanosoma brucei rhodesiense*. *Antimicrob Agents Chemother* 58(1):325–332. <https://doi.org/10.1128/AAC.01263-13>
- da Silva CF, Batista Dda G, De Araújo JS et al (2013) Activities of psilostachyin A and cynaropicrin against *Trypanosoma cruzi* *in vitro* and *in vivo*. *Antimicrob Agents Chemother* 57(11):5307–5314. <https://doi.org/10.1128/AAC.00595-13>
- da Silva EB, Oliveira E, Silva DA, Oliveira AR et al (2017) Design and synthesis of potent anti-*Trypanosoma cruzi* agents new thiazoles derivatives which induce apoptotic parasite death. *Eur J Med Chem* 130:39–50. <https://doi.org/10.1016/j.ejmech.2017.02.026>
- Singh OP, Singh B, Chakravarty J et al (2016) Current challenges in treatment options for visceral leishmaniasis in India: a public health perspective. *Infect Dis Poverty* 5:19. <https://doi.org/10.1186/s40249-016-0112-2>
- Sosa AM, Amaya S, Salamanca Capusiri E et al (2016) Active sesquiterpene lactones against *Leishmania amazonensis* and *Leishmania braziliensis*. *Nat Prod Res* 12:1–5
- Srivastava S, Shankar P, Mishra J et al (2016) Possibilities and challenges for developing a successful vaccine for leishmaniasis. *Parasit Vectors* 9(1):277. <https://doi.org/10.1186/s13071-016-1553-y>
- von Stebut E, Udey MC (2004) Requirements for Th1-dependent immunity against infection with *Leishmania major*. *Microbes Infect* 6(12):1102–1109
- Steverding D (2017) The history of leishmaniasis. *Parasit Vectors* 10(1):82. <https://doi.org/10.1186/s13071-017-2028-5>
- Sülßen VP, Frank FM, Cazorla SI et al (2008) Trypanocidal and leishmanicidal activities of sesquiterpene lactones from *Ambrosia tenuifolia* Sprengel (*Asteraceae*). *Antimicrob Agents Chemother* 52(7):2415–2419. <https://doi.org/10.1128/AAC.01630-07>
- Sülßen VP, Frank FM, Cazorla SI et al (2011) Psilostachyin C: a natural compound with trypanocidal activity. *Int J Antimicrob Agents* 37(6):536–543. <https://doi.org/10.1016/j.ijantimicag.2011.02.003>
- Sülßen VP, Cazorla SI, Frank FM et al (2013) Natural terpenoids from *Ambrosia species* are active *in vitro* and *in vivo* against human pathogenic trypanosomatids. *PLoS Negl Trop Dis* 7(10):e2494. <https://doi.org/10.1371/journal.pntd.0002494>
- Sülßen VP, Puente V, Papademetrio D et al (2016) Mode of action of the Sesquiterpene lactones Psilostachyin and Psilostachyin C on *Trypanosoma cruzi*. *PLoS One* 11(3):e0150526. <https://doi.org/10.1371/journal.pone.0150526>



- Sundar S, Chakravarty J (2013) Leishmaniasis: an update of current pharmacotherapy. *Expert Opin Pharmacother* 14(1):53–63. <https://doi.org/10.1517/14656566.2013.755515>
- Sundar S, Rai M (2002) Advances in the treatment of leishmaniasis. *Curr Opin Infect Dis* 15(6):593–598
- Teixeira AR, Hecht MM, Guimaro MC et al (2011) Pathogenesis of Chagas' disease: parasite persistence and autoimmunity. *Clin Microbiol Rev* 24(3):592–630. <https://doi.org/10.1128/CMR.00063-10>
- Thiem DA, Sneden AT, Khan SI et al (2005) Bisorriterpenes from *Salacia madagascariensis*. *J Nat Prod* 68(2):251–254
- Tiuman TS, Ueda-Nakamura T, Garcia Cortez DA et al (2005) Antileishmanial activity of parthenolide, a sesquiterpene lactone isolated from *Tanacetum parthenium*. *Antimicrob Agents Chemother* 49(1):176–182
- Tiuman TS, Ueda-Nakamura T, Alonso A et al (2014) Cell death in amastigote forms of *Leishmania amazonensis* induced by parthenolide. *BMC Microbiol* 14:152. <https://doi.org/10.1186/1471-2180-14-152>
- de Toledo JS, Ambrósio SR, Borges CH et al (2014) *In vitro* leishmanicidal activities of sesquiterpene lactones from *Tithonia diversifolia* against *Leishmania braziliensis* promastigotes and amastigotes. *Molecules* 19(5):6070–6079. doi: <https://doi.org/10.3390/molecules19056070>
- Vasconcellos Ede C, Pimentel MI, Schubach Ade O et al (2006) Intralesional meglumine antimoniate for treatment of cutaneous leishmaniasis patients with contraindication to systemic therapy from Rio de Janeiro (2000 to 2006). *Am J Trop Med Hyg* 87(2):257–260
- Veiga-Santos P, Li K, Lameira L et al (2015) SQ109, a new drug lead for Chagas disease. *Antimicrob Agents Chemother* 59(4):1950–1961. <https://doi.org/10.1128/AAC.03972-14>
- World Health Organization (WHO) (2017a) Control of Neglected Tropical Diseases. [http://www.who.int/neglected\\_diseases/en/](http://www.who.int/neglected_diseases/en/). Accessed 31 July 2017
- World Health Organization (WHO) (2017b). Leishmaniasis. Fact sheet Updated April 2017. <http://www.who.int/mediacentre/factsheets/fs375/en/>. Accessed 31 July 2017
- Wu H, Fronczek FR, Burandt CL Jr et al (2011) Antileishmanial germacranolides from *Calea zacatechichi*. *Planta Med* 77(7):749–453. <https://doi.org/10.1055/s-0030-1250584>
- Zahari Z, Jani NA, Amanah A et al (2014) Bioassay-guided isolation of a sesquiterpene lactone of deoxyelephantopin from *Elephantopus scaber* Linn active on *Trypanosoma brucei rhodesiense*. *Phytomedicine* 21(3):282–285. <https://doi.org/10.1016/j.phymed.2013.09.011>
- Zimmermann S, Kaiser M, Brun R et al (2012) Cynaropicrin: the first plant natural product with *in vivo* activity against *Trypanosoma brucei*. *Planta Med* 78(6):553–556. <https://doi.org/10.1055/s-0031-1298241>

# Chapter 9

## Antiplasmodial Activity



**Nubia Boechat, Luiz Carlos da Silva Pinheiro,  
and Flavia Fernandes da Silveira**

**Abstract** According to the World Health Organization, malaria is one of the most serious public health problems globally. Malaria is a parasitic disease caused by protozoa of the genus *Plasmodium*, which are predominant in tropical and subtropical regions. Currently, the number of safe medications for this disease is limited, mainly due to the development of drug resistance. Combination therapy is recommended by the World Health Organization to either prevent or to delay the onset of resistance. Implementing projects in the medicinal chemistry area, which include organic chemistry and biological activity investigations, is essential for the discovery of new drugs. Sesquiterpene lactones have been demonstrated to be important antimalarial drugs. Artemisinin and its derivatives are some of the most widely used sesquiterpene lactone drugs and contain an endoperoxide bridge. Due to their antimalarial properties, several new sesquiterpene lactones have been tested in clinical trials and are being studied as a new class of antimalarial agents. The activity of sesquiterpene lactones is primarily attributed to the  $\alpha$ -methylene- $\gamma$ -lactone group that is present in their structure. Molecular hybridization is a strategy that is employed by medicinal chemists for the discovery of new drugs which involves combining pharmacophore fragments with a single hybrid molecule. Several synthetic hybrid sesquiterpene lactones have shown significant antiplasmodial activity. The aim of this work is to review antiplasmodial agents featuring a sesquiterpene lactone scaffold. Particularly, the sesquiterpene lactones that are currently being used or those that are still in the development process as well as those from natural or semisynthetic origins are highlighted.

---

N. Boechat (✉) · L. C. da Silva Pinheiro  
Fundação Oswaldo Cruz, Instituto de Tecnologia em Fármacos Farmanguinhos-Fiocruz,  
Rio de Janeiro, Brazil  
e-mail: [nubia.boechat@far.fiocruz.br](mailto:nubia.boechat@far.fiocruz.br)

F. F. da Silveira  
Fundação Oswaldo Cruz, Instituto de Tecnologia em Fármacos Farmanguinhos-Fiocruz,  
Rio de Janeiro, Brazil

Programa de Pós-graduação em Química da Universidade Federal do Rio de Janeiro,  
Rio de Janeiro, Brazil

**Keywords** Malaria · Artemisinin · Antiplasmodial activity · Drug resistance · Asteraceae · Sesquiterpene lactone · Hybrid · Clinical trials

## 9.1 Introduction

### 9.1.1 Malaria

Malaria is one of the most serious public health problems globally, with almost half of the world population being at risk of transmission. Estimated data provided by the World Health Organization (WHO) in 2016 show that 212 million malaria cases were detected worldwide, with 429,000 deaths, mainly among children under 5 years of age in African countries. Malaria is present in 91 countries, which are mainly in tropical and subtropical regions of the planet. However, and as a consequence of the globalization phenomenon, malaria has been drawing the attention of virtually all countries due to the increasing number of malaria cases in first-world countries (WHO 2016).

Malaria is a potentially serious infectious parasitic disease caused by protozoa of the genus *Plasmodium*, five species of which are responsible for human infections in humans, that is, *Plasmodium falciparum*, *P. vivax*, *P. malariae*, *P. ovale* and *P. knowlesi*. This parasite is transmitted by the bite of infected female mosquitoes of the genus *Anopheles* (Garcia 2010).

The life cycle of *Plasmodium* species is quite complex because it is divided into several phases occurring in two hosts: the mosquito and a vertebrate. The infection begins with the bite of an infected female *Anopheles* mosquito. While the mosquitoes are feeding, the salivary glands release sporozoites on the skin, which after invading the bloodstream, they quickly invade liver cells, initiating the infection. In the liver cells, sporozoites will undergo differentiation and multiply into thousands of merozoites that invade the erythrocytes and continue to multiply. The symptoms of malaria appear during the phase of merozoite multiplication. The duration of the erythrocytic stage will vary according to the species: 72 h for *P. malariae* and 48 h for *P. falciparum*, *P. vivax* and *P. ovale* (Midha et al. 2015).

Not all merozoites will reproduce asexually. Some of them develop into gametocytes (sex forms) that will be ingested by the female *Anopheles* mosquito during hematophagy, initiating the sexual cycle in the mosquito's stomach. The new sporozoites migrate to the mosquito's salivary glands, and their inoculation into a new human host perpetuates the *Plasmodium* life cycle. Some merozoites evolve into hypnozoites, a latent form of the parasite whose reactivation is responsible for disease relapses (malaria caused by *P. vivax* and *P. ovale*) (Coura 2013; Midha et al. 2015).

### 9.1.2 Current Chemotherapy for Malaria

The main measures to eliminate or reduce the number of cases of malaria are vector control, vaccine development, chemoprophylaxis and chemotherapy employing antimalarial drugs (Rappuoli and Aderem 2011).

Most antimalarials operate by mechanisms that target one or two phases of the parasite's life cycle (O'Neill et al. 2010). The treatment aims at killing the parasite during the evolutionary cycle, in other words, it interrupts the schizogony, which is the life cycle step that is responsible for the clinical manifestations of the infection. It also aims at destroying the parasite during the tissue cycle, in the case of *P. vivax* and *P. ovale*, thus avoiding relapse; and interrupting parasite transmission by preventing the development of the sexual forms of the parasite. To achieve these goals, several drugs are available, each of which has a specific mechanism of action (Baio 2011).

The antimalarial chemotherapy has been focused in finding a drug that is effective against *Plasmodium* strains that are resistant to conventional drugs. One possible way of lowering costs in antimalarial drug development is to test already known therapeutic agents (Seder et al. 2013; Raj et al. 2014; Teixeira et al. 2014).

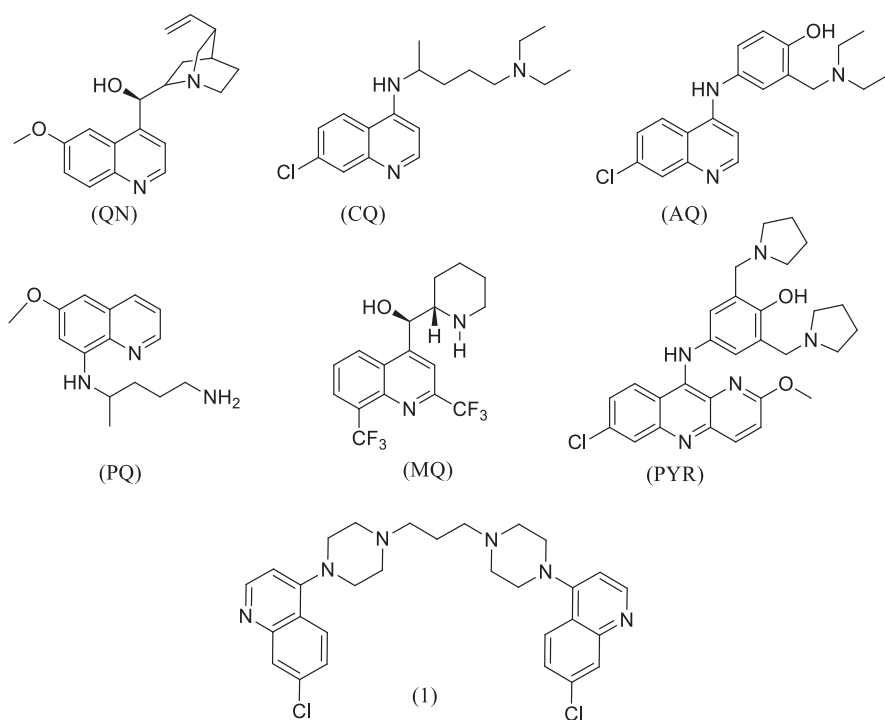


**Fig. 9.1** Quinoline derivatives used in the treatment of malaria

Antimalarial drugs are based on natural products, semisynthetic and synthetic compounds produced since the 1940s. Safe antimalarials fall into three main classes: quinoline derivatives (Fig. 9.1), antifolates (Fig. 9.2) and artemisinin derivatives (Fig. 9.3) (Leite et al. 2013).

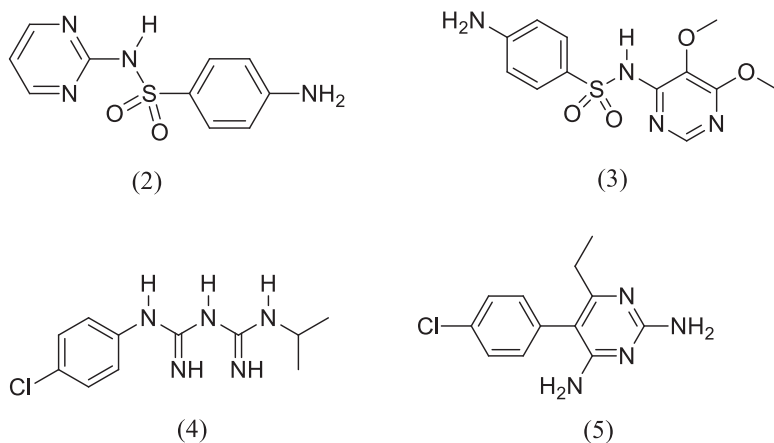


**Fig. 9.2** Antifolates used in the treatment of malaria

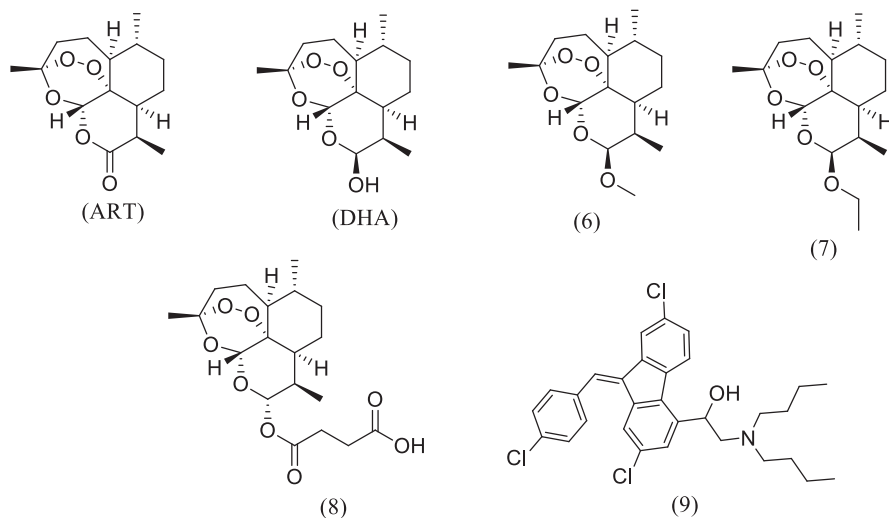


**Fig. 9.3** Artemisinic derivatives used in the treatment of malaria (ART, DHA, 6–8) and the structure of lumefantrine (9)

### 9.1.2.1 Quinoline Derivatives

Historically, quinolines are among the most widely used drugs for the treatment of malaria. Quinine (QN) (Fig. 9.1), which is an alkaloid isolated from *Cinchona* bark, was first used to treat malaria as early as the 1600s. The extraction of QN is still economically more feasible than its synthetic production (Achan et al. 2011). Due to the emergence of resistant *P. falciparum* strains and its high toxicity, its use has been reduced. However, other quinoline derivatives have been developed, such as chloroquine (CQ), amodiaquine (AQ), primaquine (PQ), mefloquine (MQ), pyronaridine (PYR) and piperazine (1) (Fig. 9.1) (Kaur et al. 2010).

Quinine, 4-aminoquinolines, 8-aminoquinolines and quinolinic alcohols are active compounds against the erythrocytic forms of *P. falciparum* and *P. vivax*. Among these, the most effective drug has been CQ, a 4-aminoquinoline employed since the early 1950s, when the WHO declared war against malaria. The employment of CQ has helped curing billions of clinical episodes, saving lives around the world. CQ is inexpensive and causes adverse effects that are tolerable, being considered safe for the treatment of pregnant women. For a long time, CQ has been the first treatment choice; however, its abusive use soon led to the emergence of CQ-resistant strains (CQR), making it ineffective in many parts of the world (Araujo et al. 2009; Cunico et al. 2008; Kaur et al. 2010).

The 8-aminoquinoline (PQ, Fig. 9.1), also inhibits the formation of gametocytes and is used against *P. vivax* and *P. ovale* hypnozoites. PQ acts against the slowly developing hepatic forms that are common in *P. vivax* that are responsible for relapses. MQ has been used in the fight against CQR *P. falciparum*; however, this drug is known to cause several side effects. Cases of resistance to MQ have also been reported (Teixeira 2011).

### 9.1.2.2 Antifolate Derivatives

Antifolates (Fig. 9.2) are a class of antimalarials that act as schizonticides in the blood. However, many of them are toxic to humans and have poor oral tolerance. They can also be used in the treatment of several other diseases, such as cancer (Gangjee et al. 2006). According to their mechanisms of action, the antifolates are divided into classes I and II: The sulfonamides sulfadiazine (2) and sulfadoxine (3) (Fig. 9.2) belong to the type I class of antifolates, which have structures that are similar to that of *p*-aminobenzoic acid (PABA) and which interrupt the formation of dihydrofolic acid by inhibiting dihydropteroate synthase (DHPS), which is necessary for the synthesis of nucleic acids. In the past, attempts were made to use DHPS inhibitors alone as antimalarial agents, but this strategy was abandoned because of its low efficacy and toxicity (Staines and Krishna 2012).

Proguanil (4) and pyrimethamine (5) belong to the type II class, which inhibit dihydrofolate reductase (DHFR) in the parasite, thus preventing the reduction of dihydrofolate (DHF) to tetrahydrofolate (THF), which is important in the synthesis of nucleic acids and amino acids. DHFR inhibitors are potent schizonticidal agents

that act on the asexual forms of the parasite (Gangjee et al. 2006). Compound **5** was initially synthesized as an anticancer drug and then identified as an antimalarial based on its structural similarity to **4**. It has been the most commonly used antifolate administered in combination with other faster acting drugs. However, the use of this class of drugs has been reduced due to the capacity of the parasites to develop resistance (Staines and Krishna 2012; Leite et al. 2013). Compound **4** was the first antifolate developed against malaria. It is a prodrug that is metabolized to cycloguanil, and its low toxicity is important for prophylaxis because it acts by destroying parasites during their passage into the bloodstream and before they invade red blood cells.

### 9.1.2.3 Artemisinin and Its Derivative Classes

Artemisinin (ART) is a sesquiterpene lactone natural product isolated for the first time in 1972 from a Chinese medicinal plant, *Artemisia annua* (an effective antimalarial herbaceous plant belonging to the Asteraceae family). ART was discovered by Youyou Tu, a Chinese scientist who was awarded half of the 2015 Nobel Prize in Medicine for her discovery. ART reduced the mortality rates of patients with malaria. This drug is widely used in the treatment of some types of fever and is indicated in cases of severe malaria. Since the discovery of the antimalarial activity of ART and its semisynthetic derivatives, these compounds have been used as first-line drugs in the treatment of malaria. (França et al. 2008; Barnett and Guy 2014; The Nobel Foundation 2015).

In 1979, ART was introduced into the rest of the world because of its potent antimalarial effect and uncommon chemical structure. There was considerable interest in exploring methods for its chemical synthesis. Thus ART was semisynthesized from artemisinic acid, while the total synthesis was achieved in 1983. Apart from malaria, the activity of ART against other parasites such as *Schistosoma* spp., *Leishmania* spp and *Toxoplasma gondii* has been reported. ART and its semisynthetic derivatives have other bioactivities, including antiviral and anticancer. It has also been considered a candidate to be used to reduce the coccidial load in chickens (Misra et al. 2014; Li and Zhou 2010)

The main sources of ART are field-grown leaves and flowering tops of *A. annua* from which the compound is isolated for commercialization. The search for increased productivity follows two approaches: (a) the search for new *Artemisia* species and (b) the development and application of new methods for genetic improvement. These approaches are based on the well-known high cost of ART synthesis. Several analytical methods have been developed for the detection and quantification of ART, such as high-performance liquid chromatography with UV or electrochemical detection, thin-layer chromatography, gas chromatography with mass spectrometric detection, and enzyme-linked immunosorbent assay, among others. However, sample preparation is time-consuming and are difficult to apply in routine analysis. Therefore, advanced methods for the extraction and determination

of ART have been evaluated, such as microwave-assisted extraction, supercritical fluid extraction (Misra et al. 2014).

There are simple and traditional techniques, including ancient Chinese methods, to produce artemisinin-rich extracts. These methods involve either soaking or pounding the fresh herb are more effective than the common ones used to prepare herbal teas from the dried herb. Even though the concentrations were up to 20-fold higher, the amount of total ART extracted by these ancient Chinese methods was much less than that extracted by the typical methods. Extracts showed potent in vitro activities against *P. falciparum*, but only the pounded juice contained the amount of ART necessary to eliminate parasitemia in *P. berghei*-infected mice (Wright et al. 2010).

Artemisinin and its derivatives, dihydroartemisinin (DHA), artemether (6), arteether (7) and artesunate (8) (Fig. 9.3), can rapidly reduce the number of parasites, killing them at an early stage of their development. However, they are poorly effective when employed as monotherapies for the treatment of malaria, due to their low bioavailability and short half-life. Additionally, resistance cases have been reported; thus, these drugs are indicated in artemisinin-based combination therapy (ACT) (WHO 2015a, 2015b).

The most important semisynthetic derivatives are artesunate (8) and the widely used artemether (6). The use of artesunate (8) is based on the rapidity with which it exerts its antimalarial effect, the low rate of resistance development and its solubility in water, which facilitates the development of formulations (Aquino 2010).

It is known that the endoperoxide bridge of these compounds can undergo reductive cleavage in the presence of the ferrous ions from the heme group of hemoglobin, generating free radicals that can either alkylate or modify the proteins of the parasite and cause its death (O'Neill et al. 2010). These drugs are blood schizonticides and act on the gametocytes, thus limiting transmission to other hosts and reducing the spread of resistant forms (Na-Bangchang and Karbwang 2009).

#### 9.1.2.4 Current Combination Chemotherapy in Malaria

In order to either prevent or minimize the occurrence of antimalarial resistance, the WHO recommends the use of combination therapies of at least two drugs. These combinations should act simultaneously through different mechanisms of action and in different biochemical targets of the parasite getting better results than monotherapy (WHO 2015a, 2015b).

All countries where *P. falciparum* is endemic have started to replace monotherapy with ACT, which includes the combination of a fast-acting ART derivative and a long-acting antimalarial with different modes of action. ART derivatives are used to treat uncomplicated malaria and are considered the pillars of the treatment of *P. falciparum* malaria. Due to the high potency and efficacy of ACT, many new pharmaceutical fixed-dose combination (FDC) formulations have been developed to treat this fatal parasitic disease (WHO 2015b).



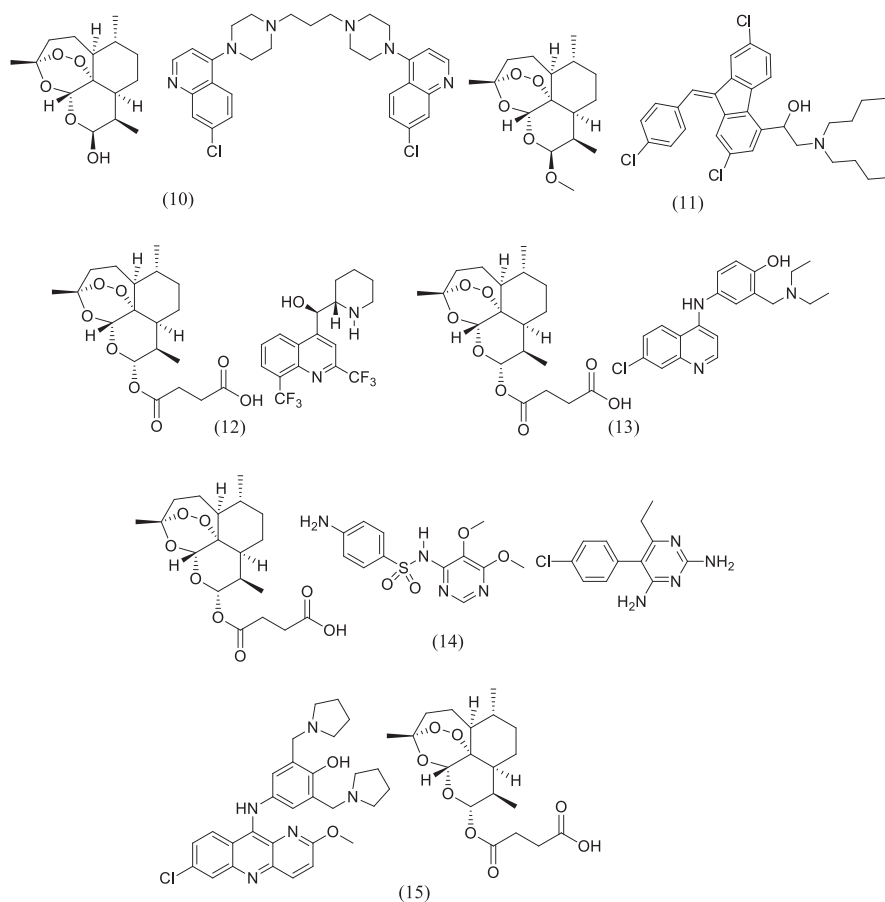


**Fig. 9.4** Sesquiterpene lactones used in combination chemotherapy to treat malaria

The ACTs employed for the treatment of malaria are (Fig. 9.4):

- Dihydroartemisinin (**DHA**) + piperazine (**1**) (**10**; Eurartesim®)
- Artemether (**6**) + lumefantrine (**9**) (**11**; Coartem®)
- Artesunate (**8**) + mefloquine (**MQ**) (**12**; ASMQ)
- Artesunate (**8**) + amodiaquine (**AQ**) (**13**; Winthrop® or Coarsucam™)
- Artesunate (**8**) + sulfadoxine (**3**) + pyrimethamine (**5**) (**14**)
- Pyronaridine (PYR) + artesunate (**8**) (**15**; Pyramax®), in development.

Mixed malaria infections are common in endemic areas. For example, patients infected with acute *P. vivax* can also have *P. falciparum* infections. In addition, acute *P. falciparum* infections can be followed by a presumed relapse of *P. vivax* malaria. The treatment of choice for these mixed infections is the ACT, as it is effective against all *Plasmodium* species (WHO 2015b).

Other combinations that do not include ART have been tested, for instance, sulfadoxine (**3**) + pyrimethamine (**5**) + AQ. This combination has been more effective than the constituent drugs used alone, but was less effective than the ACTs (WHO 2015b). However, the choice of drugs and doses for FDC therapy is a challenge, because of the differences in solubility, stability and pharmacokinetic profile of the drugs involved. In addition, clinical development is required, and drug-drug interactions can also result in toxic side effects (Srivastava and Lee 2015).

Eurartesim® (**10**) (Fig. 9.4) was developed by Sigma-Tau in partnership with Medicines for Malaria Venture (MMV) for the treatment of uncomplicated *P. falciparum* malaria in adults. A pediatric formulation of Eurartesim® for children over 5 kg is under study in a phase III clinical trial. In October 2011, the European Medicines Agency (EMA) granted marketing authorization for Eurartesim®. This formulation is administered once a day for 3 days, making it easier for patients to comply with the dosing. In addition, studies have shown that the half-life of this drug affords longer post-treatment protection. In 2015, Sigma-Tau signed an exclusive licensing agreement with Pierre Fabre to expand its ability to support country registration requirements and national adoption in 32 African countries. In October 2015, Eurartesim® was prequalified by the WHO, and a dossier for a hydrodispersible child-friendly formulation of the drug was submitted to the EMA. Through this prequalification process, the WHO assesses and approves the quality, safety and efficacy of the medicinal product (Valecha et al. 2010; Bassat et al. 2009; MMV. ORG 2017a).

DHA, the main active metabolite of Eurartesim®, reaches high concentrations in red blood cells infected with *P. falciparum*. The endoperoxide bridge of DHA is essential to its antimalarial activity, resulting in free radical damage to parasite membrane systems. The drug interferes with mitochondrial electron transport and parasite transport proteins, inhibits plasmodial sarco-endoplasmic reticulum calcium adenosine triphosphatase (SERCA), and disrupts parasite mitochondrial function. In an in vitro study in Uganda, the DHA IC<sub>50</sub> was <5 nmol/L for all sensitivities strains of *P. falciparum*. The second drug of formulation, piperazine (**1**), is a bisquinolone, and although its precise mechanism of action is unknown, it is thought to be similar to that of CQ, which is structurally similar. A study in Uganda demonstrated a mean IC<sub>50</sub> for piperazine of 6.1 nmol/l against clinical isolates of *P. falciparum*, with a maximum reported IC<sub>50</sub> of 46.2 nmol/l. Piperazine showed good in vitro activity against both chloroquine-sensitive (CQS) and CQR *P. falciparum* strains. The bulky bisquinoline structure of piperazine (**1**) is postulated to inhibit the transporter-mediated drug efflux. However, high rates of resistance to **1** have been reported in areas where it has been widely used as a monotherapy (EMA 2017b; Keating 2012). DHA is rapidly absorbed, with a time to C<sub>max</sub> (T<sub>max</sub>) of approximately 1–2 h. By contrast, **1** is slowly absorbed, with a T<sub>max</sub> of approximately 5 h. The bioavailability of DHA is increased in patients with malaria, possibly reflecting a reduced hepatic clearance in those patients. Eurartesim® is recommended to be administered in the fasting state because when administered with a high-fat/high-calorie meal, exposure to **1** was increased approximately three-fold, and DHA exposure was increased by 43%. The elimination half-life of DHA

is approximately 1 h, whereas for **1**, in adult patients with malaria, the elimination half-life of approximately 22 days. In pediatric patients, the elimination half-life of **1** is approximately 20 days. Compound **1** accumulates with repeated administration, reflecting its long elimination half-life (EMA 2017a; Nguyen et al. 2009).

Coartem® (**11**) (Fig. 9.4) is used to treat adults and children over 5 kg with uncomplicated *P. falciparum* infection, including mixed infections. Novartis and MMV have co-developed Coartem® Dispersible because children bear more than 70% of the burden of global malaria mortality and because drug metabolism and pharmacokinetics can differ between adults and children. Moreover, antimalarial tablets for adults are bitter and need to be broken up or crushed, making it difficult to give correct dosing and causing children to gag or spit out the medicine. Coartem® Dispersible is a sweet-tasting cherry-flavored tablet that disperses in a small amount of water. It is taken twice daily for 3 days. This formulation was the first prequalified child-friendly ACT and approved in over 50 endemic countries. Coartem® accounted for 73% of ACTs prescribed in 2013 (MMV.ORG 2017b; WHO 2014).

Artemether (**6**) has several proposed mechanisms of action, including interference with the plasmodial transport proteins and with mitochondrial electron transport and production of free radicals which lead to a reduction of blood levels of glutathione and other antioxidants. When used as monotherapy, artemether (**6**) has a relatively high recrudescence rate. The exact mechanism of action of lumefantrine is not well defined, but it is thought to inhibit the formation of  $\beta$ -hematin. Lumefantrine has a slower onset of action, resulting in a clearance of residual parasites and a decrease in the recrudescence rate. Lumefantrine serum concentrations 7 days after the administration of 175 ng/ml and 280 ng/ml have been associated with treatment success. This pharmaceutical formulation causes a  $10^8$  reduction in parasites after a 3-day course of therapy. The remaining  $10$ – $10^4$  parasites are cleared by lumefantrine (Stover et al. 2012; WWARN 2015).

Artemether (**6**) is rapidly absorbed after oral dosing, reaching a maximum concentration in adults after approximately 2 h. Once in systemic circulation, artemether (**6**) is hydrolyzed to DHA in the gut and liver to DHA. Lumefantrine is very slowly absorbed. Its absorption begins after a lag-phase of approximately 2 h, reaching a peak concentration approximately 6 h after an oral dose in healthy individuals. Because of this slow and erratic absorption, the bioavailability of an oral dose is variable but increases with repeated dosing. This effect stems from an increase in food intake as the acute malarial episode subsides. Once absorbed, approximately 99% of lumefantrine is bound to serum high-density lipoproteins. The elimination half-life is 4–6 days in patients with malaria, which is much longer than that of artemether (**6**), allowing the drug to remain in the system and reducing the likelihood of recrudescence after the rapid parasite reduction induced by artemether (**6**). High-fat foods contribute to the increase in the absorption of these drugs. The bioavailability of artemether (**6**) increases two-fold when given together with food, whereas the bioavailability of lumefantrine increases approximately 16-fold under these conditions (Stover et al. 2012; WWARN 2015).

ASMQ (**12**) (Fig. 9.4) is a formulation developed by Farmanguinhos/Fiocruz, which is a Brazilian government-owned pharmaceutical company working, in part-

nership with the Drugs Initiative for Neglected Diseases (DNDi). ASMQ was transferred to the Indian pharmaceutical company Cipla and was prequalified by the WHO in 2012. The ASMQ combination therapy has been one of the WHO-recommended forms of ACT for first-line treatment of uncomplicated malaria in adults and children over 5 kg. ASMQ was adopted in several countries. The fixed dose containing 100 mg artesunate and 220 mg mefloquine hydrochloride was demonstrated to be effective and safe. This combination is less commonly used in Africa because of the availability of other affordable and already registered ACTs (MMV.ORG 2017c; Wells et al. 2013; Sirima et al. 2016).

Studies have shown that ASMQ had the highest cure rate, the lowest rate of gametocyte carriage, and the most effective suppression of *P. vivax* malaria. In addition, a large phase IV trial (23,845 patients) carried out in Brazil confirmed its effectiveness for the treatment of uncomplicated *P. falciparum* infection (Sirima et al. 2016). In vitro, ASMQ has shown a broad specificity, acting against all asexual stages of *P. falciparum*, i.e., rings, trophozoites, schizonts and young forms, but not against mature gametocytes. MQ is an antimalarial agent with high schizonticidal, but not gametocidal, activity. It is active against CQR *P. falciparum*. The exact mechanism of action of MQ is not clear. However, this molecule has a high affinity for erythrocyte membranes, and has a mechanism of action that is presumably related to its interference with the polymerization of hemes. Through the combination of these drugs, efficacy improves, as the number of gametocytes is reduced, promoting a possible reduction in malaria transmission. Studies have shown high cure rates (>95%) maintained for more than 10 years, with reduced levels of transmission and increased in vitro sensitivity of MQ. In ASMQ, **8** and DHA are absorbed rapidly in the gastrointestinal tract with high bioavailability. The protein binding, mainly to albumin, is reported to be 43% for DHA and 59% for **8**. DHA is excreted primarily by urine, with less than 1% of unmetabolized **8** present in urine and feces. MQ is absorbed in the gastrointestinal tract and then is widely and rapidly distributed throughout the body. The average time for maximum concentration ranges from 6 to 24 h. Plasma levels are higher in malaria patients than in healthy people. Plasma protein binding of MQ is 98% and it is partially metabolized in the liver to carboxy-mefloquine and several other metabolites. MQ has a long half-life of 15–33 days and is eliminated primarily through the feces, although unmodified MQ (9%) is also found in the urine. The absorption rate of MQ is slowed when administered as a co-formulation; however, the total plasma exposure of MQ is comparable (ITF 2017) to that obtained when MQ is administered as a monodose.

Artesunate-amodiaquine (ASAQ), sold commercially as Winthrop® or Coarsucam™ (Fig. 9.4), was developed by the DNDi and Sanofi between 2004 and 2007 and was prequalified by the WHO in 2008. It is taken once-per day for 3 days. It has been approved in 33 countries and it has the lowest price of all the fixed-dose ACTs. It has 3 years shelf life. Serious safety issues associated with AQ administered alone at high doses for either the treatment or the long-term prophylaxis were detected in the past, with case reports of severe adverse events; therefore, ASAQ should be provided as an FDC to improve compliance (MMV.ORG 2017e).

Artesunate-amodiaquine is very well tolerated and highly efficacious (>90% genotyping-adjusted cure rates). After the emergence of parasite resistance to CQ, AQ gained prominence, as this phenyl-substituted analogue of CQ was found to have an excellent activity/toxicity profile while possibly sharing with CQ its mechanism of antimalarial action. As AQ is effective against several CQR strains, this drug remains an important component of current antimalarial combination therapies, even when used with **8**. The AS/AQ fixed-dose combination is effective in clearing *P. falciparum* parasites from infected individuals (Teixeira et al. 2014).

Artesunate-amodiaquine is rapidly absorbed and undergoes rapid and extensive metabolism to DHA and desethylamodiaquine (DEAQ). Plasma levels of both DHA and DEAQ are many times higher and persist for longer than their respective parent compounds. AQ is absorbed in the gastrointestinal tract and accumulates in the liver, kidneys, lung, and spleen. The  $T_{\max}$  of AQ ranges from 0.6 to 1.3 h in healthy volunteers, and the  $T_{\max}$  of DEAQ ranges from 3 to 5.5 h. The elimination of this drug follows a first-order kinetics, and the mean elimination half-life ranges from 5.3 to 7.9 h in healthy individuals, while that of DEAQ ranges from 9 to 18 days. Pharmacokinetic parameters of the fixed- and loose-dose AS/AQ combinations are comparable (Navaratnam et al. 2009; Adjei et al. 2010).

The combination **14**, artesunate (**8**) + sulfadoxine (**3**) + pyrimethamine (**5**) (Fig. 9.4) is used for the treatment of acute uncomplicated malaria but is not available as an FDC yet. It is available in a blister-pack containing 50 mg of artesunate (**8**) and fixed-dose combination tablets comprising 500 mg of sulfadoxine (**3**) and 25 mg of pyrimethamine (**5**). A target dose of artesunate (**8**) is given once a day for 3 days, and a single administration of a single dose of sulfadoxine-pyrimethamine is given on the first day. The FDC **3+5** is indicated in areas of moderate to high malaria transmission for treating pregnant women in the first and second pregnancy and infants. Combination **14** is the first-line therapy for uncomplicated *P. falciparum* malaria in Sudan and globally (WHO 2015a, 2015b; Matar et al. 2014). Sulfadoxine (**3**) inhibits the bacterial and protozoal dihydropteroate synthetase activity and folic acid synthesis. Pyrimethamine (**5**) inhibits protozoal dihydrofolate reductase and folic acid synthesis. Both of them act in the later development stages of asexual stages.

After administration, FDC **3+5** is absorbed in the gastrointestinal tract. Sulfadoxine (**3**) usually has a longer elimination half-life, while pyrimethamine (**5**) has a larger volume of distribution and is concentrated in the lungs, kidneys, spleen and liver. FDC **3+5** crosses the placental barrier and passes into breast milk. Furthermore, **3+5** is metabolized by the liver and excreted through the kidneys (WHO 2015b).

Pyronaridine + artesunate (PYR + **8**), known commercially as Pyramax® (**15**) (Fig. 9.4), is still in the preregistration phase but it is also an example of a fixed-dose combination of PYR and **8** co-developed by MMV and Shin Poong Pharmaceutical Co. Ltd. It is the first ACT for which the EMA has adopted a positive scientific opinion and it is the first and only ACT to be approved for the blood-stage treatment of the main strains of malaria, *P. falciparum* and *P. vivax*. It is also the first Korean product included in the WHO list of prequalified medicines for malaria. This once

daily 3-day therapy is indicated for the treatment of uncomplicated malaria in adults and children over 20 kg (tablets) and in children between 5 and 20 kg (granules) (MMV.ORG 2017d). PYR was synthesized in 1970 in China and has been used there for over 30 years for the treatment of malaria. It has high potency against *Plasmodium falciparum*, including CQR strains. Resistance to PYR appears slowly and is further retarded when used in combination with other antimalarials, particularly artesunate. Pivotal phase III comparative clinical trials were completed in 2009 (MMV.ORG 2017d; Croft et al. 2012). PYR inhibits the formation of  $\beta$ -hematin, thus preventing the malarial parasite from neutralizing heme, which is toxic to the parasite. Additionally, by forming a drug-hematin complex, PYR inhibits the glutathione-dependent degradation of hematin and enhances the hematin-induced hemolysis. These two actions lead to parasite death. In vitro, PYR combined with artesunate or DHA has shown either additive effects or weak antagonism. The  $IC_{50}$  value is similar to that of CQ (0.125  $\mu$ M). The activity of PYR against erythrocytic *P. falciparum* is greatest for the ring-form stage, followed by the schizonts, and then the trophozoites. It was more active against all of these stages than CQ (Croft et al. 2012). Studies employing pyronaridine-artesunate (PYR + **8**) (3:1 ratio) against *P. berghei* infection in mice showed that the  $ED_{50}$  (50% of effective dose) for PYR was 0.42 mg/kg, for artesunate (**8**) was 5.1 mg/kg and for the combination was 1.12 mg/kg, while the  $ED_{90}$ s were 0.8, 31.19 and 1.87 mg/kg, respectively. Several mechanisms of action have been proposed to account for the activity of AS; for example, the generation of free radicals inside the parasite food vacuole and the inhibition of the parasite's sarcoplasmic endoplasmic reticulum calcium-ATPase are widely accepted (Croft et al. 2012). PYR is generally less toxic than CQ. PYR is highly lipophilic at pH 7.4, but its lipophilicity is reduced at pH 5, as the base is more liposoluble than the salt. The blood concentration of PYR declines in a multiexponential manner with a half-life that ranges from 2 to 4 days. Intramuscularly, the half-life of PYR ranges from 2 to 3 days. In mice, rats and rabbits, the highest concentrations of radioactivity were typically located in the liver, spleen, adrenal gland, kidney and thyroid. The combination has a good safety profile. Following the administration of Pyramax tablets to healthy volunteers and patients with malaria, peak plasma concentrations were generally reached between 0.5 and 1.0 h post-dose for **8** and between 2 and 8 h post-dose for PYR. The exposure to artesunate (**8**) and PYR was increased by 34% and 20%, respectively when Pyramax was administered with a high-fat meal; however, these effects were not considered clinically significant, and thus, patients can take Pyramax tablets regardless of meals ingestion (Croft et al. 2012; MMV.ORG 2017d).

## 9.2 Sesquiterpene Lactones as Antiplasmodial Agents

Sesquiterpene lactones (STLs) have displayed several biological and pharmacological activities, such as antimicrobial, anti-inflammatory, antibacterial, antiviral, antifungal, antimalarial, cytotoxic, and central nervous and cardiovascular systems

effects. Consequently, their therapeutic effects are critical. The biological activity of SLs is primarily attributed to the presence of an  $\alpha$ -methylene- $\gamma$ -lactone group in their structure, which acts as a Michael acceptor and reacts with nucleophiles (sulfhydryl groups) in enzymes, transcription factors, and other proteins to alkylate them irreversibly (Majdi et al. 2016; Schmidt 2006; Arantes et al. 2011). Herein, the aim is to review the antiplasmodial agents with a STL scaffold. Sesquiterpene lactones in use or in development, as well those from natural or semisynthetic origins, are highlighted.

### 9.2.1 Artemisinin and its Semisynthetic Derivatives

The natural artemisinin (ART, Fig. 9.3) has a distinctive 1,2,4-trioxane ring structure that contains an endoperoxide bridge. The endoperoxide bridge is primarily responsible for the antimalarial activity of this drug class. This highly oxygenated peroxide lacks nitrogen-containing heterocyclic ring systems and, compared to conventional drugs, was found to be a superior plasmodicidal and blood schizonticidal agent. ART is a sensitive molecule for large-scale derivatization. The carbonyl group can be easily reduced to a hydroxyl group in high yields using sodium borohydride, transforming the lactone ART into the lactol DHA while preserving the crucial endoperoxide moiety. This strategy has led to the preparation of a series of semisynthetic first-generation analogues, including oil-soluble artemether (6), arteether (7) and artesunic acid, with the latter being commercially known as artesunate (8) (Fig. 9.3). These compounds share the same basic structure as ART, where the carbonyl group is replaced with different substituents. These substituents determine the solubility of each ART derivative and influence some of the pharmacokinetic properties of ART. ART is poorly soluble in both water and oil but is soluble in many aprotic organic solvents. Compound 8 has significantly greater solubility in water than ART, DHA or 7. To increase the antimalarial potency, ART dimers, trimers and tetramers have been synthesized, many of which have shown a more promising antimalarial activity than ART, thus constituting the first generation analogs (Chaturvedi 2011; Staines and Krishna 2012).

The semisynthetic derivatives of ART (ARTs) are effective against chloroquine- and mefloquine-resistant strains and are not only active against the mature ring stage of *P. falciparum*, which is the most metabolically active form, but also target the young ring stages of the parasite. Another potential benefit is that they are active against the gametocytes, which are transmitted from humans to mosquitoes. These analogs have proved to cause a significant reduction in the gametocytemia and subsequent decrease in the transmission to mosquitoes, as compared to the use of previous first-line non-artemisinin antimalarial drugs. However, these compounds are not active against the pre-erythrocytic stages or the dormant hypnozoite stages of *P. vivax* and *P. ovale* in the liver (Okell et al. 2008; Tan 2009). ARTs are capable of killing >99.9% of parasites per asexual cycle. However, to remove all parasites from the blood, the concentration of ARTs needs to be at a parasiticidal level for at least

6 days (corresponding to 3 asexual life cycles for *P. falciparum*). Therefore, when given alone, ARTs must be given as 7-day regimens to maximize the cure rate. However, compliance to 7-day treatment courses is poor, particularly when the clinical symptoms of malaria disappear within a couple days of treatment initiation. When used in combination with partner drugs with longer elimination half-lives, 3-day treatment courses are sufficient (Nyunt and Plowe 2007). As previously discussed, ARTs have a short half-life and are always used in combination with another antimalarial drug.

### 9.2.2 Other Sesquiterpene Lactones with Antiplasmodial Activity

Neuroleenin B (**16**) (Fig. 9.5) is a germacranolide sesquiterpene lactone isolated from *Neurolaena lobata* (Asteraceae), which is a plant species growing in Central America. This compound is used to treat ulcers, inflammatory skin disorders; and ringworms, fungal infections and malaria (Unger et al. 2015). Neuroleenin B has proved to be active against *P. falciparum* in vitro ( $IC_{50} = 0.62 \mu M$ ). Among the germacranolides, the double bond in the 2,3-position of the  $\alpha,\beta$ -unsaturated keto function increases their activity, suggesting that this is a structural requirement. Additionally, a free hydroxyl group increases the antiplasmodial activity (Chaturvedi 2011).

Tagitinin C (**17**) (Fig. 9.5), which was isolated from *Tithonia diversifolia* (Asteraceae), has antiplasmodial properties and it was investigated in *P. falciparum*, obtaining an  $IC_{50} = 0.33 \mu g/ml$ . Vernodalol (**18**) and 11 $\beta$ ,13-dihydrovernodalin (**19**), which were isolated from *Vernonia colorata*, exhibited antiplasmodial activity, with  $IC_{50} = 4.8$  and  $1.1 \mu g/ml$ , respectively. Among the sesquiterpene lactones obtained from *Artemisia afra*, rupicolin A-8-*O*-acetate (**20**) possessed in vitro antiplasmodial activity with  $IC_{50} = 10.8$ – $17.5 \mu g/mL$ . Helenalin (**21**) was isolated from *Arnica Montana* and showed activity against *P. falciparum* in vitro ( $IC_{50} = 0.23 \mu M$ ). Psilostachyin (**22**) and peruvín (**23**) have been evaluated against the F32 and W2 strains of *P. falciparum*. Both STLs have been isolated from the organic extract of *Ambrosia tenuifolia* and have displayed in vitro antiplasmodial activity. Among the sesquiterpene lactones obtained from *Artemisia afra*, rupicolin A-8-*O*-acetate possessed in vitro antiplasmodial activity with  $IC_{50} = 10.8$ – $17.5 \mu g/mL$ . Helenalin was isolated from *Arnica montana* and showed activity against *P. falciparum* in vitro ( $IC_{50} = 0.23 \mu M$ ). Psilostachyin (**22**) has shown activity on both strains, with  $IC_{50} = 0.6$  and  $1.8 \mu g/ml$ , respectively. Peruvín (**23**) has shown stronger activity on the F32 strain with  $IC_{50} = 0.3 \mu g/ml$ . The sesquiterpene lactones **24** and **25**, which were isolated from *Camchaya calcarea*, inhibit the growth of *P. falciparum* with  $IC_{50} = 1.2$  and  $0.3 \mu g/ml$ , respectively (Chaturvedi 2011; Sülsen et al. 2011; Kaur et al. 2009).



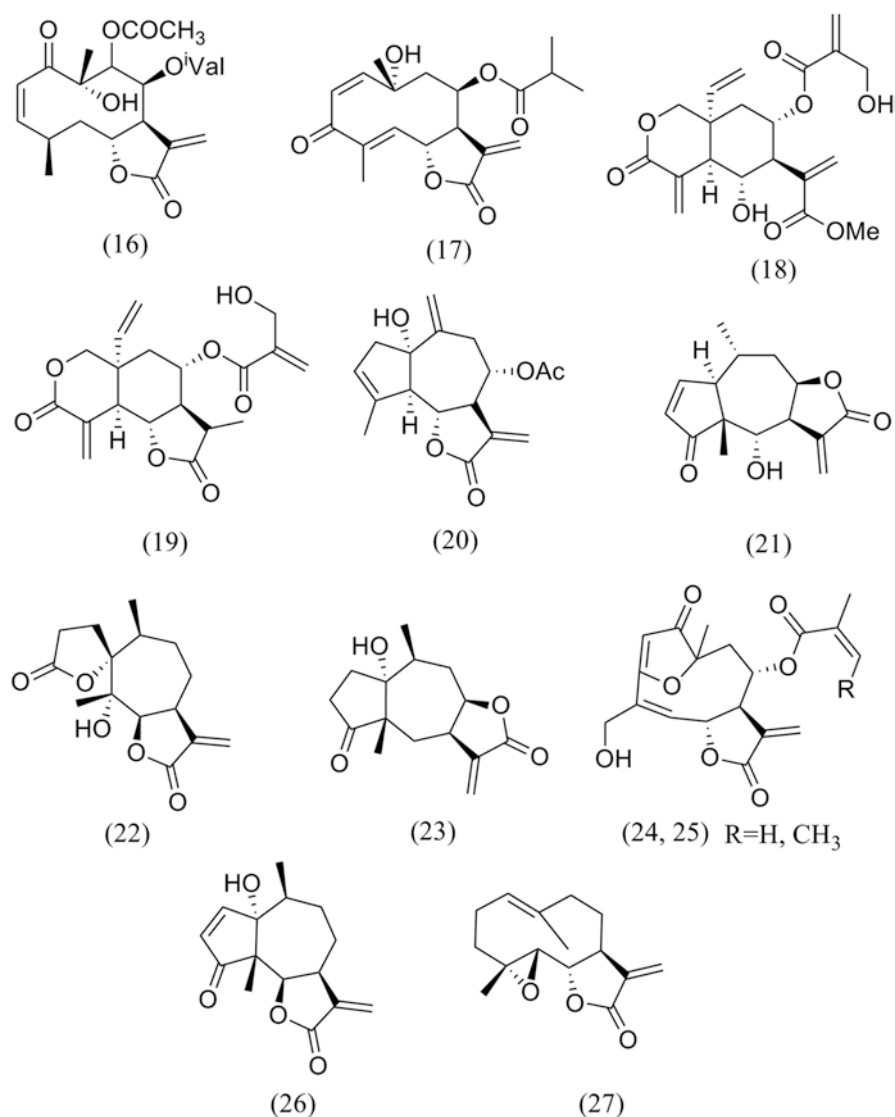


**Fig. 9.5** Structures of some antimalarial sesquiterpene lactones

Parthenin (**26**) (Fig. 9.5) is a STL isolated from *Parthenium hysterophorus*, which is an invasive flowering weed spreading worldwide. Evidences of the potential activity of parthenin against *P. falciparum* sexual stage transmission comes from studies of the sugar-feeding preferences of *Anopheles gambiae* in Kenya (Manda et al. 2007).

The exposure of *P. falciparum* gametocytes to **26** in blood meal decreases the midgut oocyst number by 40–80%; however, the infection prevalence remains high

(88–91%). The inclusion of compound **26** in blood meal effectively confirmed its transmission-blocking activity. Compound **26** decreases the number of zygotes and ookinetes in *P. falciparum* in vivo and *P. berghei* in vitro and decreases the total number of parasites prior to midgut cell invasion and oocyst formation. It also inhibits male microgamete exflagellation and inactivates mature *P. falciparum* stage V gametocytes. ART is active against early gametocyte developmental stages but not against mature forms (Balaich et al. 2016).

Parthenolide (**27**) (Fig. 9.5) is a natural product isolated from *Tanacetum parthenium*, a traditional plant that has been used for centuries for the treatment of migraine, fever, and arthritis. Compound **27** exhibits properties similar to those of parthenin (**26**). Its structure is similar to ART, it is safer for non-target cells, and it shows acceptable pharmacological properties. Compound **27** has also proved to be effective against microgamete exflagellation and gametocytes and, at the same dosing levels, this drug may be more effective than parthenin (**26**). Although ART, **26**, and **27** are derived from the same plant family, compounds **26** and **27** do not contain the endoperoxide bridge essential for the activity displayed by artemisinin (Wyrebska et al. 2012; Ghantous et al. 2013; Balaich et al. 2016).

### 9.2.3 Antimalarial Hybrids Containing Sesquiterpene Lactones

Molecular hybridization, a strategy employed in medicinal chemistry for the development of new drugs, consists of combining pharmacological fragments from two or more molecules into a single hybrid molecule. The employment of hybrid molecules instead of multicomponent therapy entails several advantages. A hybrid is a single compound that can act either by two different mechanisms or by a single one that is different from that exerted by each part of the molecule separately. The latter phenomenon may occur because the hybrid molecule constitutes a new pharmaceutical entity. A hybrid may be potentially safer, more efficient, and can have an improved cost/effectiveness relationship with lower rates of resistance development. Another advantage would be a lower risk of drug interactions, as compared to FDC (Vandekerckhove and D'hooghe 2015; Staines and Krishna 2012).

Some hybrid sesquiterpene lactones that are active against *Plasmodium* strains are shown in Fig. 9.6. Compound **28** is a conjugate hybrid between DHA and QN. The original vinyl functional group in QN was used to link both molecules (Fig. 9.3). The linkage was achieved by coupling DHA to a carboxylic acid derivative of QN via a covalent ester linkage. Studies have demonstrated that changes introduced to other sites in the QN molecule have unfavorable effects on activity. The hydroxyl group and the quinoline ring are essential for the activity, but the quinuclidine ring can be replaced by another one without loss of activity. The novel hybrid **28** was active against both sensitive (3D7;  $IC_{50} = 0.008 \mu\text{M}$ ) and resistant (FcB1;  $IC_{50} = 0.009 \mu\text{M}$ ) strains of *P. falciparum* in vitro. This finding shows that

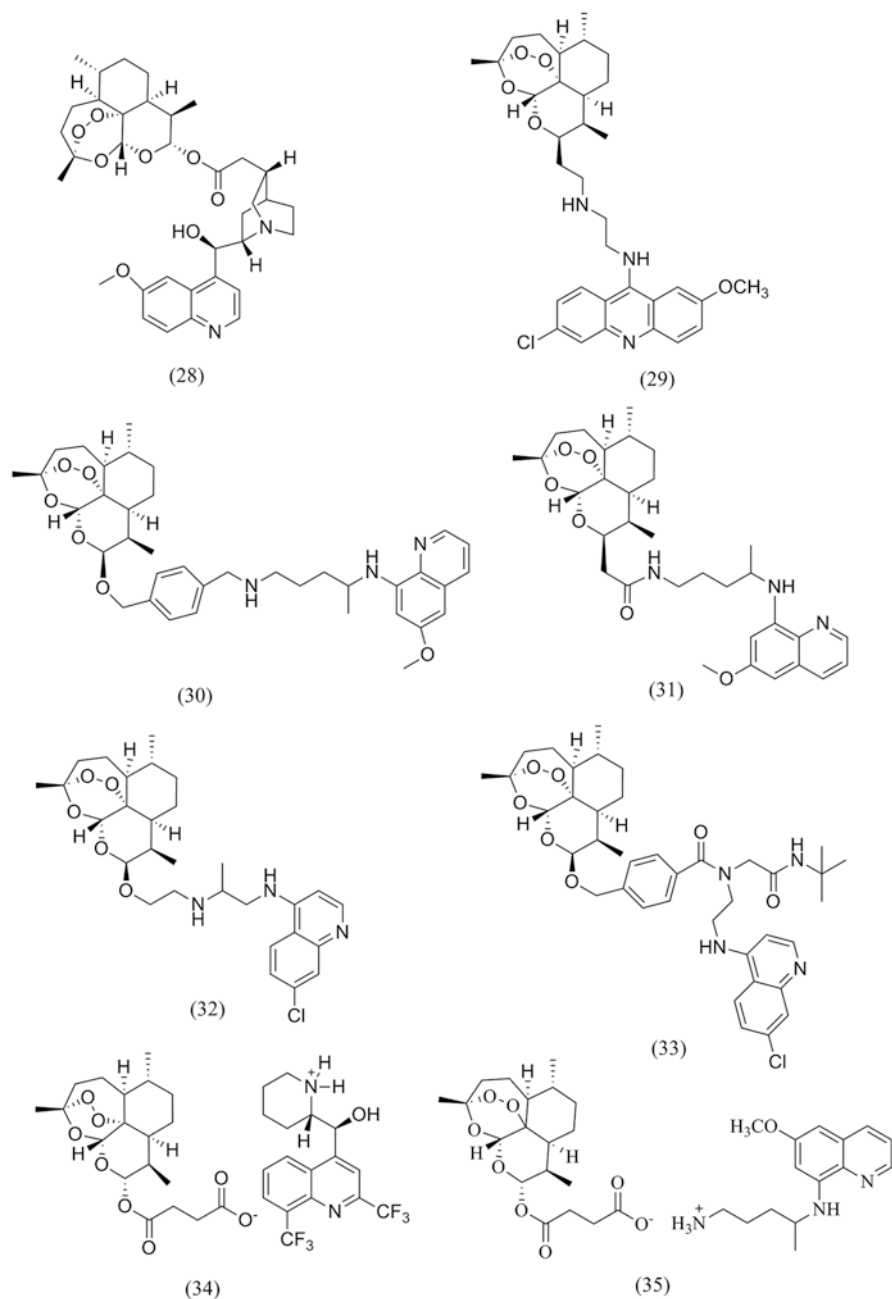


Fig. 9.6 Structures of some antimalarial hybrid sesquiterpene lactones

the hybrid has higher potency than ART (3D7, FcB1;  $IC_{50}$  = 0.049 and 0.050  $\mu$ M, respectively) and QN (3D7, FcB1;  $IC_{50}$  = 0.149 and 0.096  $\mu$ M, respectively) used as a control (Walsh et al. 2007; Muregi and Ishih 2010). Despite recent promising findings on QN surrogates, none of them seem to have been tested in clinical trials yet. Nevertheless, QN is expected to play a meaningful role in the treatment of malaria in the near future (Achan et al. 2011; Teixeira et al. 2014).

The relevance of artemisinin-based antimalarials in current clinical strategies against CQR malaria led to the exploration of several endoperoxides and derived hybrid constructs as potential antimalarial leads. One example is hybrid compound **29**, which features a metabolically stable linkage. The artemisinin derivative/quinacrine hybrid (**29**) (Fig. 9.6) was developed by Araujo et al. (2009) by joining the quinacrine acridine core with an ART derivative. This hybrid was evaluated against CQS *P. falciparum* (3D7;  $IC_{50}$  = 0.012–0.016  $\mu$ M) and CQR (K1;  $IC_{50}$  = 0.014–0.020  $\mu$ M) strains and was found to display micromolar activities against both strains, thus exhibiting no cross-resistance with CQ. In fact, this hybrid was more active than ART and was easily transformed into a water-soluble salt, making it suitable for oral and intravenous administration. Although this analogue is more potent than ART (3D7;  $IC_{50}$  = 0.011  $\mu$ M) (K1;  $IC_{50}$  = 0.009  $\mu$ M), it was not more potent than artemether (**6**) (3D7;  $IC_{50}$  = 0.003  $\mu$ M) (K1;  $IC_{50}$  = 0.001  $\mu$ M). This is surprising because the drug should accumulate within the acidic digestive vacuole much more efficiently than the parent drug through an ion-trapping mechanism. This may indicate that other targets outside the food vacuole may be more important for this class of hybrid drugs (Araujo et al. 2009).

For DHA/PQ hybrids **30** and **31** (Fig. 9.6), a double-drug approach was used by synthesizing molecular constructs where PQ is covalently bound to another potent moiety with complementary antimalarial properties. In this approach, PQ was combined with the DHA core. Hybrid compound **28** was synthesized from artelinic acid, which is a 4-methylbenzoic acid derivative of ART that has been demonstrated to be the most metabolically stable of the ARTs. Hybrid compound **30** was designed by replacing the oxygen atom with a  $CH_2$  group. This modification was intended to produce a compound with greater hydrolytic stability, a longer half-life, and, potentially, lower toxicity. Both **30** and **31** displayed enhanced in vitro activities against liver-stage *P. berghei*, as compared to their parent drugs. These compounds were also evaluated in vitro against W2 strains of *P. falciparum* ( $IC_{50}$  = 0.0125 and 0.0091  $\mu$ M, respectively), in which they were equipotent to ART ( $IC_{50}$  = 0.0082  $\mu$ M) and superior to PQ ( $IC_{50}$  = 3.3  $\mu$ M). Additional preclinical studies on these considerably promising hybrids have not been reported (Capela et al. 2011).

In order to increase the half-life of DHA, compound **32**, a DHA/4-aminoquinoline hybrid (Fig. 9.6), has been developed by Lombard et al. (2011). This hybrid was obtained by joining a DHA motif to 4-aminoquinoline via an ether/amine bond. In order to increase the solubility and stability, this hybrid was treated with oxalic acid to obtain the oxalate salt. Hybrid **32** exhibited higher potency against both CQS (D10;  $IC_{50}$  = 0.012  $\mu$ M) and CQR (Dd2;  $IC_{50}$  = 0.017  $\mu$ M) strains than CQ (D10;  $IC_{50}$  = 0.021  $\mu$ M) (Dd2;  $IC_{50}$  = 0.15  $\mu$ M). One drawback of the compound was its

lower activity than DHA (D10;  $IC_{50} = 0.005 \mu\text{M}$ ) (Dd2;  $IC_{50} = 0.002 \mu\text{M}$ ) irrespective of the *P. falciparum* strain (Lombard et al. 2011).

Artemisinin/chloroquinoline hybrid **33** (Fig. 9.6) was synthesized by Feng et al. (2011) by coupling DHA and a chloroquinoline moiety through an ether/amide bond. Compared to CQ values (D10;  $IC_{50} = 0.020 \mu\text{M}$ ) (K1;  $IC_{50} = 0.021 \mu\text{M}$ ), the compound displayed excellent in vitro antiplasmodial activities against sensitive (D10;  $IC_{50} = 0.027 \mu\text{M}$ ) and resistant (K1;  $IC_{50} = 0.019 \mu\text{M}$ ) *P. falciparum* strains. No cross-resistance with CQ was observed for this hybrid compound in CQR malaria parasites, even though it contains a CQ moiety. It has also been found that this hybrid shares the same mechanism of action with both ART and CQ, as it displayed potent activity against  $\beta$ -hematin formation and contributed to an increase in the accumulation of hemoglobin within the parasites. Despite its potent biological results, this hybrid was found to exhibit cytotoxicity against a human cervical cancer cell line (HeLa) (Feng et al. 2011).

MEFAS (**34**) (Fig. 9.6) is a hybrid salt of artesunate (**8**) and MQ that is under development by Boechat et al. (2014). MEFAS was active against *P. falciparum* CQS 3D7 and CQR W2, showing an  $IC_{50}$  value of  $0.001 \mu\text{M}$  for both strains. Studies have shown that MEFAS was at least five-fold more potent than MQ alone, more potent than **8** against 3D7, as effective as **8** against W2, and more potent than mixtures of **8** with MQ. In in vivo tests carried out in *P. berghei* infected mice, a cure was observed after treatment at a dose of 10 mg/kg, without recrudescence of parasitemia. Assessments of the in vivo cytotoxicity of MEFAS have demonstrated that its toxicity is five-fold lower than that of MQ. The FDC ASMQ was three-fold more toxic than MEFAS (Varotti et al. 2008). Antimalarial drugs target asexual parasites without reducing gametocyte formation. Drugs that are able to target both asexual parasites and gametocytes would improve malaria control. MEFAS has been demonstrated to be an active blood schizonticidal drug (Penna-Coutinho et al. 2016). The ability of MEFAS to block the infectivity of *P. falciparum* gametocytes, was evaluated to find that it was 280- and 15-fold more effective than both MQ and **8** alone, respectively.

PRIMAS (**35**) (Fig. 9.6), which has been designed using the same approach as with MEFAS, is also a hybrid salt between artesunate (**8**) and PQ under development by Boechat et al. (2014). PRIMAS was developed with the goal of minimizing the toxicity of PQ. The efficacy studies of PRIMAS hybrid salt in in vivo and in vitro models have shown that it is more active and less toxic when compared to the isolated parent drugs (Boechat et al. 2014).

### 9.2.4 Dimer, Trimer and Tetramer Sesquiterpene Lactones

The extent of antimalarial activity was thought to depend upon the number of peroxide units, which can be increased by including an additional artemisinin moiety.

Thus, dimers, trimers and tetramers of artemisinin with various lengths, stereochemistries and flexibilities have been synthesized. ART trimer and tetramer derivatives without acetal groups have also been reported (Chaturvedi et al. 2010).

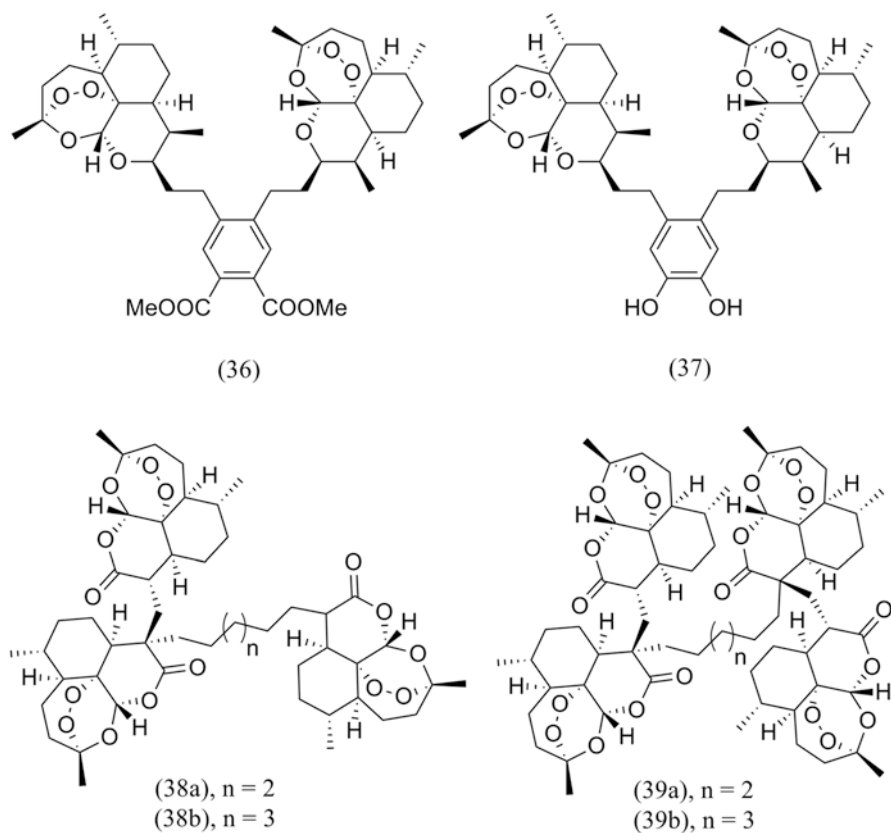


**Fig. 9.7** Structures of some dimer, trimer and tetramer antimalarial sesquiterpene lactones

Dimers **36** and **37** (Fig. 9.7) had antimalarial activities in vitro against CQS *P. falciparum* parasites and were considerably more potent antimalarials (**36**;  $IC_{50} = 0.0016 \mu\text{M}$ , **37**;  $IC_{50} = 0.00077 \mu\text{M}$ ), than ART ( $IC_{50} = 0.0066 \mu\text{M}$ ) (Paik et al. 2006).

Trimers **38a,b** and tetramers **39a,b** (Fig. 9.7) have been synthesized and their antimalarial activity evaluated. The results obtained for trimers **38a** ( $EC_{50} = 0.0024 \mu\text{M}$ ) and **38b** ( $EC_{50} = 0.0031 \mu\text{M}$ ) and tetramers **39a** ( $EC_{50} = 0.0058 \mu\text{M}$ ) and **39b** ( $EC_{50} = 0.02 \mu\text{M}$ ) were quite impressive and superior (except **39b**) in comparison to ART ( $EC_{50} = 0.012 \mu\text{M}$ ) (Chaturvedi et al. 2010).

### 9.3 Conclusion

Malaria is still one of the most serious health problems worldwide. This review describes antiplasmodial agents with an STL scaffold. Sesquiterpene lactones in use or in development, as well as those from natural or semisynthetic origins, were

highlighted. Artemisinin and its semisynthetic derivatives are the most important representatives of SLs and play an important role in the fight against this disease. Treatments based on artemisinin and its derivatives are recommended by the WHO. These derivatives and artemisinin itself can be used in combination with other antimalarials or can be combined in new hybrid molecules.

## References

- Achan J, Talisuna AO, Erhart A et al (2011) Quinine, an old anti-malarial drug in a modern world: role in the treatment of malaria. *Malar J* 10:144–156
- Adjei GO, Kudzi W, Dodo A et al (2010) Artesunate plus amodiaquine combination therapy: reviewing the evidence. *Drug Dev Res* 71:33–43
- Aquino I (2010) Efeito genotóxico da artemisinina e do artesunato em células de mamíferos. Dissertation, University of São Paulo
- Arantes FFP, Barbosa LCA, Maltha CRA et al (2011) A quantum chemical and chemometric study of sesquiterpene lactones with cytotoxicity against tumor cells. *J Chemom* 25(8):401–407
- Araujo NCP, Barton V, Jones M (2009) Semi-synthetic and synthetic 1,2,4-trioxoquinones and 1,2,4-trioxoloquinones: synthesis, preliminary SAR and comparison with acridine endoperoxide conjugates. *Bioorg Med Chem Lett* 19:2038–2043
- Baio PA (2011) A importância do conhecimento clínico e epidemiológico da malária nos países não endêmicos: perspectivas futuras para Europa. Dissertation, University of Porto, Portugal
- Balaich JN, Mathias DK, Torto B et al (2016) The nonartemisinin sesquiterpene lactones parthenin and parthenolide block *Plasmodium falciparum* sexual stage transmission. *Antimicrob Agents Chemother* 60(4):2108–2117
- Barnett DS, Guy RK (2014) Antimalarials in development in 2014. *Chem Rev* 114:11221–11241
- Bassat Q, Mulenga M, Tinto H et al (2009) Dihydroartemisinin-piperazine and artemether-lumefantrine for treating uncomplicated malaria in african children: a randomised, non-inferiority trial. *PLoS One* 4(11):e7871. <https://doi.org/10.1371/journal.pone.0007871>
- Boechat N, Souza MVN, Valverde AL et al (2014) Compounds derived from artesunate, preparation process, pharmaceutical composition and use of the respective medicine. *Us Patent* 8,802,701 B2, 12 Aug 2014
- Capela R, Cabal GG, Rosenthal PJ et al (2011) Design and evaluation of primaquine-artemisinin hybrids as a multistage antimalarial strategy. *Antimicrob Agents Chemother* 55:4698–4706
- Chaturvedi D (2011) Sesquiterpene lactones: structural diversity and their biological activities. In: Tiwari V, Mishra B (eds) *Opportunity, challenge and scope of natural products in medicinal chemistry*. Research Signpost, Kerala, pp 313–334
- Chaturvedi D, Goswami A, Saikia PP et al (2010) Artemisinin and its derivatives: a novel class of anti-malarial and anti-cancer agents. *Chem Soc Rev* 39:435–454
- Coura JR (2013) *Dinâmica das doenças infecciosas e parasitárias*, 2nd edn. Guanabara Koogan, Rio de Janeiro
- Croft SL, Duparc S, Arbe-Barnes SJ et al (2012) Review of pyronaridine anti-malarial properties and product characteristics. *Malar J* 11:270–298
- Cunico W, Carvalho SA, Gomes CRB et al (2008) Fármacos antimalariais – história e perspectivas. *Rev Bras Farm* 89:49–55
- European Medicines Agency (EMA) Science Medicine Health (2017a) [http://www.ema.europa.eu/docs/en\\_GB/document\\_library/Medicine\\_for\\_use\\_outside\\_EU/2012/06/WC500129288.pdf](http://www.ema.europa.eu/docs/en_GB/document_library/Medicine_for_use_outside_EU/2012/06/WC500129288.pdf). Accessed 31 Jan 2017
- European Medicines Agency (EMA) Science Medicine Health (2017b) Eurartesim (dihydroartemisinin/ piperazine) 20 mg/160 mg and 40 mg/320 mg film-coated tablets: EU summary of

- product characteristics. [http://www.ema.europa.eu/docs/en\\_GB/document\\_library/EPAR\\_-\\_Product\\_Information/human/001199/WC500118113.pdf](http://www.ema.europa.eu/docs/en_GB/document_library/EPAR_-_Product_Information/human/001199/WC500118113.pdf). Accessed 10 Jan 2017
- Feng TS, Guantai EM, Nell M et al (2011) Effects of highly active novel artemisinin–chloroquinoline hybrid compounds on b-hematin formation, parasite morphology and endocytosis in *Plasmodium falciparum*. *Biochem Pharmacol* 82:236–247
- França TCC, Santos MG, Figueroa-Villar JD (2008) Malária: aspectos históricos e quimioterapia. *Quim Nova* 31(5):1271–1278
- Gangjee A, Jain HD, Phan J et al (2006) Dual inhibitors of thymidylate synthase and dihydrofolate reductase as antitumour agents: design, synthesis and biological evaluation of classical and nonclassical pyrrolo[2,3-d] pyrimidine antifolates. *J Med Chem* 49:1055–1065
- Garcia LS (2010) Clinics in laboratory. *Medicine* 30:93–129
- Ghantous A, Sinjab A, Herceg Z, Darwiche N (2013) Parthenolide: from plant shoots to cancer roots. *Drug Discov Today* 18:894–905
- Instituto de Tecnologia de Farmacos (ITF), Farmanguinhos/Fiocruz (2017) [https://facilbula.com.br/pesquisabula/arquivopdf?nomeArquivo=5133402015\\_2673917\\_PROFSSIONAL.PDF](https://facilbula.com.br/pesquisabula/arquivopdf?nomeArquivo=5133402015_2673917_PROFSSIONAL.PDF). Accessed 30 Jan 2017
- Kaur K, Jain M, Kaur T, Jain R (2009) Antimalarials from nature. *Bioorg Med Chem* 17:3229–3256
- Kaur K, Jain M, Reddy RP et al (2010) Quinolines and structurally related heterocycles as antimalarials. *Eur J Med Chem* 45:3245–3264
- Keating GM (2012) Dihydroartemisinin/Piperaquine: a review of its use in the treatment of uncomplicated *Plasmodium falciparum* malaria. *Adis Drug Eval* 72(7):937–961
- Leite FHA, Fonseca A, Nunes RR et al (2013) Malaria: from old drugs to new molecular targets. *Biochem Biotechnol Rep* 2:59–76
- Li J, Zhou B (2010) Biological actions of artemisinin: insights from medicinal chemistry studies. *Molecules* 15:1378–1397
- Lombard MC, N'Da DD, Breytenbach JC et al (2011) Synthesis, *in vitro* antimalarial and cytotoxicity of artemisinin-aminoquinoline hybrids. *Bioorg Med Chem Lett* 21:1683–1686
- Majdi M, Ashengroph M, Abdollahi MR (2016) Sesquiterpene lactone engineering in microbial and plant platforms: parthenolide and artemisinin as case studies. *Appl Microbiol Biotechnol* 100:1041–1059
- Manda H, Gouagna LC, Foster WA et al (2007) Effect of discriminative plant-sugar feeding on the survival and fecundity of *Anopheles gambiae*. *Malar J* 6:113–124
- Matar KM, Awad AI, Elamin SB (2014) Pharmacokinetics of artesunate alone and in combination with sulfadoxine/Pyrimethamine in healthy sudanese volunteers. *Am J Trop Med Hyg* 90(6):1087–1093
- Medicines for malária venture (MMV) (2017a) <http://www.mmv.org/access/products-projects/eurartesim-dihydroartemisinin-piperaquine>. Accessed 28 Jan 2017
- Medicines for malária venture (MMV) (2017b) <http://www.mmv.org/access/products-projects/coartem-dispersible-artemether-lumefantrine/coartem-dispersible-facts>. Accessed 28 Dec 2016
- Medicines for malaria venture (MMV) (2017c) <http://www.mmv.org/access/products-projects/artesun-injectable-artesunate>. Accessed 29 Jan 2017
- Medicines for malária venture (MMV) (2017d) <http://www.mmv.org/access/products-projects/pyramax-pyronaridine-artesunate>. Accessed 01 Dec 2016
- Medicines for malaria venture (MMV) (2017e) <https://www.mmv.org/access/products-projects/asaq-winthrop-artesunate-amodiaquine>. Accessed 20 Jan 2017
- Midha K, Mohit, Nagpal M, Sharma A (2015) Drug-resistant malaria in south Asian countries: a review of evidence and future prospects of nanomedicine based strategies for prophylaxis and treatment. *Eur J Pharm Med Res* 2(5):231–248
- Misra H, Mehta D, Mehta BK, Jain DC (2014) Extraction of artemisinin, an active antimalarial phytopharmaceutical from dried leaves of *Artemisia annua* L., using microwaves and a validated HPTLC-visible method for its quantitative determination. *Chromatogr Res Int* 2014, Article ID 361405. <https://doi.org/10.1155/2014/361405>



- Muregi FW, Ishih A (2010) Next-generation antimalarial drugs: hybrid molecules as a new strategy in drug design. *Drug Dev Res* 71:20–32
- Na-Bangchang K, Karbwang J (2009) Review: current status of malaria chemotherapy and the role of pharmacology in antimalarial drug research and development. *Fundam Clin Pharmacol* 23:387–409
- Navaratnam V, Ramanathan S, Wahab MSA et al (2009) Tolerability and pharmacokinetics of non-fixed and fixed combinations of artesunate and amodiaquine in Malaysian healthy normal volunteers. *Eur J Clin Pharmacol* 65:809–821
- Nguyen DVH, Nguyen QP, Nguyen ND et al (2009) Pharmacokinetics and ex vivo pharmacodynamics antimalarial activity of dihydroartemisinin-piperazine in patients with uncomplicated falciparum malaria in Vietnam. *Antimicrob Agents Chemother* 53(8):3534–3537
- Nyunt MM, Plowe CV (2007) Pharmacologic advances in the global control and treatment of malaria: combination therapy and resistance. *Clin Pharmacol Ther* 82(5):601–605
- O'Neill PM, Barton VE, Ward SA (2010) The molecular mechanism of action of artemisinin—the debate continues. *Molecules* 15:1705–1721
- Okell LC, Drakeley CJ, Ghani AC et al (2008) Reduction of transmission from malaria patients by artemisinin combination therapies: a pooled analysis of six randomized trials. *Malar J* 7:125–138
- Paik IH, Xie S, Shapiro TA et al (2006) Second generation, orally active, antimalarial, artemisinin-derived trioxane dimers with high stability, efficacy, and anticancer activity. *J Med Chem* 49:2731–2734
- Penna-Coutinho J, Almela MJ, Miguel-Blanco C et al (2016) Transmission-blocking potential of MEFAS, a hybrid compound derived from artesunate and mefloquine. *Antimicrob Agents Chemother* 60(5):3145–3147
- Raj DK, Nixon CP, Nixon CE et al (2014) Antibodies to pfsen-1 block parasite egress from rbc and protect against malaria infection. *Science* 344:871–877
- Rappuoli R, Aderem A (2011) A 2020 vision for vaccines against HIV, tuberculosis and malaria. *Nature* 473:463–469
- Schmidt TJ (2006) Structure-activity relationships of sesquiterpene lactones. *Stud Nat Prod Chem* 33:309–392
- Seder RA, Chang LJ, Enama ME et al (2013) Protection against malaria by intravenous immunization with a nonreplicating sporozoite vaccine. *Science* 341:1359–1365
- Sirima SB, Ogutu B, Lusingu JPA et al (2016) Comparison of artesunate–mefloquine and artemether–lumefantrine fixed-dose combinations for treatment of uncomplicated *Plasmodium falciparum* malaria in children younger than 5 years in sub-Saharan Africa: a randomised, multicentre, phase 4 trial. *Lancet* 16:1123–1133
- Srivastava V, Lee H (2015) Chloroquine-based hybrid molecules as promising novel chemotherapeutic agents. *Eur J Pharmacol* 762:472–486
- Staines HM, Krishna S (2012) Treatment and prevention of malaria: antimalarial drug chemistry, action and use. Springer, London
- Stover KR, King ST, Robinson J (2012) Artemether-Lumefantrine: an option for malaria. *Ann Pharmacother* 46:567–577
- Sülzen V, Gutierrez Yappu D, Laurella L et al (2011) *In vitro* antiplasmodial activity of sesquiterpene lactones from *Ambrosia tenuifolia*. *Evid Based Complement Alternat Med* 2011:352938. <https://doi.org/10.1155/2011/352938>
- Tan BS (2009) Population pharmacokinetics of artesunate and its active metabolite dihydroartemisinin. Thesis, University of Iowa
- Teixeira JRM (2011) Avaliação da terapêutica da malária por *Plasmodium vivax*: perfil cinético da cloroquina e primaquina. Ph.D. thesis, University Federal of Pará, Brazil
- Teixeira C, Vale N, Pérez B et al (2014) Recycling classical drugs for malaria. *Chem Rev* 114:1164–11220
- The Nobel Foundation (2015) The Nobel prize in physiology or medicine 2015. [http://www.nobel-prize.org/nobel\\_prizes/medicine/laureates/2015/press.pdf](http://www.nobel-prize.org/nobel_prizes/medicine/laureates/2015/press.pdf). Accessed 10 Jan 2016

- Unger C, Kiss I, Vasas A et al (2015) The germacranolide sesquiterpene lactone neurolelin B of the medicinal plant *Neurolaena lobata* (L.) R.Br. ex Cass inhibits NPM/ALK-driven cell expansion and NF- $\kappa$ B-driven tumour intravasation. *Phytomedicine* 22:862–874
- Valecha N, Phyo AP, Mayxay M et al (2010) An open-label, randomised study of dihydroartemisinin-piperaquine versus artesunate-mefloquine for falciparum malaria in Asia. *PLoS One* 5(7):e11880. <https://doi.org/10.1371/journal.pone.0011880>
- Vandekerckhove S, D'hooghe M (2015) Quinoline-based antimalarial hybrid compounds. *Bioorg Med Chem* 23:5098–5119
- Varotti FP, Botelho ACC, Andrade AA et al (2008) Synthesis, antimalarial activity, and intracellular targets of Mefas, a new hybrid compound derived from mefloquine and artesunate. *Antimicrob Agents Chemother* 52:3868–3874
- Walsh JJ, Coughlan D, Heneghan N et al (2007) A novel artemisinin-quinine hybrid with potent antimalarial activity. *Bioorg Med Chem Lett* 17:3599–3602
- Wells S, Diap G, Kiechel JR et al (2013) The story of artesunate–mefloquine (ASMQ), innovative partnerships in drug development: case study. *Malar J* 12:68–78
- World Health Organization (WHO) (2014) World malaria report. WHO, Geneva. [http://www.who.int/malaria/publications/world\\_malaria\\_report\\_2014/report/en/](http://www.who.int/malaria/publications/world_malaria_report_2014/report/en/). Accessed 02 Dec 2016
- World Health Organization (WHO) (2015a) World malaria report. <http://www.who.int/malaria/publications/world-malaria-report-2015/report/en/>. Accessed 10 Jan 2016
- World Health Organization (WHO) (2015b) Guidelines for the treatment of malaria, 3rd edn. World Health Organization, Geneva. <http://www.who.int/malaria/publications/atoz/9789241549127/en/> Accessed 12 Jan 2017
- World Health Organization (WHO) (2016) World malaria report. <http://www.who.int/malaria/publications/world-malaria-report-2016/report/en/>. Accessed 16 Jan 2017
- WorldWide Antimalarial Resistance Network (WWARN) Lumefantrine PK/PD Study Group (2015) Artemether-lumefantrine treatment of uncomplicated *Plasmodium falciparum* malaria: a systematic review and meta-analysis of day 7 lumefantrine concentrations and therapeutic response using individual patient data. *BMC Med* 13:227–246
- Wright CW, Linley PA, Brun R et al (2010) Ancient chinese methods are remarkably effective for the preparation of artemisinin-rich extracts of Qing Hao with potent antimalarial activity. *Molecules* 15:804–812
- Wyrebska A, Gach K, Szemraj J et al (2012) Comparison of anti-invasive activity of parthenolide and 3-isopropyl-2-methyl-4-methyleneisoxazolidin-5-one (MZ-6) – a new compound with a-methylene-c-lactone motif – on two breast cancer cell lines. *Chem Biol Drug Des* 79:112–120

# Chapter 10

## Mode of Action on *Trypanosoma* and *Leishmania* spp.



María E. Lombardo and Alcira Batlle

**Abstract** In this chapter, the most common molecular targets and mechanisms of action of anti-trypanosomatid drugs are described: biosynthesis of sterols, trypanothione pathway, purine salvage pathway, cysteine proteinases, trans-sialidase, metalloproteases, tubulin, calcium homeostasis and pyrophosphate metabolism, heme uptake and degradation, glycolytic pathway, DNA interaction, oxidative stress and apoptosis. Interaction of the sesquiterpene lactones with heme, the induction of oxidative stress, the inhibition of enzymes as cruzipain and trypanothione reductase, the apoptosis induction and the ability of this type of compounds to inhibit sterol biosynthesis will be also discussed.

**Keywords** Anti-trypanosomatid drugs · Drug targets · Sterol biosynthesis · Trypanothione pathway · Proteinases · Trans-sialidase · Tubulin · Heme · Oxidative stress · Apoptosis

### 10.1 Introduction

Among the pathogenic parasites which affect human, trypanosomatids, such as trypanosomes and leishmanias, can be found. These parasites are the causative agents of American trypanosomiasis or Chagas' disease (*Trypanosoma cruzi*), African trypanosomiasis or sleeping sickness (*Trypanosoma brucei*) and leishmaniasis

---

M. E. Lombardo (✉)

Universidad de Buenos Aires, Facultad de Ciencias Exactas y Naturales, Departamento de Química Biológica, Buenos Aires, Argentina

CONICET – Universidad de Buenos Aires, Centro de Investigaciones sobre Porfirinas y Porfirias (CIPYP), Buenos Aires, Argentina

e-mail: [elombardo@fcen.uba.ar](mailto:elombardo@fcen.uba.ar)

A. Batlle (✉)

CONICET – Universidad de Buenos Aires, Centro de Investigaciones sobre Porfirinas y Porfirias (CIPYP), Buenos Aires, Argentina

(*Leishmania* spp.) The World Health Organization includes trypanosomiasis and leishmaniasis among the group of neglected tropical diseases. These diseases are more prevalent in poor populations, not representing an interesting market for the pharmaceutical industry; efficient vaccines have not been developed; chemotherapy is not always effective, as it presents serious side effects and drug resistance phenomena often occur. Moreover, globalization and migratory currents have favoured the expansion of these diseases into nonendemic zones. Therefore, the need for new and efficient therapeutic and diagnostic alternatives has become evident.

The ideal anti-trypanosomatid drug must attack the parasite with the higher rate of selectivity as possible, due to the fact that not harming or interacting with the host is of great importance to minimize side effects. Molecular structures used as therapeutic agents should show differences with the corresponding analogues in the mammalian host. However, selectivity is not the only parameter that guarantees drug efficiency; it is also needed that the selected target be vital for the parasite. For a target to be validated as such, the drugs (either natural products or drugs designed and optimized in silico) that interact selectively with it must show high efficiency.

The knowledge acquired about the basic parasite biochemistry, the application of genetic engineering techniques and the development of bioinformatics and computational techniques are key elements for the identification of these targets. As to *Leishmania* spp. *T. cruzi* and *T. brucei* concern, their respective genomes are known. Therefore, with this information, a comparative genomic analysis with the human genome, or between them, is of great help at the moment of postulating possible therapeutic targets (Jiang and Zhou 2005; Katsila et al. 2016).

## 10.2 Molecular Targets

Herein, the most common molecular targets for anti-trypanosomatid drugs are described, together with possible mechanisms of action for sesquiterpene lactones (STLs).

### 10.2.1 Biosynthesis of Sterols

Unlike mammalian cells, which synthesize cholesterol, in trypanosomatids, fungi and yeasts, the sterol synthesis leads to the formation of ergosterol (Fig. 10.1). Sterols (mainly ergosterol and 24-methylsterols) are essential components of the cell membrane. These sterols are not supplied by neither the vector nor the host cell. The sterol biosynthetic route with its inhibitors is schematized in Fig. 10.1.

One of the enzymes on which inhibitors have been tested is squalene synthase (SQS) that catalyses the formation of squalene from two molecules of farnesyl pyrophosphate (FPP). This enzyme is inhibited by two synthetic derivatives of quinuclidine, namely, ER-119884 and E5700 (Tsukuba Research Laboratories, Eisai

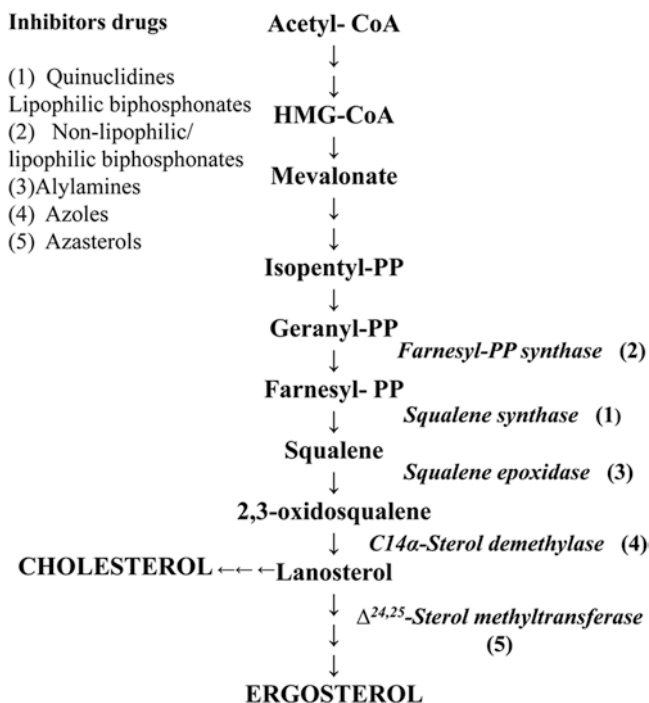


**Fig. 10.1** Sterol biosynthetic pathway in trypanosomatids. Reaction steps and the enzymes involved (indicating inhibitory drugs) in ergosterol biosynthesis are depicted. HMG-CoA 3-hydroxy-3-methyl-glutaryl-CoA, PP- pyrophosphate

Co), for which a strong antiparasitic activity against *T. cruzi* (Urbina et al. 2004) and *L. amazonensis* (Fernandes Rodrigues et al. 2008) has been reported. Other important inhibitors of this enzyme are the lipophilic bisphosphonates (Shang et al. 2014), which have also proved to have a considerable inhibitory effect on farnesyl pyrophosphate synthase (FPPS). The usefulness of lipophilic bisphosphonates has been discovered during the process of improving the inhibitory activity of nitrogen-containing bisphosphonate drugs, such as incadronate and ibandronate, which had been reported to be potent inhibitors of human FPPS and SQS (Amin et al. 1992). The nitrogen-containing bisphosphonates have great disadvantages as antiparasitic agents. Firstly, these drugs have a strong binding capacity to human bone mineral (Kavanagh et al. 2006; Mukherjee et al. 2009), and secondly, they are highly polar molecules, which makes the crossing of the plasma membrane to enter the cell difficult.

However, the capacity of lipophilic bisphosphonates to inhibit the synthesis of ergosterol (SQS and FPPS) in more than one point makes them attractive candidates to be evaluated as anti-trypanosomatids drugs. The crystallographic study of *T. cruzi* SQS has allowed not only to carry out a comparative study with human SQS but also to superimpose the molecular structure of ER-119884, E5700 and four representative lipophilic bisphosphonates (BPH-1218, BPH-1237, BPH-1325,

BPG-1344) with that of the enzyme, thus elucidating the structural requirements for these inhibitors to block the active site of SQS (Shang et al. 2014).

Another enzyme belonging to the sterol biosynthetic pathway, for which inhibitors have been tested, is the squalene epoxidase, which converts squalene into 2,3-oxidosqualene. Allylamines, such as terbinafine, are known inhibitors of the enzyme. Antiproliferative effects and ultrastructural alterations induced in vitro by terbinafine on *L. amazonensis* promastigotes and intracellular amastigotes have been reported (Vannier-Santos et al. 1995). The drug is not capable of eradicating the infection by itself, but its activity increases when combined with other inhibitors of the ergosterol pathway. The inhibition of this pathway can also be achieved at the C14 $\alpha$ -sterol demethylase level by azoles, such as ketoconazole or itraconazole, which are effective for the treatment of superficial and systematic mycoses (Buckner 2008; McCall et al. 2015). These commercially available compounds have not been efficient neither in patients nor in animal models of *T. cruzi* infection (McCabe 1988; Moreira et al. 1992; Brener et al. 1993); however, when combined with other drugs, their efficiency could be enhanced. The combination terbinafine with ketoconazole increases almost a hundredfold the activity of terbinafine alone (Vannier-Santos et al. 1995). Moreover, benznidazole, when combined with itraconazole, is more efficient than benznidazole alone in eliminating parasites from the blood. The combination, thus, allows reducing the benznidazole dosage notably (Assíria Fontes Martins et al. 2015). Amiodarone and itraconazole have also shown a synergistic activity (Paniz-Mondolfi et al. 2009). Likewise for azoles, which interact at the C14 $\alpha$ -sterol demethylase level, a series of triazole derivatives have shown great antiparasitic potency. The latter group of drugs includes posaconazole (SCG56592), ravuconazole (BMS 207, 147) and TAK-187, among others (Urbina 2001; Buckner 2008). These compounds are capable of inducing radical parasitological cure both during acute and chronic infections caused by *T. cruzi*. Besides, these drugs are active orally, and they exert little or no toxic effects in mammal cells and are active against nitrofuran- and nitroimidazole-resistant *T. cruzi* strains (Urbina 2010). In humans, posaconazole has shown a considerable synergistic effect with quinuclidine E5700 (Shang et al. 2014), amiodarone (Veiga-Santos et al. 2012) and with benznidazole. Two clinical trials, CHAGASAZOL and E1224, were carried out to analyse the effect of posaconazole and ravuconazole, respectively. In both cases these drugs were compared to benznidazole. These trials demonstrated that azoles are not effective as monotherapy for the treatment of patients in the indeterminate phase of Chagas' disease, unlike benznidazole, which proved to be an efficacious drug to maintain sustained clearance of the parasite even 1 year later (Chatelain 2015).

The enzyme  $\Delta^{24,25}$ -sterol methyltransferase is involved in the last steps of the biosynthetic ergosterol pathway. This enzyme is present in trypanosomatids but not in the mammalian host, which renders it a potential therapeutic target. Although azasterols are inhibitors of this enzyme, it has been demonstrated that, though these compounds have suppressor effect, they are ineffective to cure and to prevent disease progression (Urbina 2010).

The interference with the synthesis of sterols is a very interesting therapeutic target. The interaction of drugs with ergosterol can be detrimental to the parasite, since this interaction brings about an alteration of cell membrane permeability, causing the loss of small ions, mainly  $K^+$  and cell death. This mechanism of action would account for the antileishmanial effect of amphotericin B. Miltefosine would exert its effects by interacting with phospholipids and membrane sterols (Silva-Jardim et al. 2014).

### 10.2.2 Trypanothione Pathway

The trypanothione (N1,N8-bis(glutathionyl)-spermidine) is the main low molecular weight thiol that is exclusively present in trypanosomatids. This thiol in an equilibrium between its oxidized and reduced forms,  $TS_2$  and  $T(SH)_2$ , respectively, plays a key role in maintaining the intracellular redox state (Manta et al. 2013). Being the trypanosomatids' aerobic organisms, they are exposed to oxidative and nitrosative stress originated from the host and parasite cellular metabolisms. The trypanothione thiol groups play a key role in the parasite's antioxidative defence system. The trypanothione-based redox metabolism provides the reduction equivalents for both detoxification of peroxides by the tryparedoxin peroxidase and ascorbate peroxidase and for the biosynthesis of deoxyribonucleotides by the ribonucleotide reductase (Leroux and Krauth-Siegel 2016). The intracellular levels of  $TS_2$  and  $T(SH)_2$  are regulated by the activity of two enzymes, the trypanothione synthetase (Try-S), which is the enzyme that catalyses the synthesis of trypanothione disulphide ( $TS_2$ ), and the trypanothione reductase (Try-R), which catalyses the NADPH-dependent reduction of  $TS_2$  to  $T(SH)_2$ . In kinetoplastids, the trypanothione/Try-R system performs functions that are equivalent to the glutathione/glutathione reductase system in mammals. Since both Try-S and Try-R are specific for trypanosomatids and essential for their multiplication, they are promising targets for the development of selective inhibitors.

Kinetic studies performed on Try-S from different trypanosomatids, along with data obtained from structural analyses, have shown the low specificity of the enzyme to spermidine. This finding allows postulating the use of polyamines, which are analogous to spermidine, as inhibitors of this enzyme (Leroux and Krauth-Siegel 2016). Regarding the identification of potential inhibitors, the use of the high-throughput screening techniques has allowed to analyse compound libraries with the purpose of developing lead molecules targeting Try-S (Leroux and Krauth-Siegel 2016).

As for Try-R, three kinds of inhibitors have been considered: competitive inhibitors, irreversible inhibitors and subversive substrates. The tridimensional structure of this enzyme in its three stages (free enzyme and enzyme-substrate and enzyme-inhibitor complexes) is known and has allowed the rational design of drugs which behave as Try-R inhibitors. In addition, the differences existing between the active sites of Try-R and glutathione reductase allow the design of inhibitors that are

specific for one of them (Steenkamp 2002). Many non-structurally related compounds have shown inhibitory activity, i.e. polyamine derivatives, tricyclic aromatic compounds, amino diphenyl sulphides, peptidic derivatives and (terpyridine) platinum (II) complexes (Leroux and Krauth-Siegel 2016; Steenkamp 2002; Chawla and Madhubala 2010; Sueth-Santiago et al. 2017). Even if these compounds act as possible Try-R inhibitors, the antiparasitic activity that they have displayed correlated poorly with the inhibitory potency against Try-R. This phenomenon could be due either to the parasite being able to survive with only 10% of the enzyme activity, to limited uptake of the drug into the parasite, or to the fact that, in vivo, the inhibitor showed affinity for another target, rather than Try-R (Leroux and Krauth-Siegel 2016).

Finally, Try-S and Try-R are not the only trypanothione pathway targets; the enzymes involved in the synthesis of spermidine such as ornithine decarboxylase (ODC) and S-adenosylmethionine decarboxylase (AdoMetDC) are also considered interesting for the development of new drugs against trypanosomiasis and leishmaniasis (Heby et al. 2007).

### 10.2.3 Purine Salvage Pathway

Trypanosomatid parasites lack the enzymes necessary for the de novo synthesis of purines; therefore, they depend on the salvage pathway of purines to synthesize purine nucleotides from purine bases from the mammalian host (Fig. 10.2). In this sense, both the transport mechanisms of purine bases into the parasite cell and the enzymes of the salvage route become attractive targets to kill the parasite. Although the transporters of both the bases and their nucleosides are different from those of the host in terms of specificity, the multiplicity of transporters present in trypanosomatids (Chawla and Madhubala 2010) makes it difficult to efficiently block them to cause parasite death. As for the enzymes involved in the purine salvage pathway

**Fig. 10.2** Enzymes involved in the purine salvage pathway. PRPP phosphoribosyl pyrophosphate

- 1) **Adenine phosphoribosyl transferase (APRT)**  
Adenine + PRPP  $\rightarrow$  AMP + Ppi
- 2) **Hypoxanthine-guanine phosphoribosyl transferase (HGPRT)**  
Hypoxanthine + PRPP  $\rightarrow$  IMP + PPI  
Guanine + PRPP  $\rightarrow$  GMP + Ppi
- 3) **AMP deaminase**  
AMP  $\rightarrow$  IMP + NH<sub>3</sub>
- 4) **Adenosine deaminase**  
Adenosine  $\rightarrow$  Inosine + NH<sub>3</sub>
- 5) **Nucleoside quinase**  
Adenosine + ATP  $\rightarrow$  AMP + ADP  
Guanosine + ATP  $\rightarrow$  GMP + ADP  
Inosine + ATP  $\rightarrow$  IMP + ADP



(Fig. 10.2), they have been identified and found to differ significantly from those of the host, basically as specificity towards the substrate concerns. Allopurinol (hypoxanthine analogue) is an inhibitor of the hypoxanthine-guanine phosphoribosyl transferase (HGPRT) which has shown antiparasitic activity against *Leishmania* and *T. cruzi* (Maya et al. 2007; Raviolo et al. 2013). Allopurinol is phosphorylated by the HGPRT to be incorporated into the nucleic acids as a nonphysiological nucleotide, thus disrupting the synthesis of nucleic acids and the synthesis of proteins, leading to parasite death. Phthalic anhydride derivatives and phthalimide can also be used as structural analogues of purine bases. As trypanosomatids have many alternative pathways for the salvage of purines, the enzymes involved in this process are not essential for parasite survival; therefore, either the simultaneous blockade of more than one enzyme or the combined treatment with other antiparasitic drugs could be effective as therapeutic alternative.

#### 10.2.4 Cysteine Proteinases

In trypanosomatids, the cysteine proteinases, which are homologous to mammalian cathepsins, are the most characterized enzymes. They have become an interesting therapeutic target not only because they are structurally different from their homologues in mammals but also for their role in the host-parasite interaction as putative virulence factors.

Cruzipain is a cathepsin L cysteine proteinase present in *T. cruzi*. This enzyme is encoded by a gene whose expression is under different regulatory mechanisms in the different parasite stages suggesting specific functions for the regulation in each stage (Alvarez et al. 2012). Furthermore, the location of this enzyme varies with the stage, being located in reservosomes, lysosomes and the cell surface and in epimastigotes, trypomastigotes and amastigotes, respectively (Sueth-Santiago et al. 2017; Alvarez et al. 2012). The first designed inhibitors were peptides capable of binding irreversibly to the enzyme, such as diazomethylketone, vinyl sulfone and fluoromethylketone derivatives (Kerr et al. 2009). Non-peptidic inhibitors have also been developed, such as cyclic thiosemicarbazones, nitrile-based inhibitors, benidipine and clofazimine (Ferreira et al. 2010; Caputto et al. 2011; Sbaraglini et al. 2016; Burtoloso et al. 2017). Cruzipain inhibitors have been used in murine models of chronic and acute infections, obtaining parasitological cure with minimum toxicity; however, high doses were required due to their short half-life.

An analysis of the *Leishmania major* genome has shown the presence of about 65 cysteine proteinases, some of which are of the cathepsin L type and others of the cathepsin B type, which are involved in the host-parasite interaction (Chawla and Madhubala 2010). Moreover, a natural inhibitor of cysteine proteinases from *L. mexicana* has been characterized and has proved to be a potent inhibitor of cathepsin B cysteine proteinase. BALB/c mice infected with mutants overexpressing such inhibitors were able to resolve the infection faster than the control group infected with wild-type parasites (Bryson et al. 2009).

In *T. brucei*-infected mice treated with carbobenzoxy-phenylalanyl-alanine diazomethylketone, (Z-Phe-Ala-CHN<sub>2</sub>), which is a cathepsin B-cysteine proteinase inhibitor, it is observed that this inhibition depletes the parasite of essential nutrients necessary for DNA synthesis, preventing the progression of the cell cycle (Scory et al. 2007). This *T. brucei* cysteine proteinase has been demonstrated to have differences with its mammalian counterpart, thus being a promissory target for drug design (Kerr et al. 2010).

### 10.2.5 *Trans-sialidase*

Trans-sialidase (TS) was identified in *T. cruzi* three decades ago. This enzyme is expressed in the trypomastigote form; it is located on the external surface of the parasite and is anchored as a non-integral membrane protein to glycosylphosphatidylinositol, which promotes its secretion to the extracellular environment to act on specific phospholipases. Unlike classic sialidases that hydrolyse sialic acid residues of glycoproteins and/or glycolipids, the TS catalyses the transference of sialic acid residues between glycoconjugates. Sialic acid is not produced by the parasite, and it is one of the most important sugars in the parasite recognition of the mammalian cell. In trypomastigotes, TS allows the parasite to transfer sialic acid from the host cell to its own. In this way, the parasite is no longer recognized as a foreign agent and can then infect host cells without triggering the immune response (Dc-Rubin and Schenkman 2012; Miller and Roitberg 2013). It is known that decreased levels of TS expression could contribute to the loss of *T. cruzi* trypomastigote virulence (San Francisco et al. 2017). Since this enzyme plays a crucial role in parasite survival, a large number of genes encoding highly related but enzymatically inactive proteins are present in the parasite's genome. These proteins, which are expressed simultaneously, would serve to neutralize both antibodies and inhibitors directed to TS. This fact, added to the multiple roles that TS plays in both the biology of the parasite and in the development of Chagas' disease, renders TS difficult to inhibit. The inhibitors tested so far have proved to be weak and non-specific, with high inhibition constants that were in the millimolar order. Inhibitors of the enzymes that hydrolyse sialic acid (sialidase), sialic acid derivatives (compounds that covalently bind to Tyr342 present in the active site of the enzyme), sugar derivatives (such as lactitol, which competes with sialic acid) and sialic acid analogues capable of inhibiting their transfer were tested as inhibitors, but none of them have shown good activity (Sueth-Santiago et al. 2017). Currently, research works are still ongoing to find new chemical scaffolds to inhibit TS.

### 10.2.6 *Tubulin*

Tubulin is a protein that forms microtubules, which are cytoskeletal filaments that are responsible for maintaining the main functions of eukaryotic cells. Such functions include the segregation of chromosomes during cell division, the transport of intracellular components and the maintenance of the cell shape, cell motility and distribution of plasma membrane components (Sueth-Santiago et al. 2017). Tubulin is present in two isoforms, namely,  $\alpha$ - and  $\beta$ -tubulin, which polymerize to form a filamentous cylindrical structure called protofilament. The microtubule, which is formed from a protofilament grouping, is a dynamic structure in which polymerization/depolymerization phenomena coexist in equilibrium. Thus, the microtubule size can change to adapt to different situations, such as those arising during the cell cycle. Cell division and parasite motility are highly dependent on the polymerization/depolymerization equilibrium of tubulin and are essential for infection maintenance. In spite of the structural similarity between the tubulins of the different species, different inhibitors have shown a selective recognition. This behaviour would indicate that the small differences existing between tubulins would function as recognition sites for the different inhibitors. Since the parasite proliferation kinetics is comparable to the cancer cell and certain antineoplastic compounds bind to tubulin, they are also expected to display antiparasitic activity. Thus, anti-*T. cruzi* activity has been reported for taxol, curcumin and natural amidepiperins (Baum et al. 1981; Chakraborti et al. 2011; Sueth-Santiago et al. 2016; Freire-de-Lima et al. 2011).

### 10.2.7 *Homeostasis of Calcium and Pyrophosphate Metabolism*

In trypanosomatids,  $\text{Ca}^{2+}$  plays an important role in different cellular functions, such as flagellar movement, differentiation, depolarization of microtubules, host cell invasion and immune response evasion mechanisms, such as antigenic variation (Benaim and Garcia 2011). As in other eukaryotic cells, in trypanosomatids, the disruption of  $\text{Ca}^{2+}$  homeostasis leads to cell death by apoptosis or necrosis. As regards the intracellular regulation of  $\text{Ca}^{2+}$ , trypanosomatids possess a single mitochondrion that occupies 12% of the total volume of the parasite. In this mitochondrion large amounts of  $\text{Ca}^{2+}$  are accumulated. In addition, an endoplasmic reticulum  $\text{Ca}^{2+}$ -ATPase, a plasma membrane  $\text{Ca}^{2+}$ -ATPase and large amounts of calmodulin are also involved in the regulation of  $\text{Ca}^{2+}$  levels. Trypanosomatids also have acidocalcisomes, which are organelles that play a role in the bioenergetics of these parasites, acting as the main reservoir of  $\text{Ca}^{2+}$  ions together with polyphosphates (mostly pyrophosphate). Within the parasite, the pyrophosphate is hydrolysed by pyrophosphatases, constituting an alternative mechanism to the hydrolysis of ATP to obtain energy. Both the hydrolysis of pyrophosphate and the homeostasis of  $\text{Ca}^{2+}$  are vital

for the parasite and therefore attractive therapeutic targets. Examples of inhibitors of these events are the bisphosphonates (non-metabolizable analogues of pyrophosphate) that inhibit pyrophosphatases and reactions involving pyrophosphate (Galaka et al. 2017), crystal violet and pentamidine that inhibit the plasma membrane  $\text{Ca}^{2+}$ -ATPase and antiarrhythmic drugs (amiodarone, dronedarone) that destabilize the intracellular  $\text{Ca}^{2+}$  homeostasis by altering the mitochondrial electrochemical potential and by alkalizing acidocalcisomes (Serrano-Martín et al. 2009; Benaim et al. 2012; Benaim and Paniz Mondolfi 2012; Benaim et al. 2014).

### 10.2.8 Uptake and Degradation of Heme

Heme is a fundamental molecule for parasite survival that must be acquired from both vertebrate and invertebrate hosts, for the parasite cannot biosynthesize it (Ciccarelli et al. 2007; Tripodi et al. 2011); however, an excessive amount of free heme is known to be toxic for the parasite. Therefore, an efficient control of its uptake, transport and degradation is required in order to avoid the generation of intracellular oxidative stress. Since both excessive and deficient heme levels lead to parasite death, this molecule becomes an important target for the development of antiparasitic drugs.

In trypanosomatids, several proteins involved in the heme uptake and transport have been identified. Although the mechanism involved in heme transport across biological membranes is not fully understood, experimental data indicate the participation of ATP-binding cassette (ABC) transporters in this process (Cupello et al. 2011; Campos-Salinas et al. 2011). In *Leishmania amazonensis*, LHR1, which is a transmembrane protein that mediates the transport of extracellular heme inside the cell, has been identified (Huynh et al. 2012). Syntenic genes with high-sequence identity to LHR1 have been recognized in the genome of several *Leishmania* species, *T. cruzi* and *T. brucei* (Huynh et al. 2012). Merli et al. (2016) have identified and characterized a *T. cruzi* protein (TcHTE) with 55% of sequence homology to LHR1. TcHTE has been found to be located in the flagellar pocket, where the transport of nutrients occurs. As mentioned above, the degradation of heme is also an important event to avoid its cytotoxic effects. In this regard, both *Leishmania* spp. and *T. cruzi* have been demonstrated to have heme oxygenase activity, which transforms the heme into biliverdin, thus accomplishing heme detoxification (Ciccarelli et al. 2007; Cupello et al. 2011; Lechuga et al. 2016).

It is expected that both, heme structural analogues (which compete with heme for its uptake and/or use) and drugs that act as heme-drug complexes (which may inhibit heme degradation), would then display trypanocidal activity. Thus, vitamin B12 (cyanocobalamin) has shown marked antiparasitic activity against the three stages of *T. cruzi* in vitro and on an acute murine model of Chagas' disease (Ciccarelli et al. 2012). Likewise hemin and vitamin B12 would exert its anti-*T. cruzi* effect through the generation of reactive oxygen species.

**Table 10.1** Other possible targets to consider for the design of new anti-trypanosomatid drugs

Targets	Mechanism of action	Reference
Glycolytic pathway	Inhibition of glycolytic enzymes: phosphofructokinase, pyruvate kinase and glyceraldehyde 3-phosphate dehydrogenase	Rodenko et al. (2007), Nowicki et al. (2008), Benaim et al. (2014)
DNA topoisomerases I and II	Inhibits of kinetoplast DNA replication	Babokhov et al. (2013)
Metalloprotease	Inhibition of metalloproteases of the M32 family	Alvarez et al. (2012), Frasci et al. (2012), Alvarez et al. (2013)

Other targets considered for the search of new anti-trypanosomatid drugs are summarized in Table 10.1.

### 10.3 Oxidative Stress and Apoptosis

Oxidative stress and programmed cell death (PCD) arise as consequences of the interaction of drugs with their therapeutic targets.

Oxidative stress emerges from biologic oxidations that generate oxygen-reduction products such as  $O_2^-$ ,  $H_2O_2$  and/or  $OH^\cdot$ , which are known as reactive oxygen species (ROS). These products cause an oxidative damage that the cellular antioxidant defence system must counteract. Trypanosomatids have an antioxidant defence system (Turrens 2004) which differs notably from that of the host cell (Fig. 10.3). In the parasite, trypanothione behaves in a similar way to glutathione in the host cell. Both cell types possess superoxide dismutase, but trypanosomatids lack catalase, the role of which is replaced by peroxidases. These differences render the parasite more sensitive to the action of ROS, in comparison to the host cell. In conclusion, oxidative stress is produced as a response to a redox unbalance that the antioxidant defence system of the parasite cannot compensate. The imbalance caused by an antiparasitic drug could be the result of its intracellular reduction followed by autoxidation (yielding ROS), its interaction with the heme or with other molecules that generate ROS that the parasite cannot metabolize, or acting as a Try-R or Try-S inhibitor, which would decrease the efficacy of the antioxidant defence system.

Different types of cell death may occur in trypanosomatids, such as apoptosis or PCD (Proto et al. 2013). Although the apoptotic pathway in trypanosomatids has very similar features to that of mammalian cells, such as lipid peroxidation, increase in cytosolic  $Ca^{2+}$  levels, changes in mitochondrial membrane potential, the release of cytochrome C from the mitochondrion to the cytoplasm and induction of proteases and DNA fragmentation, trypanosomatids lack their classical effectors or regulators like the TNF-related family of receptors, Bcl-2 family members and caspases. However, they possess an endogenous basic machinery constituted by proteins that

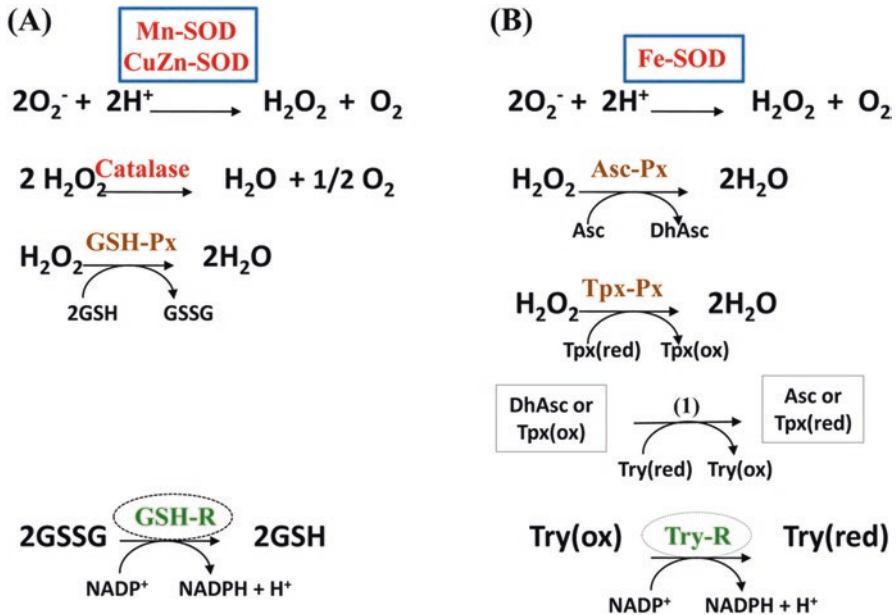


**Fig. 10.3** Antioxidant defence enzymatic system in mammalian cells (a) and trypanosomatids (b) GSH glutathione, GSSG oxidized glutathione, Try trypanothione, (ox) oxidized state, (red) reduced state, Asc ascorbate, DhAsc dehydroascorbate, (1) spontaneous reaction, SOD superoxide dismutase, GSH-Px glutathione peroxidase, GSH glutathione reductase, Asc-Px ascorbate peroxidase, Tpx-Px tryparedoxin peroxidase, Try-R trypanothione reductase

control both the cycle and cell differentiation, such as proto-oncogenes, cyclin and cyclin-dependent kinases, which lead to death in a regulated manner. Cell cycle deregulation, heat shock, antiparasitic drugs, nutrient deprivation and ROS are some of the stimuli that can lead to apoptosis in trypanosomatids (Smirlis et al. 2010). Induction of PCD is a particularly important characteristic of antichagasic drugs, due to the fact that apoptosis suppresses the inflammatory response. Taking into consideration that the major cause of myocarditis in chagasic chronic patients is the maintenance of a pro-inflammatory response (Vieira et al. 2012), an antiparasitic drug that induces PCD would not only kill the parasite but also would have a beneficial effect on the host.

## 10.4 Natural Sesquiterpene Lactones: Parasitic Effects and Probable Targets in Trypanosomatids

Although there are a significant number of reports that describe the anti-trypanosomatid activity of different natural sesquiterpene lactones (Brenagio et al. 2000; Schmidt et al. 2002; Jimenez-Ortiz et al. 2005; Saúde-Guimarães et al. 2007;

**Table 10.2** Mechanism of action reported for anti-trypanosomatid sesquiterpene lactones

Sesquiterpene lactones	Mechanism	Parasite tested	References
Dehydroleucodine	Intracellular redox imbalance	<i>Trypanosoma cruzi</i>	Brengio et al. (2000)
Mexicanin Helenalin	Intracellular redox imbalance different from dehydroleucodine	<i>Trypanosoma cruzi</i>	Jimenez-Ortiz et al. (2005)
Mexicanin I Dehydroleucodine Psilostachyin	Oxidative stress induction	<i>Leishmania mexicana</i>	Barrera et al. (2013)
Dehydroleucodine Helenalin	Programmed cell death Induction	<i>Trypanosoma cruzi</i>	Jimenez et al. (2014)
Psilostachyin Psilostachyin C	Hemin interaction Ergosterol biosynthesis inhibition	<i>Trypanosoma cruzi</i>	Sülsen et al. (2016)

Sülsen et al. 2008; Karioti et al. 2009; Sülsen et al. 2011; Barrera et al. 2013; Sülsen et al. 2013; Jimenez et al. 2014; Sülsen et al. 2016), little is known about neither their mechanisms of action nor the molecular targets. The mechanisms of action of STLs are summarized in Table 10.2.

Brengio et al. (2000) have demonstrated that the anti-*T. cruzi* effect of dehydroleucodine (DhL) could be blocked by the presence of reducing substrates such as glutathione or dithiothreitol. However, these agents were not able to reverse the effect of DhL if they were added 2 days after the beginning of drug exposure. Based on these results, an intracellular redox imbalance has been proposed to explain the antiparasitic effect of DhL.

The STLs, mexicanin I (Mxn) and helenalin (Hln), have been reported to be equally active against the trypomastigote and epimastigote forms of *T. cruzi* (Schmidt et al. 2002; Jimenez-Ortiz et al. 2005). Since the reducing agents dithiothreitol and beta-mercaptoethanol were not able to reverse the trypanocidal effect of both compounds, it was concluded that Mxn I and Hln are deleterious for *T. cruzi* epimastigotes and that their mode of action would be different than that of the related STL DhL.

To explain the antiproliferative effect of Mxn, DhL and psilostachyin (Psi) on *Leishmania mexicana* promastigotes, Barrera et al. (2013) postulated a direct interaction of the drugs with intracellular sulfhydryl groups. This interaction would alter the non-enzymatic antioxidant defence system, which generates an oxidative stress leading to parasite death. After a short-time treatment (3 h), the induction of oxidative stress would be at least one of the mechanisms of action of DhL, Mxn and Psi, but not for psilostachyin C (PsiC) that would act through another mechanism (Barrera et al. 2013).

Jimenez et al. (2014) have postulated PCD as a possible new therapeutic target. In this sense, they have investigated the induction of PCD in *T. cruzi* by DhL and Hln in comparison with the two conventional drugs, benznidazole and nifurtimox. Both STLs induced PCD in epimastigotes and trypomastigotes, while the conventional drugs did not. This fact could indicate that STLs could act through a different

mechanism of action to kill the parasite. When combined with either benznidazole or nifurtimox, DhL displayed an increased trypanocidal activity. Therefore, the use of both DhL and Hln alone or combined with conventional drugs may be proposed as a potential new therapeutic schedule for the treatment of Chagas' disease.

Artemisinin is an STL that is used as an antimalarial drug, which exerts its activity through heme binding (Schmidt et al. 2012). Taking this phenomenon into consideration, Psi and PsiC, two STLs isolated from plants of the genus *Ambrosia*, have been tested for hemin binding (Sülsen et al. 2016). The results obtained by Sülsen et al. (2016) have shown that both STLs were capable of interacting with hemin, with this interaction leading to an inhibition of heme detoxification and the generation of oxidative stress within the parasite. After a 4-h treatment of *T. cruzi*, Psi induced a fivefold increase in ROS levels. Conversely, PsiC induced a 1.5-fold increase in ROS levels. These results are in agreement with those obtained by Barrera et al. (2013) in experiments performed on *Leishmania mexicana* in which Psi, but not PsiC, in short-time treatment, increased the generation of ROS inside the parasites. Only PsiC was able to inhibit ergosterol biosynthesis, causing an accumulation of squalene upon inhibition of squalene epoxidase. Neither Psi nor PsiC (up to 50  $\mu$ M) inhibited cruzipain and Try-R. It can be concluded that despite their structural similarity, both STLs exerted their anti-*T. cruzi* activity through the interaction with different targets. Psi accomplished its antiparasitic effect by interacting with hemin, while PsiC interfered with sterol synthesis. Both STLs induced parasite death by apoptosis. The same type of cell death was observed by Jimenez et al. (2014) for epimastigotes and trypomastigotes of *T. cruzi* treated with DhL or Hln.

Further studies need to be performed in order to characterize the mechanism of action that accounts for the antiprotozoal activity of STLs.

## References

- Alvarez VE, Niemirowicz GT, Cazzulo JJ (2012) The peptidases of *Trypanosoma cruzi*: digestive enzymes, virulence factors, and mediators of autophagy and programmed cell death. *Biochim Biophys Acta* 1824:195–206
- Alvarez VE, Niemirowicz GT, Cazzulo JJ (2013) Metacaspases, autophagins and metalloproteases: potential new targets for chemotherapy of the trypanosomiasis. *Curr Med Chem* 20:3069–3077. Review
- Amin D, Cornell SA, Gustafson SK et al (1992) Bisphosphonates used for the treatment of bone disorders inhibit squalene synthase and cholesterol biosynthesis. *J Lipid Res* 33:1657–1663
- Assíria Fontes Martins T, de Figueiredo Diniz L, Mazzeti AL et al (2015) Benznidazole/itraconazole combination treatment enhances anti-*Trypanosoma cruzi* activity in experimental Chagas disease. *PLoS One* 10:e0128707
- Babokhov P, Sanyaolu AO, Oyibo WA et al (2013) A current analysis of chemotherapy strategies for the treatment of human African trypanosomiasis. *Pathog Glob Health* 107:242–252
- Barrera P, Sülsen VP, Lozano E et al (2013) Natural sesquiterpene lactones induce oxidative stress in *Leishmania mexicana*. *Evid Based Complement Alternat Med* 2013:163404



- Baum SG, Wittner M, Nadler JP et al (1981) Taxol, a microtubule stabilizing agent, blocks the replication of *Trypanosoma cruzi*. Proc Natl Acad Sci U S A 78:4571–4575
- Benaim B, Garcia CR (2011) Targeting calcium homeostasis as the therapy of Chagas' disease and leishmaniasis – a review. Trop Biomed 28:471–481
- Benaim G, Paniz Mondolfi AE (2012) The emerging role of amiodarone and dronedarone in Chagas disease. Nat Rev Cardiol 9:605–609
- Benaim G, Hernandez-Rodriguez V, Mujica-Gonzalez S et al (2012) In vitro anti-*Trypanosoma cruzi* activity of dronedarone, a novel amiodarone derivative with an improved safety profile. Antimicrob Agents Chemother 56:3720–3725
- Benaim G, Casanova P, Hernandez-Rodriguez V et al (2014) Dronedarone, an amiodarone analog with improved anti-*Leishmania mexicana* efficacy. Antimicrob Agents Chemother 58:2295–2303
- Brener Z, Cañado JR, Galvão LM et al (1993) An experimental and clinical assay with ketoconazole in the treatment of Chagas disease. Mem Inst Oswaldo Cruz 88:149–153
- Bregio S, Belmonte S, Guerreiro E et al (2000) The sesquiterpene lactone dehydroleucodine (DhL) affects the growth of cultured epimastigotes of *Trypanosoma cruzi*. J Parasitol 86:407–412
- Bryson K, Besteiro S, McGachy HA et al (2009) Overexpression of the natural inhibitor of cysteine peptidases in *Leishmania mexicana* leads to reduced virulence and a Th1 response. Infect Immun 77:2971–2978
- Buckner FS (2008) Sterol 14-demethylase inhibitors for *Trypanosoma cruzi* infections. Adv Exp Med Biol 625:61–80
- Burtoloso AC, de Albuquerque S, Furber M et al (2017) Anti-trypanosomal activity of non-peptidic nitrile-based cysteine protease inhibitors. PLoS Negl Trop Dis 11:e0005343
- Campos-Salinas J, Cabello-Donayre M, García-Hernández R et al (2011) A new ATP-binding cassette protein is involved in intracellular haem trafficking in *Leishmania*. Mol Microbiol 79:1430–1444
- Caputto ME, Fabian LE, Benítez D et al (2011) Thiosemicarbazones derived from 1-indanones as new anti-*Trypanosoma cruzi* agents. Bioorg Med Chem 19:6818–6826
- Chakraborti S, Das L, Kapoor N et al (2011) Curcumin recognizes a unique binding site of tubulin. J Med Chem 54:6183–6196
- Chatelain E (2015) Chagas disease drug discovery: toward a new era. J Biomol Screen 20:22–35
- Chawla B, Madhubala R (2010) Drug targets in *Leishmania*. J Parasit Dis 34:1–13
- Ciccarelli A, Araujo L, Batlle A et al (2007) Effect of haemin on growth, protein content and the antioxidant defence system in *Trypanosoma cruzi*. Parasitology 134:959–965
- Ciccarelli AB, Frank FM, Puente V et al (2012) Antiparasitic effect of vitamin B12 on *Trypanosoma cruzi*. Antimicrob Agents Chemother 56:5315–5320
- Cupello MP, Souza CF, Buchensky C et al (2011) The heme uptake process in *Trypanosoma cruzi* epimastigotes is inhibited by heme analogues and by inhibitors of ABC transporters. Acta Trop 120:211–218
- Dc-Rubin SS, Schenkman S (2012) *Trypanosoma crWuzi* trans-sialidase as a multifunctional enzyme in Chagas' disease. Cell Microbiol 14:1522–1530
- Fernandes Rodrigues JC, Concepcion JL, Rodrigues C et al (2008) In vitro activities of ER-119884 and E5700, two potent squalene synthase inhibitors, against *Leishmania amazonensis*: antiproliferative, biochemical, and ultrastructural effects. Antimicrob Agents Chemother 52:4098–4114
- Ferreira RS, Simeonov A, Jadhav A et al (2010) Complementarity between a docking and a high-throughput screen in discovering new cruzain inhibitors. J Med Chem 53:4891–4905
- Frasch AP, Carmona AK, Juliano L et al (2012) Characterization of the M32 metallo-carboxypeptidase of *Trypanosoma brucei*: differences and similarities with its orthologue in *Trypanosoma cruzi*. Mol Biochem Parasitol 184:63–70
- Freire-de-Lima L, Ribeiro TS, Rocha GM et al (2011) The toxic effects of piperine against *Trypanosoma cruzi*: ultrastructural alterations and reversible blockage of cytokinesis in epimastigote forms. Parasitol Res 102:1059–1067

- Galaka T, Ferrer Casal M, Storey M et al (2017) Antiparasitic activity of sulfur- and fluorine-containing bisphosphonates against trypanosomatids and apicomplexan parasites. *Molecules* 22(1):82. <https://doi.org/10.3390/molecules22010082>
- Heby O, Persson L, Rentala M (2007) Targeting the polyamine biosynthetic enzymes: a promising approach to therapy of African sleeping sickness, Chagas' disease, and leishmaniasis. *Amino Acids* 33:359–366
- Huynh C, Yuan X, Miguel DC et al (2012) Heme uptake by *Leishmania amazonensis* is mediated by the transmembrane protein LHR1. *PLoS Pathog* 8:e1002795
- Jiang Z, Zhou Y (2005) Using bioinformatics for drug target identification from the genome. *Am J Pharmacogenomics* 5:387–396. Review
- Jimenez V, Kemmerling U, Paredes R et al (2014) Natural sesquiterpene lactones induce programmed cell death in *Trypanosoma cruzi*: a new therapeutic target? *Phytomedicine* 21:1411–1418
- Jimenez-Ortiz V, Brengio SD, Giordano O et al (2005) The trypanocidal effect of sesquiterpene lactones helenalin and mexicanin on cultured epimastigotes. *J Parasitol* 91:170–174
- Karioti A, Skaltsa H, Kaiser M et al (2009) Trypanocidal, leishmanicidal and cytotoxic effects of anthecotulide-type linear sesquiterpene lactones from *Anthemis auriculata*. *Phytomedicine* 16:783–787
- Katsila T, Spyroulias GA, Patrinos GP et al (2016) Computational approaches in target identification and drug discovery. *Comput Struct Biotechnol J* 14:177–184. Review
- Kavanagh KL, Guo K, Dunford JE et al (2006) The molecular mechanism of nitrogen-containing bisphosphonates as antiosteoporosis drugs. *Proc Natl Acad Sci* 103:7829–7834
- Kerr ID, Lee JH, Farady CJ et al (2009) Vinyl sulfones as antiparasitic agents and a structural basis for drug design. *J Biol Chem* 284:25697–25703
- Kerr ID, Wu P, Marion-Tsukamaki R et al (2010) Crystal structures of TbCatB and rhodesain, potential chemotherapeutic targets and major cysteine proteases of *Trypanosoma brucei*. *PLoS Negl Trop Dis* 4:e701
- Lechuga GC, Borges JC, Calvet CM et al (2016) Interactions between 4-aminoquinoline and heme: promising mechanism against *Trypanosoma cruzi*. *Int J Parasitol Drugs Drug Resist* 6:154–164
- Leroux AE, Krauth-Siegel RL (2016) Thiol redox biology of trypanosomatids and potential targets for chemotherapy. *Mol Biochem Parasitol* 206:67–74
- Manta B, Comini M, Medeiros A et al (2013) Trypanothione: a unique bis-glutathionyl derivative in trypanosomatids. *Biochim Biophys Acta* 1830:3199–3216
- Maya JD, Cassels BK, Iturriaga-Vásquez P et al (2007) Mode of action of natural and synthetic drugs against *Trypanosoma cruzi* and their interaction with the mammalian host. *Comp Biochem Physiol A Mol Integr Physiol* 146:601–620
- McCabe R (1988) Failure of ketoconazole to cure chronic murine Chagas' disease. *J Infect Dis* 158:1408–1409
- McCall LI, El Aroussi A, Choi JY et al (2015) Targeting ergosterol biosynthesis in *Leishmania donovani*: essentiality of sterol 14 alpha-demethylase. *PLoS Negl Trop Dis* 9:e0003588
- Merli ML, Pagura L, Hernández J et al (2016) The *Trypanosoma cruzi* protein TcHTE is critical for heme uptake. *PLoS Negl Trop Dis* 10:e0004359
- Miller BR, Roitberg AE (2013) *Trypanosoma cruzi* trans-sialidase as a drug target against Chagas disease (American trypanosomiasis). *Future Med Chem* 5:1889–1900
- Moreira AA, de Souza HB, Amato Neto V et al (1992) Evaluation of the therapeutic activity of itraconazole in chronic infections, experimental and human, by *Trypanosoma cruzi*. *Rev Inst Med Trop Sao Paulo* 34:177–180
- Mukherjee S, Huang C, Guerra F et al (2009) Thermodynamics of bisphosphonates binding to human bone: a two-site model. *J Am Chem Soc* 131:8374–8375
- Nowicki MW, Tulloch LB, Worrall L et al (2008) Design, synthesis and trypanocidal activity of lead compounds based on inhibitors of parasite glycolysis. *Bioorg Med Chem* 16:5050–5061

- Paniz-Mondolfi AE, Pérez-Alvarez AM, Lanza G et al (2009) Amiodarone and itraconazole: a rational therapeutic approach for the treatment of chronic Chagas' disease. *Chemotherapy* 55:228–233
- Proto WR, Coombs GH, Mottram JC (2013) Cell death in parasitic protozoa: regulated or incidental? *Nat Rev Microbiol* 11:58–66
- Raviolo MA, Solana ME, Novoa MM et al (2013) Synthesis, physicochemical properties of allopurinol derivatives and their biological activity against *Trypanosoma cruzi*. *Eur J Med Chem* 69:455–464
- Rodenko B, van der Burg AM, Wanner MJ et al (2007) 2,N 6-disubstituted adenosine analogs with antitrypanosomal and antimalarial activities. *Antimicrob Agents Chemother* 51:3796–3802
- San Francisco J, Barría I, Gutiérrez B et al (2017) Decreased cruzipain and gp85/trans-sialidase family protein expression contributes to loss of *Trypanosoma cruzi* trypomastigote virulence. *Microbes Infect* 19:55–61
- Saúde-Guimarães DA, Perry KS, Raslan DS et al (2007) Complete assignments of <sup>1</sup>H and <sup>13</sup>C NMR data for trypanocidal eremantholide C oxide derivatives. *Magn Reson Chem* 45:1084–1087
- Sbaraglini ML, Bellera CL, Fraccaroli L et al (2016) Novel cruzipain inhibitors for the chemotherapy of chronic Chagas disease. *Int J Antimicrob Agents* 48:91–95
- Schmidt TJ, Brun R, Willuhn G et al (2002) Anti-trypanosomal activity of helenalin and some structurally related sesquiterpene lactones. *Planta Med* 68:750–751
- Schmidt TJ, Khalid SA, Romanha AJ et al (2012) The potential of secondary metabolites from plants as drugs or leads against protozoan neglected diseases - part I. *Curr Med Chem* 19:2128–2175
- Scory S, Stierhof YD, Caffrey CR et al (2007) The cysteine proteinase inhibitor Z-Phe-Ala-CHN2 alters cell morphology and cell division activity of *Trypanosoma brucei* bloodstream forms *in vivo*. *Kinetoplastid Biol Dis* 6:2. <https://doi.org/10.1186/1475-9292-6-2>
- Serrano-Martín X, García-Marchan Y, Fernandez A et al (2009) Amiodarone destabilizes intracellular Ca<sup>2+</sup> homeostasis and biosynthesis of sterols in *Leishmania mexicana*. *Antimicrob Agents Chemother* 53:1403–1410
- Shang N, Li Q, Ko TP et al (2014) Squalene synthase as target for Chagas disease therapeutics. *PLoS Pathog* 10:e1004114
- Silva-Jardim I, Thiemann OH, Anibal F de F (2014) Leishmaniasis and Chagas disease chemotherapy: a critical review. *J Braz Chem Soc* 25:1810–1823
- Smirlis D, Duszzenko M, Ruiz AJ (2010) Targeting essential pathways in trypanosomatids gives insights into protozoan mechanisms of cell death. *Parasit Vectors* 3:107. Review
- Steenkamp DJ (2002) Thiol metabolism of the trypanosomatids as potential drug targets. *IUBMB Life* 53:243–248
- Sueth-Santiago V, Moraes JB, Sobral Alves ES et al (2016) The effectiveness of natural diarylheptanoids against *Trypanosoma cruzi*: cytotoxicity, ultrastructural alterations and molecular modeling studies. *PLoS One* 11:e0162926
- Sueth-Santiago V, Decote-Ricardo D, Morrot A et al (2017) Challenges in the chemotherapy of Chagas disease: looking for possibilities related to the differences and similarities between the parasite and host. *World J Biol Chem* 8:57–80
- Sülsen VP, Frank FM, Cazorla SI et al (2008) Trypanocidal and leishmanicidal activities of sesquiterpene lactones from *Ambrosia tenuifolia* Sprengel (Asteraceae). *Antimicrob Agents Chemother* 52:2415–2419
- Sülsen VP, Frank FM, Cazorla SI et al (2011) Psilostachyin C: a natural compound with trypanocidal activity. *Int J Antimicrob Agents* 37:536–543
- Sülsen VP, Cazorla SI, Frank FM et al (2013) Natural terpenoids from *Ambrosia* species are active *in vitro* and *in vivo* against human pathogenic trypanosomatids. *PLoS Negl Trop Dis* 7:e2494
- Sülsen VP, Puente V, Papademetrio D et al (2016) Mode of action of the sesquiterpene lactones psilostachyin and psilostachyin C on *Trypanosoma cruzi*. *PLoS One* 11:e0150526

- Tripodi KE, Menendez Bravo SM, Cricco JA (2011) Role of heme and heme-proteins in trypanosomatid essential metabolic pathways. *Enzyme Res* 201:873230. <https://doi.org/10.4061/2011/87323>
- Turrens JF (2004) Oxidative stress and antioxidant defences: a target for the treatment of diseases caused by parasitic protozoa. *Mol Asp Med* 25:211–220
- Urbina JA (2001) Specific treatment of Chagas disease: current status and new developments. *Curr Opin Infect Dis* 14:733–741
- Urbina JA (2010) Specific chemotherapy of Chagas disease: relevance, current limitations and new approaches. *Acta Trop* 115:55–68
- Urbina JA, Concepcion JL, Caldera A et al (2004) *In vitro* and *in vivo* activities of E5700 and ER-119884, two novel orally active squalene synthase inhibitors, against *Trypanosoma cruzi*. *Antimicrob Agents Chemother* 48:2379–2387
- Vannier-Santos MA, Urbina JA, Martiny A et al (1995) Alterations induced by the antifungal compounds ketoconazole and terbinafine in *Leishmania*. *J Eukaryot Microbiol* 42:337–346
- Veiga-Santos P, Barrias ES, Santos JF et al (2012) Effects of amiodarone and posaconazole on the growth and ultrastructure of *Trypanosoma cruzi*. *Int J Antimicrob Agents* 40:61–71
- Vieira PM, Francisco AF, Machado EM et al (2012) Different infective forms trigger distinct immune response in experimental Chagas disease. *PLoS One* 7:e32912

# Chapter 11

## Contribution of Microscopy for Understanding the Mechanism of Action Against Trypanosomatids



Esteban Lozano, Renata Spina, Patricia Barrera, Carlos Tonn,  
and Miguel A. Sosa

**Abstract** Transmission electron microscopy (TEM) has proved to be a useful tool to study the ultrastructural alterations and the target organelles of new antitrypanosomatid drugs. Thus, it has been observed that sesquiterpene lactones induce diverse ultrastructural alterations in both *T. cruzi* and *Leishmania* spp., such as cytoplasmic vacuolization, appearance of multilamellar structures, condensation of nuclear DNA, and, in some cases, an important accumulation of lipid vacuoles. This accumulation could be related to apoptotic events. Some of the sesquiterpene lactones (e.g., psilostachyin) have also been demonstrated to cause an intense mitochondrial swelling accompanied by a visible kinetoplast deformation as well as the appearance of multivesicular bodies. This mitochondrial swelling could be related to the generation of oxidative stress and associated to alterations in the ergosterol metabolism. The appearance of multilamellar structures and multiple kinetoplasts and flagella induced by the sesquiterpene lactone psilostachyin C indicates that this compound would act at the parasite cell cycle level, in an intermediate stage between kinetoplast segregation and nuclear division. In turn, the diterpene lactone icetexane has proved to induce the external membrane budding on *T. cruzi* together with an apparent disorganization of the pericellular cytoskeleton. Thus, ultrastructural TEM studies allow elucidating the possible mechanisms and the subsequent identification of molecular targets for the action of natural compounds on trypanosomatids.

**Keywords** Natural compounds · Terpenes · Bioactive molecules · Trypanosomatids · Trypanosomatid ultrastructure · Neglected tropical diseases

---

E. Lozano

Laboratorio de Inmunología y Desarrollo de Vacunas, Instituto de Medicina y Biología Experimental de Cuyo (IMBECU, CCT-CONICET), Mendoza, Argentina

R. Spina · P. Barrera · M. A. Sosa (✉)

Laboratorio de Biología y Fisiología Celular Dr. Francisco Bertini, Instituto de Histología y Embriología (IHEM-CONICET), Mendoza, Argentina

e-mail: [msosa@fcm.uncu.edu.ar](mailto:msosa@fcm.uncu.edu.ar)

C. Tonn

Instituto de Investigación en Tecnología Química (INTEQUI), Facultad de Química Bioquímica y Farmacia, Universidad Nacional de San Luis, San Luis, Argentina

## 11.1 Introduction

*Trypanosoma cruzi* is the hemoflagellate parasite causative of Chagas' disease. About 6–7 million people are estimated to be infected worldwide, being an endemic disease in Latin America (Andrade et al. 2014; WHO 2017). Both invertebrate (triatomine bugs) and vertebrate (mammals, including man) hosts are needed to complete the parasite's life cycle. *T. cruzi* has three parasite stages: (a) the amastigote (or spheromastigote), (b) the epimastigote, and (c) the trypomastigote (3). The amastigote is a rounded flagellated form of 2–4  $\mu\text{m}$  diameter which is infective for vertebrate cells (De Souza 2002). The epimastigote is a spindle-shaped organism, 20–40  $\mu\text{m}$  long, with a kinetoplast located in the anterior portion of the parasite. The epimastigote can be found in the hindgut of the insect vector and maintained in vitro in axenic cultures. Both the amastigote and the epimastigote are the replicative forms of the parasite. The trypomastigote is the non-replicative form and can be found in the tissues and in the bloodstream of the vertebrates and also in the hindgut, the urine, and the feces of the insect vector. In this stage, the kinetoplast is located in the posterior region in relation to the nucleus.

### 11.1.1 Life Cycle of *Trypanosoma cruzi*

As mentioned above, both invertebrate and vertebrate hosts are needed to complete the life cycle of *T. cruzi*. When the insect vector ingests the trypomastigote-containing blood from infected mammals, parasites differentiate into replicative epimastigotes within the vector's digestive tract. In the intestine, epimastigotes divide by binary fission and attach themselves to the arthropod's intestinal epithelial cell lining by means of hemidesmosome-like structures. Afterward, a number of epimastigotes undergo metacyclogenesis in the vector's hindgut. Thus, metacyclic trypomastigotes are then eliminated in the feces or the urine (Brack 1968; Garcia and Azambuja 1991; Zeledon et al. 1977; Kolien and Schaub 2000). Following the entrance into the vertebrate host's cells through the bite lesion, trypomastigotes invade neighboring cells and differentiate into amastigotes, and after several cycles of replication, they transform into trypomastigotes, which are responsible for the elimination of the infection.

### 11.1.2 Infection and Disease

In humans, *T. cruzi* can invade any tissue derived either from the embryonic mesoderm, endoderm, or neuroectoderm. However, the extent of the infection depends on the host's genetic background and the parasite strain (Campbell et al. 2004). Mesoderm-derived tissues, such as smooth and striated muscles, bone marrow and the phagocytic mononuclear system, as well as gonadal cells, can be heavily parasitized. Instead, endoderm-derived tissues (liver, kidney, and thyroid gland, among

others) are seldom parasitized, and even less frequent is the invasion of the neuroectodermal-derived tissues (Campbell et al. 2004). If parasites reach the nervous system, they mostly invade astrocytes (Campbell et al. 2004).

The initial phase (acute phase) of *T. cruzi* infection lasts between 4 and 8 weeks, whereas the chronic phase persists throughout the patient's lifetime. In addition, the acute phase is mostly asymptomatic or might present as a self-limiting febrile illness. These mild symptoms appear usually about 1–2 weeks after exposure to the infected vector or up to a few months after transfusion with infected blood (Laranja et al. 1956; Dias 1984; WHO 2002).

The treatment with antiparasitic drugs, such as benznidazole, is known to be effective against the acute phase, preventing subsequent chronic manifestations (Rassi and Luquetti 1992; Pinto et al. 2009). Death in the acute phase occurs occasionally (<10% of symptomatic cases) as a result of severe myocarditis and/or meningoencephalitis. Manifestations of the acute disease resolve spontaneously in about 90% of infected individuals, even if the infection is not treated with trypanocidal drugs. Furthermore, about 60–70% of these patients never develop a clinical infection, and they enter an “indeterminate form” of chronic Chagas' disease featuring the presence of serum antibodies to the parasite but without clinical manifestations. After 10–30 years after the initial infection, some patients (30–40%) may develop a chronic disease, characterized by cardiac and/or digestive dysfunction (megaesophagus or megacolon) (Dias 1995).

### 11.1.3 Morphology and Ultrastructure of *T. cruzi*

#### 11.1.3.1 First Transmission Electron Microscopy Studies on *T. cruzi*

Since the initial description of *T. cruzi* by Carlos Chagas in 1909, the morphology of the parasite stages has been the subject of numerous studies. It is noteworthy that *T. cruzi* has been one of the first cells to be observed by transmission electron microscopy (TEM), and it has been the most studied organism with the techniques developed over the last 50 years (De Souza 2008). Thus, the first electron microscope (60 kV) images of *T. cruzi* were taken by Hertha Meyer and Keith Porter in 1954 (Fig. 11.1) (Meyer and Porter 1954).

However, at that time, the images were of low resolution, and only some peripheral fibrous structures could be observed (Fig. 11.1).

By 1978, samples were examined with a high-voltage electron microscope (1000 kV) (Fig. 11.2) (De Souza 2008), with which the kinetoplast and the attachment of the flagellum to the cell body could be observed. These methods also allowed identifying the unique and highly branched mitochondrion within the parasite.

Over the years, the resolution of the microscope was improved, and the methods became more reliable. Thus, other organelles and structures such as acidocalcisomes, glycosomes, reservosomes, lipid inclusions, and membranous components of the endocytic and secretory machinery could be identified (De Souza 2009).

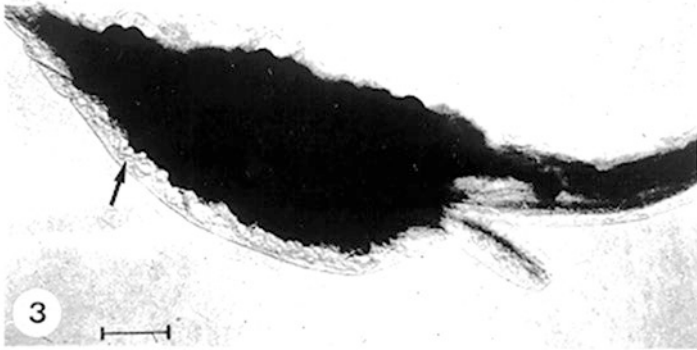


**Fig. 11.1** Electron micrograph of the whole epimastigote form of *Trypanosoma cruzi* dried on the grid. This image was obtained by H Meyer and KR Porter and published in 1954. The arrow indicates peripheral fibrillary structures. Magnification  $\times 10,000$



**Fig. 11.2** *Trypanosoma cruzi* trypomastigote observed by high-voltage electron microscopy. Structures such as the kinetoplast (K), the nucleus (N), and areas of adhesion of the flagellum to the cell body (arrows) were identified. Magnification  $\times 12,000$  (De Souza 1999)

### 11.1.3.2 The Ultrastructure of *T. cruzi*

**The nucleus** The nucleus of *T. cruzi* and other trypanosomatids has a structural organization that is similar to that of other eukaryotic cells. This organelle is localized centrally in the cell body in the trypomastigote and is elongated, whereas in the amastigote and the epimastigote, it exhibits a more rounded shape (Fig. 11.3). Chromosomal structures have been difficult to describe in *T. cruzi* due to their incomplete condensation during the mitotic metaphase. The development of novel methods such as the pulsed-field gel electrophoresis (PFGE) has allowed determin-





**Fig. 11.3** Transmission electron microscopy of a thin section of an epimastigote form of *Trypanosoma cruzi*. N nucleus, FP flagellar pocket, F flagellum, K kinetoplast, magnification  $\times 20,000$

ing the structure of chromosomes, to find that the whole parasite's genome (43–50 Mb) renders about 30–40 chromosomal bands ranging from 0.45 to 4.0 Mb (Johnston et al. 1999).

**The flagellum** All members of the *Trypanosomatidae* family have a single flagellum that emerges from an invagination called the “flagellar pocket” (FP). The flagellum of *T. cruzi* has a basic structure (9 + 2) of axonemal microtubules which is similar to the typical flagella of other flagellated cells (Fig. 11.3). In trypanosomatids, the length of the flagellum varies in each parasite stage. For example, the amastigote form has a very short flagellum (1  $\mu\text{m}$ ); however, in the other stages, the parasite elongates, and the flagellum can reach up to about 20  $\mu\text{m}$  (Martinez-Palomo et al. 1976; De Souza et al. 1978). The flagellum of trypanosomatids is usually attached to the cell body in a specific region. When the flagellum begins to beat, a wave propagates toward its free end, inducing an apparent swing of the parasite body like an undulating membrane. A specialization of the flagellar membrane was described by freeze-fracture at the zone where the flagellum emerges from the cell body both in epimastigotes and trypomastigotes (Martinez-Palomo et al. 1976; De Souza et al. 1978).

**The flagellar pocket** All trypanosomatids have a FP which is as a depression located at the front of the cell from where the flagellum emerges (Webster and Russel 1993). As shown in Fig. 11.3, the FP is an invagination of the plasma membrane in continuity with the flagellar membrane. Since the plasma and flagellar membranes establish a tight contact at the zone of the flagellum emergence, the FP

can be considered a special extracellular compartment. There are morphological and biochemical evidences supporting the idea that the FP is a highly specialized compartment of the parasite: (a) the FP is the only area that lacks subpellicular microtubules, (b) its membrane protein composition differs substantially from the plasma membrane surrounding the cell body, and (c) an intense endocytic and exocytic activity occurs in that area (Simpson 1972).

**The kinetoplast-mitochondrion complex** Early electron microscopy studies had identified an electron dense and slightly bent structure named kinetonucleus (Meyer et al. 1958). Later on, this structure was termed the kinetoplast. This structure is located close to the nucleus, and its shape and the structural organization vary according to parasite stage (Fig. 11.3). Not until the late 1960s was the molecular configuration of kinetoplast DNA unveiled (Shapiro and Englund 1995; Lukes et al. 2002). It is now well established that trypanosomatids have a single and highly branched mitochondrion, whose DNA (k-DNA) forms the dense structure of the kinetoplast. The first images obtained using thin sections clearly revealed the special organization of the k-DNA located in a specialized zone of the mitochondrial matrix, perpendicular to the flagellum axis. In addition, filamentous structures connect the kinetoplast to the basal body (Souto-Padron et al. 1984; Ogbadoiyi et al. 2003).

Other cytochemistry studies, using the ethanolic phosphotungstic acid technique and ammoniacal silver, have demonstrated the presence of basic proteins in the kinetoplast, suggesting that these proteins may neutralize the negatively charged DNA molecules packed within this structure (Souto-Padron and De Souza 1978; Souto-Padron and De Souza 1979). More recently, the presence of these basic proteins was confirmed by biochemical and molecular studies and indicated that H1 histone-like proteins participate in the condensation of k-DNA in *Crithidia fasciculata* and *T. cruzi* (De Souza and Cavalcanti 2008).

Two types of DNA rings are present in the kinetoplast: the minicircles and the maxicircles. There are several thousand minicircles which range in size from about 0.5 to 2.5 kb (depending on the species) and a few dozen maxicircles, usually varying from 20 to 40 kb (Shapiro and Englund 1995; De Souza and Cavalcanti 2008). These DNA rings encode guide RNAs that modify maxicircle transcripts by extensive uridylyate insertion or deletion, a process known as “RNA editing.” In turn, the maxicircles are structurally and functionally analogous to the mitochondrial DNA of higher eukaryotes, which encodes rRNAs and the subunits of respiratory chain complexes.

**The endomembrane system** In trypanosomatids, the endoplasmic reticulum (ER) is observed throughout the protozoan cytoplasm. In some cases the ER reaches the cell periphery establishing contact with the plasma membrane and the subpellicular microtubules (Pimenta and De Souza 1983). In turn, cisternae of the Golgi complex, which vary in size according to the species, are observed near the kinetoplast and the FP (Fig. 11.4). These cisternae are oriented perpendicularly to the kinetoplast and parallel to the FP. Vesicle budding from the *trans*-Golgi is also observed in the vicinity of the FP. It has been demonstrated that an increase in the number of Golgi

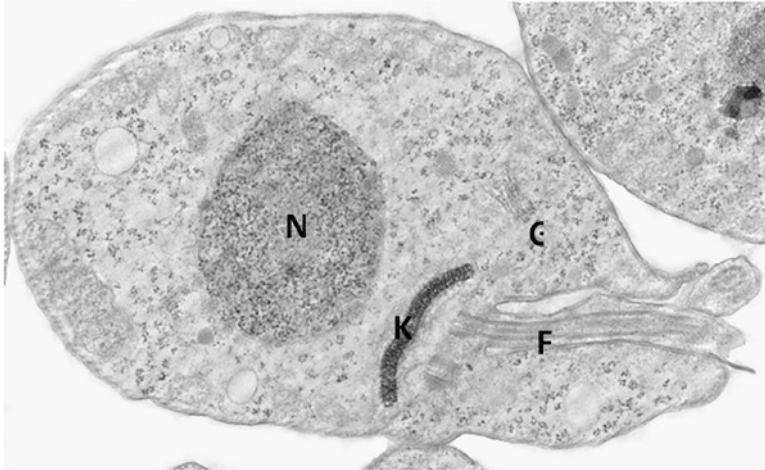


**Fig. 11.4** Transmission electron microscopy of a thin section of an epimastigote form of *Trypanosoma cruzi*. N nucleus, F flagellum, K kinetoplast, G Golgi complex. Magnification  $\times 20,000$

cisternae is related to the acquisition of epimastigote resistance to a cysteine protease inhibitor (Engel et al. 2000).

**The glycosome** In several species of trypanosomatids, ultrastructural studies have revealed the presence of spherical structures that have a homogeneous matrix and are surrounded by a single membrane. Initially, these structures were named microbodies, in analogy with similar structures described in mammalian cells. Interestingly, in trypanosomatids, most of the glycolytic pathway is carried out in this organelle, whereas in other eukaryotic cells the glycolysis occurs in the cytoplasm. Thus, these microbodies were eventually named glycosomes (Oppenoes and Borst 1977). Biochemical studies have demonstrated that glycosomes contain enzymes of high isoelectric point (Souto-Padron and De Souza 1978). There is also evidence that in trypanosomatids, additional metabolic pathways, such as carbon dioxide fixation, purine salvage and de novo pyrimidine biosynthesis, fatty acid elongation, isoprenoid biosynthesis, and sterol biosynthesis, take place in the glycosomes, while these processes occur in the cytosol of other cell types (Oppenoes 1987; Oppenoes and Cotton 1982).

**The acidocalcisome** Observations of thin sections of *T. cruzi* and other trypanosomatids have revealed some vacuolar structures containing electron-dense deposits. These structures were first identified as polyphosphate or volutin granules. In 1994, this organelle was demonstrated to transport protons and calcium, and therefore, it was named the acidocalcisome (Docampo et al. 2005). The appearance of this organelle depends on the method used to prepare the samples for electron microscopy. If conventional methods are used, it appears that the electron-dense deposits

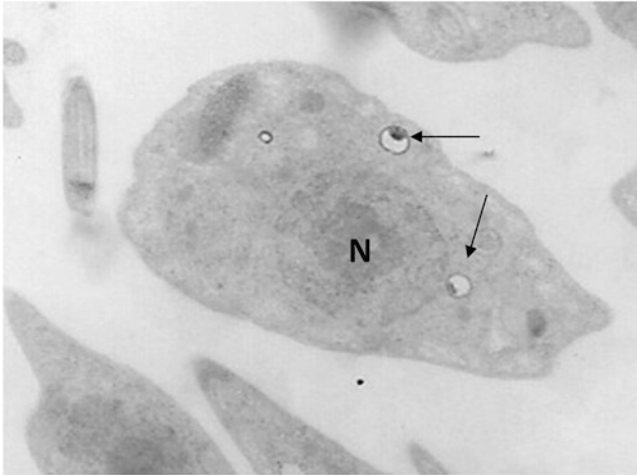


**Fig. 11.5** Transmission electron microscopy of a thin section of an epimastigote form of *Trypanosoma cruzi*. N nucleus. Arrows indicate the acidocalcisomes. Magnification  $\times 5,000$

shrink to such an extent that only a small dark spot is observed inside the organelle (Fig. 11.5). Instead, most of the electron-dense deposits are preserved if cryofixation is used or when cells are quick frozen using a high-pressure freezing technique and subjected to freeze-substitution (Miranda et al. 2000). The best strategy to visualize the acidocalcisome is to observe the whole cells dried on a grid under an electron microscope with an energy filter. Furthermore, the electron microscopy microanalysis has played a key role in determining the ionic composition of the acidocalcisome. At present, it is known that the acidocalcisome contains calcium, phosphorous, sodium, potassium, and zinc, and in some trypanosomatids (such as *T. cruzi*, *T. brucei*, *L. amazonensis*, and *L. donovani*), iron has also been found (Miranda et al. 2004). Therefore, it is postulated that the acidocalcisome is involved in functions such as (i) the storage of calcium, magnesium, sodium, potassium, zinc, iron, and phosphorous compounds, especially inorganic pyrophosphate and polyphosphate, (ii) the pH balance, and (iii) the osmoregulation, possibly acting in close association with a contractile vacuole (Docampo et al. 2005).

**The contractile vacuole** This structure is formed by several tubules connected to a central vacuole located close to the FP (Linder and Staehelin 1977). More recently, aquaporin, a protein involved in water transport, was identified in both, the acidocalcisome and the contractile vacuole of *T. cruzi* epimastigotes (Montalvetti et al. 2004). These structures appear to be involved in osmoregulation processes.

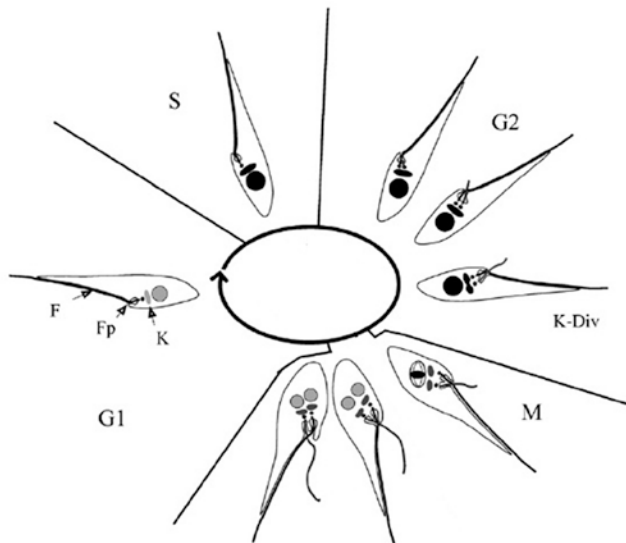


**Fig. 11.6** Schematic representation of morphological changes during the *Trypanosoma cruzi* cell cycle. The stages of the nuclear cell cycle are indicated as G1, S, G2, and M (mitosis). The shading inside the nucleus and kinetoplast is proportional to the DNA content. The new flagellum is shown in gray and the old in black. The new flagellum emerges from the flagellar pocket when cells are in the G2 stage, and at this stage, the kinetoplast segregates. Mitosis occurs, the flagellar pocket segregates, and the cell undergoes cytokinesis, producing two identical cells. N nucleus, K kinetoplast, F flagellum, FP flagellar pocket (Elias et al. 2007)

### 11.1.3.3 Ultrastructure of *T. cruzi* During Cell Division

Unlike other cell types, a disruption of the nuclear membrane has not been observed in *T. cruzi* during cell division (Fig. 11.6), making it difficult to distinguish the typical mitosis steps. In spite of this drawback, the formation of a mitotic spindle has been observed inside the parasite's nucleus. At the beginning of division, the first signals can be observed in the nucleus; the chromatin material localized below the inner nuclear membrane and the nucleolus disappear. This occurs immediately after replication of the basal body, when the kinetoplast still shows no morphological signs of division. The nucleus changes from a spherical to an oval form (De Souza and Meyer 1975; Solari 1980).

Likewise, during division, small electron-dense plaques are observed between and connected with the intranuclear microtubules (De Souza and Meyer 1975; Solari 1980). A more detailed description of the nuclear division of *T. cruzi* epimastigotes arises from serial sections and a three-dimensional reconstruction of each stage (Solari 1980). The mitotic spindle is formed by approximately 120 microtubules arranged in two sets of about 60, running from each pole to the dense plaques and divided into discreet bundles which reach a single plaque. Each plaque has a

symmetrical structure formed by transverse bands. Before nuclear elongation occurs, the dense plaques split in two halves and begin to migrate to the polar regions. At this time no microtubules are seen between the two halves of each plaque. All microtubules are localized between the plaques and the poles of the nucleus. The nature and functional roles of the dense plaques are not yet clear. It has been suggested that they could represent specialized parts of uncondensed chromosomes (Solari 1980). However, there are no data supporting this hypothesis. They could also represent kinetochore-like structures which would play an important role in separation of the nuclear material between two new cells. When the division is completed, the chromatin and the nucleolus reorganize and assume the position seen in interphase cells, whereas the microtubules disappear. During the whole process of division, the nuclear membrane remains intact, albeit with a more irregular folding. Recent studies have shown that a nucleolus is not observed in the trypomastigote and that there is a decrease in the transcription rates by RNA polymerases I and II from the epimastigote to the trypomastigote form (Elias et al. 2001).

## 11.2 How Vulnerable Is *T. cruzi*?

Chagas' disease is a widely distributed illness that affects many people and whose cure is far from being achieved. Traditionally, the development of new drugs has been based on the screening of natural compounds or extracts containing bioactive molecules against certain pathogens, including *T. cruzi*. Over the years, this random approach has been conducted without prior knowledge neither of the molecular targets on the pathogen nor of the mechanism of action of drugs. Nowadays, the search for antiparasitic molecules is accompanied by more extensive studies in order to know the impact of the compound on certain molecular targets. Making use of the extensive knowledge of the *T. cruzi* genome and its biochemistry, the mechanism of action of the new bioactive molecules could be better understood (El Sayed et al. 2005). Thereafter, the molecular targets have been selected on the basis of their role in the parasite growth and survival. In recent years, the gene knockout technology has been employed to study the function of a particular gene, thus being an excellent method for selecting and validating a molecular target. Afterward, inhibitory molecules are designed for these molecular targets (Majumder 2008).

### 11.2.1 Some Molecular Targets for Trypanocidal Agents

#### 11.2.1.1 Ergosterol Biosynthesis

Since trypanosomatid parasites lack the abundant supply of cholesterol present in the mammalian host cells (Urbina 1997; Urbina 2000; Urbina 2001; Urbina 2002), they have a strict requirement for specific endogenous sterols (e.g.,

ergosterol and analogs) for survival and growth. Inhibitors of the ergosterol biosynthesis can induce radical parasitological cure in animal models suffering both acute and chronic experimental *T. cruzi* infection and are also active against several forms of leishmaniasis (Urbina 1997; Urbina 2000; Urbina 2001; Urbina 2002). One of the crucial enzymes that regulates the sterol synthesis is the squalene synthase (SQS), which catalyzes the dimerization of farnesyl pyrophosphate (FPP) in a two-step reaction to form squalene (Gonzalez-Pacanowska et al. 1988). Therefore, SQS is currently under intense study, since it is a possible molecular target for the action of compounds that interfere with the synthesis of cholesterol in humans (Bergstrom et al. 1995). Studies in vertebrates and yeasts have demonstrated that the levels of SQS mRNA change in response to exogenous sources of sterols and also to 3-hydroxy-3-methylglutaryl coenzyme A (HMG-CoA) reductase inhibitors.

### 11.2.1.2 The Thiols Metabolism and the Defense Against Free Radicals

In *T. cruzi*, the defense mechanisms against the oxidative stress are deficient when compared to that of mammals. This feature is due to a low superoxide dismutase activity (Turrens 2004) and the absence of glutathione peroxidase, catalase (Turrens 2004; Wilkinson and Kelly 2003),  $\alpha$ -tocopherol, and  $\beta$ -carotene (Aldunate and Morello 1993) in trypanosomatids. Thus, the defense against oxidative stress is limited to GSH and trypanothione (N1, N8-bis (glutathionyl) spermidine) (T(SH)<sub>2</sub>), the latter being exclusive of trypanosomatids and indispensable for glutathione reduction (Ariyanayagam and Fairlamb 2001; Turrens 2004). This characteristic makes *T. cruzi* more vulnerable than the host cells to the oxidative stress. This is the basis of the action of nifurtimox and benznidazole, which, through electrophilic conjugation, these drugs block the thiol groups in the parasites (Ariyanayagam et al. 2003; Maya et al. 1997). In mammals, however, the eventual decrease of GSH caused by these compounds is compensated by  $\alpha$ -tocopherol,  $\beta$ -carotene, and ascorbate, among others.

### 11.2.1.3 Cruzipain

Cruzipain (Cz) is a cysteine protease (CP) that belongs to the papain superfamily in mammals. This enzyme contains an unusual C-terminal extension, as other CPs from trypanosomatids. This glycoprotein is synthesized as a zymogen that is activated by cleavage of the N-terminal pro-domain to generate the mature protease (Eakin et al. 1992). The mature enzyme consists of a catalytic moiety at the N-terminus, displaying a high homology with cathepsin L, and a C-terminus showing 36% homology with that of type 1 CPs from other protozoans (Campetella et al. 1992; Mottram et al. 1998). Cz seems to be important for the survival of the parasite and for the growth and cellular differentiation (dos Reis et al. 2006; McKerrow et al. 2006). This enzyme has endopeptidase activity and

hydrolyzes the IgG Fc fragment, endowing the parasite with an escape mechanism from the host's immune attack (Bontempi and Cazzulo 1990). Cz has also been demonstrated to play a role in the internalization of the parasite into mammalian cells, a process for which specific enzyme inhibitors have been found, thus inhibiting *T. cruzi* intracellular replication (Souto-Padron et al. 1990; Meirelles et al. 1992).

#### 11.2.1.4 Nucleotide Metabolism

It is known that trypanosomatids cannot synthesize purines de novo. However, they have developed effective mechanisms for self-delivery of preformed purines and nucleosides. Through the salvage pathway, the parasite is able to concentrate pyrazolopyrimidines and transform them into purines for the synthesis of nucleic acids (Gutteridge and Davies 1981).

The pyrazolopyrimidine base allopurinol (4-hydroxypyrazolo [3,4-a] pyrimidine, HPP) is activated by the phosphoribosyl transferase into the ribonucleotide-5' monophosphate (HPPR-MP). HPPR-MP is then aminated to 4-aminopyrazolopyrimidine ribonucleotide (APPR-MP) and subsequently phosphorylated to form the triphosphate form. The growth of *T. cruzi* epimastigotes is inhibited by allopurinol; however, some strains are not sensitive to this compound, suggesting that these strains have different metabolic routes (Avila et al. 1984; Avila and Avila 1981; Marr et al. 1978). On the other hand, pyrimidines can be synthesized by trypanosomes de novo, and it is known that some of the enzymes involved in such pathways are located in glycosomes, whereas the analogous enzymes in mammals are cytosolic (Hammond et al. 1981).

### 11.3 In the Search for a Solution Against Parasitic Diseases

Chagas' disease and leishmaniasis cause significant morbidity and mortality in Latin America and are extending worldwide. According to the World Health Organization (WHO), these diseases are considered neglected tropical diseases (NTDs), affecting people in developing countries.

Most of the drugs currently used for the treatment of Chagas' disease and leishmaniasis have severe side effects. Currently, the treatments against Chagas' disease are limited to benznidazole and nifurtimox, which have been available since the 1970s. These two drugs are effective only in the acute phase of the disease. On the other hand, the current antileishmanial therapy includes the use of pentavalent antimonials (amphotericin B, miltefosine, and paromomycin), which also present several disadvantages such as the route of administration, the development of parasite resistance, the high costs, the teratogenic effects, and the treatment duration and



associated toxicity. Among the natural compounds, the members of the large family of terpenoids display a wide range of biological activities such as anticancer and anti-inflammatory and are effective against various infective agents such as viruses, bacteria, and parasites (Sepúlveda-Boza and Cassels 1996). In fact, several terpenoids have proved to be active against *T. cruzi* and *Leishmania* spp., thus being attractive compounds as future therapeutic agents for Chagas' disease and leishmaniasis (Barrera et al. 2008). Besides, terpenoids are widely distributed in the plant kingdom. In the following sections, we will review the antiprotozoal activity of natural terpenoid compounds and derivatives isolated from plants in Argentina.

Terpenes are made up of isoprene ( $C_5H_8$ ) units. According to the number of linked isoprenes, several terpene families are defined. Among them, sesquiterpenes that contain three ( $C_{15}H_{24}$ ) and diterpenes that contain four ( $C_{20}H_{32}$ ) isoprene units are the aim of this revision.

### 11.3.1 Sesquiterpene Lactones

Dehydroleucodine (DHL) is a sesquiterpene lactone (STL) belonging to the guaianolide group (Fig. 11.7). This compound has been isolated and purified at concentrations >1% from the aerial parts of *Artemisia douglasiana*, which is a widespread medicinal plant commonly used in Argentina (Giordano et al. 1990). In addition, other biological activities have been described for this compound (Penissi et al. 2003; Costantino et al. 2016). *Mexicanin* (MXN) is a STL isolated from the aerial parts of *Gaillardia megapota mica* (Jimenez-Ortiz et al. 2005) (Fig. 11.7).

Psilostachyin (Psi) and psilostachyin C (Psi C) have been isolated by bioassay-guided fractionation from *Ambrosia tenuifolia* and *Ambrosia scabra* (Asteraceae), respectively. These medicinal species are popularly known as “ajeno del campo” and traditionally used against intermittent fevers and worm infections (Sülsen et al. 2006; Muschietti et al. 2008). Parthenolide has been isolated and purified from the aerial parts of *Tanacetum parthenium* (Tiuman et al. 2005). Cynaropicrin has been isolated from aerial parts of *Cynara cardunculus* var. *scolymus* (“globe artichoke”), which belongs to the Asteraceae family (da Silva et al. 2013) (Fig. 11.7).

### 11.3.2 Diterpenes

5-epi-icetexone (ICTX) is a diterpene isolated from the aerial parts of *Salvia gilliesii* as an orange solid (Nieto et al. 2000). Abietane (12-hydroxy-11,14-diketo-6,8,12-abietatrien-19,20-olide) (HABTO) has been isolated from the aerial parts of *Salvia cuspidata*. This compound has a diterpene structure belonging to the abietane group (Lozano et al. 2015) (Fig. 11.8).

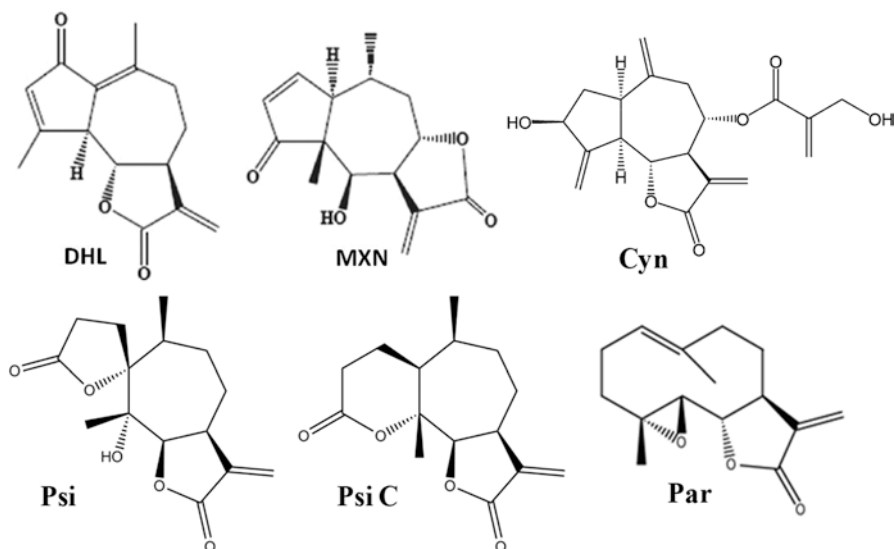
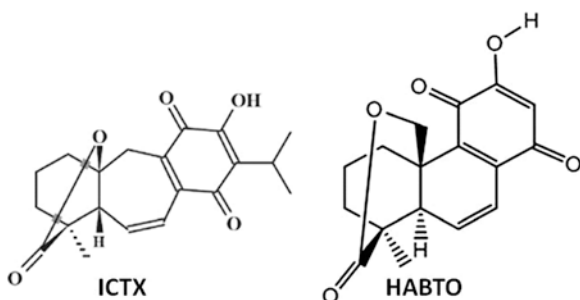


**Fig. 11.7** Chemical structure of sesquiterpene lactones. DHL Dehydroleucodine, MXN Mexicanin, Cyn Cynaropicrin, Psi Psilostachyin, Psi C Psilostachyin C, Par Parthenolide

**Fig. 11.8** Chemical structure of natural diterpenes. 5-epi-icetexone (ICTX) and abietane (12-hydroxy-11,14-diketo-6,8,12-abietatrien-19,20-olide) (HABTO)



### 11.3.3 Effect of Sesquiterpene Lactones and Diterpenes on *Trypanosoma cruzi*

All the compounds mentioned above are active against different stages of *T. cruzi*, inhibiting their growth and viability and with a very low toxicity on mammalian cells (Bregio et al. 2000; Jimenez-Ortiz et al. 2005; Lozano et al. 2012b). Because of this, these molecules could be potential therapeutic agents against these parasitic diseases. Sesquiterpene lactones have proved to have oxidative effects on the parasites, and this effect could be ascribed to the presence of the  $\gamma$ -lactone group (Giordano et al. 1992; Jimenez-Ortiz et al. 2005). Several studies

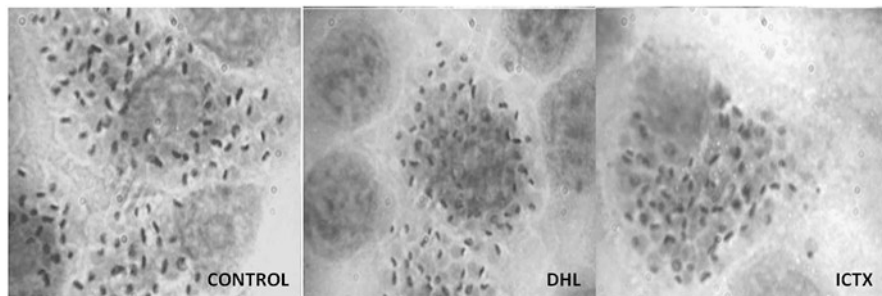


**Fig. 11.9** Vero cells infected with *Trypanosoma cruzi*, subjected to different treatments with dehydroleucodine (DHL) or 5-epi-icetexone (ICTX) (Lozano et al. 2012b)

have suggested that STLs and ICTX may act through multiple mechanisms on different parasite molecular targets (Barrera et al. 2008; Jimenez-Ortiz et al. 2005; Lozano et al. 2012a). DHL and ICTX have also effect on the growth of intracellular forms of *T. cruzi*, without affecting the viability of the host cell (Fig. 11.9) (Lozano et al. 2012b). In animal models, it has been demonstrated that ICTX can protect mice from *T. cruzi*, at least during the early stages of infection (Fig. 11.10) (Lozano et al. 2016).

Morphological and ultrastructural studies have been very helpful in elucidating the possible mechanisms of action of drugs on trypanosomatids. Some examples of the action of STL and diterpenes on *T. cruzi* epimastigotes are described in the following sections.

While DHL does not induce major changes on the morphology or the ultrastructure of the parasites (Fig. 11.11), MXN has been demonstrated to induce vacuolization in the cytoplasm, which precedes parasite death (Fig. 11.12).

The nuclear disorganization observed by TEM may show an apoptotic effect of the drugs on the parasites. It is feasible that MXN causes irreversible damage to the parasite DNA, since interactions of STLs with DNA have been reported (Lee et al. 1977). However, it was not possible to discern whether this nuclear disorganization preceded other effects, such as vacuolization and changes in morphology, or if all these drastic changes occurred simultaneously.

Psilostachyins, isolated from *Ambrosia tenuifolia* (Sülsen et al. 2010), have been found to be active against *T. cruzi* epimastigotes. This STL induced drastic ultrastructural changes, such as cytoplasmic vacuolization, a slight increase in multivesicular bodies, and, especially, mitochondrial swelling accompanied by a visible deformity of the kinetoplast (Fig. 11.13). The mitochondrial swelling may be attributed to alterations in ergosterol metabolism, as reported by others (Lazardi et al. 1990).

Psilostachyin C, isolated from *Ambrosia scabra*, is also active against *T. cruzi* epimastigotes since it induces alterations on *T. cruzi* ultrastructure, such as cytoplasmic vacuolization, at a concentration of 2.5  $\mu\text{g/ml}$ . Moreover, the compound promoted the appearance of membranous structures resembling cytoplasmic multivesicular bodies (Fig. 11.14d). The appearance of multilamellar structures was

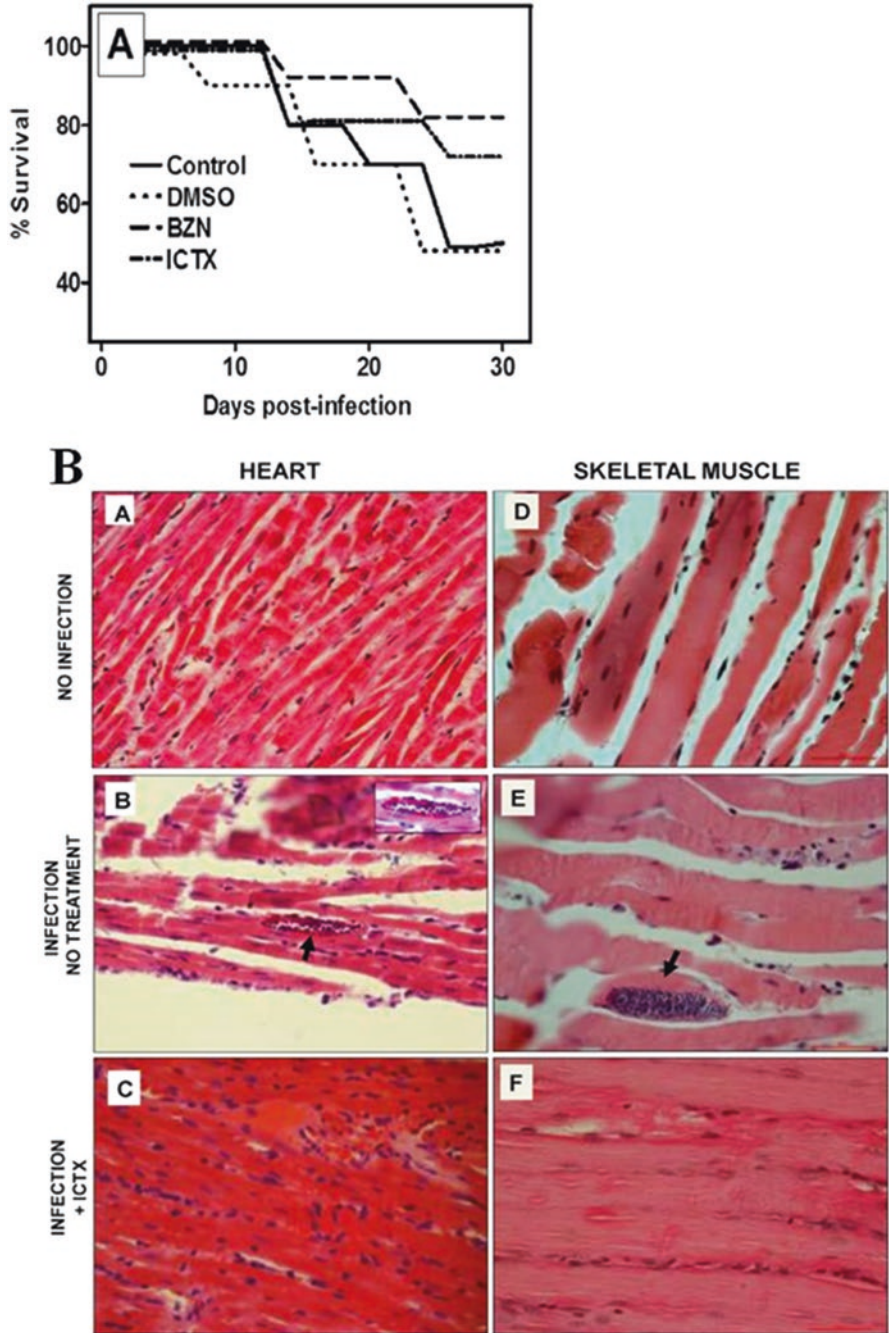


**Fig. 11.10** (a) Survival of mice infected with *T. cruzi* and treated with either benznidazole (BZN) or 5-epi-icetexone (ICTX). (b) Histological analysis of cardiac muscle (a–c) or skeletal muscle of the hind leg (d–f) in mice inoculated with *T. cruzi* and treated or not with either BZN or ICTX on day 35 after infection. Amastigote nests (b, arrow and inset, e arrow) can be observed in control animals. Magnification  $\times 400$  (Lozano et al. 2016)

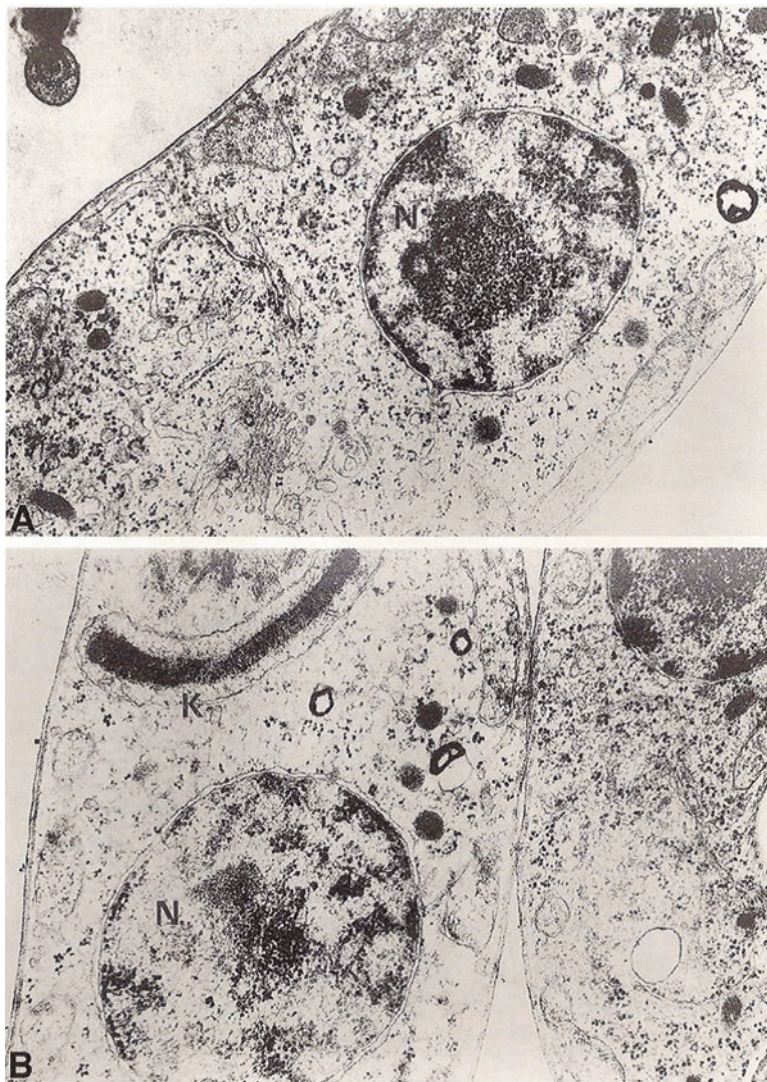


**Fig. 11.11** Ultrastructural aspect of cultured *Trypanosoma cruzi* on the second day of growth in culture medium. (a) Control cells and (b) cells incubated with 10 µg/ml dehydroleucodine (DHL). N nucleus, K kinetoplast (Breggio et al. 2000)

also observed. Although some parasites exhibited redistribution of nuclear chromatin, the compound did not induce changes on cellular or nuclear morphology. Interestingly, some parasites (ca. 10%) exhibited abnormalities such as the presence of more than two flagella and kinetoplasts (Fig. 11.14b, c), suggesting a possible effect of the compound on cytokinesis (Sülsen et al. 2011).

Ultrastructural analysis of cynaropicrin-treated bloodstream trypomastigotes (BT) demonstrated that while untreated parasites exhibited normal morphology for the mitochondrion, nucleus, endoplasmic reticulum, and kinetoplast (Fig. 11.15a, b),

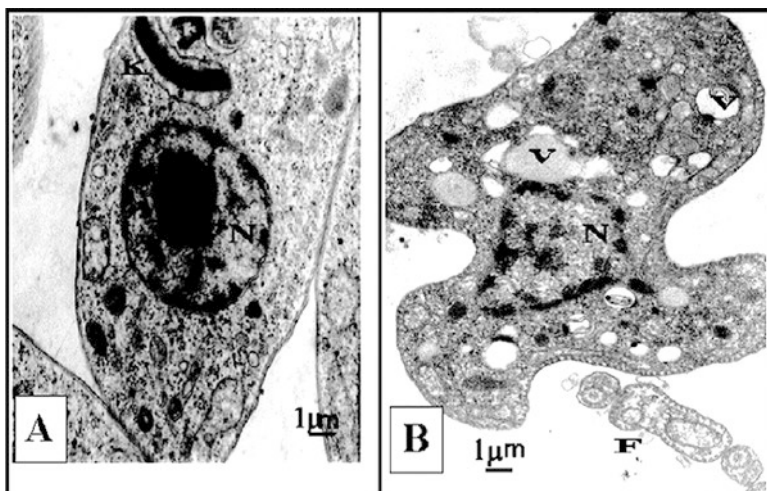


**Fig. 11.12** Ultrastructure of *Trypanosoma cruzi* epimastigotes on the second day of growth in culture medium. (a) Control cells or (b) cells incubated with 1.9  $\mu$ M Mexicanin (MXN). N nucleus, K kinetoplast, F flagellum, V vacuoles. Magnification 35,000 (Jimenez-Ortiz et al. 2005)

cynaropicrin-treated BT showed intense intracellular vacuolization, with a great number of membrane blebs and with shedding of the intracellular contents, alongside the occurrence of large multivesicular bodies (Fig. 11.15c–f) (da Silva et al. 2013).

Some diterpenes containing icetexane skeleton, such as 5-epi-icetexone (ICTX), are also active against *T. cruzi*. Interestingly, after 24 h of exposure to ICTX, some parasites exhibit an external vesiculization and an apparent disorganization of the pericellular cytoskeleton although cell integrity is apparently preserved (Fig. 11.16c). At longer times of exposure to the drug, the parasites showed an intense vacuolization in the cytoplasm and exhibited a nuclear disorganization, as a signal of the deleterious effect of the compound (Fig. 11.16d). The external vesiculization observed at 24 h of exposure may be related to a disorganization of the cytoskeleton surrounding the parasites. It is known that the presence of a microtubules layer localized below the parasite plasma membrane confers rigidity and high resistance to mechanical traction. The vacuolization may be related to strong alterations of metabolism and/or the ionic equilibrium, as well as membrane disruptions due to lipid peroxidation (Breggio et al. 2000).

As mentioned above, it has been difficult to detail the stages of cell division of the parasites because of the insufficient chromatin condensation, the maintenance of the nuclear envelope, and the lack of a visible mitotic spindle. Nevertheless, it has been possible to specify a sequence of events that precede the cellular division: duplication of the flagellum, followed by kinetoplast duplication and finally the nuclear division (De Souza and Meyer 1975; Elias et al. 2001). In axenic cultures, the parasites grow asynchronously, and therefore, strategies have to be used to achieve growth synchronization, such as the use of hydroxyurea (HU). By this strat-

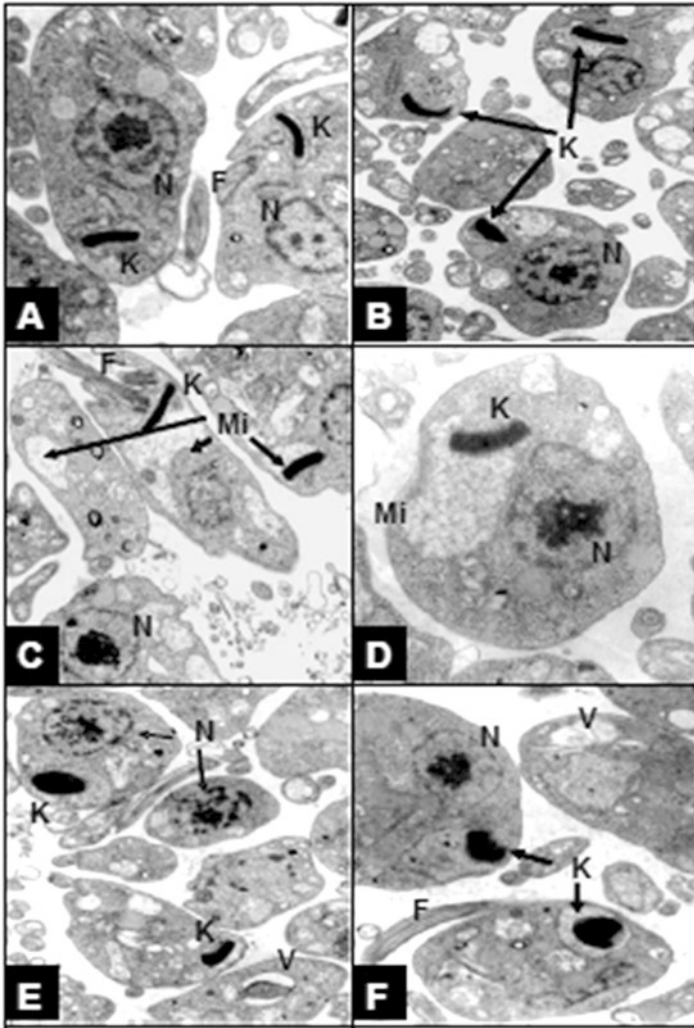


**Fig. 11.13** Effect of psilostachyin on the ultrastructure of *Trypanosoma cruzi* epimastigotes. Parasites were incubated in Diamond's medium alone (a) or with the addition of 0.5 (b, c), 1.0 (d, e) or 2.5 (f) µg/ml of psilostachyin. N nucleus, K kinetoplast, F flagellum, V vacuoles, Mi mitochondrion. Magnification ×2500 (B, C, E), ×2800 (a, f), and ×3000 (d) (Sülsen et al. 2010)

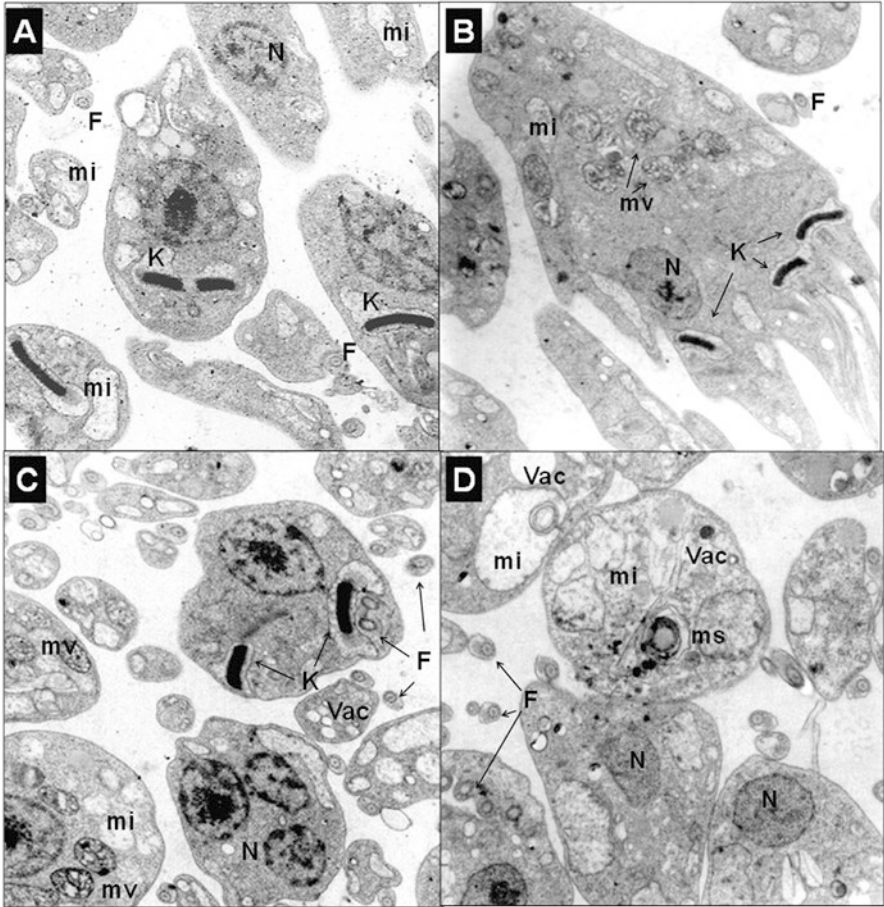


**Fig. 11.14** Ultrastructural effects of psilostachyin C on *Trypanosoma cruzi* epimastigotes. Parasites were incubated with (a) Diamond's medium alone or with (b) 0.5 µg/ml psilostachyin C, (c) 1.0 µg/mL psilostachyin C, or (d) 2.5 µg/ml psilostachyin C. N nucleus, K kinetoplast, F flagellum, Vac vacuoles, mi mitochondria, ms multilamellar structures, mv multivesicular bodies. Magnification  $\times 2500$  (Sülsen et al. 2011)



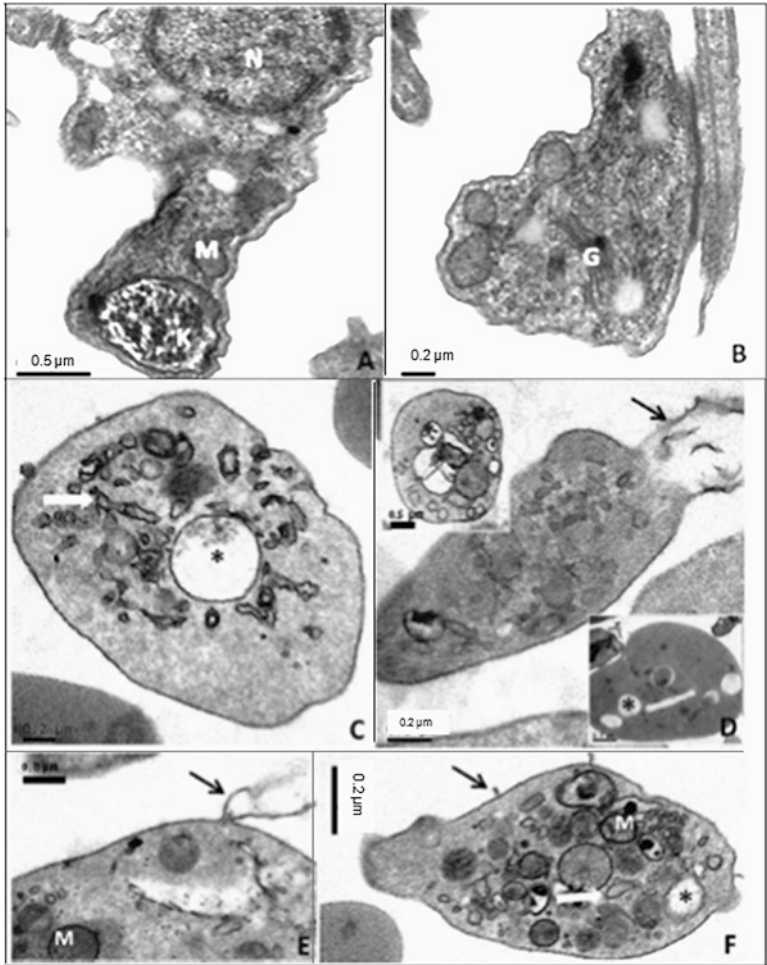


**Fig. 11.15** Transmission electron microscopy analysis of the effect of cynaropicrin on blood-stream trypomastigotes. BT were left untreated (**a** and **b**) or exposed to this STL ( $EC_{50}/24$  h) for 2 h (**c–f**). Untreated parasites displayed typical morphology, while cynaropicrin-treated parasites showed vacuolization (\*), swelling of the mitochondrion and endoplasmic reticulum (white arrows), and plasma membrane shedding (black arrows). M mitochondrion, G Golgi complex, N nucleus (da Silva et al. 2013)

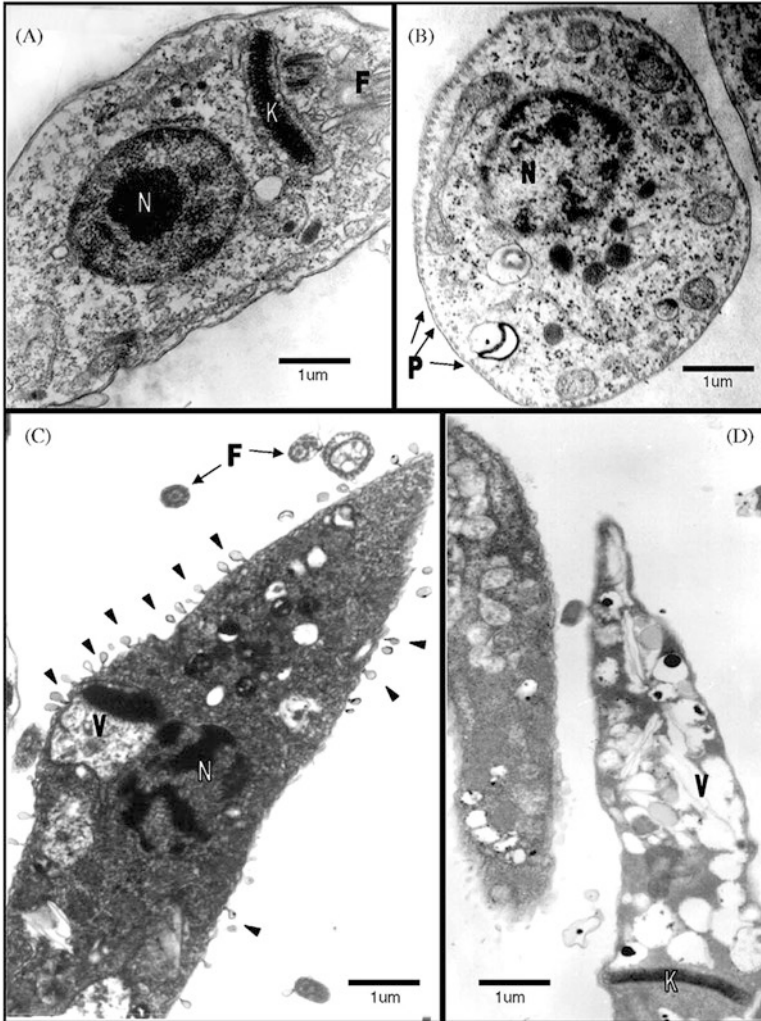


**Fig. 11.16** Effect of 5-epi-icetexone (ICTX) on the ultrastructure of *Trypanosoma cruzi* epimastigotes after incubation for 24 h (c) or 48 h (d) in the presence of 4.3  $\mu$ M of ICTX. (a and b): untreated controls. N nucleus, K kinetoplast, P pericellar cytoskeleton, V vacuoles, F flagellum. Arrowheads indicate vesiculation processes. Magnification:  $\times 5000$  (a and b);  $\times 4500$  (c);  $\times 3500$  (d) (Sanchez et al. 2006)

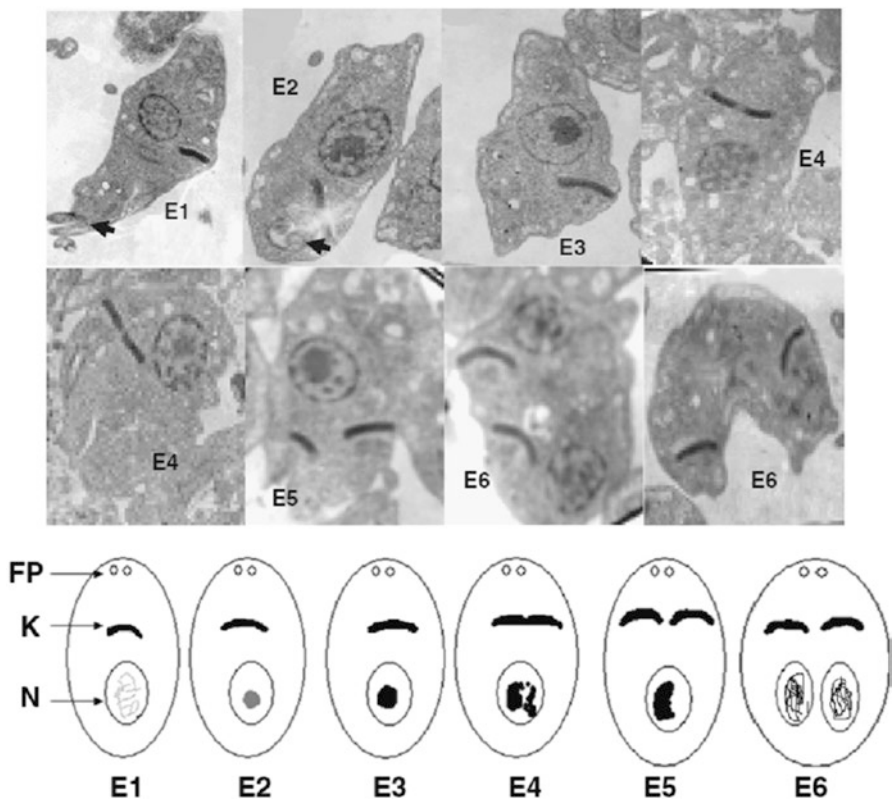


**Fig. 11.17** Ultrastructural aspects of *Trypanosoma cruzi* epimastigotes after 18 h of hydroxyurea (HU) removal. The figure shows the sequential stages during cell division, which are schematized in the bottom panel. FP flagellar pocket, K kinetoplast, N nucleus. Arrow: flagellum. Magnification:  $\times 2000$  (Lozano et al. 2012a)

egy it has been possible to determine that around 18 h after synchronization, the events of the cell division of the parasites begin. Taking into account the number of flagella, kinetoplasts and chromatin condensation, six stages of parasites would be found, which have been ordered sequentially as shown in Fig. 11.17. From this assumption, we observed that the treatment with ICTX ( $4.3 \mu\text{M}$ ) interferes with early steps of the cell division. It is noteworthy that at 18 h 30 min, a number of control parasites had progressed to the E6 stage, while most of the treated parasites remained in the E1 stage. This wave of division was maintained until 20 h, and probably until 21 h, since an increase of parasites in the E1 stage observed in the controls could be a possible E7 stage (occurring after cell division), which would be indistinguishable from E1 (Fig. 11.18).

More recently, a new diterpene, 12-hydroxy-11,14-diketo-6,8,12-abietatrien-19,20-olide) (HABTO,  $\text{IC}_{50} \sim 14 \mu\text{M}$ ) belonging to the abietane group and some derivatives, proved to be active against epimastigotes, inhibiting parasite growth

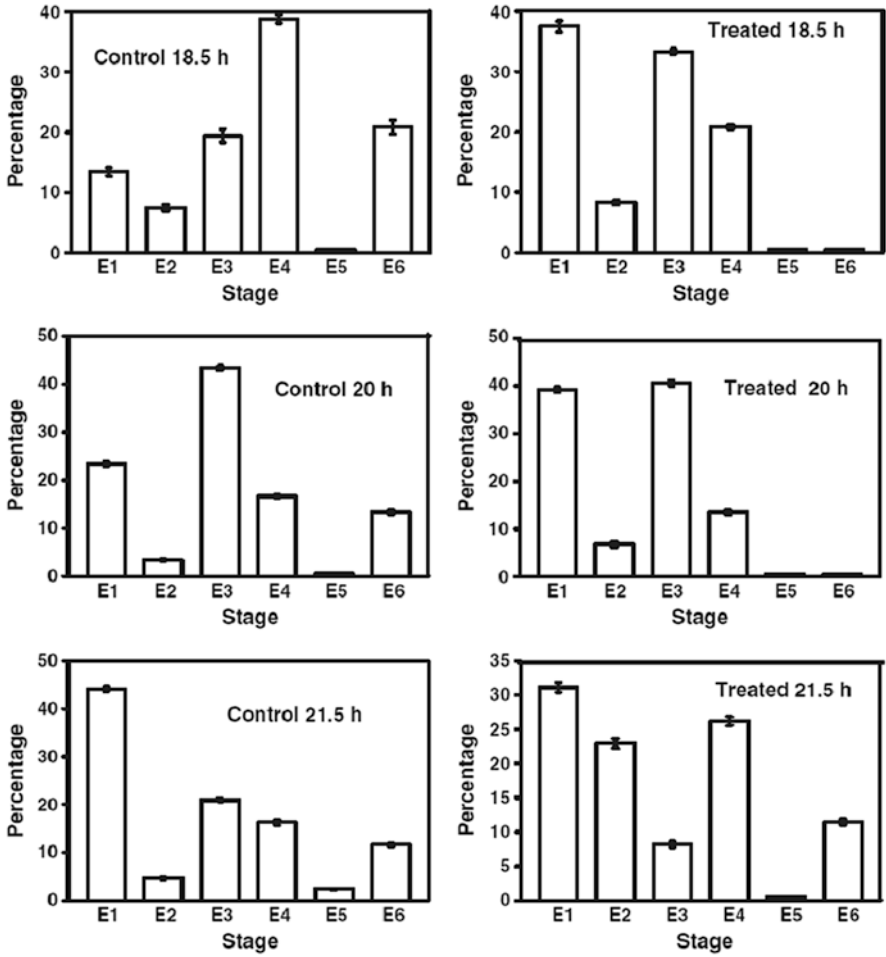


**Fig. 11.18** Quantification of the different parasite stages in control cultures or in cultures treated with 5-epi-icetexone (ICTX) long after the removal of hydroxyurea (HU). Graphs show the distribution of each stage in control cultures and in cultures treated at different times (18.5, 20, and 21.5 h after removal of HU). Bars represent the percentages of each stage  $\pm$ SD from three independent experiments (Lozano et al. 2012a)

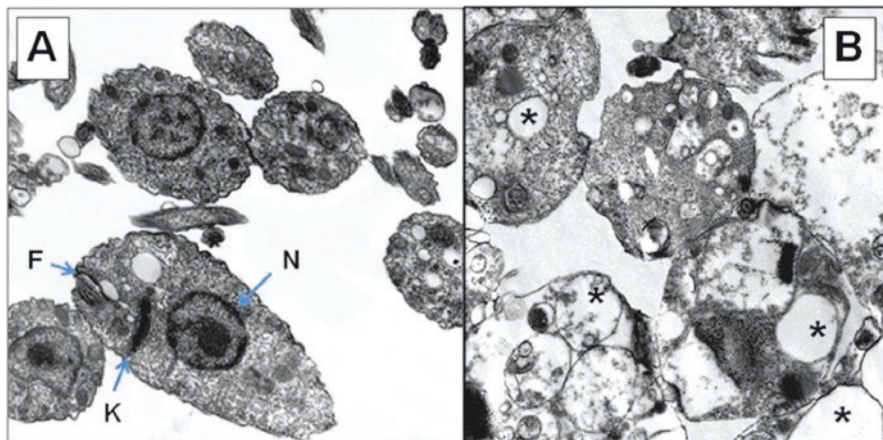


**Fig. 11.19** The effect of 12-hydroxy-11,14-diketo-6,8,12-abietatrien-19,20-olide (HABTO) on the ultrastructure of *Trypanosoma cruzi* epimastigotes at 48 h of treatment. (a) Control culture and (b) culture treated with 14  $\mu$ M HABTO (N nucleus, K kinetoplast, F flagellum). Asterisks: vacuolization. Magnification:  $\times 3000$  (a);  $\times 3500$  (b) (Lozano et al. 2015)

(Lozano et al. 2015). As observed in Fig. 11.19, HABTO can induce an intense vacuolization similar to that observed with other terpenes.

### 11.3.4 Effect of Sesquiterpene Lactones on *Leishmania* spp.

DHL, MXN, and also helenalin (HLN) have also been found to be active against this trypanosomatid, since they inhibited parasite growth and induced strong vacuolization, HLN being more deleterious than the others (Fig. 11.20).

*Leishmania amazonensis* parasites treated with 1  $\mu$ g/ml of parthenolide showed significant morphological alterations. An intense exocytic activity was observed in the region of the flagellar pocket, which appeared in the form of protrusions of the cell body toward the flagellar pocket and concentric membranes within the pocket (Fig. 11.21b, c). Moreover, some structures similar to large lysosomes were observed in the cytoplasm (Fig. 11.1d) (Tiuman et al. 2005).

De Toledo showed, for the first time, that *Tithonia diversifolia* dichloromethane leaf rinse extract (LRE) presents strong in vitro antileishmanial activity. Notably, LRE is a rich source of STL. The LRE showed a LD<sub>50</sub> value of  $1.5 \pm 0.50$   $\mu$ g/mL. Through scanning electron microscopy (SEM), morphological analysis of promastigotes revealed noticeable differences between the treated parasites and the control group (Fig. 11.22). When parasites were incubated with LRE, they lost two major promastigote characteristics: (i) their fusiform morphology changed to a rounded shape, and (ii) the flagellum in the majority of the cells was missing. All

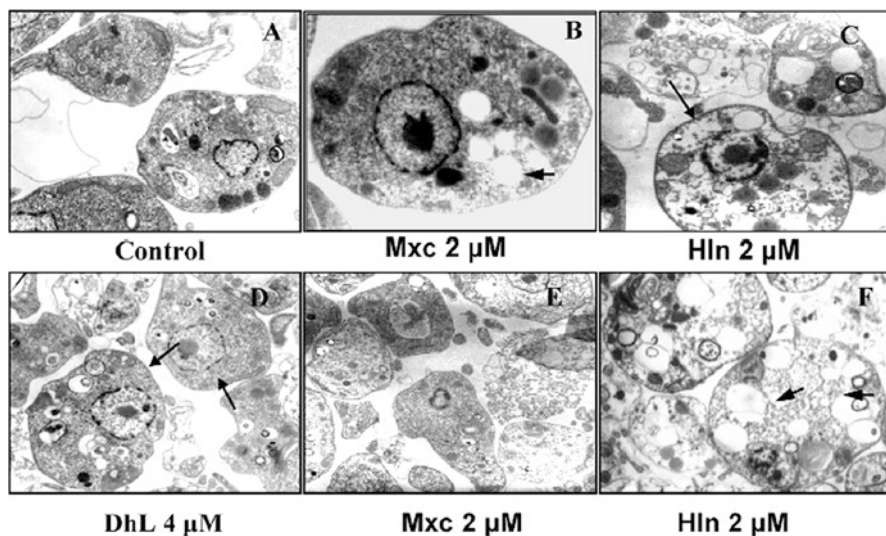


**Fig. 11.20** Ultrastructure of *Leishmania mexicana* after incubation with or without the STLs at the indicated concentrations. Parasites were incubated for 24 (a–c) or 48 h (d–f) and then fixed and processed for TEM. Arrows, pericellular microtubules; arrowheads, vacuoles. Magnification:  $\times 15,000$  (a, c, d, and f);  $\times 30,000$  (b);  $\times 9,000$  (f) (Barrera et al. 2008)

this information suggests that the LRE is a potential source of natural compounds with leishmanicidal activity.

Eight STL (Fig. 11.23), from LREs, were investigated for activity against promastigote forms of *L. braziliensis* (Table 11.1). STL 3 was the only compound that did not show an in vitro leishmanicidal effect in the evaluated concentrations and displayed an  $LD_{50}$  value that was higher than  $50 \mu\text{g}\cdot\text{mL}^{-1}$  (Table 11.1). Still, compounds 1, 2, and 4–8 displayed very effective  $LD_{50}$  values ranging from  $6.0 \pm 2.5$  to  $37.4 \pm 7.1 \mu\text{M}$  (see Table 11.1). The antiprotozoal activities, displayed by STL, correlate with their cytotoxicity, which are promoted by a Michael-type addition reaction of free thiol groups (usually from cysteine residues) from proteins with  $\alpha,\beta$ -unsaturated carbonyls from the  $\alpha$ -methylene- $\gamma$ -lactone group. Cytotoxicity assays against macrophages for the effective compounds (Table 11.1) show that only compound 1 (tagitinin C), the major STL present in LRE, causes significant cytotoxic effects while displaying low selectivity ( $SI = 1.4$ ). Interestingly, the chemical structure of 1 (Fig. 11.23) has an  $\alpha,\beta$ -unsaturated carbonyl group in the  $\gamma$ -lactone ring and a carbonyl group conjugated with two different double bonds in the germacranolide ring; therefore, there are three reactive sites. On the other hand, the other STL, which have only one or two  $\alpha,\beta$ -unsaturated carbonyl groups (compounds 4–8 and 2, respectively), did not show significant toxicity in macrophages and displayed a high level of selectivity (Table 11.1) (De Toledo et al. 2014).

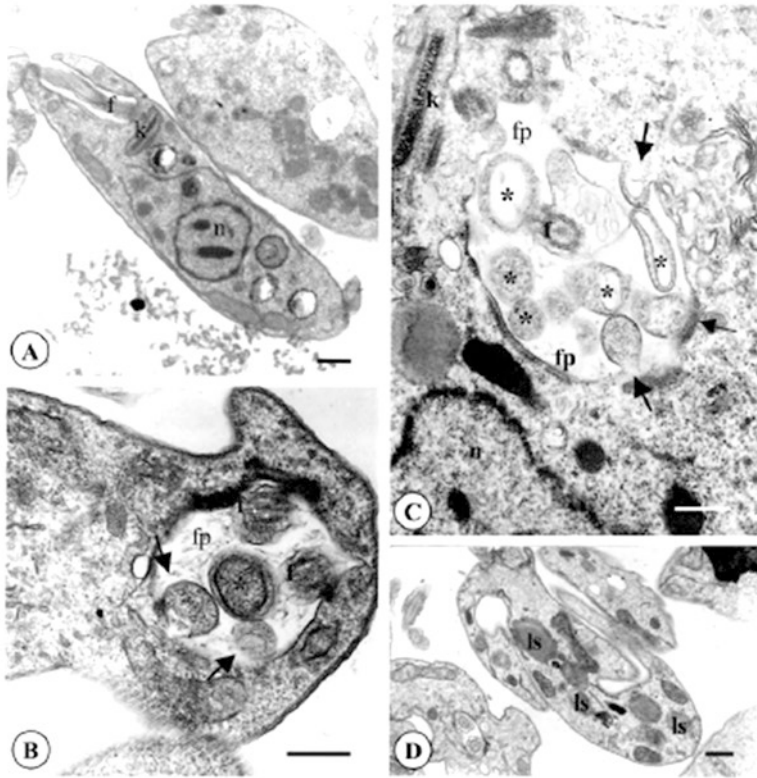


**Fig. 11.21** Ultrastructural effects of parthenolide on promastigote forms of *L. amazonensis*. Parasites were incubated with DMSO or medium alone (a) or with 1  $\mu\text{g}$  of parthenolide/ml (the  $\text{IC}_{50}$ ) (b to d) for 72 h. (a) Section showing the normal aspect of the nucleus, the flagellum in the flagellar pocket, and the mitochondrion containing the kinetoplast. (b and c) Promastigote showing intense exocytic activity. The arrows indicate the protrusions of the cell body toward the flagellar pocket; the asterisks indicate the vesicles located in the flagellar pocket. (d) The promastigotes also showed some structures similar to large lysosomes in the cytoplasm. fp flagellar pocket, f flagellum, k kinetoplast, n nucleus, ls lysosome. Bars, 1  $\mu\text{m}$  (Tiuman et al. 2005)

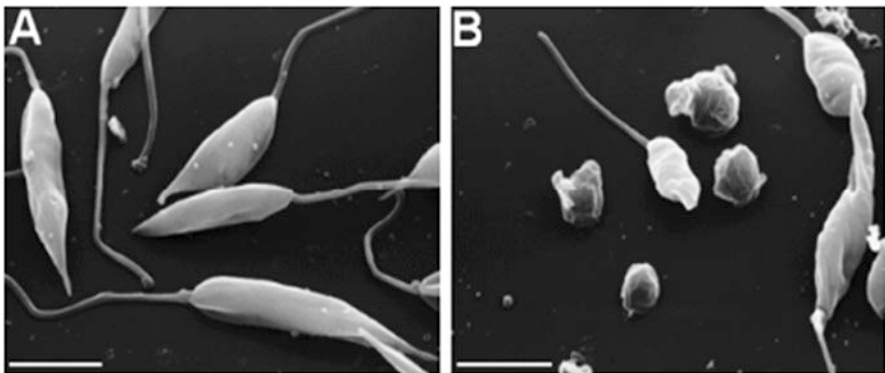


**Fig. 11.22** Scanning electron microscopy of untreated (a) and 10  $\mu\text{g}/\text{mL}$  *Tithonia diversifolia* dichloromethane leaf rinse extract (b) *Leishmania braziliensis* promastigotes. Bar, 5  $\mu\text{m}$  (De Toledo et al. 2014)

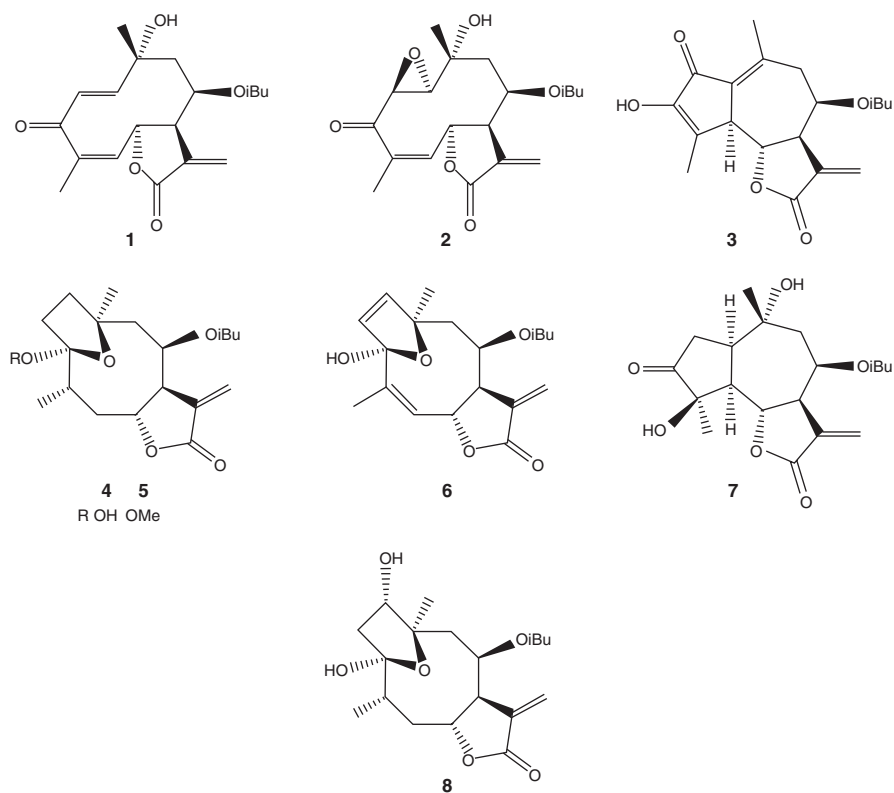


**Fig. 11.23** Chemical structures of sesquiterpene lactones isolated from the leaves of *Tithonia diversifolia*

**Table 11.1** In vitro antileishmanial activities of sesquiterpene lactones of *Tithonia diversifolia* against *Leishmania braziliensis* promastigotes and cytotoxic effects on peritoneal macrophages

Compounds	LD <sub>50</sub> for <i>L. braziliensis</i> μg.mL <sup>-1</sup> / μM	LD <sub>50</sub> for macrophages μg.mL <sup>-1</sup>	Selectivity index
1	3.2 ± 0.5/9.2 ± 1.4	4.5 ± 0.9	1.4
2	2.2 ± 0.9/0.6 ± 2.5	>50.0	>22.7
3	>50.0	>50.0	–
4	8.7 ± 1.9/24.7 ± 5.4	24.9 ± 1.1	2.9
5	13.7 ± 2.6/37.4 ± 7.1	>50.0	>3.6
6	7.4 ± 2.8/21.2 ± 8.0	>50.0	>6.7
7	9.0 ± 1.2/24.6 ± 3.3	>50.0	>5.5
8	7.5 ± 3.2/20.4 ± 8.7	>50.0	>6.6



## 11.4 Conclusion

Taking into account all these findings, compounds from the terpene family emerge as promising alternatives for therapeutic use against parasitic diseases, and the studies on parasite ultrastructure became an important tool to elucidate the mechanisms of action and the identification of molecular targets for the drugs.

## References

- Aldunate J, Morello A (1993) Free radicals in the mode of action of parasitic drugs. In: Aruoma OI (ed) Free radicals in tropical diseases. Harwood Academic Publishers, London, pp 137–165
- Andrade DV, Gollob KJ, Dutra WO (2014) Acute chagas disease: new global challenges for an old neglected disease. *PLoS Negl Trop Dis* 8:e3010. <https://doi.org/10.1371/journal.pntd.0003010>
- Ariyanayagam MR, Fairlamb AH (2001) Ovothiol and trypanothione as antioxidants in trypanosomatids. *Mol Biochem Parasitol* 115:189–198
- Ariyanayagam MR, Oza SL, Mehlert A et al (2003) Bis (glutathionyl) spermine and other novel trypanothione analogues in *Trypanosoma cruzi*. *J Biol Chem* 278:27612–27619
- Avila JL, Avila A (1981) *Trypanosoma cruzi*: allopurinol in the treatment of mice with experimental acute Chagas disease. *Exp Parasitol* 5:204–208
- Avila JL, Avila A, Monzón H (1984) Differences in allopurinol and 4-aminopyrazolo(3,4-d)pyrimidine metabolism in drug-sensitive and insensitive strains of *Trypanosoma cruzi*. *Mol Biochem Parasitol* 1:51–60
- Barrera P, Jimenez-Ortiz V, Giordano O et al (2008) Natural sesquiterpene lactones are active against *Leishmania mexicana* possible by multiple effects. *J Parasitol* 94:1143–1149
- Bergstrom JD, Dufresne C, Bills GF et al (1995) Discovery, synthesis and mechanism of action of the zaragozic acids: potent inhibitors of squalene synthase. *Annu Rev Microbiol* 49:607–639
- Bontempi E, Cazzulo J (1990) Digestion of human immunoglobulin G by the major cysteine proteinase (cruzipain) from *Trypanosoma cruzi*. *FEMS Microbiol Lett* 58:337–341
- Brack C (1968) Electron microscopic studies on the life cycle of *Trypanosoma cruzi* with special reference to developmental forms in the vector *Rhodnius prolixus*. *Acta Trop* 25:289–356
- Brengio SD, Belmonte S, Guerreiro E et al (2000) The sesquiterpene lactone dehydroleucodine (DHL) affects the growth of cultured epimastigotes of *Trypanosoma cruzi*. *J Parasitol* 86:407–412
- Campbell DA, Westenberger SJ, Sturm NR (2004) The determinants of Chagas disease: connecting parasite and host genetics. *Curr Mol Med* 4:549–562
- Campetella O, Henriksson J, Aslund L et al (1992) The major cysteine proteinase (cruzipain) from *Trypanosoma cruzi* is encoded by multiple polymorphic tandemly organized genes located on different chromosomes. *Mol Biochem Parasitol* 50:225–234
- Costantino VV, Lobos-Gonzalez L, Ibañez J et al (2016) Dehydroleucodine inhibits tumor growth in a preclinical melanoma model by inducing cell cycle arrest, senescence and apoptosis. *Cancer Lett* 372(1):10–23
- Da Silva CF, Batista DGJ, De Araújo JS et al (2013) Activities of psilostachyin A and cynaropicrin against *Trypanosoma cruzi* *in vitro* and *in vivo*. *Antimicrob Agents Chemother* 57(11):5307–5314
- De Souza W (2002) Basic cell biology of *Trypanosoma cruzi*. *Curr Pharm Des* 8:269–285
- De Souza W (2008) Electron microscopy of trypanosomes – a historical view. *Mem Inst Oswaldo Cruz* 103(4):313–325
- De Souza W (2009) Structural organization of *Trypanosoma cruzi*. *Mem Inst Oswaldo Cruz* 104:89–100

- De Souza W, Cavalcanti DP (2008) DNA-containing organelles in pathogenic protozoa: a review. *Trends Cell Mol Biol* 2:89–104
- De Souza W, Meyer HJ (1975) An electron microscopic and cytochemical study of the cell coat of *Trypanosoma cruzi* in tissue cultures. *Z Parasitenkd* 46(3):179–187
- De Souza W, Martinez-Palomo A, Gonzales-Robbles A (1978) The cell surface of *Trypanosoma cruzi*: cytochemistry and freeze-fracture. *J Cell Sci* 33:285–299
- Dias JCP (1984) Acute Chagas' disease. *Mem Inst Oswaldo Cruz* 79(suppl):85–91
- Dias JCP (1995) Natural history of Chagas' disease. *Arq Bras Cardiol* 65:359–366
- Docampo R, De Souza W, Miranda K et al (2005) Acidocalcisomes – conserved from bacteria to man. *Nat Rev Microbiol* 3:251–261
- Dos Reis F, Judice W, Juliano M et al (2006) The substrate specificity of cruzipain 2, a cysteine protease isoform from *Trypanosoma cruzi*. *FEMS Microbiol Lett* 259:215–220
- Eakin AE, Mills AA, Harth G et al (1992) The sequence, organization, and expression of the major cysteine protease (cruzain) from *Trypanosoma cruzi*. *J Biol Chem* 267:7411–7420
- El Sayed NM, Myler PJ, Blandin G et al (2005) Comparative genomics of trypanosomatid parasitic Protozoa. *Science* 309:404–409
- Elias MCQB, Marques-Porto R, Freymuller E et al (2001) Transcription rate modulation through the *Trypanosoma cruzi* life cycle occurs in parallel with changes in nuclear organization. *Mol Biochem Parasitol* 112:79–90
- Elias MC, Da Cunha JPC, De Faria FP et al (2007) Morphological events during the *Trypanosoma cruzi* cell cycle. *Protist* 158:147–157
- Engel JC, Garcia CT, Hsieh I et al (2000) Upregulation of the secretory pathway in cysteine protease inhibitor-resistant *Trypanosoma cruzi*. *J Cell Sci* 113:1345–1354
- Garcia ES, Azambuja P (1991) Development and interactions of *Trypanosoma cruzi* within the insect vector. *Parasitol Today* 7:240–244
- Giordano OS, Guerreiro E, Pestchanker MJ et al (1990) The gastric cytoprotective effect of several sesquiterpene lactones. *J Nat Prod* 53:803–809. <https://doi.org/10.1021/np50070a004>
- Giordano OS, Pestchanker MJ, Guerreiro E et al (1992) Structure-activity relationship in the gastric cytoprotective effect of several sesquiterpene lactones. *J Med Chem* 35:2452–2458
- Gonzalez-Pacanowska D, Arison B, Havel CM et al (1988) Isopentenoid synthesis in isolated embryonic *Drosophila* cells. Farnesol catabolism and v-oxidation. *J Biol Chem* 263:1301–1306
- Gutteridge WE, Davies MJ (1981) Enzymes of purine salvage in *Trypanosoma cruzi*. *FEBS Lett* 127:211–214
- Hammond DJ, Gutteridge WE, Opperdoes FR (1981) A novel location for two enzymes of de novo pyrimidine biosynthesis in trypanosomes and *Leishmania*. *FEBS Lett* 128:27–29
- Jimenez-Ortiz V, Brengio SD, Giordano O et al (2005) The trypanocidal effect of sesquiterpene lactones helenalin and mexicanin on cultured epimastigotes. *J Parasitol* 91:170–174
- Johnston DA, Blaxter ML, Degraeve WM (1999) Genomics and the biology of parasites. *BioEssays* 21:131–147
- de Toledo J, Ambrósio S, Borges C, et al (2014) In Vitro Leishmanicidal Activities of Sesquiterpene Lactones from *Tithonia diversifolia* against *Leishmania braziliensis* Promastigotes and Amastigotes. *Molecules* 19 (5):6070-6079.
- Kolien AH, Schaub GA (2000) The development of *Trypanosoma cruzi* in triatomine. *Parasitol Today* 16:381–387
- Laranja FS, Dias E, Nobrega G et al (1956) Chagas' disease; a clinical, epidemiologic, and pathologic study. *Circulation* 14:1035–1060
- Lazardi K, Urbina JA, De Souza W (1990) Ultrastructural alterations induced by two ergosterol biosynthesis inhibitors, ketoconazole and terbinafine, on epimastigotes and amastigotes of *Trypanosoma* (Schizotrypanum) *cruzi*. *Antimicrob Agents Chemother* 34:2097–2105
- Lee KH, Hall IH, Mar EC et al (1977) Sesquiterpene antitumor agents: inhibitors of cellular metabolism. *Science* 196:533–535
- Linder JC, Staehelin LA (1977) Plasma membrane specialization in a trypanosomatid flagellate. *J Ultrastruct Res* 60:246–262

- Lozano E, Barrera P, Tonn C et al (2012a) The effect of the diterpene 5-epi-icetexone on the cell cycle of *Trypanosoma cruzi*. *Parasitol Int* 61:275–279
- Lozano E, Barrera P, Salinas R et al (2012b) Sesquiterpene lactones and the diterpene 5-epi-icetexone affect the intracellular and extracellular stages of *Trypanosoma cruzi*. *Parasitol Int* 61:628–633
- Lozano ES, Spina RM, Tonn CE et al (2015) An abietane diterpene from *Salvia cuspidata* and some new derivatives are active against *Trypanosoma cruzi*. *Bioorg Med Chem Lett* 25:5481–5484
- Lozano E, Strauss M, Spina R et al (2016) The *in vivo* trypanocidal effect of the diterpene 5-epi-icetexone obtained from *Salvia gilliesii*. *Parasitol Int* 65:23–26
- Lukes J, Guilbride DL, Votýpka J et al (2002) Kinetoplast DNA network: evolution of an improbable structure. *Eukaryot Cell* 1:495–502
- Majumder HK (2008) Drug targets in kinetoplastid parasites (Advances in experimental medicine and biology). Vol 625 ISBN: 978-0-387-77569-2 (Print) 978-0-387-77570-8 (Online), Springer Verlag, New York
- Marr JJ, Berens RL, Nelson DJ (1978) Antitrypanosomal effect of allopurinol: conversion *in vivo* to aminopyrazolopyrimidine nucleotides by *Trypanosoma cruzi*. *Science* 201:1018–1020
- Martinez-Palomo A, De Souza W, Gonzales-Robles AJ (1976) Topographical differences in the distribution of surface coat components and intramembranous particles. *J Cell Biol* 69:507–513
- Maya JD, Repetto Y, Agosin M et al (1997) Effects of nifurtimox and benznidazole upon glutathione and trypanothione content in epimastigote, trypomastigote and amastigote forms of *Trypanosoma cruzi*. *Mol Biochem Parasitol* 86:101–106
- McKerrow J, Caffrey C, Kelly B et al (2006) Proteases in parasitic diseases. *Annu Rev Pathol* 1:497–536
- Meirelles M, Juliano L, Carmona E et al (1992) Inhibitors of the major cysteinyl proteinase (GP57/51) impair host cell invasion and arrest the intracellular development of *Trypanosoma cruzi in vitro*. *Mol Biochem Parasitol* 52:175–184
- Meyer H, Porter KR (1954) A study of *Trypanosoma cruzi* with the electron microscope. *Parasitology* 44:1–2
- Meyer H, Oliveira Musacchio M, Andrade Mendonça I (1958) Electron microscopy study of *Trypanosoma cruzi* in thin sections of infected tissue cultures and blood agar forms. *Parasitology* 48:1–8
- Miranda K, Benchimol M, Docampo R et al (2000) The fine structure of acidocalcisomes in *Trypanosoma cruzi*. *Parasitol Res* 86:373–384
- Miranda K, Docampo R, Grillo O et al (2004) Acidocalcisomes of trypanosomatids have species-specific elemental composition. *Protist* 155:395–340
- Montalvetti A, Rohloff P, Docampo R (2004) A functional aquaporin co-localizes with the vacuolar proton pyrophosphatase to acidocalcisomes and the contractile vacuole complex of *Trypanosoma cruzi*. *J Biol Chem* 279:38673–38682
- Mottram J, Brooks D, Coombs G (1998) Roles of cysteine proteinases of trypanosomes and *Leishmania* in host-parasite interactions. *Curr Opin Microbiol* 1:455–460
- Muschietti LV, Sülsen VP, Martino V (2008) Trypanocidal and leishmanicidal activities of south American medicinal plants. In: Martino VS, Muschietti LV (eds) South American medicinal plants as a potential source of bioactive compounds. Transworld Research, Kerala, pp 149–180
- Nieto M, Garcia EE, Giordano OS et al (2000) Icetexane and abietane diterpenoids from *Salvia gilliesii*. *Phytochemistry* 53:911–915
- Ogbadoyi EO, Robinson DR, Gull K (2003) A high-order trans-membrane structural linkage is responsible for mitochondrial genome positioning and segregation by flagellar basal bodies in trypanosomes. *Mol Biol Cell* 14:1769–1779
- Opperdoes FR (1987) Compartmentalization of carbohydrate metabolism in trypanosomes. *Annu Rev Microbiol* 41:127–151
- Opperdoes FR, Borst P (1977) Localization of nine glycolytic enzymes in a microbody-like organelle in *Trypanosoma brucei*. *FEBS Lett* 80:360–364
- Opperdoes FR, Cotton D (1982) Involvement of the glycosome of *Trypanosoma brucei* in carbon dioxide fixation. *FEBS Lett* 143:60–64

- Penissi AB, Rudolph MI, Piezzi RS (2003) Role of mast cells in gastrointestinal mucosal defense. *Biocell* 27(2):163–172
- Pimenta PF, De Souza WJ (1983) *Leishmania mexicana amazonensis*: surface charge of amastigote and promastigote forms. *Exp Parasitol* 56(2):194–206
- Pinto AY, Ferreira AG Jr, Valente Vda C et al (2009) Urban outbreak of acute Chagas disease in Amazon region of Brazil: four-year follow-up after treatment with benznidazole. *Rev Panam Salud Pública* 25:77–83
- Rassi A, Luquetti AO (1992) Therapy of Chagas disease. In: Wendel S, Brener Z, Camargo ME, Rassi A (eds) Chagas disease (American Trypanosomiasis): its impact on transfusion and clinical medicine. ISBT, Sao Paulo, pp 237–247
- Sánchez AM, Jiménez-Ortiz V, Sartor T et al (2006) A novel icetexane diterpene, 5-epi-icetexone from *Salvia gilliessi* is active against *Trypanosoma cruzi*. *Acta Trop* 98:118–124
- Sepúlveda-Boza S, Cassels BK (1996) Plant metabolites active against *Trypanosoma cruzi*. *Planta Med* 62:98–105
- Shapiro TA, Englund PT (1995) The structure and replication of kinetoplast DNA. *Annu Rev Microbiol* 49:117–143
- Simpson L (1972) The kinetoplast DNA of the hemoflagellate protozoa. *Int Rev Cytol* 32:139–207
- Solari AJ (1980) The 3-dimensional fine structure of the mitotic spindle in *Trypanosoma cruzi*. *Chromosoma* 78:239–255
- Souto-Padron T, De Souza W (1978) Ultrastructural localization of basic proteins in *Trypanosoma cruzi*. *J Histochem Cytochem* 26:349–356
- Souto-Padron T, De Souza W (1979) Cytochemical analysis at the fine-structural level of trypanosomatids stained with phosphotungstic acid. *J Protozool* 26:551–557
- Souto-Padron T, De Souza W, Heuser JE (1984) Quick-freeze, deep-etch rotary replication of *Trypanosoma cruzi* and *Herpetomonas megaseliae*. *J Cell Sci* 69:167–168
- Souto-Padron T, Campetella O, Cazzulo J et al (1990) Cysteine proteinase in *Trypanosoma cruzi*: immunocytochemical localization and involvement in parasite-host cell interaction. *J Cell Sci* 96:485–490
- De Souza W (1999) A short review on the morphology of *Trypanosoma cruzi*: from 1909 to 1999. *Mem Inst Oswaldo Cruz* 94(Suppl) I:17–36
- Sülsen VP, Güida C, Coussio J et al (2006) *In vitro* evaluation of trypanocidal activity in plants used in Argentine traditional medicine. *Parasitol Res* 98:370–374
- Sülsen V, Barrera P, Muschiatti L et al (2010) Antiproliferative effect and Ultrastructural alterations induced by Psilostachyin on *Trypanosoma cruzi*. *Molecules* 15:545–553. <https://doi.org/10.3390/molecules15010545>
- Sülsen VP, Frank FM, Cazorla SI et al (2011) Psilostachyin C: a natural compound with trypanocidal activity. *Int J Antimicrob Agents* 37:536–543
- Tiuman TS, Ueda-Nakamura T, Garcia Cortez DA et al (2005) Antileishmanial activity of parthenolide, a sesquiterpene lactone isolated from *Tanacetum parthenium*. *Antimicrob Agents Chemother* 49(1):176–182
- Turrens JF (2004) Oxidative stress and antioxidant defenses: a target for the treatment of diseases caused by parasitic protozoa. *Mol Asp Med* 25:211–220
- Urbina JA (1997) Lipid biosynthesis pathways as chemotherapeutic targets in kinetoplastid parasites. *Parasitology* 117:S91–S99
- Urbina JA (2000) Sterol biosynthesis inhibitors for Chagas' disease. *Curr Opin Anti-Infect Inv Drugs* 2:40–46
- Urbina JA (2001) Specific treatment of Chagas disease: current status and new developments. *Curr Opin Infect Dis* 14:733–741
- Urbina JA (2002) Chemotherapy of Chagas disease. *Curr Pharm Des* 8:287–295
- Webster P, Russel DG (1993) The flagellar pocket of trypanosomatids. *Parasitol Today* 9:201–206

- Wilkinson SR, Kelly JM (2003) The role of glutathione peroxidases in trypanosomatids. *Biol Chem* 384:517–525
- World Health Organization (WHO) (2002) Control of Chagas' disease. Tech Rep Ser 905:i–vi. World Health Organization, Geneva
- World Health Organization (WHO) (2017) Chagas disease (American trypanosomiasis). Fact sheet Updated March 2017. <http://www.who.int/mediacentre/factsheets/fs340/en/>. Accessed 2 Nov 2017
- Zeledón R, Alvarenga NJ, Schosinsky K (1977) Ecology of *Trypanosoma cruzi* in the insect vector. In: Pan American Health Organization (ed) Chagas' Disease. Scientific Publication No. 347, Pan American Health Organization, Washington, pp 59–70

# Chapter 12

## Effects on Other Microorganisms



María Victoria Castelli and Silvia Noelí López

**Abstract** Sesquiterpene lactones (STLs) are natural and semisynthetic compounds displaying interesting biological activities, including antiprotozoal, anti-inflammatory, and cytotoxic among the most studied. Some compounds belonging to this group have recently been described as promising antimicrobial hits. In this chapter, the antifungal, antibacterial, and antiviral properties will be discussed, taking into account their basic chemical scaffolds.

**Keywords** Sesquiterpene lactones · Antimicrobial · Antifungal · Antibacterial · Antiviral

### Abbreviations

ATCC	American Type Culture Collection
DNA	Deoxyribonucleic acid
EC <sub>50</sub>	Half maximal effective concentration
HBeAg	Hepatitis B e antigen
HBsAg	Hepatitis B virus surface antigen
HBV	Hepatitis B virus
IC <sub>50</sub>	Half-maximal inhibitory concentration
MIC	Minimum inhibitory concentration
MTCC	Microbial Type Culture Collection

---

M. V. Castelli (✉) · S. N. López (✉)  
Farmacognosia – Facultad de Ciencias Bioquímicas y Farmacéuticas – CONICET –  
Universidad Nacional de Rosario. Suipacha 531, (S2002LRK) - Rosario, Argentina  
e-mail: [mcastel@fbioyf.unr.edu.ar](mailto:mcastel@fbioyf.unr.edu.ar); [slopez@fbioyf.unr.edu.ar](mailto:slopez@fbioyf.unr.edu.ar)

## 12.1 Introduction

Sesquiterpene lactones (STLs) constitute a large group of secondary plant metabolites comprising about 8000 members, mostly isolated from the Asteraceae family (Macias et al. 2013; Zhang et al. 2012). They have been described as the active constituents of several medicinal plants traditionally used to treat inflammatory diseases. However, not only do they have anti-inflammatory properties but also a broad spectrum of biological activities, including antimicrobial, antifungal, antiviral, antiparasitic (anthelmintic, antimalarial), uterus contracting, cytotoxic, antifeedant, and anticancer, among others (Merfort 2011).

Microorganisms, fungi, and bacteria have been in contact with humans since ancient times (Hancock 2007). Although some of them are beneficial to humans, a small fraction of them is responsible for devastating diseases affecting crops, food security, and human health. The continuous development of antibiotic resistance by microbes is alarming; therefore, there is an urgent need for new active molecules to fight such microorganisms (Demain and Sanchez 2009). The main classes of antibiotic drugs in current use were mainly discovered through empirical screening programs carried out more than 50 years ago. Most drugs currently in use ( $\beta$ -lactamic, azoles, etc.) derive from these precursors and encompass a limited number of chemical skeletons, offering, in some cases, few improvements over existing therapies. The increasing emergence of fungal and bacterial diseases is further promoted by human activity, primarily through global trade, and may be exacerbated by the impact of climate change (Jampilek 2016).

Viruses are responsible for a number of human diseases including cancer. Due to globalization, epidemic outbreaks caused by emerging and reemerging viruses (e.g. dengue virus, influenza virus, severe acute respiratory syndrome virus, etc.) represent a threat to public health. Despite progress has been made in the development of immunization therapies and antiviral drug development, vaccines to prevent infections and efficient antiviral therapies against many viral infections are still lacking. In addition, drug-resistant mutants can arise, especially when viral enzyme-specific inhibitors are employed (Lin et al. 2014).

Taking this information into account, it can be deduced that the need for new drugs to target emerging multidrug-resistant microorganisms is imperative. These drugs should also be less toxic and cheaper than the existing ones. In this sense, nature continues to provide an unparalleled source of small molecules that may be useful to comply with this need.

In this chapter, the antifungal, antibacterial, and antiviral properties of natural sesquiterpene lactones, including some examples of semisynthetic derivatives, will be discussed.

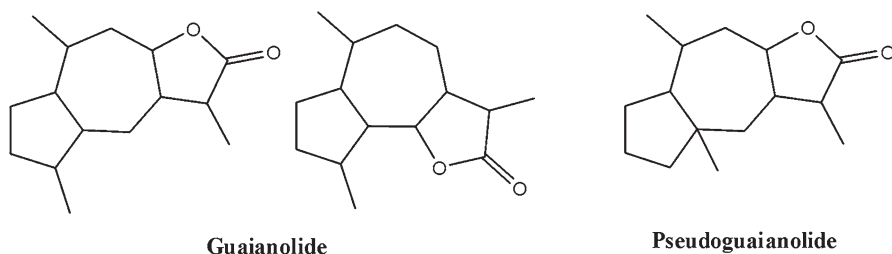


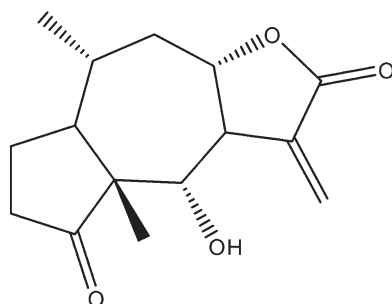
**Fig. 12.1** Guaianolide and pseudoguaianolide skeleton

## 12.2 Antifungal, Antibacterial, and Antiviral Activity

### 12.2.1 *Guaianolides and Pseudoguaianolides*

Guaianolides and pseudoguaianolides (Fig. 12.1) are regular tricyclic sesquiterpene lactones that contain a five-membered  $\gamma$ -lactone ring fused to a seven-membered carbocycle in positions 6,7 or 7,8 (*cis* or *trans* configurations, respectively), which in turn, is fused to a five-member carbocycle (Macías et al. 2013; Zhang et al. 2015). Pseudoguaianolides contain methylated *trans*-perhydroazulene scaffolds.

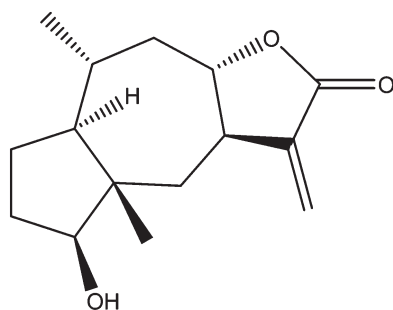
Carpesiolin (**1**) is a pseudoguaianolide sesquiterpene lactone isolated from the ethanolic extract of *Carpesium abrotanoides* L. (Asteraceae) along with other eudesmanolide sesquiterpene lactones (see below). The bioassay-guided fractionation of the extract has shown that carpesiolin has a potent activity against *Cochliobolus miyabeanus* and *Xanthomonas oryzae*, which are two infectious agents of rice cultures (Maruyama and Shibata 1975; Maruyama and Omura 1977).



**carpesiolin (1)**

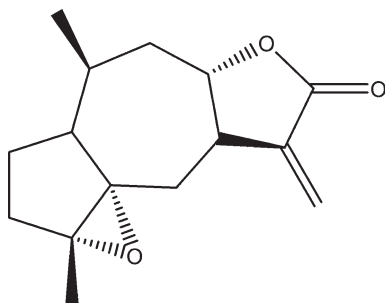
Further studies performed on the same plant have led to the isolation of 2-desoxy-4-epi-pulchellin (**2**), which has shown significant antimycobacterial activity (MIC: 7.6  $\mu$ M) (Wang et al. 2015).





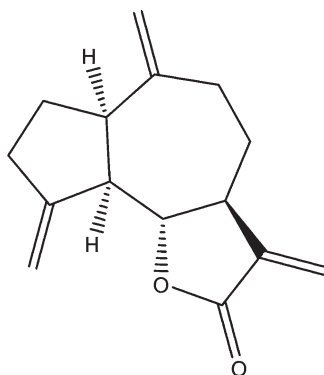
**2-desoxy-4-epi-pulchellin (2)**

The guaianolide  $4\alpha,5\alpha$ -epoxy- $10\alpha,14H$ -1-epi-inuviscolide (**3**) has been isolated from *Carpesium macrocephalum* Franch. & Sav. (Asteraceae), which is a widely distributed plant in China and Korea used as fungicide against phytopathogenic fungi. When the antifungal activity was tested in vitro against *Candida albicans*, it did not show activity at 256  $\mu\text{g/ml}$ . However, in an anti-virulence assay, the compound strongly inhibited biofilm formation with an  $\text{IC}_{50}$  value of 38  $\mu\text{g/ml}$ , also inhibiting the yeast to hyphae morphogenetic transition with an  $\text{IC}_{50}$  value of 106.5  $\mu\text{g/ml}$  (Xie et al. 2015).



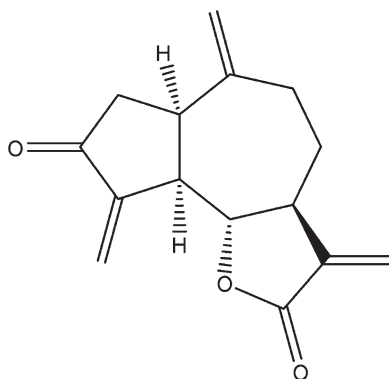
**$4\alpha,5\alpha$ -epoxy- $10\alpha,14H$ -1-epi-inuviscolide (3)**

When (-)-dehydrocostuslactone (**4**), which was isolated from a commercially available roots extract of *Saussurea lappa* (Asteraceae), was tested against *Cunninghamella echinulata*, the lactone inhibited fungal growth with an  $\text{EC}_{50}$  value of 6  $\mu\text{g/ml}$ , which is a value that is similar to that obtained with ketoconazole ( $\text{EC}_{50}$  1.5  $\mu\text{g/ml}$ ) (Barrero et al. 2000).



(-)-dehydro-costuslactone (4)

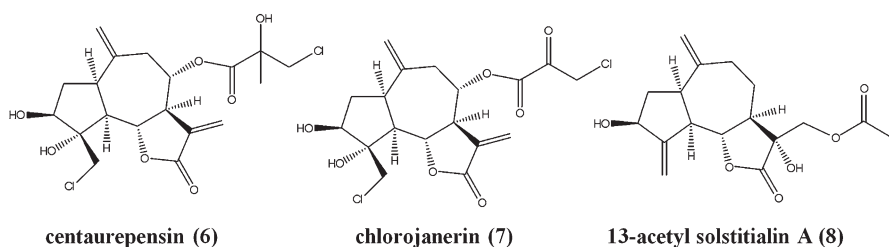
Dehydrozalizanin C (5) has been isolated from many different species from the Asteraceae family; however, this compound can also be semisynthesized from dehydrocostus lactone (Macías et al. 2000; Galindo et al. 1999). In a bioautographic assay, compound (5) has shown fungicidal activity against *Colletotrichum gloeosporioides*, *Colletotrichum acutatum*, *Colletotrichum fragariae*, *Phomopsis* sp., and *Botrytis cinerea*. When evaluated in a 96-well bioassay system, dehydrozalizanin C (30  $\mu$ M) inhibited the growth of *C. fragariae*, *C. gloeosporioides*, and *C. acutatum* by 90%, 89%, and 29%, respectively (Wedge et al. 2000).



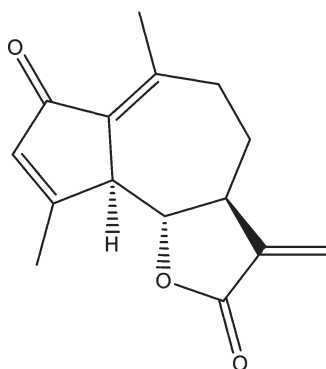
dehydrozalizanin C (5)

The genus *Centaurea* (Asteraceae) comprises many species that are used in folk medicine. Plants belonging to this genus have sesquiterpene lactones as characteristic constituents (Ciric et al. 2012). *Centaurea solstitialis* L. subsp. *solstitialis* is commonly used in Turkish folk medicine to treat orofacial herpes infections, peptic ulcer, malaria, common colds, and stomach and abdominal pain (Honda et al. 1996). Three sesquiterpene lactones centaurepensin (6), chlorojanerin (7), and 13-acetyl solstitialin A (8) have been isolated from the aerial parts as major

constituents, and their antimicrobial, antifungal, and antiviral profiles have been determined (Özçelik et al. 2009). These compounds have been tested against *Escherichia coli*, *Pseudomonas aeruginosa*, *Enterococcus faecalis*, *Staphylococcus aureus*, *Candida albicans*, and *Candida parapsilosis* by the microdilution method and against type 1 herpes simplex virus (HSV-1) and parainfluenza virus using Vero cells. These compounds have shown weak activity against fungi (MIC = 64 µg/ml), Gram-negative bacteria (MIC = 64–256 µg/ml), and Gram-positive *E. faecalis* (MIC = 64–128 µg/ml). However, 13-acetyl solstitialin A (**8**) and to a lesser degree centaurepensin (**6**) and chlorojanerin (**7**) have shown moderate activity on standard and isolated strains of *S. aureus* (MIC = 16 and 32 µg/ml, respectively). These compounds were also active against HSV-1, being **8** the most active when tested in a microdilution antiviral test using Vero cells (MIC ≤ 60 pg/ml).



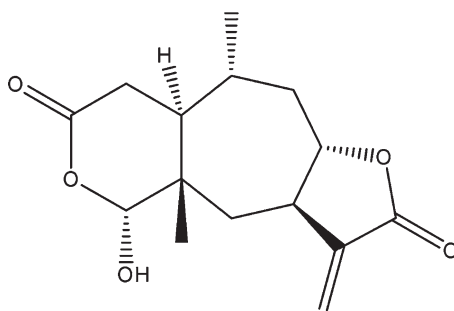
*Artemisia douglasiana* (Asteraceae) leaves, also known as “matico,” are used in Argentinian folk medicine for their beneficial effects against gastroduodenal disorders like peptic ulcer and for the treatment of external sores (Vega et al. 2009). Dehydroleucodine (**9**) is the main active cytoprotective principle isolated from the plant, which has been demonstrated to increase the synthesis of glycoproteins of the gastric mucosa and to prevent the formation of gastric mucous lesions induced by absolute ethanol or other necrotizing agents. The compound has been tested for its in vitro antibacterial activity on one *Helicobacter pylori* reference strain (NCTC 11638) and six antral biopsy clinical isolates by the agar dilution method. Dehydroleucodine (**9**) was active against all strains tested, with MIC values ranging from 1 to 8 µg/ml.



**dehydroleucodine (9)**

*Seco*-pseudoguaianolides are common compounds found in the genus *Hymenoxys* (Asteraceae). Herz (1977) categorized *seco*-pseudoguaianolides at the fourth level of biogenetic complexity (from 1 to 4). The biosynthesis of these compounds starts by a cyclization of either a germacrolide precursor or melampolide precursor (see below), which generates the guaianolide skeleton. After a number of structural rearrangements, the guaianolide is transformed into a pseudoguaianolide skeleton followed by a five-membered ring opening to produce the *seco*-pseudoguaianolide one. Generally, the lower complexity level skeletons have broader distributions within the family than the higher complexity level skeletons (Herz 1977, 1978).

Vermeerin (**10**) and other sesquiterpene lactones presenting a *seco*-pseudoguaianolide backbone have been isolated from *Hymenoxys robusta* (Rusby) K.F. Parker, also known in Bolivia as “q’illu q’illu” (Fortuna et al. 2011). When these *seco*-pseudoguaianolide sesquiterpene lactones were tested against a panel of bacterial and fungal pathogen strains, only vermeerin (**10**) was found to be active, showing a specific antibacterial activity on *S. aureus* with a MIC value of 10 µg/ml.



vermeerin (**10**)

### 12.2.2 Eudesmanolides

As for the antimicrobial activity, eudesmane sesquiterpene lactones constitute the most represented group among sesquiterpene lactones. They are tricyclic sesquiterpenoid lactones containing a five-membered  $\gamma$ -butyrolactone ring (Fig. 12.2) and can be divided in two structural classes according to the lactone ring annulation, 6,12- or 8,12-olides (Zhang et al. 2015).

Granilin (**11**) is an eudesmane-type sesquiterpene lactone which has been isolated from a methanolic extract of the whole *C. abrotanoides* plant and has shown in vitro activity against *Cochliobolus miyabeanus* and *Xanthomonas oryzae* (Maruyama and Shibata 1975).

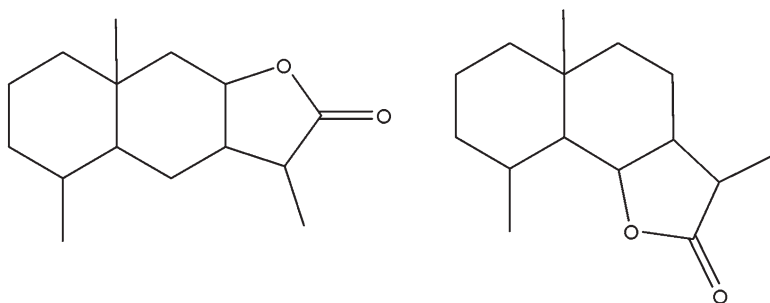
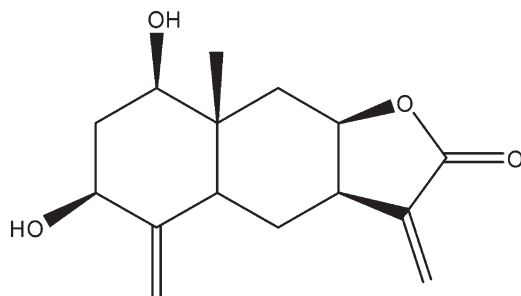


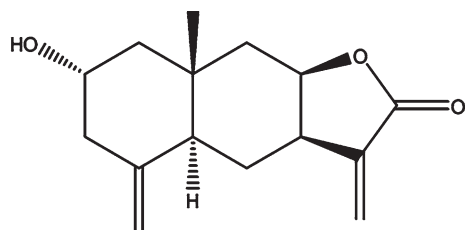
**Fig. 12.2** Eudesmanolide skeletons



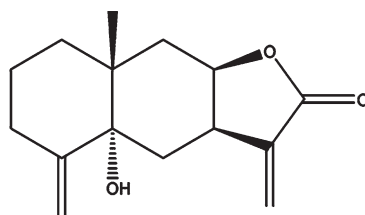
**granilin (11)**

Ten eudesmanolide sesquiterpene lactones have been isolated from the seeds of *C. macrocephalum*. Six of them have been tested for their antibacterial activity against *Bacillus subtilis*, *S. aureus*, and *E. coli*. Ivalin (**12**), telekin (**13**), and 2-( $\beta$ -D-glucopyranosyloxy)-5,11(H-eudesma-4(15)-en-12,8- $\beta$ -olide (**14**) have shown moderate antibacterial activity, while telekin (**13**) and ivalin (**12**) strongly inhibited *C. albicans* biofilm formation with  $IC_{50}$  values ranging from 15.4 to 36.0  $\mu\text{g/ml}$  (Yang et al. 2002; Xie et al. 2015).

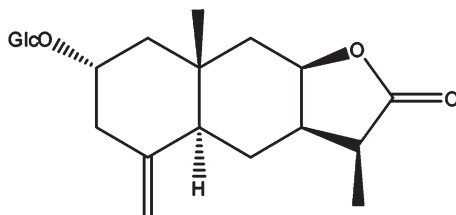
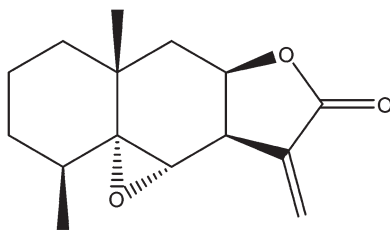
Other sesquiterpene lactones also isolated from *C. macrocephalum* have also been evaluated in vitro for their antifungal capacity to inhibit growth, biofilm formation, and yeast-hyphal transition of *C. albicans*. The eudesmane 5 $\alpha$ -epoxyalantolactone (**15**) did not show neither antifungal activity ( $MIC_{50} > 256 \mu\text{g/ml}$ ) nor inhibitory capacity on biofilm formation ( $IC_{50} > 128 \mu\text{g/ml}$ ); however, the compound inhibited the morphogenetic transition yeast-to-hyphae with an  $IC_{50}$  value of 118.4  $\mu\text{g/ml}$  (Xie et al. 2015).



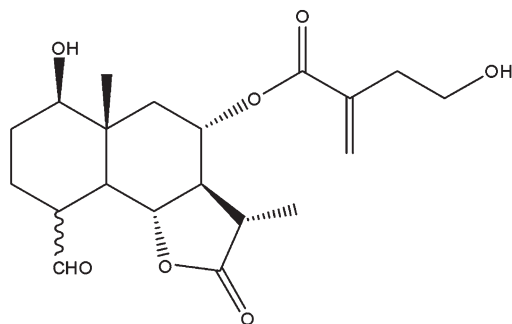
ivalin (12)



telekin (13)

2 $\alpha$ -( $\beta$ -D-Glucopyranosyloxy)-5 $\alpha$ ,11 $\alpha$ H-eudesma-4(15)-en-12,8- $\beta$ -olide (14)5 $\alpha$ -epoxyalantolactone (15)

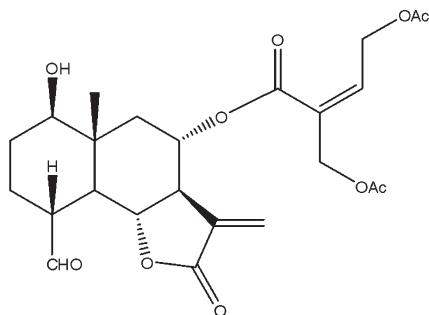
Antimicrobial eudesmane sesquiterpene lactones have been isolated from the aerial parts of *Centaurea pullata* (Djeddi et al. 2007). Two eudesmanolides (**16**) and (**17**), which had not previously been described, showed in vitro antibacterial and antifungal activities when tested against Gram-negative bacteria such as *Pseudomonas tolaasii* and *E. coli* ATCC 35210; Gram-positive bacteria such as *B. subtilis* ATCC 10907, *Micrococcus flavus* ATCC 10240, and *Staphylococcus epidermidis* ATCC 12228; and eight fungi (*Aspergillus niger* ATCC 6275, *Aspergillus ochraceus* ATCC 12066, *Aspergillus flavus* ATCC 9643, *Penicillium ochrochloron* ATCC 9112, *Penicillium funiculosum* ATCC 36839, *Trichoderma viride* IAM 5061, *Fusarium tricinctum* CBS 514478, and *Alternaria alternata* DSM 2006). Minimum inhibitory bactericidal or fungicidal concentrations obtained using the microdilution method ranged from 0.2 to 0.5  $\mu\text{g/ml}$ , being the compounds more potent than the positive controls streptomycin and miconazole.



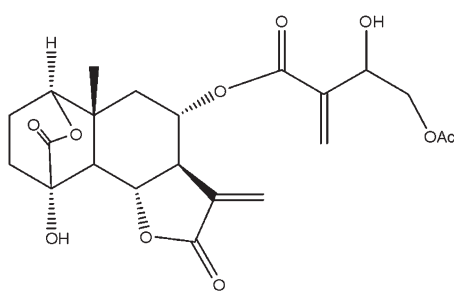
$\alpha$ -CHO 8 $\alpha$ -O-(4-hydroxy-2-methylenebutanoyloxy)-11 $\beta$ ,13-dihydrosonchucarpolide (**16**)

$\beta$ -CHO 8 $\alpha$ -O-(4-hydroxy-2-methylenebutanoyloxy)-11 $\beta$ ,13-dihydro-4-epi-sonchucarpolide (**17**)

The sesquiterpene lactones 8 $\alpha$ -O-(4,5-diacetoxyangeloyl)sonchucarpolide (**18**) and zuccarinin (**19**) have been isolated from *Centaurea zuccariniana* and evaluated by the broth microdilution method against Gram-negative bacteria (*E. coli*, *Proteus mirabilis*, *P. aeruginosa*, *Salmonella typhimurium*), Gram-positive bacteria (*Bacillus cereus*, *Micrococcus flavus*, *Listeria monocytogenes*, *S. aureus*), and fungi (*Aspergillus niger*, *Aspergillus versicolor*, *A. flavus*, *Aspergillus fumigatus*, *C. albicans*, *Penicillium funiculosum*, *Penicillium ochrochloron*, *T. viride*). The tested compounds exhibited moderate antibacterial activity when compared to streptomycin and amoxicillin, with MIC values ranging from 222 to 450 nmol/ml, and similar or higher antifungal activities than the fungicides, bifonazole, and ketoconazole (MIC = 222 to 900 nmol/ml) (Ciric et al. 2012).



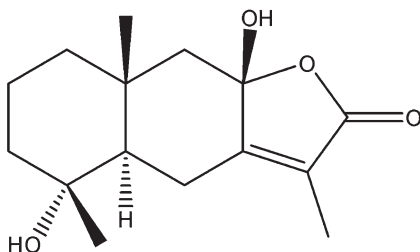
8 $\alpha$ -O-(4,5-diacetoxyangeloyl)sonchucarpolide (**18**)



zuccarinin (**19**)

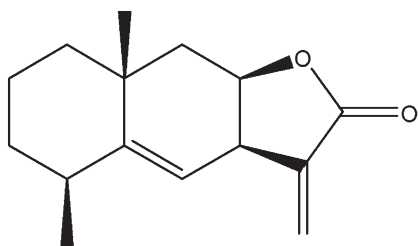
Plants from the genus *Chloranthus* (Chloranthaceae) such as *C. angustifolius* have been used as herbal medicines in China for the treatment of traumatic injury, blood stasis, and *tinea* infections (Yang et al. 2014). Sesquiterpenes and their dimers have been described as the major secondary metabolites in this genus, exhibiting a variety of biological activities like antifungal and cytotoxic, among others (Xu 2013). A bioassay-guided phytochemical investigation

carried out on *C. angustifolius* roots has led to the isolation of the eudesmane sesquiterpene lactone 4 $\alpha$ ,8 $\beta$ -dihydroxy-5 $\alpha$ (H)-eudesm-7(11)-en-8,12-olide (**20**), among others. When tested against a panel of five bacterial and six fungal strains, the lactone exhibited moderate inhibitory activity on *C. albicans* with a MIC value of 16  $\mu$ g/ml.

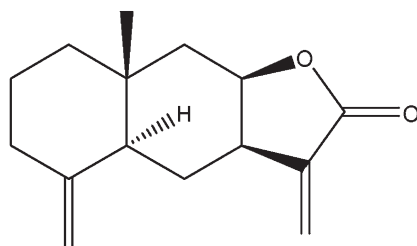


4 $\alpha$ ,8 $\beta$ -dihydroxy-5 $\alpha$ (H)-eudesm-7(11)-en-8,12-olide (**20**)

The sesquiterpene lactones alantolactone (**21**) and isoalantolactone (**22**) have been isolated from *Inula helenium* (Asteraceae). Actually, these compounds have been isolated from their natural source as a mixture known as helenin (Gökbulut and Şarer 2013). These lactones have been reported to inhibit the growth of dermatophytes *Microsporum gypseum*, *Trichophyton acuminatum*, and *Epidermophyton* sp. When tested against a panel of 16 fungi in a macrodilution agar test, both lactones showed antifungal activity against all fungi tested at least at the highest concentration used (1000  $\mu$ g/ml), being strongly active against *Microsporum cookei* and *Trichophyton mentagrophytes*, whose growth was completely inhibited when used at 10  $\mu$ g/ml (Picman 1983).



alantolactone (**21**)



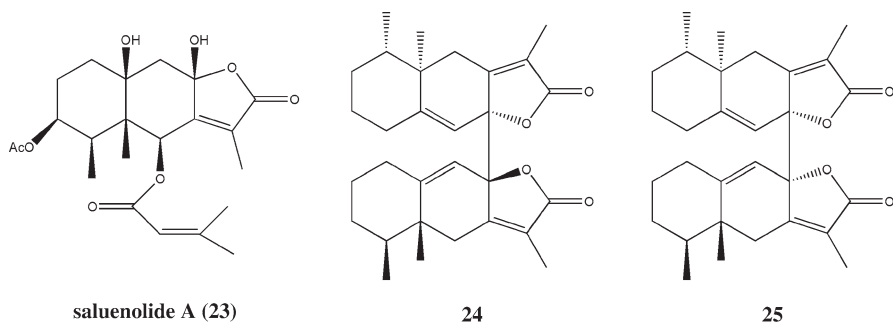
iso-alantolactone (**22**)

Alantolactone (**21**) has also shown antiviral activity in vitro on herpes simplex virus 1 (HSV-1) (Rezeng et al. 2015). The effect of the compound was determined using a cytopathic effect-based assay, and results indicated that alantolactone markedly inhibited viral infections at 0.01-1  $\mu$ g/ml, showing the more potent antiviral activity at 0.1  $\mu$ g/ml. Besides Vero cells viability was not affected at concentrations below 1  $\mu$ g/ml.

Plants of the genus *Senecio* L. (Asteraceae) are traditionally used in China for the treatment of hepatitis B, dermatosis, and inflammation. Studies performed on extracts



from *S. tsoongianus* and *S. saluenensis* have shown a suppressor activity on the secretion of hepatitis B virus surface antigen (HBsAg) and hepatitis B virus e antigen (HBeAg) in HepG2.2.15 cells. The bioguided fractionation of *S. saluenensis* has led to the isolation of saluenolide A (**23**) and compounds **24** and **25** from *S. tsoongianus*. These compounds displayed significant inhibitory activity on the expression of HBsAg and HBeAg in HepG2.2.15 and reduced the hepatitis B virus (HBV) DNA in the culture medium without inhibiting intracellular HBV DNA, suggesting that these compounds may interfere with virion release from cells (Li et al. 2005).

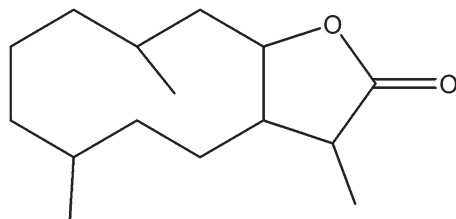


### 12.2.3 Germacranolides and Other Related Structures

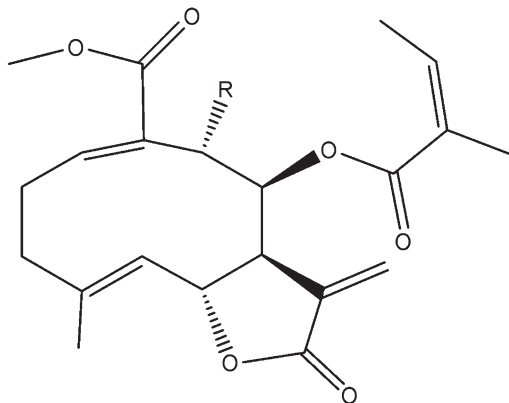
The parent nucleus of the germacrane contains a special ten-member ring (Fig. 12.3), thus creating a complex and diverse stereo configuration. The Asteraceae family presents several types of germacranolides (Zhang et al. 2015).

*Smallanthus sonchifolius* (Poepp.) H. Rob. (Asteraceae), also known as “yacon,” is a medicinal plant originally cultivated in the Andean highlands. It has been reported that its tubers contain high amounts of oligofructans and polyphenols, and that the leaf extract has antidiabetic effects. Its tubers are also used as food, whereas the aerial parts are used as fodder for animals (Inoue et al. 1995). Since for the cultivation of “yacon,” it is not necessary to use antifungal and pesticide compounds; it has been suggested that the aerial parts of the plant should contain some antifungal and pesticide compounds (Lin et al. 2003). The ethanolic extract of yacon leaves has been studied by a bioassay-guided fractionation using a spore suspension of

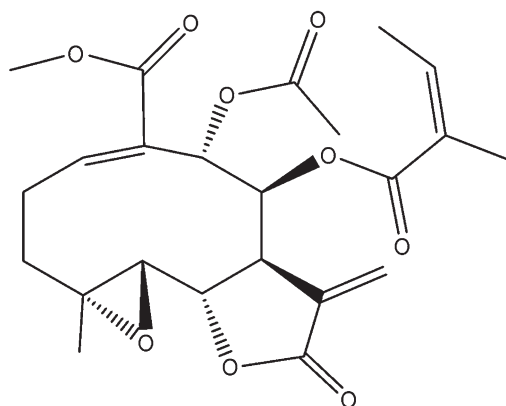
**Fig. 12.3** Germacranolide skeleton



*Pyricularia oryzae* (Akatsuka et al. 1985). The active fractions obtained proved to contain the melampolides sonchifolin (26) and polymatin B (27), among other melampolides. The complete inhibition of spore germination was obtained at 100 ppm and 250 ppm for sonchifolin (26) and polymatin B (27), respectively.

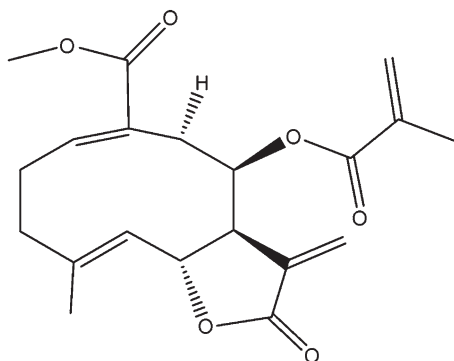


R=H sonchifolin (26), R=OAc polymatin B (27)



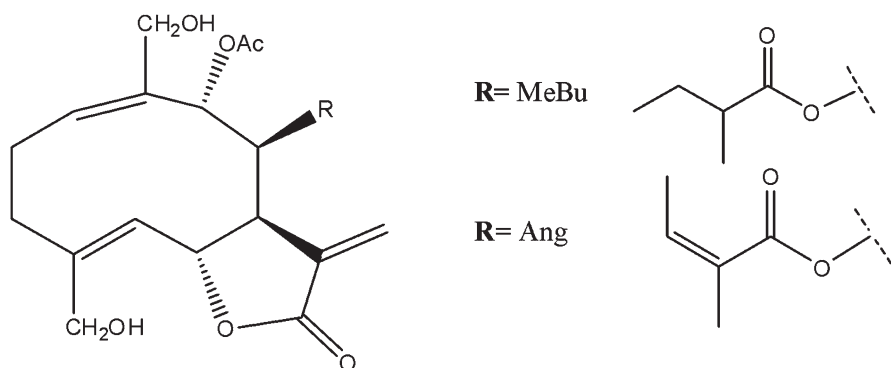
fluctuanin (28)

The extraction and chromatographic separation of “yacon” leaves extract yielded two melampolide-type sesquiterpene lactones that had not previously been described and the known melampolides sonchifolin (26), fluctuanin (28), uvedalin, and enhydrin (structures not shown) (Lin et al. 2003). These compounds were tested for their antibacterial activity against *B. subtilis* and for their antifungal properties against *P. oryzae*. The new compound 8 $\beta$ -methacryloyloxymelampolid-14-oic acid methyl ester (29) and sonchifolin (26) exhibited potent antifungal activity on *P. oryzae*, inhibiting 100% of spore germination at 200 ppm. Fluctuanin (28) was the most active compound on *B. subtilis*, and the minimum inhibitory weight to give a bacterial growth inhibition zone greater than 10 mm diameter was 25  $\mu$ g.



**8β-methacryloyloxy melampolid-14-oic acid methyl ester (29)**

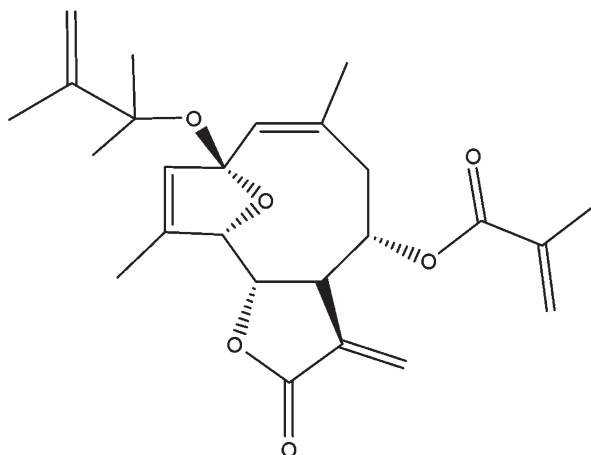
The dihydroxy melampolides (**30**) and (**31**) isolated from *Acanthospermum hispidum* (Asteraceae) have shown activity on *P. aeruginosa* biofilm formation. These compounds were active at the two concentrations tested (0.25 μg/ml and 2.5 μg/ml), reducing biofilm formation by roughly 50%, when compared to the control after 1 or 6 h of bacteria-compound contact (Cartagena et al. 2007).



**R=MeBu** 9α-acetyloxy-14,15-dihydroxy-8β-(2-methylbutanoyloxy)-acanthospermolide (**30**)

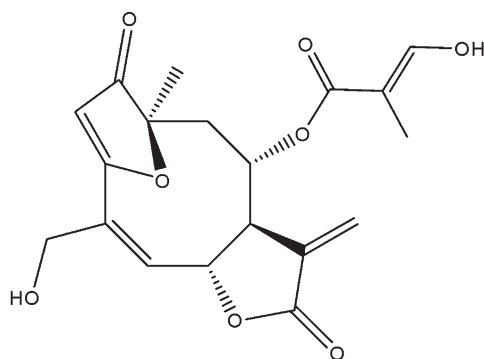
**R= Ang** 9α-acetyloxy-14,15-dihydroxy-8β-(2-angeloyloxy)-acanthospermolide (**31**)

*Elephantopus tomentosus* (Asteraceae) is a traditional plant medicine growing in the south of China. The whole plant is used for the treatment of hepatitis, bronchitis, fever, the cough associated with pneumonia, and arthralgia. Three germacranolide sesquiterpene lactones have been isolated from the whole plant and their antibacterial properties evaluated by the agar diffusion assay on *S. aureus* employing kanamycin sulfate as positive control. Tomenphantopin H (**32**), 2β-methoxy-2-de-ethoxy-8-O-deacylphanto-molin-8-O-tigilate, and 2-de-ethoxy-2-hydroxyphantomolin (structure not shown) inhibited the growth of *S. aureus* at 500 μg/disk with inhibition halos of 14.2 mm, 13.4 mm, and 31.0 mm, respectively (positive control 6.4 μg/disk, 32.6 mm) (Wang et al. 2012).



**tomenphantopin H (32)**

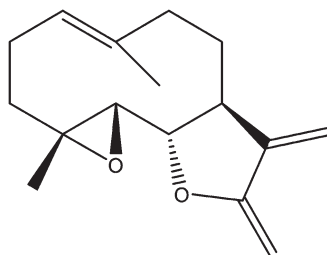
Six sesquiterpene lactones of the goyazensolide-type and the isogoyazensolide-type have been isolated from *Centratherum punctatum* subsp. *punctatum* (Asteraceae). The compounds were tested for their inhibitory capacity on *P. aeruginosa* biofilm formation, elastase activity, and production of N-acyl-homoserinelactones, which act as intercellular signal molecules. All the compounds assayed inhibited bacterial growth at the highest concentration tested. At 200  $\mu\text{g/ml}$  the inhibitory effect of the compounds ranged from 11% to 71%. The biofilm formation and N-acyl-homoserinelactones production were also inhibited by all the compounds tested, being 1-oxo-3,10-epoxy-8-epoxymethacryloyloxy-15-hydroxygermacra-2,4,11(13)-trien-6,12-olide (**33**) the most potent compound causing a 42% inhibition of biofilm formation at 0.5  $\mu\text{g/ml}$  and 66% inhibition on N-acyl-homoserinelactones production at 200  $\mu\text{g/ml}$  (Amaya et al. 2012).



**1-oxo-3,10-epoxy-8-epoxymethacryloyloxy-15-hydroxygermacra-2,4,11(13)-trien-6,12-olide(33)**

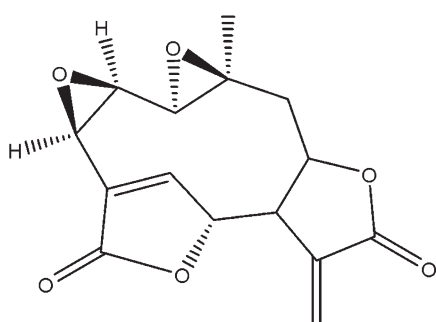
Parthenolide-like sesquiterpene lactones are germacranolides which bear a ten-membered ring with a five-membered fused lactone, an  $\alpha$ -methylene group in the lactone ring, and a  $\text{C}_4\text{-C}_5$  epoxide ring (Seca et al. 2017). Parthenolide (**34**) was the first

sesquiterpene lactone isolated from feverfew leaves, *Tanacetum parthenium* (Asteraceae), and from other asteraceous species such as *Tarhonanthus camphoratus*. The species *T. camphoratus* is used in Yemen to treat wounds and urinary tract infections, while in South Africa, the plant is used to relieve toothache and to treat respiratory disorders. Parthenolide has been tested for its in vitro growth inhibitory activity against *C. albicans* ATCC 2091, *S. aureus* ATCC 6538P, *B. subtilis* ATCC 6633, *Mycobacterium smegmatis* ATCC 14468, *E. coli* ATCC 25922, and *P. aeruginosa* MTCC 741. The molecule showed activity against *S. aureus* and *B. subtilis* with MIC values of 25  $\mu\text{g/ml}$ , while the MIC for *C. albicans* was 300  $\mu\text{g/ml}$  (Jamal et al. 2014).

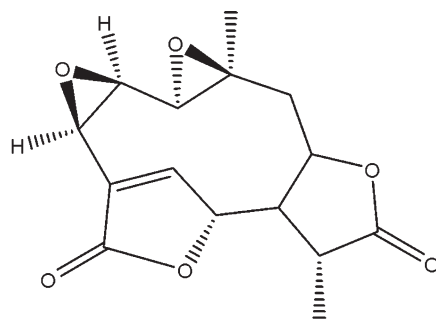


parthenolide (34)

The plant *Mikania micrantha* (Asteraceae) is an extremely fast growing perennial creeping weed native to Central and South America, where it is traditionally used to treat skin diseases and athlete's foot (Rios et al. 2014). Sesquiterpene lactones of the germacrane type have been described as constituents of the plant. Mikanolide (35) and dihydromikanolide (36) have been isolated from the aerial parts as the major constituents which are responsible for the antimicrobial activity of the plant. In an agar diffusion test, both compounds showed antibacterial and antifungal activities on *S. aureus* (45–48 mg/disc) and *C. albicans* (6–42 mg/disc), being the dihydro derivative seven times more active against *C. albicans* (Facey et al. 1999).



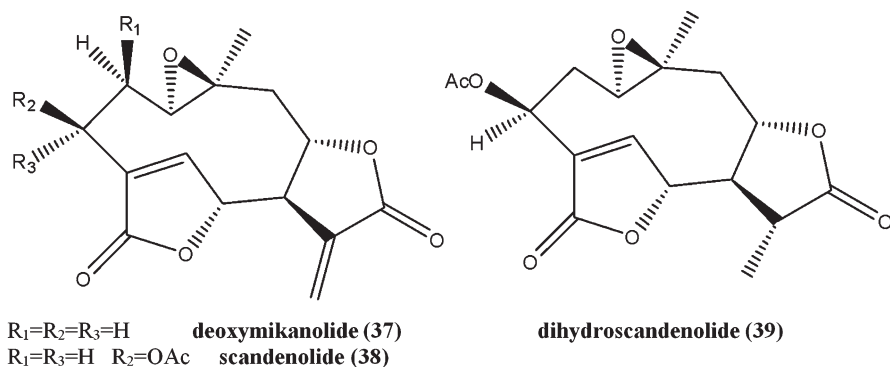
mikanolide (35)



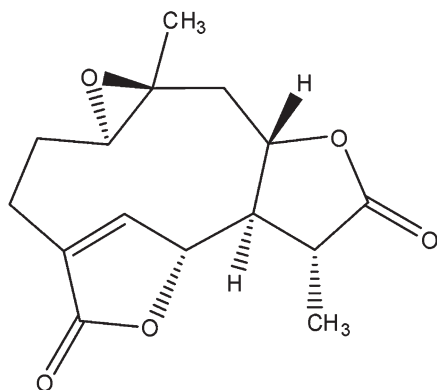
dihydromikanolide (36)

Further studies have led to the isolation of deoxymikanolide (37), scandenolide (38), and dihydroscandenolide (39) in addition to mikanolide (35) and dihydromikanolide (36). The compounds were evaluated by the hypha growth inhibition and

the spore germination inhibition methods against eight phytopathogenic fungal strains. All compounds showed antimicrobial activity, and the MIC values for the tested strains (*S. aureus*, *B. subtilis*, *Micrococcus luteus*, *Bacillus cereus*, *Ralstonia dolaanacearum*, *Xanthomonas oryzae* pv. *oryza*, *Xanthomonas campestris* pv. *vesicatoria*, *Xanthomonas campestris* pv. *citri*) ranged from 62.5 to 125  $\mu\text{g/ml}$ . In the hypha growth inhibition method,  $\text{EC}_{50}$  values for the four strains tested (*Fusarium solani*, *Rhizoctonia solani*, *Pythium aphanidermatum*, *Phytophthora parasitica*) ranged from 82.4 to 347.33  $\mu\text{g/ml}$ . Deoxymikanolide (**37**) was the most active compound in the spore germination assay, and the  $\text{IC}_{50}$  ranged from 21.44 to 53.18  $\mu\text{g/ml}$  for the four strains tested (*Exserohilum turcicum*, *Botrytis cinerea*, *Pseudoperonospora cubensis*, *Colletotrichum lagenarium*) (Li et al. 2013).

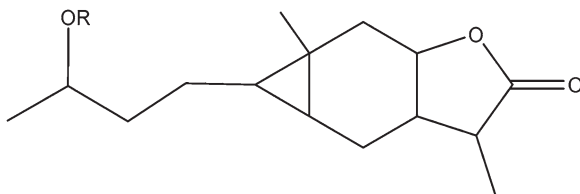


In another study (But et al. 2009), the methanolic extract from the dried aerial parts of *M. micrantha* has shown inhibitory activity on respiratory syncytial virus (RSV) with an  $\text{IC}_{50}$  of 60  $\mu\text{g/ml}$ . Further studies led to the isolation of sesquiterpene lactones **36**, **39**, and **40**. These sesquiterpene lactones showed weak antitype A influenza activities, while compound **40** showed moderate activity against RSV ( $\text{IC}_{50} = 37.4 \mu\text{M}$ ) and parainfluenza type 3 virus ( $\text{IC}_{50} = 37.4 \mu\text{M}$ ) with a therapeutic index of 10 for both viruses.



**1,10-epox-4-germacrane-12,8;15,6-diolide (40)**

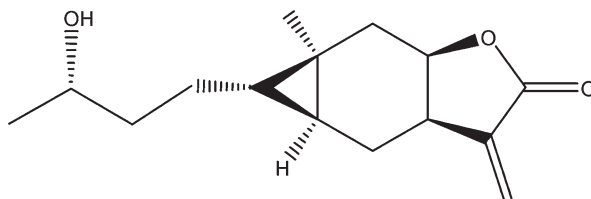
**Fig. 12.4** Carabranolide skeleton



### 12.2.4 Carabranolides

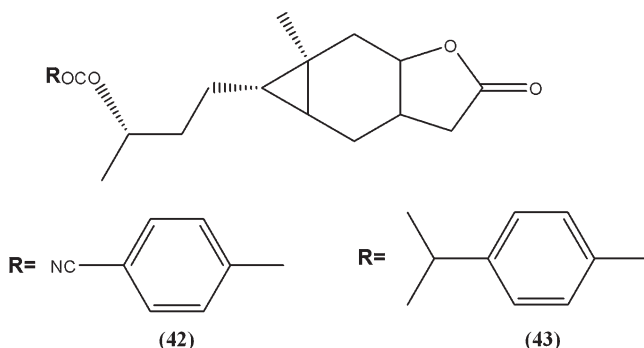
Carabranolide sesquiterpene lactones (Fig. 12.4) are secoregular sesquiterpenoids that can be biosynthesized from a xanthanolide carbon skeleton by creating a bond between C-5 and C-10 to form a ring (Zhang et al. 2015). Interestingly, carabrol (**41**) is the only compound presenting antimicrobial activity (see below).

The sesquiterpene lactone carabrol (**41**) has been isolated from *C. abrotanoides*. This compound has shown antifungal activity against *Colletotrichum lagenarium* with an  $IC_{50}$  value of 20.14  $\mu\text{g/ml}$  in a spore germination assay. The fungus *C. lagenarium* is the causative agent of anthracnose of leaves and fruits of cucurbit crops, resulting in severe yield losses and reduction in the quality of the fruits (Feng et al. 2012).



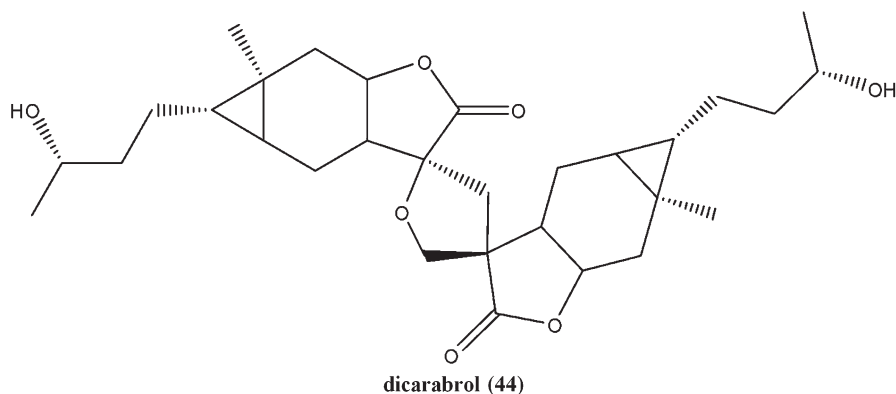
**carabrol (41)**

Because carabrol has great potential as a template for developing more effective fungicides that may be environmentally safe, Feng et al. (2012) prepared 38 ester derivatives and tested them on *C. lagenarium*, 16 of which showed higher antifungal activity than that of carabrol. The authors found that the C-4 position of carabrol was key for the biological activity. When that position was substituted by a phenyl ring, the ester derivatives bearing electron-attracting groups showed higher activity than those bearing electron-donating ones. Two ester derivatives, carabryl 4-cyanobenzoate (**42**,  $IC_{50} = 2.70 \mu\text{g/ml}$ ) and carabryl 4-isopropylbenzoate (**43**,  $IC_{50} = 2.82 \mu\text{g/ml}$ ), showed an antifungal activity that was near to chlorothalonil used as positive control ( $IC_{50} = 0.87 \mu\text{g/ml}$ ) (Feng et al. 2012).



### 12.2.5 Dimeric Sesquiterpene Lactones

Sesquiterpene dimers, which are also called disesquiterpenoids, can be classified into three major classes based on their biosynthetic origins, namely, true disesquiterpenoids, pseudo-disesquiterpenoids, and dimerosesquiterpenoids. Sesquiterpene dimers are mainly synthesized by Diels-Alder, hetero-Diels-Alder, [2 + 2] cycloaddition, or free-radical coupling reactions (Zhang et al. 2015). Sesquiterpenoid dimers with unusual carbon skeletons have been reported. The complex linkage patterns, along with their multiple chiral centers, make them to exhibit more “biologically friendly” and “drug-like” molecular features than the corresponding monomers (Wu et al. 2017), as is the case of dimeric sesquiterpene lactones.

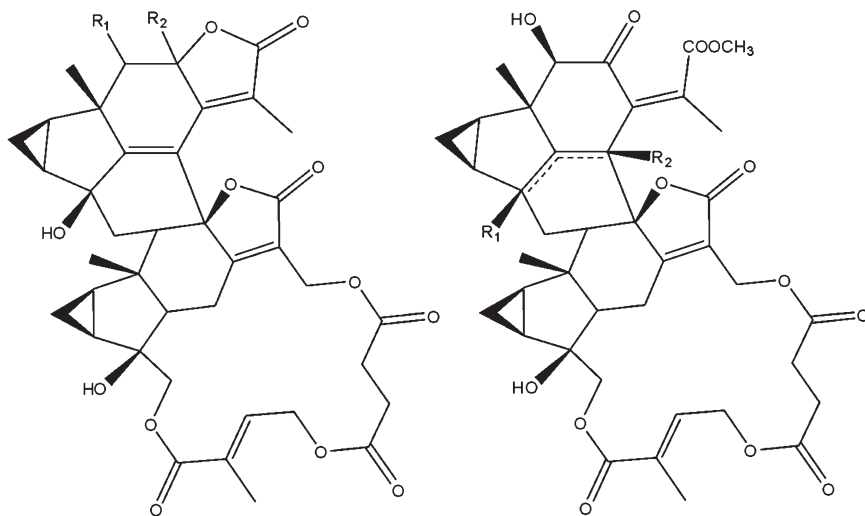


Dicarabrol (**44**) is a dimeric sesquiterpene lactone which has been isolated from *C. abrotanoides* along with other dimeric and monomeric sesquiterpene lactones. Dicarabrol (**44**) possesses an unusual carbon skeleton with two carabranolide moieties linked through a spiro-tetrahydrofuran ring, presumably generated by a [4 + 2]



cycloaddition (Wu et al. 2015). The molecule displayed significant antimycobacterial activity on *Mycobacterium tuberculosis* H37Rv with an  $IC_{50}$  value of 3.7  $\mu$ M (1.91  $\mu$ g/ml), control isoniazid  $IC_{50}$  = 2.0  $\mu$ M (0.2  $\mu$ g/ml) employing the alamar blue microdilution test (Wang et al. 2015).

*Mycobacterium tuberculosis* has been a major human pathogen since the dawn of modern human existence. The prognosis for patients with tuberculosis has improved dramatically with the discovery and introduction of antitubercular drugs, starting with streptomycin in 1946 and subsequent research that produced today's frontline therapies for drug-sensitive *M. tuberculosis*. Despite having an effective treatment regimen, tuberculosis is still causing millions of infections and deaths. There are a few drugs that are currently being assessed in clinical trials. Besides, major pharmacological redundancies exist, with many of the new agents in the pipeline that share a similar mechanism of action, cross-resistance, and/or side effect profiles, which makes them unsuitable to be used in combination (Hoagland et al. 2016). Taking into account these facts, the search for new drugs within the plant kingdom can certainly give interesting results, as occurs with dicarabrol.



	R <sub>1</sub>	R <sub>2</sub>		R <sub>1</sub>	R <sub>2</sub>	$\Delta$
<b>henriol A (45)</b>	$\beta$ -OH	$\alpha$ -OH	<b>chloramultilide A (49)</b>	OH	--	5,6
<b>spicachlorantin A (46)</b>	=O	$\alpha$ -OH	<b>shizukaol B (50)</b>	--	H	4,5
<b>8-tianmushanol (47)</b>	$\beta$ -OH	$\beta$ -OH				
<b>8-O-methyltianmushanol (48)</b>	$\beta$ -OH	$\beta$ -OCH <sub>3</sub>				

The dimeric carabranolide sesquiterpene lactones henriol A (45), spirachlorantin A (46), 8-tianmushanol (47), 8-O-methyltianmushanol (48), chloramultilide A (49), and shizukaol B (50) have been isolated from *C. angustifolius*, which was cited above as a producer of antimicrobial eudesmanolide sesquiterpene lactones. The compounds were tested in vitro using a microdilution assay against a panel of five bacterial strains including *S. aureus* (ATCC 29213), *E. coli* (ATCC 25922),

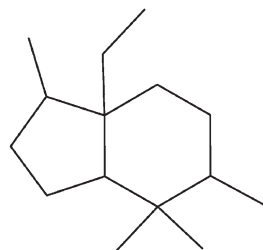
*S. typhimurium* (ATCC 13311), *P. aeruginosa* (ATCC 27853), and *Klebsiella pneumoniae* (ATCC 18433), as well as six fungal strains including *C. albicans* (ATCC 90028), *C. neoformans* (ATCC 22402), *Candida glabrata* (ATCC 90030), *Candida krusei* (ATCC 6258), *Candida parapsilosis* (ATCC 22019), and *Aspergillus* spp. (ATCC 293). None of the compounds were active on bacteria at 256 µg/ml; however, the compounds showed activity on the fungal strains tested. All compounds displayed significant antifungal activity against *C. albicans*, with MIC values ranging from 4 to 8 µg/ml (MIC itraconazole = 0.125 µg/ml). Shizukaol B (**37**) was active on *C. neoformans* (MIC itraconazole = 2.0 µg/ml) and on *Aspergillus* spp. with a MIC value of 8 µg/ml (MIC itraconazole = 2.0 µg/ml) (Yang et al. 2014).

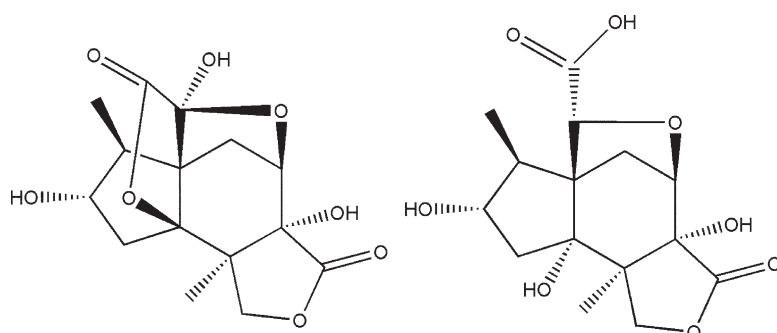
### 12.2.6 *Seco-prezizaane Sesquiterpene Lactones*

Seco-prezizaane-type sesquiterpenoids (Fig. 12.5) constitute a biosynthetically fascinating, architecturally variegated, and rapidly growing class of natural products that are found as characteristic chemical markers of *Illicium* spp. (Schisandraceae) (Liu et al. 2015). This genus is widely distributed in southern regions of China.

The cortex and root bark of *Illicium* spp. such as *I. merrillianum*, *I. jiadifengpi*, and *I. minwanense* have been used in folk medicine for the treatment of rheumatoid arthritis. Studies performed on the ethanolic extract of the fruits of *I. jiadifengpi*, a tree found in South China, led to the isolation of two new *seco*-prezizaane sesquiterpene lactones 2*S*-hydroxyl-jiadifenolide (**51**) and jiadifenlactone acid (**52**) along with other known *seco*-prezizaane sesquiterpene lactones (**53** and **54**). The compounds were tested for their potential anti-HBV activities regarding their capacity to inhibit the secretion of HBsAg and HBeAg to the culture medium of HBV-infected HepG2.2.15 cells under non-cytotoxic concentrations (Liu et al. 2015). The compounds **53** and **54** were the most active, inhibiting 15.53 to 37.93% of HBeAg and HBsAg expression at 64.94 and 61.35 µM, respectively. These results suggest that the carbonyl group at position 2 enhanced the antiviral activity (Liu et al. 2015).

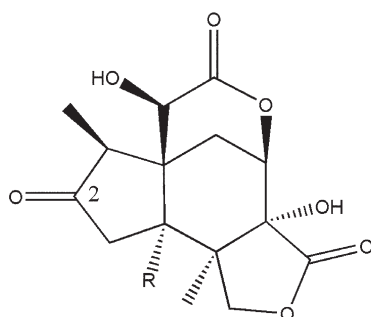
**Fig. 12.5** Seco-prezizaane skeleton





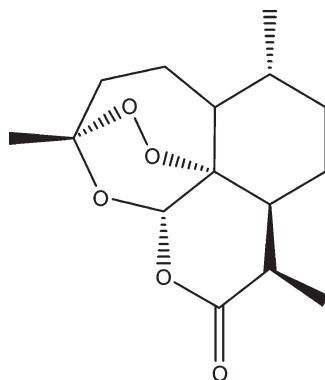
2S-hydroxyl-jiadifenolide (51)

jiadifenlactone acid (52)

R=OH 2-oxoneomajucin (53)  
2-oxo-3,4-dehydroxoneomajucin (54)

### 12.2.7 Cadinanolides

*Artemisia annua* (Asteraceae), also known as “sweet wormwood,” is a traditional Chinese herbal medicine which has been used for hundreds of years for its antimalarial properties, among others. Artemisinin (**55**), a cadinane-type sesquiterpene containing a unique peroxide bridge, has been identified in China in 1972 as the active compound (Efferth et al. 2008); and since then, artemisinin and its derivatives have been used against multidrug-resistant *Plasmodium falciparum* strains.

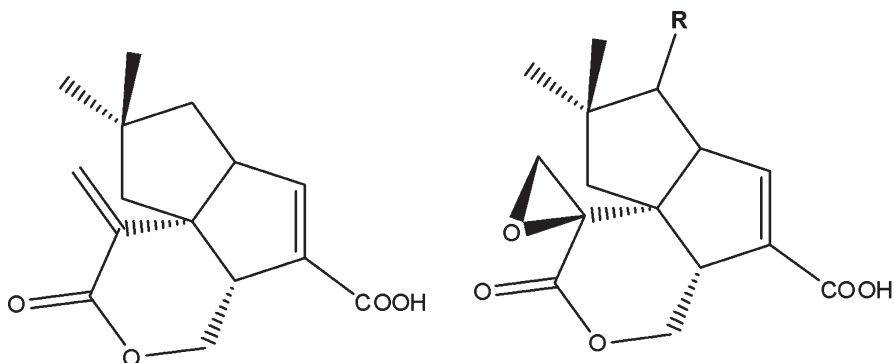


artemisinin (55)

Apart from its potent antimalarial activity, artemisinin has immunomodulatory and antitumor properties. In addition, several *in vitro* studies have demonstrated that the compound has also antiviral activities (Goswami et al. 2012, Ivanescu et al. 2015). Artemisinin (55) has shown considerable anti-HBV activity, when tested on HBV-transfected HepG2 2.2.15 cells, inhibiting HBsAg secretion with an  $IC_{50} = 55 \mu\text{g/ml}$  (Romero et al. 2005). The compound inhibited HCV replication in Huh5-2 cells, with an  $EC_{50} = 78 \mu\text{M}$  (Paeshuyse et al. 2006). The compound has also demonstrated strong activity against *Helicobacter pylori*, which is one of the causative agents of peptic ulcer disease. When tested against standard strains and clinical isolates of *H. pylori*, artemisinin (55) generated a 1.5 to 2.5 cm inhibition zone diameter at a dose of 1 to 5  $\mu\text{g/disc}$  and MIC values that ranged from 0.5 to  $\geq 8 \mu\text{g/ml}$  (Goswami et al. 2012).

### 12.2.8 Microbial Sesquiterpene Lactones

Pentalenolactones, also known as arenaemycins, are a sesquiterpenoid family of antibiotics discovered in 1957 in the culture extracts of *Streptomyces roseogriseus* and subsequently isolated from numerous *Streptomyces* species such as *S. avermitilis* and *S. arenae* (Takamatsu et al. 2011).



**pentalenolactone E (56)**

R=H **pentalenolactone F (57)**

R=O **pentalenolactone G (58)**

R=OH **pentalenolactone H (59)**

Pentalenolactones (**56–59**) are active against both Gram-positive and Gram-negative bacteria, as well as pathogenic and saprophytic fungi (Takamatsu et al. 2011). The mechanism of action of pentalenolactone E (**56**) has been reported by Hartmann et al. (1978). These authors have demonstrated that pentalenolactone exerts its antimicrobial activity by selective irreversible inhibition of glyceraldehyde-3-phosphate dehydrogenase (EC 1.2.1.12), an enzyme from the glycolytic pathway, with no affectation of other glycolytic reactions or enzymes of the intermediary metabolism. The study showed that pentalenolactone E (**56**) inhibits the enzyme of both prokaryotic and eukaryotic organisms (Hartmann et al. 1978).

## 12.3 Conclusion

Sesquiterpene lactones constitute a great group of natural products with an outstanding chemical diversity. Derived from the common biosynthetic precursor farnesyl diphosphate (FPP), they can undergo many chemical changes to produce several different backbones.

The antimicrobial and antiviral properties of 59 natural and semisynthetic sesquiterpene lactones were included in this chapter. All the natural structures discussed herein have been isolated from plants, with the exception of pentalenolactones, which are the only sesquiterpene lactones of microbial origin. Semisynthetic molecules dehydrozaluzanin and carabrol esters have also been included, and their antimicrobial properties were discussed.

As for the sesquiterpene lactones isolated from plants, most of them were from the Asteraceae family, followed by a few molecules from the Chloranthaceae and Schisandraceae families. These compounds may play a role in the defense of these

plants against pathogens, herbivorous insects, and mammals and in competition with other plants. Regarding sesquiterpene lactones of bacterial origin, they were from *Streptomyces* spp.

Different methods have been used to evaluate the antibacterial or antifungal activity of sesquiterpene lactones. It is known that the use of standardized methods is extremely important in order to perform comparisons of antimicrobial activities both intra- and inter-laboratory. It must be taken into account that the results corresponding to each research have been presented in different units. In addition, in many examples included in this chapter, no information regarding the values obtained for positive controls was provided. Thus, comparison of antimicrobial activities to establish valid relationships becomes difficult.

The biological activities of sesquiterpene lactones, including the antimicrobial activity, are generally the result of their interaction with the thiol groups present in proteins. When the relationship between the biological activity and the chemical structure was studied, no major generalizations could be obtained. In addition to the  $\alpha$ -methylene- $\gamma$ -lactone moiety, suspected to be responsible for many activities, other functionalities and their position on a skeleton and/or configuration may also enhance or reduce the activity of sesquiterpene lactones. Differences in the physiology and biochemistry among the target organisms must also be considered in order to draw valid conclusions.

## References

- Akatsuka T, Kodama O, Sekido H et al (1985) Novel phytoalexins (oryzalexins A, B and C) isolated from rice blast leaves infected with *Pyricularia oryzae*. Part I: Isolation, characterization and biological activities of oryzalexins. *Agric Biol Chem* 49:1689–1694
- Amaya S, Pereira JA, Borkosky SA et al (2012) Inhibition of quorum sensing in *Pseudomonas aeruginosa* by sesquiterpene lactones. *Phytomedicine* 19:1173–1177
- Barrero A, Oltra JE, Álvarez M et al (2000) New sources and antifungal activity of sesquiterpene lactones. *Fitoterapia* 71:60–64
- But PHH, He ZD, Ma SC et al (2009) Antiviral constituents against respiratory viruses from *Mikania micrantha*. *J Nat Prod* 72:925–928
- Cartagena E, Colom OA, Neske A et al (2007) Effects of plant lactones on the production of biofilm of *Pseudomonas aeruginosa*. *Chem Pharm Bull* 55:22–25
- Ciric A, Karioti A, Koukoulitsa C et al (2012) Sesquiterpene lactones from *Centaurea zaccarini-ana* and their antimicrobial activity. *Chem Biodivers* 9:2843–2853
- Demain AL, Sanchez S (2009) Microbial drug discovery: 80 years of progress. *J Antibiot* 62:5–16
- Djeddi S, Karioti A, Sokovic M et al (2007) Minor sesquiterpene lactones from *Centaurea pullata* and their antimicrobial activity. *J Nat Prod* 70:1796–1799
- Efferth T, Romero MR, Wolf DG et al (2008) The antiviral activities of artemisinin and artesunate. *Clin Infect Dis* 47:804–811
- Facey P, Pascoe KO, Porter RB et al (1999) Investigation of plants used in Jamaican folk medicine for anti-bacterial activity. *J Pharm Pharmacol* 51:1555–1560
- Feng JT, Wang H, Ren SX et al (2012) Synthesis and antifungal activities of carabrol ester derivatives. *J Agric Food Chem* 60:3817–3823
- Fortuna AM, Juárez ZN, Bach H et al (2011) Antimicrobial activities of sesquiterpene lactones and inositol derivatives from *Hymenoxys robusta*. *Phytochemistry* 72:2413–2418

- Galindo JCG, Hernández A, Dayan FE et al (1999) Dehydrozaluzanin C, a natural sesquiterpenoid, causes plasma membrane leakage. *Phytochemistry* 52:805–813
- Gökbulut A, Şarer E (2013) Isolation and quantification of alantolactone/isoalantolactone from the roots of *Inula helenium* subsp *turcoracemosa*. *Turk J Pharm Sci* 10:447–452
- Goswami S, Bhakuni RS, Chinniah A et al (2012) Anti-*Helicobacter pylori* potential of artemisinin and its derivatives. *Antimicrob Agents Chemother* 56:4594–4607
- Hancock REW (2007) The end of an era? *Nat Rev Drug Discov* 6:28
- Hartmann S, Neeff J, Heer U et al (1978) Arenaemycin (pentalenolactone): a specific inhibitor of glycolysis. *FEBS Lett* 93:339–342
- Herz W (1977) Biogenetic aspects of sesquiterpene lactone chemistry. *Isr J Chem* 16:32–44
- Herz W (1978) Sesquiterpene lactones in the Compositae. In: Heywood VH, Harborne JB, Turner BL (eds) *The biology and chemistry of the Compositae*, vol 1. Academic Press, London, pp 337–357
- Hoagland DT, Liu J, Lee RB et al (2016) New agents for the treatment of drug-resistant *Mycobacterium tuberculosis*. *Adv Drug Deliv Rev* 102:55–72
- Honda G, Yeşilada E, Tabata M et al (1996) Traditional medicine in Turkey VI. Folk medicine in West Anatolia: Afyon, Kiiyahya, Denizli, Mu la, Aydin provinces. *J Ethnopharmacol* 53:75–87
- Inoue A, Tamogami S, Kato H et al (1995) Antifungal melampolides from leaf extracts of *Smallanthus sonchifolius*. *Phytochemistry* 39:845–848
- Ivanescu B, Miron A, Corciova A (2015) Sesquiterpene lactones from *Artemisia* Genus: biological activities and methods of analysis. *J Anal Methods Chem.*, Article ID 247685, 21. <https://doi.org/10.1155/2015/247685>
- Jamal W, Bari A, Mothana RA et al (2014) Antimicrobial evaluation and crystal structure of parthenolide from *Tarchonanthus camphoratus* collected in Saudi Arabia. *Asian J Chem* 26:5183–5185
- Jampilek J (2016) Potential of agricultural fungicides for antifungal drug discovery. *Expert Opin Drug Discovery* 11:1–9
- Li H, Zhou C, Zhou L et al (2005) *In vitro* antiviral activity of three enantiomeric sesquiterpene lactones from *Senecio* species against hepatitis B virus. *Antivir Chem Chemother* 16:277–282
- Li Y, Li J, Wang X et al (2013) Antimicrobial constituents of the leaves of *Mikania micrantha* H. B. K. *PLoS One* 8(10):e76725
- Lin F, Hasegawa M, Kodama O (2003) Purification and identification of antimicrobial sesquiterpene lactones from Yacon (*Smallanthus sonchifolius*) leaves. *Biosci Biotechnol Biochem* 67:2154–2159
- Lin LT, Hsu WC, Lin CC (2014) Antiviral natural products and herbal medicines. *J Tradit Complement Med* 4:24–35
- Liu JF, Wang L, Wang YF et al (2015) Sesquiterpenes from the fruits of *Illicium jiadifengpi* and their anti-hepatitis B virus activities. *Fitoterapia* 104:41–44
- Macías FA, Galindo JCG, Molinillo JMG et al (2000) Dehydrozaluzanin C: a potent plant growth regulator with potential use as a natural herbicide template. *Phytochemistry* 54:165–171
- Macías FA, Santana A, Durán AG et al (2013) Guaianolides for multipurpose molecular design. In: Beck J, Coats J, Duke S, Koivunen M (eds) *Pest management with natural products*, vol 1141. ACS, New York, pp 167–188. <https://doi.org/10.1021/bk-2013-1141.ch012>
- Maruyama M, Omura S (1977) Carpesiolin from *Carpesium abrotanoides*. *Phytochemistry* 16:782–783
- Maruyama M, Shibata F (1975) Stereochemistry of granilin isolated from *Carpesium abrotanoides*. *Phytochemistry* 14:2247–2248
- Merfort I (2011) Perspectives on sesquiterpene lactones in inflammation and cancer. *Curr Drug Targets* 12:1560–1573
- Özçelik B, Gürbüz I, Karaoglu T et al (2009) Antiviral and antimicrobial activities of three sesquiterpene lactones from *Centaurea solstitialis* L. ssp. *solstitialis*. *Microbiol Res* 164:545–552
- Paeshuyse J, Coelmont L, Vliegen I et al (2006) Hemin potentiates the anti-hepatitis C virus activity of the antimalarial drug artemisinin. *Biochem Biophys Res Commun* 348:139–144

- Picman A (1983) Antifungal activity of helenin and isohelenin. *Biochem Syst Ecol* 11:183–281
- Rezeng C, Yuan D, Long J et al (2015) Alantolactone exhibited anti-herpes simplex virus 1 (HSV-1) action *in vitro*. *Biosci Trends* 9:420–422
- Rios VE, León A, Chávez MI et al (2014) Sesquiterpene lactones from *Mikania micrantha* and *Mikania cordifolia* and their cytotoxic and anti-inflammatory evaluation. *Fitoterapia* 94:155–163
- Romero MR, Efferth O, Serrano MA et al (2005) Effect of artemisinin/artesunate as inhibitors of hepatitis B virus production in an “in vitro” replicative system. *Antivir Res* 68(2005):75–83
- Seca AML, Silva MAS, Pinto DCG (2017) Parthenolide and parthenolide like sesquiterpene lactones as multiple target drugs: current knowledge and new developments. In: Atta-ur-Rahman (ed) *Studies in natural products chemistry*, vol 54. Elsevier, Amsterdam, pp 337–352
- Takamatsu S, Xu LH, Fushinobu S et al (2011) Pentalenic acid is a shunt metabolite in the biosynthesis of the pentalenolactone family of metabolites: hydroxylation of 1-deoxypentalenic acid mediated by CYP105D7 (SAV\_7469) of *Streptomyces avermitilis*. *J Antibiot* 64:65–71
- Vega AE, Wendel GH, Maria AOE et al (2009) Antimicrobial activity of *Artemisia douglasiana* and dehydroleucodine against *Helicobacter pylori*. *J Ethnopharmacol* 124:653–655
- Wang JF, He WJ et al (2015) Dicarabrol, a new dimeric sesquiterpene from *Carpesium abrotanoides* L. *Bioorg Med Chem Lett* 25:4082–4084
- Wang B, Mei WL, Zeng YB et al (2012) A new sesquiterpene lactone from *Elephantopus tomentosus*. *J Asian Nat Prod Res* 14:700–703
- Wedge DE, Galindo JCG, Macías FA (2000) Fungicidal activity of natural and synthetic sesquiterpene lactone analogs. *Phytochemistry* 53:747–757
- Wu J, Tang C, Chen L et al (2015) Dicarabrones A and B, a pair of new epimers dimerized from sesquiterpene lactones via a [3 + 2] cycloaddition from *Carpesium abrotanoides*. *Org Lett* 17:1656–1659
- Wu JW, Tang C, Ke CQ et al (2017) Dicarabrol A, dicarabrone C and dipulchellin A, unique sesquiterpene lactone dimers from *Carpesium abrotanoides*. *RSC Adv* 7:4639–4644
- Xie C, Sun L, Meng L et al (2015) Sesquiterpenes from *Carpesium macrocephalum* inhibit *Candida albicans* biofilm formation and dimorphism. *Bioorg Med Chem Lett* 25:5409–5411
- Xu YJ (2013) Phytochemical and biological studies of *Chloranthus* medicinal plants. *Chem Biodivers* 10:1754
- Yang C, Shi YP, Jia ZJ (2002) Sesquiterpene lactone glycosides, eudesmanolides, and other constituents from *Carpesium macrocephalum*. *Planta Med* 68:626–630
- Yang X, Wang C, Yang J et al (2014) Antimicrobial sesquiterpenes from the Chinese medicinal plant, *Chloranthus angustifolius*. *Tetrahedron Lett* 55:5632–5634
- Zhang Q, Lu Y, Ding Y et al (2012) Guaianolide sesquiterpene lactones, a source to discover agents that selectively inhibit acute myelogenous leukemia stem and progenitor cells. *J Med Chem* 55:8757–8769
- Zhang JP, Wang GW et al (2015) The genus *Carpesium*: a review of its ethnopharmacology, phytochemistry and pharmacology. *J Ethnopharmacol* 163:173–191



# Chapter 13

## Antiproliferative and Cytotoxic Activities



Claudia A. Anesini, María Rosario Alonso, and Renzo F. Martino

**Abstract** Cancer is a genetic disease, affecting many people worldwide. Chemotherapy is routinely used for cancer treatment. However, this therapeutic approach is not always effective due to the development of cell resistance and toxic effects. Plants are a reservoir of natural chemicals with chemoprotective potential against cancer and with low adverse effects. While some drugs from natural origin are currently used for cancer treatment, others are being studied. Among the compounds isolated from plants, sesquiterpene lactones are very promising anticancer agents, which are widely being studied in different models of cancer in vitro and in vivo, and some clinical trials are being performed. Sesquiterpene lactones are very attractive compounds to be used as antitumoral therapy due to the diverse mechanisms of action through which they exert their effects. Among such mechanisms are their capacity to interfere with the generation of reactive oxygen species, the epigenetic modulation of gene expression, the targeting of the sarco-/endoplasmic reticulum calcium ATPase pump, and the activation of the NF- $\kappa$ B and the p53 signaling pathways. The latter mechanisms could be important to reduce the development of drug resistance by tumor cells. Sesquiterpene lactones can also inhibit angiogenesis and metastasis.

**Keywords** Cancer · Sesquiterpene lactones · Mechanism of action · In vitro studies · In vivo studies · Clinical trials

---

C. A. Anesini (✉)

Universidad de Buenos Aires, Facultad de Farmacia y Bioquímica, Departamento de Farmacología, Cátedra de Farmacognosia, Buenos Aires, Argentina

CONICET – Universidad de Buenos Aires, Instituto de Química y Metabolismo del Fármaco (IQUIMEFA), Buenos Aires, Argentina

M. R. Alonso

Universidad de Buenos Aires, Facultad de Farmacia y Bioquímica, Departamento de Farmacología, Cátedra de Farmacognosia, Buenos Aires, Argentina

CONICET – Universidad de Buenos Aires, Instituto de Química y Metabolismo del Fármaco (IQUIMEFA), Buenos Aires, Argentina

R. F. Martino

Universidad de Buenos Aires, Facultad de Farmacia y Bioquímica, Departamento de Microbiología, Inmunología y Biotecnología, Cátedra de Inmunología, Buenos Aires, Argentina

## Abbreviations

ALCLs	Anaplastic large cell lymphomas
ALL	Acute lymphoblastic leukemia
AML	Acute myeloid leukemia
APL	Acute promyelocytic leukemia
Bax	Apoptosis regulator BAX
Bcl- 2	B-cell CLL/lymphoma 2
Bid	BH3 interacting domain death agonist
BL	Burkitt lymphoma
BZLF1	Human herpes virus (E'stein-Barr virus) gene
Caspases	Cysteine aspartate-specific proteases
CCRF-CEM cells	Cellosaurus acute lymphoblastic leukemia cell line
CCRF/ADR 5000	Cellosaurus cell line, a doxorubicin-resistant sub-line derived from drug-sensitive, parental CCRF-CEM cells
Cdc2	Cell division control protein 2
c-FLIP	Cellular FLICE-like inhibitory protein
CLL	Chronic lymphocytic leukemia
CML	Chronic myeloid leukemia
c-Src	Proto-oncogene tyrosine-protein kinase
C/EBP	CHOP homologous protein
GADD 153	DNA damage inducible gene 153
DU-145	Human prostate carcinoma cell line
EGFR	EGFR/PI3K/Akt signaling pathway
EBV	Raji cell line: Epstein Barr virus (EBV)-positive Burkitt lymphoma (BL) cell line
ER	Endoplasmic reticulum
ERK	Extracellular signal-regulated kinase
HDAC1	Histone deacetylase 1
HeLa	Immortal cell line
HepG2	Human liver cancer cell line
HIN-1	Histidine nucleotide-binding protein 1
HL	Hodgkin lymphoma
HL-60	Acute myeloid leukemia
HSCs	Healthy hematopoietic stem cells
HT 29	Human colorectal adenocarcinoma
CML	Human chronic myeloid leukemia (CML) K562 cells
HL	Human leukemia HL-60 cells
IκB	Inhibitor of NF-κB
IKK	NF-κB kinase
JNK	C-Jun N-terminal kinase
Jun B	Transcription factor of the tyrosine receptor kinase PDGF-Rβ
LSCs	Leukemic stem cells

MAPK	Mitogen activated protein kinases
MCF-7	Breast cancer cells
MCF7	Human breast adenocarcinoma cell line
MDA-MB 435	Melanoma cell line
MDA-MB-231	Human breast cancer cell line
MDM2	Mouse double minute 2 homolog protein
MIA-PaCa-2 cells	Human pancreatic carcinoma cell lines
MDR P-gp CEM/ADR5000 cells	Multidrug-resistant P-gp over expressing CEM/ADR5000 leukemic cells
NF- $\kappa$ B	Nuclear factor kappa-light-chain-enhancer of activated B cells
NHL	Non-Hodgkin lymphoma
NIH/3T3	Normal fibroblast cell line
NPM-ALK	Nucleophosmin-anaplastic lymphoma kinase
p21	Protein P21
P-38	Protein kinase P-38
p53	Protein P53
PARP 1	Poly-(ADP-ribose) polymerase 1
PBMC	Peripheral blood mononuclear cells
PC-3	Human prostate grade IV adenocarcinoma cell line
PDGF-R $\beta$	Beta-type platelet-derived growth factor receptor
PI3K	Phosphatidylinositol-3-kinase
PKC $\alpha$	Protein kinase C alpha
PKC $\beta$ II	Protein kinase $\beta$
RIPK1	Receptor interacting protein kinase 1
ROS	Reactive oxygen species
SW872	Cellosaurus cell line SW 872, liposarcoma
SW982	Cellosaurus cell line SW 982, biphasic synovial sarcoma
TE-671	Cellosaurus cell line T-671, a human rhabdomyosarcoma
SER	Sarcoplasmic/endoplasmic reticulum
SERCA	Sarco/endoplasmic reticulum calcium ATPase
Smac/Diablo	Mitochondria-derived activator of caspases
SMMC-7721	Human hepatocarcinoma cell line
STAT	Signal transducer and activator of transcription
TNF $\alpha$	Tumor necrosis factor- $\alpha$
TRAIL	TNF-related apoptosis-inducing ligand
U251MG	Glioblastoma cell line
U937	Histiocytic lymphoma cell line
Ub	Ubiquitin
UPR	Unfolded protein response
Walker-256	Rat breast carcinoma cell line

## 13.1 Introduction

Cancer is a genetic disease causing high morbidity and mortality, with approximately 14 million new cases arising in 2012. The number of cases is expected to rise to almost 19 million by 2024. After cardiovascular disease, cancer represents the second leading cause of death in the world, having been responsible for 8.8 million deaths in 2015 (WHO 2017), which means that nearly 1 out of 6 deaths is due to this disease.

Cancer is caused by the deregulation of genes controlling cell growth, division, and death. The genetic changes that contribute to the development of cancer affect three main types of genes: proto-oncogenes, tumor suppressor genes, and DNA repair genes. These changes are sometimes called “drivers” of cancer. The final consequence is the generation of an imbalance between growth and death causing cells to proliferate and migrate toward distant organs, a phenomenon known as metastasis. Cancer may be either hereditary, may be the consequence of errors that occur during cell division, or may be due to DNA damage caused by certain environmental noxious agents such as the chemicals present in tobacco smoke or radiation such as ultraviolet rays (WHO 2005; Ferlay et al. 2015). Normal and tumor cells present a number of differences such as the lack of specialization of the latter, which causes them to divide continuously. Cancer cells have also lost their capacity to respond to the intracellular signals that regulate cell growth and apoptosis. Tumors are known to establish a relationship with the microenvironment, mainly through contact with normal cells, nearby molecules, and surrounding blood vessels that serve as nutrient source. Besides, tumor cells have developed mechanisms for immune evasion.

Cancers can be classified according to the organs or tissues where they originate. Thus, carcinomas are the most common type, which are constituted by epithelial cells; sarcomas are cancers generated in bones and soft tissues, including muscle, fat, blood vessels, lymph vessels, and fibrous tissue (such as tendons and ligaments); melanomas are made up of melanocyte precursors; and multiple myeloma is a cancer type of plasma cells.

Leukemia and lymphoma are a group of heterogeneous neoplastic disorders of white blood cells characterized by the uncontrolled proliferation and the blockage in the differentiation process of hematopoietic cells. While lymphomas are characterized by an abnormal lymphocyte proliferation developing as a solid tumor, most commonly in the lymph nodes of the neck, chest, armpit, or groin (Jaffe 2009), leukemias develop in the bone marrow and do not form solid tumors.

Leukemia and lymphoma stand at the fifth place of cancer-related deaths over the world (Armitage 2012). Leukemia includes acute lymphoblastic leukemia (ALL), acute myeloid leukemia (AML), chronic lymphocytic leukemia (CLL), and chronic myeloid leukemia (CML). AML is the most common acute leukemia in adult patients, which progresses rapidly and may be lethal within weeks or months. Based on the cytogenetic/genetic features of AML, and according to the 2008 revised WHO classification system, patients can be broadly classified into three different

risk groups. Treatment strategies and prognoses vary among these subtypes and are further influenced by patient-specific factors (Zeisig et al. 2012).

As stated above, lymphomas involve the uncontrolled growth of lymphocytes (T cells or B cells) and include two types: Hodgkin lymphoma (HL) and non-Hodgkin lymphoma (NHL), the latter is subdivided into two main types depending on the cell growth rate, that is, high-grade (or “aggressive”) and low-grade (or “indolent”) NHLs.

Taking into account patient-specific characteristics, such as age and overall health status, and each tumor type, it is obvious that the treatment strategies spectrum to be applied will be broad.

Chemotherapy is routinely used for cancer treatment; however, this strategy is not always effective due to the development of cell resistance phenomena and toxic effects (Hopfinger et al. 2012). For example, 5-fluorouracil, a common chemotherapeutic agent, is known to cause myelotoxicity and cardiotoxicity. Doxorubicin, which is another widely used drug, is known to cause cardiotoxicity, nephrotoxicity, and myelotoxicity. Similarly, bleomycin, a well-known chemotherapeutic agent, is known for its pulmonary toxicity. In addition, bleomycin causes cutaneous toxicity. Cyclophosphamide, a drug used to treat many malignant conditions, has been demonstrated to cause bladder toxicity in the form of hemorrhagic cystitis, immunosuppression, alopecia, and, at high doses, cardiotoxicity (Chabner et al. 2006).

All AML subtypes, except for the acute promyelocytic leukemia (APL), are typically treated with an induction chemotherapy using a “3 + 7” combination of daunorubicin and cytarabine (Zeisig et al. 2012). Almost all APL patients can achieve complete remission after treatment with all-*trans*-retinoic acid, which can effectively induce APL cell differentiation (Degos and Wang 2001). Conversely, although treatment strategies for AML have substantially progressed in recent decades, effective therapies for non-APL subtypes of AML are still urgently needed.

In this context, plants have enormous potential as a source of new drugs, constituting a reservoir of natural chemicals with low toxicity chemoprotective properties against cancer. There are four classes of commercially available plant-derived anti-cancer agents: the vinca alkaloids (vinblastine, vincristine, and vindesine), the epipodophyllo toxins (etoposide and teniposide), the taxanes (paclitaxel and docetaxel), and the camptothecin derivatives (camptothecin and irinotecan). The mechanisms of action of these drugs include cell cycle arrest, the induction of cell differentiation, or the induction of cell death through the activation and sensitization of the intrinsic and extrinsic pathways of apoptosis, respectively. Some drugs also interact with the cytoskeleton by either inhibiting the polymerization or by inducing depolymerization of microtubules. The latter effects also lead to a cell cycle arrest and apoptosis (Balunas and Kingborn 2005; Cragg et al. 2009).

Sesquiterpene lactones are a group of plant secondary metabolites that are abundant in members of the Asteraceae family (Merfort 2011). The  $\alpha$ ,  $\beta$  unsaturated carbonyl function of STLs is important to exert the antiproliferative effect of these compounds. Among cytotoxic STLs, costunolide, eupatolide, parthenolide, dehydrocostuslactone, and thapsigargin can be mentioned (Fig. 13.1).

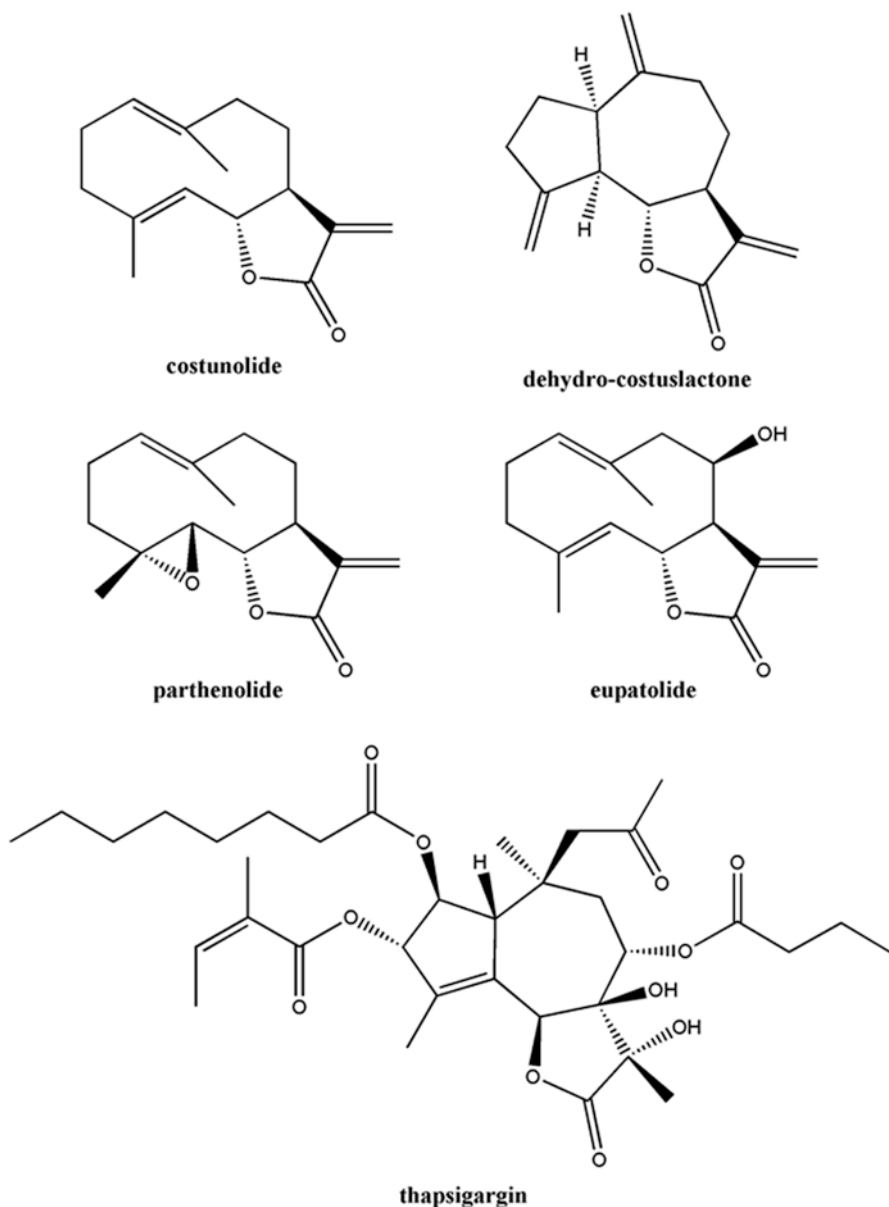


**Fig. 13.1** Chemical structure of cytotoxic sesquiterpene lactones

In this chapter, the cytotoxic and antitumor effects and mechanisms of action of STLs will be summarized, focusing on their effects on leukemias, lymphomas, and myelomas. Besides, some clinical trials assessing the effect of this type of compounds in other tumors will also be described. The remission obtained after the co-treatment with STLs and conventional chemotherapeutics will also be addressed.

## 13.2 In Vitro Studies and Mechanism of Action

There are two mechanisms by which natural compounds can induce cytotoxicity, namely, cell death and cell differentiation.

Three types of cell death are recognized: apoptosis, necrosis, and autophagy. Apoptosis is characterized by the activation of cysteine aspartate-specific proteases (caspases), chromatin condensation, cell shrinking, and blebbing of the cell membrane. Autophagy is characterized by the formation of intracellular vacuoles, organelle degradation, and, finally, cell death. In contrast, in necrotic cells, the endoplasmic reticulum (ER), mitochondria, and cytosol continue to swell until the cell bursts and releases its contents (Krysko et al. 2003). Apoptosis is the most common mechanism of cell death by which natural compounds exert their cytotoxic effects.

Apoptosis can occur through an extrinsic pathway activated by the binding of ligands to death receptors on the cell membrane and involves caspase-8 and caspase-3 or through an intrinsic pathway activated by other stimuli involving the release of mitochondrial proteins and the activation of the caspase-9 and caspase-3. The extrinsic and intrinsic pathways are interconnected, for example, the cleavage of BH3 interacting domain death agonist (Bid) by caspase-8 results in the formation of pro-apoptotic truncated Bid (tBid), which activates the intrinsic pathway (Krysko and Vandenabeele 2009).

The mechanisms leading to the activation of apoptosis are diverse: the direct activation of caspases, the direct effect on mitochondria (cytochrome release) and consequent caspase activation, a redox imbalance and the generation of oxidative stress, a disturbance in cell cycle progression, the induction of ER stress, the activation of transcription factors that promote apoptotic proteins, the inhibition of transcription factors related to survival and proliferation such as NF- $\kappa$ B and STATs, and the inhibition or activation of mitogen-activated protein kinases (MAPK), which transmit extracellular signals to regulate cell growth, proliferation differentiation, and apoptosis. Three major MAPK families have been described: P-38, the extracellular signal-regulated kinase (ERK), and C-Jun N-terminal kinase (JNK). When cells are exposed to stressors, one of the major outcomes of MAPK activation is the induction of apoptosis, a process in which the transcription of the Bcl-2 family proteins, such as Bax and Bcl-2 takes place. While the inhibition of DNA methylation is related to cell differentiation and apoptosis, the inhibition of histone deacetylase 1 (HDAC1) induces apoptosis through the activation of p21 and p53 proteins.

The induction of apoptosis through the generation of oxidative stress is a mechanism by which many STLs produce either cytostatic or cytotoxic effects in tumors involving the participation of mitochondria. The mitochondrial events involve the release of apoptotic factors, including cytochrome C and second mitochondria-derived activator of caspases (Smac/Diablo). Usually, the permeabilization of the mitochondrial outer membrane leading to the release of these components is controlled by the balance between pro-apoptotic and anti-apoptotic members of the B-cell CLL/lymphoma 2 (Bcl-2) superfamily.

Over the last 5 years, many studies have been performed to assess the antiproliferative activity of STLs. It has been demonstrated that the treatment of tumor cells with STLs disrupts their redox status and causes oxidative stress, with the subsequent initiation of the intrinsic apoptosis pathway (Sun et al. 2010). For example, the treatment of tumor cells with parthenolide increases the generation of reactive oxygen species (ROS) in tumor cells through diverse mechanisms such as the reduction of the cysteine sulfhydryl group of the nonprotein antioxidant molecule glutathione (Ralstin et al. 2006), the activation of NADPH oxidase, and the downregulation of the antioxidant enzymes manganese superoxide dismutase and catalase.

Other STLs produce apoptosis by interfering with the cell cycle progression and by arresting cells in the G2/M phase (Rozenblat et al. 2008) together with an increase in the sub-G0 fraction or, conversely, by arresting the cells in the G1/S phase with the appearance of a broad sub-G1 peak (Cho et al. 2004). The activation of p53 and the subsequent inactivation of cell division control protein 2 (Cdc2) are responsible for the G2/M arrest, whereas the G1/S arrest involves the modulation of cyclin-dependent kinases and their activating partners, cyclins. Other STLs trigger apoptosis by increasing the levels of ROS, leading to the activation of either the extrinsic or the intrinsic pathway. Psilostachyin, psilostachyin C, peruvine, and cumanine exert an antiproliferative effect by inducing apoptosis on the BW5147 murine lymphoma cell line. Psilostachyin C has proved to be the most active and the less toxic pro-apoptotic compound. These effects are achieved through an impairment in the mitochondrial membrane potential and the generation of ROS. These phenomena are related to a modulation of the activity of antioxidant enzymes and by inducing cell cycle arrest in the S phase (Martino et al. 2015). Besides, psilostachyin and psilostachyin C are considered novel checkpoint inhibitors, since they cause the arrest of other cell types such as breast cancer cells (MCF-7) in the G2 phase (Sturgeon et al. 2005).

In addition, the STL EM23, isolated from *Elephantopus mollis*, which is a traditional herbal medicine with multiple pharmacological activities, inhibits the proliferation of human chronic myeloid leukemia (CML) K562 cells and acute myeloid leukemia (AML) HL-60 cells through the induction of apoptosis involving the translocation of the membrane-associated phospholipid phosphatidylserine, changes in cell morphology, the activation of caspases, and the cleavage of poly-(ADP-ribose) polymerase1 (PARP 1). The disruptions in the mitochondrial membrane potential observed have allowed suggesting the involvement of the mitochondrial pathway in EM23-mediated apoptosis. Mechanistic studies have indicated that EM23 caused a marked increase in the levels of ROS (Li et al. 2016).

Furthermore, five melampolide STLs (uvedalin, enhydrin, polymatin B, sonchifolin, and fluctuanin) isolated from the leaves of *Smilax sonchifolia* have been demonstrated to exert poor cytotoxic effects on peripheral blood mononuclear cells (PBMC) of healthy human subjects while being strongly cytotoxic against human T-cell acute lymphoblastic leukemia (CCRF-CEM) cells, CEM-ADR5000, and pancreatic cancer cells. These effects were achieved by triggering the generation of oxidative stress. These findings suggest that these STLs display a certain selectivity for tumor cells. It has been reported that the generation of ROS entails the induc-



tion of apoptosis in CCRF-CEM and CEM-ADR5000 cells through the activation of receptor-interacting protein kinase 1 (RIP1K). Neither apoptosis nor necroptosis was observed in human pancreatic carcinoma cell lines (MIA-PaCa-2 cells (de Ford et al. 2015)).

The dimeric STLs uvedafolin and enhydrofolin, also isolated from *S. sonchifolius*, have been demonstrated to have cytotoxic activity on HeLa cells with low  $IC_{50}$  values (2.96 and 3.17 mM, respectively) after 24 h of treatment, displaying low toxicity on normal NIH/3 T3 cells. These STLs caused cell cycle arrest in the G2/M phase and induced apoptosis through the activation of the mitochondrial pathway, with the participation of caspase-9 and caspase-3/7. In addition, the STL 2,3-dehydrosilostachyn isolated from the *n*-butanolic extract of *Ambrosia cumanensis* Kunth. has shown cytotoxic activity with different potencies in HeLa, Jurkat, and U937 cell lines. This STL was found to cause arrest in the G2/M cell cycle block (Del Socorro Jimenez-Usuga et al. 2016).

Another mechanism through which STLs activate the apoptotic intrinsic pathway is the interaction with ER through the ER stress-dependent and ER stress-independent pathways related to proteasome inhibition. The ER is responsible for the folding and the posttranslational modification of secreted proteins. When the ER becomes stressed due to the accumulation of newly synthesized unfolded or misfolded proteins, a complex intracellular signal transduction pathway, named the unfolded protein response (UPR), is activated, leading to the activation of the intrinsic pathway of apoptosis by phosphorylation and inactivation of Bcl-2, repression of Bcl-2 expression, or translocation of Bax/Bak to the mitochondria (Krysko and Vandenabeele 2009). The dehydrocostus lactone activates the ER-resident transmembrane protein sensors, which lead to the activation of a transcription factor that regulates UPR target gene expression and upregulates the pro-apoptotic transcription factor growth arrest and GADD153/C/EBP protein (Hung et al. 2010). The guaianolide thapsigargin induces ER stress by decreasing the  $Ca^{2+}$  concentration in the ER by blocking the capacity of the sarco-/endoplasmic reticulum calcium ATPase (SERCA) pump to transfer  $Ca^{2+}$  from the cytosol to the ER, thus increasing the cytosolic  $Ca^{2+}$  concentration. The latter phenomenon leads to the generation of ROS and subsequent cell death (Denmeade and Isaacs 2005).

Costunolide has antiproliferative effects on human bone osteosarcoma epithelial cells (U2OS) by inducing the loss of the mitochondrial transmembrane potential. This STL decreases the Bcl-2/Bax ratio, induces cytochrome C release, and activates caspases. All these effects are related to the generation of ROS and the ER stress-induced mitochondrial dysfunction, which activate kinases such as c-Jun N-terminal kinase (JNK) and induce apoptosis (Zhang et al. 2016).

It has also been demonstrated that the balance between apoptosis and survival can be affected by the reactivation of tumor suppressor genes. Tumor suppressor genes are silenced in tumor cells by hypermethylation. Therefore, inhibition of DNA methylation results either in the differentiation of cancer cells or in apoptosis. In this sense, the inhibition of DNA methyl transferase 1 by parthenolide results in significant hypomethylation and reactivation of histidine nucleotide-binding protein 1 (HIN-1) suppressor gene (Liu et al. 2009). Moreover, the activation of HIN-1

results in the inhibition of AKT signaling, which leads to the dephosphorylation of Bad, allowing it to bind anti-apoptotic Bcl-2 members to neutralize them. Parthenolide also affects histone acetylation by inhibiting histone deacetylase 1 (HDAC1), leading to p21 and p53 activation and subsequent apoptosis (Gopal et al. 2009).

It has also been demonstrated that rapidly proliferating cancer cells express elevated levels of transferrin receptors on their cell surface and have higher amounts of intracellular iron than normal or slowly proliferating cells. In this regard, artemisinin has an endoperoxide bridge that is cleaved upon binding to Fe (II), producing toxic C-4 and seco-C-4 free radicals that destroy tumor cells. The addition of holotransferrin and iron sources to artemisinin increases its antitumor properties and targeted delivery (Nakase et al. 2009).

It is noteworthy that some STLs produce sensitization of the extrinsic pathway of apoptosis. This pathway is activated upon binding of membrane death receptors to their extracellular ligands, such as TNF and TNF-related apoptosis-inducing ligand (TRAIL). For example, the germacranolide eupatolide sensitizes cancer cells to TRAIL-induced apoptosis by downregulating the cellular FLICE-like inhibitory protein (c-FLIP). The treatment of human breast cancer cells with TRAIL in combination with subtoxic concentrations of eupatolide enhanced the TRAIL-induced cytotoxicity, as compared with the effect exerted by each STL alone (Lee et al. 2010). Dehydrocostus lactone renders human leukemia HL-60 cells susceptible to TNF-induced apoptosis by enhancing caspase-3 and caspase-8 activities (Oh et al. 2004). Parthenolide sensitizes cancer cells for TNF-induced apoptosis by downregulating anti-apoptotic genes and sensitizes hepatocellular carcinoma cells to TRAIL by inducing the expression of death receptors through the inhibition of STAT3 (Carlisi et al. 2011).

However, the most important mechanism by which STLs exert their antiproliferative effect and apoptosis involves the inhibition of NF- $\kappa$ B or STATs transcription factors. NF- $\kappa$ B and STAT3 are two important pathways involved in cell survival and proliferation that are constitutively activated in neoplastic cells in response to autocrine and paracrine factors that are produced within the tumor microenvironment (Takeuchi and Akira 2010). The NF- $\kappa$ B activation favors angiogenesis and tumorigenesis and plays a key role in the expression of several inflammatory genes and anti-apoptotic genes. Thus, NF- $\kappa$ B has been considered an important link between inflammation and cancer.

Parthenolide is one STL that is capable of inhibiting NF- $\kappa$ B transcription, presenting antiproliferative activity on leukemia cells. This STL can be found in different medicinal plants, particularly in feverfew (*Tanacetum parthenium*). It has been demonstrated that parthenolide induces apoptosis in acute myeloid leukemia (AML) stem and progenitor cells, without causing significant toxicity to normal hematopoietic stem cells (HSCs). AML growth is hierarchical and originates from leukemic stem cells (LSCs). All these findings have anointed parthenolide as the prototypical member of next-generation therapies for the elimination of LSCs (Guzman et al. 2005).

Parthenolide also suppresses the growth of the Raji cell line and activates the transcription of BZLF1 by inhibiting the activity of NF- $\kappa$ B. BL has been reported to be strongly associated with EBV infection. When parthenolide was used in combination with ganciclovir, the cytotoxic effect of first drug was enhanced. These data suggest that the induction of EBV-mediated lysis achieved with this drugs combination may constitute an efficient viral-targeted therapy for EBV-associated BL (Li et al. 2012). In addition, the STLs honokiol, magnolol, and parthenolide, isolated from *Magnolia grandiflora*, have proved to induce apoptosis and to exert cytotoxic effects in vitro on the atypical lymphocytes follicular Non-Hodgkin lymphoma cells (NHL) obtained from a patient (Marin et al. 2013). The increase in I $\kappa$ B and the consequent decrease in NF- $\kappa$ B DNA binding, the inhibition of the EGFR/PI3K/Akt signaling pathway, and the inhibition of telomerase are possible mechanisms proposed by the authors to explain this effect. The same authors had previously demonstrated that parthenolide has an antitumor activity in a lymphocyte malignancy animal model.

Another antitumor mechanism exerted by STLs involves NF- $\kappa$ B-driven transcription of matrix metalloproteinase 9, a crucial angiogenesis-related transcript that is suppressed by treatment with parthenolide (Oka et al. 2007) and by the germacranolide deoxyelephantopin (Huang et al. 2010). These antiangiogenic treatments reduce the occurrence of metastasis.

More recently, the chemical optimization of parthenolide on the  $\alpha$ -methylene- $\gamma$ -butyrolactone has been done to improve the potency and pharmacokinetic parameters. The modification in C1-C10 olefinic groups of parthenolide leads to the generation of the parthenolide analogues cyclopropane 4 and micheliolide, which were found to have inhibitory activity on drug resistant AML cells and low toxicity to healthy bone marrow cells. These analogues are also known to induce the generation of ROS (Kempema et al. 2015).

Not only do STLs inhibit NF- $\kappa$ B, but also they exert inhibition of STATs. Using the luciferase reporter system, some authors have observed that two STLs, damsine and coronopilin, isolated from *Ambrosia arborescens*, are capable of inhibiting NF- $\kappa$ B and STAT3 transcriptional activities in Jurkat and HeLa cells. The expression of NF- $\kappa$ B and STAT3 were induced by TNF $\alpha$  and IFN $\gamma$ , respectively. In both cases, the IC<sub>50</sub> values for damsine were lower than those of coronopilin, indicating that damsine is more effective than coronopilin. The authors hypothesized that the NF- $\kappa$ B signaling pathway can be inhibited by multiple mechanisms, including the activation of the inhibitor of NF- $\kappa$ B kinase (IKK) activity, the activation of the inhibitor of NF- $\kappa$ B (I $\kappa$ B) phosphorylation through I $\kappa$ B degradation, and DNA binding. Some STLs, such as ergolide, artemisinin, costunolide, and zerumbone, have also been reported to have inhibitory effects on the NF- $\kappa$ B pathway (Villagomez et al. 2013).

Leptocarpin (LTC) is a STL isolated from a native Chilean plant, *Leptocarpha rivularis*, which has been widely used in traditional medicine by Mapuche peoples. It decreases cell viability of cancer cell lines (such as HT-29, PC-3, DU-145, MCF7, and MDA-MB-231) by inducing caspase-dependent apoptosis and through the inhibition of the NF- $\kappa$ B factor, the latter effect being associated with a decreased DNA-

binding capacity of this transcription factor. However, the specific mechanism underlying this effect remains unknown (Bosio et al. 2015). Four new STLs, 8 $\alpha$ -(2'Z-tigloyloxy)-hirsutinolide, 8 $\alpha$ -(2'Z-tigloyloxy)-hirsutinolide-13-O-acetate, 8 $\alpha$ -(4-hydroxytigloyloxy)-hirsutinolide, and 8 $\alpha$ -hydroxy-13-O-tigloyl-hirsutinolide, isolated from *Vernonia cinerea* leaves and stems, are capable of inhibiting the proliferation of U251MG glioblastoma and MDA-MB-231 breast cancer cells by inhibiting aberrant active STAT3 (Joung Youn et al. 2014).

It has been observed that the inhibition of NF- $\kappa$ B and STATs by STLs sensitize tumoral cells to the action of chemotherapeutic agents. When STLs are combined with other treatments, they also sensitize the extrinsic apoptosis pathway by interfering with anti-apoptotic gene expression or by increasing the expression of death receptors. Parthenolide has potent antitumor activity against cancer stem cells (Guzman et al. 2005) and acts synergistically with the treatment of pancreatic adenocarcinoma and on a xenograft model of breast cancer when used in combination with docetaxel or sulindac, respectively (Yip-Schneider et al. 2005; Sweeney et al. 2005).

It is noteworthy that STLs are active on cells that have become resistant to many chemotherapeutic agents. The multidrug resistance is a prevailing phenomenon leading to chemotherapy treatment failure in cancer patients. In this regard, two STLs, neoambrosin and damsine, isolated from *Ambrosia maritima* (Asteraceae), have been studied on MDR P-gp CEM/ADR 5000 cells P-gp-overexpressing CEM/ADR5000 leukemic cells. The compounds inhibited cell proliferation by silencing the proto-oncogene tyrosine kinase (c-Src) which is a non-receptor tyrosine kinase protein that in humans is encoded by the SRC gene. This protein phosphorylates specific tyrosine residues in other proteins, for example, in tumor cells, the overexpression of c-Src leads to the constitutive activation of PI3K (phosphatidylinositol-3-kinase)/Akt-NF- $\kappa$ B and STATs (STAT3 and STAT5) pathways. As described above, this activation governs cancer development and progression (Saeed et al. 2015).

Sesquiterpene lactones can also exert antiproliferative effects through the inhibition of oncogenes or the inhibition of tumor suppressor gene p53 (related to apoptosis). It has been demonstrated that STLs inhibit the oncogene *nucleophosmin*-anaplastic lymphoma kinase (NPM/ALK) chimera, which is involved in the majority of anaplastic large cell lymphomas (ALCLs). The furanoheliangolide STL lobatin B, isolated from *Neurolaena lobata*, downregulates NPM-ALK, and as a consequence, an inhibition of expression of Jun B (which is a transcription factor of the tyrosine receptor kinase PDGF-R $\beta$ ) is observed (Kiss et al. 2015).

The other mechanism by which STLs induce death is necrosis. Through this mechanism, some STLs, such as the pseudoguanolide helenalin, kill apoptosis-resistant cells. Helenalin induces necrosis in three cell lines overexpressing Bcl-2 by mechanisms involving free intracellular iron, ROS, and inhibition of NF- $\kappa$ B. This form of necrosis has proved to be independent of receptor-interacting protein kinase 1 (RIPK1) and poly-(ADP-ribose) polymerase1 (PARP1) (Hoffmann et al. 2011).

Differentiation is another mechanism exerted by antitumoral drugs. The STL arsanin, present in *Artemisia santolina*, induces cell differentiation of the human promyelocytic leukemia HL-60 cell line in a concentration-dependent manner. A cytofluorometric analysis indicated that arsanin induces HL-60 cell differentiation predominantly into granulocytes by increasing the levels of protein kinase C alpha (PKC $\alpha$ ) and protein kinase  $\beta$  (PKC $\beta$ II) isoforms and by increasing the phosphorylation rate MAPKs in HL-60 cells. In addition, arsanin synergistically enhanced the differentiation of HL-60 cells in a dose-dependent manner when combined with low doses of 1–25-(OH) $_2$ D3 (Kweon et al. 2015).

In many cases, the antiproliferative activity of STLs in leukemic cells is shown without describing the mechanism of action. This is a case of an amino conjugate of a sulfated guaiane STL isolated from the roots of *Scorzonera divaricata*. This STL exhibits significant in vitro cytotoxic activity against human cancer cell lines such HL60, HeLa, HepG2, and SMMC-7721, among others (Yang et al. 2016).

In addition, the STL dehydroleucodine, isolated from *Gynoxys verrucosa*, a species used in traditional medicine in Southern Ecuador, has proved to have an antiproliferative effect against eight acute myeloid leukemia (AML) cell lines, with LD $_{50}$  values ranging from 5.0 to 18.9  $\mu$ M. Besides, this STL was active against human AML cell samples from five patients, with an average LD $_{50}$  of 9.4  $\mu$ M. It is noteworthy that the compound does not affect the proliferation of normal peripheral blood mononuclear cells. The authors concluded that an exocyclic methylene in the lactone ring is required for the cytotoxic activity (Ordóñez et al. 2016).

The mechanism of action of the three more studied STLs, parthenolide, artemisinin, and thapsigargin, is shown in Fig. 13.2.

Apart from blood cell malignancies, STLs also have activity on other tumors. For example, parthenolide presents activity against breast cancer and pancreatic carcinoma (Carlisi et al. 2016; Liu et al. 2017); the prodrug of thapsigargin, mipsagargin, has proved to induce apoptosis in prostatic tumors (Mahalingam et al. 2016).

Moreover, eupatolide induces apoptosis in breast cancer cells, and artemisinin is being evaluated in clinical trials for breast and colorectal cancer (see below).

Furthermore, dehydrocostus lactone and costunolide are active on hepatocellular carcinoma and on sarcomas (SW-872, SW-982, and TE-671) (Lohberger et al. 2013). Furthermore, deoxyelephantopin exerts antitumoral activity on breast adenocarcinoma in mice (Kreuger et al. 2012; Merfort 2011). Psilostachyin, psilostachyin C, helenalin, and mexicanin I are active on different tumor cells apart from white blood cells (Martino et al. 2015; Kreuger et al. 2012; Merfort 2011; Sturgeon et al. 2005; Bujnicki et al. 2012).

### 13.3 In Vivo Studies

The “in vivo” antitumoral activity of STLs had been demonstrated in animal models. For example, goyazensolide exerts antitumoral activity in an in vivo hollow fiber assay employing HT 29 and MDA-MB 435 human tumoral cells. The fibers

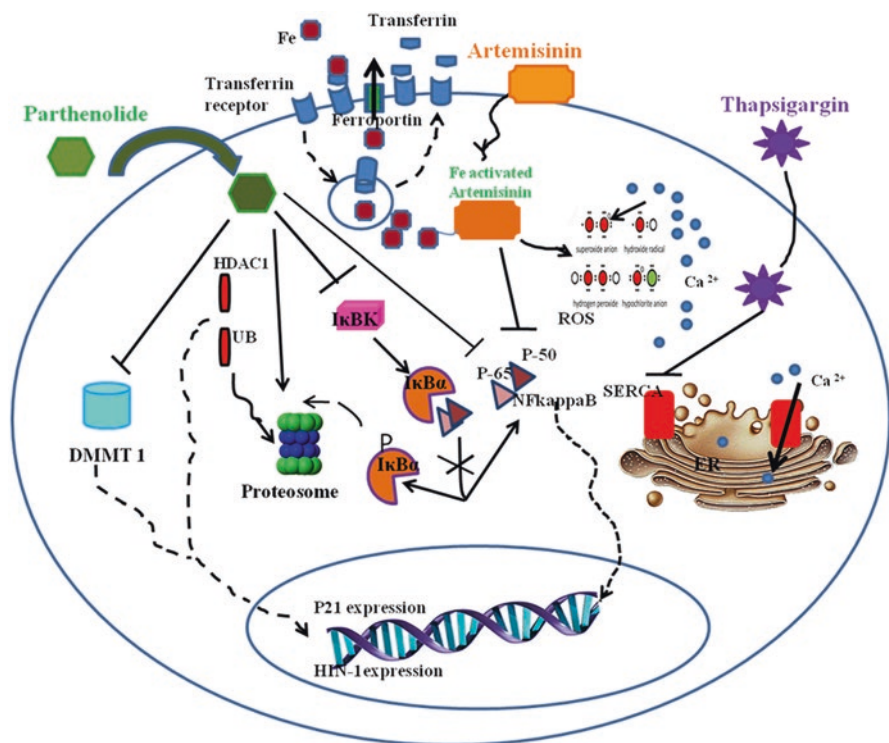


**Fig. 13.2** Mechanism of action of sesquiterpene lactones on tumoral cells. The mechanism of action of the three more studied STLs is shown. STLs diffuse through the plasma membrane and selectively target the SERCA pump, high iron content and cell surface transferrin receptors, NF- $\kappa$ B signaling, and epigenetic mechanisms. Thapsigargin can diffuse into the SERCA pump blocking its ability to transfer  $\text{Ca}^{2+}$  from the cytosol into the ER. High cytosolic  $\text{Ca}^{2+}$  concentrations lead to the generation of ROS and subsequent cell death. Many tumoral cells have high intracellular  $\text{Fe}^{2+}$  contents and high levels of transferrin receptors. The cytosolic  $\text{Fe}^{2+}$  binds to the endoperoxide bridge of artemisinin, leading to its activation and the consequent generation of toxic ROS. Parthenolide directly inhibits DNMT1 and causes ubiquitin-mediated proteasomal degradation of HDAC1, leading to expression of HIN-1 and p21, respectively. Parthenolide directly inhibits the NF- $\kappa$ B p65 subunit and the IKK complex preventing IKK-mediated phosphorylation and proteasomal degradation of I $\kappa$ B. Artemisinin also inhibits NF- $\kappa$ B activity. Abbreviations: ER sarcoplasmic/endoplasmic reticulum, HDAC1 histone deacetylase 1, IKK, I $\kappa$ B kinase, I $\kappa$ B inhibitor of NF- $\kappa$ B, NF- $\kappa$ B nuclear factor- $\kappa$ B, ROS reactive oxygen species, SERCA, ER calcium ATPase, Ub ubiquitin. Dashed and solid lines indicate translocation and activation, respectively

were implanted into immunodeficient female NCr nu/nu mice. On the contrary, the STLs 15-deoxygoyazensolide and ereglomerulide did not present antitumoral activity in the same system (Muñoz Acuña et al. 2013). Japonicone A, which is found in the traditional herb *Inula japonica*, is considered a promising compound. This STL has proved to have potent *in vitro* and *in vivo* antitumor activity against Burkitt's lymphoma cells (Wang et al. 2014). Besides, it has been demonstrated that the treatment of BALB/c mice bearing Ehrlich tumors with a daily dose of the STL diacetyl

piptocarphol, isolated from *Vernonia scorpioides*, produced a decrease on the tumor size and prevented the development of the ascitic tumor. Furthermore, the dichloromethane fraction of *Moquiniastrum polymorphum* subsp. *floccosum*, which is rich in STLs, has shown activity against Walker-256 carcinosarcoma in rats. The treatment with the fraction significantly reduced the tumor volume and weight. The fraction also modified hepatic glutathione and superoxide dismutase levels and normalized plasma glucose, alkaline phosphatase, and amylase and the nitric oxide levels in the tumoral tissue. Moreover, the fraction induced apoptosis through the upregulation of the p53 and Bax gene expression. It is noteworthy that no clinical signs of toxicity or death were observed in the rats treated with the fraction (Gomes Martins et al. 2015)

Angiogenesis and metastasis are also two important targets for antitumoral drugs in vivo. Artemisinin has proved to prevent angiogenesis by inhibiting human vein endothelial cell proliferation and vascular endothelial growth factor and receptor expression. DNA microarray analysis correlates tumor inhibition exerted by artemisinin with the reduced expression of crucial angiogenesis-related transcripts, namely, vascular endothelial growth factor, fibroblast growth factor, several matrix metalloproteinases, and hypoxia-inducing factor (Anfosso et al. 2006). Thapsigargin also inhibits microvessel formation and proliferation of human artery endothelial cells in vitro (Shukla et al. 2001). Furthermore, parthenolide has been found to inhibit the expression of matrix metalloproteinase-9 and urinary plasminogen activator and the migration of carcinoma cells in vitro, as well as osteolytic bone metastasis in vivo (Idris et al. 2009).

### 13.4 Clinical Trials

Nowadays, some STLs such as artemisinin from *Artemisia annua*, thapsigargin from *Thapsia* genus (Apiaceae), and parthenolide from *Tanacetum parthenium* (feverfew) and/or many of their synthetic derivatives are under evaluation in clinical trials.

These compounds have been selected for their selectivity, which is attributed to their ability to target the sarco-/endoplasmic reticulum (ER) calcium ATPase (SERCA) pump, particular proteases secreted by cancer cells, high iron content and cell surface transferrin receptors, nuclear factor-kB (NF-kB) signaling, MDM2 degradation and p53 activation, angiogenesis, metastasis, and epigenetic mechanisms.

Clinical evidence indicates that artemisinin-derived drugs are promising for laryngeal carcinoma, uveal melanoma, and pituitary macroadenoma. These drugs are in phase I–II trials against lupus nephritis and breast, colorectal, and non-small cell lung cancers (Singh and Panwar 2006). In addition, the artemisinin derivatives, artemether and artesunate, have been subjected for evaluation in cancer clinical trials (Chen et al. 2004). Besides, artesunate was then also incorporated in several clinical trials: in 2008, it was evaluated for the treatment of metastatic breast cancer (Table 13.1); in 2015, a study was undertaken to assess the effect of artesunate

**Table 13.1** Sesquiterpene lactones evaluated in clinical trials

Sesquiterpene lactones or derivatives	Cancer or inflammation condition	References
Artemisinin	Lupus nephritis Metastatic breast cancer Colorectal cancer	Chen et al. (2004) Clinical trial gov.: NCT 00764036 <a href="http://Isrctn.org.ISRCTN05203252">Isrctn.org.ISRCTN05203252</a>
Artesunate	Non-small cell lung cancer, metastatic uveal melanoma, laryngeal squamous cell carcinoma Hepatocellular carcinoma Metastatic breast cancer Intraepithelial neoplasia (CIN2/3) Colorectal cancer (not yet recruiting) Colorectal cancer, stage II/III bowel cancer (currently recruiting) Solid tumors	Singh and Panwar(2006) <a href="http://ClinicalTrials.gov">ClinicalTrials.gov</a> : NCT02304289 <a href="http://ClinicalTrials.gov">ClinicalTrials.gov</a> : NCT00764036 <a href="http://ClinicalTrials.gov">ClinicalTrials.gov</a> : NCT02354534 <a href="http://ClinicalTrials.gov">ClinicalTrials.gov</a> : NCT03093129 <a href="http://ClinicalTrials.gov">ClinicalTrials.gov</a> : NCT02633098 <a href="http://ClinicalTrials.gov">ClinicalTrials.gov</a> : NCT02353026
Artemether	Pituitary macroadenoma Solid tumors (not yet recruiting)	<a href="http://ClinicalTrials.gov">ClinicalTrials.gov</a> : NCT03093129
Thapsigargin (G-202: mipsagargin)	Advanced solid tumors Advanced adult hepatocellular carcinoma Multiform glioblastoma Clear renal cell carcinoma Prostatic neoplasms	Phase I clinical trial Clinicaltrials. gov.:NCT01056029 <a href="http://ClinicalTrials.gov">ClinicalTrials.gov</a> : NCT01777594 <a href="http://ClinicalTrials.gov">ClinicalTrials.gov</a> : NCT02067156 <a href="http://ClinicalTrials.gov">ClinicalTrials.gov</a> : NCT02607553 <a href="http://ClinicalTrials.gov">ClinicalTrials.gov</a> : NCT02381236

Adapted from Ghantous et al. (2010)

administered intravaginally for the HPV-positive high-grade cervical intraepithelial neoplasia (CIN2/3) (Table 13.1); and in 2016, this STL was incorporated in a phase I study involving patients with solid tumors to evaluate its effect after intravenous administration (Table 13.1). In the same year, the safety and pharmacokinetics parameters of artesunate were evaluated in a phase I dose-escalation study in patients with hepatocellular carcinoma. The study was completed in December 2016; however, the results have not been published (Table 13.1). Artesunate will also be evaluated in two clinical trials: one of the trials is not in the recruiting phase yet (March 2017), and the other is already recruiting participants (October 2016) to study the safety and effectiveness of this STL on colorectal cancer and stage II/III bowel cancer (Table 13.1). Furthermore, artemether will also be assessed in a clinical trial (not yet recruiting participants, March 2017) to study its effect on solid tumors (Table 13.1). The orally bioavailable parthenolide analogue dimethyl amino-



parthenolide or LC-1 has been subjected to phase I clinical trials against acute myeloid leukemia (AML), acute lymphoblastic leukemia (ALL), and other blood and lymph node cancers (Guzman et al. 2007).

Thapsigargin-derived drugs are currently being studied in phase I clinical trials for breast, kidney, and prostate cancer treatments. For example, a thapsigargin pro-drug (G-202 mipsagargin, which consists of a thapsigargin molecule coupled with a masking peptide that is cleaved at the tumor site) is in phase I clinical trials for advanced solid tumors (Christensen et al. 2009). Mipsagargin has also been evaluated in several clinical trials for the treatment of multiform glioblastoma, advanced adult hepatocellular carcinoma, clear renal cell carcinoma, and prostatic neoplasm (Table 13.1) (Quynh Doan and Christensen 2015). For example, in a study carried out with patients affected with solid tumors [14 patients (32%) with colorectal, 9 (20%) with prostate, and 6 (14%) with hepatocellular carcinoma], the drug presented a good pharmacokinetic profile and was well tolerated. Only 12 (28.6%) of the patients presented a disease stabilization (Mahalingam et al. 2016). The clinical trials with STLs are shown in Table 13.1.

Some other STLs are currently being used for the treatment of different cancer types, for example, arglabin, isolated from *Artemisia glabella* (Asteraceae), is used for liver, breast, ovarian, and uterus cancer (Adekenov 2016).

## 13.5 Conclusion

Sesquiterpene lactones are very attractive compounds to be used in antitumor therapy due to the diverse mechanisms of action they exert, such as ROS generation, epigenetic modulation of gene expression, and targeting of the sarco-/endoplasmic reticulum calcium ATPase (SERCA) pump, the NF- $\kappa$ B signaling pathway, and the p53 pathway. Because of this, sesquiterpene lactones could be useful to treat resistant tumors. In addition, sesquiterpene lactones have proved to inhibit angiogenesis and metastasis. Promising results have also been achieved in animal models, and some sesquiterpene lactones are under study in clinical trials.

It can be concluded that sesquiterpene lactones can exert the antitumor activity mainly by inducing apoptosis through different pathways. All these considerations make these compounds very attractive to be used as antitumor drugs to be used either alone or in combination with other traditional chemotherapeutic drugs.

## References

- Adekenov SM (2016) Chemical modification of arglabin and biological activity of its new derivatives. *Fitoterapia* 110:196–205
- Anfosso L, Efferth T, Albini A et al (2006) Microarray expression profiles of angiogenesis-related genes predict tumor cell response to artemisinins. *Pharmacogenomics J* 6:269–278

- Armitage JO (2012) The aggressive peripheral T-cell lymphomas: update on diagnosis, risk stratification and management. *Am J Hematol* 87:511–519
- Balunas MJ, Kingborn AD (2005) Drug discovery from medicinal plants. *Life Sci* 78:431–441
- Bosio C, Tomasoni G, Martínez R et al (2015) Cytotoxic and apoptotic effects of leptocarpin, a plant-derived sesquiterpene lactone, on human cancer cell lines. *Chem Biol Interact* 242:415–421
- Bujnicki T, Wilczek C, Schomburg C et al (2012) Inhibition of Myb-dependent gene expression by the sesquiterpene lactone mexicanin-I. *Leukemia* 26(4):615–622
- Carlisi D, D'Anneo A, Angileri L et al (2011) Parthenolide sensitizes hepatocellular carcinoma cells to TRAIL by inducing the expression of death receptors through inhibition of STAT3 activation. *J Cell Physiol* 226:1632–1641
- Carlisi D, Buttitta G, Di Fiore R et al (2016) Parthenolide and DMAPT exert cytotoxic effects on breast cancer stem-like cells by inducing oxidative stress, mitochondrial dysfunction and necrosis. *Cell Death Dis* 7(4):e2194
- Chabner BA, Amrein PC, Druker BJ et al (2006) Antineoplastic agents. In: Goodman, Gilman's (eds) *The pharmacological basis of the therapeutics*, 11th edn. The McGraw-Hill Companies Inc, New York, pp 1731–1755
- Chen HH, Zhou HJ, Wu GD et al (2004) Inhibitory effects of artesunate on angiogenesis and on expressions of vascular endothelial growth factor and VEGF receptor KDR/flk-1. *Pharmacology* 71:1–9
- Cho JY, Kim AR, Jung JH et al (2004) Cytotoxic and pro-apoptotic activities of cynaropicrin, a sesquiterpene lactone on the viability of leukocyte cancer cell lines. *Eur J Pharmacol* 492:85–94
- Christensen SB, Skytte DM, Denmeade SR et al (2009) A trojan horse in drug development: targeting of thapsigargin towards prostate cancer cells. *Anti Cancer Agents Med Chem* 9:276–294
- Cragg GM, Grothaus PG, Newman DJ (2009) Impact of natural products on developing new anticancer agents. *Chem Rev* 109:3012–3043
- De Ford C, Ulloa JL, Catalán CA et al (2015) The sesquiterpene lactone polymatin B from *Smallanthus sonchifolius* induces different cell death mechanisms in three cancer cell lines. *Phytochemistry* 117:332–339. <https://doi.org/10.1016/j.phytochem.2015.06.020>
- Degos L, Wang ZY (2001) All trans retinoic acid in acute promyelocytic leukemia. *Oncogene* 20:7140–7145. <https://doi.org/10.1038/sj.onc.1204763>
- Del Socorro Jimenez Usuga N, Malafronte N, Osorio Durango EJ et al (2016) Phytochemical investigation of *Pseudelephantopus spiralis* (Less.) Cronquist. *Phytochem Lett* 15:256–259
- Denmeade SR, Isaacs JT (2005) The SERCA pump as a therapeutic target: making a 'smart bomb' for prostate cancer. *Cancer Biol Ther* 4:14–22
- Ferlay J, Soerjomataram I, Dikshit R et al (2015) Cancer incidence and mortality worldwide: sources, methods and major patterns in GLOBOCAN 2012. *Int J Cancer* 136(5):E359–E386
- Ghantous A, Gali-Muhtasib H, Vuorela H et al (2010) What made sesquiterpene lactones reach cancer clinical trials? *Drug Discov Today* 15:668–678
- Gomes Martins G, dos Reis Lívero FA, Stolf AM et al (2015) Sesquiterpene lactones of *Moquiniastrum polymorpha* subsp. *floccosum* have antineoplastic effects in Walker-256 tumor-bearing rats. *Chem Biol Interact* 228:46–56
- Gopal YN, Chanchorn E, Van Dyke MW (2009) Parthenolide promotes the ubiquitination of MDM2 and activates p53 cellular functions. *Mol Cancer Ther* 8:552–562
- Guzman ML, Rossi RM, Karnischky L et al (2005) The sesquiterpene lactone parthenolide induces apoptosis of human acute myelogenous leukemia stem and progenitor cells. *Blood* 105:4163–4169
- Guzman ML, Rossi RM, Neelakantan S et al (2007) An orally bioavailable parthenolide analog selectively eradicates acute myelogenous leukemia stem and progenitor cells. *Blood* 110:4427–4435
- Hoffmann R, von Schwarzenberg K, Lopez-Anton N et al (2011) Helenalin by passes Bcl-2-mediated cell death resistance by inhibiting NF-kappaB and promoting reactive oxygen species generation. *Biochem Pharmacol* 82:453–463

- Hopfinger G, Griessl R, Sift E et al (2012) Novel treatment avenues for peripheral T-cell lymphomas. *Expert Opin Drug Discovery* 7:1149–1163
- Huang CC, Lo CP, Chiu CY et al (2010) Deoxyelephantopin, a novel multifunctional agent, suppresses mammary tumour growth and lungmetastasis and doubles survival time in mice. *Br J Pharmacol* 159:856–871
- Hung JY, Hsu YL, Ni WC et al (2010) Oxidative and endoplasmic reticulum stress signaling are involved in dehydrocostuslactone-mediated apoptosis in human non-small cell lungcancer cells. *Lung Cancer* 68:355–365
- Idris AI, Libouban H, Nyangoga H et al (2009) Pharmacologic inhibitors of IkappaB kinase suppress growth and migration of mammary carcinosarcoma cells *in vitro* and prevent osteolyticbone metastasis *in vivo*. *Mol Cancer Ther* 8:2339–2347
- Jaffe ES (2009) The 2008 WHO classification of lymphomas: implications for clinical practice and translational research. *Hematology Am Soc Hematol Educ Program*:523–531. <https://doi.org/10.1182/asheducation-2009.1.523>
- JoungYoun U, Miklossy G, Chai X et al (2014) Bioactive sesquiterpene lactones and other compounds isolated from *Vernonia cinerea*. *Fitoterapia* 93:194–200
- Kempema AM, Widen JC, Hexum JK et al (2015) Synthesis and antileukemic activities of C1–C10-modifiedparthenolide analogues. *Bioorg Med Chem* 23:4737–4745
- Kiss I, Unger C, Huu CN et al (2015) Lobatin B inhibits NPM/ALK and NF- $\kappa$ B attenuating anaplastic-large cell-lymphomagenesis and lymph endothelial tumour in trasvasation. *Cancer Lett* 356:994–1006
- Kreuger M, Grootjans S, Biavatti MW et al (2012) Sesquiterpene lactones as drugs with multiple targets in cancer treatment: focus on parthenolide. *Anti-Cancer Drugs* 23(9):883–896
- Krysko DV, Vandenabeele P (2009) Part I-molecular mechanisms of phagocytosis of dying cells. In: Krysko DV, Vandenabeele P (eds) *Phagocytosis of dying cells from molecular mechanisms to human diseases*. Springer, Dordrecht, pp 3–31
- Krysko DV, Brouckaert G, Kalai M et al (2003) Mechanisms of internalization of apoptotic and necrotic L929 cells by amacrophage cell line studied by electron microscopy. *J Morphol* 258:336–345
- Kweon SH, Song JH, Kim HJ et al (2015) Induction of human leukemia cell differentiation via PKC/MAPK pathways by arsanitin, a sesquiterpene lactone from *Artemisia santolina*. *Arch Pharm Res* 38(11):2020–2028. <https://doi.org/10.1007/s12272-015-0609-4>
- Lee J, Hwangbo C, Lee JJ et al (2010) The sesquiterpene lactone eupatolide sensitizes breast cancer cells to TRAIL through down-regulationof c-FLIP expression. *Oncol Rep* 23:229–237
- Li Y, Zhang Y, Fu M et al (2012) Parthenolide induces apoptosis and lytic cytotoxicity in Epstein-Barr virus-positive Burkitt lymphoma. *Mol Med Rep* 6:477–482
- Li H, Li M, Wang G et al (2016) EM23, a natural sesquiterpene lactone from *Elephantopus mollis*, induces apoptosis in human myeloid leukemia cells through thioredoxin- and reactive oxygen species-mediated signaling pathways. *Front Pharmacol*. <https://doi.org/10.3389/fphar.2016.00077>
- Liu Z, Liu S, Xie Z et al (2009) Modulation of DNA methylation by a sesquiterpene lactone parthenolide. *J Pharmacol Exp Ther* 329:505–514
- Liu W, Wang X, Sun J et al (2017) Parthenolide suppresses pancreatic cell growth by autophagy-mediated apoptosis. *Onco Targets Ther* 10:453–461
- Lohberger B, Rinner B, Stuedl N et al (2013) Sesquiterpene lactones downregulate G2/M cell cycle regulator proteins and affect the invasive potential of human soft tissue sarcoma cells. *PLoS One* 8:1–9
- Mahalingam D, Wilding G, Denmeade S et al (2016) Mipsagargin, a novel thapsigargin-based PSMA-activated prodrug: results of a first-in-man phase I clinical trial in patients with refractory, advanced or metastatic solid tumours. *Br J Cancer* 114:986–994. <https://doi.org/10.1038/bjc.2016.72>

- Marin GH, Mansilla E, Ciocchini S et al (2013) Sesquiterpene lactone extract from native American herbs demonstrated antineoplastic activity against non Hodgkin lymphoma cells. *Annalen der Chemi Forschung* 1(2):50–55
- Martino R, Beer MF, Anesini C et al (2015) Sesquiterpene lactones from *Ambrosia* spp. are active against a murine lymphoma cell line by inducing apoptosis and cell cycle arrest. *Toxicol In Vitro* 29:1529–1536
- Merfort I (2011) Perspectives on sesquiterpene lactones in inflammation and cancer. *Curr Drug Targets* 12:1560–1573
- Muñoz Acuña U, Shen Q, Ren Y et al (2013) Goyazensolide induces apoptosis in cancer cells *in vitro* and *in vivo*. *Int J Cancer Res* 9(2):36–53. <https://doi.org/10.3923/ijcr.2013.36.53>
- Nakase I, Gallis B, Takatani-Nakase T et al (2009) Transferrin receptor-dependent cytotoxicity of artemisinin–transferrin conjugates on prostate cancer cells and induction of apoptosis. *Cancer Lett* 274:290–298
- Oh GS, Pae HO, Chung HT et al (2004) Dehydrocostuslactone enhances tumor necrosis factor- $\alpha$ -induced apoptosis of human leukemia HL-60 cells. *Immunopharmacol Immunotoxicol* 26:163–175
- Oka D, Nishimura K, Shiba M et al (2007) Sesquiterpene lactone parthenolide suppresses tumor growth in xenograft model of renal cell carcinoma by inhibiting the activation of NF- $\kappa$ B. *Int J Cancer* 120:2576–2581
- Ordóñez PE, Sharma KK, Bystrom LM et al (2016) Dehydroleucodine, a sesquiterpene lactone from *Gynoxys verrucosa*, demonstrates cytotoxic activity against Human Leukemia Cells. *J Nat Prod* 79(4):691–696
- Quynh D NT, Christensen SB (2015). Thapsigargin, Origin, Chemistry, Structure-Activity Relationships and Prodrug Development. *Curr Pharm Des.* 21(38):5501–5517
- Ralstin MC, Gage EA, Yip-Schneider MT et al (2006) Parthenolide cooperates with NS398 to inhibit growth of human hepatocellular carcinoma cells through effects on apoptosis and G0-G1 cell cycle arrest. *Mol Cancer Res* 4:387–399
- Rozenblat S, Grossman S, Bergman M et al (2008) Induction of G2/M arrest and apoptosis by sesquiterpene lactones in human melanoma cell lines. *Biochem Pharmacol* 75:369–382
- Saeed M, Jacob S, Sandjo LP et al (2015) Cytotoxicity of the sesquiterpene lactones neoambrosin and damsine from *Ambrosia maritime* against multidrug-resistant cancer cells. *Front Pharmacol* 6:267. <https://doi.org/10.3389/fphar.2015.00267>
- Shukla N, Freeman N, Gadsdon P et al (2001) Thapsigargin inhibits angiogenesis in the rat isolated aorta: studies on the role of intracellular calcium pools. *Cardiovasc Res* 49:681–689
- Singh NP, Panwar VK (2006) Case report of a pituitary macro adenoma treated with artemether. *Integr Cancer Ther* 5:391–394
- Sturgeon CM, Craig K, Brown C et al (2005) Modulation of the G2 cell cycle checkpoint by sesquiterpene lactones psilostachyins A and C isolated from the common ragweed *Ambrosia artemisiifolia*. *Planta Med* 71(10):938–943
- Sun Y, St Clair DK, Xu Y et al (2010) A NADPH oxidase dependent redox signaling pathway mediates the selective radio sensitization effect of parthenolide in prostate cancer cells. *Cancer Res* 70:2880–2890
- Sweeney CJ, Mehrotra S, Sadaria MR et al (2005) The sesquiterpene lactone parthenolide in combination with docetaxel reduces metastasis and improves survival in a xenograft model of breast cancer. *Mol Cancer Ther* 4:1004–1012
- Takeuchi O, Akira S (2010) Pattern recognition receptors and inflammation. *Cell* 140:805–820
- Villagomez R, Rodrigo GC, Collado IG et al (2013) Multiple anticancer effects of damsine and coronopilin isolated from *Ambrosia arborescens* on cell cultures. *Int J Anticancer Res* 33:3799–3806
- Wang GW, Qin JJ, Cheng XR et al (2014) *Inula* sesquiterpenoids: structural diversity, cytotoxicity and anti-tumor activity. *Expert Opin Investig Drugs* 23(3):317–345. <https://doi.org/10.1517/13543784.2014.868882>

- World Health Organization (WHO) (2005) Preventing chronic diseases: a vital investment. Geneva: WHO Global report. [http://www.who.int/chp/chronic\\_disease\\_report/en/](http://www.who.int/chp/chronic_disease_report/en/). Accessed 14 Aug 2017
- World Health Organization (WHO) (2017) <http://www.who.int/cancer/en/>. Accessed 14 Aug 2017
- Yang YJ, Yao J, Jin X et al (2016) Sesquiterpenoids and tirucallane triterpenoids from the roots of *Scorzonera divaricata*. *Phytochemistry* 124:86–98
- Yip-Schneider MT, Nakshatri H, Sweeney CJ et al (2005) Parthenolide and sulindac cooperate to mediate growth suppression and inhibit the nuclear factor- $\kappa$ B pathway in pancreatic carcinoma cells. *Mol Cancer Ther* 4:587–594
- Zeisig BB, Kulasekararaj AG, Mufti GJ et al (2012) Snap shot: acute myeloid leukemia. *Cancer Cell* 22:691–698. <https://doi.org/10.1016/j.ccr.2012.10.017>
- Zhang C, Lu T, Wang GD et al (2016) Costunolide, an active sesquiterpene lactone, induced apoptosis via ROS-mediated ER stress and JNK pathway in human U2OS cells. *Biomed Pharmacother* 80:253–259

# Chapter 14

## Anti-inflammatory Activity



María Rosario Alonso, Claudia A. Anesini, and Renzo F. Martino

**Abstract** It is known that inflammation involves a complex series of protective and reparative responses to tissue injury caused by either mechanical and autoimmune stimuli or infection. Inflammation can be either acute or chronic. In the acute phase, in the early stages of inflammation, neutrophils, macrophages, and dendritic cells contribute to cytokine production that spreads the inflammatory events. Although inflammation has a protective role, many diseases have the etiological origin in inflammatory processes such as atherosclerosis, arthritis, cancer, and ischemic heart disease. There are many pathways involving the synthesis and secretion of pro-inflammatory mediators. In this chapter we analyze different intracellular signaling routes related to inflammation. There are two principal types of anti-inflammatory drugs, namely, steroidal anti-inflammatory drugs, which reduce inflammation by binding to cortisol receptors and nonsteroidal anti-inflammatory drugs, which decrease damage by inhibition of cyclooxygenase enzymes. These anti-inflammatory drugs entail many risks, in particular, gastrointestinal ulceration, bleeding, and hepatotoxicity. Over the last decades, the potential of sesquiterpene lactones as anti-inflammatory agents has been pointed out by different authors.

---

M. R. Alonso (✉)

Universidad de Buenos Aires, Facultad de Farmacia y Bioquímica, Departamento de Farmacología, Cátedra de Farmacología, Buenos Aires, Argentina

CONICET – Universidad de Buenos Aires, Instituto de Química y Metabolismo del Fármaco (IQUIMEFA), Buenos Aires, Argentina

e-mail: [mralonso@ffyb.uba.ar](mailto:mralonso@ffyb.uba.ar)

C. A. Anesini

CONICET – Universidad de Buenos Aires, Instituto de Química y Metabolismo del Fármaco (IQUIMEFA), Buenos Aires, Argentina

Universidad de Buenos Aires, Facultad de Farmacia y Bioquímica, Departamento de Farmacología, Cátedra de Farmacognosia, Buenos Aires, Argentina

R. F. Martino

Universidad de Buenos Aires, Facultad de Farmacia y Bioquímica, Departamento de Microbiología, Inmunología y Biotecnología, Cátedra de Inmunología, Buenos Aires, Argentina

**Keywords** Acute inflammation · Chronic inflammation · Pro-inflammatory mediators · Intracellular signaling routes · Anti-inflammatory activity · Sesquiterpene lactones

## Abbreviations

AP-1	activator protein-1
ARE	antioxidant response element
C	complement component
Chemokine R	chemokine receptors
COX-2	ciclooxigenase 2
CR	complement receptor
CysLTs	cysteinyl leukotrienes
Cytokine R	cytokine receptors
DAMPs	damage-associated molecular patterns
ERK	extracellular signal-regulated kinase
HO-1	heme oxygenase 1
IFN- $\gamma$	interferon- $\gamma$
IKK	I $\kappa$ B kinase
IL	interleukins
IL-1ra	IL-1 receptor antagonist
IL-1RAcP	IL-1 receptor accessory protein
IL-1RI	IL-1 type 1 receptor
IL-1RII	IL-1 type 2 receptor
iNOS	inducible type-2 isoform of nitric oxide synthase NOS-2
JAKs	Janus kinases
JNK	c-Jun N-terminal kinase
LPS	lipopolysaccharide
LTs	leukotrienes
MAPKs	mitogen-activated protein kinases
MCP-1	monocyte chemoattractant protein 1
MSU	monosodium urate
NF- $\kappa$ B	nuclear factor kappa B
NLRP3	inflammasome complex Nod-like receptor family pyrin domain containing 3
NLRs	Nucleotide-binding oligomerization-domain protein-like receptors
Nrf2	factor (erythroid-derived 2)-related factor 2
NSAIDs	Nonsteroidal anti-inflammatory drugs
PAMPs	pathogen-associated molecular patterns
PGs	prostaglandins

PLA2	phospholipase A2
PMNs	polymorphonuclear neutrophils
Purine R	purine receptors
RLRs	RIG-I-like (retinoic acid inducible gene 1) receptor family
RNS	reactive nitrogen species
ROS	reactive oxygen species
STATs	signal transducers and activators of transcription
STLs	sesquiterpene lactones
TGF	tumor growth factor
Th	helper T cells
TLRs	Toll-like receptors
TNF- $\alpha$	tumor necrosis factor alpha
TXs	thromboxanes
TyK2	tyrosine kinase 2

## 14.1 Introduction

Inflammation is a complex biological response of vascular tissues to harmful stimuli (Ferrero-Miliani et al. 2007; Davicino et al. 2015). This complex reaction is initiated and organized by mediators of different chemical classes derived from plasma proteins or secreted by cells (Robbins et al. 2010). The inflammation process can be classified as either acute or chronic. In the acute phase, the early stages of inflammation are mediated by tissue-resident macrophages and mast cells, Toll-like receptors (TLRs), and nucleotide-binding oligomerization-domain protein-like receptors (NLRs) present in these cells. These components are activated and are responsible for the activation of transcription factors and the production of pro-inflammatory molecules (Medzhitov 2008). Neutrophils, monocytes, and eosinophils access and migrate to the site of infection or injury and contribute to cytokine production tumor necrosis factor alpha (TNF- $\alpha$ ) and interleukin-6 (IL-6), which spread inflammatory events. Neutrophils release reactive nitrogen species (RNS), reactive oxygen species (ROS), and enzymes such as proteinase and elastase, which destroy invading microorganisms or necrotic tissues. On the other hand, some interleukins, such as IL-4, IL-9, IL-10, IL-11, IL-13, and IL-19 have anti-inflammatory effects. Interleukin-10 (IL-10) is the most widely studied of the anti-inflammatory interleukins related to the suppression of pro-inflammatory mediators (Zhao et al. 2014). It is noteworthy that a successful acute inflammatory response is followed by resolution and repair. However, if the inflammatory stimulus persists, the acute process progresses to chronic diseases such as cancer, arthritis, atherosclerosis, and ischemic heart disease. The prevention of inflammation and pain is of significant concern particularly for those patients afflicted with arthritis and other musculoskeletal ailments (Fig. 14.1).



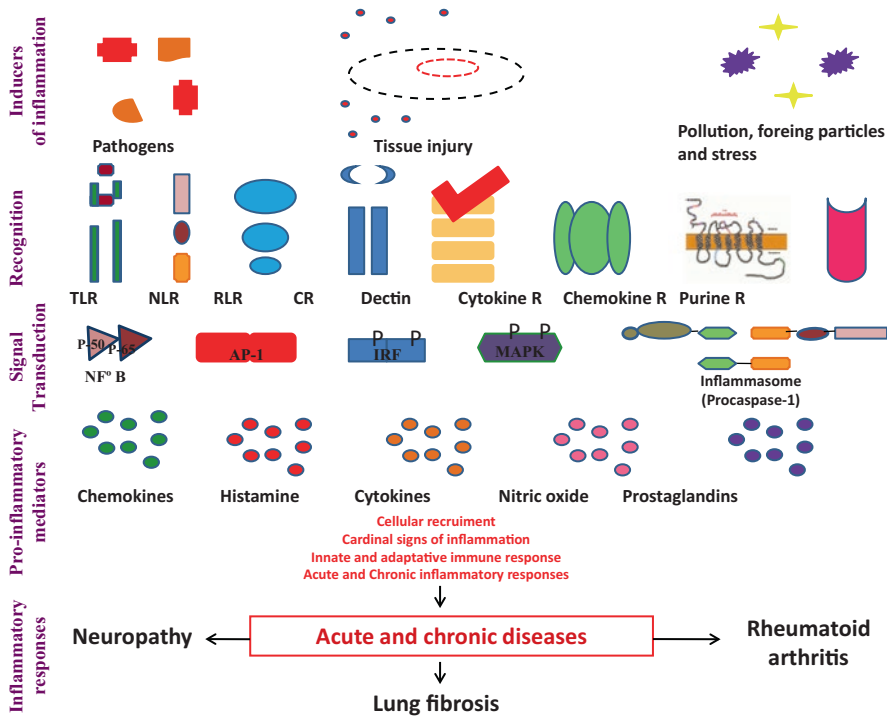


**Fig. 14.1** *Summary of inflammatory mediators.* Overview of inflammatory mediators. Firstly, inflammatory stimuli are recognized by specific cell receptors, for example, Toll-like receptors (TLRs), nucleotide-binding oligomerization-domain protein (NOD)-like receptors or NLRs, cytokine receptors (cytokine R), chemokine receptors (chemokine R), purine receptors (purine R), RIG-I-like (retinoic acid-inducible gene 1) receptor family (RLRs), and complement receptor (CR), among others. After recognition, intracellular signaling pathways are activated, such as nuclear factor kappa B (NF- $\kappa$ B) and mitogen-activated protein kinases (MAPKs), which culminate in the activation of transcription factors NF- $\kappa$ B and activator protein-1 (AP-1) upregulation of transcription and, consequently, production of a series of pro-inflammatory mediators (chemokines, cytokines, histamine, prostanoids, and nitric oxide). These molecules mediate responses that are involved in acute and chronic inflammatory conditions, such as leukocyte recruitment, the generation of local exudates, the appearance of cardinal signs of inflammation, immune responses, and consequent diseases. (Adapted from Hohmann et al. 2016)

## 14.2 Inflammatory Pathways Serving as Pharmacological Targets in Inflammatory Diseases

There are many pathways that involve the synthesis and secretion of pro-inflammatory mediators. In this chapter, we analyze, summarize, and discuss different intracellular signaling routes (Fig. 14.2).

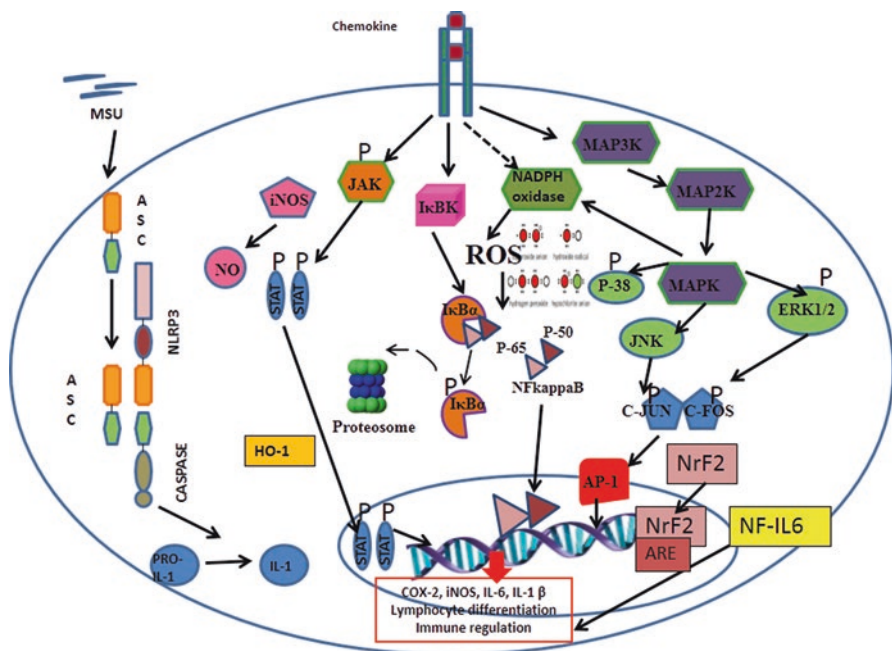


**Fig. 14.2** *The most important pathways involved in inflammation.* Activation of nuclear factor kappa B (NF-κB) translocation into nucleus, the expression of NF-IL6; the production of nitric oxide (NO) through the upregulation of iNOS; the activation of extracellular signal-regulated kinase (ERK) 1/2 and activation of the phosphorylation of inhibitor IκBα by IKK, activation of oxidative stress through the inhibition of phase II detoxification genes, such as HO-1, activation of Janus kinase (JAK)/ signal transducer, activation of transcription (STAT) and mitogen-activated protein kinases (MAPK) activation; the activation of inflammasome caspase-1 and NLRP3; and activation of the nuclear factor E2-related factor 2 (Nrf2)/antioxidant response element (ARE). MSU monosodium urate

### 14.2.1 Inflammatory Cytokines

Cytokines are small secreted proteins, produced predominately by helper T cells (Th) and macrophages, which have a specific effect on the interaction and communication between cells. They can act either on the cells that secrete them (autocrine action), or on nearby cells (paracrine action), or in some instances, on distant cells (endocrine action). They are often produced in a cascade, as one cytokine stimulates its target cells to secrete additional cytokines. Cytokines can also act either synergistically or antagonistically. They are produced as a consequence of physiological or pathological processes. Pro-inflammatory cytokines are produced predominantly by activated macrophages and are involved in the upregulation of inflammatory reactions. Among pro-inflammatory cytokines, interleukins (IL) such as IL-1α and IL-β, IL-6, and TNF-α can be mentioned (Zhang and An 2007).

### 14.2.1.1 Interleukin-1 $\alpha$ and Interleukin- $\beta$

IL-1 $\alpha$  and IL- $\beta$  are prototypic pro-inflammatory cytokines that exert pleiotropic effects on a variety of cells and play key roles in acute and chronic inflammatory and autoimmune disorders. There are two IL-1 receptors, namely, type 1 IL-1 receptor (IL-1RI) and type 2 IL-1 receptor (IL-1 RII). The inflammatory action is mediated by the interaction with IL-1RI, while the binding to IL-1RII does not lead to cell signaling, and it is therefore considered a decoy receptor.

Upon the binding of IL-1 to IL-1RI, a second receptor termed IL-1 receptor accessory protein (IL-1RAcP) is recruited at the cell membrane to form a high-affinity binding receptor complex that triggers the intracellular signaling cascade. A third IL-1 family member, IL-1 receptor antagonist (IL-1ra), binds to IL-1 receptors and prevents the interaction of IL-1 with its receptors, acting as a natural IL-1 inhibitor (Dinarello 1996; Braddock and Quinn 2004). In healthy organisms, IL-1 $\beta$  has important homeostatic functions, such as the regulation of feeding, sleep, and body temperature; however, its overproduction is implicated in the pathophysiological changes that occur during different diseases such as rheumatoid arthritis, neuropathic pain, inflammatory bowel disease, osteoarthritis, vascular disease, multiple sclerosis, and Alzheimer's disease (Braddock and Quinn, 2004; Dinarello 2004).

### 14.2.1.2 Interleukin-6

IL-6 is the principal stimulator for the production of most acute phase proteins (Gitlin and Colten et al. 1987); it participates in the recruitment of leucocytes *in vivo*, and it is capable of crossing the blood-brain barrier (Banks et al. 1994) to stimulate the synthesis of PGE<sub>2</sub> in the hypothalamus, thereby regulating the body temperature. The IL-6-sIL-6R $\alpha$  complex can activate endothelial cells to secrete IL-8 and monocyte chemoattractant protein (MCP)-1 and induce expression of adhesion molecules (Romano et al. 1997). IL-6, in combination with its soluble receptor sIL-6R $\alpha$ , regulates the transition from acute to chronic inflammation by changing the nature of leucocyte infiltrates (from polymorphonuclear neutrophils to monocyte/macrophages). In addition, IL-6 exerts stimulatory effects on T- and B-cells, thus favoring chronic inflammatory responses. IL-6 signals through a cell-surface type I cytokine receptor complex consisting of the ligand-binding IL-6R $\alpha$  chain (CD126) and the signal-transducing component gp130 (also named CD130). As IL-6 interacts with its receptor, it triggers the gp130 and IL-6R proteins to form a complex, thus activating the receptor. These complexes bring together the intracellular regions of gp130 to initiate a signal transduction cascade through the transcription factors Janus kinases (JAKs) and signal transducers and activators of transcription (STATs) (Heinrich et al. 1998).

Strategies targeting IL-6 and IL-6 signaling pathways have led to the effective prophylaxis and treatment of rheumatoid arthritis and other chronic inflammatory diseases in animal models.

### 14.2.1.3 Tumor Necrosis Factor Alpha

Tumor necrosis factor alpha (TNF- $\alpha$ ) is a soluble 17 kDa protein comprising three identical subunits. It is produced by macrophages in response to inflammatory stimuli or infection; TNF- $\alpha$  binds to receptors present on almost all cell types (Vargas Salazar 2009; Bazzoni and Beutler 1996). These receptors are designated p55 and p75, which consist of two identical subunits of transmembrane proteins that form dimers on the cell surface where they bind a TNF- $\alpha$  trimeric form (Mease 2002). The classical inflammatory response attributed to TNF- $\alpha$ , through interaction with p55 and p75, involves thymocyte proliferation, skin necrosis, and apoptosis of activated mature lymphocytes (Peschon et al. 1998). High levels of systemically released TNF- $\alpha$  can modify the anticoagulant properties of endothelial cells, activate neutrophils, and induce the release of other inflammatory cytokines. On the other hand, chronically sustained low levels of TNF- $\alpha$  contribute to the development of the inflammatory response (Choy and Panayi 2001). In this sense the abnormal regulation of TNF- $\alpha$  function plays an important role in the development of chronic inflammatory diseases and infections (Vargas Salazar 2009; Bazzoni and Beutler 1996).

### 14.2.2 *Caspase-1 and the Inflammasome Complex Nod-Like Receptor Family Pyrin Domain Containing the Complex NLRP3*

These factors are related to the modulation of cytokine maturation and release. It has been demonstrated that the inhibition of caspase-1 and the complex NLRP3 reduces the maturation rate of pro-inflammatory cytokines IL-1 $\beta$  and IL-18 (Mathema et al. 2012). The inflammasome is a receptor for endogenous danger signals such as ATP, precipitation of monosodium urate (MSU), cholesterol crystals, and  $\beta$ -amyloid. The inappropriate activation of NLRP3 has been demonstrated to be involved in the pathogenesis of different human diseases such as gouty arthritis and atherosclerosis (Li et al. 2014; Kingsbury et al. 2011). This is particularly relevant in patients with chronic inflammation, with chronic or remittent viral or bacterial infections, and with atherosclerosis, since in those conditions, inflammasomes may become activated through damage-associated molecular patterns (DAMPs) or pathogen-associated molecular patterns (PAMPs). In gout, pro-inflammatory cytokines have an important role in orchestrating the inflammatory reaction to MSU crystals. Recent studies have demonstrated that IL-1 $\beta$  plays a key role by promoting a neutrophil influx into the synovium and joint fluid, which is the pathological expression of the acute attack (Landis and Haskard 2001).

### ***14.2.3 Nuclear Factor Kappa-Light-Chain-Enhancer of Activated B Cells***

Nuclear factor kappa-light-chain-enhancer of activated B cells (NF- $\kappa$ B) is a ubiquitous transcription factor that plays an important role in many inflammatory diseases (Baeuerle and Henkel 1994). NF- $\kappa$ B consists of two subunits: the p50 subunit (NF- $\kappa$ B1) and the p65 subunit (RelA). Under physiological conditions, NF- $\kappa$ B is present in the cytoplasm associated with its inhibitory subunit I $\kappa$ B $\alpha$ . In response to different pro-inflammatory stimuli such as stress, cytokines, free radicals, ultraviolet radiation, bacterial, or viral antigens, the I $\kappa$ B kinase (IKK) is activated to phosphorylate I $\kappa$ B $\alpha$  at serine/threonine residues, leading to the release of NF- $\kappa$ B from I $\kappa$ B $\alpha$ . As a consequence, NF- $\kappa$ B translocates into the nucleus, binds to specific sequences in the promoter regions of genes related to inflammation, and activates their transcription (Gilmore 2006).

Antioxidants, which reduce the levels of ROS and RNS, can suppress the activation of NF- $\kappa$ B. The inhibition of NF- $\kappa$ B activation may provide a pharmacological basis to prevent these acute processes.

### ***14.2.4 The Janus Kinase (Jak)/Signal Transducers and Activators of Transcription (STATs) Pathway***

Inflammatory cytokines are involved in the activation of these pathways. After the cytokine binds to the corresponding receptor, the JAK tyrosine kinases JAK1, JAK2, and tyrosine kinase 2 (Tyk2) are activated and proceed to tyrosine-phosphorylate cytosolic inert STATs. The phosphorylated STATs homo- or hetero-dimerize and translocate into the nucleus. In addition to tyrosine phosphorylation, STATs may also be phosphorylated on serine residues located on their carboxyl-terminal transactivation domains (Butturini et al. 2011; Decker and Kovarik 2000). The pleiotropic cytokine IL-6 predominantly activates STAT3 binding to gp130 cytokine receptor complex and modulates the expression of genes encoding mediators for the classic physiological acute phase response and for the activation of the apoptotic pathway (Kamimura et al. 2003). The activation of STAT3 leads to the physiological response. The deregulation of this transduction cascade may trigger tissue damage either directly or indirectly, leading to the development of chronic diseases such as psoriasis and Crohn's disease, among others. These diseases are characterized by the hyperactivation of STAT3 (Danese and Mantovani 2010; Atreya and Neurath 2008; Mariotto et al. 2008). Therefore, any treatment aimed at blocking the JAK/STAT pathway will have an anti-inflammatory effect, thus representing a novel anti-inflammatory strategy (de Prati et al. 2005).

### 14.2.5 Nitric Oxide

Nitric oxide (NO) is synthesized by many cell types involved in immunity and inflammation. The principal enzyme involved in its synthesis is the inducible type-2 isoform of nitric oxide synthase NOS-2 (iNOS), whose expression is mediated by NF- $\kappa$ B. This enzyme produces high sustained levels of NO. Resting cells do not express iNOS, but it is induced by immunological stimuli such as bacterial lipopolysaccharide (LPS) or cytokines such as IL-1, TNF- $\alpha$ , or interferon- $\gamma$  (IFN- $\gamma$ ). NO is important as a toxic defense molecule against infectious agents, and it also regulates the functional activity, growth, and death of many immune and inflammatory cell types including macrophages, T lymphocytes, antigen-presenting cells, mast cells, neutrophils, and natural killer cells. NO does not act through a receptor, and its target cell specificity depends on its concentration, its chemical reactivity, the vicinity of target cells, and the way that target cells are programmed to respond. At high concentrations, as generated by iNOS, NO is rapidly oxidized to reactive nitrogen oxide species (RNOS) that mediate most of the immunological effects. RNOS can nitrosate thiols to modify key signaling molecules such as kinases and transcription factors. Several key enzymes in mitochondrial respiration are also inhibited by RNOS, and this inhibition leads to a depletion of ATP and cellular energy. NO acts as a pro-inflammatory mediator by inducing vasodilatation and the recruitment of neutrophils, whereas at high concentrations, it downregulates the expression of adhesion molecules and suppresses the activation-inducing apoptosis of inflammatory cells (Ross and Reske-Kunz 2001).

### 14.2.6 Reactive Oxygen Species

Reactive oxygen species (ROS) are defined as partially reduced oxygen metabolites that have strong oxidizing capacity. While at high concentrations, ROS are deleterious to cells; at low concentrations, they serve complex signaling functions. They are injurious, because they oxidize protein and lipid cellular constituents and damage the DNA, as occurs in the progression of inflammatory disorders where an enhanced ROS generation by polymorphonuclear neutrophils (PMNs) at the site of inflammation causes endothelial dysfunction and tissue injury. The superoxide anion ( $O_2^{\cdot-}$ ), the hydroxyl radical (OH $\cdot$ ), hydrogen peroxide ( $H_2O_2$ ), and hypochlorous acid (HOCl) can be mentioned among ROS. The superoxide anion can modulate the activity of kinases upstream NF- $\kappa$ B, resulting in its activation and consequent pro-inflammatory cytokine production and COX-2 expression. If ROS are scavenged, the activation of NF- $\kappa$ B does not occur, with the consequent decrease of inflammation (Mittal et al. 2014). When antioxidant enzymes, such as superoxide dismutase, glutathione peroxidase, and catalase, or nonenzymatic antioxidants such as ascorbic

acid (vitamin C),  $\alpha$ -tocopherol (vitamin E), reduced glutathione, carotenoids, flavonoids, and other antioxidants are at low levels, an imbalance occurs leading to the generation of oxidative stress. The synthesis of antioxidant enzymes is induced by the nuclear factor (erythroid-derived 2)-related factor 2 (Nrf2), which is a stress-responsive transcription factor present in the cytoplasm that plays a key role in the induction of stress resistance genes which encode  $\gamma$ -glutamylcysteine synthetase, glutathione peroxidase, glutathione S-transferase, and heme oxygenase-1 (HO-1) through the activation of the antioxidant response element (ARE) (Nakamura et al. 2004; Umemura et al. 2008).

### ***14.2.7 Mitogen-Activated Protein Kinases***

The main three mitogen-activated protein kinases (MAPKs), c-Jun N-terminal kinase (JNK), extracellular signal-regulated kinase (ERK), and p38 MAPK, are involved in the inflammatory process. MAPKs represent a significant common point for many signaling pathways in the immune response, cell death, and proliferation. MAPKs regulate the activation of downstream transcriptional factors that are important in inflammation. For instance, ERK and JNK and p38 activate the transcription factor activator protein-1 (AP-1) and NF- $\kappa$ B, respectively. On the other hand, anti-inflammatory pathways can also be activated through MAPKs. Another molecule associated with MAPK is Nrf2. When MAPKs are activated, they can activate Nrf2, which is translocated into the nucleus to induce gene expression of heme oxygenase 1 (HO-1). HO-1 plays a key role in the regulation of biological responses such as oxidative stress (where it has cytoprotective/antioxidant roles) and inflammation (Robbins et al. 2010; Haddad 2002).

### ***14.2.8 Lipid Mediators***

Lipid mediators are chemical messengers that are released in response to tissue injury, helping tissues to eliminate harmful invaders, such as bacteria. Current evidence suggests that lipid mediators, including prostaglandins (PGs), leukotrienes (LTs), and lipoxins, play an essential role in the different phases of inflammation. The arachidonic acid pathway is involved in the synthesis of PGs, thromboxanes (TXs), and leukotrienes (LTs). The enzymes phospholipase A2 (PLA2) and cyclooxygenase 2 (COX-2) release and metabolize phospholipids from membranes (Teixeira et al. 2003). When cells are activated, phospholipase A2 (PLA2) hydrolyzes glycerophospholipid membranes releasing, among other fatty acids, arachidonic acid, which in turn, is converted into PGs and TXs by COX, and into LTs by the lipoxygenase (LOX) pathways. For example, prostaglandins are generated during inflammation processes by the inducible COX-2 enzyme through the activation of early genes. Though COX-2 is the dominant source of prostaglandins in

inflammation, recent evidences suggest that both COX-1 and COX-2 may contribute to prostanoid production during both acute inflammatory responses and the resolution phase of inflammation (Li et al. 2015; Scarponi et al. 2014).

These mediators are responsible for important events in inflammation such as vasodilatation, increase of vascular permeability, chemotaxis, pain, leucocyte recruitment, and immune modulation. For example, PGE<sub>2</sub> and cysteinyl leukotrienes (cysLTs) promote the increase of early vascular permeability, and leukotriene B<sub>4</sub> (LTB<sub>4</sub>) stimulates leucocyte chemotaxis. PGs also play additional roles during the acute inflammatory response, including the regulation of local changes in blood flow and pain sensitization (Verri et al. 2006; Xie et al. 2015).

### 14.3 Which Are the Most Currently Used Drugs to Treat Inflammation?

Nowadays, there are two principal types of anti-inflammatory drugs: the steroidal anti-inflammatory drugs, also known as corticosteroids, which reduce inflammation by binding to cortisol receptors, and the nonsteroidal anti-inflammatory drugs (NSAIDs), which alleviate pain and decrease inflammation signs by inhibition of COX. The use of NSAIDs entails many risks, in particular, the development of gastrointestinal ulcers, bleeding, and hepatotoxicity. The gastrointestinal adverse effects are due to the nonselective capacity of NSAIDs to inhibit both COX-1 and COX-2. Besides, most NSAIDs are organic acids, being their ulcerogenic potential related to their pKa and lipophilicity. NSAIDs with pKa values ranging from 2.8 to 4.4 are most likely to cause ulcers, as they are lipophilic drugs that interact with phospholipids and disrupt gastric mucosal membranes. In contrast, most selective COX-2 inhibitors are not acidic and have much higher pKa values, thus, they are less likely to cause gastrointestinal mucosal irritation (Scarpignato and Hunt 2010; Park et al. 2015; Kim et al. 2011). Nevertheless, selective COX-2 inhibitors are still associated with the potential to cause serious gastrointestinal events in high-risk patients, as these inhibitors block the synthesis of gastroduodenal epithelial COX-2-dependent prostanoid synthesis that accelerate ulcer healing (Robbins et al. 2010). In addition, when COX pathways are blocked by NSAIDs, some arachidonic acid is diverted through the lipoxygenase (LOX) pathway, which increases leukotriene synthesis, which can further propagate mucosal damage. The participation of cytokines, principally an increase in serum TNF- $\alpha$ , has been extensively documented in NSAID-induced gastric injury in rats after the administration of indomethacin (Choy and Panayi 2001). Moreover, selective COX-2 inhibitors have been found to be associated with an increased risk of cardiovascular events, such as risk of recurrent myocardial infarction and death. These adverse effects have been observed even after short-term use (i.e., <1 week), as in the case of the management of acute gouty arthritis flares (Schjerning Olsen et al. 2011). Furthermore, the suppression of COX-2-derived prostacyclin by both nonselective NSAIDs and selective COX-2 inhibitors increases the risk of thrombosis, hypertension, atherosclerosis, and myocardial



infarction (Funk and FitzGerald 2007; Smyth et al. 2009). These drugs also have adverse effects at the renal level, provoking sodium retention, edema, and exacerbation of hypertension. Moreover, they can decrease platelets and red and white blood cells counts, thus increasing the risk of bleeding, anemia, or infection, respectively (Peschon et al. 1998). Furthermore, the side effects of corticosteroids are mainly due to the ability of the steroid-activated glucocorticoid receptor to activate target genes involved in the metabolism of sugars, proteins, fats, muscles, and bones via transactivation and suppression of the hypothalamic-pituitary-adrenal axis via trans repression (De Bosscher and Haegeman 2009; Schäcke et al. 2002). For example, the most common adverse effects associated with steroid use for the management of acute gouty arthritis attacks are hyperglycemia due to the stimulation of gluconeogenesis (related to glucocorticoid-induced upregulation in glucose synthesis, consequence of transactivation of a complex network of hepatic enzymes), mobilization and degradation of proteins, and increased glycogen storage in the liver (De Bosscher and Haegeman 2009; Schäcke et al. 2002). The glucocorticoid therapy is also associated with adverse cardiovascular effects, most notably, hypertension, dyslipidemia, and reduced fibrinolytic potential. Moreover, the acute corticosteroids therapy can cause psychiatric disorders and aggravation of preexisting psychoses, also affecting memory and cognition. Other effects observed with these drugs include an increase in the hemoglobin concentration and red blood cell counts, possibly by retarding erythrophagocytosis. The treatment with corticosteroid also causes an increase of polymorphonuclear leucocytes in blood. In contrast, lymphocytes, eosinophils, monocytes, and basophils decrease in number after administration of glucocorticoids.

Taking into account the role of IL-1 $\beta$  in inflammation, it is clear that the agents that target IL-1 $\beta$ , or prevent the action of IL-1 $\beta$  on cells, are likely to be useful therapies for the treatment or prevention of acute gouty attacks. For example, riloncept is a recombinant dimeric fusion protein consisting of fragments of interleukin-1 receptor (IL-1R) and the IL-1R accessory protein linked to the Fc portion (fragment crystallizable region) of immunoglobulin G1, which acts as a receptor to neutralize both IL-1 $\beta$  and IL-1 $\alpha$  and as a soluble decoy receptor. Canakinumab is a fully human monoclonal antibody that binds to human IL-1 $\beta$  and neutralizes its activity by blocking its interaction with IL-1 receptors. Nakinra is an IL-1R antagonist that binds to IL-1R1 and blocks IL-1 $\beta$  and IL-1 $\alpha$ . These drugs cause adverse effects such as infections, injection-site reactions, hypertension, and headache.

Another drug that is specifically used to treat gouty arthritis is colchicine, which is an antimetabolic alkaloid that binds to specific sites on the cytoskeletal protein tubulin and disrupts microtubule polymerization. This disruption of normal cytoskeletal assembly results in a range of biologic effects on essential cell functions, including inhibition of intracellular vesicle transport, decreased secretion of chemokines and cytokines, impairment of cell migration, and inhibition of cell division (Nuki 2008). Colchicine has a narrow therapeutic index between efficacy and treatment-limiting gastrointestinal adverse effects, including diarrhea and abdominal pain caused by increased peristaltic activity (Fig. 14.3).

Since the beginning of human history, plant extracts have been the basis for medical treatments, and such traditional medicine is still widely practiced today.

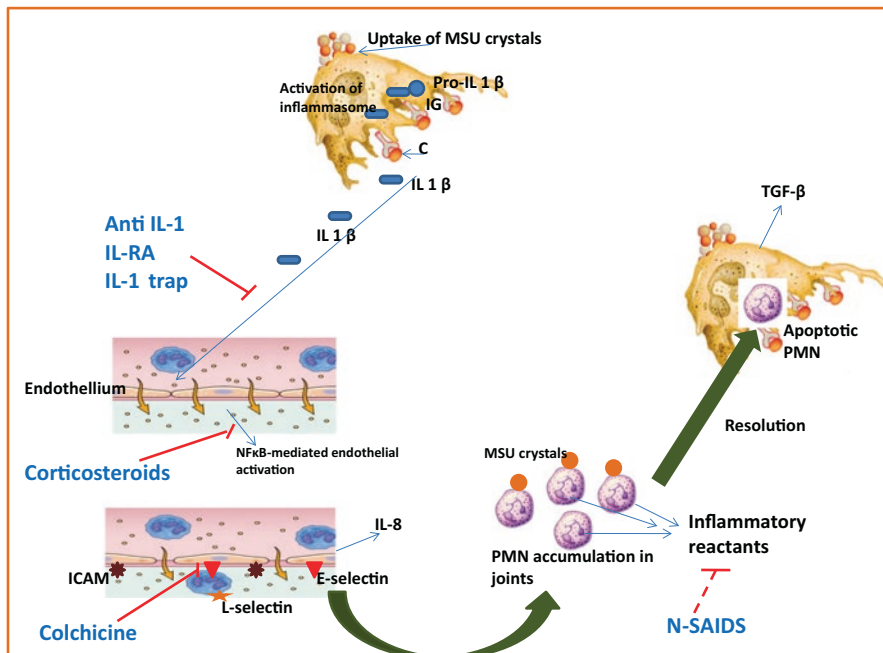


**Fig. 14.3** Mechanism of action of the most commonly anti-inflammatory drugs. The most common mechanisms of therapeutic anti-inflammatory action of gouty arthritis drugs are colchicine, nonsteroidal anti-inflammatory drugs (NSAIDs), and glucocorticoids which act on many different molecular targets. The mechanisms displayed herein are the most likely targets for reduction of MSU crystal-induced inflammation when these drugs are administered at the recommended therapeutic doses. Anti-IL-1, IL-1RA, and IL-1 trap therapies act specifically to block IL-1 $\beta$ . MSU monosodium urate monohydrate, ICAM intracellular adhesion molecule, IL-1 interleukin-1, IL-1RA, IL-1 receptor antagonist, IL-1 trap, IL-1 antagonist, PMN polymorphonuclear leukocytes, TGF tumor growth factor, NF- $\kappa$ B nuclear factor  $\kappa$ B, C complement component

Medicinal plants produce chemical compounds as part of their normal metabolic activity, including secondary metabolites which not only are involved in the plant defense against pathogens but also they have effects on humans. Some authors state that plant extracts are more effective and innocuous than synthetic drugs. Among the compounds isolated from plants, sesquiterpene lactones (STLs) are very promising due to their interesting biological activities.

Taking this into account, the aim of this chapter is to review the anti-inflammatory activity and the mechanisms of action of STLs that are used as anti-inflammatory agents, with special interest in their interaction with the cytokine network, lipid mediator production, their effect on the production of reactive oxygen and nitrogen species, their antioxidant capacity, and the effect on the intracellular signaling pathways activated during inflammation. Sesquiterpene lactones can interfere with the production of molecules that initiate and amplify inflammation. Thus, these compounds can modulate events present in both acute and chronic inflammation processes.

## 14.4 Effects of Sesquiterpene Lactones on Inflammatory Pathways

The effect of some STLs on the inflammatory pathways is reviewed below (Fig. 14.4 and Table 14.1).

### 14.4.1 Effects on the NF- $\kappa$ B Pathway

One of the most important anti-inflammatory effects exerted by STLs is the inhibition of NF- $\kappa$ B signaling pathway (Siedle et al. 2004; Rummel et al. 2011). Some studies show that STLs can inhibit the NF- $\kappa$ B activity by blocking I $\kappa$ B $\alpha$  degradation

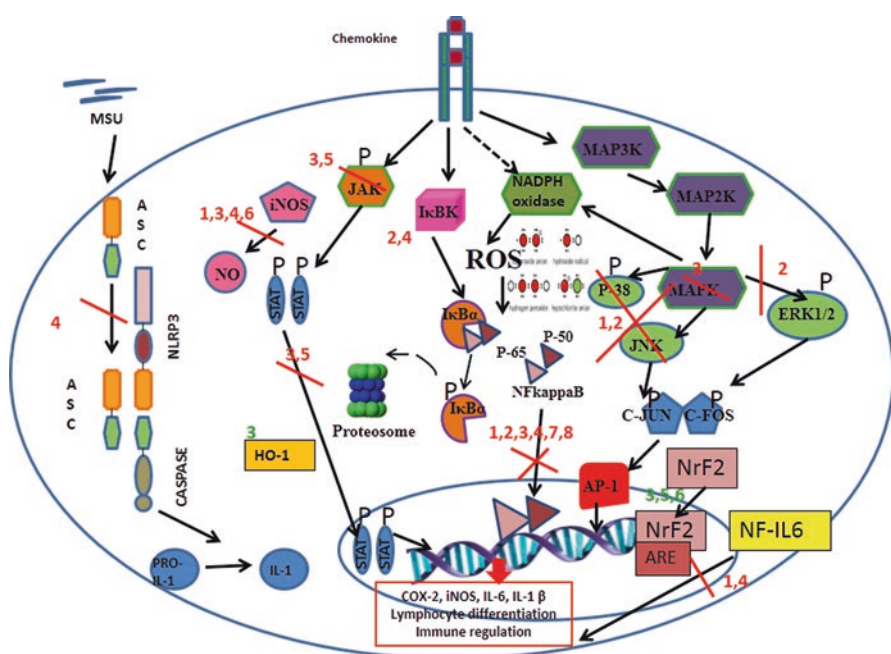


**Fig. 14.4** The anti-inflammatory mechanisms of action of some sesquiterpene lactones. Attractylenolide I and III (represented as 1) and artemisinin (2) suppress p-38 and c-Jun N-terminal kinase (JNK) activation; 1, 2, costunolide (3), parthenolide (4), budlein A (7), and helenalin (8) inhibit nuclear factor kappa B (NF- $\kappa$ B) induction by targeting p65 subunit; 1 and 4 reduce the expression of NF-IL6; 1, 3, 4, and guaianolide (6) can inhibit the production of NO by downregulating the expression of iNOS; 2 inhibits the activation of extracellular signal-regulated kinase (ERK) 1/2 and decreases the phosphorylation of the inhibitor I $\kappa$ B $\alpha$  by IKK and thus, NF- $\kappa$ B translocation into nucleus. A similar action is observed for 4; 3 suppresses oxidative stress through the induction of phase II detoxification genes, such as HO-1, and inhibits Janus kinase (JAK)/ signal transducer and activator of transcription (STAT) and mitogen-activated protein kinases (MAPK) activation; dehydrocostus lactone (5) inhibits JAK/STAT activation; 4 also reduces the activation of caspase-1 and NLRP3; 3, 5, and 6 increase the nuclear factor E2-related factor 2 (Nrf2)/ antioxidant response element (ARE) activation. MSU, monosodium urate. (Adapted from Hohmann et al. 2016)

**Table 14.1** Examples of sesquiterpene lactones with anti-inflammatory effect present in plants and their mechanism of action

Mechanism of action	Sesquiterpene lactones
Inhibition of TNF- $\alpha$	Artemisinin Budlein A
Inhibition of NF- $\kappa$ B	Atractylenolide I/III Artemisinin Costunolide Parthenolide Mehydrocostus lactone Budlein A Helenalin
Inhibition of JAK-STAT	Costunolide Dehydrocostus lactone
Caspase-1/NLRP3	Parthenolide
Inhibition of NO	Atractylenolide I/III Costunolide Parthenolide Guaianolide
Inhibition of COX	Budlein A Costunolide Artemisinin and parthenolide (mRMA expression of COX-2)
Inhibition of cytokine production (TNF- $\alpha$ , IL-1 $\beta$ )	Parthenolide Budlein A
Inhibition of NF- $\kappa$ B and MAPK	Costunolide Atractylenolide III Artemisinin derivative (SM905)
Effect on the production of lipid mediators: PGs, TX, and LT	Costunolide Parthenolide

or NF- $\kappa$ B translocation into the nucleus, being the latter the most frequent effect (Lyss et al. 1998).

The degradation of I $\kappa$ B $\alpha$  can be blocked by  $\alpha$ ,  $\beta$ -unsaturated carbonyl moieties of  $\alpha$ -methylene- $\gamma$ -lactones, which react with thiol groups of critical cysteine (Cys-179) in the IKK through a Michael-type addition (Tamura et al. 2012). On the other hand, the prevention of nuclear translocation or DNA binding of NF- $\kappa$ B occurs by alkylation of the critical cysteine residues (Cys38) in the DNA-binding domain of the p65 subunit of NF- $\kappa$ B (Lyss et al. 1998; Tamura et al. 2012). Atractylenolide III, artemisinin, costunolide, budlein A, helenalin, and parthenolide are some examples of STLs that can modulate inflammation by targeting NF- $\kappa$ B activation. For example, it has been demonstrated that costunolide downregulates the LPS-induced expression of TNF- $\alpha$ , IL-1, IL-6, iNOS, monocyte chemotactic protein (MCP)-1, and COX-2 in activated microglia by inhibiting NF- $\kappa$ B and mitogen-activated protein kinases (MAPK) activation, thus reducing brain inflammation (Rayan et al. 2011). Furthermore, costunolide and dehydrocostus lactone reduce the pleural inflammation induced by carrageenan through the inhibition of ICAM-1, P-selectin, NF- $\kappa$ B, and STAT3 upregulation (Butturini et al. 2014). Nevertheless, other mechanisms of

action, apart from the inhibition of NF- $\kappa$ B activation, are involved in the anti-inflammatory action of STLs, for example, atractylenolide III also suppresses receptor-interacting protein-2 (RIP-2) activation and decreases caspase-1 activation and activity, and IL-1 $\beta$  secretion in phorbol-12-myristate 13-acetate plus calcium ionophore A23187 (PMACI)-induced mast cells (Kang et al. 2011). Budlein A inhibits NF- $\kappa$ B DNA binding at very low concentrations (Siedle et al. 2004).

In addition, parthenolide can also suppress the production of inflammatory mediators by inhibiting I $\kappa$ B degradation (Rummel et al. 2011; Siedle et al. 2004; Dai et al. 2010). In vitro studies have shown that parthenolide and artemisinin inhibit the phosphorylation of IKK and RelA/p65, NF- $\kappa$ B translocation into nucleus, and RelA/p65 binding to DNA, which results in significant reduction in cytokine (TNF- $\alpha$ , IL-1 $\beta$ , IL-6, and IL-8) levels and COX-2 mRNA expression (Wang et al. 2011). Moreover, not only does parthenolide attenuate LPS-induced fever, COX-2 expression, and the levels of circulating TNF- $\alpha$  and IL-6 but also reduces the LPS-induced expression of markers for hypothalamic inflammation, such as NF- $\kappa$ B and the nuclear factor for IL-6 expression (NF-IL6) signaling pathways (Rummel et al. 2011).

#### ***14.4.2 Effects on Janus Kinase (Jak)/Signal Transducers and Activators of Transcription (STATs) Pathway***

It has been demonstrated that dehydrocostus lactone and costunolide inhibit the JAK1 and JAK2 phosphorylation and STAT3 DNA-binding activity in IL-6-activated THP-1 cells (human acute monocytic leukemia cell line). Therefore, STLs also reduce cytokine production and signaling by targeting JAK/STAT (Butturini et al. 2011), thus leading to a significant anti-inflammatory effect.

#### ***14.4.3 Effects on Cytokine Production, Maturation, and Release***

It has been demonstrated that parthenolide can reduce the maturation of pro-inflammatory cytokines IL-1 $\beta$  and IL-18 by inhibiting the activation of caspase-1 and the inflammasome complex NLRP3 (Mathema et al. 2012). In an experimental stroke model in rats, parthenolide also exerted a protective effect which was partially attributed to a downregulation of caspase-1 expression (Dong et al. 2013). It has been demonstrated that parthenolide can inhibit the proteolysis of pro-IL-1 $\beta$  into active IL-1 $\beta$  through the interaction with caspase-1 by direct alkylation of the active site (Cys285) of the p20 subunit (Juliana et al. 2010). Moreover, this STL inhibits the activation of the NLRP3 inflammasome, possibly by inhibiting its ATPase activity. The ATPase activity of NLRP3 is required to oligomerize the inflammasome protein adaptor ASC and to activate procaspase-1 (Juliana et al. 2010).

Furthermore, budlein A, isolated from *Viguiera robusta* (Asteraceae), can inhibit carrageenan-induced mice paw edema, mechanical hyperalgesia (pain), myeloperoxidase activity, and neutrophil recruitment to the peritoneal cavity by a mechanism

related to inhibition of cytokine production (TNF- $\alpha$ , IL-1 $\beta$ , and CXCL1). This STL neither induces the gastric mucosal damage (increased myeloperoxidase activity in the stomach tissue) that is observed after the administration of indomethacin over a 7-day treatment protocol nor the adverse effects provoked by glucocorticosteroids (Valerio et al. 2007). Other authors have also found that budlein A inhibits leukocyte recruitment, adhesion molecule expression, and cytokine production (IL-1 $\beta$ , TNF- $\alpha$ ) in vitro (Nicolete et al. 2009).

#### ***14.4.4 Effect on Nitric Oxide, Reactive Oxygen Species, Reactive Nitrogen Species, and Antioxidant Contents***

It has been demonstrated that STLs exert anti-inflammatory effects by controlling the levels of ROS, RNS, and NO by different mechanisms. Some STLs act by modulating NO levels through the downregulation of iNOS expression, in many cases, through the inhibition of NF- $\kappa$ B and/or MAPK activation. Other STLs control ROS and RNS levels by enhancing antioxidant defenses, which can be either enzymatic or nonenzymatic, via Nrf2/ARE activation. In this sense, parthenolide, costunolide, and atractylenolide I and III are capable of counteracting inflammation by inhibiting the production of NO through the inhibition of NF- $\kappa$ B and/or MAPKs activation (Rayan et al. 2011; Li et al. 2006; Wong and Menendez 1999; Matsuda et al. 2003). The effect on NO production can be studied in vitro on macrophages 264.7, in which the levels of NO can be increased by the action of lipopolysaccharide (LPS). With this model, the anti-inflammatory effect of guaianolides has been demonstrated (Qin et al. 2011).

As for antioxidant enzymes, costunolide and parthenolide, for example, suppress oxidative stress through the increase of endogenous antioxidants such as reduced glutathione and the increase in the activity of the phase II xenobiotic-metabolizing enzymes ( $\gamma$ -glutamylcysteine synthetase, glutathione peroxidase, glutathione S-transferase). These enzymatic activities are induced by the activation of Nrf2/ARE (Jeong et al. 2005).

The antioxidant effect of parthenolide is achieved at low doses, while high doses increase oxidative stress; this effect is responsible for the antiproliferative effect exerted by this compound (Li-Weber et al. 2005). Rummel et al. (2011) have demonstrated that parthenolide exerts antioxidant effects on the rat hypothalamus by reducing LPS-induced mRNA expression of hypothalamic oxidative stress markers (PGC1 $\alpha$ /NRF1/TFAM).

#### ***14.4.5 Effect on the Production of Lipid Mediators***

Some STLs can reduce inflammation by modulating the production of lipid mediators such as PGs, TX, and LT by the inhibition of the enzymes involved in their synthesis. For example, costunolide inhibits the production of PGE2 by suppressing

COX-2 expression (Rodriguez et al. 1976). Sumner et al. (1992) have also demonstrated that parthenolide inhibits TX and LT generation in rat peritoneal leucocytes stimulated with the calcium ionophore A23187 (PMACI).

#### ***14.4.6 Effects on Mitogen-Activated Protein Kinase***

It has been demonstrated that atractylenolide III can diminish the phosphorylation rate of p38 MAPK and JNK, NF- $\kappa$ B activation, and IL-6 secretion in mast cells induced by phorbol-12-myristate 13-acetate plus the calcium ionophore PMACI (Kang et al. 2011). In addition, an artemisinin derivative (SM905) has proved to inhibit the phosphorylation of ERK, p-38, and JNK and decrease the TNF- $\alpha$ , IL-1 $\beta$ , and IL-6 production induced by LPS in a mouse peritoneal macrophage cell line (Wang et al. 2009; Jung et al. 2010; Lee et al. 2010). In these cases, the inhibition of MAPKs by STLs results in the reduction of cytokine production. As mentioned above, there is a connection between MAPKs and the Nrf2 pathway; for example, costunolide can control TNF- $\alpha$  and IL-6 production induced by LPS by increasing Nrf2 and HO-1 expression (Pae et al. 2007).

### **14.5 Conclusion**

One of the most important mechanisms by which STLs exert anti-inflammatory effects is the inhibition of NF- $\kappa$ B. The inhibition of this nuclear transcription factor leads to the inhibition of the production of pro-inflammatory molecules, such as cytokines and enzymes. As a consequence, inhibition of hypernociception and neutrophil migration occurs, thus achieving control of the inflammation scenario.

The most clinically used inhibitors of NF- $\kappa$ B are the glucocorticosteroids such as dexamethasone, which exerts anti-inflammatory effects. However, this drug is known to cause serious side effects, including osteoporosis, aseptic joint necrosis, adrenal insufficiency, gastrointestinal, hepatic, and ophthalmologic disorders, hyperlipidemia, growth suppression, and probably, congenital malformations.

Sesquiterpene lactones can also exert anti-inflammatory effects by inhibiting the production of lipid mediators by inhibition of COX-2 and LX. The main inhibitors of COX-2 and LX are the nonsteroidal anti-inflammatory drugs (non-NSAID) which are one of the most widely prescribed medications together with corticosteroids. Even though the benefits of NSAIDs are related to their anti-inflammatory and analgesic effects, the use of these agents is not innocuous since they mainly increase the risk of gastrointestinal (GI) and cardiovascular complications. Conversely, sesquiterpene lactones appear to have less side adverse effects.

In summary, sesquiterpene lactones can modulate different inflammatory pathways besides NF- $\kappa$ B inhibition without causing adverse effects, as compared to nonsteroidal and steroidal anti-inflammatory drugs. Therefore, many of these molecules are regarded as promising drug candidates for the treatment of inflammatory diseases.

## References

- Atreya R, Neurath MF (2008) Signaling molecules: the pathogenic role of the IL6/STAT-3 trans signaling pathway in intestinal inflammation and in colonic cancer. *Curr Drug Targets* 9:369–374
- Baeuerle PA, Henkel T (1994) Function and activation of NF- $\kappa$ B in the immune system. *Rev Immunol* 12:141–179
- Banks WA, Kastin AJ, Gutierrez EG (1994) Penetration of interleukin-6 across the murine blood-brain barrier. *Neurosci Lett* 179:53–56. [https://doi.org/10.1016/0304-3940\(94\)90933-4](https://doi.org/10.1016/0304-3940(94)90933-4). PMID 7845624
- Bazzoni F, Beutler B (1996) The tumor necrosis factor ligand and receptor families. *N Engl J Med* 334:1717–1725
- Braddock M, Quinn A (2004) Targeting IL-1 in inflammatory disease: new opportunities for therapeutic intervention. *Nat Rev Drug Discov* 3:1–10
- Butturini E, Cavalieri E, de Prati AC et al (2011) Two naturally occurring terpenes, dehydrocostuslactone and costunolide, decrease intracellular GSH content and inhibit STAT3 activation. *PLoS One* 6:e20174. <https://doi.org/10.1371/journal.pone.0020174>
- Butturini E, Paola RD, Suzuki H (2014) Costunolide and dehydrocostuslactone, two natural sesquiterpene lactones, ameliorate the inflammatory process associated to experimental pleurisy in mice. *Eur J Pharmacol* 730:107–115
- Choy EHS, Panayi GS (2001) Cytokine 9 pathways and joint inflammation in rheumatoid arthritis. *N Engl J Med* 344:907–916. <https://doi.org/10.1056/NEJM200103223441207>
- Dai Y, Guzman ML, Chen S et al (2010) The NF (Nuclear factor)- $\kappa$ B inhibitor parthenolide interacts with histone deacetylase inhibitors to induce MKK7/JNK1-dependent apoptosis in human acute myeloid leukaemia cells. *Br J Haematol* 151:70–83
- Danese S, Mantovani A (2010) Inflammatory bowel disease and intestinal cancer: a paradigm of the Yin-Yang interplay between inflammation and cancer. *Oncogene* 29:3313–3323
- Davicino R, Alonso MR, Anesini C et al (2015) Preventive anti-inflammatory activity of an aqueous extract of *larrea divaricata cav.* and digestive and hematological toxicity. *Int J Pharm Sci Res* 6:3215–3223
- De Bosscher K, Haegeman G (2009) Minireview: latest perspectives on antiinflammatory actions of glucocorticoids. *Mol Endocrinol* 23:281–291
- de Prati AC, Ciampa AR, Cavalieri E et al (2005) STAT1 as a new molecular target of anti-inflammatory treatment. *Curr Med Chem* 12:1819–1828
- Decker T, Kovarik P (2000) Serine phosphorylation of STATs. *Oncogene* 19:2628–2637
- Dinarello CA (1996) Biological basis for Interleukin-1 in disease. *Blood* 87:2095–2147
- Dinarello CA (2004) Therapeutic strategies to reduce IL-1 activity in treating local and systemic inflammation. *Curr Opin Pharmacol* 4:378–385
- Dong L, Qiao H, Zhang X et al (2013) Parthenolide is neuroprotective in rat experimental stroke model: downregulating NF- $\kappa$ B, phospho-p38MAPK, and caspase-1 and ameliorating BBB permeability. *Mediat Inflamm* 2013:370804. <https://doi.org/10.1155/2013/370804>
- Ferrero-Miliani L, Nielsen OH, Andersen PS et al (2007) Chronic inflammation: importance of nod2 and nalp3 in interleukin-1 $\beta$  generation. *Clin Exp Immunol* 147:227–235
- Funk CD, FitzGerald GA (2007) COX-2 inhibitors and cardiovascular risk. *J Cardiovasc Pharmacol* 50:470–479
- Gilmore TD (2006) Introduction to NF- $\kappa$ B: players, pathways, perspectives. *Oncogene* 25:6680–6684
- Gitlin JD, Colten HR (1987) Molecular biology of acute phase plasma proteins. In: Pick F (ed) *Lymphokines*, vol 14. Academic Press, San Diego, pp 123–153
- Haddad JJ (2002) Antioxidant and prooxidant mechanisms in the regulation of redox(y)-sensitive transcription factors. *Cell Signal* 14:879–897
- Heinrich PC, Behrmann I, Müller-Newen G et al (1998) Interleukin-6-type cytokine signalling through the gp130/Jak/STAT pathway. *Biochem J* 334:297–314. <https://doi.org/10.1042/bj3340297>



- Hohmann MS, Longhi-Balbinot DT, Guazelli CF et al (2016) Sesquiterpene lactones: structural diversity and perspectives as anti-inflammatory molecules. In: Atta-ur-Rahman (ed) *Studies in natural products chemistry*, vol 49. Elsevier, Amsterdam, pp 243–264
- Jeong WS, Keum YS, Chen C et al (2005) Differential expression and stability of endogenous nuclear factor E2-related factor 2 (Nrf2) by natural chemopreventive compounds in HepG2 human hepatoma cells. *Biochem Mol Biol* 38:167–176
- Juliana C, Fernandes-Alnemri T, Wu J et al (2010) Anti-inflammatory compounds parthenolide and bay 11-7082 are direct inhibitors of the inflammasome. *J Biol Chem* 285:9792–9802
- Jung HW, Mahesh R, Park JH et al (2010) Effect of *Sesbania grandiflora* on lung antioxidant defense system in cigarette smoke exposed rats. *Int Immunopharmacol* 10:155–162
- Kamimura D, Ishihara K, Hirano T (2003) IL-6 signal transduction and its physiological roles: the signal orchestration model. *Rev Physiol Biochem Pharmacol* 149:1–38
- Kang T, Han N, Kim H et al (2011) Blockade of IL-6 secretion pathway by the sesquiterpenoid atractylenolide III. *J Nat Prod* 74:223–227
- Kim SJ, Park YS, Paik HD et al (2011) Effect of anthocyanins on expression of matrix metalloproteinase-2 in naproxen-induced gastric ulcers. *Br J Nutr* 106:1792–1801
- Kingsbury S, Conaghan P, McDermott MF (2011) The role of the NLRP3 inflammasome in gout. *J Inflamm Res* 4:39–49
- Landis RC, Haskard DO (2001) Pathogenesis of crystal-induced inflammation. *Curr Rheumatol Rep* 1:36–41
- Lee J, Tae N, Lee JJ et al (2010) Effect of MF on NO production and iNOS expression levels in LPS-stimulated RAW264.7 cells. *Eur J Pharmacol* 636:173–180
- Li X, Cui X, Li Y et al (2006) Parthenolide has limited effects on nuclear factor-kappa beta increases and worsens survival in lipopolysaccharide-challenged C57BL/6J mice. *Cytokine* 33:299–308
- Li X, Zhang Y, Xia M et al (2014) Activation of Nlrp3 inflammasomes enhances macrophage lipid-deposition and migration: implication of a novel role of inflammasome in atherogenesis. *PLoS One* 9:e87552. <https://doi.org/10.1371/journal.pone.0087552>
- Li X, Peng Z, Su C (2015) Potential anti-cancer activities and mechanisms of costunolide and dehydrocostuslactone. *Int J Mol Sci* 16:10888–10906
- Li-Weber M, Palfi K, Giaisi M et al (2005) Dual role of the anti-inflammatory sesquiterpene lactone: regulation of life and death by parthenolide. *Cell Death Differ* 12:408–409
- Lyss G, Knorre A, Schmidt TJ et al (1998) The anti-inflammatory sesquiterpene lactone hel-enalin inhibits the transcription factor NF-kappaB by directly targeting p65. *J Biol Chem* 273:33508–33516
- Mariotto S, Esposito E, Di Paola R et al (2008) Protective effect of *Arbutus unedo* aqueous extract in carrageenan-induced lung inflammation in mice. *Pharmacol Res* 57:110–124
- Mathema VB, Koh Y, Thakuri B et al (2012) Parthenolide, a sesquiterpene lactone, expresses multiple anti-cancer and anti-inflammatory activities. *Inflammation* 35:560–565
- Matsuda H, Toguchida I, Ninomiya K et al (2003) Effects of sesquiterpenes and amino acid-sesquiterpene conjugates from the roots of *Saussurea lappa* on inducible nitric oxide synthase and heat shock protein in lipopolysaccharide-activated macrophages. *Bioorg Med Chem* 11:709–715
- Mease P (2002) Tumor necrosis factor (TNF) 36. In psoriatic arthritis: pathophysiology and treatment with TNF inhibitors. *Ann Rheum Dis* 61:298–304
- Medzhitov R (2008) Origin and physiological roles of inflammation. *Nature* 454:28–435
- Mittal M, Siddiqui MR, Tran K et al (2014) Reactive oxygen species in inflammation and tissue injury. *Antioxid Redox Signal* 20:1126–1167
- Nakamura Y, Yoshida C, Murakami A et al (2004) Zerumbone, a tropical ginger sesquiterpene, activates phase II drug metabolizing enzymes. *FEBS Lett* 572:245–250
- Nicolette R, Arakawa NS, Rius C et al (2009) Budlein a from *Viguiera robusta* inhibits leukocyte-endothelial cell interactions, adhesion molecule expression and inflammatory mediators release. *Phytomedicine* 16:904–915
- Nuki G (2008) Colchicine: its mechanism of action and efficacy in crystal-induced inflammation. *Curr Rheumatol Rep* 10:218–227

- Pae HO, Jeong GS, Kim HS et al (2007) Costunolide inhibits production of tumor necrosis factor- $\alpha$  and interleukin-6 by inducing heme oxygenase-1 in RAW264.7 macrophages. *Inflamm Res* 56:520–526
- Park EH, Han YM, Jeong M et al (2015) Omega-3 polyunsaturated fatty acids as an angelus custos to rescue patients from NSAID-induced gastroduodenal damage. *J Gastroenterol* 50:614–625. <https://doi.org/10.1007/s00535-014-1034>
- Peschon JJ, Torrance DS, Stocking KL et al (1998) TNF receptor-deficient mice reveals divergent roles for p55 and p75 in several models of inflammation. *J Immunol* 160:943–952
- Qin JJ, Wang LY, Zhu JX et al (2011) Neojaponicone A, a bioactive sesquiterpene lactone dimer with an unprecedented carbon skeleton from *Inula japonica*. *Chem Commun* 47:1222–1224
- Rayan NA, Baby N, Pitchai D et al (2011) Costunolide inhibits proinflammatory cytokines and iNOS in activated murine BV2 microglia. *Front Biosci* 3:1079–1091
- Robbins SL, Kumar V, Abbas A et al (2010) *Patologia bases patológicas das doenças*, 8th edn. Elsevier, Rio de Janeiro
- Rodríguez E, Towers GHN, Mitchell JC (1976) Biological activities of sesquiterpene lactones. *Phytochemistry* 15:1573–1580
- Romano M, Sironi M, Toniatti C et al (1997) Role of IL-6 and its soluble receptor in induction of chemokines and leukocyte recruitment. *Immunity* 6:315–325
- Ross R, Reske-Kunz AB (2001) The role of nitric oxide in contact hypersensitivity. *Int Immunopharmacol* 1:1469–1478
- Rummel C, Gerstberger R, Roth J et al (2011) Parthenolide attenuates LPS-induced fever, circulating cytokines and markers of brain inflammation in rats. *Cytokine* 56:739–748
- Scarpignato C, Hunt RH (2010) Nonsteroidal antiinflammatory drug-related injury to the gastrointestinal tract: clinical picture, pathogenesis, and prevention. *Gastroenterol Clin North Am* 39:433–464
- Scarponi C, Butturini E, Sestito R et al (2014) Inhibition of inflammatory and proliferative responses of human keratinocytes exposed to the sesquiterpene lactones dehydrocostuslactone and costunolide. *PLoS One* 16:e107904
- Schäcke H, Döcke WD, Asadullah K (2002) Mechanisms involved in the side effects of glucocorticoids. *Pharmacol Ther* 96:23–43
- Schjerning Olsen AM, Fosbol EL, Lindhardsen J et al (2011) Duration of treatment with nonsteroidal anti-inflammatory drugs and impact on risk of death and recurrent myocardial infarction in patients with prior myocardial infarction: a nationwide cohort study. *Circulation* 123:2226–2235
- Siedle B, Garcia-Piñeres AJ, Murillo R et al (2004) Quantitative structure-activity relationship of sesquiterpene lactones as inhibitors of the transcription factor NF- $\kappa$ B. *Med Chem* 47:6042–6054
- Smyth EM, Grosser T, Wang M et al (2009) Prostanoids in health and disease. *J Lipid Res* 50:S423–S428
- Sumner H, Salan U, Knight DW et al (1992) Inhibition of 5-lipoxygenase and cyclo-oxygenase in leukocytes by feverfew. Involvement of sesquiterpene lactones and other components. *Biochem Pharmacol* 43:2313–2320
- Tamura R, Chen Y, Shinozaki M et al (2012) Eudesmane-type sesquiterpene lactones inhibit multiple steps in the NF- $\kappa$ B signaling pathway induced by inflammatory cytokines. *Bioorg Med Chem Lett* 22:207–211
- Teixeira C, Landucci E, Antunes E et al (2003) Inflammatory effects of snake venom myotoxic phospholipases A2. *Toxicol* 42:947–962
- Umemura K, Itoh T, Hamada N et al (2008) Preconditioning by sesquiterpene lactone enhances H<sub>2</sub>O<sub>2</sub>-induced Nrf2/ARE activation. *Biochem Biophys Res Commun* 368:948–954
- Valerio DA, Cunha TM, Arakawa NS et al (2007) Anti-inflammatory and analgesic effects of the sesquiterpene lactone budlein A in mice: inhibition of cytokine production-dependent mechanism. *Eur J Pharmacol* 562:155–163
- Vargas Salazar M (2009) El factor de necrosis tumoral-alfa (fnt- $\alpha$ ) en la patogénesis de la artritis reumatoide y el riesgo de tuberculosis con infliximab. *Revista Médica de Costa Rica y Centroamérica* LXVII 590:345–351

- Verri WA, Cunha TM, Parada CA et al (2006) Hypernociceptive role of cytokines and chemokines: targets for analgesic drug development? *Pharmacol Ther* 112:116–138
- Wang JX, Hou LF, Yang Y et al (2009) SM905, an artemisinin derivative, inhibited NO and pro-inflammatory cytokine production by suppressing MAPK and NF- $\kappa$ B pathways in RAW 264.7 macrophages. *Acta Pharmacol Sin* 30:1428–1435
- Wang Y, Huang Z, Wang L et al (2011) Artemisinin inhibits monocyte adhesion to HUVECs through the NF- $\kappa$ B and MAPK pathways *in vitro*. *Int J Mol Med* 27:233–241
- Wong HR, Menendez IY (1999) Sesquiterpene lactones inhibit inducible nitric oxide synthase gene expression in cultured rat aortic smooth muscle cells. *Biochem Bio Res Commun* 262:375–380
- Xie C, Li X, Wu J et al (2015) Anti-inflammatory activity of magnesium isoglycyrrhizinate through inhibition of phospholipase A2/arachidonic acid pathway. *Inflammation* 38:1639–1648
- Zhang JM, An J (2007) Cytokines, inflammation and pain. *Int Anesthesiol Clin* 45:27–37
- Zhao HQ, Li WM, Lu ZQ et al (2014) The growing spectrum of anti-inflammatory interleukins and their potential roles in the development of sepsis. *J Interf Cytokine Res* 35:242–251

**Part III**  
**Sesquiterpene Lactones: Medicinal**  
**Chemistry Approach**

# Chapter 15

## Structure-Activity and Activity-Activity Relationships of Sesquiterpene Lactones



Thomas J. Schmidt

**Abstract** It has long been recognized that many sesquiterpene lactones possess very prominent anti-infective as well as antitumour potential. The structure-activity relationships underlying these as well as many other aspects of their biological activity have been reviewed extensively. Since 2006, a variety of new data have emerged that warrant an update. The activity of sesquiterpene lactones against “protozoan” parasites has been the topic of studies from various laboratories, and the current chapter will attempt a synopsis of the existing biological data related to inhibitory effects on parasites of the genera *Trypanosoma*, *Leishmania* and *Plasmodium* as causative agents of major tropical diseases. Besides some recent new mechanistic evidence to explain the strong anti-trypanosomal activity of certain sesquiterpene lactones, a main focus will be on quantitative structure-activity relationship studies which have recently led to the discovery of certain furanoheliangolide-type compounds as extremely potent agents against *Trypanosoma brucei*, the pathogen responsible for human African trypanosomiasis or “sleeping sickness”. Investigations on the long-known antitumoural potential of sesquiterpene lactones have recently received new impetus by the finding that certain compounds of this class possess a hitherto unknown mechanism of action that may make them interesting leads, or even therapeutic agents, against certain types of leukaemia and some other tumours known to be characterized by an excessive activity of the transcription factor c-Myb. This factor plays important roles in cell proliferation and differentiation and has been identified as an interesting drug target. Sesquiterpene lactones were discovered as the first type of low-molecular-weight inhibitors of c-Myb and C/EBP transcriptional activity. Besides extensive QSAR studies on this new activity of sesquiterpene lactones, the chapter will also focus on very recent mechanistic studies into the peculiar mode of action of the most active sesquiterpene lactones on the transcriptional activity of c-Myb and C/EBP.

**Keywords** Sesquiterpene lactone · *Trypanosoma* · *Leishmania* · *Plasmodium* · Cytotoxicity · Cancer · Inflammation · Structure-activity-relationship · QSAR

---

T. J. Schmidt (✉)

Institute of Pharmaceutical Biology and Phytochemistry (IPBP),  
University of Münster, PharmaCampus – Corrensstrasse 48, D-48149 Münster, Germany  
e-mail: [thomschm@uni-muenster.de](mailto:thomschm@uni-muenster.de)

## 15.1 Introduction

More than a decade has passed since my last comprehensive overview on structure-activity relationships (SAR) of sesquiterpene lactones (STLs) (Schmidt 2006). Over the years, the number of known STLs has further increased, and a lot of new information has been accumulated with respect to the biological activities of this huge class of terpenoids. The present chapter will summarize studies that have emerged over the past 10 years on SAR of STLs with respect to selected bioactivities, namely, their anti-infective potential against “protozoan” parasites, their antitumour potential as well as their anti-inflammatory activity.

## 15.2 Structure-Antiprotozoal Activity Relationships

In 2006 when the last general review on SAR of STLs (Schmidt 2006) was published, some knowledge already existed on antiplasmodial, anti-trypanosomal and anti-leishmanial activities of STLs, i.e. their activity against unicellular eukaryotic parasites responsible for several severe infectious diseases, namely, malaria tropica (*Plasmodium falciparum*), human African trypanosomiasis (*Trypanosoma brucei*), Chagas disease (*T. cruzi*) and visceral leishmaniasis (*Leishmania donovani*). The main structural requirements for these activities had already been recognized, albeit on the basis of relatively few compounds. As in case of many other biological activities, the most important factor appeared to be the presence of potentially reactive structure elements, namely,  $\alpha,\beta$ -unsaturated carbonyl groups. At that time, it had already been observed that the presence of more than one such structure element in the molecule was essential for high activity and a notable degree of selective toxicity for the unicellular parasites in comparison with mammalian cells. Although coherent data on the activity against different parasites and mammalian cells were only available for a relatively small number of STLs, it had been observed that there is a significant correlation between antiparasitic and cytotoxic activities, yet at a lower degree than that observed between the various antiparasitic effects. Since then, the number of compounds with comparable activity data has greatly increased so that structure-activity relationships and activity-activity correlations can now be established on a more solid statistical basis. Many aspects of the activity of STLs against protozoan parasites have been reviewed by members of ResNet NPND in 2012 (Schmidt et al. 2012). Very recently, the group of M. T. Scotti has published a comprehensive review on in silico approaches to understand the underlying SAR (Acevedo et al. 2017).

### 15.2.1 Anti-trypanosomatid Activity: *Trypanosoma brucei*

Based on our finding that helenalin (**1**) has very potent activity against African trypanosomes (*Trypanosoma brucei*, aetiologic agent of human African trypanosomiasis, HAT or “sleeping sickness”), which was first published in 2002

(Schmidt et al. 2002), our group has, since then, isolated and tested a wide array of further STLs against *Trypanosoma brucei rhodesiense* (*Tbr*; responsible of the East African form of HAT) (Schmidt et al. 2009, 2014; Nour et al. 2009; Maas et al. 2014; Gökbulut et al. 2012; Kimani et al. 2017, 2018a, b; Nogueira 2016).

In 2009, we published the first QSAR study for STLs' anti-trypanosomal activity (Schmidt et al. 2009). Already at that time, it became clear that the antiparasitic activity is closely related to the general cytotoxicity of this class of compounds. Very similar QSAR models were obtained using PLS2 regression on a dataset of 40 STLs (1–40; structures; see Fig. 15.1) and their in vitro anti-*Tbr* activity and cytotoxicity data determined on L6 rat skeletal myoblasts. Out of a set of 44 2D and 3D descriptors considered in this study, those dominantly explaining both biological effects were related to chemical reactivity (descriptors AM1\_LUMO and ENONCS) representing the electrophilicity of the molecules as Michael acceptors and the corresponding accessible surface area of reactive carbon atoms. This finding was another confirmation that the biological activity of STLs in many, if not most cases, depends directly on their capability to engage in Michael-type additions to biological nucleophiles, for which a large body of evidence exists and which has been reviewed extensively (Schmidt 2006, 2009; Schmidt 1999a). Compounds such as helenalin (1) and its esters contain two such potential addition sites, namely, a cyclopentenone moiety in addition to the frequent  $\alpha$ -methylene- $\gamma$ -lactone structure, which correlates with their particularly high activity (not only in the case of anti-trypanosomal activity). Other structural influences on the biological effects under study (factors related to molecular size, hydrophobicity and charge distribution) have been found to be rather of modulatory nature. Although the models for anti-trypanosomal and cytotoxic activity were rather similar (i.e. used the same descriptors but to different extents), it was nevertheless also demonstrated already in this study (Schmidt et al. 2009) that the selectivity towards trypanosomes observed for the more active STLs is directly correlated with the anti-trypanosomal activity and not with cytotoxicity. Cytotoxicity does not proportionally increase with the anti-trypanosomal activity so that the most active compounds are increasingly more selective towards *T. brucei*. Plots of anti-*Tbr* activity and of cytotoxicity vs. the selectivity index (SI, i.e. the ratio of cytotoxic over anti-trypanosomal  $IC_{50}$  values), as shown in Fig. 15.2, display a (weak) linear relationship of the anti-*Tbr* activity and selectivity and the essential absence of any relationship of SI with the cytotoxic activity. A certain degree of selectivity that only depends on the strength of the desirable activity has prompted us to continue the search for even more potent STLs.

Thus, in 2014, the number of tested compounds in our series had increased to over 60 (Fig. 15.1). It is noteworthy that, up to this point, not a single STL in the whole array had outmatched helenalin (1), the first compound in our series ever tested against *Tbr* which had shown an  $IC_{50}$  value of 0.05  $\mu$ M. A QSAR study was conducted for this extended set of STLs regarding their anti-*Tbr* activity, along with some other compounds that had been tested in the same laboratory. Thus, a total of 69 STL structures (1–69) were investigated (Schmidt et al. 2014) expanding the range of compounds and taking into consideration a much larger chemical diversity than had been evaluated in our study performed in 2009 (Schmidt et al. 2009). The study, performed by using a combination of a genetic algorithm with a multiple

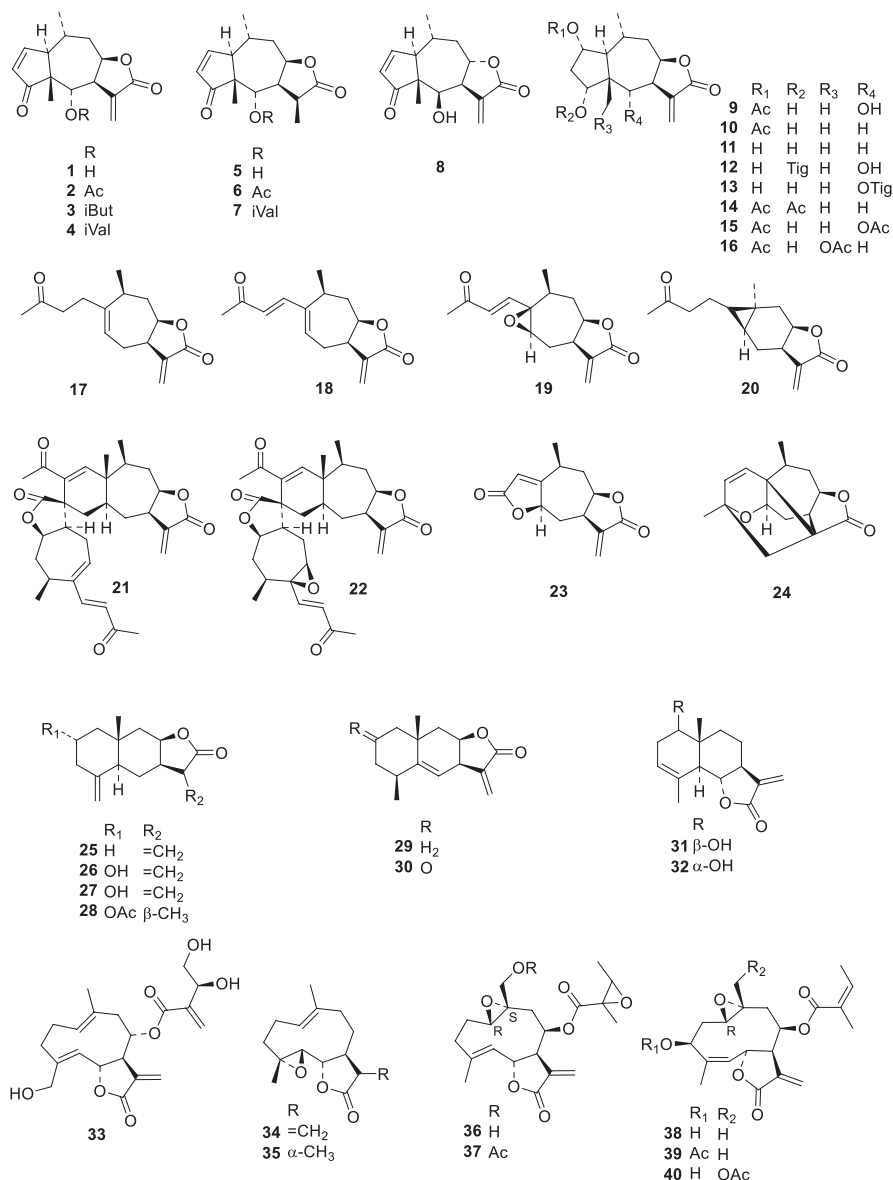


**Fig. 15.1** Structures of sesquiterpene lactones tested for antiprotozoal activity. Most of the compounds were analyzed in our QSAR studies 1–40 (Schmidt et al. 2009; Trossini et al. 2014), 1–73 (Schmidt et al. 2014)

linear regression on a set of 123 2D and 3D descriptors, led to a refined model in which the importance of descriptors related with electrophilic reactivity was emphasized, and aspects of hydrogen bond accepting as well as hydrophobic properties were also found to be of importance. Most importantly, this model showed not only good explanatory and internal predictive quality for the training set ( $n = 46$  molecules



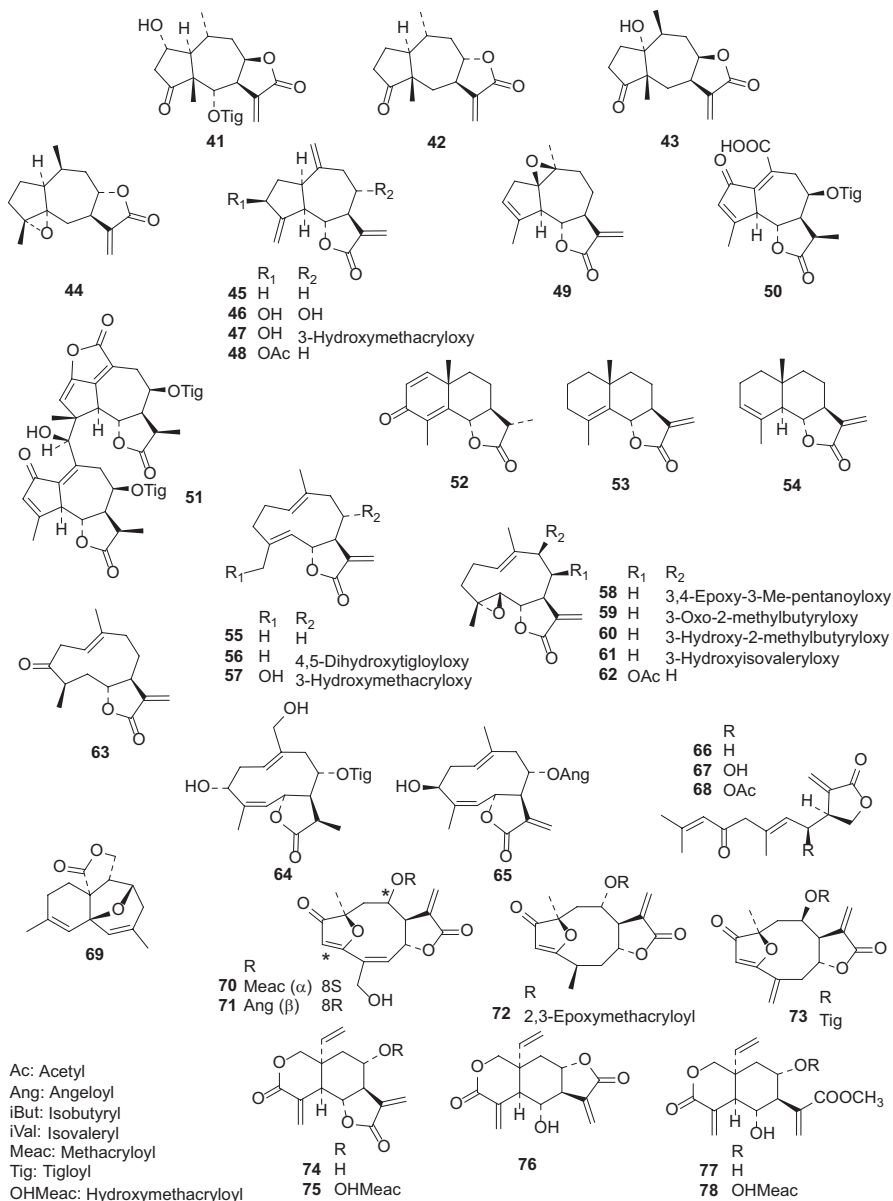
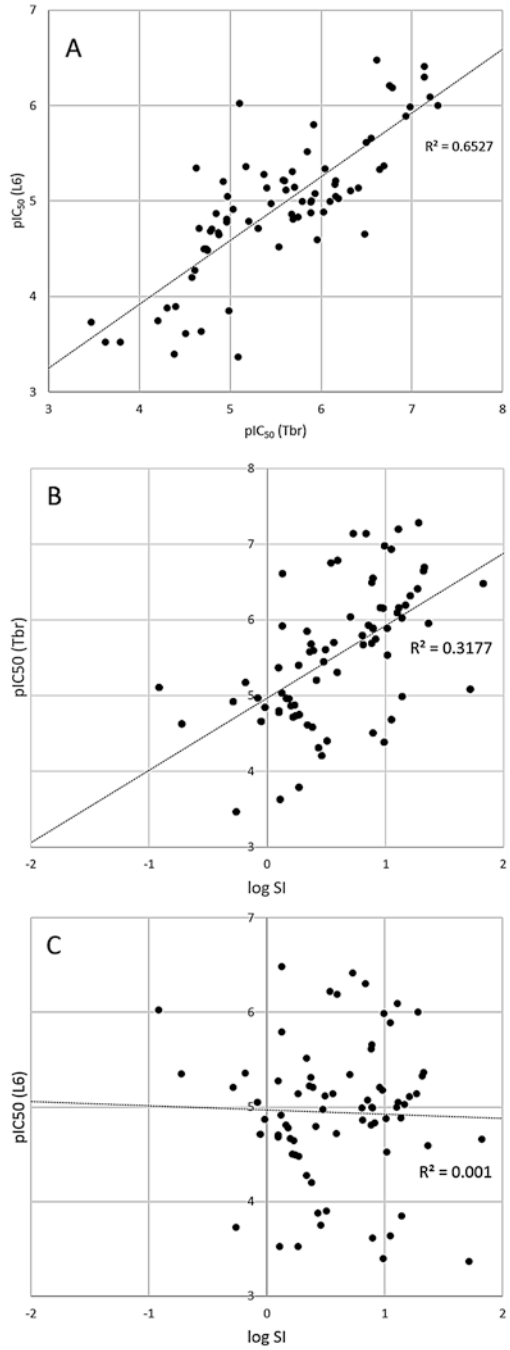


Fig. 15.1 (continued)

used to generate the model) but it also presented a good performance predicting the activity of an external test set of 23 compounds that had not been included in the model building process.

The external predictions for the test set thus led us to apply this new QSAR model to predict the activity of a large number of structurally diverse and previously untested STLs in a virtual database. Of the 1750 STLs for which predictions were

**Fig. 15.2** (a): Plot of activity data ( $pIC_{50}$  [M]) of 75 STLs for cytotoxicity (L6 rat skeletal myoblasts) vs. *T. brucei rhodesiense* (bloodstream forms) showing the linear relationship between the effects. (b): Plot of anti-*Tbr* activity vs. log SI; (c): Plot of cytotoxicity vs. log SI, demonstrating that the selectivity is related to high anti-trypanosomal activity but unrelated to cytotoxicity. (Data from Schmidt et al. (2009, 2014))



made, 71 were predicted to have  $IC_{50}$  values below  $0.1 \mu\text{M}$  and, quite conspicuously, over 30 of these compounds belonged to the subclass of furanoheliangolide-type STLs. Consequently, a number of such compounds (**70–73**) were obtained and tested. These compounds were indeed found to exhibit a strong anti-*Tbr* activity. Thus, goyazensolide (**70**) and budlein A (**71**), which contain an  $\alpha,\beta,\gamma,\delta$ -unsaturated ketone structure as a potential reactive site in addition to the  $\alpha$ -methylene- $\gamma$ -lactone moiety and which have  $IC_{50}$  values of  $0.07 \mu\text{M}$ , exhibited activity values that were close to those of helenalin (**1**). Compound **72**, which bears a “truncated” enone system in comparison with its congeners **70** and **71**, was found to be three times less active ( $IC_{50} = 0.20$ ) than **70** and **71**, thus highlighting the importance of the conjugated ketone group that represents a viable Michael acceptor structure. Most strikingly, 4,15-isoatriplicolide tiglate (**73**), a structural analogue with the  $\gamma,\delta$ -double bond in an exocyclic position that renders it more sensitive to nucleophilic attack, presented an  $IC_{50}$  of only  $0.015 \mu\text{M}$ , thus being the most active compound in our series so far (Schmidt et al. 2014). The latter constitutes a good example of how a careful QSAR analysis can lead to the discovery of very potent new lead compounds. As stated above, there are parallels to the antiproliferative activity: the pseudoguaianolide helenalin (**1**) and its esters and 1-oxo-furanoheliangolides in which the ketone group is conjugated with two double bonds ( $\alpha,\beta,\gamma,\delta$ -unsaturated ketone as in **70**, **71** and **73**) are the most active compounds. Indeed, a high degree of similarity between these two STLs is found, which becomes most evident if not only the structural diagram, but the 3D structure and the molecular shape and surface are considered (see Fig. 15.6, Sect. 15.3).

Our collection of STLs tested against *Tbr* has been further expanded to almost 100 compounds. We have recently isolated some elemanolide derivatives (**74–79**) from the African Asteraceae plant *Vernonia lasiopus*. These derivatives have displayed considerable anti-*Tbr* activity. Interestingly, the most active compounds found in this plant, vernolepin (**74**), vernodalol (**78**) and vernomenin (**76**) ( $IC_{50}$  values of  $0.19$ ,  $0.26$  and  $0.51 \mu\text{M}$ , respectively) also have two potentially reactive structure elements, namely, an  $\alpha$ -methylene- $\delta$ -lactone moiety in combination with an  $\alpha$ -methylene- $\gamma$ -lactone or an  $\alpha$ -methylene carboxylic acid ester (Kimani et al. 2017). Other STLs, including some hitherto untested skeletal types, have been obtained by our research group from various Brazilian (Nogueira 2016) as well as some African plants belonging to the Asteraceae family (Kimani et al. 2018a, b) which will widen the existing knowledge on anti-trypanosomal SAR. Since these further extended QSAR results are yet unpublished, they are not included in this chapter.

In view of such interesting activity against trypanosomes in phenotypic whole-cell assays, the question arising is whether such natural compounds have therapeutic potential. Indeed, the findings published so far are not very promising. Of the many compounds isolated by our research group, several have been tested in vivo in an early stage model (parasites in the bloodstream) with *T. brucei*-infected mice, but none of them showed sufficient in vivo activity to warrant further development. Although helenalin (**1**) did not cure the infected mice, it did not show toxicity at  $20 \text{ mg/kg}$  administered i.p. over 4 days [R. Brun, personal communication].

Compounds of various structural subclasses and with different levels of in vitro activity (**2**, **5**, **49**, **62**, **70**, **71**, **73**) were then tested in this model. Arglablin (**49**), lipiferolide (**62**) and budlein A (**71**) led to clearance of parasitemia in most animals after 4 days of i.p. treatment with 80 mg/kg, 50 mg/kg and 10 mg/kg, respectively. With these dosages, 4/4 (**49**), 3/3 (**62**) and 3/4 (**71**) animals, respectively, showed 100% clearance of the parasitemia; however, relapse occurred in all cases 3 days after the end of the treatment, and the animals generally showed signs of morbidity during or after the treatment. The other tested STLs either had no curative effect or, in several cases, displayed toxicity levels that precluded further treatment (R. Brun, M. Kaiser, personal communication).

The group of Matthias Hamburger and Michael Adams reported that the guaianolide cynaropicrin (**47**) displayed some in vivo activity (Zimmermann et al. 2012). This compound showed a significantly lower in vitro activity than STLs such as **1** or **73**; nevertheless, it was reported to exert a curative effect in the above-mentioned mouse model. When treated with 5 and 10 mg/kg of **47** over 4 days, the animals were cleared of 83 and 92% of the parasitemia 3 days after the end of the treatment. However, the animals only showed a slight increase of survival time since they apparently suffered from a relapse as well. Thus, it may be concluded that **47** did not present much advantage over the compounds mentioned above. Subsequent attempts to use a semi-synthetic dimethylamino adduct of **47** led to a decrease in toxicity but also to a loss of in vivo anti-trypanosomal activity (Zimmermann et al. 2014).

In the same study (Zimmermann et al. 2014), the authors also investigated the anti-*Tbr* potential of 34 natural and semi-synthetic STL derivatives obtained by addition of various amino substituents to the exocyclic methylene groups. The general structural determinants for high activity found in that study were, once more, related to the presence of alkylant structure elements. Interestingly enough, it has been reported that the semi-synthetic addition of morpholino and dimethylamino groups to the exocyclic methylene group of the parent STLs did not reduce but rather enhance the in vitro activity. Tyramino-, 2-(4-chlorophenyl)ethylamino or 1-(2-chlorophenyl)piperazyl derivatives were found to be two- to fourfold more active than their parent compounds that do not bear an enoate moiety. These derivatives, however, also displayed high toxicity levels (Zimmermann et al. 2014).

Quite interestingly, not so much is known about the mechanism underlying the anti-*Tbr* activity of STLs. Due to the well-known fact that STLs are particularly reactive towards thiol groups, in our first report on the activity of STLs against African trypanosomes (Schmidt et al. 2002), we hypothesized that the effect exerted by these compounds was related to the peculiar thiol metabolism of trypanosomatids, i.e. to the trypanothione system. Therefore, in 2002, helenalin was tested for its potential inhibitory capacity on trypanothione reductase (TR) to find it inactive (L. Krauth-Siegel, personal communication). More recently, the inhibition of trypanothione synthetase (TS) was also excluded as a mechanism of action, since no significant effects of helenalin and some other STLs were observed against TS of various trypanosomatids, including *Tbr* (M. Comini, personal communication).

Another mechanism related to the reaction with free thiols is the inhibition of cysteine proteases, particularly, rhodesain in case of *Tbr*. Since docking studies

gave promising results, helenalin and some other STLs were therefore tested for inhibition of this protease but were found to be inactive (W. Setzer, personal communication). Similarly, mexicanin I was found to be inactive when tested against *T. cruzi* cruzain (A. Do Amaral, personal communication).

Based on the finding that cynaropicrin (**47**) had shown some *in vivo* activity, Zimmermann et al. have investigated its potential mechanism of action (Zimmermann et al. 2013). As expected, **47** (50  $\mu\text{M}$ ) was found to form covalent adducts with trypanothione, thus depleting the intracellular thiol pool. Studies on inhibition of trypanothione-related enzymes by **47** have demonstrated that neither TR nor TS are significantly affected by the STL even when used at higher concentrations. However, an inhibitory effect on ornithine decarboxylase (ODC, which is known as the molecular target of the clinically used drug eflornithine and catalyzes an important step in trypanothione biosynthesis) was found. However, since these experiments were conducted at concentrations that were more than a hundred times higher than the effective  $\text{IC}_{50}$  of **47** against *Tbr* (0.4  $\mu\text{M}$ ), it may be questioned whether this mechanism may fully account for the anti-trypanosomal activity.

Based on our discovery of 4,15-isoatriplicolide tiglate (**73**) as an extremely potent anti-*Tbr* agent (Schmidt et al. 2014), we have recently renewed our interest in the trypanothione system as a potential target of STLs. We have found that this compound has inhibitory capacity on *Trypanosoma brucei* (*Tb*) and *T. cruzi* TR, which are very similar to each other. This property distinguishes 4,15-isoatriplicolide tiglate (**73**) from a series of other STLs (**2**, **8**, **34**, **62**, **70**, **71**) that were also tested against these enzymes and were found to be inactive (Lenz et al. 2015). Helenalin acetate (**2**), which is one of the inactive STLs in this test, confirmed the earlier observation with unesterified **1** (see above). Even though the activity of 4,15-isoatriplicolide esters (the tiglate **73** as well as the congeneric methacrylate and isobutyrate) against *Tb*TR was relatively low ( $\text{IC}_{50}$  values of about 20  $\mu\text{M}$  for **73**, after 15 min preincubation with the STL), it appears conceivable that the inhibition of this crucial enzyme under cellular conditions may at least contribute to these particular compounds' considerable anti-*Tbr* activity. This hypothesis is supported by the fact that the inhibition was found to be irreversible, thus indicating that the STLs cause a covalent modification of the cysteines of the enzyme's active site (Lenz et al. 2015). The fact that helenalin acetate, under the same conditions, was inactive against TR also indicates, on the other hand, that other targets have to be considered in order to fully explain the exceptional antiparasite activity of these compounds as well as that presented by some other STLs. The mechanistic studies in this direction are therefore currently being intensified.

### 15.2.2 Anti-trypanosomatid Activity: *Trypanosoma cruzi*

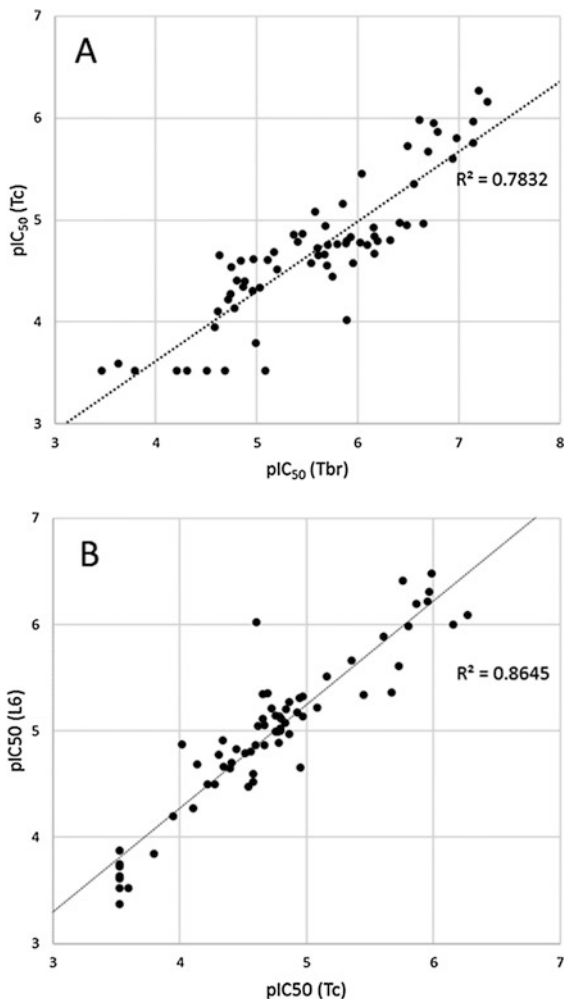
A variety of studies, including our own, have assessed the activity of STLs against *T. cruzi* (*Tc*), the causative agent of Chagas disease. According to our experience, this parasite is generally less susceptible to drugs, probably due to its intracellular

localization. In infected patients, *Tc* invades cells (e.g. muscle cells) where it persists over decades, thus evading the immune system attack. Drug activity is therefore frequently assessed on the intracellular amastigote form, in case of the data obtained in the laboratory of Swiss TPH, Basle, in rat skeletal myoblasts (L6 cell line). Over the years, we have obtained results working with the set of STLs described above (Schmidt et al. 2009, 2014) to find that the most active compounds were helenalin (**1**) and helenalin acetate (**2**;  $IC_{50} = 0.70$  and  $0.54 \mu\text{M}$ , respectively). The activity against *Tc* was about 10 times lower than that against *Tbr* and in a similar range as the cytotoxic activity determined with L6 cells. Similarly, the strong anti-*Tbr* agents of the furanoheliangolide type (**70**, **71**, **73**) were not selective for *Tc* (Schmidt et al. 2014). Therefore, further studies to assess the activity of our STLs against this parasite would not appear reasonable. A variety of other studies on the activity of STLs have been published over the years by other groups, as reviewed in (Acevedo et al. 2017).

As for structure-activity relationships, it would appear likely that similar factors as those described above for *Tbr* will be important for the anti-*Tc* activity of STLs. Accordingly, Sülsen et al. have created a QSAR model to explain the activity of 15 STLs of the pseudoguaianolide, guaianolide, germacranolide and eudesmanolide types against *Tc* epimastigotes (Fabian et al. 2013). Some of the compounds have shown quite low  $IC_{50}$  values (e.g.  $0.24 \mu\text{M}$  for the guaianolide estafietin, which was found to be the most active compound) and also very promising SI values obtained with Vero cells ( $SI = 1789$ ). A QSAR study was then performed using a variety of 1-, 2- and 3D molecular descriptors. Interestingly, it was found that, besides a weighted holistic invariant molecular (WHIM) descriptor related to molecular volume/shape, an indicator variable (“LAC”) encoding the presence/absence (1/0) of an  $\alpha$ -methylene- $\gamma$ -lactone moiety was required to obtain a model with good explanatory and predictive capacities. This finding is in line with our QSAR investigations on the anti-*Tbr* activity of STLs, in which reactivity-related descriptors were found to be the most important determinants of activity. Indicator variables such as the one used in (Fabian et al. 2013) were already used successfully in our work performed on 40 STLs (Schmidt et al. 2009) and in preceding QSAR studies on the cytotoxicity of STLs (Schmidt 1999a, b; Schmidt and Heilmann 2002). Even though the set of compounds investigated in this SAR study for *Tc* was small, and the activity data was obtained with epimastigotes and not with the clinically more relevant intracellular forms, it may hence be concluded that similar mechanisms are at work when STLs act on either *Trypanosoma* species. This also becomes obvious when the activity data obtained over the years in our group are plotted against each other (Fig. 15.3) where a high degree of linear correlation is observed between the two sets of anti-trypanosomal activity data indicating a related mechanism of action. On the other hand, a high degree of correlation is observed when the activity data for *Tc*, determined for amastigotes in rat skeletal myoblasts (L6 cell line), are compared with the cytotoxicity against the same uninfected host cells. The very strong correlation between these effects may indicate that the observed anti-*Tc*-activity is indeed not only related to but possibly caused by the cytotoxic effect on the host cells.

Even though a variety of STLs have been reported to show in vitro activity against *Tc* (Schmidt et al. 2012), not many of these compounds have been tested

**Fig. 15.3** (a): Plot of activity data ( $pIC_{50}$  [M]) of 67 STLs against *T. cruzi* (intracellular amastigotes in L6 cells) vs. *T. brucei* rhodesiense (bloodstream forms) showing the significant linear relationship between the effects. (b): Plot of activity data ( $pIC_{50}$  [M]) obtained with the same STLs for cytotoxicity (L6 cells) vs. *T. cruzi* (intracellular amastigotes in the same cells) showing the strong linear relationship between the effects. (Data from Schmidt et al. 2009, 2014)



against *Tc* in animal models, and only few have been reported to be active in vivo (references cited in Schmidt et al. 2012). However, some recent reports on the furanoheliangolide lychnopholide encapsulated in a nano-formulation have shown in vivo activity against *Tc* in infected mice (Branquinho et al. 2014), which opens a promising way to fully exploit the potential of STLs against this parasite and, maybe, others as well.

### 15.2.3 Anti-trypanosomatid Activity: *Leishmania* Species

Several SAR studies on the anti-leishmanial activity of STLs have been performed over the last years, as summarized by the group of M.T. Scotti (Acevedo et al. 2017). Data from our own investigations, obtained with most of the compounds of the

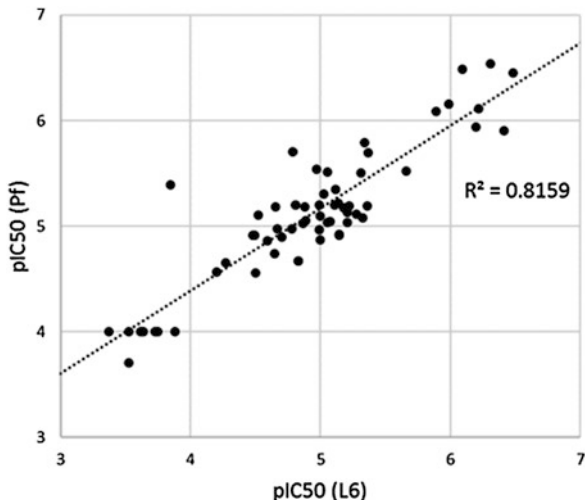
above-mentioned set of STLs (**1–78**) tested against axenically cultured amastigotes of *L. donovani* (*Ld*; causative pathogen of “Old World” visceral leishmaniasis, VL), indicate a significant but relatively low degree of correlation with toxicity to mammalian L6 cells. However, in the few instances where the more promising compounds of this series were tested against intracellular forms (in infected macrophages), no significant selectivity was observed; therefore, none of the compounds seem to be useful as anti-*Ld* drugs. These observations, however, may not hold true for other *Leishmania* species. In a recent study, helenalin acetate (**2**), mexicanin I (**5**) and some further compounds from our set have been tested against *L. major*, which is the causative agent of VL in the Americas. The tested compounds, in particular **2** and **5**, showed a marked selectivity for the intramacrophage forms of the parasite, which were about three times more susceptible ( $IC_{50}$  1.2 and 1.7  $\mu$ M, respectively) than the extracellular promastigote forms. The selectivity indices (SI) in relation to mammalian cytotoxicity (tested on murine NCTC fibroblasts) were in the range of 7 and 5, respectively (Wulsten et al. 2017). In search for more promising selectivities, studies with other *Leishmania* species, such as those causing cutaneous leishmaniasis, are now ongoing.

#### **15.2.4 Antiplasmodial Activity and SAR (Excluding Artemisinin and Derivatives)**

The discovery of the STL artemisinin as a potent antimalarial, the SAR studies of artemisinin congeners and their mechanism of action as well as the development of the semi-synthetic derivatives artemether and artesunate, now standard therapeutics against tropical malaria caused by *Plasmodium falciparum* (*Pf*), have been reviewed extensively in many previous articles (Schmidt 2006; Ojha and Roy 2015; Teixeira et al. 2012; Sun and Zhou 2016; Wang et al. 2015) so that this class of compounds are excluded from this short review. A number of studies have assessed the antiplasmodial activity of the more common STLs (i.e. such as those without the cyclic endoperoxide moiety that is required for artemisinin activity). Most of these studies are reviewed in (Schmidt et al. 2012). The presence of Michael acceptor structural elements is generally required to achieve a significant antiplasmodial activity. The frequently observed structural requirement of more than one of such moieties is confirmed by the results of a recent study performed with the eudesmanolide dehydrobrachylaenolide. This compound, which contains an  $\alpha$ -methylene- $\gamma$ -lactone as well as an exocyclic double bond conjugated with a keto function, was compared with a few congeners containing only one or no Michael acceptor site to find that this compound was the only significantly active compound in this series (Becker et al. 2011). This study also demonstrated that the mechanism of action of the mentioned compound differs from that of artesunate, since a gene expression profile analysis after treatment with this STL showed that only a very small fraction (7.65%) of almost 400 affected parasite genes affected by each compound were identical. However, the authors also noticed a relationship between the antimalarial activity and the compound's cytotoxicity.



**Fig. 15.4** Activity data ( $\text{pIC}_{50}$  [M]) of antiplasmodial activity of STLs (*P. falciparum*, intraerythrocytic forms, K1 and NF54 strains) against their cytotoxicity (L6 cells). (Data from Schmidt et al. 2009, 2014)



Our own investigations with largely the same set of STLs mentioned in the previous sections, tested against intraerythrocytic forms of *Pf*, indicate that there is a high degree of correlation between the compounds' activity and their cytotoxic effect. The data of anti-*Pf* activity and the cytotoxicity of over 50 of our compounds show a squared correlation coefficient  $R^2$  of almost 0.82 (Fig. 15.4), and the highest SI observed among these compounds is 35. However, unfortunately, this SI value was obtained with **59**, a compound displaying quite low anti-*Pf* activity ( $\text{IC}_{50} = 4.1 \mu\text{M}$ ). Similarly to *Tc*, the selectivity is probably too low to warrant further efforts to develop these compounds as antimalarial drugs.

Finally, it is worth mentioning that to date, only one study has succeeded in establishing statistically reasonable models to assess anti-trypanosomal (*Tbr* and *Tc*), anti-leishmanial (*Ld*) and antiplasmodial (*Pf*) activities together with cytotoxicity (L6 cells). In this study, Trossini et al. (2014) have applied the hologram-QSAR (HQSAR) approach to the data set of 40 STLs published by our research group in 2009 (Schmidt et al. 2009). HQSAR is based on breaking down the molecular structures into various 2D fragments of variable size and searching, through multivariate regression, those fragments that contribute most significantly to the overall variance in activity. Having identified these fragments, they can be mapped back into the 3D molecular structure in order to identify their possible contributions to the biological activity. Thereby, relatively subtle differences between related but not identical biological effects (such as toxicity vs. the various parasites under study) can be explained. These differences could not be explained through other methods. Trossini et al. have succeeded in constructing HQSAR models of comparably good quality for all mentioned sets of activity data of the STLs under study and could highlight the differential effect of certain structure elements on activity against these parasites. This interesting approach is being further exploited by our research group.

### 15.3 Structure-Antitumour Activity Relationships

The antitumoural potential of STLs has been under study for many decades. It has long been known that many of these compounds exert a cytotoxic activity at low concentrations and that some of them show a certain degree of selectivity against tumour cells (Schmidt 1999a, 2006; Merfort 2011; Kreuger et al. 2012). It is well-established that STLs have multiple targets to induce cell death and often do so at low concentrations by inducing apoptosis. Many reviews have described in detail the mechanisms involved and the various known potential molecular targets responsible for this activity (Schmidt 1999a, 2006; Merfort 2011; Kreuger et al. 2012). SARs with respect to cytotoxicity have also been reviewed extensively (Schmidt 1999a, 2006; Merfort 2011), and it is undoubted that the alkylant properties of STLs play the most important role also in this biological activity. However, in spite of the intense research carried out over the past 30–40 years, no STL has been developed into an anticancer drug for clinical use, except for one compound, the guaianolide arglabin (**49**) which – after its introduction in 1999 in the form of a semi-synthetic dimethylammonium hydrochloride derivative – has been used in cancer treatment in Kazakhstan (literature cited in Lone et al. 2015). No conclusive data, however, are publicly available on its clinical efficacy and safety.

As mentioned above, it is known that the induction of apoptosis by STLs is governed by various mechanisms, ranging from inhibition of enzymes that are vital for cell metabolism, to the inhibition of various cellular signalling cascades. It is not clear whether it would be possible to separate a tumour-selective activity from the general cytotoxicity of this class of compounds (Schmidt 1999a, 2006; Merfort 2011; Kreuger et al. 2012). In a very recent work, however, a novel and probably very important new mechanism for antitumoural activity of STLs has been discovered. This mechanism, as will be pointed out, is directed very specifically towards a particular assembly of transcription factors related to cell differentiation and proliferation, namely, c-Myb- and C/EBP-related transcription.

The c-myb gene is a proto-oncogene encoding a transcription factor (c-Myb) that has important regulatory functions in the expression of genes that determine cell lineage, proliferation and differentiation (Weston 1998; Lipsick and Wang 1999; Oh and Ready 1999; Ramsay and Gonda 2008). The c-myb gene is of crucial importance in the haematopoietic system, and it has been demonstrated to play an essential role for the development of most haematopoietic cell lineages (Mucenski et al. 1991; Emambokus et al. 2003; Bender et al. 2004; Carpinelli et al. 2004; Sandberg et al. 2005; Thomas et al. 2005). This gene is expressed with highest intensity in immature haematopoietic progenitor cells of all lineages. For their terminal differentiation, it is essential that c-myb be gradually downregulated. The c-myb gene is also expressed in some other tissues (Sitzmann et al. 1995) such as colonic crypt progenitor cells, where it also plays a role in the proliferation (Malaterre et al. 2007). The c-Myb transcription factor is involved in the regulation of a large variety of genes, particularly those related to differentiation, proliferation and cell survival (Rushton et al. 2003; Lang et al. 2005; Liu et al. 2006; Berge et al. 2007). It has been

demonstrated that a deregulation of c-Myb is involved in the development of certain leukaemias, as well as breast- and colon tumours. Therefore, the inhibition or suppression of c-Myb-induced gene transcription might be an interesting new anticancer therapeutic approach (Ramsay and Gonda 2008).

In a co-operative research work carried out by our laboratory and K.H. Klemppnauer's group, it was demonstrated that various STLs can inhibit c-Myb-induced transcription and are thus able to interfere with the function of the transcription machinery associated with it. After the initial finding that the pseudoguaianolides helenalin (**1**), mexicanin I (**5**), and, to a lesser extent, also the germacranolide parthenolide (**34**), the guaianolide dehydrocostus lactone (**45**) and the eudesmanolide isoalantolactone (**54**) inhibit c-Myb related transcription in a dose-dependent manner (Bujnicki et al. 2012), we undertook a SAR study with 60 STLs from our library, covering a considerable chemical diversity and displaying  $IC_{50}$  values between 0.6 and  $>30 \mu\text{M}$  (Schomburg et al. 2013). The plots shown in Fig. 15.5 show that his activity is only weakly related to unspecific cytotoxicity. Once more, as in so many other cases before, those compounds lacking any potential Michael acceptor structure element were inactive. However, the mere presence of such a reactive site alone did not warrant the inhibitory activity either. Compounds of the helenalin type (**1-4** and, in particular, the acetate **2** as most active derivative) combining the  $\alpha$ -methylene- $\gamma$ -lactone and cyclopentenone moieties were among the most active STLs and much more potent than either the 2,3- or 11,13-dihydro-derivatives tested. Therefore it could be concluded that the presence of two reactive sites was crucial for a high activity. It was an interesting finding, however, that synthetic cyclopent-2-enone and  $\alpha$ -methylene- $\gamma$ -lactone, tested as model chemicals separately and also in a 1:1 mixture, did not show any inhibitory effect in the transcriptional assay. It was therefore concluded that the two reactive centres must be connected in a suitable relative orientation, which is obviously constituted by the STL skeleton. Quite interestingly, goyazensolide (**70**), a furanoheliangolide STL with a structure appearing rather dissimilar from that of the pseudoguaianolides, was even slightly more potent than helenalin acetate. A detailed comparison of the 3D structures of these two most potent transcription inhibitors has revealed that they are more similar than the analysis of their structural diagrams would indicate (see Fig. 15.6) and that they share a rather similar molecular shape, distribution of hydrophilic/hydrophobic surface and electrostatic properties. In particular, their reactive structure elements are in a rather similar relative orientation towards each other. Based on the alignment of these two STLs, a 3D pharmacophore hypothesis could then be established, which was used to construct a 3D QSAR model explaining about 83% of the variance in the measured biological data within a training set of 40 compounds and giving reasonably good external predictions for a test set of 20 compounds. The underlying common pharmacophore consisted of several regions in space in which Michael acceptor structures, some hydrogen bonding substituents as well as hydrophobic elements were located in the two most active molecules. After an overlay of all tested compounds with this pharmacophore description (Fig. 15.6c, d), the presence/absence of matching structure elements in each molecule for each pharmacophore region was noted as 1/0 descriptor variable and submitted, along with some other descriptors, to PLS regression.

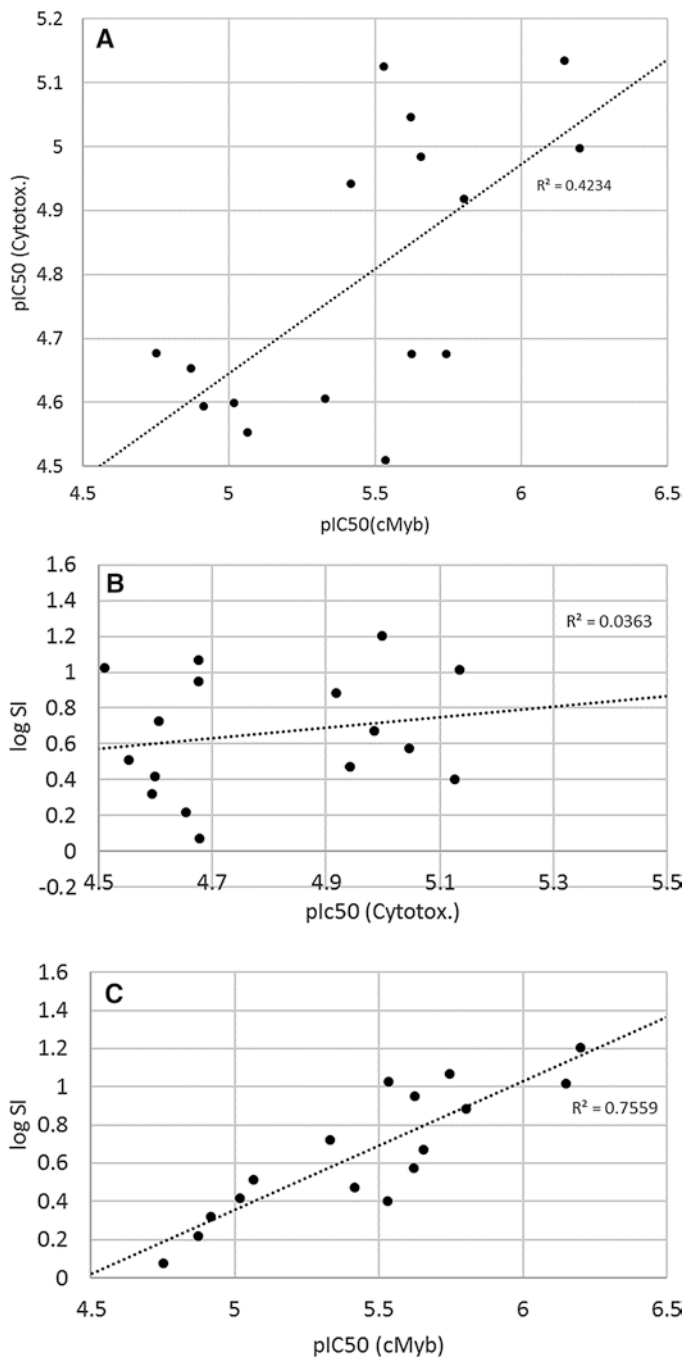


**Fig. 15.5** (a): Activity data ( $pIC_{50}$  [M]) of STLs cytotoxicity (MTS assay) on cells used in the c-Myb assay vs. inhibition of cMyb-related transcription in a fluorescence-based reporter gene assay. Only a weak correlation between cytotoxicity and inhibition of c-Myb exists. (b): Selectivity index (log SI) vs. cytotoxic activity and (c): log SI vs. c-Myb inhibitory activity. No correlation of selectivity with

**Fig. 15.6** (a): Surface representations of helenalin acetate (**2**, left) and goyazensolide (**70**, right), coloured by electrostatic potential (red, electronegative; blue, electropositive); (b): The same structures coloured by hydrophobicity (green, hydrophobic; blue, hydrophilic). (c): Superimposition of both molecular structures with their common pharmacophore model; (d): Structures of 60 STLs, superimposed with the pharmacophore. The fit of each molecule with each of the pharmacophore features was used to construct the descriptors for the QSAR study in Schomburg et al. (2013)

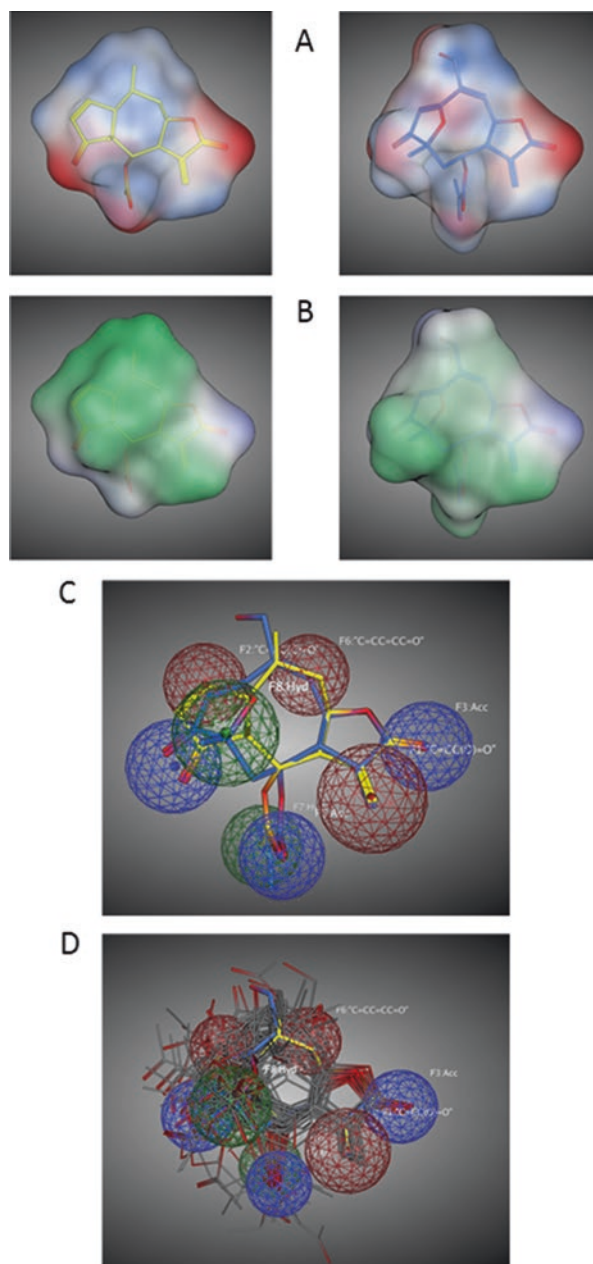


**Fig. 15.5** (continued) cytotoxicity, but a strong correlation of SI with the c-Myb inhibition exists. The plots cover only those compounds ( $n = 16$ ) for which IC<sub>50</sub> values could be obtained in both assays. (Data from Schomburg et al. 2013)

After selection of the most relevant variables, pharmacophore features encoding the respective Michael acceptor centres were found to yield highly significant contributions to the overall linear regression model. It was also shown that the good fit of this QSAR model was not merely related to the presence or absence of these Michael acceptor sites but was clearly dependent on their relative orientation in space, which points towards a highly specific interaction with the putative common binding site at the target protein, then believed to be c-Myb (Schomburg et al. 2013).

It has recently been discovered in more detailed mechanistic studies that the activity of STLs observed in the above-mentioned assay system is more complex than believed at the time when the QSAR study was conducted. It is known that c-Myb exerts its transcriptional activity in close cooperation with several other transcription factors. Through a series of conclusive biochemical experiments, it was found that helenalin acetate is actually an inhibitor of the CCAAT-box/enhancer-binding protein beta (C/EBP $\beta$ ), more specifically, of the interaction of this protein with the co-activator p300. This interaction is required for an efficient interaction with and activation of c-Myb transcriptional activity so that the previous observations (Bujnicki et al. 2012; Schomburg et al. 2013) can be attributed to a disruption of the interaction between this pair of cooperating proteins and not to a direct activity on c-Myb (Jakobs et al. 2016a, b).

Interestingly enough, this activity was found to be related to a particular amino acid sequence in the N-terminal region of the so-called LAP\* isoform of C/EBP $\beta$ , and it has been shown that the interaction of this region with a particular domain (Taz2) of p300 is disrupted by helenalin acetate. Through site-directed mutagenesis experiments, it has been demonstrated, however, that none of the cysteines in the respective region of C/EBP $\beta$  is likely to be alkylated by helenalin acetate and there is evidence that the binding of the STL to the C/EBP $\beta$  protein might be reversible (Jakobs et al. 2016a). In view of the clear evidence obtained from the comparison of so many different STLs' activities and the QSAR model described above (Schomburg et al. 2013), alternative mechanisms which unite all experimental results must hence be taken into consideration. A renewed QSAR study focusing specifically on the C/EBP $\beta$ -p300 interaction is now envisaged, which could help to shed light on such, yet not elucidated, mechanisms. In these studies, to investigate the differential activity of the various STLs on C/EBP $\beta$  and the closely related C/EBP $\alpha$  will also be important, since some preliminary evidence has been obtained that some, but not all, STLs inhibiting C/EBP $\beta$  can also influence the  $\alpha$ -orthologue to a certain extent (Klempnauer KH, personal communication).

As stated above, the full potential of STLs as antitumour agents could not be exploited yet, mainly due to a lack of selectivity. However, the concentrations of helenalin acetate and goyazensolide needed to inhibit c-Myb-related transcription and blockage of the C/EBP $\beta$  function are in the submicromolar range, and we could show selectivity of this effect in comparison with an unspecific cytotoxicity (Schomburg et al. 2013). Furthermore, and most importantly, helenalin acetate (Jakobs et al. 2016a) and also mexicanin I (Bujnicki et al. 2012) have proved to have selective toxicity towards human acute myeloid leukaemia (AML) leukaemic blasts at concentrations that did essentially not affect healthy bone marrow cells. First

experiments with a leukaemic mouse model have, moreover, yielded good evidence that helenalin acetate may indeed have a curative effect (Jakobs et al. 2016a) so that further research in this direction is now being pursued with high priority.

This interesting and novel mechanism of action of STLs on C/EBP $\beta$  and the related transcriptional machinery is currently giving a new boost to the research on STLs as anticancer agents. These findings, finally, are also of great importance with respect to the well-known anti-inflammatory activity of STLs as will be discussed in the following section.

## 15.4 Structure-Anti-inflammatory Activity Relationship

Sesquiterpene lactones have long been known as active principles in a variety of medicinal plants used to treat inflammatory conditions (Schmidt 2006; Merfort 2011). The anti-inflammatory mechanisms of action have been under intense research for decades, and the hitherto most influential discovery in this field has probably been their inhibitory effect on nuclear transcription factor  $\kappa$ B, discovered almost 20 years ago, in the late 1990s and early 2000s (Lyss et al. 1997; Lyss et al. 1998; Rungeler et al. 1999; Garcia Pineres et al. 2001). This transcription factor is a pivotal regulator of many genes involved in the immune response and inflammation so that the discovery of its inhibition by STLs, for the first time, gave a satisfactory explanation to their multiple effects on inflammatory processes.

The first SAR models describing the anti-NF- $\kappa$ B activity of STLs, beginning with the seminal work of Rungeler et al. (1999), were summarized in my 2006 review and a first QSAR model covering all STLs investigated at that time (a series of 21 compounds studied already in Rungeler et al. (1999) was presented there (Schmidt 2006)). A detailed QSAR study on the NF- $\kappa$ B inhibition by 103 STLs was then published by the group of Irmgard Merfort, who also performed QSAR studies on 24 STLs influencing the IL-8 production and others, and the main findings were summarized in her 2011 review (Merfort 2011). Not surprisingly, the main structural determinant of STLs responsible for a strong inhibition of NF- $\kappa$ B, as in other cases described above and elsewhere, was their reactivity as alkylants. Along the same line, a more recent study has investigated SAR for the inhibition of NF- $\kappa$ B:DNA complex formation of a series of 27 natural and semi-synthetic 7(12),6-lactonized pseudoguaianolides. Even though no QSAR was performed, the authors could confirm the fact that, in their series, the presence of an  $\alpha$ -methylene- $\gamma$ -lactone moiety was essential for strong inhibitory activity and that a carbonyl oxygen substituent at C-3 of the pseudoguaianolide moiety enhanced this effect (Villagomez et al. 2015).

Similarly, as stated above for the antitumour activity, it has been questioned whether the anti-inflammatory and cytotoxic effects of STLs could be separated at all since both are based on the same basic chemical phenomenon, namely, Michael addition to biological nucleophiles (Merfort 2011). On this background, our new findings on the inhibition of C/EBP $\beta$  activity (Bujnicki et al. 2012; Schomburg et al. 2013; Jakobs et al. 2016a, b; see previous section) are worth mentioning. Besides its

functions in cell proliferation and differentiation, it is well established that this factor, and the transcriptional machinery associated with it, is also intimately involved in the inflammatory response. In particular, C/EBP $\beta$  (also termed, nuclear factor-IL6) is involved in interleukin signalling such as the TNF- $\alpha$ - and IL-17-induced pathways (see, e.g. the respective pathway maps at <http://www.kegg.jp> and Natsuka et al. 1992; Davydov et al. 1995; van Dijk et al. 1999; Greenwel et al. 2000). At this point it is important to emphasize that the inhibitory activity of helenalin and helenalin acetate on C/EBP $\beta$  was determined to be at least 10 times stronger than that for NF- $\kappa$ B (EC<sub>50</sub> between 0.1 and 0.4  $\mu$ M for C/EBP $\beta$  vs. 4  $\mu$ M for NF- $\kappa$ B) (Jakobs et al. 2016a). Although this issue has only been investigated in detail for these two important and well-known anti-inflammatory STLs (responsible for the well-established clinical efficacy of anti-inflammatory herbal medicines containing Arnica flowers (Lyss et al. 1999)), it may be conceived that the C/EBP $\beta$  inhibition is indeed a major determinant of their anti-inflammatory action and possibly even more important than the anti-NF- $\kappa$ B-activity. Our ongoing collaborative research on SAR of STLs and their C/EBP-inhibitory activity is hence of twofold impact since it sheds, at the same time, new light on their anticancer and anti-inflammatory activities.

## 15.5 Conclusion

This chapter attempted to give a short overview on the more recent developments and newer findings on SARs of STLs, with a focus on the most prominent biological activities of this large class of secondary plant metabolites. As it can be appreciated, STLs still remain a field of very active pharmacological research. It is particularly interesting to see that, in many instances, great progress has been achieved with respect to the mechanisms of action, which opens new perspectives also in the direction of research on more specific SARs. In the antiprotozoal field, promising results with cynaropicrin have shown that STLs may indeed have a potential as drugs against African trypanosomiasis. Our QSAR studies have led the way to highly potent furanoheliangolides, which are now being studied mechanistically in order to find possibilities to improve their *in vivo* efficacy. The new mechanistic findings on the c-Myb and C/EBP transcription system open new perspectives to exploit more efficiently the anticancer and, probably, anti-inflammatory activity of STLs. Many exciting further discoveries are very likely yet to emerge, and thus this chapter may end with the same words as my review of 2006: “Sesquiterpene lactones certainly deserve to remain an active field of natural products research for many years.”

**Acknowledgements** I feel deeply grateful to all the co-workers, mainly doctoral students, who have contributed over the years to STL research in my group. Not all my students have been working on the discovery of new STLs but even those who did not have – in different ways – contributed to this work.



Very cordial thanks are due to Marcel Kaiser and Reto Brun of the Swiss Tropical and Public Health Institute, Basel, and to Karl-Heinz Klempnauer of the Institute of Biochemistry, University of Münster, for their continuous and very fruitful cooperation over many years. I also thank the many collaborators within the Research Network Natural Products against Neglected Diseases (<http://www.ResNetNPND.org>), who contributed bigger or smaller pieces to STL research in the past or present: Sami A. Khalid, Fernando B. Da Costa, Norberto P. Lopes, Luise Krauth-Siegel, William Setzer, Marcelo Comini, Antonia Do Amaral and, most recently, Valeria Sülsen. Thanks also to all others who cooperate with me, but not only on the study of STLs. Finally, I would like to acknowledge gratefully once more the support and inspiration by my former mentor and Doktorvater Günter Willuhn (formerly University of Düsseldorf). Thank you for awakening my interest in this fascinating class of natural products: sesquiterpene lactones.

## References

- Acevedo CH, Scotti L, Alves MF et al (2017) Computer-aided drug design using sesquiterpene lactones as sources of new structures with potential activity against infectious neglected diseases. *Molecules* 22:79
- Becker JW, van der Merwe MM, van Brummelen AC et al (2011) *In vitro* anti-plasmodial activity of *Dicoma anomala* subsp. *gerrardii* (Asteraceae): identification of its main active constituent, structure-activity relationship studies and gene expression profiling. *Malar J* 10:295
- Bender TP, Kremer CS, Kraus M et al (2004) Critical functions for c-Myb at three checkpoints during thymocyte development. *Nat Immunol* 5:721–729
- Berge T, Matre V, Brendeford EM et al (2007) Revisiting a selection of target genes for the hematopoietic transcription factor c-Myb using chromatin immunoprecipitation and c-Myb knock-down. *Blood Cells Mol Dis* 39:278–286
- Branquinho RT, Mosqueira VC, de Oliveira-Silva JC et al (2014) Sesquiterpene lactone in nanostructured parenteral dosage form is efficacious in experimental Chagas disease. *Antimicrob Agents Chemother* 58:2067–2075
- Bujnicki T, Wilczek C, Schomburg C et al (2012) Inhibition of Myb-dependent gene expression by the sesquiterpene lactone mexicanin-I. *Leukemia* 26:615–622
- Carpinelli MR, Hilton GJ, Metcalf D et al (2004) Suppressor screen in Mpl/mice: c-Myb mutation causes supraphysiological production of platelets in the absence of thrombopoietin signaling. *Proc Natl Acad Sci USA* 101:6553–6558
- Davydov IV, Krammer PH, Li-Weber M (1995) Nuclear factor-IL6 activates the human IL-4 promoter in T cells. *J Immunol* 155:5273–5279
- Emambokus N, Vegiopoulos A, Harman B et al (2003) Progression through key stages of haemopoiesis is dependent on distinct threshold levels of c-Myb. *EMBO J* 22:4478–4488
- Fabian L, Sülsen V, Frank F et al (2013) In silico study of structural and geometrical requirements of natural sesquiterpene lactones with trypanocidal activity. *Mini Rev Med Chem* 13:1407–1414
- Garcia-Pineres AJ, Castro V, Mora G et al (2001) Sesquiterpene lactones inhibit the transcription factor NF-kappa B by alkylating its p65 subunit. *J Biol Chem* 276:39713–39720
- Gökbulut A, Kaiser M, Brun R et al (2012) 9 $\beta$ -Hydroxypartenolide esters from *Inula montbretiana* DC and their antiprotozoal activity. *Planta Med* 78:225–229
- Greenwel P, Tanaka S, Penkov D et al (2000) Tumor necrosis factor alpha inhibits type I collagen synthesis through repressive ccaat/enhancer-binding proteins. *Mol Cell Biol* 20:912–918
- Jakobs A, Uttarkar S, Schomburg C et al (2016a) An isoform-specific C/EBP $\beta$  inhibitor targets acute myeloid leukemia cells. *Leukemia* 30:1612–1615
- Jakobs A, Steinmann S, Henrich SM et al (2016b) Helenalin acetate, a natural sesquiterpene lactone with anti-inflammatory and anti-cancer activity, disrupts the cooperation of CCAAT-box/enhancer-binding protein beta (C/EBP $\beta$ ) and co-activator p300. *J Biol Chem* 291:26098–26108

- Kimani NM, Matasyoh JC, Kaiser M, Brun R, Schmidt TJ (2018a) Antiprotozoal sesquiterpene lactones and Other Constituents from *Tarhconanthus camphoratus* and *Schkuhria pinnata*. *J. Nat. Prod.* 81:124–130
- Kimani MN, Matasyoh JC, Kaiser M, Brun R, Schmidt TJ (2018b) Sesquiterpene lactones from *Vernonia cinerascens* Sch. Bip. and their in vitro antitrypanosomal activity. *Molecules* 23:248
- Kimani NM, Matasyoh JC, Kaiser M et al (2017) Anti-trypanosomatid elemanolide sesquiterpene lactones from *Vernonia lasiopus* O. Hoffm. *Molecules* 22:597
- Kreuger MRO, Grootjans S, Biavatti MW et al (2012) Sesquiterpene lactones as drugs with multiple targets in cancer treatment: focus on parthenolide. *Anti-Cancer Drugs* 23:883–896
- Lang G, White JR, Argent-Katwala MJ et al (2005) Myb proteins regulate the expression of diverse target genes. *Oncogene* 24:1375–1384
- Lenz M, Krauth-Siegel L, Schmidt TJ (2015) 4,15–isoatropicolide-esters: new inhibitors of trypanothione reductase. *Planta Med* 81:PM\_102. <https://doi.org/10.1055/s-0035-1565479>
- Lipsick JS, Wang DM (1999) Transformation by v-Myb. *Oncogene* 18:3047–3055
- Liu F, Lei W, O'Rourke JP et al (2006) Oncogenic mutations cause dramatic, qualitative changes in the transcriptional activity of c-Myb. *Oncogene* 25:5795–5805
- Lone SH, Bhat KA, Khuroo MA (2015) Arglabin: from isolation to antitumor evaluation. *Chem Biol Interact* 240:180–198
- Lyss G, Schmidt TJ, Merfort I et al (1997) Helenalin, an anti-inflammatory sesquiterpene lactone from *Arnica* selectively inhibits transcription factor NF-kappaB. *Biol Chem* 378:951–961
- Lyss G, Knorre A, Schmidt TJ et al (1998) The anti-inflammatory sesquiterpene lactone helenalin inhibits the transcription factor NF-kappa B by directly targeting p65. *J Biol Chem* 273:33508–33516
- Lyss G, Schmidt TJ, Pahl HL et al (1999) Studies for the anti-inflammatory activity of *Arnica* tincture using the transcription factor NF-kappa B as molecular target. *Pharm Pharmacol Lett* 9:5–8
- Maas M, Hensel A, da Costa FB et al (2014) An unusual dimeric guaianolide with antiprotozoal activity and further sesquiterpene lactones from *Eupatorium perfoliatum*. *Phytochemistry* 72:635–644
- Malaterre J, Carpinelli M, Ernst M et al (2007) c-Myb is required for progenitor cell homeostasis in colonic crypts. *Proc Natl Acad Sci USA* 104:3829–3834
- Merfort I (2011) Perspectives on sesquiterpene lactones in inflammation and cancer. *Current Drug Targets* 12:1560–1573
- Mucenski ML, McLain K, Kier AB et al (1991) A functional c-myb gene is required for normal murine fetal hepatic hematopoiesis. *Cell* 65:677–689
- Natsuka S, Akira S, Nishio Y et al (1992) Macrophage differentiation-specific expression of NF-IL6, a transcription factor for interleukin-6. *Blood* 79:460–466
- Nogueira MS (2016) The use of Chemometric and Chemoinformatic Tools for Identification and Targeted Isolation of Compounds from Asteraceae with Antiprotozoal Activity. Dr. rer. nat. thesis, University of Münster
- Nour AMM, Khalid SA, Brun R et al (2009) The antiprotozoal activity of sixteen Asteraceae species native to Sudan and bioactivity-guided isolation of xanthanolides from *Xanthium brasili-cum*. *Planta Med* 75:1363–1368
- Oh IH, Reddy EP (1999) The myb gene family in cell growth, differentiation and apoptosis. *Oncogene* 18:3017–3033
- Ojha PK, Roy K (2015) The current status of antimalarial drug research with special reference to application of QSAR models. *Comb Chem High Throughput Screen* 18:91–128
- Ramsay RJ, Gonda TJ (2008) Myb function in normal and cancer cells. *Nat Rev Cancer* 8:523–534
- Rüngeler P, Castro V, Mora G et al (1999) Inhibition of transcription factor NF-kappa B by sesquiterpene lactones – a proposed molecular mechanism of action. *Bioorg Med Chem* 7:2343–2352
- Rushton JJ, Davis LM, Lei W et al (2003) Distinct changes in gene expression induced by A-Myb, B-Myb and c-Myb proteins. *Oncogene* 22:308–313
- Sandberg ML, Sutton SE, Pletcher MT et al (2005) c-Myb and p300 regulate hematopoietic stem cell proliferation and differentiation. *Dev Cell* 8:153–166

- Schmidt TJ (1999a) Quantitative structure-cytotoxicity relationships within a series of helenanolide type sesquiterpene lactones. (Helenanolide type sesquiterpene lactones IV). *Pharm Pharmacol Lett* 9:9–13
- Schmidt TJ (1999b) Toxic activities of sesquiterpene lactones – structural and biochemical aspects. *Curr Org Chem* 3:577–605
- Schmidt TJ (2006) Structure-activity relationships of sesquiterpene lactones. In: Atta-ur-Rahman (ed) *Studies in natural products chemistry*, vol 33. Elsevier, Amsterdam, pp 309–392
- Schmidt TJ, Heilmann J (2002) Quantitative structure-cytotoxicity relationships of sesquiterpene lactones derived from partial charge (Q)-based fractional accessible surface area descriptors (Q\_frASAs). *Quant Struct-Act Relat* 21:276–287
- Schmidt TJ, Willuhn G, Brun R et al (2002) Antitrypanosomal activity of helenalin and some related sesquiterpene lactones. *Planta Med* 68:750–751
- Schmidt TJ, Nour AMM, Khalid SA et al (2009) Quantitative structure-antiprotozoal activity relationships of sesquiterpene lactones. *Molecules* 14:2062–2076
- Schmidt TJ, Khalid SA, Romanha AJ et al (2012) The potential of secondary metabolites from plants as drugs or leads against protozoan neglected diseases – Part I. *Current Med Chem* 19:2128–2175
- Schmidt TJ, Da Costa FB, Lopes NP et al (2014) In silico prediction and experimental evaluation of furanohelianiogolide sesquiterpene lactones as potent agents against *Trypanosoma brucei* rhodesiense. *Antimicrob Agents Chemother* 58:325–332
- Schomburg C, Schuehly W, Da Costa FB et al (2013) Natural sesquiterpene lactones as inhibitors of Myb-dependent gene expression: structure-activity relationships. *Eur J Med Chem* 63:313–320
- Sitzmann J, Noben-Trauth K, Klempnauer K-H (1995) Expression of mouse c-myc during embryonic development. *Oncogene* 11:2273–2279
- Sun C, Zhou B (2016) The molecular and cellular action properties of artemisinins: what has yeast told us? *Microb Cell* 3:196–205
- Teixeira RR, Carneiro JW, Araújo MT et al (2012) A critical view on antimalarial endoperoxide QSAR studies. *Mini Rev Med Chem* 12:562–572
- Thomas MD, Kremer CS, Ravichandran KS et al (2005) c-Myb is critical for B cell development and maintenance of follicular B cells. *Immunity* 23:275–286
- Trossini GHG, Maltarollo VG, Schmidt TJ (2014) Hologram QSAR studies of antiprotozoal activities of sesquiterpene lactones. *Molecules* 19:10546–10562
- van Dijk TB, Baltus B, Raaijmakers JA et al (1999) A composite C/EBP binding site is essential for the activity of the promoter of the IL-3/IL-5/granulocyte-macrophage colony-stimulating factor receptor beta c gene. *J Immunol* 163:2674–2680
- Villagomez R, Hatti-Kaul R, Sterner O et al (2015) Effect of natural and semisynthetic pseudoguanolides on the stability of NF-κB: DNA complex studied by agarose gel electrophoresis. *PLoS One*. <https://doi.org/10.1371/journal.pone.0115819>
- Wang J, Zhang CJ, Chia WN et al (2015) Haem-activated promiscuous targeting of artemisinin in *Plasmodium falciparum*. *Nat Commun* 6:10111
- Weston K (1998) Myb proteins in life, death and differentiation. *Curr Opin Genet Dev* 8:76–81
- Wulsten IF, Costa-Silva TA, Mesquita JT et al (2017) Investigation of the anti-*Leishmania* (*Leishmania*) *infantum* activity of some natural sesquiterpene lactones. *Molecules* 22:685
- Zimmermann S, Kaiser M, Brun R et al (2012) Cynaropicrin: the first plant natural product with *in vivo* activity against *Trypanosoma brucei*. *Planta Med* 78:553–556
- Zimmermann S, Oufir M, Leroux A et al (2013) Cynaropicrin targets the trypanothione redox system in *Trypanosoma brucei*. *Bioorg Med Chem* 21:7202–7209
- Zimmermann S, Fouché G, De Mieri M et al (2014) Structure-activity relationship study of sesquiterpene lactones and their semi-synthetic amino derivatives as potential antitrypanosomal products. *Molecules* 19:3523–3538